UNIVERSITY OF CATANIA

Department of Civil Engineering and Architecture (DICAR)

PhD in *Evaluation and Mitigation of Urban and Land Risks* (*XXXI Cycle)*

NDT application in Transport Asset Management

QA/QC performance specifications in pavement construction and maintenance

PhD Dissertation

CAPACE BRUNELLA

Supervisor: Prof. Cafiso Salvatore

Co-supervisors: Prof. Di Graziano Alessandro

Prof. Motta Ernesto

PhD Coordinator: Prof. Cuomo Massimo

ABSTRACT (ENG)

NDT application in Transport Asset Management. QA/QC performance specifications in pavement construction and maintenance

Nowadays, in Transport Asset Management, there is the need to identify measures to guarantee high levels of performance over time. The application of Non-Destructive Techniques, through high-efficiency equipment, turns out to be an optimal solution to ensure the quality of transport infrastructures.
Asset Management take into account the importance of monitoring the performance characteristics of the transport infrastructures and QA/QC performance-based contracts' specifications in order to guarantee the preservation of environmental, social and economic resources, as well.
This study consists of two parts of research activity: in field tests and numerical simulations.
The first part consists of in situ experimental activities to investigate both road and rail transport infrastructures. The tests have shown the versatility of high-performance instruments, such as FWD, LWD, GPR and ARAN, in railway monitoring, in the evaluation of ballast conditions and sleeper/ballast interaction, and also in the reuse of volcanic ashes that after stabilization can be used in road subbase layers. The high-efficiency equipment allow a faster execution of the tests with the possibility of a higher number of measurements, the combination of several instruments at the same time with a continuous mapping of the infrastructures, performance measures and a significant cost reduction.
In the second part, the study focuses more specifically on road pavements. Considering several flexible pavements pulled out from the Italian Catalog, numerical simulations of FWD tests were carried out in the hypothesis of multilayer elastic theory with the aim to develop performance-based criteria and specifications for QC of pavement construction work.
The results allow to estimate effects of structural deficits in the perspective of future performance and Life Cycle Cost Analysis in order to quantify penalties to restore expected higher maintenance costs.

Keywords: *pavement engineering, railway track, Non Destructive Tests, QA/QC, performance based specifications, Falling Weight Deflectometer, Ground Penetrating Radar*

ABSTRACT (ITA)

Applicazione di controlli non distruttivi nella gestione delle infrastrutture di trasporto. Specifiche prestazionali di controllo della qualità in costruzione e manutenzione

Al giorno d'oggi, nel Transport Asset Management, c'è la necessità di identificare misure atte a garantire elevati livelli prestazionali nel tempo. L'applicazione di tecniche non distruttive, attraverso strumenti ad alta efficienza, risulta essere una soluzione ottimale per garantire la qualità delle infrastrutture di trasporto.
L'Asset Management tiene conto dell'importanza del monitoraggio delle caratteristiche di performance delle infrastrutture di trasporto e delle specifiche QA/QC dei capitolati basati sulle prestazioni al fine di garantire la conservazione delle risorse ambientali, sociali ed economiche.
Questo studio si compone di due parti di attività di ricerca: test sul campo e simulazioni numeriche.
La prima parte consiste in attività sperimentali in situ per investigare sia sulle infrastrutture stradali che su quelle ferroviarie. I test hanno dimostrato la versatilità degli strumenti ad alte prestazioni, come FWD, LWD, GPR e ARAN, nel monitoraggio ferroviario, nella valutazione delle condizioni del ballast e l'interazione traversa/ballast, e anche nel riutilizzo delle ceneri vulcaniche che dopo la stabilizzazione possono essere utilizzate in strati di fondazione stradale. Le apparecchiature ad alta efficienza consentono un'esecuzione più rapida dei test con la possibilità di un numero maggiore di misurazioni, la combinazione di più strumenti contemporaneamente con una mappatura continua delle infrastrutture, misure di performance e una significativa riduzione dei costi.
Nella seconda parte, lo studio si concentra più specificamente sulle pavimentazioni stradali. Considerando diverse pavimentazioni flessibili estratte dal Catalogo Italiano, sono state effettuate simulazioni numeriche di test FWD nell'ipotesi della teoria del multistrato elastico allo scopo di sviluppare criteri e specifiche basati sulle prestazioni per il controllo di qualità QC dei lavori di costruzione delle pavimentazioni.
I risultati consentono di stimare gli effetti dei deficit strutturali nella prospettiva delle prestazioni future e dell'analisi dei costi nel ciclo di vita al fine di quantificare le penali per ripristinare i costi previsti di manutenzione più elevati.

GENERAL INDEX

INDEX OF FIGURES

INDEX OF TABLES

INDEX OF FIGURES

INDEX OF TABLES

INTRODUCTION

Road performance in today's society is essential for all users. The functionality of road pavements, with a long-term performance approach throughout the life cycle, certainly allows greater economic competitiveness, an improvement in the quality of life and a sustainable economic-social-environmental development.

The objective of the research is part of the field of *Transport Asset Management* with particular emphasis on performance specifications and the operational techniques and activities that are used to fulfill requirements for roads quality, considering a sustainable evolution of the network.

It concerns the study of the pavements performance with the goal to find new performance specifications in particular in Quality processes (QA/QC) to ensure the high quality and efficiency of road network with sustainable and reliable technical strategies from the moment where the road is built. The high quality of an infrastructure is determined by the satisfaction of all the technical requirements of Quality assurance QA and Quality Control QC.

Quality Assurance refers to all those planned and systematic actions necessary to provide confidence that a road infrastructure will perform satisfactorily in service in the most efficient, economical, and satisfactory manner possible. QA involves continued evaluation of the activities of planning, design, development of plans and specifications, advertising and awarding of contracts, construction, and maintenance, and the interactions of these activities.

Quality Control is comprehensive of those QA actions and considerations necessary to assess and adjust production and construction processes so as to control the level of quality being produced in the end product.

The aim of the PhD research is to develop specifications and models related to the use of high-efficiency equipment, highlighting also the opportunities of including non-destructive test during the acceptance quality control phase of work that concern new constructions of the Transport Infrastructures. In particular, the knowledge of relationship between measurable Quality Control parameters and long term performance is essential in assessing the quality of any construction work of an infrastructure that allow the development of a methodology based on performance indicators of the road pavement. For these reasons, it’s crucial to find correlations between different design methods with in-field measurable performance indicators for the introduction of new specification during the acceptance phase of construction works.

The use of advanced high-efficiency testing technologies, the definition of performance indicators in the field of QC processes, open a new and important upgrade scenario and evolution of road pavement engineering techniques, considering the possibility to transfer models on other transport infrastructures.

The possibility of using such advanced tools allows to have an overall knowledge of the performance of road pavements, both in terms of surface characteristics such as grip, macrotexture, unevennes, and deep characteristics as thicknesses and bearing capacity.

The latter in particular derive from technologies like Falling Weight Deflectometer and Georadar, which allow to investigate both the stratigraphy of the pavement and its composition and to derive the deflections that are generated with the traffic. Precisely from the knowledge of these deflections it is possible not only to calculate Basin Indexes that derive from relations between them, but also to develop correlations with parameters such as the Residual Life and the Structural Number for a performance-based knowledge of the entire road pavement structure.

Reliability, measurement repeatability and transferability are key-works for the development of the present research work.
In the chapters that follow, various research themes have been explored.
In Chapter 1 the issues of sustainable development, road quality and NDT techiques in high efficiency were deepened with a literature review at international and national level level from the major Road Authority and Organizations up to the ANAS Performance Specifications in Italy.
Starting from these bases, several experimental tests have been made and exposed in Chapter 2, on various transport infrastructures, thanks to the modern high-efficiency equipment of the "*Transport Infrastructure Laboratory TILab*" of the University of Catania with the possibility of performing performance surveys with ARAN, Falling Weight Deflectometer, Light Weight Deflectometer and Ground Penetrating Radar, which are among the most advanced non-destructive test devices at the state of the art in the field of QC.
The TILab is one of the most advanced in Europe in terms of high performance equipment, so their knowledge and their use in research on road paving is certainly an added value and a great opportunity of study in this area. In this way it is important to move the specifications from a traditional approach to a performance-based approach that allows to include new techniques and materials that normally do not find application based on traditional acceptance criteria.
The topic was further investigated in Chapter 3, dedicated to Quality Control experimental applications for Performance Based Specifications.
On a database created of road pavements, representative of the categories present in Italy, were simulated numerically FWD tests of load-bearing capacity.
Basin Indexes were calculated from the deflections, to overcome the intricate approach of the back-analysis, which allowed to develop statistical models of prediction of design life and the Structural number.
All this aimed at implementing and therefore improving in detail our Italian specifications with new indicators of the performance characteristics of pavements and the consequent introduction of new Penalty/Bonus systems in the acceptance requirements during the construction phase of new roads, with the aim of reducing as much as possible unplanned maintenance costs deriving from initial construction deficits.
The importance of a change in the point of view from a traditional to a performance-based approach is crucial with high efficiency equipment and quality control testing. The need for this change is consequential with such modern and advanced equipment, thanks to which it is possible to measure performance with faster tests, to map road superstructures continuously and not punctually, to use alternative materials with a low environmental impact that are not normally accepted in traditional specifications and consequently a significant reduction in economic costs and an increase in social benefits.
Ultimately, this PhD work that will be exposed, underlines how fundamental and equally well known is the perfect compatibility, in the construction of a road, between the project of the technicians and the construction. This concept is exposed starting from the reflection that a road that is not built in a workmanlike manner, can therefore present performance and initial structural deficit, which not only occur over time with anticipated degradation, but leads to intervene with unplanned maintenance that they are expensive both in economic and social terms.

The simple respect of the project is a guarantee of functionality and reliability of the work over time for the benefit of all. From designers and construction companies in technical and economic terms, to road users who must be able to move in complete safety and comfort in daily journeys.
Today, roads are the most important route for connecting users to the various transport infrastructures (railways, airports) that allow journeys from short to long distances, and this is precisely why research must increasingly focus on performance- based targeted studies.

CHAPTER 1

NDT PERFORMANCE TESTS

This chapter analyzes the state of art at international and national level on the sustainable development of transport infrastructures, the Quality Assurance and Control using Non-Destructive Techniques and the Italian situation in terms of technical specifications in road works.
Paragraph 1.1 of this chapter is an introduction to the topic of Transport Asset Management, and represents the motivations of the research that led to the choice to study NDT applications on road infrastructures.
The quality requirements of the road infrastructures were investigated in paragraph 1.2, in which are analyzed the topics of Quality Assurance and Quality Control, the types of performance specifications, the concepts of Performance Pay Factors and the significance of non-destructive techniques.
Paragraph 1.3 deals with NDT techniques that are used more frequently in quality controls of road pavements and which were useful for carrying out experimental tests subsequently presented in this thesis in Chapter 2, such as Falling Weight Deflectometer FWD, Light Weight Deflectometer LWD, Ground Penetrating Radar GPR. The use of these high-efficiency equipment was possible thanks to their availability at the Transport Infrastructure Laboratory of the University of Catania.
The Italian technical standards, and therefore the ANAS Performance Specifications, are described in paragraph 1.4, in which the most important parameters for the knowledge of the state of health of road pavements are analyzed: grip and texture, unevenness, thicknesses of the pavement layers and bearing capacity.
Overall, the chapter investigates the issue of Transport Asset Management with a literature review both internationally and nationally, and starting from those that are the trends of Horizon 2020 and the major international Road Authority and ANAS nationwide in Italy, has been made a choice of the research field within the performance-based specifications and that led to experimental field tests and quality control applications in construction and maintenance.

1.1 Introduction to Transport Asset Management: State of art

The motivation of this study arises from the consideration that roads are the core of an integrated transport system and their performance is essential for all citizens in terms of quality of life, safety, economic competitiveness and sustainable development.
There is the need to provide recommendations for Asset Management leading identify and prioritize measures that effectively address Mobility, Safety and Environmental Sustainability (Carlson et al., 2014).
Asset Management is a systematic process which allows for the maintenance, upgrading and operation of the physical assets, based on a continuous physical inventory and condition assessment, to provide an agreed level of service and safety in the most cost effective manner for present and future communities. Its objective is to maximise asset service delivery potential and manage related risks and costs over their entire lives (Local Gov. Victoria, 2015).

In this context fits the concept of **Sustainability** that has many meanings and fields of application. In particular, in the field of pavements it refers to materials, the paving life cycle, all the methodologies aimed at reducing emissions, costs, intervention times, and control techniques on

materials also non-traditional with non-destructive and high efficiency tests that benefit the environment and the economy of road agencies.
In fact, the issue of Sustainability is increasingly topical nowadays and has great relevance at international level in the transport sector, this is demonstrated by the in progress activities and future goals of the main Road Research Organization in the world (e.g. IRF, ERF, PIARC, TRB) that in the Asset Management take into account the importance of **monitoring the performance characteristics of the transport infrastructures** with **QA/QC approaches** combined with the preservation of environmental, social and economic resources.

The aim of the research project fits with the Horizon 2020 Work Programme 2014-2015, 2016-2017, 2018-2020 "Smart, green and integrated transport" in which it refers to the importance of "*safe roads and of maintenance during construction and operativeness, well-designed infrastructure, sustainability and quality of life of users, which are all essential components of the management of road assets*".
In the **Horizon 2020 Work Programme 2014-2015**, in particular one of the core of the call "Mobility for Growth" in the section "Infrastructure[1]" faced with the reduction of the impact of infrastructure on the environment.
At the same time, the resources available to maintain and upgrade transport infrastructure have been declining. As a result, many elements of the surface transport infrastructure are in a deteriorating condition. In view of the expected growth in traffic between EU Member States, the investment required to complete and modernize the transport network is challenging and the approach needs to be sustainable.
Research in this domain should aim at "*validation of innovative solutions for infrastructures where either new construction for the completion of an efficient transport network is needed, or advanced maintenance systems are necessary to improve and extend the capacity of the existing network and to increase the performance, robustness and efficiency of infrastructure*.
New procedures and technologies in using Green Infrastructure to make transport infrastructure more resilient, less-carbon intense, maximizing multiple ecosystem services and minimizing fragmentation effects have to be developed and tested."
In the international context, the EU Member States are moving towards the following activities:

- Advanced, quick, cost-effective and flexible (modular) design, manufacturing, construction, maintenance, rehabilitation and retrofitting systems/techniques and materials.
- Performance specifications with QA/QC approaches.
- Self-monitoring, self-reporting, non-intrusive inspection and testing methods, including advanced predictive modelling.
- Reuse and recycling methods for low energy construction and maintenance of existing infrastructure.
- Innovative, harmonized and lean procurement processes, accompanied by adequate monitoring systems, contracting and tendering methods; management tools to provide help in innovation delivery.

[1] HORIZON 2020, Work Programme 2014-2015: Call "Mobility for Growth", "Infrastucture": MG.8.1-2014. *Smarter design, construction and maintenance*; MG.8.2-2014. *Next generation transport infrastructure: resource efficient, smarter and safer*; MG.8.3-2014. *Facilitating market take up of innovative transport infrastructure solutions*; MG.8.4-2014. *Smart governance, network resilience and streamlined delivery of infrastructure innovation.*

- Solutions for optimal cost-effectiveness, including network resilience, mapping of climate risk hot-spots, including under climate change, together with appropriate adaptation measures and cross-modal implementation strategies.
- Solutions for advanced asset management, advanced investment strategies and innovation governance, including smart monitoring systems adequate indicators for cost and quality.

In the **Horizon 2020 Work Programme 2016-2017**, in particular in the call "2016-2017 Mobility for Growth" in the section "Infrastructure" is emphasized that *"research studies must necessarily cover strategic application of new materials, techniques and systems for the construction, operation and maintenance, in order to ensure the sustainability and reliable network availability in unfavorable conditions"*.

Relevant topics for environmental sustainability to be considered in Transport Asset Management include not only use of recycled and **environmentally-friendly construction materials** but also water pollution, best practices for road testing through reliable equipment as **NDT**, **performance specifications** for new and existing infrastructures.

In **Horizon 2020 Work Programme 2018- 2020[2],** "Smart, green and integrated transport, call 2018-2020 Mobility for Growth" is underlined that the overall performance of the transport system depends on the performance of infrastructure, means of transport, traffic management systems and on user behavior.

The priorities identified in this Work Programme will continue to pursue Societal Challenge (SC4)'s overall objective of achieving a European transport system that is resilient, resource efficient, climate and environmentally-friendly, safe and seamless for the benefit of all citizens, the economy and society. In fact, aiming at sustainability as an indispensable element for a transport network, *"the incorporation of economic, social and environmental dimensions is important in order to improve the current transport system, increase its robustness and support safety, security and quality of life. It is also essential to consider aspects of infrastructure construction and maintenance based on innovative solutions*".

Europe is faced with a growing need to make transport infrastructure more resilient, and to keep pace with the changing mobility needs and aspirations of people and businesses and to reduce the impact of infrastructure on the environment. It is urgent to find innovative solutions to upgrade transport infrastructure ensuring an adequate performance level that reflects also vehicle and ICT developments.

National Transport Authorities are facing a change in their role from infrastructure managers to service providers and a number of relevant activities are being carried out at national and international level.

With regard to the broader international sustainability and climate change agenda, activities funded under Societal Challenge 'Smart, green and integrated transport' are expected to contribute to

[2] HORIZON 2020, Work Programme 2018-2020: "Smart, green and integrated transport", Call "Mobility for Growth", "2. Safe, Integrated and Resilient Transport Systems". This Work Programme covers 2018, 2019 and 2020. The parts that relate to 2019 and 2020 are provided at this stage on an indicative basis. Such Work Programme parts will be decided during 2018 and/or 2019.

reaching the global climate targets set by the COP 21 Paris Agreement[3] and have an impact on the implementation of the United Nations (UN)[4] Sustainable Development Goals SDGs[5].

The concept of **Sustainable Development** in transport infrastructures, that is now the most important issue to be developed in the environmental, economic and social field, was defined for the first time in 1987 by Gro Harlem Brundtland, chairman of the **World Commission on Environment and Development[6]**, in the report *Our Common Future* as *"development that meets the needs of the present without compromising the ability of future generations to meet their own needs"*. This definition is focused on the concept of "needs" and the idea of limitations imposed by the state of technology and social organization on the environment's ability to meet present and future needs. In a shorter version of this, sustainability is often described as being made up of the three components of environmental, social, and economic needs, collectively referred to as the "triple-bottom line."
It refers to economic and social growth coupled with environmental protection, with one reinforcing the other. This entails three dimensions[7]:

[3] The Paris Agreement (Accord de Paris), Paris climate accord or Paris climate agreement is an agreement within the United Nations Framework Convention on Climate Change (UNFCCC) dealing with greenhouse gas emissions mitigation, adaptation, and finance starting in the year 2020. The language of the agreement was negotiated by representatives of 196 parties at the 21st Conference of the Parties of the UNFCCC in Paris and adopted by consensus on 12 December 2015. As of February 2018, 195 UNFCCC members have signed the agreement, and 175 have become party to it. The Agreement aims to respond to the global climate change threat by keeping a global temperature rise this century well below 2 degrees Celsius above pre-industrial levels and to pursue efforts to limit the temperature increase even further to 1.5 degrees Celsius.
In the Paris Agreement, each country determines, plans and regularly reports its own contribution it should make in order to mitigate global warming. There is no mechanism to force a country to set a specific target by a specific date, but each target should go beyond previously set targets.

[4] The United Nations is an international organization founded in 1945. It is currently made up of 193 Member States. The mission and work of the United Nations are guided by the purposes and principles contained in its founding Charter.

[5] The Sustainable Development Goals (SDGs), otherwise known as the Global Goals, are a universal call to action to end poverty, protect the planet and ensure that all people enjoy peace and prosperity.
These 17 Goals build on the successes of the Millennium Development Goals, while including new areas such as climate change, economic inequality, innovation, sustainable consumption, peace and justice, among other priorities. The goals are interconnected – often the key to success on one will involve tackling issues more commonly associated with another. The SDGs work in the spirit of partnership and pragmatism to make the right choices now to improve life, in a sustainable way, for future generations. They provide clear guidelines and targets for all countries to adopt in accordance with their own priorities and the environmental challenges of the world at large. The SDGs are an inclusive agenda.

[6] Formally known as the World Commission on Environment and Development (WCED), the Brundtland Commission's mission is to unite countries to pursue sustainable development together. The Chairman of the Commission, Gro Harlem Brundtland, was appointed by Javier Pérez de Cuéllar, former Secretary General of the United Nations, in December 1983. At the time, the UN General Assembly realized that there was a heavy deterioration of the human environment and natural resources. To rally countries to work and pursue sustainable development together, the UN decided to establish the Brundtland Commission. Gro Harlem Brundtland was the former Prime Minister of Norway and was chosen due to her strong background in the sciences and public health.

[7] Definition of the three dimensions in road transport made by UNESCAP in a chapter: "The challenge: sustainable road transport" available online. Source: http://www.unescap.org/sites/default/files/roadprice_ch1.pdf

1. ***economic sustainability (economic efficiency):*** although public debate about sustainability often focuses on ecological goals, in fact, a sustainable development cannot be achieved unless the effects on the economy, employment and the provision of goods are considered;
2. ***environmental sustainability (ecological stability):*** this requires that the environmental balance is not overburdened by human emissions and resource use in order to guarantee the functional stability of present eco-systems, both on a local and global scale;
3. ***social sustainability (distributional/social equity):*** social and distributional needs are met by ensuring a fair distribution of resources, poverty reduction, stable human development, public participation, and democratic policy formation

The essence of this form of development is a stable relationship between human activities and the natural world such that future generations are able to enjoy a quality of life that is at least as good as the present one. The concept of sustainable development is so powerful in the Brundtland report, which cannot be ignored for the development of a mature and healthy society, nor can it be left out in the transport sector as it is one of the most important and has always allowed cultural, economic and social exchanges between people and things.

PIARC (2008) defines **Road Asset Management** as: "*A systematic process of maintaining, upgrading and operating assets, combining engineering principles with sound business practice and economic rationale, and providing tools to facilitate a more organized and flexible approach to making the decisions necessary to achieve the public's expectations*". This definition is clear that can be extended to all Transport Infrastructures, the transferability of the concept is an important element in a research study.

FHWA-USA (2009) defines, in the traditional way, asset management as a strategic and systematic process of operating, maintaining, and improving physical assets, with a focus on engineering and economic analysis based upon quality information, to identify a structured sequence of maintenance, preservation, repair, rehabilitation, and replacement actions that will achieve and sustain a desired state of good repair over the lifecycle of the assets at minimum practicable cost.

European Union Road Federation ERF and **International Road Federation IRF** (2009) defines sustainable roads as "*Effectively and efficiently planned, designed, built, operated, upgraded and preserved roads by means of integrated policies respecting the environment and still providing the expected socio-economic services in terms of mobility and safety*". Furthermore, it is emphasized that it is important to have both sustainable roads and more sustainable transport as well: "*Sustainable roads together with more sustainable transport can help Europe and its Member States face the critical challenge of sustainable mobility without jeopardizing national economies and people's well-being"*.

"Sustainable" in the context of pavements refers to system characteristics that encompasses a pavement's ability to:

- achieve the engineering goals for which it was constructed;
- preserve and (ideally) restore surrounding ecosystems;
- use financial, human, and environmental resources economically;

- meet basic human needs such as health, safety, equity, employment, comfort, and happiness.

For many years, the economic component has been the dominant decision factor, but more recent years have seen the growing emergence of both the environmental and social components (even though there are some current limitations associated with their measurement and assessment).

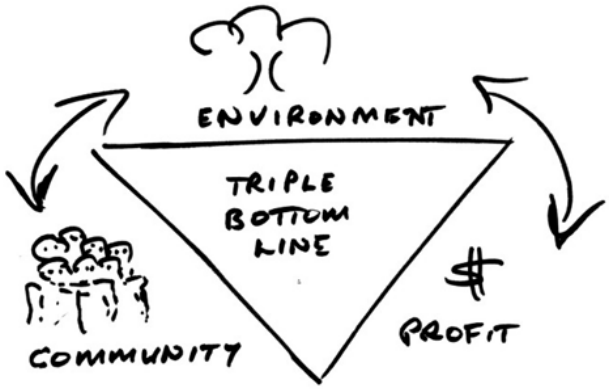

Figure 1 - Triple bottom line - components of sustainability.
Source: https://sourceable.net/investing-in-triple-bottom-line/

A focus on sustainability in Figure 1 can then be interpreted in such a way that all **Triple-Bottom Line** components are considered important, but the relative importance of these factors (and how each are considered) are case sensitive, very much driven by the goals, demands, characteristics, and constraints of a given project.

A whole-life consideration of sustainability and energy efficiency has to be considered and decision-making tools with practical application to all stages of road planning, design, construction and maintenance should be developed with specifications of performance characteristics of pavements to ensure good quality of infrastructure in the acceptance of works considering new and existing constructions.

Making an analysis on the **European road network,** it consists of 5.5 million Km mainly managed under local and regional responsibility.
Studies conducted by the European Union Road Federation show that the majority of road works, the 90%, concern the maintenance and modernization of existing roads and the remaining 10% of road construction works involve new constructions.
Moreover, the annual maintenance spending in road infrastructures in the European Union (EU 25), like in other developed countries, accounts for a share of about 40% of the total road expenditure with an annual budget of about 30 billion euro (ERF, 2013).
Despite this huge amount of expenditure, lack of information and political awareness on the importance of sufficient and appropriate investments for the maintenance of the road infrastructure lead to its chronic underfinancing and deterioration (ERF, 2014).
Some efforts are currently being made to identify low Greenhouse gas (GHG) emission solutions and life cycle energy reduction in road planning, design and construction. However, for most Road Authorities (RAs) this is still an area for considerable development especially in the framework of the management of the road network.
Road Authorities (RAs) to effectively contribute to the long-term vision of sustainable development should identify and prioritize measures in Figure 2 that effectively address:

- ***Accessibility and Mobility:*** Roads must maintain their essential role in the global future transport framework.
- ***Safety:*** reduction of number and severity of crashes for all the road users.
- ***Environmental sustainability:*** reduced energy consumption and associated reduced GHG emissions from road transport.

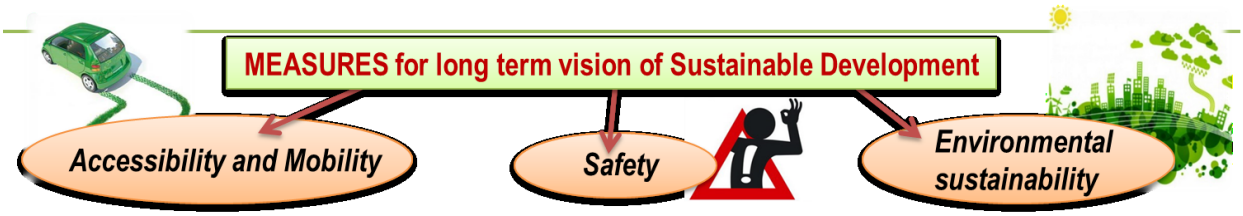

Figure 2 - Road Authorities measures for long term vision of Sustainable Development.

Maintenance and preservation of new and existing infrastructures impacts sustainability factors such as performance life, durability, life-cycle costs, construction (e.g., constructability, sequencing, schedule), and materials use (Van Dam et al., 2015). In Figure 3 is presented the pavement life cycle from the construction and material transportation to the end of life.

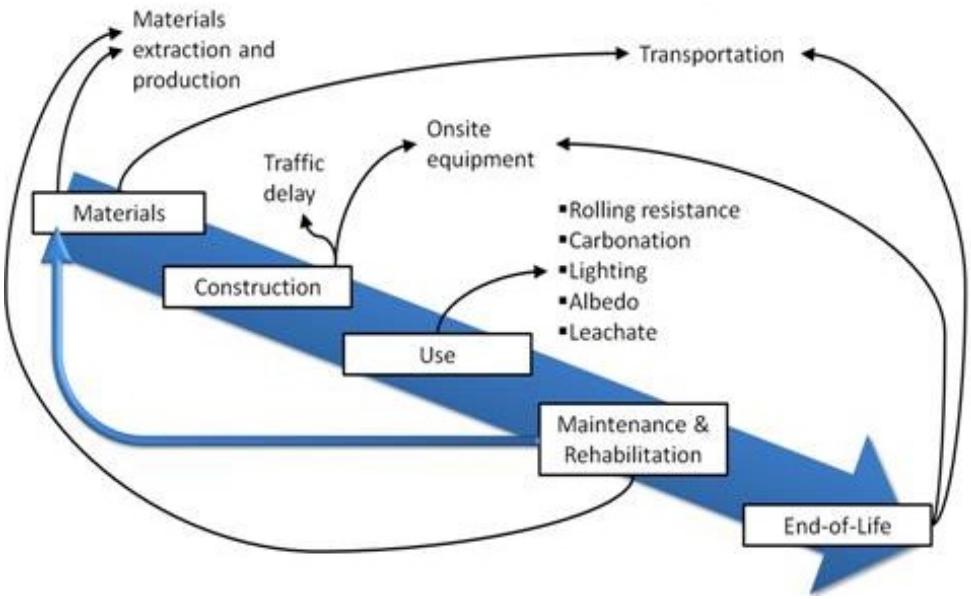

Figure 3 - The Pavement Life Cycle. Source: http://www.dot.ca.gov/research/roadway/pavement_lca/index.htm

In this context, and as already mentioned previously, it is important to underline the evolution of the concept of Sustainable Development over time which took place in 2015 with the **Sustainable Development Goals SDGs**, that are defined as 17 Goals to Transform Our World (Figure 4).
In 2015, in fact, countries adopted the 2030 Agenda for Sustainable Development and its 17 Sustainable Development Goals, that are reported in the following figure. In 2016, the Paris Agreement on climate change entered into force, addressing the need to limit the rise of global temperatures.
Governments, businesses and civil society together with the United Nations are mobilizing efforts to achieve the Sustainable Development Agenda by 2030. Universal, inclusive and indivisible, the Agenda calls for action by all countries to improve the lives of people everywhere.

Figure 4 - Sustainable Development goals.
Source: https://www.un.org/sustainabledevelopment/sustainable-development-goals/

The Goal n.9 "Industry, innovation and Infrastructure", shows how is important *"Build resilient infrastructure, promote sustainable industrialization and foster innovation"*. Investments in infrastructure – transport, irrigation, energy and information and communication technology – are crucial to achieving sustainable development and empowering communities in many countries. It has long been recognized that growth in productivity and incomes, and improvements in health and education outcomes require investment in infrastructure. In this infrastructural field, but also in the world industrial and economic innovation, Goal n. 9 sets important targets, which are configured as essential elements to be achieved:

- Develop quality, reliable, sustainable and resilient infrastructure, including regional and transborder infrastructure, to support economic development and human well-being, with a focus on affordable and equitable access for all
- Promote inclusive and sustainable industrialization and, by 2030, significantly raise industry's share of employment and gross domestic product, in line with national circumstances, and double its share in least developed countries
- Increase the access of small-scale industrial and other enterprises, in particular in developing countries, to financial services, including affordable credit, and their integration into value chains and markets
- By 2030, upgrade infrastructure and retrofit industries to make them sustainable, with increased resource-use efficiency and greater adoption of clean and environmentally sound technologies and industrial processes, with all countries taking action in accordance with their respective capabilities
- Enhance scientific research, upgrade the technological capabilities of industrial sectors in all countries, in particular developing countries, including, by 2030, encouraging innovation and substantially increasing the number of research and development workers per 1 million people and public and private research and development spending

- Facilitate sustainable and resilient infrastructure development in developing countries through enhanced financial, technological and technical support to African countries, least developed countries, landlocked developing countries and small island developing States 18
- Support domestic technology development, research and innovation in developing countries, including by ensuring a conducive policy environment for, inter alia, industrial diversification and value addition to commodities
- Significantly increase access to information and communications technology and strive to provide universal and affordable access to the Internet in least developed countries by 2020.

This means, for **Austroads**, that the process of defining **performance measures** leads to a greater understanding of customer needs and hence increases the ability to meet them.
In performance measurements are crucial the following observations:

- Monitor strategies regularly
- Make adjustments at the right stage of the asset's life cycle to achieve the balance between cost and level of service
- Use benchmarks to determine performance of assets

Consequently, the main consideration is that performance contracts require the translation of customer needs into **documented performance measures**. Performance contracts impose a discipline on all involved, which facilitates greater communication and discussion of customer needs (Austroads, 2003).
In this framework, the aim of the PhD research project is to develop performance specifications in Quality Assurance and Quality Control processes (QA/QC) with the use of high-efficiency equipment, highlighting also the possibility of including non-destructive test during the acceptance phase of work, considering bonuses and penalties, that concern new constructions and road maintenance.

1.2 Quality requirements of road infrastructures: QA/QC

In an international context where sustainable social-economic-environmental development is the cornerstone for the growth of transport infrastructures, the quality requirement is essential today to guarantee high levels of road performance and quality.
In fact, a comprehensive understanding of issues pertaining to the quality of a project is needed in order to achieve high quality that not only gives acceptable return value to society but also satisfies the needs of all the stakeholders of infrastructure projects (Warsame, 2013).
The quality requirements for road infrastructures with a complete technical description are detailed below, in order to have a more complete picture of what Quality is today and the importance of performance for road transport infrastructure Specifications.

In **NCHRP Report n. 626** (2009) is underlined that traditional pavement construction quality control and quality acceptance (QC/QA) procedures include a variety of laboratory and field test methods that measure volumetric and surface properties of pavement materials. The test methods to measure the volumetric properties have changed little within the past couple of decades.
More recently, nondestructive testing (NDT) methods, including ground-penetrating radar (GPR), Falling weight Deflectometers (FWD), Light Weight Deflectometers (LWD) and laser technologies (LCMS) have been improved significantly and have shown potential for use in the QC/QA of

flexible pavement construction. These methods correspond to the most important performance indicators of an infrastructure that are: bearing capacity, IRI, layer thicknesses of pavements.
First of all, it's important to define the concept of QA/QC in an approach aimed at defining and measuring pavement performance, centerpiece of this PhD research, with the consequent use of high-efficiency equipment.
Highway Quality Assurance (QA), like many other specialized subject areas, has its own unique language containing numerous technical terms or expressions having very specific meanings. Some of these terms are not well understood, and their use is subject to a variety of different interpretations. The highway QA language, moreover, is continually changing to keep pace with advances in QA. As new terms come into general use, older terms must often be perceived in a new light. The terminology has grown and evolved steadily since the mid-60s, when much of it was first introduced to the highway community; however, its growth and evolution have been to a large degree uncontrolled (TRB Circular E-C074, 2005).
The following are the major quality elements that are in literature, useful to a better understanding of the field of study:
Quality assurance (QA) refers to all those planned and systematic actions necessary to provide confidence that a product or facility will perform satisfactorily in service.
QA addresses the overall problem of obtaining the quality of a service, product, or facility in the most efficient, economical, and satisfactory manner possible.
Within this broad context, QA involves continued evaluation of the activities of planning, design, development of plans and specifications, advertising and awarding of contracts, construction, and maintenance, and the interactions of these activities.
Quality assurance specifications are a combination of end result specifications and materials and methods specifications. The contractor is responsible for QC (process control), and the highway agency is responsible for acceptance of the product. QA specifications typically are statistically based specifications that use methods such as random sampling and lot-by-lot testing, which let the contractor know if the operations are producing an acceptable product.
Quality control (QC) is also called process control. Those QA actions and considerations necessary to assess and adjust production and construction processes so as to control the level of quality being produced in the end product. QC can have the following uses:

- Individual Materials: Soil, Gravel, Aggregate, Binder
- Mixes: Gradation of Aggregates, Mix Proportion, Mixed Design Properties
- During Construction Process: Spreading, Segregation, Temperature – Mixing, Laying, Rolling
- Test on Compacted Layer: Mixed Proportion (Unbound Layers), Density, Mix proportion and Gradation
- Finished Surface: Bearing Capacity, Longitudinal Profile, Transverse Profile, Cross Slope, Texture

In Table 1 are summarized the differences between QA and QC:

Table 1 – QA versus QC. (Willenbrock et al., 1976; AASHTO, 2004)

Quality Assurance	Quality Control
Making sure the quality of a product is what it should be	Making the quality of a product what it should be
A highway agency responsibility.	A producer/contractor responsibility.
Includes QC.	A part of QA.
Doing the right things.	Doing things right.
Motivates good QC practices.	Motivated by QA and acceptance procedures.

The result of all these consideration is that:

QA+QC= High Quality Infrastructures

The elements of a QA system are schematized in Figure 5. The Quality Assurance cycle includes various work activities for the construction of road pavements, such as: planning, design, plans and specifications, advertise e award of contract, construction and maintenance. In particular, the QA process under construction includes the Quality Control process that requires both acceptance procedures and independent assurance. The acceptance is the process of deciding, through inspection, whether to accept or reject a product, including what pay factor to apply. The independent assurance is a management tool that requires a third party, not directly responsible for process control or acceptance, to provide an independent assessment of the product or the reliability of test results, or both, obtained from process control and acceptance.

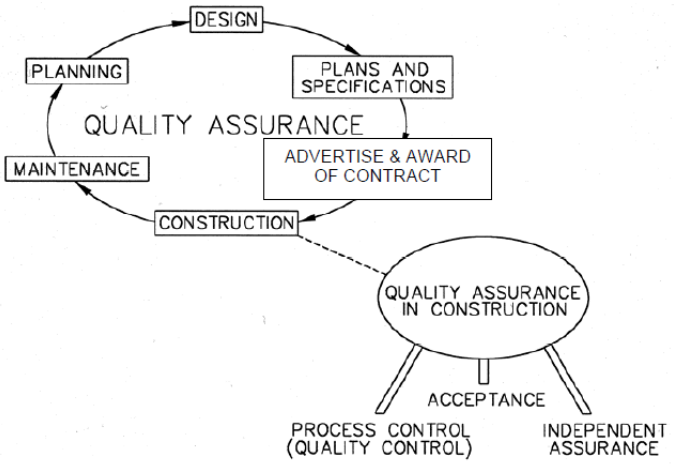

Figure 5 - QA system elements (Willenbrock et al., 1976; Burati et al. 1993)

In particular, ***Performance Specifications*** are specifications that describe how the finished product should perform over time.

For highways, performance is typically described in terms of changes in physical condition of the surface and its response to load, or in terms of the cumulative traffic required to bring the pavement to a condition defined as “failure”.

Specifications containing warranty/guarantee clauses are a form of performance specifications. Other than the warranty/guarantee type, performance specifications have not been used for major highway pavement components (subgrades, bases, riding surfaces) because there have not been suitable nondestructive tests to measure long-term performance immediately after construction. They have been used for some products (e.g., highway lighting, electrical components, and joint sealant materials) for which there are suitable tests of performance.

There are two types of Performance Specifications, defined by the TRB Circular E-C074, 2005:

1) ***Performance-based specifications*:** QA specifications that describe the desired levels of fundamental engineering properties (e.g., resilient modulus, creep properties, and fatigue properties) that are predictors of performance and appear in primary prediction relationships (i.e., models that can be used to predict pavement stress, distress, or performance from combinations of predictors that represent traffic, environmental, roadbed, and structural conditions). Because most fundamental engineering properties associated with pavements are currently not amenable to timely acceptance testing, performance-based specifications have not found application in highway construction.
   So we understand how with tests that are done promptly on road construction, then the performance-based specifications can be widely applied, this means that it is important to perform tests in high efficiency and, as has been studied later in Chapter 3 with models in this thesis, that it's essential to make predictions on different parameters that can give the technicians an indication of what future performances will be, fully respecting the projects.

2) ***Performance-related specifications:*** QA specifications that describe the desired levels of key materials and construction quality characteristics that have been found to correlate with fundamental engineering properties that predict performance.
   These characteristics (for example, air voids in AC and compressive strength of PCC) are amenable to acceptance testing at the time of construction.
   True performance-related specifications not only describe the desired levels of these quality characteristics, but also employ the quantified relationships containing the characteristics to predict as-constructed pavement performance.
   They thus provide the basis for rational acceptance/pay adjustment decisions.

In Figure 6, Kopac (1993) developed a scheme who has applied for the classification of highway construction specifications that is a good method to classify quality specifications.
Highway construction specifications, according to Kopac scheme (1993), may be classified according to:

(I) who is responsible for the quality of construction: from the 0% to the 100% contractor responsibility, which varies from the choice of materials and methods to QAs specifications and results.
(II) the type of sampling employed
(III) the relationship between quality criteria and constructed product performance.

Thus, a QA specification according to classification I, for example, might be a statistical specification for classification II, and contain intuitive specification limits and pay adjustments for classification III.
A specification might also, and usually do, contain one or more features within the same classification.
For example, a specification that is primarily performance-related might contain some performance-based acceptance criteria and some intuitively developed acceptance criteria.

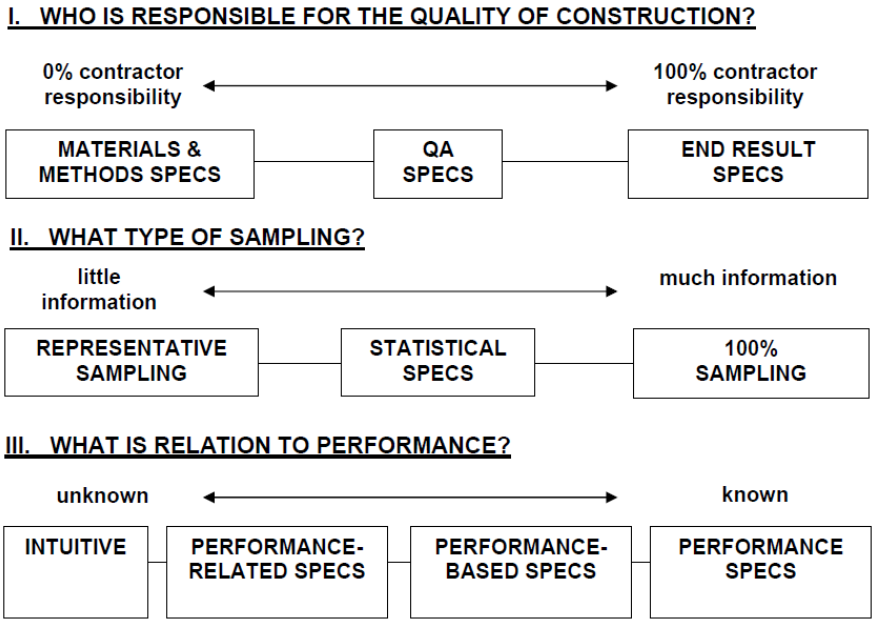

Figure 6 - Classifying quality specifications (Kopac, 1993)

It is therefore clear that this model can be transferred to any quality procedure in the transport sector.

In **NCHRP Report n.704** (2011) these concepts are emphasized, as in recent years in recent years there has been interest in the paving industry in defining the quality of the mix and pavement in terms of performance, where the contractor responsible for production and placement would then be paid on the basis of the difference in service life between the as-designed and as-built pavement. In this case, the specifications state the **acceptance quality characteristics AQC** as a measure of pavement performance. Such a specification describes how the finished product should perform over time. Warranty or guarantee specifications, by which the contractor agrees to build and maintain the pavement for a specified period of time, are also used. In these types of specifications, a time period is identified during which the acceptance quality characteristics are expected to be maintained at satisfactory levels. In general, this approach to specifications has not yet been widely accepted in the industry. A performance-related specification is defined as a quality acceptance (QA) specification that describes the desired levels of key acceptance quality characteristics that have been found to correlate with fundamental engineering properties that predict performance.
The selection of a particular AQC by itself does not make the specification performance related. Rather, there must be a direct connection to performance through field validated empirical or mechanistic prediction models that account for the effect of deviations of the as-built AQC level from the as-designed AQC level.
Other factors such as environment, traffic, pavement cross section, and variability also must be considered in a comprehensive **Performance Related Specification PRS**. To implement the PRS, pavement performance must be predicted based on the initial design (as-designed) and the as built properties. The difference in predicted performance between the as-designed and as-built pavement then is used as a basis for acceptance. In this regard, the National Cooperative Highway Research Program has developed a QRSS software "Quality-Related Specification Software" to carry out pay adjustment factor and payment computations by comparing the as-built pavement performance with that of the as-designed pavement.

The following is presented for a greater understanding of the issue in terms of penalties to be applied when a project is implemented in a manner inconsistent with the probabilistic methodology for the development of NCHRP **Performance Pay Factors** founded on several important concepts:

1. The concept of effective temperature is used to evaluate the climatic effects on the HMA dynamic modulus and so predict the anticipated deformation and fatigue distresses for a particular pavement structure and project location.
2. Simulation of the MEPDG (Mechanistic-Empirical Pavement Design Guide) distress prediction is the basis for developing closed form solutions for the three major distresses: rutting, fatigue cracking, and thermal cracking.
3. For the job mix formula (JMF), heretofore referred to as the as-designed mix, a Monte Carlo simulation is conducted on the dynamic modulus using the mean and historical variance of the HMA volumetric properties and aggregate gradation. This is done separately for rutting and fatigue cracking. An alternative type of simulation, the Rosenblueth point estimate method, is conducted on the creep compliance for thermal cracking.
4. From the closed form solutions and the two simulations, the pavement distresses for the as-designed mix are estimated.
5. A relationship is developed between each predicted distress level and pavement life. These relationships are then used to estimate the pavement life of the as-designed mix.
6. Similarly, for the constructed mix, heretofore referred to as the as-built mix, the lot data (daily production) are used in the simulations to estimate each distress and predict pavement life for each lot.
7. The cumulative probability distributions of the as-designed and as-built pavement lives are compared to calculate the **pavement life difference (PLD)** for each lot.
8. The Pay Factor Penalty/Bonus is then estimated from the PLD for each lot. The criterion for each distress between the PLD and Pay Factor is solely defined by the user agency. The summation of the pay factors for the lots will provide the total project pay factor.
9. The QRSS methodology developed in NCHRP Project 9-22 is based on simplifying assumptions compared to the comprehensive MEPDG solution. The assumptions are:
    - Traffic is represented by ESALs.
    - No seasonal changes are allowed for the unsaturated modulus of any unbound layer (base, subbase, or subgrade). Rather, an effective modulus of all unbound layers is estimated.
    - The accuracy of the closed form solution is almost equivalent to that of the MEPDG. However, the MEPDG will give the more accurate distress predictions.
    - The QRSS will predict one value of each distress at the end of the design life.

Therefore, as part of the application of penalties on a project, an important element that emerges is definitely the **Predicted Life Difference**, because the life of an infrastructure when a project is not carried out in a workmanlike manner is certainly the key element that comes to change with respect to the project forecasts. In fact, the variable Predicted Life Difference (PLD) is introduced to assess the difference between the as-designed and as built distributions.

The PLD is defined as the difference in predicted service life between the as-designed mix and the as-built mix. This parameter has a unique algebraic sign, depending upon whether the as-built

mix is of greater or lesser quality (Service Life) than the as-designed mix. Finally, this PLD is used as the basis for establishing the **Pay Factor Penalty/Bonus** for each distress type.

The purpose of a Performance Related Specification is to promote the construction of a quality pavement by measuring and evaluating characteristics directly related to its performance.
Undoubtedly NDT technologies[8] allow to carry out evaluations on road paving, but in general also on other types of infrastructures, which are based on performance and which therefore contribute to giving important results within the specifications. In the following paragraph 1.3 NDT techniques will be investigated in terms of high efficiency equipment.

1.3 NDT Techniques

Non-destructive testing (NDT) methods, more recently, have been improved significantly in civil engineering and in particular in the transportation sector and have shown a huge potential for use in the Quality Control processes and performance specifications. Non-destructive tests (NDT) represent an efficient monitoring tool, as they allow to evaluate infrastructure characteristics in a continuous or quasi-continuous way, saving time and costs, enabling to make changes if tests results do not comply with the project requirements.
In particular, in the road sector, the measurement of the structural characteristics of pavements, as the load-bearing capacity are made with the Falling and Light Weight Deflectometer; instead the thickness measurement is carried out with Ground Penetrating Radar.
These devices represent very advanced NDT measurement performance techniques, which will be detailed in the following paragraphs in which will also be introduced the advanced and modern "TILab" Road Test Laboratory of the University of Catania.

1.3.1 Falling Weight Deflectometer

A traditional device for the measurement of pavement stiffness and bearing capacity is the Falling Weight Deflectometer (FWD) and it's intended for network asset evaluation, rehabilitation design, construction quality control and for the collection of more data that is always necessary for the targeted quality control of unbound pavement layers. The international reference for FWD is the **ASTM D4694-96** *Standard Test Method for Deflections with a Falling-Weight-Type Impulse Load Device.*

Figure 7 - Falling Weight Deflectometer 8000 (University of Catania)

[8] Non-destructive testing (NDT) is a wide group of analysis techniques used in science and technology industry to evaluate the properties of a material, component or system without causing damage (Louis, 1995).

The FWD, which is shown in Figure 7, is a non-destructive field plate bearing test that has been widely used in the evaluation of pavement layers and it's designed to simulate deflection of a pavement surface caused by a fast-moving truck.
The FWD test implies applying an impulse load by dropping a weight from a certain height on a buffer system and is transmitted through a 300 mm or a 450 mm circular loading plate, in Figure 8, that can be solid or segmented and in contact with the surface of the test section.

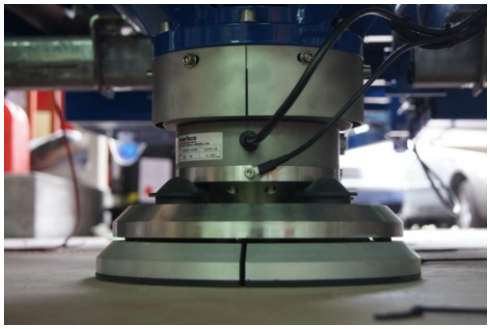

Figure 8 - Loading plate of 300 mm. FWD Dynatest 8000 (University of Catania)

The load cell[9] is used to measure the applied load on each impact and shall be placed in a position to minimize the mass between the load cell and the pavement.
The test apparatus may be mounted in a vehicle or on a suitable trailer towed by a vehicle that is brought to a stop with the loading plate positioned over the desired test location.
Different load magnitudes can be generated by varying the mass of weight and drop height.
The load pulse generated by the FWD momentarily deforms the pavement under the load plate into a dish or bowl shape. The shape of the deformed pavement surface is a deflection basin.

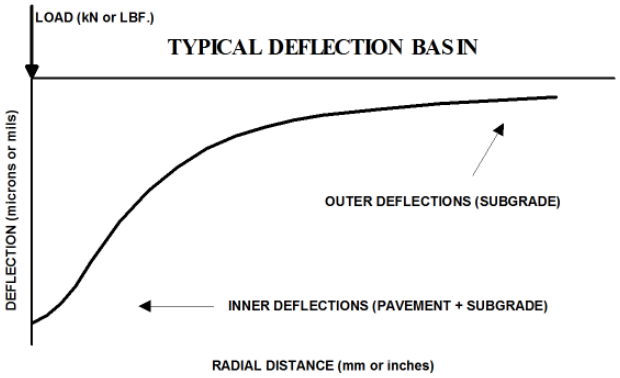

Figure 9 - Typical Deflection Basin

Based on the force imparted to the pavement and the shape of the deflection basin and if the thickness of the individual layers is also known, the stiffness of those layers can be calculated by using various computational methods.
The resulting force pulse transmitted to the pavement with the test shall be reproducible within some requirements:

- Prior to load and deflection sensor calibration, pre-condition the device by dropping the weight at least five times and checking the relative difference in each loading;

[9] The load cell shall be positioned in such a way that it does not restrict the ability to obtain deflection measurements under the center of the load plate. It shall be water resistant, and shall be resistant to mechanical shocks from road impacts during testing or travelling, or both.

- Loading shall not vary from each other more than 3%;
- If the variations exceed this tolerance, the height of the drop, cleanliness of the track, as well as any springs or rubber pads that are used to condition the load shall be checked;
- Improperly operating parts shall be replaced or repaired prior to calibration to ensure that the horizontal forces are minimized.

The force pulse shall approximate the shape of a haversine or half-sine wave, and a peak force of approximately 50 kN (11000 lbf) shall be achievable.
An FWD has two types of primary measurement devices: the load cell and the deflection sensor.
In detail, the peak force imparted by the falling weight is measured by the load cell and recorded, as the force in kN or lbf or mean stress (the load divided by the plate area) in kN/m2 or psi as appropriate.
Considering the deflection sensor, the weight is raised to the height that, when dropped, will impart the desired force to the pavement. Multiple tests at the same or different heights of drop may be performed before the apparatus is then raised and moved to the next test site.
During the test (Figure 10) the plate and deflection sensors are lowered to the pavement surface.

Figure 10 - Geophones bar. FWD Dynatest 8000 (University of Catania)

Deflection sensors are called geophones and are mounted radially from the center of the load plate to measure the deformation of the pavement in response to the load. They measure the maximum vertical movement of the pavement and mounted in such a manner as to minimize angular rotation with respect to its measuring plane at the maximum expected movement.
The number of spacing of the sensors is optional and will depend upon the purpose of the test: a sensor spacing of 300 mm (12 in.) is frequently used. Some typical offsets for tests on road pavements are 0mm, 200mm, 300mm, 450mm, 600mm, 900mm, 1200mm 1500mm, 1800 mm.
The peak pavement deflections measured at these sensors are termed D0, D200, D300 etc., and recorded in micrometres, millimetres, mils, or inches, as appropriate.
It's also important to know the temperature of the materials in the pavement structure. All this because for example, asphalt is hard and brittle at very low temperatures and soft and ductile at very high temperatures; therefore, the stiffness calculated from FWD data for these materials must be corrected for these temperature effects (FHWA, 2006). Temperature dependency is usually used with bitumen bound materials, and allows the asphalt modulus to be corrected to a reference temperature. This is important to do before any design because the temperature usually vary a lot over the day and over the year, and because the stiffness of the bitumen is very sensitive to the temperature.
Considering the instrument exposed to elements (outside the vehicle), it shall be operable in the temperature range of -10 to 50°C (10 to 120°F) and shall tolerate relatively high humidity, rain or spray, and all othe adverse conditions such as dust, shock, or vibrations that may normally be

encountered. Considering the FWD not exposed to elements (inside the vehicle), shall be operable in the temperature range of 5 to 40°C (40 to 105°F).

As already stated, the traditional method to analyze the FWD data implies the use of the maximum deflections of each point of measurement by geophones and, according to the distance, they represent a basin of deflections (Ullidtz, 1998).
A numerical optimization method is employed so that this basin agrees with the deflections given by a numerical model. The optimization process is an iterative method which modifies the elastic modulus of the pavement layers until a better adjustment is produced. Several **backcalculation** programs were developed like: MODULUS, ELSYM5, KENLAYER, ELMOD[10].

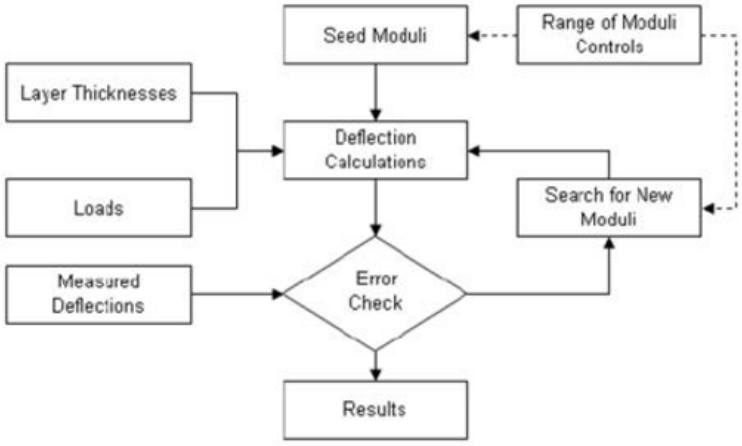

Figure 11 - Elmod optimization process of backcalculation to estimate moduli.

ELMOD, developed by Dynatest Consulting Inc., is a software with 3 possible modes of backcalculation to estimate Moduli:

1) *Radius of Curvature RoC:* this option uses the radius of curvature along with the actual or apparent non-linear subgrade properties to determine moduli within the pavement system. Initially, the subgrade material properties, stiffness and non-linearity, are calculated using the deflections from the outer geophones. The "radius od curvature" from the central geophones can be used to assess the stiffness of the upper pavement layer. The stiffness of remaining layers is then calculated based on the overall pavement response to the applied load. This ensures that the proposed pavement structure results in the correct central deflection under the measured load.

2) *Deflection Basin Fit DBF*: it goes beyond the radius of curvature method, strictly following the calculation of the deflection profile and the measured deviation profile. The percentage difference between the calculated value and the measured value can be specified as a convergence criterion in the iteration. This method uses an approach with additional iterations until the deflections calculated from the measured deflections reach the specified tolerance.

[10] In this thesis work, the backcalculation methods of ELMOD will be exposed, the licensed software available at the Transport Infrastructure Laboratory of the University of Catania together with the Falling Weight Deflectometer Dynatest 8000.

3) *FEM/LET/MET*[11]: with this option, the backcalculation can be performed with the finite element method (FEM), with the linear elastic theory (LET) or with the method of equivalent thickness (MET). Before FEM can be used, however, the finite element mesh must be set, ie the mesh and the nodes must be defined. If no texture is generated, the program creates a mesh based on the default values. With LET all layers are treated as an elastic-linear half-space and with MET only the subgrade can be non-linear.

Depending on the needs and types of road pavements to be analyzed, the RoC, DBF or FEM/LET/MET modes can be selected, with the backcalculation algorithm shown in Figure 11.
In all methods, Poisson's ratio is assumed to be 0.35, except in the FEM/LET/MET option, in which it is possible to assign this coefficient with different values to each layer.
So specifically, ELMOD calculates the modulus of each layer in two, three, four or five-layer pavement systems using either the "Radius of Curvature" - Odemark-Boussinesq transformed section approach, the "Deflection Basin Fit" method normally used with numerical integration techniques or using the "FEM/LET/MET" option which allows the user to select either the Finite Element Method, Linear Elastic Theory or the Method of Equivalent Thicknesses.
The backcalculation provides the apparent moduli for the as-measured deflections at each FWD test point, and taking the non-linearity of the subgrade (or all layers with FEM) into consideration.
With this software is also possible to calculate the residual life of pavements and a Life Cycle Cost Analysis.
In particular, with reference to the theory used to calculate the layer moduli, ELMOD is the traditional Dynatest FWD model which uses the Boussinesq–Odemark method based on the assumption of the equivalent thickness by supposing that the strains within layers depends only on stiffness (Elmod Dynatest Manual, 1998).
The backcalculation process for FWD considering flexible pavements, is based on models that are set out below: Boussinesq, Odemark-Boussinesq, Ullidtz.
Boussinesq developed a set of equations to calculate the stress, strain and displacement conditions in a homogeneous, isotropic, linear elastic semi-infinite space under a point load. The modulus of a semi-infinite space may be calculated from:

$$E = \frac{f(1-\nu^2)\sigma_0 . a}{d_0}$$

where: E = surface modulus at equivalent depth r (MPa); f = factor that depends on the stress distribution (Table 2); ν= Poisson's Ratio; σ_0 = pressure under loading plate; a = radius of the loading plate; d_0 = deflection at the center of the circular load.

Table 2 - Stress distribution factor f

STRESS DISTRIBUTION	**f**
Uniform	2
Rigid plate	π/2
Parabolic, granular	8/3
Parabolic, cohesive	4/3

[11] The FEM (Finite Element Module) makes use of an axial symmetric finite element program. The LET (Linear Elastic Theory) option makes use of the Waterways Experiment Station's program (WESLEA), and MET is similar to the Deflection Basin fit, but with a simpler use of adjustment factors. Where Elmod applies adjustment factors directly on the calculated responses, MET makes use of the traditional Odemark adjustment factors directly on the layer thicknesses. Source: Dynatest International, 1998. *ELMOD Quick Start Manual*.

Considering that the Poisson ratio, in road pavements, may range from 0.1 to 0.5 depending on the layer and the material of which it is composed) and that the stress distribution factor can assume the values expressed in Table 2, then the combined effect of this two parameter give the result that the factor $f(1-\nu^2)$ may range[12] from 1 to 2.67.

In Figure 12 there are the distributions of stress for granular and cohesive materials.

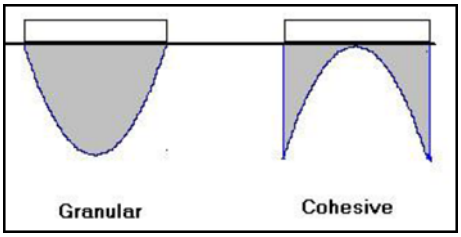

Figure 12 - Stress distribution of granular and cohesive materials

This very large uncertainty can be reduced by measuring the deflections at different distances from the load. The deflections caused by a point load are very close to the deflections under a circular load, for distances of more than two radii from the center of the load. The modulus may, therefore, be calculated from:

$$E= ((1-\nu^2)\sigma 0.\ a^2)/(r \cdot d0(r))$$

Where d0(r) is the deflection at distance r from the load center.

Boussinesq's equations are only applicable to a homogeneous layer. In practice, most pavement structures are not homogeneous but are layered systems.

Odemark developed an approximate method to transform a system consisting of layers with different moduli into an equivalent system where the thicknesses of the layers are altered but all layers have the same modulus (Figure 13). This is known as the Method of Equivalent Thickness.

Odemark's method is based on the assumption that the stresses and strains below a layer depend on the stiffness of that layer only. If the thickness, modulus and Poisson's ratio of a layer are changed, but the stiffness remains unchanged, the stresses and strains below the layer should also remain (relatively) unchanged.

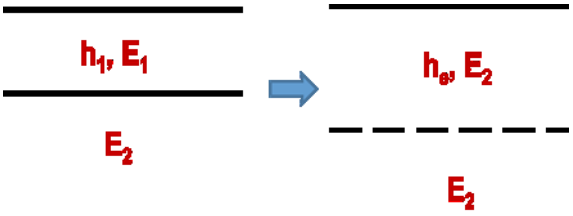

Figure 13 - Odemark's transformation of a layered system

The stiffness of a layer is proportional to: $(h^3E)/(1-\nu^2)$ where h is the thickness of the layer. With the Odemark transformation:

$$\frac{h_1^3 E_1}{1-\nu_1^2} = \frac{h_e^3 E_2}{1-\nu_2^2}$$

[12] In fact, if neither stress distribution nor Poisson's ratio is known, then the factor $f(1-\nu^2)$ may range from 1 to 2.67 (Ullidtz, 1998).

where he is the known as the “equivalent” thickness. The transformed system is a semi-infinite half space on which Boussinesq’s equations may be used, but only for stresses, strains and displacement below the interface.
Correlation with the elastic theory: If it is desirable to obtain results close to the theory of elasticity, when using Odemark’s method, a correction factor, f, may be introduced.
If, in addition, Poisson’s ratio is assumed to be the same for all layers (and in practice Poisson’s ratio is seldom known with any degree of accuracy and may be larger than 0.5 for some layers), the transformation may be written as:

$$h_e = f \cdot h_1 \cdot \sqrt[3]{\frac{E_1}{E_2}}$$

Reasonably good agreement with the theory of elasticity is obtained with a correction factor f of 0.8, except for the first interface where a factor of 0.9 is used for a two-layer system and 1.0 for a multi-layer system.
If measured values of stresses and strains, in real pavements, are available, these should be used to "calibrate" Odemark’s method, rather than values from the theory of elasticity.
For a multi-layer system, the equivalent thickness of the upper n-1 layers with respect to the modulus of layer n, may be calculated from:

$$h_{e,n} = f * \sum_{i=1}^{n-1} h_1 * \sqrt[3]{\frac{E_1}{E_n}}$$

According to Ullidtz (1998), this method gives acceptable results but two conditions have to be given. First, the modulus decreases with the depth and then equivalent thickness of each layer is taller than the loading area. Moreover, ELMOD takes into account the non-linear behavior of the platform. Alternatively, the program is able to detect the depth of a rigid layer and considers the effect of this layer on the deflections. Since the determination of the modulus of the various layers is controlled by the modulus of platform, ELMOD checks if this last one is modified while moving away from the central line of the load to check the existence of a rigid layer. In this case, the distance can be calculated and this layer is supposed infinitely rigid.
If no rigid layer is detected, deflections are then used to calculate two coefficients (C and n) according to the Ullidtz theory:

$$E = C\,(\sigma/\sigma a)^n$$

Where: E = subgrade modulus; σ = stress level; σa = reference stress level, (atmspheric pressure is used); C = Modulus at reference stress levelt; n = exponent for non-linearity (n>0 granular subgrade, n<0 cohesive subgrade).

In synthesis the main field of application of this tool are: QC of pavements and subgrades, estimation of dynamic modules of the pavement layers and of the subgrades through back calculation, LCCA.

1.3.2 Light Weight Deflectometer

The light weight deflectometer (LWD), also known as the light falling weight deflectometer, light drop weight tester, and dynamic plate load test, is a hand portable device that was developed in Germany to measure the soil in situ LWD dynamic modulus (Isola et al.,2013).

The international reference for LWD is the **ASTM E 2583-07** *Standard Test Method for Measuring Deflections with a Light Weight Deflectometer (LWD).*
In Figure 14 is shown the Light Weight Deflectometer available at the Transport Infrastructure Laboratory of the University of Catania and used for in field experimental tests.

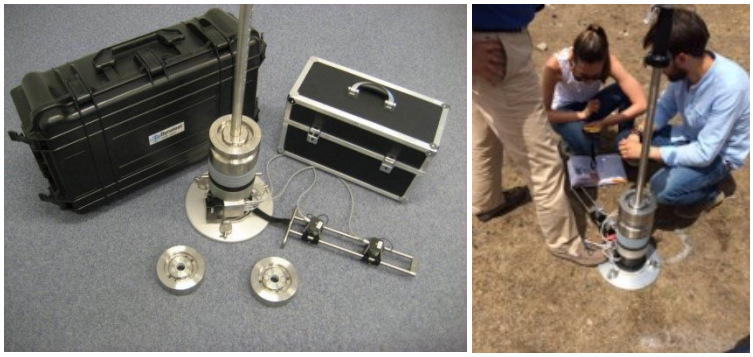

Figure 14 - LWD Dynatest 3031. University of Catania.

This test method, that is a type of plate-bearing test, covers the determination of surface deflections as a result of the application of an impulse load.
The resulting deflections are measured at the center of the applied load and may also be measured at various distances away from the load. Deflections may be either correlated directly to pavement performance or used to determine in-situ material characteristics of the pavement layers.
Generally, the LWD is used for testing unbound pavement layers. Some uses of data include quality control and quality assurance of compacted layers, structural evaluation of load carrying capacity, and determination of thickness requirements for highway and airfield pavements.
The LWD consists of a circular plate (150, 200, 300 mm) loaded by a falling mass (10 - 15 - 20 kg). The load is a force pulse generated by a falling weight (mass) dropped on a buffer system, in Figure 15 that transmits the load pulse through a plate resting on the material to be tested. The test apparatus may be hand held or moved around with a dolly type device.

Figure 15 - Buffer configurations at 10 - 15 - 20 kg. Dynatest LWD 3031, University of Catania

The load plate is capable of an approximately uniform distribution of the impulse load on the surface. The instrument shall be suitably constructed to allow pavement deflection measurements at the center of the point of impact, through a hole in the center of the load plate.
The weight is raised to the height that, when dropped, will impart the desired force pulse. The weight is dropped and the resulting vertical movement or deflection of the surface is measured

using suitable instrumentation. Multiple tests at the same drop height (different heights are optional) may be performed at the same location.
The peak deflection resulting from the force pulse at each location is recorded in micrometres, millimetres, mils or inches, as appropriate. The LWD is a portable version of the FWD. The LWD uses a load cell and geophones with the same accuracy as the FWD. The LWD had one geophone positioned in the center of the plate and 2 additional geophones that can be used for specific measures. The deflection sensors are capable of measuring the maximum vertical movement and mounted in such a manner as to minimize angular rotation with respect to its measuring plane at the maximum expected movement.
The number and spacing of the sensors is optional and will depend upon the purpose of the test and the pavement layer characteristics. Surface modulus can be calculated according to Boussinesq theory already exposed for the FWD and it is the modulus of an equivalent single layer system, which would give the same surface deflection as the measured deflections.
Therefore, it is a composite value with the contribution of all underlying layers.
In literature, the influence of depth of LWD tests is considered to be 1–1.5 diameters of the plate.
Subgrade modulus can be calculated with Ullidtz theory.

As regards the procedure for using the tool, it can be summarized in a few steps:

- Position the instrument over the desired test point. The test surface shall be as clean and smooth as possible with loose granules and protruding material removed. For gravel surfaces it is recommended that a thin layer of fine sand be placed over the test point. This helps in obtaining uniform contact between the load plate and the surface. A suitable rubber pad may be used for improving the load distribution.
- Place the loading plate and the sensors to ensure they are resting on a firm and stable test surface. The precision requirement for the deflection sensors is ± 2 μm (0.08 mils). The precision requirement for the load cell is ± 0.1 kN (22 lbf) or better. The bias requirement for both the deflection sensors and the load cell is ± 2 % or better.
- Raise the weight to the desired height and allow it to fall freely[13].
- Record the resulting peak surface deflection(s) and the peak load.
- Perform at least two falling weight sequences and compare the results. If the difference is greater than ± 3% for any sensor, note the variability in the report. Additional tests may be run at the same or at different load levels.

For data processing and storage system, load and deflection data shall be displayed and recorded. Supporting information such as air temperature, surface temperature, distance measurements, and identification data for each test point may be recorded either automatically or manually.
Different types of LWD are available (Marradi et al., 2014): the main differences are related to the height of the dropping masses (adjustable or fixed), the presence of the load cell and the different way to measure deflections produced by the dynamic load (geophone directly in contact with the tested surface or accelerometer on the top of the loading plate).
The LWD can be used to test thin asphaltic pavements, recycled materials bound with foamed bitumen and directly test the unbound subbase and subgrade. It can also be used to identify weaknesses, leading to further tests using FWDs and other material analysis techniques.

[13] It may be advantageous to use the first one or two drops for seating and use the subsequent drops for analysis.

1.3.3 Ground Penetrating Radar

The Ground Penetrating Radar (GPR), also known as Georadar, is a geophysical radar system with antennas and receivers used to perform non-destructive investigations of under-ground characteristics with high resolution and in depth (up to 3.2 m from the surface).
This system uses discrete pulses of radar energy with a central frequency varying from 10 MHz up to 2.5 GHz to detect objects or interfaces buried under the earth surface.
The GPR system is usually composed by: one or more antennas, a control unit, a computer, and accessory equipment. A control unit enables to collect the data, to control the radar operation, to display and save the results. After the data are collected, they're transferred to a pc for processing.
In general, a radar works with two fixed antennas, one transmitter and one receiver, by sending electromagnetic waves into the ground and when a target is detected, part of the wave is reflected; then the receiver, located near the transmitter, picks up the reflected energy and gives information for detection. In Figure 16 is shown a typical operation of a GPR system.
The distance to the detected object is determined by time gap between the moment of pulse emission and the moment of receiving of its echo.

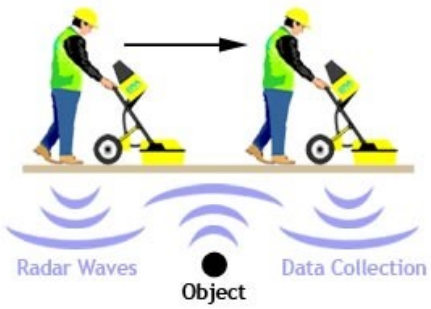

Figure 16 - Typical operation of a Ground Penetrating Radar.
Source: https://cefloyd.com/uploads/images/Blog%20Photos/GPR-Image.jpg

GPR is based on the same principle of conventional radars, but there are some differences:

- in conventional radar, the emitted electromagnetic wave propagates in air, while in the radar applied for ground introspection, wave propagates in soil or other solid materials (De Chiara, 2014);
- conventional radars use a single antenna while most GPR systems use two separate antennas;
- Unlike conventional radars that identify targets at long distance (some kilometers), GPR presents only a limited penetration in order of centimeters or few meters (IDS, 2013);
- Resolution also changes: for conventional radars it can reach up to some hundreds of meters, while GPR can detect with precision some centimeters (IDS, 2013).

It is a versatile instrument that allows obtaining, with high precision, a continuous profile of the medium investigated, that can be either a natural soil, or a road pavement, or a wall, from which it is possible to acquire a lot of information in a short time. In fact, it detects and localizes the presence of objects, buried structures, cavities, or of any discontinuity in the soil texture.
The propagation and reflection of the radar pulses is controlled by the electrical properties of the materials, which comprise:

- magnetic susceptibility, that is magnetism of the material;

- relative dielectric permittivity;
- electrical conductivity.

The magnetic susceptibility of a soil or road material is regarded as equal to the value of the vacuum, and thus does not affect the GPR pulse propagation.
The GPR system provides a fast, nondestructive measurement technique for evaluating the superstructure conditions in the field of Transport Asset Management: thicknesses of layers, underground density, moisture and utilities.
The equipment present different characteristics depending on the area where are applied, an important aspect is the choice of the two antennas because their frequency and configuration is crucial in each survey planning.
The choice of the antennas depends on target dimensions, characteristics of the surface, electrical properties of the medium, testing zone and possible limitations in access for the equipment. In fact, for each use of the equipment it is essential to plan the survey in order to ensure the best possible system output according to the aspects listed above.
It's important to underline that the success of a radar survey is dependent upon many factors, but the most important is surely the competency of the persons responsible for planning, carrying out the survey, and interpreting the data understanding the theory, field procedures and methods for interpretation of GPR data.
Penetration and resolution of GPR depend primarily on the transmitting frequency of the equipment, the antenna characteristics, the electrical properties of the ground or of the surveyed material, and the contrasting electrical properties of the targets with respect to the surrounding medium. Generally, there is a direct relationship between the transmitter frequency (determining the wavelength) and the resolution that can be obtained; conversely there is an inverse relationship between frequency and penetration depth (Pajewski et al., 2013). A transmitting GPR antenna converts an excitation in the form of a voltage pulse or wave train into electromagnetic waves. A receiving GPR antenna converts energy contained in electromagnetic waves into voltages, which are regarded as GPR data.
In Figure 17 is exposed a schematic diagram typical GPR traces from ASTM D6432-11.

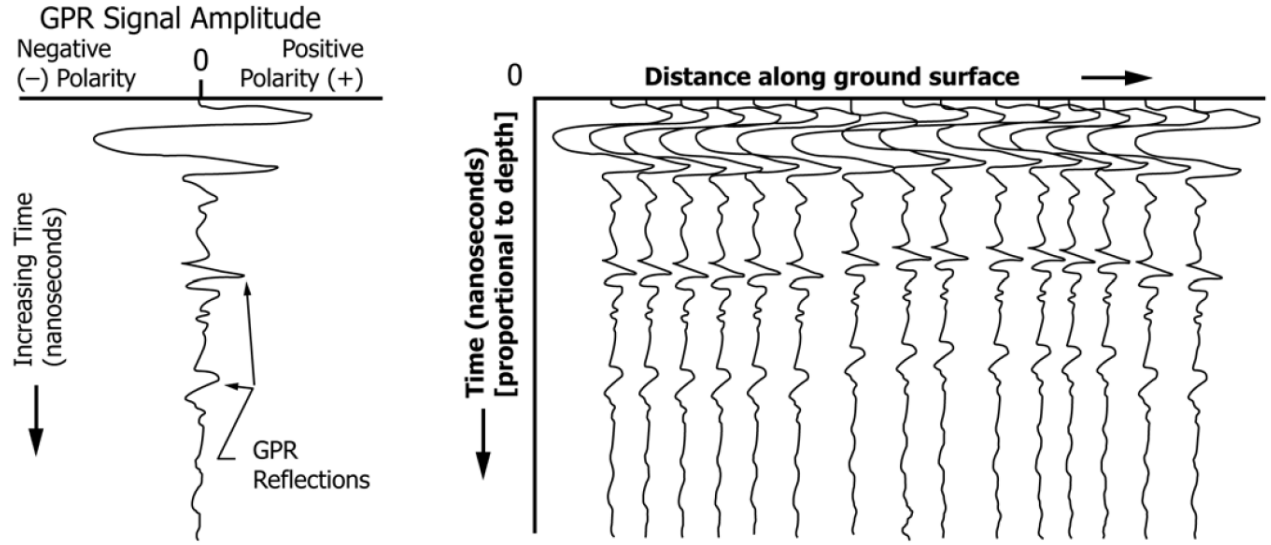

Figure 17 - Schematic diagram showing a typical GPR trace, and a series of GPR traces collected at specific distances to form a GPR profile line or cross section. Source: ASTM D6432-11

Generally, the GPR antennas consist of a transmitter and a receiver and they are classified in different manners. One important classification is based on the antenna location relative to the ground, in fact they are distinguished in:

- ground-coupled;
- air-coupled.

The center frequencies of commercial GPR antennae typically range from 25 MHz to 4 GHz.

Ground-coupled antennas present a frequency ranging from 80 to 2000 MHz, their signal is very strong enabling to achieve greater depth of penetration, up to 30 m.

In transport infrastructures studies, frequencies between 400 MHz and 1500 MHz are generally used with good results.

During surveys, the ground-coupled antennas are in contact with pavement, or very close to its surface, reaching a test speed between 5-30 km/h. Special attention should be paid to the gap between the antenna and the surface, in fact with a smaller air gap the results are better. If the ground-antennas are not in contact with the pavement, the distance to structure surface must be kept constant because the coupling changes as a function of distance.

The clear advantage of ground-coupled systems is the better signal penetration compared with the air-coupled, although surface coupling and antenna ringing present problems, which make it difficult to obtain any quantitative information from the near surface without signal processing. Another advantage is better vertical resolution compared with air coupled antenna systems, which allows these antennas to be used, for example, to detect pavement cracks, cables and reinforcement bars in concrete structures (Jol H. M., 2008).

Ground-coupled antennas main manufacturers for road and railway infrastructures assessment are GSSI (USA), IDS (Italy), MALA (Sweden), Penetraradar Corporation (USA), Sensors and Software (Canada) and UTSI Electronics (United Kingdom). In Figure 18 the Ground Coupled GPR of the Transport Infrastructure Laboratory of the University of Catania and used for in field experimental tests for this PhD dissertation.

Figure 18 - Ground Coupled GPR IDS. University of Catania

The air coupled GPR systems are increasingly being used to evaluate the upper part of the pavement structure. They produce relatively clean signals and can operate at close to highway speed.

Air coupled antenna systems are pulse radar systems and they generally operate in the range from 500 MHz to 2.5 GHz, the most common central frequency being 1.0 GHz. Their depth penetration is typically 0.5–0.9 m. During data acquisition these antennas are suspended 0.3–0.5 meters above the pavement surface. Most air coupled antenna types are transversal electromagnetic (TEM) horn antennas but hemispherical butterfly dipole (HBD) types have also been used in road surveys. The greatest advantage of air coupled systems is their repeatability because antenna coupling does not change with the changes in pavement properties.

Figure 19 - Air coupled horn antenna. Source: http://www.ndt.net/article/ndtce03/papers/v110/fig2.jpg

This allows them to be used for measuring changes in material properties for instance in asphalt quality control surveys (Saarenketo, 1998). Another advantage is, because they are mounted above the pavement, data collection can be done at full speed (up to 100 km/h) without interfering with traffic. Currently, horn antenna type air coupled systems are manufactured by GSSI, Penetradar; Pulse Radar and Wavebounce, all from USA, and butterfly dipole systems by Radar Team Sweden Ab. Euradar air-coupled GPR systems have also been used in pavement surveys in the Netherlands (Jol H. M., 2008).

An important reference for the correct use of GPR and internationally recognized is the **ASTM D6432-11** *Standard Guide for Using the Surface Ground Penetrating Radar Method for Subsurface Investigations*, in this guide is exposed working principle of the instrument according to the Maxwell electromagnetic theory[14].

A GPR trace is the record of the amplitude of electromagnetic energy that has been reflecte
d from interfaces between materials possessing different electromagnetic properties and recorded as a function of two-way travel time.

The relative permittivity of the material ε_r through which the electromagnetic pulse propagates mostly determines the propagation velocity of the electromagnetic wave.

The propagation velocity through the material is approximated using this relationship:

$$V_m = c/\sqrt{\varepsilon r}$$

[14] GPR operation principle is based on electromagnetic theory, its functioning consists in sending short electromagnetic pulses into a medium and when pulses achieve an interface they are reflected back partially and collected by the receiving antenna.
The reflected energy is displayed in wave-forms and the greatest amplitudes represent the interfaces between layers with distinct dielectric characteristics (Daniels, 2004; Saarenketo, 2006).
GPR measures the travel time between the transmission of the energy pulses and its reception. Transmission and reception of radar pulses are performed from one or more antennas that are moved on the investigated medium (Sussmann et al., 2003).

where: c = propagation velocity in free space (3×10^8m/s), V_m = propagation velocity through the material, and ε_r = relative permittivity, or dielectric constant.

Table 3 lists the relative permittivities and radar propagation velocities for various materials.

Table 3 - Approximate electromagnetic properties of various materials. Source: ASTM D6432-11

NOTE 1—
d = function of density,
w = function of porosity and water content,
f = function of frequency,
t = function of temperature
s = function of salinity, and
p = function of pressure.

Material	Relative Permittivity, K	Pulse Velocities, m/Ns	Conductivity, mS/m
Air	1	0.3	0
Fresh water (f,t)	81	0.033	0.10 - 30
Sea water (f,t,s)	70	0.033	400
Sand (dry) (d)	4-6	0.15-0.12	0.0001 - 1
Sand (saturated) (d,w,f)	25	0.055	0.1 - 1
Silt (saturated) (d,w,f)	10	0.095	1 - 10
Clay (saturated) (d,w,f)	8-12	0.106-0.087	100 - 1000
Dry sandy coastal land (d)	10	0.095	2
Fresh water ice (f,t)	4	0.15	0.1 - 10
Permafrost (f,t,p)	4-8	0.15-0.106	0.01 - 10
Granite (dry)	5	0.134	0.00001
Limestone (dry)	7-9	0.113-0.1	0.000001
Dolomite	6-8	0.122-0.106	
Quartz	4	0.15	
Coal (d,w,f, ash content)	4-5	0.15-0.134	
Concrete (w,f, age)	5-10	0.134-0.095	
Asphalt	3-5	0.173-0.134	
Sea ice (s,f,t)	4-12	0.15-0.087	
PVC, epoxy, polyesters vinyls, rubber (f,t)	3	0.173	

If the relative permittivity is unknown, as is normally the case, it may be necessary to estimate velocity or use a reflector of known depth to calculate the velocity. The propagation velocity, Vm, is calculated from the relationship:

$$V_m = (2D)/t$$

where: D = measured depth to reflecting interface, and t = two-way travel time of an electromagnetic pulse.

An accurate estimation of layer dielectric values or signal velocities is a key issue in successful traffic infrastructure GPR data processing. An interpreter, analyzing traffic infrastructure data, needs information concerning the dielectric properties of structures and subgrade soils in order to:

- calculate the correct layer thickness of structural layers and subgrade soil layers,
- calculate the moisture content,
- calculate the asphalt air voids content,
- estimate the moisture susceptibility and sensitivity which is directly relate to permanent deformation of unbound materials,
- estimate the frost susceptibility of subgrade soils,
- estimate the compressibility of subgrade soils,
- estimate the homogeneity and fatigue of bound layers.

In many surveys, especially in QA/QC (quality assurance/quality control) projects, there are major economic factors attached to the survey's results and as such there is a requirement for high quality data.
The GPR is used in various areas[15] ranging from civil engineering to geology, archaeology to environment, therefore equipment has to be built "ad hoc" for its different uses, enabling the user to make the best choice (Daniels, 2004).
In particular in civil engineering, and with reference to this PhD work, GPR can be used for studies on transportation infrastructures in terms of layer thicknesses or changes in structure: road, railways and airfields.
Experimental in field tests conducted with the GPR system will be exposed in Chapter 2.

1.3.4 Transport Infrastructure Laboratory "TI Lab", University of Catania

The Laboratory of Transport Infrastructure "TI Lab", of the Department of Civil Engineering and Architecture (DICAR) at University of Catania, is one of the most advanced laboratories in Europe in the field of Asset Management.
The laboratory is equipped with high-efficiency equipment and the related software, that allows to collect data related to pavements (layer thicknesses, bearing capacity, friction, unevenness, macro texture, subgrade) and road asset inventory (horizontal and vertical alignment, cross section, signs and markings, barriers, accesses, etc.).
The main application fields are referred to Transport Asset Management: Inventory, quality and performance controls of pavement, either in construction or maintenance management.
The Laboratory is equipped with top level system (Figure 20): Automatic Road Analyzer - ARAN 9000, Mobile Laboratory with Falling Weight Deflectometer - FWD 8000, Ground Penetrating Radar - GPR IDS, Laser Profilometer, Grip Tester Findlay Irvine GT 209, Light Weight Deflectometer - LWD 3031.
In this framework, the use of the equipment available at the TI Lab is of considerable importance for reaching innovative research results.
The versatility and the vanguard of these devices makes it possible to develop a consistent research work not only on roads, but also on railways and in other transport infrastructures, even for the transferability of models, in the deepening of the sustainable Transport Asset Management issue.

[15] Specific areas and uses of the GPR:

- *Geology:* determination of subsoil nature and geometry, localization of rocky masses, rocky boulders, karst cavities, etc.; measurement of ice sheet thickness; *i*dentification of discontinuities (faults, fractures, joints, etc.); sealing checks on polluted landfills, location of illegal landfills; identification of the piezometric surface; identification of areas characterized by polluted soils.
- *Archaeology:* discovery of masonry structures, artifacts, burial chambers, catacombs, cisterns, findings of different types; testing and evaluations for licenses granting in archeological restricted areas; identification of burial chambers.
- *Civil Engineering:* studies of transportation infrastructures in terms of layer thicknesses or changes in structure (road, railways and airfields); location of various types of underground utilities (metal or plastic pipes, electric cables, optical fiber cables, sewers, etc.); structural controls on artifacts, identifying cracks, detached surfaces, areas of materials degradation; detection and recognition of types of reinforcements and inspection of structures (such as tunnels, viaducts, bridges, dams, etc.); research and identification of buried structures for planning excavation and reconstruction works; investigations on frescoes, walls and floors; quality control on building structures.

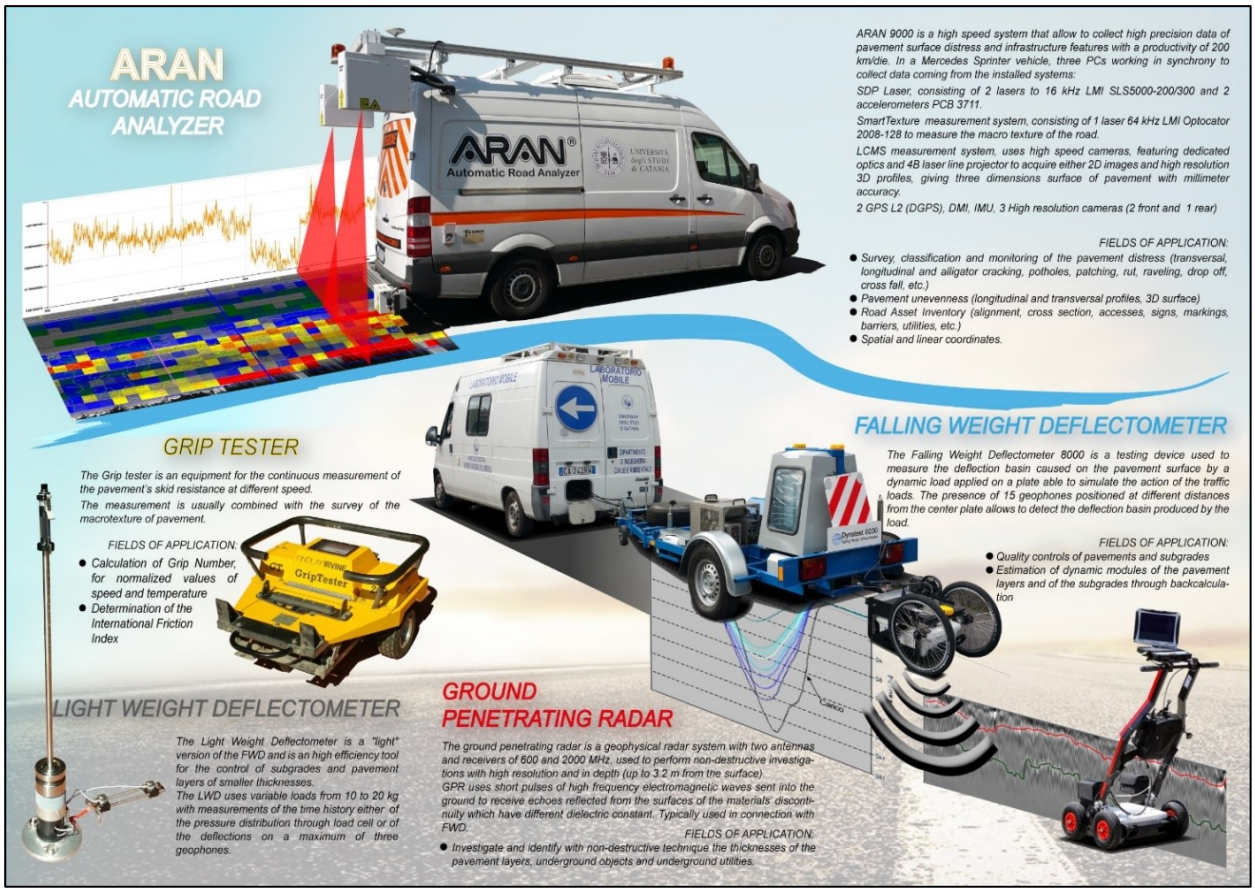

Figure 20 - Equipment of the TI Lab at DICAR. University of Catania

The experimental research works developed are part of sustainable Transport Asset Management topic and in particular regards the QA/QC that have been made in the road and railway environment with the high performance NDT equipment of the University of Catania.

Dipartimento Ingegneria Civile e Architettura
TI Lab
Transport Infrastructure Laboratory

Figure 21- TI Lab Laboratory of Transport Infrastructures. University of Catania, Department of Civil Engineering and Architecture (DICAR).

In Chapter 2 will be treated all the experimental tests that were conducted with the high-efficiency equipment of the University of Catania and that have also been the subject of scientific publications.

In particular, experiments in the railway field and in subgrade soils have been published, and experiments have also been carried out on volcanic ash from Etna eruptions, evaluating their reuse in the road sector for the deeper layers.

1.4 The Italian Road Authority: technical performance standards of the ANAS Specifications

In Italy, the **ANAS**[16] Road Authority has published guidelines and performance specifications[17] better known as *"Capitolato Speciale D'Appalto"* in which it explains the project methodologies of the mixtures and the performance control policies in the road paving maintenance and construction work. The ANAS Performance Specifications for the pavements includes a catalog of solutions, a manual for the design of mixtures, for maintenances and new constructions, and the prescriptions true for the benefits to be obtained on road, according to predefined values (indicators) measured with well-defined machines, that can also be high-efficiency machines.
ANAS S.p.A. is the Company that operates and maintains the main Italian road network.
ANAS S.p.A., *"Azienda Nazionale Autonoma delle Strade"* or *"National Autonomous Roads Corporation"*, is an Italian government-owned company deputed to the construction and maintenance of Italian motorways and state highways under the control of Italian Ministry of Infrastructure and Transport. In Figure 22 the ANAS head office in Rome.

Figure 22 - ANAS spa logo and head office in Rome. Source: http://www.stradeanas.it

The management of an infrastructure network so extensive and articulated poses serious and complex problems, especially in the vital sector of pavements preservation.
The current industrial process derives from having systematically pursued the transfer of the results of the research on the pavements to the methods and materials used in the operational practice, so that they became the patrimony of the administrations that had to build and maintain the roads.
The technical standards preceding the "ANAS Performance Specifications", however, had not well enucleated the meaning of the word "performance" because they linked it to the characteristics to be measured on the individual components rather than to a characteristic of the finished product, as we do today.

---

[16] **ANAS**: Founded on June 27, 1946, the company took immediately a government granting for the reconstruction of Italian road network, seriously damaged in the aftermath of World War II.
Thanks to the wealth of experience accumulated over 80 years of activities and to the knowledge of their management and technical personnel, Anas has expanded the range of services offered during the years, being able to play a supporting role to government agencies and offer themselves as a catalyst in Italy and abroad in the services of design, construction and road maintenance. The share capital of Anas S.p.A. amounts to EUR 2,269,892,000.00.
The present total extension of the Italian road network is about 25,000 km, which is added the network under concession to the motorway companies that is about 6,000 km, with regard to which ANAS s.p.a. exercises a function of control and monitoring.

[17] "Linee Guida di Progetto e Norme Tecniche Prestazionali" (2008), "Capitolato Speciale D'Appalto - Norme Tecniche" (2009), "Capitolato Speciale D'Appalto - Norme Tecniche per l'esecuzione del contratto Parte 2" (Coordinamento Territoriale/Direzione IT.PRL.05.21).

In fact, the measure of performance, the "performance", is what must leave no doubt about the functioning of the built object, so much so that it was introduced to allow the assessment, and payment, all or in part, the road work.
Faced with the problems related to the management of road pavements, in an extended network and articulated as the Italian network, new solutions in terms of *guarantee of performance* are represented by ***measurements performed in "High Efficiency",*** as new policies and new instruments of measurement from new *performance indicators* and *new control methods*, all it made operational and integrated into specific operational implementing rules (Cesolini et al., Anas S.p.A).
Product excellence consists of knowledge on materials and methods to measure their effectiveness with machines that make this process operational. It is to be considered that the guidelines of Anas cover a part of the issues that had been addressed at the international level considering that the infrastructure sector is constantly evolving and updating.
In the following, a parenthesis is dedicated to the indications of Anas, which are nowadays considered as an Italian normative reference, to be seen from a viewpoint of knowledge, renewal and improvement, just as was thought for the development of this PhD thesis.
Road pavements, constituted by materials at visco plasto-elastic behavior must be preserved in their basic qualities, i.e. be subdivided into *superficial*, in direct contact with the wheels of the vehicles, and *deeper*, related to the bearing capacity of the complex package which constitutes them.
The peculiar features of the measures planned by Anas guidelines and performance specifications for the formulation and testing of materials to be used, are:

- Dimensioning of the road structure through the use of rational methods of calculation using specific fatigue curves that allow to calculate the service life of the intervention.
- Maximum possible reuse of milled materials and other easily available materials on the place of intervention, evaluated and verified in the fatigue life calculations, and to reduce transport costs and preserve the environment.
- Definition of general working criteria to consider the problems of practical application on roads in service; the expected thicknesses are related to the need for bearing capacity and also connected to the feasibility with the techniques used.
- Use of modified bitumen, to increase the durations with certainty of result.
- Definition of *performance testing methods*, on individual materials, mixtures and complete works. For the latter are assigned levels of performance, measurable with *High Efficiency tools* that easily can give performance index.

The materials that will be used in the work will have to respect the performance requirements listed in the Anas specifications and the bituminous mixes (mixed hot asphalts) will have to be provided with CE marking to be considered suitable and employable.
According to ANAS, two are the cornerstones of the technical scientific process:

1. The non-destructive global verification of the result on the road is as characteristics superficial (with procedures already tested in Italian use), which as a load-bearing capacity and therefore duration in service, which completes the performances required for a paving.
2. The use of all the materials available also of a marginal type, thanks to the possible global fatigue check to be carried out before the work is carried out.

As part of road pavements management, the main problems can essentially be summarized in three key points (Cesolini et al., Anas S.p.A):

1. ***Evaluation of the state of pavements****:* primarily aimed to the preparation of maintenance plans scheduled with the goal of the optimal management of available resources, including the gradual improvement of the road functions in time;
2. ***Project of road pavements:*** pavements must be effectively dimensioned on the expected traffic, environmental conditions, the materials used and the duration of the planned project;
3. ***Verification and control work****:* for efficient testing and which final results of planned maintenance in the planning stage. Repeated measures allow to control the evolution of the paving over time performance, so it is possible to know, not only the performance at time zero (occurs during testing), but also their durability.

ANAS performance specifications are related to the execution of works for the pavement superstructure; the work may be of **3 types of intervention**:

1. ***Ordinary Maintenance (MO):*** works for interventions on existing pavements for routine maintenance of them that are localized and confined to restore the original state of the pavements
2. ***Extraordinary Maintenance (MS):*** works for interventions on existing pavements for their recovery, and/or reinforcement with interventions of superficial (RS) or deep rehabilitations (RP);
3. ***New Constructions (NC):*** work on pavements of new construction (roads and motorways) or upgrading of existing roads.

In particular, for the control of the pavements acceptance requirements, some premises must be made:

- The control for the pavements acceptance requirements, and the evaluation of any deductions or penalties to be applied, are based on always prescriptive checks for the MO type work.
- The control for the pavements acceptance requirements, and the evaluation of any deductions or penalties to be applied, are based on controls always of a performance type for MS and NC works.
- At the discretion of the DL (Works Direction), even in the case of work type MO, performance checks may be requested on the characteristics of grip, texture, and thickness ratings, which may result, by the DL, deductions or penalties as foreseen in the activities MS and NC.

With regard to traditional performance checks some indications on mixtures to be used for road paving must be observed, in terms of percentages of bitumen, voids, aggregates.
The companies that perform the work must provide all the data for: mixture and production plant, aggregates (percentages, granulometries, PSV, CLA), volumetric and mechanical characteristics, percentages of binder (bitumen or emulsion), performance data and technical data sheets of the supplier.

During the execution of the works all the checks are made by the company (Table 4 and Table 5), but the client can carry out checks at any time through his laboratories and can request all the documentation. All the design curves for the bituminous conglomerates must be verified by using a rotary press.

Table 4 - Anas specifications for traditional controls of the mixture: particle size analysis, % bitumen, thicknesses

Sieves opening (mm)	Particle size (passing %)									
	Wear a (US)		Wear b (US)		Binder (BI)		Basebinder (°) (Bb)		Base (BA)	
31,5							100	100	100	100
20					100	100	78	100	68	88
16	100	100			90	100	66	86	55	78
12,5	90	100	100	100	66	86	-	-	-	-
8	70	88	90	100	52	72	42	62	36	60
4	40	58	44	64	34	54	30	50	25	48
2	25	38	28	42	25	40	20	38	18	38
0,5	10	20	12	24	10	22	8	21	8	21
0,25	8	16	8	18	6	16	5	16	5	16
0,063	6	10	6	10	4	8	4	8	4	8
% bitumen referred to the mixture (12697-1 and 39)	4,5 - 6,1		4,5 - 6,1		4,1 - 5,5		4,0 –5,3		3,8-5,2	
Thicknesses (cm)	4 – 6		3		4 - 8		7-12		8-18	

Table 5 - Anas specifications for % voids

	Base and basebinder			Binder			Wear A and B			% voids (Vm UNI EN 12697-8)
	TQ	Sf	HD	TQ	Sf	HD	TQ	Sf	HD	
N1	10	10	10	10	10	10	10	10	10	11-15
N2	100	110	120	100	110	120	120	130	140	3-6
N3	180	190	200	180	190	200	210	220	230	≥ 2

Where: TQ=unmodified bitumen, Sf=bitumen modified soft, HD=bitumen modified hard, N1,N2,N3= three levels of revolutions (initial, average, final) for the verification of the percentage of voids with girate press

Regarding the application of penal deductions, on the quality and percentage of bitumen, the characteristics in the specifications regarding penetration, ball and ring, and viscosity at 160 ° C on the bitumen taken in the plant must be respected, with a tolerance of 10% on the range (for example if the expected penetration is 50-70 dmm, then the penalty thresholds are 50-0.1 * 50 = 45dmm and 70 + 0.1 * 70dmm). Also for the purposes of application of the penalty, compliance with the percentage of binder detected by extraction must be respected compared to the approved (design) percentage contained in the studies to formulate the mixture in question. With respect to the project bitumen content, a tolerance of + 0.3% is allowed for the application of the penalty.

The percentage of bitumen must always be reported by weight with respect to the mixture and can be measured on cores performed on the pavement or from loose conglomerate taken in the laying phase and will be performed according to UNI EN 12697-1 or 39. The DL can apply the penalty even if only one of the above variables results out of the tolerances described. Should one or more

of the quantities listed above not be within the ranges, a standard CM amount of bituminous conglomerate will be deducted by 15% at a PS price, calculated according to the following method:

$$CM\ (m^3) = Q / (2.3 * 0.045)$$
$$D\ (€) = 0.15 * CM * PS$$

Where: CM is the quantity of AC (in m^3) realized with the supply of Q tons of bitumen; Q is the quantity in tons of the bitumen supply to which the levy refers, if is not possible to go back to the Q quantity of bitumen or the parameter to be penalized (out of tolerance) both the percentage of the bitumen will be considered Q = 20ton; PS is the price in €/m^3 for the awarding of the works of the AC realized with the bitumen in question; and finally D is the value to be deducted in euros (€).
If the same bitumen is used for more types of AC, then the AC with the highest price will be used.
Essential element to frame correctly all these problems is, therefore, the definition of performance indicators characteristics of the surface and deep of the pavement, and also the identification of appropriate measuring instruments, which make it possible expeditious and extensive measurements, i.e. able to monitor all the construction lanes, maybe even with repeated trials.
Have been identified, and are in current use, the following performance indicators of ***surface characteristics*****:**

- Coefficient of transversal adherence **CAT** to assess **grip**
- Average height of macrotexture **MPD** for assessing **macrotexture**
- International Index **IRI** to assess the **unevennes**

Subsequently were identified new performance indicators of the ***deep characteristics*****:**

- **Thicknesses** of the pavement layers
- **Structural Index IS** for the evaluation of the **bearing capacity.**

Below, Table 6 shows the performance type controls that evaluate the surface and structural characteristics of the pavements.

Table 6 - Performance controls in ANAS Specification. Source: "Capitolato Speciale D'Appalto - Norme Tecniche per l'esecuzione del contratto Parte 2" (Coordinamento Territoriale/Direzione IT.PRL.05.21).

Type of processing	**% bitumen and quality**	**Thicknesses**	**CAT20**	**HS**	**IRI**	**IS300**	**IS200**
article	7.4	7.4 and 10.5	10.2	10.2	10.3	10.4	10.4
RSS *(rescue superficial repairs)*	yes	yes	Yes if extended ≥ 500 m	Yes if extended ≥ 500 m	no	no	no
TS *(surface treatments)*	yes	yes	yes	Yes	yes	no	no
RS *(superficial renovations)*	yes	yes	yes	Yes	yes	no	yes
RP *(deep renovations)*	yes	yes	yes	Yes	yes	yes	not applicable
NC *(new constructions)*	yes	yes	yes	Yes	yes	yes	not applicable

As far as concerns the acceptance requirements of the road pavements, with reference to the penalties, it's also important to highlight what Anas does when it is necessary to apply multiple penalties.
The presence of more deductions will lead to the application of the most severe penalty, excluding the penalty on the thickness and bitumen (percentage and quality) that, if present, will always be applied in addition, except in special cases that will be judged by the DL.
The maximum value of the total deduction cannot exceed 20% of the total amount of pavements work. In cases where the awarding of the works has taken place with a reduction of more than 30%, the maximum value of the total deduction will be raised up to a maximum of 30%.

In the following part, the ANAS specifications for the superficial and structural deep features will be explained in detail. The reference below will be "Capitolato Speciale D'Appalto - Norme Tecniche per l'esecuzione del contratto Parte 2 - (Coordinamento Territoriale/Direzione IT.PRL.05.21)", then the current specifications will be reported.

It is good to remember that that this thesis work, as will be seen in the following chapters and paragraphs, focuses more on the structural characteristics of the road pavements in terms of thickness and bearing capacity, detailed in paragraphs 1.4.3, 1.4.4 and 1.4.5.
For the sake of completeness in dealing with the topic related to the performance specifications in the road sector, in paragraphs 1.4.1 and 1.4.2 a summary of the surface characteristics indicators was made: grip, texture and unnevenness.

1.4.1 Grip and Texture in ANAS specifications

The values of GRIP and TEXTURE constitute the surface performance data, the values to be obtained are dependent on:

- The types of material used for the execution of the surface layer;
- The plano-altimetric conditions of the section in every point;
- The type of prevailing traffic and its intensity.

The coefficient of Transversal Grip "CAT" will be measured by the SCRIM equipment, SUMMS or ERMES according to CNR Standard B.U. No. 147 of 14/12/92.
The geometric texture "HS" intended as surface macrotexture, will be measured in terms of MPD by SCRIM, SUMMS or ERMES according to UNI EN ISO 13473-1 (2004), where:

$$HS=0,2+0,8\cdot MPD.$$

The CAT indicators, reported to the air reference temperature of 20°C, will have to be greater than or equal to values which depend on types of material, indicated in the tables of the performance specifications, in terms of CAT_{20} and HS.
The CAT at the reference temperature is calculated with the following formula: $CAT_{20}=CATt/(0.548+(44.69/t+80))$, where: CAT20 is the value of CAT at the reference temperature of 20°C; CATt is the value of CAT at test conditions; t is the air temperature at test condition in °C.
In Table 7 CAT and HS indicators in Anas Specifications.

Table 7- CAT and HS indicators in ANAS Specifications

Type of processing	**CAT_{20}**	**HS (mm)**
AC for wear layers	58	0.4
AC for temporary wear layers (binder)	50	0.3
AC for wear layers with expanded clay	62	0.4
Draining AC	53	1.0
Draining AC with expanded clay	56	0.8
Cold surface treatments macroseal type 6 mm thick	62	0.5
Hot surface treatments	55	0.3
Mechanical roughening irradiance (shot peening)	5 points of CAT more than the existing CAT	not applicable

ANAS also indicates the period of time within which the CAT and HS measurements must be made, ie between the 15th and the 180th day of opening to traffic, with some exceptions for different particular materials. Moreover, the speed of relief must be kept as constant as possible and equal to 60 ± 5 km/h, the measurement step must be 10 m over the entire length of the interventions.

1.4.2 Unevenness in ANAS specifications

The UNEVENNESS values constitute the data surface performance together with GRIP and TEXTURE.

The unevenness can be measured with high-performance equipment with inertial laser profilometer Class 1 according to ASTM E950-98 (2004) and calculated through the IRI[18] International Roughness Index (Figure 23) as defined by the WORLD Bank in 1986[19] "The International Road Roughness Experiment".

In Table 8 the ANAS specifications for IRI.

[18] IRI: The **International Roughness Index** is the roughness index most commonly obtained from measured longitudinal road profiles. It is calculated using a quarter-car vehicle math model, whose response is accumulated to yield a roughness index with units of slope (in/mi, m/km, etc.). Since its introduction in 1986, IRI has become the road roughness index most commonly used worldwide for evaluating and managing road systems. The measurement of IRI is required for data provided to the United States Federal Highway Administration, and is covered in several standards from ASTM International: ASTM E1926 - 08, ASTM E1364 - 95(2005), and others. IRI is also used to evaluate new pavement construction, to determine penalties or bonus payments based on smoothness.
In the early 1980s the highway engineering community identified road roughness as the primary indicator of the utility of a highway network to road users. However, existing methods used to characterize roughness were not reproducible by different agencies using different measuring equipment and methods. Even with a given agency, the methods were not necessarily repeatable. Nor were they stable with time. The United States National Cooperative Highway Research Program (NCHRP) initiated a research project to help state agencies improve their use of roughness measuring equipment. The work was continued by the World Bank to determine how to compare or convert data obtained from different countries (mostly developing countries) involved in World Bank projects. Findings from the World Bank testing showed that most equipment in use could produce useful roughness measures on a single scale if methods were standardized. The roughness scale that was defined and tested was eventually named the International Roughness Index.

[19] World Bank Technical Paper Number 45 and 46, 1986.

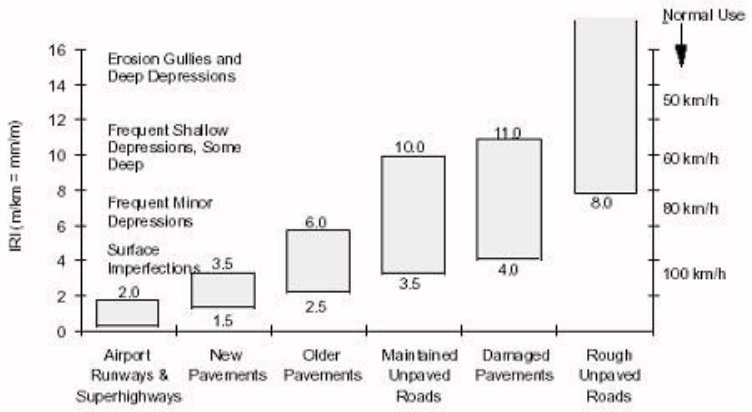

Figure 23- IRI roughness scale. Source: http://www.pavementinteractive.org/wp-content/uploads/2007/08/Iri1.jpg

Table 8 - IRI in ANAS Specifications

Type of intervention	**IRI (mm/m)**
RS, RP, NC	2.5
RSS, TS	not applicable

Following in 1.4.3, 1.4.4, 1.4.5 the ANAS directions for *structural characteristics*, that will be of particular interest and detailed in this PhD thesis.

1.4.3 Thicknesses of the pavement layers in ANAS specifications with Ground Penetrating Radar

The measurement of the thickness for the bituminous layers may be carried out as well as with cores, even with systems with high-efficiency appliances with Radar Penetrometric (GPR) suitably calibrated with control cores.
The thicknesses of the pavement layers, measured with the Ground Penetrating Radar high-efficiency system, constitute the structural performance data.
The antennas to be used will be of at least 1 GHz and the acquisition system must guarantee a resolution in the measurement of the thickness on the order of 1 centimeter; while the spatial sampling step should be of at least 50 cm.
The values of thicknesses will be deducted from the examination of radargrams obtained with the Ground Penetrating Radar equipment.
The exam can be done visually or through dedicated software; before the examination must be operated a calibration of the measures using control cores (indicatively not less than 3 cores/km per lane) or alternatively evaluation of the thickness through the use of borescopes or video endoscopes on holes made on the pavement with the same cadence of core samples.
The entire length of the intervention realized by each individual site must be recorded; the thickness measurements, made with georadar, must be returned with a measuring step of 2 m and then analyzed for homogeneous sections.
It is also essential to check the thicknesses, for a homogeneous section: the average values of the thicknesses obtained with the equipment must be greater than or equal to the project thicknesses.

Deductions

In the case of control measures carried out with georadar the asphalt concrete will be evaluated in thickness as a whole without distinguishing between the component layers.

The deduction will be applied in percentage points on the contract price of the entire rebuilt package, determined as the sum of the prices of the individual component layers on the basis of the relative project thicknesses; this deduction will be valid for the whole homogeneous stretch to which it refers.

The deduction will correspond to three times the percentage points of which the overall thickness, regardless of its composition, differs in decrease compared to the project values, admitting a maximum tolerance of 7% (exemplifying, if the difference is 10% compared to the value of project, the penalty will be ((10 - 7) · 3)% = 9%); if, on the other hand, the difference reaches 25%, excluding tolerance, the D.L., even taking into account the effective extension and distribution of the homogeneous sections lacking, may request its remaking at complete care and expense of the Contractor. In Figure 24 there are the Penalties applied by ANAS for the percentage differences in thicknesses with Ground Penetrating Radar.

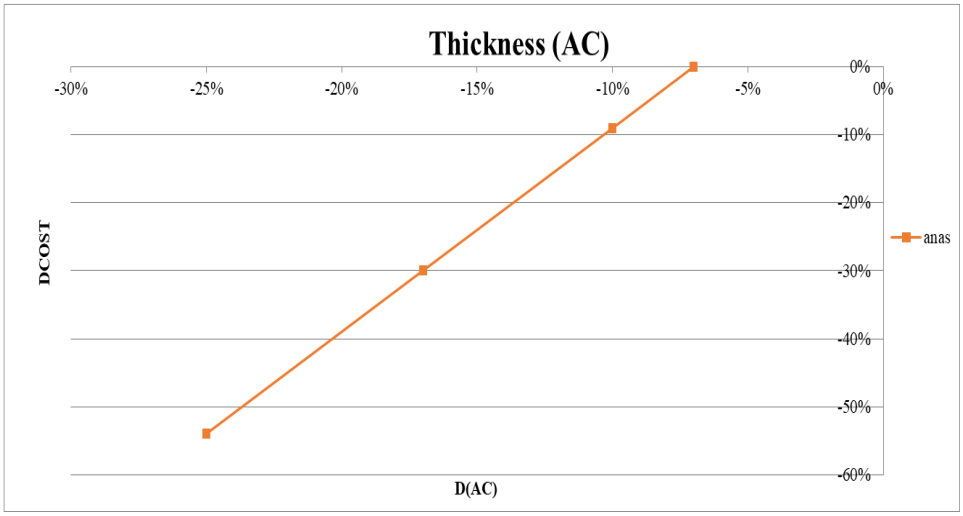

Figure 24 - Penalties for the percentage differences in thicknesses in ANAS specifications with Ground Penetrating Radar

1.4.4 Bearing Capacity in ANAS Specifications with Falling Weight Deflectometer and TSD

Bearing capacity values represents the *structural performance data*. The measurement of the bearing capacity is obtained by evaluating the effective dynamic deflection basin of the pavement due to the application of a dynamic load imposed by a Falling Weight Deflectometer (FWD) and/or a mobile machine with 12 t measuring axis (Traffic Speed Deflectometer).
The FWD equipment (Figure 25) to be used should be equipped with minimum 7, preferably 9, deflection measuring devices (geophones) mounted in line at a predetermined distance from the loading plate The distances in mm from the plate center are: 0, 200, 300, 450, 600, 900, 1200, 1500, 1800.

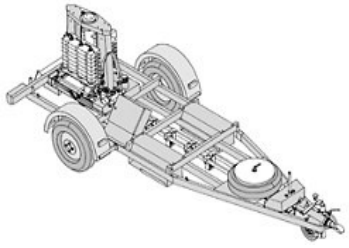

Figure 25 - A typical FWD used for bearing capacity measurements

The measurements will normally be carried out on an alignment placed centrally with respect to the width of the intervention, or, in case of doubts about the success at the edges, it can also be carried out in the side at least 50 cm from the edge, however, the results will be worth for the acceptance of the full intervention width. Alternatively, the 700 kg Heavy Weight Deflectometer HWD (Figure 26) with at least 7, preferably 9, sensors fitted with the distances indicated above may be used, however the applied mass shall be adjusted to 350 kg.

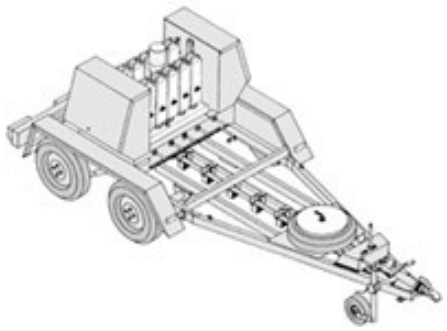

Figure 26 - A typical HWD used for bearing capacity measurements

The high-performance mobile equipment, for the survey performed in speed, must provide basin values at least at the wheel axis and at 200, 300, 900 and 1500 mm from the axis, or at least provide the IS300, IS200 and ISFOND indicators directly, specified below.

The indicative value of the basin, to be used as reference data for the deep rehabilitations or new pavements, is the one called Structural Index 300 (IS300) obtained as the difference between the maximum deflection recorded at the center of the FWD plate and 300 mm from this center, and the values, however, to be registered, of the other drops can only be used for study purposes and not for contractual assessments in the way described below.

The expression of the Structural Index 300 is:

$$IS300=D_0-D_{300}$$

The indicative value of the basin, to be used as reference data for superficial rehabilitations, is called structural index 200 (IS200) obtained as the difference between the maximum deflection recorded at the center of the FWD plate and 200 mm from this center:

$$IS200=D_0-D_{200}$$

Evaluations are typically made on finished pavements, and it is on these values that will operate for verification in contractual terms; other measures, carried out during the work on the lower and/or intermediate layers, may be used by the works management (DL) to give directions to the company executor, who will still be assessed on the final result.

The Superficial Rescue Repairs (RSS) and the Surface Treatments (TS) do not provide acceptance on bearing capacity.

Measurements with FWD will have a minimum cadence of an evaluation every 20 or 50 meters, depending on the actual extension of the intervention.

For each measurement station will have to perform 3 drops of load assigned by imposing a stress of 1700 kPa, the reference basin is the basin recorded in the third repetition.

The measures will be extended to the entire tract of the intervention. With the new speed measurement equipment such as Traffic Speed Deflectometer (Figure 27), the detection of the structural parameter will take place continuously and at high speed.

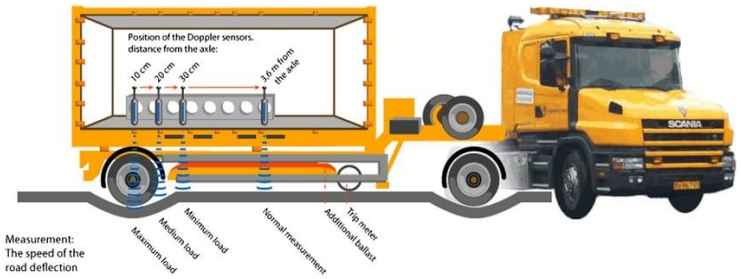

Figure 27 - Traffic Speed Deflectometer. Source: Baltzer et al, 2010.

For each type of intervention, the characteristics of bearing capacity were evaluated, and therefore the deflection basins, which are obtained by soliciting the expected materials with a given effort. These calculations made it possible to determine the permissible limits for the IS300 Structural Index, according to the test conditions, which will be subsequently shown in the table.
The test conditions are evaluated through the effective air temperature at the time of the test and the possible degree of maturation of the process compared to the time of execution of the test itself.
The tests are normally carried out at a given Air Reference Temperature (14°), but in any case will be considered valid if it is contained within the temperature ranges between 8 and 25°C, over such intervals the data will still registered, but it will not constitute binding conditions for acceptance.
In case of FWD tests performed with a different load value imposed will require an adjustment of the control diagrams.
The evaluations of bearing capacity carried out on roads of new constructions, or on existing roads, take into account the different working conditions objectively linked to the presence or absence of road traffic. As part of the Deep Rehabilitation (RP) or New Construction (NC) the bearing capacity will be evaluated through the structural indicator IS300, corrected with the air temperature as described in Table 9, evaluated and detected, with the same methods and equipment described above but judged through the following control table.

Table 9 - Bearing capacity evaluation with IS300 in Anas Specifications

Type of processing	$IS300_{14°C}$ FWD measure with a pressure of 1700 Kpa			$IS300_{14°C}$ TSD measure with a pressure of 850 Kpa		
	1 month	6 months	1 year	1 month	6 months	1 year
RPA1	84	72	67	48	41	39
RPA2	88	80	77	50	46	44
RPA3	67			39		
RPB1	106	86	76	59	48	44
RPB2	102	89	83	58	51	47
RPB3	76			44		
NC1	76	66	61	43	37	35
NC2	98	79	70	54	44	40

The different values of $IS300_{14°C}$ relating to the RP (Deep Rehabilitation) and the NC (New Construction), that can have layers of foamed binder and/or linked to the emulsion or layers that are not bonded to cement, are referred to the various moments of maturation of these materials in which the measurement can be performed (in a month, 6 months and 1 year after the last coat).

In the case of a cement binder use, the measures will be made at least 3 days after coating.
The acceptance measurements are made on the pavements at the latest one year after the last coat.
As part of the Surface Rehabilitation (RS), the bearing capacity will be evaluated through the IS200, corrected with the air temperature as described below, evaluated and detected, with the same procedures and equipment described above but judged through the following control Table 10.

Table 10 - Bearing capacity evaluation with IS200 in Anas Specifications

Type of processing	$IS200_{14°C}$ FWD measure with a pressure of 1700 Kpa	$IS200_{14°C}$ TSD measure with a pressure of 850 Kpa
RSA1	138	55
RSB1	171	67
RSA2	133	53
RSB2	158	63

For the calculation of the Structural Index 200 (IS200) it is also necessary to record the deflection at 900 and 1500 mm from the center of the load from which the corrective factor of the subgrade is obtained.
The correct value with the subgrade IS200cf is provided by the following expression:

$$IS200cf/IS200 = (f - 0.50 \cdot LOG(IS_{FOND}))$$

Where: IS_{FOND} = D900 – D1500, f is a correction factor (f=1.94 for FWD and HWD test, f=1.77 for TSD test). IS_{FOND} represents the behavior of the subgrade, therefore it is a measure of the bearing capacity provided by the unbounded lower layers.
The measurements of the Structural index (IS) will be analyzed for homogeneous sections. Before this analysis, all the values of IS300 and IS200 measured must be brought back to the reference air temperature of 14°C with the following expression:

$$IS_{14°C}/IS_T = e^{c\cdot(14-T)}$$

Where: $IS_{14°C}$= Structural Index at the Air Reference Temperature (14°C); IS_T= Structural Index measured in the test conditions; T= air temperature in the test conditions; c= coefficient which is 0.037 for interventions of new construction and deeper rehabilitation; and is 0.022 for interventions of superficial rehabilitation

Deductions

The deduction will be applied in percentage points on the contract price of the entire reconstructed package (intended consisting of foundation, base, binder and wear), determined as the sum of the prices of the individual component layers on the basis of the relative project thicknesses; this deduction will be valid for the whole homogeneous stretch to which it refers.
The deduction will correspond to half the percentage points of which the Structural Index, at the reference temperature of 14°C, differs with respect to the limit value prescribed for the type of intervention and the maturation time (exemplifying, if the difference is 6% compared to the prescribed value, the penalty will be 3%).
If the differences of the IS reach 40%, the work will not be considered acceptable, and the Works Management, even taking into account the extension and distribution of the homogeneous sections missing, may request its remake at the complete care and expense of the Contractor.

Requests for measures with higher maturation times will not be accepted if the measures taken at lower maturation times have given negative results, except in special cases certified by the Works Management.

1.4.5 Bearing Capacity in ANAS Specifications with Light Weight Deflectometer

The LWD tests, in ANAS specifications, must be made for layers of granular material, then subbases in extraordinary maintenance (MS) or in new constructions (NC) in cases of lesser importance roads, moreover they can also be done on subgrades.
The LWD tests must comply with the ASTM Standards E2583-07[20] and will be performed applying a stress of approximately 70 KPa while the duration of load impulse will be approximately 30 msec. This configuration is obtained by using the 10 kg load with a fall height (distance between ground and load base) equal to 100 cm.
The measures of the LWD, as indicated in the Standard, must be repeated until admitting a gap between the center plate deflections ≤ 3%; while respecting the required elastic modulus limit, if the gap limit is not reached between two consecutive deflections after 4 drops for more than 5 measuring points spaced at least 5 meters apart, the layer will be recompacted.
The tests carried out, which can be saved on file, must record at least the applied pressure, the application time of the load, the deflection at the plate center and the elastic module which must be calculated with the following expression $E = f \cdot (1-h2) \cdot s \cdot r / d0$ with f = 2, h = 0.35, s = applied stress (around 70 KPa), r = 150 mm (plate radius), and d0 = deflection measured at the plate center.

1.5 References

- AASHTO Designation R 9-97, Standard Recommended Practice for Acceptance Sampling Plans for Highway Construction, *Standard Specifications for Transportation Materials and Methods of Sampling and Testing, Part I Specifications*, 24th Edition. AASHTO, Washington, D.C., 2004.

- ANAS S.p.A., *Capitolato Speciale D'Appalto - Norme Tecniche per l'esecuzione del contratto Parte 2,* Coordinamento Territoriale/Direzione IT.PRL.05.21., 2016.

- ANAS S.p.A., *Capitolato Speciale D'Appalto. Norme Tecniche*, IT.CDGT.C.05.16-Rev.0-24/04/2009.

- ANAS S.p.A., *Gestione delle pavimentazioni stradali. Linee guida di progetto e norme tecniche prestazionali*, Ricerca & Innovazione – Centro Sperimentale Stradale, Novembre 2008.

- ASTM D4694-96, *Standard Test Method for Deflections with a Falling-Weight-Type Impulse Load Device.*

- ASTM D6432-11, *Standard Guide for Using the Surface Ground Penetrating Radar Method for Subsurface.*

[20] Standard Test Method for Measuring Deflections with a Light Weight Deflectometer (LWD)

- Austroads, *Development of Performance Contracts and Specifications - Full Report*, ISBN 0 85588 670 6, Austroads Project No. T&E.P.N.506, Austroads Publication No. AP–T25.1/03, Published by Austroads Incorporated, Sidney, 2003.

- Baltzer, S., Pratt, D., Weligamage, J., Adamsen, J., and Hildebrand, G., *Continuous bearing capacity profile of 18,000 km Australian road network in 5 months*, 24th ARRB conference proceedings, Melbourne, Australia, 2010.

- Burati, J. L., and C. S. Hughes. *Construction Quality Management for Managers*. Demonstration Project 89, Publication Number FHWA-SA-94-044. FHWA, Dec. 1993.

- Carlson A., Folkeson L., *Sustainability and Energy Efficient Management of Roads*, ERA-NET Road – Energy, May 2014.

- Cesolini E., Drusin S., *La capacità portante delle pavimentazioni misurata ad alto rendimento e collegata al capitolato d'appalto prestazionale*, Anas S.p.A., Centro Sperimentale Stradale – Cesano (Roma), Italy.

- Corsaro G., *Compressione, compattazione e portanza di ceneri vulcaniche per il riutilizzo in ambito geotecnico e stradale*, Tesi di Laurea in Ingegneria Civile e Ambientale - Università di Catania, Relatori: Prof. Ing. Ernesto Motta, Prof. Ing. Salvatore Cafiso, Correlatori: Dott. Ing. Piera Paola Capilleri, Dott. Ing. Grazia La Cava, A.A. 2015/2016.

- Decreto Legislativo 3 Aprile 2006, n. 152, *Norme in materia ambientale*, (G.U. n. 88 del 14 aprile 2006).

- Dynatest International, 1998. *ELMOD Quick Start Manual*.

- European Union Road Federation (ERF), International Road Federation (IRF), *Sustainable Roads and Optimal Mobility*, ERF Discussion paper, October 2009.

- European Union Road Federation, *European Road Statistics*, 11th edition ERF, 2013.

- European Union Road Federation, *Road Asset Management - An ERF position paper for maintaining and improving a sustainable and efficient road network*, 2014.

- FHWA, *Long-Term Pavement Performance Program Manual for Falling Weight Deflectometer Measurements*, Publication No. FHWA-HRT-06-132, December 2006.

- FHWA, *MAP-21, the Moving Ahead for Progress in the 21st Century Act in USA*, source: http://www.fhwa.dot.gov/asset/plans.cfm, 2009.

- Horizon 2020, Work Programme 2014-2015, *Smart, green and integrated transport.*

- Horizon 2020, Work Programme 2016-2017, *Smart, green and integrated transport.*

- Horizon 2020, Work Programme 2018-2020, *Smart, green and integrated transport.*

- IDS Ingegneria dei sistemi, *K2 Fast Wave v. 02.00 – User manual,* Pisa, 2013.
- Isola M., Betti G., Marradi A., Tebaldi G., *Evaluation of cement treated mixtures with high percentage of reclaimed asphalt pavement*, Construction and Building Materials 48 (2013) 238–247, 2013.
- Jol H. M., *Ground Penetrating Radar Theory and Applications*, 1st Edition, eBook ISBN 9780080951843, Hardcover ISBN 9780444533487, Elsevier Science, December 2008.
- Kopac, P. A. *Performance-Related Quality Assurance Specifications*. Presented at the ASCE Convention, Dallas, Tex., Oct. 1993.
- Local Government Victoria, *Local Government Asset Management Better Practice Guide*, http://www.delwp.vic.gov.au, 2015.
- Louis, Cartz, *Nondestructive Testing,* A S M International, ISBN 978-0-87170-517-4, 1995.
- NCHRP, Report *626: NDT Technology for Quality Assurance of HMA Pavement Construction,* Research sponsored by the American Association of State Highway and Transportation Officials in cooperation with the Federal Highway Administration, Transportation Research Board, Washington D.C., 2009.
- NCHRP Report 704, *A Performance-Related Specification for Hot-Mixed Asphalt*, TRB, Washington D.C., 2011.
- Pajewski L., Benedetto A., Loizos A., Slob E., Tosti F., *Civil Engineering Applications of Ground Penetrating Radar: Research Perspectives in COST Action TU1208*, Geophysical Research Abstracts Vol. 15, EGU2013-13941, 2013.
- PIARC, *Asset Management Practice*, Technical Committee C4.1 Management of road infrastructure assets, Paris, 2008.
- Saaranketo T., *Electrical properties of road materials and subgrade soils and the use of ground penetrating radar in traffic infrastructure surveys* (PhD Thesis). University of Oulu, 2006.
- Sanfilippo M., *Caratterizzazione in sito di ceneri vulcaniche stabilizzate a cemento per sottofondi stradale,* Tesi di Laurea in Ingegneria Civile e Ambientale - Università di Catania, Relatore: Prof. Ing. Salvatore Cafiso, Correlatori: Dott.ssa Ing. Brunella Capace, Dott. Ing. Carmelo D'Agostino, Dott. Ing. Emanuele Delfino, A.A. 2016/2017.
- Tranchina G., *Riutilizzo di ceneri vulcaniche in ambito geotecnico-stradale mediante stabilizzazione a cemento*, Tesi di Laurea in Ingegneria Civile e Ambientale - Università di Catania, *Relatori:* Prof. Ing. Ernesto Motta, Prof. Ing. Salvatore Cafiso, *Correlatori:* Dott. Ing. Piera Paola Capilleri, Dott. Ing. Grazia La Cava, A.A. 2015/2016.
- Transportation Research Circular E-C074, *Glossary of Highway Quality Assurance Terms*, Transportation Research Board, Washington D.C., May 2005.
- Ullidtz P. *Modelling flexible pavement response and performance*, Copenhagen: Polyteknisk Forlag; 1998.

- Uzarski, D.R., Brown, D.G., Harris, R.W. & Plotkin, D.E., *Maintenance Management of U.S. Army Railroad Networks-the RAILER System: Detailed Track Inspection Manual*. Champaign, IL: US Army Corps of Engineers; Construction Engineering Research Laboratories, 1993.

- Van Dam Thomas J., Harvey John T., Muench Stephen T., Smith Kurt D., Snyder Mark B., Al-Qadi Imad L., Ozer Hasan, Meijer Joep, V. Ram Prashant, R. Roesier Jeffery, Kendall Alissa, *Towards Sustainable Pavement Systems: A Reference Document*, FHWA-HIF-15-002, January 2015.

- Varrica R., *Caratterizzazione di laboratorio per la stabilizzazione a cemento delle ceneri vulcaniche dell'Etna,* Tesi di Laurea in Ingegneria Civile e Ambientale - Università di Catania, Relatore: Prof. Ing. Salvatore Damiano Cafiso, Correlatori: Dott. Ing. Emanuele Delfino, Dott. Ing. Piera Paola Capilleri, A.A. 2015/2016.

- Warsame A., *Framework for Quality Improvement of Infrastructure Projects*, Journal of Civil Engineering and Architecture, ISSN 1934-7359, Volume 7, No. 12 (Serial No. 73), pp. 1529-1539, USA, Dec. 2013.

- Willenbrock, J. H., *Statistical Quality Control of Highway Construction*, Volume 2. FHWA, Jan. 1976.

- World Commission on Environment and Development, *Our Common Future*, ISBN 019282080X, Oxford University press, 1987.

CHAPTER 2

IN FIELD EXPERIMENTAL TESTS WITH NDT

In this chapter the experimental tests that have been conducted with the "TI Lab" equipment of the University of Catania will be illustrated and detailed.
The following paragraphs 2.1, 2.2 and 2.3 deal essentially with three experiments investigating with NDT techniques: rail maintenance, the stiffness of the subgrades, and the possibility of re-using Etna's volcanic ash for road subbases or subgrades with a sustainable approach and the acceptance possibility of a material that would not be applied in traditional specifications.
Moreover, the first two studies, in 2.1 and 2.2, that will be exhibited, on railway and pavement subgrade stiffness, have already been the subject of several scientific publications during the PhD period[21].
In 2.1 the experimental tests that have been done on a railway in Sicily are shown through FWD, LWD, LCMS and GPR, in order to be able to evaluate the application of these NDT techniques and to carry out quality checks and maintenance of the infrastructure.
In paragraph 2.2, also subject to a scientific publication indexed on Scopus, there is a comparison of in situ device (FWD, LWD and DCP test) for the assessment of pavement subgrade stiffness.
Paragraph 2.3 deals with an innovative experiment, thanks to which it has been possible to demonstrate that cement-stabilized ashes from the Etna volcano can be reused for the realization of subgrades and subbase layers. This is an example of material that, normally discarded in traditional specifications, can instead be used, and find application in the road sector, if stabilized to concrete as it has improved its performance.
For each case study are exposed the models used, the detailed presentation of the problem under study, the framing of the analysis in the framework of international scientific research, the developments, the results and their critical analysis.

2.1 Application of NDT and maintenance strategies on railway track

One of the major problems that railroads have faced since the earliest days is the prevention of service failures in track. There is an increasing importance in obtaining a consistent relative measure of trackbed stiffness in the physical and time restrictions applicable on live track for assessing potential maintenance requirement and subsequent design of remedial measures.

[21] Scientific publications:

- Cafiso S., Capace B., D'Agostino C., Delfino E., Di Graziano A., *Introduction of new systems for evaluation of ballast bearing capacity*, *BCRRA 2017* Tenth International Conference on the Bearing Capacity of Roads, Railways and Airfields, Athens, June 28/30, 2017.
- Cafiso, S., Capace, B., D'Agostino, C., Delfino, M., Di Graziano A., *Monitoring of railway track with light high efficiency systems*. International congress on transport infrastructure and systems 10th – 12th April 2017 Rome (Italy), 2017.
- Cafiso, S., Capace, B., D'Agostino, C., Delfino, M., Di Graziano A., *Application of NDT to railway track inspection*. International Conference on Traffic and Transport Engineering, 24th – 25th November 2016, Belgrade (Serbia), 2016.
- Cafiso, S., D'Agostino, C., Capace, B., Motta, E., Capilleri, P., *Comparison of in situ devices for the assessment of pavement subgrade stiffness*. 1st IMEKO TC4 International Workshop on Metrology for Geotechnics Benevento, Italy, March 17-18, 2016.

The stiffness assessment of the trackbed should include an assessment of ballast, sub-ballast and formation (e.g. sub-ballast depth, groundwater profile). The performance of railway track is highly dependent upon the magnitude and variation of differential track geometry.
Furthermore, a lack of a systematic monitoring brings to the impossibility to produce an effective long term track management system, by allocating budget where emergencies come. Latest technology can improve the rail inspection with higher cost of the equipment. The great advantage is related to the speed and precision of the measurement, avoiding to interfere with the normal use of the infrastructure. Moreover, in the case of local railway track with narrow gauge, the use of the traditional high speed track monitoring systems is not feasible.
In this framework the monitoring of the track with alternative non-destructive techniques (NDT) are promising for ballast and track stiffness inspections in the early stage of investigations. This research study details a site investigation comprising trial Ground Penetrating Radar (GPR), Light Weight Deflectometer (LWD), Falling Weight Deflectometer (FWD) and Laser Measurement System (LCMS) testing. In recent decades, these devices have already proven their effectiveness in the field of road pavement engineering and prospects are the same in the rail sector which is increasingly growing. Literature review and trial site testing are used to identify Strengths, Weaknesses, Opportunities, and Threats (SWOT analysis) of the application of the high speed systems (GPR, LWD, FWD and LCMS) of the DICAR in Catania for the assessment of trackbed stiffness and superstructure conditions (geometry) presenting also an infield experience and tracking the direction of future work. The use of NDTs in railways is expected to affectively contribute to a creation of a reliable monitoring system for preventive **maintenance strategies of railway asset** and **Quality Control of track works**, as well.

Railway lines are investments with very long life. Typical lifetimes for rails are 30 – 60 years and turnouts 20 – 30 years (Sundquist H., Byggande, 2000). Today many tracks are over 100 years old. However, to ensure this long life a large amount of maintenance is necessary.
There are several reasons for maintenance:

- *Safety:* the probability for accidents needs to be low on railways;
- *Comfort:* it is important, both for passengers and freight as well as for the environment in terms of noise and vibration;
- *Serviceability*: with lots of failures and speed restrictions the serviceability of the track will be low;
- *Economy*: a track with low quality is cost driving, since the deterioration of both track and trains will be higher. Optimization and Life Cycle Cost (LCC) planning is needed.

Nowadays more trains occupy the track and the competition with other means of transportation becomes harder. There is a clear trend towards higher speeds and higher capacity (more trains on the tracks and heavier trains).
To face the new circumstances, more effort has to be put on track maintenance to ensure the issues of safety, comfort, serviceability and economy.
Theoretically, the number one solution for optimal maintenance is to do the right measure at the right time to fulfil the requirements of safety, comfort and serviceability in terms of Life Cycle Cost. This task is practically difficult, since it requires complete knowledge about the current condition of the track and what effect different kinds of maintenance, or no maintenance, will have

on the track. Instead, the goal of condition based maintenance is to come as close to this optimum as possible.

This could be done with the help of measurements of important parameters which are analyzed to give knowledge about the condition of the track. But clearly, again this kind of approach require a control of the network, or of those parameters able to represent the real condition of the track and substructure.

2.1.1 Control test in railway

Track failures is one of the main problems that railroads have faced since the earliest days is the prevention of service.
To keep railroads safe and prevent any high maintenance costs caused by failures on the railroads, scheduled inspections must be performed on rail tracks, soil, and bridges. There are several types of track inspections such as soil inspection, railroad bridge inspection, and railroad inspection, and each track inspection type has their subcategories shown in Figure 28.

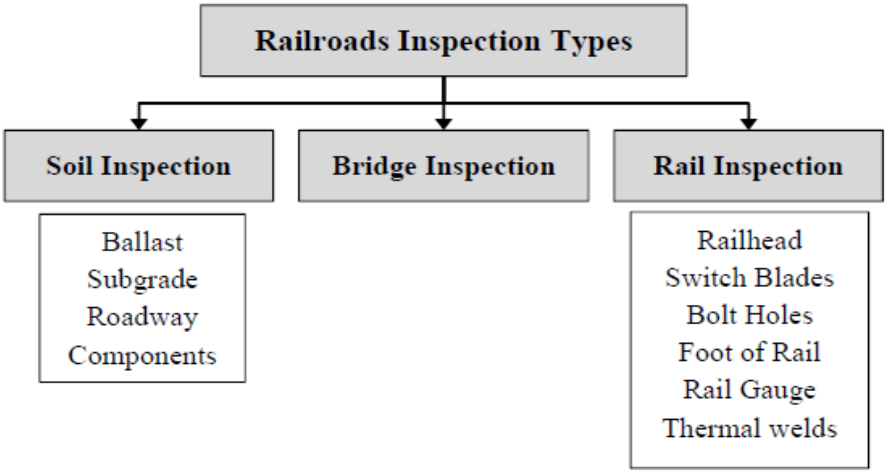

Figure 28 - Types of track inspections in a railroad

Soil inspection investigates the Ballast, Subgrade, and Roadway (BSR) component, which includes all earthen materials on the track structure, tracks, and embankments (Uzarski et al., 1993).
It focuses on the thickness of the ballast, subsoil material and geotechnical properties of subgrade. In addition, the inspection is executed mainly by digging trenches at evenly spaced intervals and in locations of special interest (Hugenschmid, 2000).
Soil inspection also investigates the plants on the railroads. For instance, Eriksen et al. (2004) tried to improve the reliability of soil inspection by adding the investigation of plant growth in the inspection process. Rail inspection investigates the rail heads, switch blades, bolt holes, foot of the rail, rail gauge, thermite welds, etc. (NDT H., 2014). Latest technology can improve the rail inspection with higher cost of the equipment (Cerniglia et al., 2006).
This technology is mainly developed directly from the railway Agency to monitor their network. The great advantage is related to the speed and precision of the measurement, avoiding to interfere with the normal use of the infrastructure. Generally local railways have not the most advanced equipment to survey the network as well as the economic possibility for a systematic global survey. The result is that the maintenance is carried out to avoid track failures with visual and manual inspection of the track based on the experience of the technicians (Cafiso et al. 2016a, 2017a, b).

Local railway tracks, usually with narrow gauge cannot afford the expenses to buy high efficiency monitoring systems. Unfortunately, the lack of a systematic control and the economic difficulties, especially in local railway track, lead to the impossibility of producing a long-term effective track management system. Specifically, in presence of local tracks with narrow gauge, the use of traditional monitoring systems track at high speed is not feasible. In this framework the preventive monitoring of the track with alternative non-destructive techniques (NDT), such as GPR, LWD and FWD are promising for soil and rail inspection and to plan a preventive maintenance from the early stage of investigations. In recent decades, these devices have already proven their effectiveness in the field of road pavement engineering and prospects are the same in the rail sector which is increasingly growing.

2.1.2 SWOT Analysis

Because of the interest in the introduction of new NDT for the investigation of railway track, a SWOT analysis will be performed basing on the literature review and trial tests of GPR, LWD and LCMS. Originated by Albert S. Humphrey in the 1960s, SWOT analysis is a basic, straightforward model that assesses what an organization can and cannot do as well as its potential opportunities and threats. It is an extremely useful tool for understanding and decision-making for all sorts of situations and disciplines in project planning, management and business for investigating problems from a strategic perspective.

SWOT, in Figure 29, is an acronym for Strengths, Weaknesses, Opportunities and Threats that, specifically, takes information from an environmental analysis and separates it into internal strengths and weaknesses, as well as its external opportunities and threats.

SWOT Analyses are often arranged as a 2 by 2 matrices with the lists of strength and weaknesses in the first two boxes in the first row and the lists of opportunities and threats in the second row. By arranging the analysis this fashion, the lists are separated into internal factors that can affect a project on the first row and external factors on the second row. In addition, the first column consists of the positive factors (strengths and opportunities) and the second column consists of negative actors (weaknesses and threats.). This method provides a simple framework to keep lists organized and conceptualize how the lists are related. SWOT analysis is presented in the present research work, for the application of GPR, LWD and LCMS to survey a railway track. The analysis was conducted for each single equipment after a trial on a real railway environment and post processing of the results.

Figure 29 - SWOT Analysis, general schema

SWOT analysis resulted particularly interesting to evaluate the feasibility of application of those equipment in a different context than their usual test environment. Subsequently, in the case study, the SWOT analysis conducted for the individual equipment will be exposed.

2.1.3 Equipment on railway track

GPR on railway track: The ground penetrating radar is a geophysical radar system with two antennas and receivers used to perform non-destructive investigations of underground characteristics with high resolution and in depth (up to 3.2 m from the surface).
Main application of GPR in railway track are:

- monitoring the condition of railway ballast, and detect zones of clay fouling leading to track instability;
- mapping soil, rock or fill layers in geological and geotechnical investigations, or for foundation design.

The track substructure, consisting of the ballast, sub ballast, and subgrade layers, has a profound influence on track performance.
The substructure performance is significantly affected by moisture accumulation and thickness of the roadbed layers (Selig & Waters, 1994).
Accurate knowledge of the substructure condition is important in effectively assessing the potential for service interruptions and the need for slow orders. A significant part of a railroad's track maintenance budget is allocated to correct rough track that is caused by movements in the substructure under repeated train loading. In this field, the GPR method seems to be a good alternative to traditional core inspection techniques. Methods of applying GPR to railways are being developed to provide a continuous evaluation of the track substructure conditions relative to subsurface layering, material type, moisture content and density.
GPR application to railways, during construction and monitoring phase, is relatively recent. In Germany, Göbel et al. (1994) referred by Saarenketo performed GPR tests for determining: ballast thickness, layers interfaces, ballast pockets and mudholes location. Jack and Jackson (1999) studied ballast layer along a track using two antennas with different frequencies, they found: clearer ballast interfaces indicating a clean ballast and thickness variations, affirmed GPR as a useful tool for identifying track sections with urgent necessity of rehabilitation.
Gallagher et al. (1999) researches found positive results for survey of ballast/subgrade interface, such as anomalies detection. Hugenschmidt (2000) reports a study developed on different alignments, evaluating the ballast thickness, fouled zones and ballast/subgrade interface depth. Their conclusion was that radar survey is useful combined with traditional inspection methods. Recently, to determine the correlation between water content or fouling of a railroad track and GPR signals, a full-scale railway track model was designed and constructed at the University of Massachusetts Amherst (Hamed et al. 2016). Different models were tested with moisture content conditions of dry, saturated and two points between these extremes. 450 MHz and 2 GHz frequency antennas were used to evaluate the different conditions. The results shown that the dielectric permittivity and frequency spectrum can be used as an indicator of fouling percentage and moisture content in a track. In addition, a linear correlation is observed between the fouling percentage and moisture content under saturation conditions.

LWD and FWD on railway track: With regard to the railway track investigations concerning load bearing capacity, LWD and FWD were used.
The LWD, used for the trial test, had one geophone positioned in the center of the plate and 2 additional geophones that can be used for specific measures outside the plate. With the same theoretical principles but with higher loads, the Falling Weight Deflectometer (FWD) used in the present study, specific for railway track is equipped with a loading plate of 300 mm diameter and a geophone under the plate, a load of 250 kg and 4 different heights able to produce a stress of 300-1200 kPa.
Neupane et al. (2016) from the university of Kansas estimated with LWD the resilient modulus of the substructure considering different combination of fouled ballast (10-40% by weight) and moisture content (1-10%). The test was conducted by reproducing in laboratory the real condition. Considering the various combination, they concluded that moisture content has the highest influence in reducing the bearing capacity.
Hornícek et al (2014) used the LWD for the long-term evaluation of the condition of trial sections with the application of under-ballast geocomposites useful to avoid long-term problems of the track geometric position caused by the pushing of fine-grained soil from the subballast into the ballast bed (so-called pumping effect) and by the missing base layer between the ballast and the subgrade.
The exploitation potential of the Lightweight Falling Deflectometer is still increasing, and the results are aptly combined with other analytical and mathematical methods (Fernandes, et al., 2012; Burrow et al, 2007). In some cases, the impact device is used for a specific assessment of spots with problems resulting from the unstable geometric track position (Sharpe & Govan, 2014).

LCMS on railway track: The LCMS system employs high speed cameras, custom optics, and laser line projectors to acquire 2D images and high resolution transversal profiles of road surfaces 4 meters wide. LCMS was originally for automatic detection of cracks, rut depth, macrotexture and other road pavement distress. The LCMS can be operated at speeds of up to 100km/h.
The only experimental trials of LCMS on railway tracks were carried out by Pavemetrics ®. The surveys were conducted by using a multifunction vehicle adapted for running on a railway track with standard gauge in Figure 30.

Figure 30 - Multifunctional vehicles used by Pavemetrics to test the LCMS performance on surveying railway tracks

That configuration minimizes the needs for sensors placement representing the optimum in terms of sensor distances from the ground DMI synchronization. There are not yet other experiences reported in literature. Most probably it is related to two key factors: (i) the technology of LCMS was developed only in the last decade and (ii) the high cost of equipment does not allow a widespread diffusion in a such short time.

2.1.4 Field Trials

The trial site chosen for the trial run of the equipment is part of the Circumetnea railway track, that manage about 120 km of local railway track in Sicily, by circumnavigating Etna volcano. The track is characterized by narrow gauge (950 mm instead the 1435 mm of the European standard) and a different composition of the superstructure which is going to be modernized with new concrete sleepers, new fasting system and the tamping of ballast. The area selected for testing is close to the Adrano Nord railway station. It has the different conditions of tamped and not tamped ballast, wooden and concrete sleepers and cribs full with ballast or a complete lack of ballast in cribs.
The test was conducted on about 290 m of railway line.
Specifically, the trial was conducted on three different sites:

- ***Site A:*** ballast with partial renovation and tamping;
- ***Site B:*** ballast in bad conditions;
- ***Site C:*** ballast recently replaced.

Thanks to this variety it was possible to test different railway track composition to test the ability of the equipment to catch the possible differences in: ballast layer thicknesses and their changes along the line (based on the presence of tamped ballast or old ballast), difference material for the sleepers, lack of presence of ballast in the cribs, different stiffness of the substructure based on the sleepers and ballast conditions. In the present experimental research work, an operative description of the equipment for the railway tests is presented. Preliminary results are used to draw potential field of application to provide a framework about the use of the equipment for railway track monitoring.

<u>*GPR in field trials:*</u> The wheel system of the GPR of the "TI Lab" (University of Catania) used in the trial, in Figure 31, was adapted for the test by modifying the wheels and the DMI configuration from road to railway application. Wheels are built with cone shape and made with resin for running on the railway track and avoiding electrical interferences. The chassis was adapted to the ground technology positioning the antennas very close to the surface of ballast (e.g. less than 10 cm). In this configuration it was easy pushing the cart at a walking speed, but the system should be able to work at a speed up to 30 km/h.

Figure 31- Ground Penetrating Radar adapted for rail inspection

Figure 32 reports the image of the radargram and the identification of the ballast layers.
To obtain this image the filters applied to radar map are:

- Identification of "zero point", i.e.the transition air/ground. This operation is mainly used when scans are performed with antennas not in contact with the surface;

- Background removal: This command applies the Clear-X filtering algorithm used to remove continuous components along the X axis (horizontal direction) following user preset parameters, Depth min [m]=0 and Depth max [m]=10;
- Bandpass filter: this command applies a filter onto a frequency interval;
- Linear gain: is used to apply a filtering algorithm of the power equalization along a sweep to a selected radar map on the basis of an estimated linear attenuation.

In the radargrams are reported the layer of the three sites investigated (A, B and C) that show respectively:

- Site A: from the top composed by the presence of renewed ballast, fouled ballast and subgrade;
- Site B: composed by a thin layer of ballast in bad conditions and subgrade;
- Site C: composed by ballast recently replaced with a deeper layer than the other sites.

The results comply with data from literature by identifying mixed and spent ballast conditions as follow. In the radargram in Figure 32 of the three sites, the transition between the different layers is marked by a clear signal indicative of differences in dielectric constant in the renewed and fouled ballast/subgrade interface of site A, in the bad ballast/subgrade interface of site B and the replaced ballast/subgrade interface of the site C.

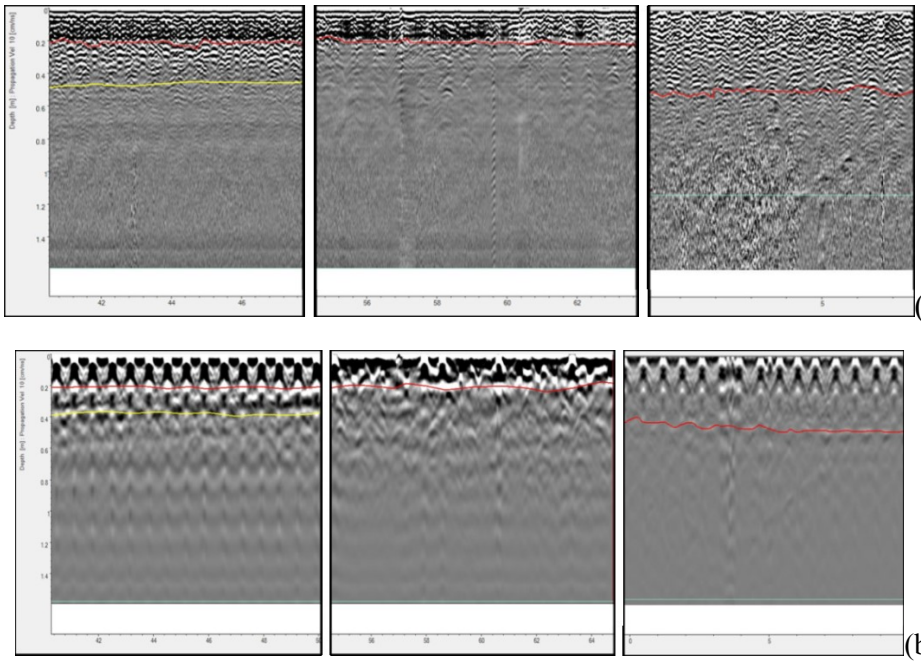
(a)

(b)

Figure 32 - Radar scans of the trial test with 2 GHz (a) and 600 MHz (b) for site A, B, C

The presence of layers' interfaces at different depths was detected by 600 and 2000 MHz antennas, as well. As expected 2000 MHz is more effective in identifying layer's interface at shallower depths that in this ballast application resulted limited at about 40 cm.
To identify deeper interfaces (e.g. ballast fouling), sub-ballast and subgrade moisture conditions the 600 MHz antenna resulted effective up to a depth of 1.5 m. Also it's clear the signal different between the wooden (site B) and concrete sleepers (sites A and C). The wooden sleepers give a greater dispersion of the signal.

Considering the tests performed the results obtained with the two antennas of the GPR at different frequencies, a SWOT analysis in Table 11 was elaborated, which provides strengths, weaknesses, opportunities and threats in the possible use of this equipment for railway maintenance.

Table 11 - SWOT Analysis for GPR System

STRENGHT *(internal, positive factor)*	**WEAKNESSES** *(internal, negative factor)*
▪ Reliable and established technology ▪ NDT testing ▪ Speed of execution ▪ Reduced number of operators ▪ More issues investigated ▪ Potential data on the whole structure	▪ Radar analysis subject to interpretation of the operator ▪ Still provisional models ▪ Need of technologically and advanced equipment ▪ Need of calibration tests for data deduction ▪ Interference of magnetic materials
OPPORTUNITIES *(external, positive factor)*	**THREATS** *(external, negative factor)*
▪ Development of new models for extrapolation of results. ▪ Approach to a field of engineering technique that is not " saturated " ▪ Possibility of agreements with public authorities or private companies that need of an advanced know-how for the development of its own procedures	▪ Results distorted by unexpected and/or unforeseen conditions ▪ Difficulties in the interpretation of the data obtained ▪ Ignorance and mistrust of the Public Administrations in the use of these devices for NDT on railways

LWD and FWD in field trials: LWD (Figure 33) and FWD (Figure 34) were used to estimate the stiffness of track foundation and sleeper support, as well.
The use of FWD, considering that railways are generally subjected to the heavy loads produced by the trains, was carried out to take into account the reduced load induced by LWD.
Specifically, tests were carried out positioning the loading plate in the middle of the sleeper (FWD and LWD) and directly on the ballast between sleepers and at the side of rail (LWD).

Figure 33 - LWD test with plate in crib position and with plate on the sleeper with additional geophones

Figure 34 - FWD test position

Results of drops on the sleeper with LWD, reported in Figure 35, show a clear variability in the measured deflections among the sites with different ballast conditions. Site with ballast of good quality (site C) reports lower deflections and higher uniformity.

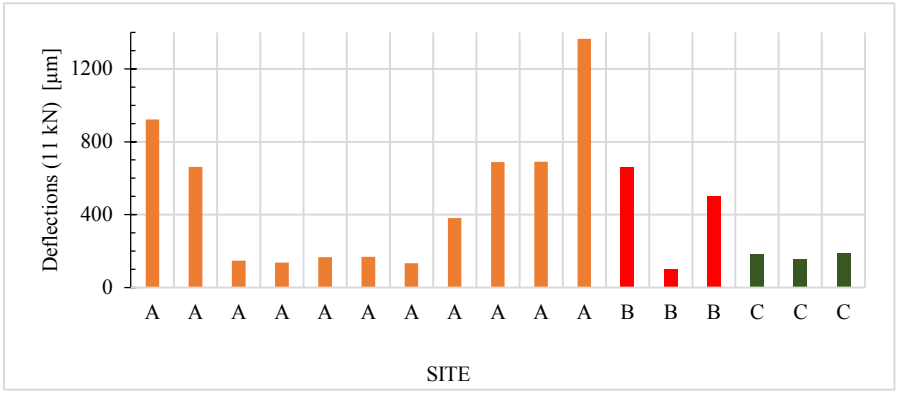

Figure 35 - Deflection from LWD at different site

Deflection and load data can be used to calculate the track modulus. The track modulus, u, is defined as the applied force per unit length of rail per unit deflection (δ) (unit Pa) (Selig et al., 1994): $u = q/\delta$; where q is the vertical foundation supporting force per unit length.

When the load is applied at the center of the sleeper, a simplified model of uniform vertical foundation supporting force per unit length can be assumed. This assumption is sustained by the uniform deflection of the sleeper detected during the test.

In the graph in Figure 36 are reported the deflections at the center of the loading plate Def1 (x axis) and the deflections Def2 and Def3 (y axis) that are measured at 20 and 30 cm of distance from the loading plate. The comparison between this different deflections, with a load of 11 kN, detect a negligible sleeper rotation that is of the 0.01% on average.

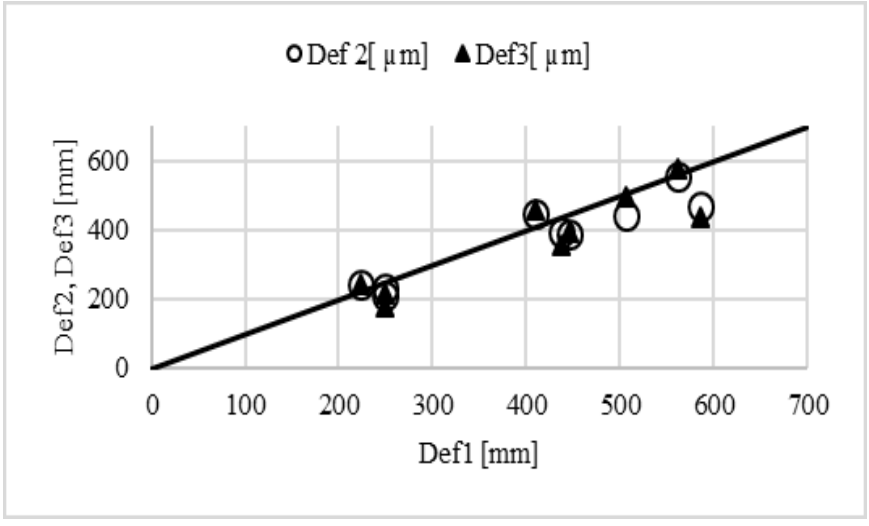

Figure 36 - Deflection at the center of the loading plate (Def1) vs. deflections at 20 (Def2) and 30 cm (Def3) (load 11 kN)

The use of FWD, as expected, produced higher deflections with a dual behavior as it is clear from Figure 37.

At lower load, at 11 kN with the LWD tests, deflection has a linear relationship with load with a certain module. At higher loads, with FWD tests in a range from about 30 to 90 kN, modules suddenly increase, by showing a sharing of the entire system (sleeper, track and fastclip) to the response at the impulsive load.

Although the present research work represents the first stage of the investigation, further applications of FWD need to assess the use of LWD in identification of lack of bearing capacity, as comparative analysis, given by the response of the sleeper at lower loads.

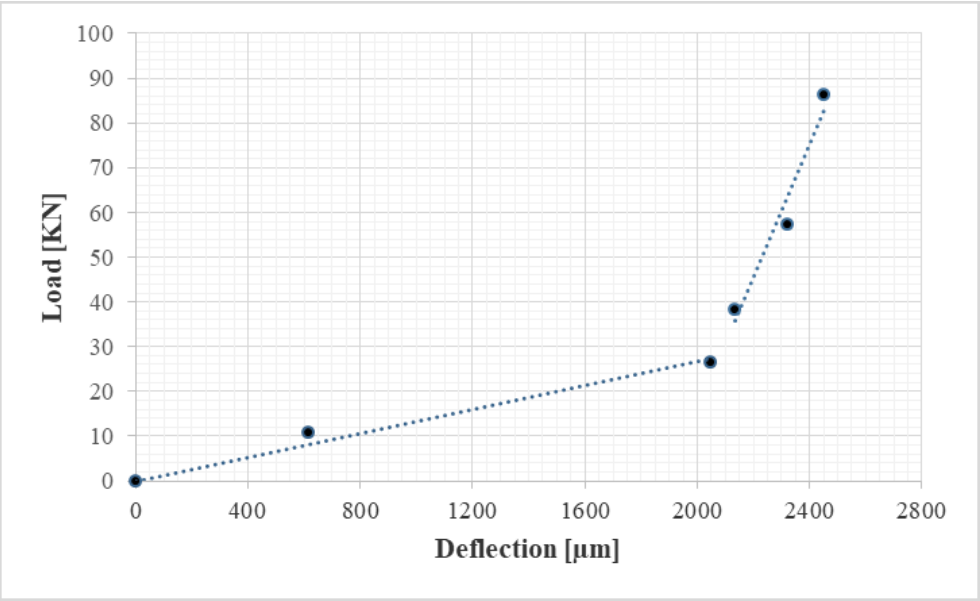

Figure 37 - Load-Deflection diagram of LWD (11 kN) and FWD test (30-90 kN) on a sleeper

The SWOT analysis for LWD and FWD is reported in Table 12. Also in this case, as already done for GPR, a careful analysis of this type allows us to understand how the use of FWD and LWD for railway monitoring is very advantageous: in fact, there are considerable strengths and opportunities given by the fact that high-efficiency surveys give high precision data in a non-destructive way and an approach that is certainly innovative. Weaknesses and threats are only related to ignorance in the knowledge of these devices and operators that clearly must be highly specialized.

Table 12 - SWOT Analysis for LWD and FWD system.

STRENGHT *(internal, positive factor)*	**WEAKNESSES** *(internal, negative factor)*
▪ Reliable technology ▪ NDT testing ▪ Reduced number of operators ▪ Possibility to investigate the various components of the infrastructure ▪ Application of mathematical and analytical models	▪ Techniques of analysis often subject to comparison ▪ Variability of the results ▪ Loads insufficient for the optimal evaluation of the ballast bearing capacity (only LWD) ▪ Need of calibration tests for the data acquisition ▪ Speed of execution (only FWD)
OPPORTUNITIES *(external, positive factor)*	**THREATS** *(external, negative factor)*
▪ Development of new models for the interpretation of the results ▪ Approach to a field of engineering technique that is not " saturated " ▪ Possibility of agreements with public authorities or private companies that need an advanced know-how for development of its own procedures	▪ Results distorted by unexpected and/or unforeseen conditions and on-board effects cannot be assessed ▪ Returning of untruthful data about the bearing capacity of the superstructure (only LWD) ▪ Ignorance and mistrust of the Public Administrations in the use of these devices for NDT on railways

LCMS in field trials: LCMS are actually installed on the Automatic Road Analyzer of the Department of Civil Engineering & Architecture of University of Catania.
The test was conducted putting ARAN on ad hoc prepared railway wagon in Figure 38.

This configuration is not the optimum can be achieved because of the increased distance of the laser from the track, but, at this stage of the research, that was the only configuration available to survey the reduced railway gauge which does not allow ARAN to travel with its own wheel on the railroad track. Another issue to be solved, was the coupling of LCMS with the DMI which control the frequency of acquisition.

Figure 38 - LCMS configuration and DMI installed on the rail wagon wheel

A medium resolution DMI (2048 pulse/round) was installed and connected with the acquisition unit in ARAN. Before the trial the system was re-calibrated for taking into account the new configuration (LCMS height and DMI resolution).
As mentioned above, basic LCMS output are images and cross section profiles. High resolution images can be used to replace a visual rail inspection (e.g. sleepers, fast, ballast). Cross section profile allows to detect gauge values and track geometry.
A sample output of is reported in Figure 39.

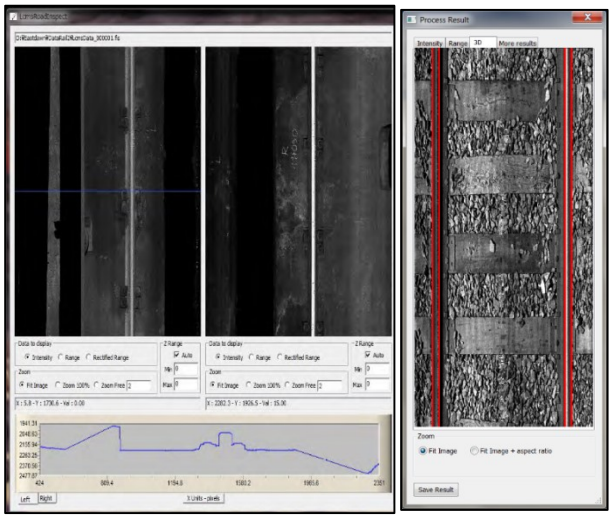

Figure 39 - Output from LCMS survey.

Due to the laser height and DMI resolution the resolution of output was of 3 mm in transversal profile with a longitudinal acquisition step of 5 mm.
Coupling the system with an Inertial Measurement Unit (IMU) it will be possible to correct the undesired wagon motion (roll, pitch, yaw) joining the successive section to obtain a complete 3D scan of the track.

This data can be combined (Figure 40) with the digital images with surprising results in terms of resolution and details.

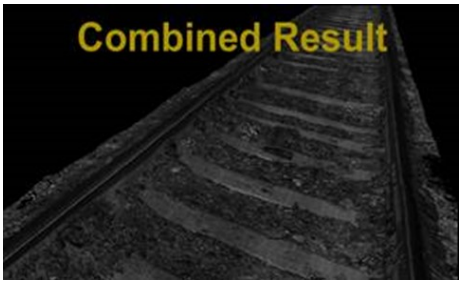

Figure 40 - 3D rendering of railroad track (courtesy of Pavemetrics)

Table 13 - SWOT Analysis for LCMS system.

STRENGHT *(internal, positive factor)*	**WEAKNESSES** *(internal, negative factor)*
▪ Established technology with increasing diffusion ▪ NDT testing ▪ High performance in surveys and post-analysis ▪ Reduced number of operators ▪ Chance to investigate more features of the infrastructure ▪ Data or information about the most important track issues ▪ Higher precision of data	▪ Technologically advanced equipment (expensive and complex) ▪ Require high operator training for survey and post elaboration ▪ difficulty adapting configurations used in road surveys to railway tracks ▪ Not suitable for adverse climatic conditions
OPPORTUNITIES *(external, positive factor)*	**THREATS** *(external, negative factor)*
▪ Development of new models for the extrapolation of indirect index from surveys data ▪ Approach to a field of engineering technique that is not "saturated" ▪ Possibility of agreements with public authorities or private companies that need of an advanced know-how for the development of its own procedures	▪ Ignorance and mistrust of the Public Administrations in the use of these devices for NDT on railways ▪ Partial lack of interest of railway companies to use new technologies

2.1.5 Conclusions and future skills

This work of research has explored new and promising solutions for rail track monitoring by using the equipment well known for road pavement monitoring, but not yet diffused in the railway management. Particularly this research study focused on the adaptation needed to use GPR, LWD and FWD on a railway track to test the bearing capacity and quality of ballast. The results are presented in terms of a SWOT analysis based literature review and on site trials.
More specifically, the field tests were carried out on a local railway with narrow gauge of 950 mm.
That condition gave the opportunity to test the system in an environment open to the introduction of such system, but posed also specific limitations for the use of the systems.
GPR and LWD are not new in such application and confirmed the suitability of the equipment for testing the quality of ballast. More specifically, LWD, despite of the limited load (6 kN in the trial test) applied directly on the sleeper, was able to detect defects in the bearing capacity at the Sleeper/Ballast interface. The limitation of loads can be overcome with the heavier FWD, which unfortunately, presents some physical limitation for the access in railway track. GPR was able to detect the presence of layers' interfaces at different depths. Fouling phenomena are the main causes of changing in the layer dielectric proprieties within the ballast thickness.

Results highlighted as each equipment should be able to detect only specific defects of the sleeper/ballast system. Therefore a combined use of all the equipment is needed for in depth monitoring of bearing capacity of rail track. This is because having information on both the geometry and the fouling phenomena, combining them with the load-bearing capacity, make it possible to identify the structural deficits of the railway in a very precise manner, thus also identifying the places where maintenance is required, which consequently, on the whole, it can be programmed over time, even with considerable economic savings, because in this way it is possible to prevent it.
Further research with FWD on railway can validate the use of LWD in identification of lack of bearing capacity of the sleepers or system in general. That is the case if the behavior in the response of railway track, even changing modulus does not change in a comparative analysis of more sleepers.

2.2 Comparison of in situ devices for the assessment of pavement subgrade stiffness

The subgrade is the top surface of a roadbed upon which the pavement structure is constructed. The purpose is to provide a platform for construction of the pavement and to support the pavement without unwanted deflection that would reduce its performance. For those reasons subgrade bearing capacity have to be investigated during the construction process as a quality control, based on the design results. The dynamic in situ Falling Weight Deflectometer (FWD) tests are nowadays considered the most reliable approach to determine bearing capacity of road pavements and elastic moduli. In addition, the use of the Light Weight Deflectometer (LWD) takes the advantage of the dynamic application of load, and the flexibility of the handling of the equipment on construction area and unbound layer. In this research study, a wide literature review is presented on the topic of correlation between different subgrade bearing capacity in situ tests. In order to assess the transferability of LWD measures, these results were compared with FWD test and Dynamic Cone Penetrometer (DCP) test. Soil samples, taken from the site, have also been investigated in laboratory to relate geotechnical and in situ test results.

2.2.1 Introduction to subgrade bearing capacity and tests

In recent years, mechanistic-empirical design procedures have attracted the attention of both pavement engineers and researchers. These design procedures require knowledge of the mechanical properties of the materials that make up the pavement structure. In this framework, the resilient modulus (M_r) has become the basic parameter to characterize unbound pavement materials because a large amount of evidence has shown that the elastic (resilient) pavement deflection provides a better correlation to field performance than the total pavement deflection (George, 2003). Resilient modulus is defined as the ratio of deviator stress, σ_d, to the recoverable strain, ε_r: $M_r = \sigma_d/\varepsilon_r$.
Meanwhile, the complexity of the laboratory test procedures has prompted highway agencies to explore other test methods, especially in-situ field tests. Deflection measurements with the Falling Weight Deflectometer (FWD) and Light Weight Deflectometer (LWD) and penetration test with Dynamic Cone Penetrometer (DCP) have been routinely employed in evaluating pavement layers, and the underlying subgrade. On the other hand, considering the differences between on situ test and laboratory tests, the modulus of a multilayer system, calculated from surface deflections employing a backcalculation routine, is referred to as "backcalculated modulus," E_{back}, in contrast to

"resilient modulus," Mr, which results from a laboratory test. When using forward calculation, employing surface deflections and Boussinesq equations, the modulus resulting is designated "elastic modulus," E.

In the Minnesota Research Road Project (Mn/ROAD), Van Deusen et al. (1994) reported difficulties in analyzing FWD measurements performed directly on subgrade surfaces. Their results showed a weak correlation between laboratory and backcalculated (E_{back}) moduli. On the contrary, an investigation, conducted by George (2003), showed that E_{back} moduli obtained from testing directly on the subgrade are in satisfactory agreement with the laboratory values with certain restrictions. In this framework, Nazzal et al (2016) conducted a linear regression analysis on collected field test data to relate the elastic modulus calculated by using the Light Weight Deflectometer (ELWD) and the FWD back-calculated modulus (MFWD), by obtaining the following regression model: MFWD = 0.964 ELWD with $R^2 = 0.94$. This result suggests that the LWD and FWD yield close modulus values. This model is similar to the one proposed by Fleming et al. (2000) based on the results of several field tests conducted on different subgrade soils, which is: MFWD= 1.031 ELWD.

As the Dynamic Cone Penetration (DCP) test is concerned, a number of correlations have been developed between the penetration index (DPI) and the Elastic modulus of subgrade.

Chen et al. (2005) found a strong correlation between 30 DCP test results and E_{back} elastic modulus from FWD in mostly clayey and silty soils in Kansas. The DCP results were corrected to take into account the effect of overburden pressure in case of conducting the test through a drilled hole in the asphalt layer with the equation: Es= 537.8*(DPI)-0.664.

Siekmeier et al. (2009) proposed the minimum required DCPi values to be used for construction quality assurance based on tests conducted on granular and fine-grained soil samples for different range of moisture contents and densities and for those found the relationship with E that is: $E_{DPI}=10^{3.04758-1.06166\log(DPI)}$.

In this framework, the focus of the present research work is to investigate the viability of in situ tests performed with FWD, LWD and DCP for deriving the Elastic modulus of pavements' subgrade. To this aim via the correlation between FWD, LWD modulus and DCP index was tested and validated. The interpretation of in situ tests were supported by laboratory tests.

The tests were carried out at the University of Catania Campus.

The site, with a surface of 2.5 x 2.5 m and subdivided in 9 sampling points (Figure 41), is characterized by alluvial deposits of different depositional environments, consisting in an alternating sequence of silty-clayey layers of alluvial plain and volcanic rock at the basement.

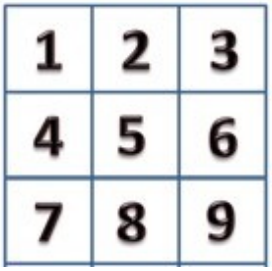

Figure 41 - Test point codes

Several conventional laboratory tests were performed, that in order are: grain size distribution, index properties, shear strength and resilient modulus.

The results of all the tests are in the following part. The gradation characteristics of each sample were investigated by performing sieve analysis, according to ASTM method[22]. The following Figure 42 shows the grain size distribution curves for some of the samples tested: from 1 to 5.

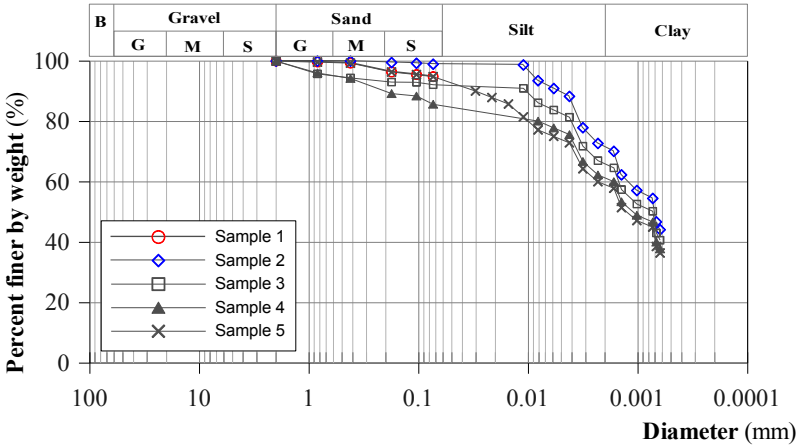

Figure 42 - Grain size distribution curves of sample tested

The values of the natural moisture content wn range from between 18.46 and 24.04%. Characteristic values for the Atterberg limits[23] are: wL = 58.07 – 61.91 % and wP = 30 - 40 %, with a plasticity index of PI = 23 - 30 %, with the specific gravity Gs[24] that varying from 2.71 to 2.74.
The laboratory results on the samples tested indicate a reasonable degree of homogeneity of the deposit.

To define subgrade soil stiffness dynamic loading plate test were performed.
These include Falling Weight Deflectometer (FWD), Light Weight Deflectometer (LWD) and the equations developed by Boussinesq allow to calculate the stress, strain and displacement conditions in a homogeneous, isotropic, linear elastic semi-infinite space under a circular loading area, and to evaluate the modulus of a semi-infinite space.
Subgrades are typically non-linear elastic, for which a use the use of a linear elastic approach may result in incorrect layer moduli. In fact, a typical outcome is that the modulus of the subgrade is overestimated. Mallela & George (1994) showed that when measured stresses and strains were compared to theoretical values it was found that a static analysis, assuming a non-linear subgrade, gave the best agreement. Subgrade non-linearity was investigated by Ullidtz (1998) by using a formula that is function of σ_1 that is the major principle stress from the external loading, pa that is a reference stress, often taken equal to atmospheric pressure (0.1 MPa) and two constants C and n. Under this assumption, it was also found that the strains and displacements in the non-linear elastic half-space could be calculated using Boussinesq's equations for the center line, under a point load P, with the modulus substituted by a non-linear function of the major principal stress. As result, a plate loading test on the surface of a material with the modulus described by Boussinesq would give the surface modulus:

$$E_0 = (1-2n)\cdot C\cdot\left(\frac{\sigma_0}{p_a}\right)^n$$

[22] For the gradation characteristics (particle size analysis), sieve analysis was made according to ASTM D 422-63.
[23] The Atterberg limits were calculated according to ASTM D4318-84.
[24] The specific gravity was obtained according to ASTM D 854-F12 and A.G.I. 1994.

where σ_o is the uniformly distributed stress under the plate.
The nonlinear behavior of the subgrade was investigated by the way of a cyclic triaxial test in the laboratory of the University of Catania.
Since the pavement subgrades are subjected to a series of distinct load pulses, a laboratory test duplicating this condition is desirable. In the laboratory tests that were carried out, cylindrical specimens of soil were subjected to a series of cyclic loading with different deviatoric stress, simulating the multiple wheels moving over the pavement. A constant confining pressure applied on the specimens simulated the lateral stresses caused by the overburden pressure and the applied wheel load.
The recoverable axial deformation of the specimens due to the cyclic loading was used to calculate the resilient modulus of the material.
Axial deformation of the specimen was recorded by two externally mounted Linear Variable Differential Transducers (LVDT). Some plots of cyclic triaxial laboratory tests relating axial strain and deviatoric stress are shown in Figure 43 (a).

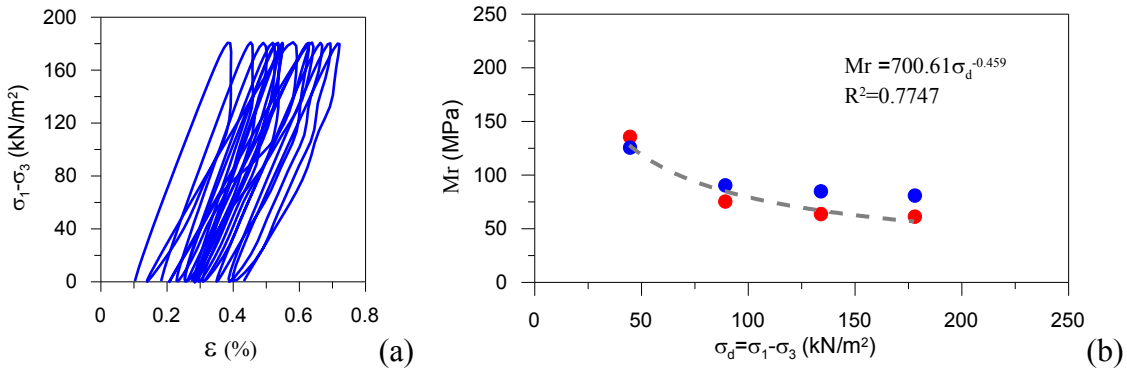

Figure 43 - Triaxial test results: stress-strain curves(a) and resilient modulus vs. deviator stress (b)

Figure 43(b) shows the variation of the resilient modulus with the applied deviator stress for two specimen analyzed (in red and blue)[25], ranging from 50 to 180 kPa. Each point represents a cycle of the cyclic triaxial test to which corresponds the deviatoric stress and from that the resilient module was calculated, as a ratio between the deviatoric stress σ_d and the deformation ε. A reduction in the resilient modulus is out lied by the regression curve.

2.2.2 Loading plate and DCP test

Both FWD and LWD test were performed in the present study.
The FWD used in the present study is the Dynatest 8000 equipped with a loading plate of 300 mm diameter and 15 geophones with a different offset from the loading plate (the farthest is located at 2100 mm on the beam), a load of 150 kg and heights able to produce a stress of 230-240 kPa.
Due to the dimension of the equipment only position 2, 5 and 8 were tested with FWD.
The LWD device used in the present work (Dynatest 3031) is equipped with 2 additional geophones that can be used for measurement of deflections outside the loading plate and an additional load cell positioned under the loading plate. The LWD tests were conducted with two configuration of plate diameter: 150 mm and 300mm with a weight of 15 Kg and respectively a height of 13" and 17". LWD data are mainly used to calculate Surface Modulus of the tested materials by means of

[25] The two specimen were taken from the site of the University of Catania Campus, sampling point n. 1 (Figure 41).

Boussinesq equation; more recently some particular procedures, specifically developed to estimate the material compaction level achieved on site, are also starting to be used (Marradi et al. 2014). LWD test was performed in each of the 9 positions.
Basing on the cyclic triaxial laboratory tests, a no-linearity for the subgrade was assumed for determining the elastic modulus E with loading plate in situ tests.
From the exponent of the regression equation reported in Figure 43, a value of n=-0.46 can be assumed as seed value, as coefficient of non-linearity in the calculation of the moduli. This non-linearity value was used as seed value for all tests, and the consequent calculations that were made, since a reasonable degree of homogeneity of the deposit was obtained from the laboratory tests on the tested samples.
Seed values are the start values in the iteration procedure that uses the results of load and deflection of FWD and LWD in situ test that are in Table 14.
It is therefore important to enter these values as realistic as possible. Analogously, the stress distribution factor f was assumed equal to $\pi/2$, according to the literature for stress distribution on cohesive soils.
With the Dynamic Cone Penetrometer (DCP) it was possible to calculate the DCP penetration index (PI).
The penetration index can be plotted versus depth to identify thicknesses and strengths of different pavement layers or can be correlated to other soil parameters such as the California Bearing Ratio CBR (Minnesota Department of Transportation) and the Modulus of subgrades. DCP test was performed in each of the 9 positions.

2.2.3 Results and conclusions of in situ tests

The results of in situ tests are reported in Table 14 for the test positions n. 2, 5 and 8 as regards to FWD and for the test positions from 1 to 9 for LWD and DCP.

Table 14 - FWD, LWD and DCP results

	FWD (300)				LWD (150)				LWD (300)				DCP
Position	Stress (kPa)	E (MPa)	C	n	Stress (kPa)	E (Mpa)	C	n	Stress (kPa)	E (MPa)	C	n	DPI (mm/blow)
1	-	-	-	-	397	26	55	-0.55	159	34	42	-0.43	-
2	238	26	30	-0.15	404	27	50	-0.45	151	27	30	-0.28	28.50
3	-	-	-	-	414	27	50	-0.43	159	20	23	-0.35	25.00
4	-	-	-	-	410	28	45	-0.34	158	21	25	-0.34	19.00
5	234	23	31	-0.36	406	24	44	-0.42	159	23	27	-0.33	13.00
6	-	-	-	-	390	22	42	-0.49	153	17	20	-0.4	-
7	-	-	-	-	412	31	65	-0.52	161	36	46	-0.5	3.45
8	239	24	28	-0.18	398	23	27	-0.33	158	22	42	-0.49	31.00
9	-	-	-	-	158	35	50	-0.26	159	26	32	-0.47	15.00

Looking at the results, there is good agreement between the moduli computed with FWD and LWD tests. This latter was used in a double configuration with plate diameters of 150 or 300 mm.

Figure 44 reports the correlation between FWD and LWD calculation of moduli.

Both the FWD and LWD moduli were computed by using a no-linear response of the subgrade.

Load, deflection at the center of the plate recorded for each of the test positions and E modulus with parameters C, n carried out by the back-calculation are reported in Table 14. As far as the DCP test is considered, Table 1 reports the results of the DCP tests on the same test position of the LWD tests.

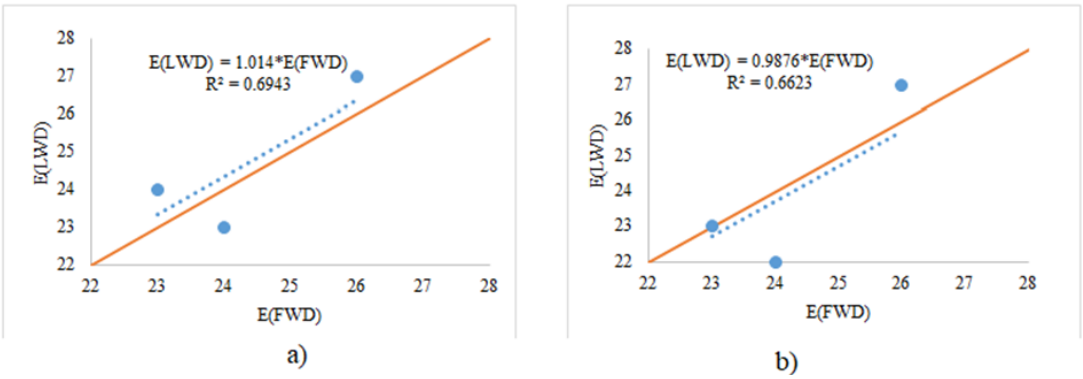

Figure 44 - Sugrade moduli: a) comparison of FWD and LWD (150); b) comparison of FWD and LWD (300)

The following equations and Figure 45 shows the correlation between the LWD with the 300 and 150 mm plate configuration respectively and the penetration index (DPI) evaluated from DCP test. According to ASTM D6951-03, a cumulate of penetration each 5 blows for normal soil was used for the computation of DPIs. The average value of DPIs for a total depth of 60 cm (excluding the first series of seating blows) was considered for comparison with LWD. In fact, in agreement with the literature, acceptable correlations were identified between log(E) and log(DPI):

$$E_{DPI(300mm)} = 10^{1.528-0.0841\log(DPI)}$$

$$E_{DPI(150mm)} = 10^{1.6433-0.2098\log(DPI)}$$

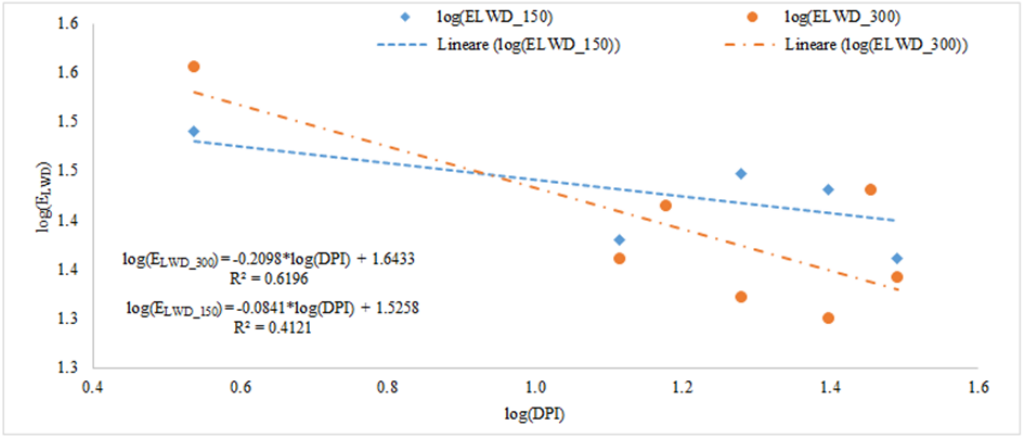

Figure 45 - DPI-Modulus correlations

The best correlation between the E_{LWD} module of LWD and the Penetration Index DPI, is that obtained by considering the LWD test conducted with the 300 mm loading plate in terms of highest R^2. This result can be justified by the deeper stress distribution produced by larger plates (in this case 300 mm), and consequently the subgrade depth results more comparable with the DCP penetration in the soil.

Resilient modulus of subgrade soil is an important material property, a requisite parameter to input in the design of pavements with mechanistic approaches. For many years the repeated load triaxial compression test (AASHTO TP 46) has been the basic test procedure to evaluate resilient modulus of cohesive and granular materials for pavement design applications. Despite several improvements made over the years, Seed et al. (ASTM STP 1375) cited a series of uncertainties as well as limitations associated with the test procedure. Because laboratory resilient modulus sample is not completely representative of in-situ conditions because of sample disturbance and differences in aggregate orientation, moisture content and level of compaction, an in situ determination test may be more representative.Results pointed out a good correlation among different in situ devices which can be used to determine directly (e.g. FWD, LWD) or indirectly (e.g. DCP) the subgrade modulus. The use of triaxial laboratory test can be complimentary to the in situ test as proposed in the present paper to determine the soil proprieties and behavior. It is possible, also, to check the assumption that the measurements are done on a semi-infinite, linear elastic half space by measuring the deflections at different distances from the load. For this application, the system must be equipped with more geophones than the center plate one. This configuration is typical for FWD but less diffused for LWD. LWD equipment showed its high usability in sites with accessibility restrains for heavier and larger equipment like FWD. DPI, has the advantage to explore the soil more in depth, but needs an in site pre-calibration to determine the subgrade modulus. To this aim LWD test with larger loading plates (e.g. 200-300 mm diameters) are recommended.

2.3 Cement Stabilization of Volcanic Ashes and Bearing Capacity In-Situ Tests with Light Weight Deflectometer Technology

The volcanic materials have long been considered an important resource in engineering, getting several applications in various contexts. For the Sicilian territory and beyond, Etna is an extremely important resource, although sometimes the exuberance of its activity is creating major inconvenience to neighboring towns that are often submerged by the ash resulting from its eruptive activity (Figure 46). From the research study carried out, it has emerged that the stabilization of cement of volcanic ash can be an important resource in the field of quality control and reuse for subgrades and subbases layers of road infrastructures. In fact, the ashes stabilized with cement responded well to the treatment in the maturing times and the results are encouraging in terms of bearing capacity of layers and therefore of modulus.
The reuse of ashes in the road environment is an important means of achieving economic, social and environmental sustainability. Volcanic ashes can thus be considered and re-evaluated as a material that is no longer a waste but a resource for our society.

Figure 46 - Ashes in the municipalities of Etna.
Source: http://catania.livesicilia.it/2013/04/20/etna-violentissima-eruzione-lampo-molti-i-danni-per-la-pioggia-di-lapilli-e-pietre_238058/ and http://www.cataniatoday.it/cronaca/comuni-etnei-etna-emergenza-cenere-acireale-divieto-circolazione.html

The ashes, especially those on the road and which are therefore polluting, represent a waste to be disposed to landfills. With regard to the financial aspect, it is necessary to consider both the damage caused by the phenomenon, and the costs to be incurred for cleaning, storage and landfill.
The reuse of volcanic ash, a porous material with poor resistance characteristics, requires the introduction of techniques aimed at increasing its performance so that it can be used in the road field. The service life of a road pavement is strongly conditioned by the bearing capacity of the subgrade and of the deeper layers; during its construction is not uncommon to come across land not suitable to guarantee the characteristics of bearing capacity necessary to ensure a satisfactory durability of the superstructure. In the past, the solution to this problem was represented by the replacement of a certain natural soil thickness present in the site with appropriate quarry material, with adequate characteristics to withstand the loads without the occurrence of excessive deformations.
One of the most satisfactory techniques that allows material reuse and at the same time the increase in performance characteristics is the stabilization with hydraulic binders applied extensively in northern Europe, that would represent a valid solution to the needs of land with high geotechnical characteristics especially for companies for which the supply from quarries is a significant budget item. It's an advantageous technology and able to guarantee considerable savings, which must, however, be supported by in situ and laboratory research studies.
The aim of this research work is to determine whether a material is considered to be waste, and should therefore be treated as waste and stored in special landfills, can instead be reused in road and geotechnical field, taking advantage of the stabilization methods by means hydraulic binders, such as cement, which will improve the properties.
The tests carried out in laboratory on ashes have allowed us to use cement as a hydraulic binder to achieve the increase in performance characteristics and get it in road field that is a good solution for granular materials such as ashes.
It is clear that the use of ashes in the road field is of crucial importance since it is a material easy to find, low cost, and low environmental impact for the intended purpose.
However, at the same time, in order to allow the use of ashes, they must have characteristics of strength and bearing capacity typical of the materials used in the unbound layers of road pavements.

2.3.1 Recovery and transportation of volcanic ashes at the University of Catania

The recovery of local low-quality materials for use in road sector and others has a double meaning: economic and environmental. Currently, the limitations imposed by the extractives plans and the growing attention to environmental issues, have shifted the interest of the field on alternative methods such as soil stabilization considered waste with hydraulic binders.
With this background it is clear how is important at economically and environmentally level the reuse of treated waste volcanic ashes and their stabilization with cement.
For all of these reasons were made considerations aimed at a sustainability perspective and it was chosen the material that could best perform these needs.
In fact, the material used for the development of this study was Etna volcanic ash (called "Etna 10") and was picked up in the territory of Santa Venerina in province of Catania (Italy) in a space dedicated to the collection of building material approximately at 325 meters above sea level in Figure 47.

Figure 47- Localization of the site dedicated to the collection of volcanic ashes in Santa Venerina

Figure 48 - Collection phase of volcanic ashes from the storage site in Santa Venerina

The material was collected (Figure 48) and transported to the University of Catania (Figure 49) at the Department of Civil Engineering and Architecture (DICAR), and then was submitted to laboratory and in-situ tests.

Figure 49 - Ashes transported at the University of Catania. Department of Civil Engineering and Architecture (DICAR)

2.3.2 Laboratory analysis on volcanic ashes

The volcanic material collected and transported to the Department of Civil Engineering and Architecture (DICAR) of the University of Catania and as a first thing was submitted to laboratory tests[26]. The ashes, which are dark in color typical of volcanic materials, were subjected to Particle Size Analysis for sieving, Proctor test, Micro-Deval abrasion test and CBR test.

Particle Size Analysis: The gradation characteristics of each sample were investigated by performing sieve analyses, according to ASTM method. The particle size analysis was carried out by means of sieves of the ASTM series characterized by different opening meshes and sieving was made by stacking one on the other the various sieves with a downward slit opening up to the sieve ASTM 200. The equipment is very simple for this type of test and is constituted by ASTM sieves and a balance that allows measurement of the material with a sensitivity of 0,1 g. The test was then carried out with a mechanical sieve that produces vibrations for a period of 3-5 minutes.

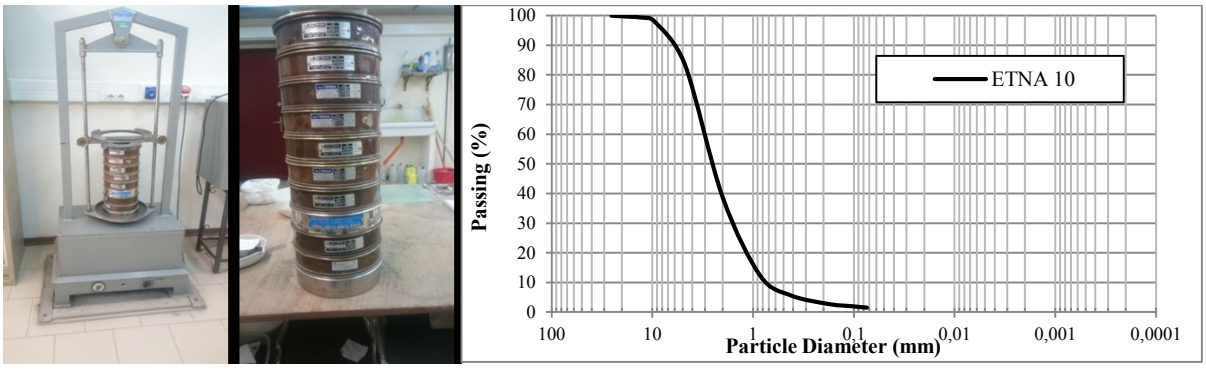

Figure 50- Equipment for particle size analysis at DICAR (University of Catania) and grain size distribution

From the results obtained, and illustrated in Figure 50, the material analyzed consists of gravel (61%), sand (37%) and silt (2%), so it is classified as "Gravel with sand" and as soil of group A2 according to HRB-AASHTO CNR UNI 10006 classification with a specific weight of grains Gs = 2.78 g/cm3 for the ASTM D 854.

Proctor Compaction Test and post-Proctor Particle Size Analysis: Each soil under load reduces its volume, which means that a soil is compressible, both for its granular constitution and for the presence of voids and water. Land compressibility is of paramount importance in road constructions: in particular, in the realization of roads or walls support, there are often disadvantages resulting from the settling of the ground and after the construction of the work.
The Proctor compaction test is a laboratory geotechnical testing method used to determine the soil compaction properties, specifically, to determine the optimal water content at which soil can reach its maximum dry density.
It's necessary to carry out appropriate surveys to ascertain the characteristics of the soil which, at an initial assessment, are not considered fit and which will insist on road works. In fact, the ashes were tested with Proctor Modified Test with 5-Layer and 56 shots per layer by means of automatic compressor and the optimum water content was reached at 20%.

[26] Laboratory tests were carried out at the DICAR of the University of Catania, at the geotechnical and road testing laboratories. Some of the tests conducted were also useful for the realization of some degree theses (Tranchina, Corsaro, Varrica, Sanfilippo, 2016) and of support for the deepening in this PhD thesis with subsequent detailed tests that allowed to study the possibility of reuse the volcanic ash in the road field with NDT (LWD).

Clearly, due to the compaction resulting from 56 shots of the mechanical compactor, a particle size variation was observed for finer particles that occurred precisely because the ash object of study had larger grains characterized by the presence of pores and hence easily crushed (Figure 51). In fact, compared to the first particle size analysis, the percentage of silt changes from 1-2% to 9% and the amount of gravel has drastically reduced.

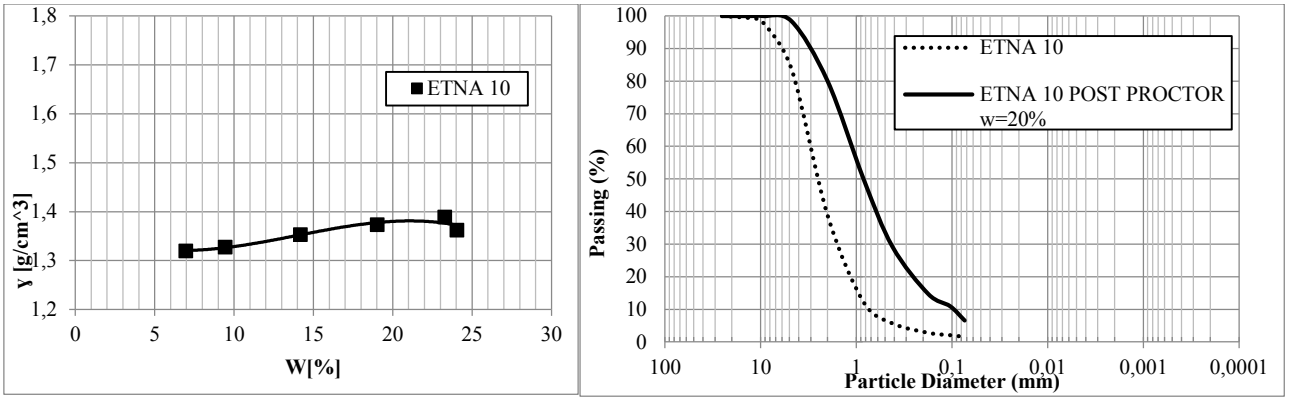

Figure 51 - Proctor Modified Test on Etna volcanic ashes and pre and post-proctor grain size distribution comparison

Micro-Deval Abrasion Test: The Micro-Deval test was conducted for a fuller understanding of the physical and mechanical characteristics of the aggregates. The purpose of the test is to determine the wear resistance of a sample of stone aggregates, this test is applicable to both natural and artificial aggregates, excluding fillers.

The test is normally performed on the particle size class between 10mm and 14mm and the sample of volcanic ash meets these requirements. Since the Micro-Deval Coefficient is defined as the percentage of material produced by the action of steel balls inside cylinders, it is deduced that when the MDE value is lower, the wear resistance of the aggregates is better.

Initially, a Micro-Deval Standard test was performed in wet conditions, as described in UNI EN 1097-1, which led to a Micro-Deval MDE coefficient of 88.55. Subsequently, it was decided to proceed with a new 4-6.30mm particle size range, with an alternative Micro-Deval test with which an MDE coefficient of 98 was found. Such high values of Micro-Deval coefficient, resulting from the tests carried out, confirm the very low wear resistance of this type of aggregates and therefore of volcanic ashes. Inside the cylinders the material has been completely reduced to sludge by impact with the spheres. During the cleaning of the spheres it was noted that there was a clear electrostatic interaction between the spheres and the aggregate; along with the high grain weight this could mean a considerable iron content in the chemical composition of the volcanic ashes studied.

It's evident that the volcanic ashes examined with a glassy and porous structure are not suitable for the construction of the most superficial layer of the road surface due to their extreme wearability and if used in the underlying layers of the road superstructures they need a stabilization.

California Bearing Ratio (CBR) Test and hydraulic stabilization with cement: Bearing capacity depends on a number of factors such as: nature, porosity and water content of the soil, entity, imprint area and speed of load application, as well as application number of the load itself.

An important aspect of this study is the evaluation of the *California Bearing Ratio* ash index to measure the resistance that this material offers to deformations and definitively the decision, given the characteristics of the material and the lack of pozzolanic component, of what stabilization type is most suitable for use in the road and in what percentage the hydraulic binder must be present.

The CBR test, developed by the California Department of Transportation (Caltrans)[27] before World War II, measures the bearing capacity of a soil under certain densities and humidity conditions and provides an index that, together with traffic data, can be used for the dimensioning of the layers of flexible pavements. The test was performed on the compacted material and the interpretation of the results was carried out through the analysis of the load-penetration curve in accordance with AASHTO T 193 and ASTM D 1883.

Tests on Etna ashes have been conducted to reach 35% water content due to its porosity and consequently the ability to absorb large amounts of water. In particular, the resistance values of the material range around 14-17 kN with water percentages ranging from 19 to 20% with a CBR index of 60%.

Table 15 - Results of CBR on volcanic ashes

Water content W [%]	**CBR 2,5 mm**	**CBR 5,0 mm**	**CBR Index [%]**
5	0.24	0.29	29
10	0.43	0.45	45
15	0.39	0.38	40
20	0.52	0.58	60
25	0.77	0.81	85
27	0.59	0.69	70
30	0.71	0.84	85
35	0.46	0.69	70

Note: The criterion for calculating the CBR index, in accordance with UNI EN 13286-47 is to assume the greater of the two values (CBR 2.5 mm and CBR 5.0 mm), the immediate bearing index value is 0.5% in CBR range from 0 to 9, 1% from 10 to 29, and 5% for values major to 29.

From the values of CBR indexes found, in Table 15, it can be said that the volcanic ash, although presenting issues such as the fragility of the grains and the extreme porosity, if properly compacted succeed in reaching of good bearing capacity levels.

Bearing capacity could therefore be improved by an appropriate stabilization process and choosing cement as a hydraulic binder results from the fact that the material studied has no pozzolanic component so this is definitely the best choice. Since the pozzolanic composition with lime produces grip, it is precisely by the absence of this material that results in the choice of discarding lime as a binder in stabilization.

In particular, were conducted two types of tests that are showed in Figure 52: on Etna ashes and on the ashes stabilized with 5% and 7% of cement content.

In case of CBR made on the mix with 5% cement content and water equal to the optimum of the proctor test, 2 specimens (called Stabilized 1 and Stabilized 2) were analyzed at 14 and 28 days of curing.

The same was made with the 7% cement content, water content equal to the optimum of the proctor test and 2 specimens at 7 and 14 days of curing.

[27] Caltrans manages more than 50,000 miles of California's highway and freeway lanes, provides inter-city rail services, permits more than 400 public-use airports and special-use hospital heliports, and works with local agencies. Caltrans carries out its mission of providing a safe, sustainable, integrated and efficient transportation system to enhance California's economy and livability, with six primary programs: Aeronautics, Highway Transportation, Mass Transportation, Transportation Planning, Administration and the Equipment Service Center. Source: http://www.ca.gov

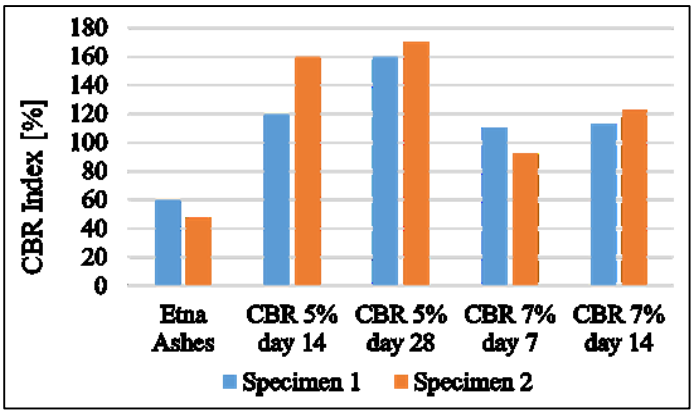

Figure 52 - CBR tests on ashes and on stabilized with a cement content of 5% and 7% in different days of curing

The presence of cement has shown a significant improvement in the characteristics of volcanic ash, bringing CBR at about 120% after 14 days of curing (comparable values in 5-7% cases), so half of the normal ripening time there were positive performance results, it was then decided to build the stabilized block with a cement percentage of 7%.
It was clearly more important to conduct stabilized ash tests, because this has allowed to decide on the percentage of cement to be used for the construction of the stabilized layer, and therefore the tests carried out in situ, confirming the importance of stabilizing the ash material for possible use in the road field.

2.3.3 In-situ bearing capacity tests

In-situ tests were conducted at the University of Catania in a test area of the Department of Civil Engineering and Architecture (DICAR) in Figure 53. After transporting the ash from the storage of Santa Venerina to the test site of the University of Catania, steps were taken to the removal of a small sample to be dried in the oven, so as to recognize the water content of the soil and to dose the water that need to be added for the stabilization.
As noted by the performance of the Proctor curve, thanks to the test performed in the laboratory, the optimal water content which allowed the maximum densification further to the compaction was equal to 19%.
The field trial was object of a first preliminary analysis to verify that it was possible to lay the ash to be stabilized in a sufficiently large area.
Having done this, it has been possible proceed with the realization of a block of compacted volcanic ash. The element, of square base, with a side of about 1,20 meters and a thickness of 20 cm, was obtained through the construction of four successive layers with thickness of about 5cm each, each of which was hydrated with a suitable amount of water and subsequently compacted using a roller compactor manual, constructed at the DICAR, consisting of three rotating cylinders in cement connected together and driven by means of suitable thrust system (Figure 54).

Figure 53 - Test area and manual roller compactor of the University of Catania

Figure 54 - Laying of the layers, hydration with water and compacted ash

At this point, were carried out the first LWD tests on the compacted block of ashes to derive the modules of the two layers, ash and subgrade.
In Figure 55 is possible to see how the LWD plate placed on the block of ashes (a), on which is placed a wooden board where a hole was made to allow the realization of the bearing capacity test (b). This moment was called "Day 0".

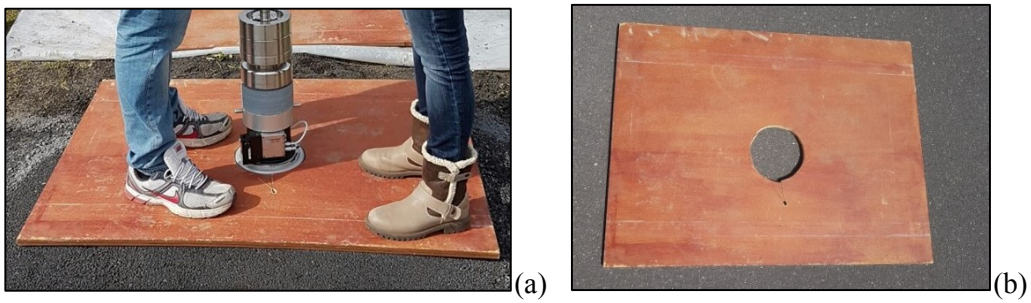

(a) (b)

Figure 55 - LWD tests on the compacted block of ash (a) and wooden board used during the realization of the tests(b)

Subsequently to these tests was possible to begin the stabilization phase of volcanic ashes with cement (Figure 56). It was decided, after careful analysis of Proctor and CBR laboratory tests carried out, to employ a cement content of 7% that is about 5 Kg/m^3. The procedures carried out for the realization of the new block have been entirely analogous to the previous case with the addition, for each layer, of the quantity of cement calculated and subsequent mixing.

Figure 56 - Cement mixing and stabilized block (1.20x1.20x0.20 m)

In order to protect the sample from atmospheric agents and to ensure an adequate maturation, it was placed a protection system consisting of wooden plank on the block and protective sheet of plastic, that is showed in Figure 57.

Figure 57 - Protection system to ensure an adequate curing

The following images in Figure 58 are relative to the layer of stabilized in different days of maturation.

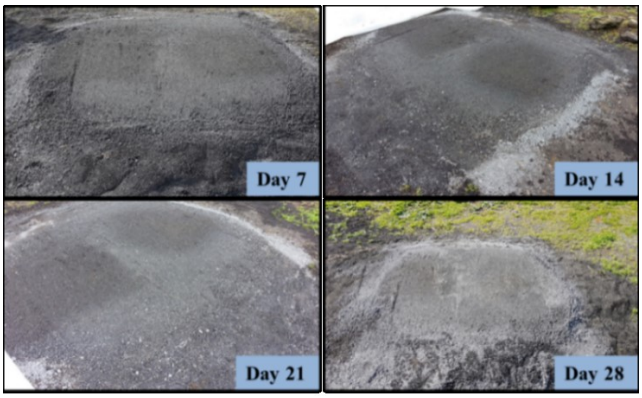

Figure 58 - Ashes cement stabilized at days 7-14-21-28

The survey covered the analysis, in different time instants (0, 7, 14, 21, 28, 35, 42 days), of the bearing characteristics of a prismatic element of volcanic ash compacted and stabilized with a cement content of 7 % and, as noted by the performance of the Proctor curve, an optimal water content of 19-20%. Treating a soil with cement stabilization means to improve its level of resistance and bearing capacity thanks to the design of a mixture composed of soil and by certain percentages of cement and water. The treatment should take place in a short time to avoid the start of the step of cement setting before the end of the mass in work operations. In the different time instants, after mixing with cement, were made tests with Light Weight Deflectometer (LWD) in Figure 59, which provided the necessary data, analyzed and processed in order to understand if the way undertaken is factually correct. In fact, the LWD was used for the calculation of the layers' modulus, and then to monitor the realized stratification and the resulting aging of the cement on days 0, 7, 14, 21, 28, 35, 42.

Figure 59 - Light Weight Deflectometer in the area test of the University of Catania

2.3.4 Models and conclusions

Before exposing the experimental methodology and the numerical part of the case study that has been developed, it's essential to make some premises about the theory of elasticity[28] that have been

[28] The theory of elasticity is the most widely used model for pavement design and it has been described by Ullidtz in 1998 in his "Modelling Flexible Pavement Response and Performance".

used with particular reference to Boussinesq's equations applied for the centre line of a circular load that is uniformly distributed and Odemark's method for a multi-layer system.
In particular, the closed form solutions proposed by Boussinesq for the centre line of a circular load, was applied in this case study of the NDT test performed with a LWD on a concrete stabilized soil area realized in "Cittadella Universitaria of Catania" at DICAR. The vertical stress σ_z is:

$$\sigma_z = \sigma_o \left[1 - \frac{1}{\left(\sqrt{1 + \left(\frac{a}{z} \right)^2} \right)^3} \right]$$

where: σ_o is the mean value of the stress, a is the plate radius, z is the thickness that in the specific case study is the "equivalent thickness" which will be explained with the Odemark's method.
In case of load transferred via a completely rigid circular plate σ_z is:

$$\sigma_z = \frac{\sigma_o}{2} \frac{1 + 3\left(\frac{z}{a} \right)^2}{\left[1 + \left(\frac{z}{a} \right)^2 \right]^2}$$

The total deflection Dz of a two layer-system, as the case study, is calculated as the sum of two contributions dz1 and dz2: $Dz = dz_1 + dz_2$

$$dz_1 = \frac{(1+\vartheta_1)\cdot P \cdot a}{E_1} \cdot \left[2\cdot(1-\vartheta_1) - \left\{ \left(1 + \left(\frac{h_1}{a} \right)^2 \right)^{-0.5} + (1-2\cdot\vartheta_1)\cdot \left(\left(1 + \left(\frac{h_1}{a} \right)^2 \right)^{0.5} - \frac{h_1}{a} \right) \right\} \right]$$

$$dz_2 = \frac{(1+\vartheta_2)\cdot P \cdot a}{E_2} \cdot \left[\left\{ \left(1 + \left(\frac{h_e}{a} \right)^2 \right)^{-0.5} + (1-2\cdot\vartheta_2)\cdot \left(\left(1 + \left(\frac{h_e}{a} \right)^2 \right)^{0.5} - \frac{h_e}{a} \right) \right\} \right]$$

Where: h_1 is the thickness of the first layer and h_e is the equivalent thickness, that is explained below.
For the calculation of the module E are used the Boussinesq equations, already exposed in Chapter 1 (paragraph 1.3.1), under a point load and at different distances from the centre of the load.
Boussinesq's equations are only applicable to a homogeneous layer. The assumption on which the theory of elasticity is based are never fulfilled by real pavement materials or pavement structures. The loads are not static but dynamic and LWD is an NDT dynamic test. In practice, most pavement structures are not homogeneous but are layered systems.
In fact, Odemark developed the Method of Equivalent Thickness (Chapter 1, paragraph 1.3.1) to transform a system consisting of layers with different moduli into an equivalent system where the thicknesses of the layers are altered but all layers have the same modulus.
According to Ullidtz this method gives acceptable results, but two conditions have to be given. With the correction factor f given above Odemark's method will give answers reasonably close to the theory of elasticity provided that modulus decreases with the depth ($E_i/E_{i+1}>2$), and then equivalent thickness of each layer is larger than the radius of the loaded area.

These theoretical considerations have been fundamental because they represent the basis for the understanding of the models that have been applied to the case study due to uniformly distributed load and a multi-layer system as consisting of two layers: a layer 1 with a thickness of 200 mm which is constituted by ashes that have been stabilized with cement, a layer 2 which is the subgrade. Furthermore, BISAR and LWDmod programs were supportive in the numerical iterations performed. With BISAR, a software developed by Shell, stresses, strains and displacements can be calculated in an elastic multi-layer system which is defined by the following configuration and material behavior:

- the system consists of horizontal layers of uniform thickness resting on a semi-infinite base or half space;
- the layers extend infinitely in horizontal directions;
- the material of each layer is homogeneous and isotropic;
- the materials are elastic and have a linear stress-strain relationship.

The system is loaded on top of the structure by one or more circular loads, with a uniform stress distribution over the loaded area. The program offers the possibility to calculate the effect of vertical and horizontal stresses and includes an option to account for the effect of (partial) slip between the layers, via a shear spring compliance at the interface.
BISAR calculations require the following input: the number of layers with their moduli, Poison's ratios, thickness (except for the semi-infinite base layer), the interface shear spring compliance at each interface, the number of loads, the co-ordinates of the position of the centre of the loads, one of the following combinations to indicate the vertical normal component of the load (stress and load, load and radius, stress and radius), the co-ordinates of the positions for which output is required. The detailed output comprises the following information for each selected position in the structure under consideration: the components of the stress tensor (normal and shear), the components of the strain tensor (normal and shear), the components of the displacement vector.
In this specific case study BISAR was used to simulate the LWD tests, and in particular to validate the results of design methods and in-situ campaign of analysis.
The numerical simulation is used to integrate in field tests. In particular, significant benefits can result from an elevation of the standards of design and effectiveness of the controls carried out easily and extensively.
The software Dynatest LWDmod concern data organization, analysis and reporting: imports data into a project database, allowing organization of multiple files into one database; graphical features to view test results, and to eliminate selected drops or points from the file; editing features; automated selection of drops to be used in the analysis; calculation of surface moduli; back-calculation of layer moduli for multi-layer systems, using the results of multiple tests; calculation of subgrade non-linearity; calculation of needed overlay thickness, based on design surface moduli; analysis of load/deflection time histories; graphical presentation of all analysis results; capability to export results tables and graphics. In this case study the program was used to calculate the modulus of the layer realized with ashes stabilized with cement within an iterative procedure which has been tested on this work.

Results

The Light Weight Deflectometer tests were performed, as explained before, on days 0, 7, 14, 21, 28, 35, 42. More specifically were made:

- Test at day 0 on the ash as it is not mixed with water and cement;
- Tests in densification and maturation days 7, 14, 21, 28;
- Testing on days 28, 35, 42 after the destruction with hand roller.

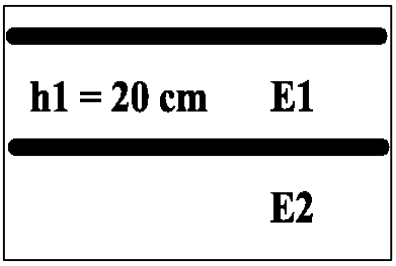

Figure 60 - Two-layer system object of study

All of these tests were useful to develop the methodology of numerical calculation of the modules and to overcome the problem of those tests carried out simply with a geophone for which it is not possible to obtain engineering acceptable solutions.
The tools that have allowed to develop simulations and iterative processes on the two-layer system (Figure 60) realized in the test area of the University of Catania were: the elasticity theories with Boussinesq relationships and those for stress and displacements, the BISAR calculation software multilayer system and LWDmod that has proved useful for backcalculation.
After a careful phase of study and the collection of all data within 42 days, it has been developed an equation with the pressure parameters and substrate module that allows to find at the variation of the pressures the corresponding subgrade module.
The curve, which then later on will be seen in what context of calculations has been useful, has been realized by means of two types of tests:

1) Tests carried out directly on the subgrade at different pressures σ and drop heights h (5", 11", 15") with a single geophone, for which it was easily to derive the subgrade modulus values E2 with the Boussinesq formula for a plate load test:

$$E2 = \frac{f(1-\nu^2)\sigma_0 . a}{d_0}$$

with: f=2, ν=0,35, a=100 mm. The LWD configuration was: plate diameter=200 mm, weight=20Kg, h=5"-11"-15". In Table 16 there are the values of the subgrade modulus E2:

Table 16 - Pressure and Modulus carried out directly on the subgrade with LWD tests

	σ [KPa]	**E2** [MPa]
5"	110	196
11"	140	224

2) Two tests at 28 and 35 days of curing and carried out on the two-layer system with three geophones (at distances 0, 200 mm and 300 mm from the center of the circular plate), for which the models of the two layers were formed easily in back calculation with LWDmod with Boussinesq's equation and then each test was simulated with BISAR to know the interface stresses to which corresponds the modulus of the subgrade.
The LWD configuration for each test was: plate diameter=200 mm, weight=20Kg, h=17".
The values obtained at 28 days were: E1=438 MPa, E2=123 MPa; at 35 days: E1=210 MPa, E2=135 MPa. The modules E1 and E2 calculated with LWDmod were used as inputs on

BISAR, along with loads, pressures, radius of the plate and position of the geophones; in this way it was simulated LWD the test carried out in situ and with BISAR was possible to obtain the interface stress between the two layers (at 0.20 m of depth) to which corresponds E2 previously obtained. The interface stresses σzz between the two layers at 28 and 35 days respectively were: $\sigma zz_{28\ days}$= 51.22 KPa and $\sigma zz_{35\ days}$= 69.38 KPa.

From the results of the two types of tests it was possible to derive the curve stress-subgrade modulus. And at the same time were calculated the stress at the interface with the relations exposed before in the cases of uniformly distributed load and load transferred via a completely rigid circular plate; this was done to compare the results at the interfaces and select the curve with the better value of R^2. The results are summarized Table 17 and Figure 61.

Table 17 - Results of the two types of tests for σ and E2

	σ [KPa]	**E2 [MPa]**	**σ [KPa]**	**E2 [MPa]**	**σ [KPa]**	**E2 [MPa]**
	Test at the top of subgrade					
h= 5"	110	196	110	196	110	154
h=11"	140	224	140	224	140	176
h= 15"	159	239	159	239	159	188
	Test at the top of the ash layer					
35 days	**69**	135	**73.6**	135	**67.7**	135
28 days	**51**	123	**47.1**	123	**44.8**	123
	Bisar σ uniform		Odemark **σ uniform**		Odemark **σ rigid**	

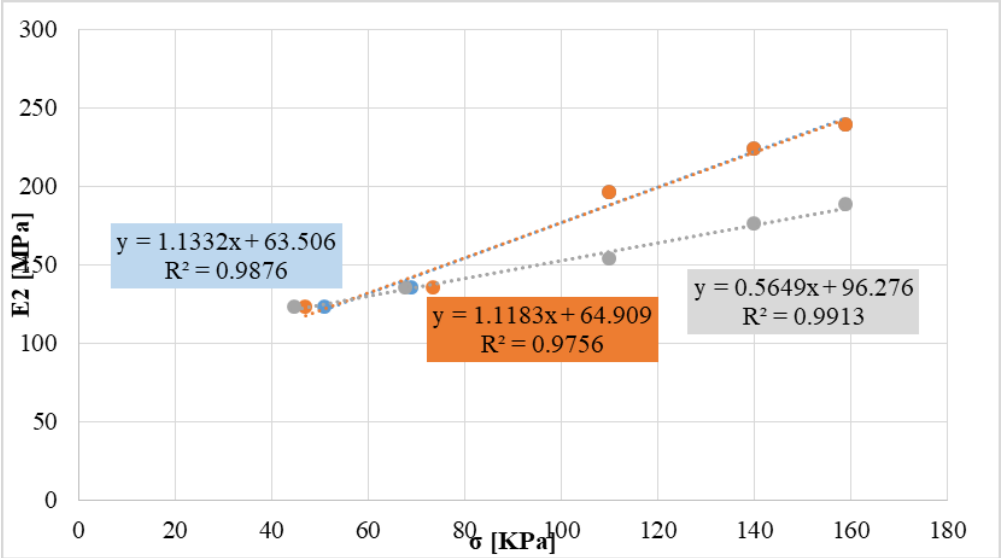

Figure 61- Curves stress-subgrade modulus with their equation

The curve selected is the one with the value of R^2 = 0.9876 and equation y = 1.1332 x + 63.506, which it is below.

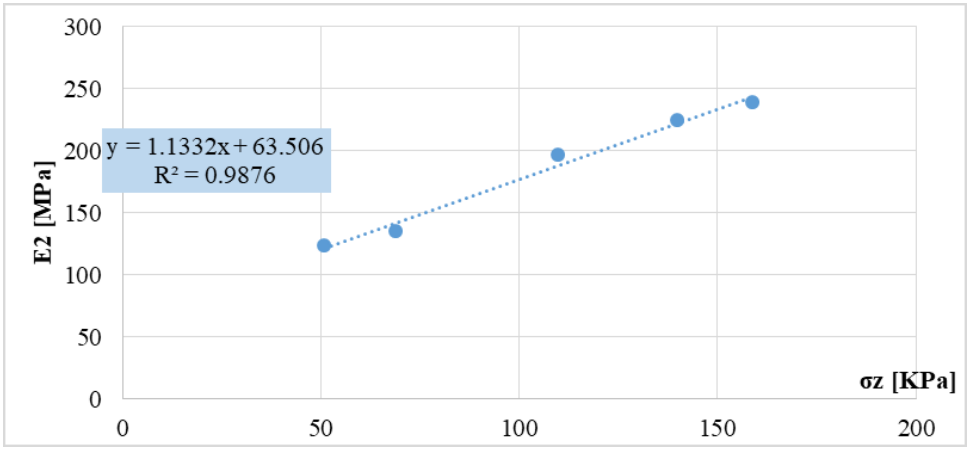

Figure 62 - Curve stress-subgrade modulus selected for the numerical calculations of the case study

The equation in Figure 62, y = 1.332 x + 63.506 ➔ E2equation= 1.332 σz + 63.506 was then used, for iterative calculations that short below will be exposed, for the calculation of "E2equation" subgrade modules. The following calculations make use of iterative processes and have been developed to overcome the problem of the calculation of the modules of a two-layer system with just one geophone, the calculation method uses Odemark-Boussinesq models, is supported by Bisar and LWDmod programs and by the application of the equation of curve stress-subgrade for E2equation value. This iterative process has been developed to test data for 7-14-21-28 days.
The results for "Day 7" are shown in Table 18 and then explained.

Table 18 - Day 7

$E1_m$	ν1	h1	**$E2_m$**	ν2	f	P lwd	a	he	**σz**	**E2 equation**	dz1	dz2	**Dz**	$D_{lwdtest}$
MPa	-	mm	**MPa**	-	-	MPa	mm	mm	**KPa**	**MPa**	mm	mm	**µm**	µm
210	0.35	200	**146**	0.35	0.9	0.274	100	203	**76**	**149.7**	0.083	0.20	**264.1**	288.17

Where: E1 and E2 are input data of the iterative process, ν1 and ν2 are the Poisson ratios for the 2 layers, h1 is the real thickness of the stabilized layer, he is the equivalent thickness from Odemark model with f=0.9 (factor for a two-layer system to have good agreement with the theory of elasticity), a is the radius of the LWD circular plate used in the tests, Plwd is the total stress of the LWD test, Dlwdtest is the deflection recorded with one geophone with the LWD tool.
In red there are the values calculated, and clearly form part of the iterative process: the value of the stress σz (at the depth of 200 mm) and Dz, were calculated from the theory of elasticity with the closed form solution for the center line of a circular load previously described.
E2equation, as extensively described, was calculated by the curve stress-subgrade modulus.
From this calculation was possible to see the differences in percentages of the results of the calculation models (Δ) for E2 modules and the deflections (calculated deflections "Dz" and measured by LWD "D lwd test"), and with the iterations it is tried to reduce as much as possible the value of Δ.
In fact, ΔE2=2% and ΔDz=8.4%.
With this input data, in BISAR were obtained the following results:

σz_{bisar}= 70.3 KPa
Dz_{bisar} =258 µm

At this point, the E2 obtained from the model $E2_m$=146 MPa was used as a fixed input value in LWDmod toghether with the deflection Dlwd test of the previous table and was obtained a new value of E1 (useful for comparison), in fact $E1_{lwdmod}$=188 MPa.

With this values in Bisar was obtained a deflection $Dz_{bisarbis}$= 277 µm and a $\sigma z_{bisarbis}$= 72.7 KPa

The same procedure was used in the days 14-21-28 and the results are in Table 19, Table 20 ans Table 21. In general, the schema used was:

a) Calculation with the iterative method with Odemark-Boussinesq theories ($E1_m$, $E2_m$, σz, Dz) → Bisar (σz_{bisar}, Dz_{bisar})
b) Backcalculation with LWDmod ($E2_m$, $E1_{lwdmod}$, $D_{lwdtest}$) → Bisar ($Dz_{bisarbis}$)

Table 19 - Day 14

$E1_m$	ν1	h1	**$E2_m$**	ν2	f	P lwd	a	he	**σz**	**E2 equation**	dz1	dz2	**Dz**	$D_{lwdtest}$
MPa	-	mm	**Mpa**	-	-	MPa	mm	mm	**KPa**	**MPa**	mm	mm	**µm**	µm
225	0.35	200	**147**	0.35	0.9	0.277	100	207	**75**	**148.0**	0.078	0.21	**257**	278.01

With:

a) ΔE2=1%; ΔDz=7.5% → Bisar: σz_{bisar}= 69.8 KPa; Dz_{bisar} =249 µm
b) $E2_m$=147 MPa; $E1_{lwdmod}$=201 MPa; $D_{lwdtest}$=278 µm → Bisar: $Dz_{bisarbis}$=268 µm

Table 20 - Day 21

$E1_m$	ν1	h1	**$E2_m$**	ν2	f	P lwd	a	he	**σz**	**E2 equation**	dz1	dz2	**Dz**	$D_{lwdtest}$
MPa	-	mm	**MPa**	-	-	MPa	mm	mm	**KPa**	**MPa**	mm	mm	**µm**	µm
230	0.35	200	**146**	0.35	0.9	0.275	100	209	**73**	**146.1**	0.076	0.21	**253**	270.01

With:

a) ΔE2=0.1% ΔDz=6.3% → Bisar: σz_{bisar}= 68.9 KPa; Dz_{bisar} =246 µm
b) $E2_m$=146 MPa; $E1_{lwdmod}$=201 MPa; $D_{lwdtest}$=270 µm → Bisar: $Dz_{bisarbis}$=261 µm

Table 21 - Day 28

$E1_m$	ν1	h1	**$E2_m$**	ν2	f	P lwd	a	he	**σz**	**E2 equation**	dz1	dz2	**Dz**	$D_{lwdtest}$
MPa	-	mm	**MPa**	-	-	MPa	mm	mm	**KPa**	**MPa**	mm	mm	**µm**	µm
270	0.35	200	**135**	0.35	0.9	0.275	100	227	**64**	**136.4**	0.064	0.21	**234.5**	235.0

With:

a) ΔE2=1% and ΔDz=0.2% → Bisar: σz_{bisar}= 63.3 KPa; Dz_{bisar} =228.9 µm
b) $E2_m$=135 MPa; $E1_{lwdmod}$=270 MPa; $D_{lwdtest}$=235 µm → Bisar: $Dz_{bisarbis}$=228.9 µm

After completing the iterative model Odemark-Boussinesq working with the equation of the subgrade resulting from the curve stress-subgrade modulus and verified the test with Bisar (σz_{bisar}, Dz_{bisar}), the model was calibrated and refined further. Changing the coefficient f, the factor of a two-layer system of the equation of the equivalent thickness "he" (fixed in the just exposed model at 0.9), as to obtain the values of σz_{bisar}, it was found an equation for the calculation of the factor "f" of a two-layers system (now regarded as a value that varies) that is a function of the ratio of the modules $E1_m/E2_m$. The calculations for obtaining the equation of the factor f are summarized in Table 22.

Table 22 - Modules and variation of the factor f for a two-layer system

E1	E2	E1/E2	f	1/f	σZbisar	σZOdemark	Dzbisar	DzOdemark
210	146	1.4	0.95	1.05	70.3	70	258	264.4
225	147	1.5	0.94	1.06	69.8	70	249	257.3
230	146	1.6	0.93	1.08	68.9	69	246	253.1
270	135	2.0	0.91	1.10	63.3	63	228.9	234.5
		2.5	0.90	1.11	-	-	-	-

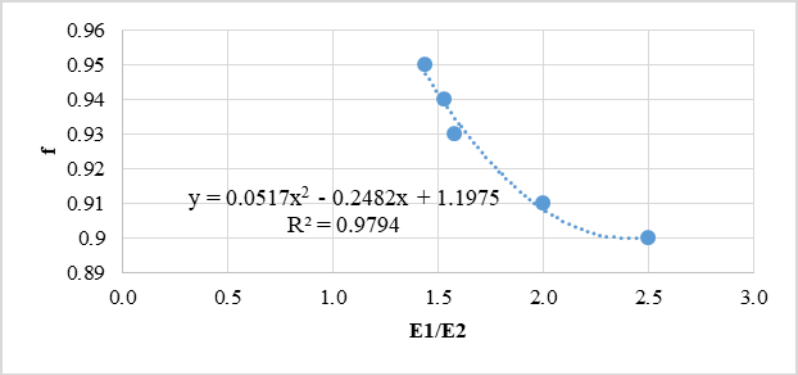

Figure 63 - Curve for the calculation of the factor f for a two-layer system

The curve obtained (Figure 63) has equation $y = 0.0517\ x^2 - 0.2482\ x + 1.1975$ and therefore:

$$\rightarrow f = 0.0517\ (E1/E2)^2 - 0.2482\ (E1/E2) + 1.1975$$

So knowing the value of f, by now no longer fixed on, the model is calibrated in a more specific way and consequently it is no longer necessary to use Bisar, whose elaboration is now overtaken.
At this point the calculation of the modules of the various layers becomes more precise, by iterating the calculation model Odemark-Boussinesq developed and perfected with the factor f and the interface stresses, and with the aid of LWDmod is possible to easily derive the subgrade module E2 and verify the percentage difference (accepting a maximum of 2 %) and so consequently also get the module of the first layer E1 which is in this case stabilized ash with cement.
This procedure was applied in 7-14-21-28 days of maturation of the cement and the following results in Table 23 were obtained:

Table 23 - Calculations of modulus with the model developed in days 7-14-21-28

	E1m	ν1	h1	**E2m**	ν2	f	P lwd	a	he	**σz**	**E2 equation**	Δ E2	Dz Odemark	Dz Lwd test	ΔDz
	MPa	-	mm	**Mpa**	-	-	MPa	mm	mm	**KPa**	**MPa**		μm	μm	
Day 7	188	0.35	200	145.6	0.35	0.963	0.274	100	209.8	72.5	145.7	0.1%	280.6	288.17	2.6%
Day 14	203	0.35	200	144.6	0.35	0.951	0.277	100	213.0	71.6	144.6	0%	271.3	278.01	2.4%
Day 21	211	0.35	200	143	0.35	0.944	0.275	100	214.9	70.0	142.9	0.1%	264.4	270.01	2.1%
Day 28	269	0.35	200	136	0.35	0.909	0.275	100	228.2	63.7	135.7	0.2%	234.9	235	0%

From the values obtained for the stabilized it has a 43% increase of the module from day 7 to day 28, this is certainly positive as there was a binding action of the cement, the modules of the substrate have an average value of 142 MPa.
Then the model has proved useful to monitor the experiment of Quality Control with the LWD tool which has demonstrated quite versatile in the tests.

At the twenty-eighth of the cement maturation day, after making the LWD tests already described, the stabilized block has been cracked by the passage of a hand roller, and what has been done to monitor even a bit the modules and therefore the consistency of the material and its bearing capacity. So have been made yet three other LWD tests (Table 24) on days 28, 35, 42 and was again applied the calculation model developed for the calculation of the modules, obtaining:

Table 24 - Calculations of modulus with the model developed in days 28-35-42

	$E1_m$	ν1	h1	**$E2_m$**	ν2	f	P lwd	a	he	**σz**	**E2 equation**	Δ E2	Dz Odemark	Dz Lwd test	ΔDz
	MPa	-	mm	**Mpa**	-	-	MPa	mm	mm	**KPa**	**MPa**		µm	µm	
Day 28	218	0.35	200	143	0.35	0.939	0.278	100	216.2	70.1	143.0	0%	262.1	266.71	1.7%
Day 35	192	0.35	200	145	0.35	0.959	0.275	100	210.7	72.2	145.3	0.2%	278	285.26	2.6%
Day 42	199	0.35	200	144.3	0.35	0.954	0.274	100	212.3	71.3	144.3	0%	272.3	267.10	2.0%

After the partial destruction of the stabilized block, of course, there is a decrease in the stabilized modules, but it is still not very high and this is definitely a positive fact.
Important considerations must also be made on Day 0, at this time we had only ashes in his state that had been collected from the storage area, so it was considered appropriate to carry out tests on this layer and also know the modules of the ashes and the subgrade.
The Odemark-Boussinesq theory cannot be applied for the stratification object of study no stabilized ashes-subgrade, because the no stabilized ashes have lower modules of the substrate under examination.
Whereas this theory is applicable on condition that the modules decrease with depth, then have been made iterations with Bisar and considering the equation previously calculated for the subgrade module E2, obtaining with three iterations exposed in Table 25:

Table 25 - Calculation of modules at Day 0 and iteration process

1)

E2	$E1_{lwdmod}$
145	70

σz bisar	**E2**	E1	**Dz bisar E2=145**	$Dz_{testlwd}$	ΔDz	ΔE2
89.6	**165.0**	68	**638.3**	646.08	1.2 %	12.1 %

2)

E2	$E1_{lwdmod}$
165	68

σz bisar	**E2**	E1	**Dz bisar E2=165**	$Dz_{testlwd}$	ΔDz	ΔE2	Δσz
91.7	**167.4**	68	**640.1**	646.08	0.9 %	1.4%	2%

3)

E2	$E1_{lwdmod}$
167.4	68

σz bisar	**E2**	E1	**Dz bisar E2=167.4**	$Dz_{testlwd}$	ΔDz	ΔE2	Δσz
91.9	**167.6**	68	**638.9**	646.08	1.1 %	0.1%	0.2 %

The module of the ash layer is 68 MPa, it has a lower value of the subgrade.
In synthesis, with this research study and the calculation method developed, the data found in several weeks are (Table 26):

Table 26 - Results for the two-layer system in the different days

	E1 [Mpa]	E2 [Mpa]
Day 0	68	167
Day 7	188	145.6
Day 14	203	144.6
Day 21	211	143
Day 28	269	136
Day 28 (2)	218	143
Day 35	192	145
Day 42	199	144.3

The stabilization of cement produced within 28 days a considerable increase of the E1 modules relative to the first layer (Figure 64), with a 43% increase of the module from day 7 to day 28, then there was a good binding action in the mix.

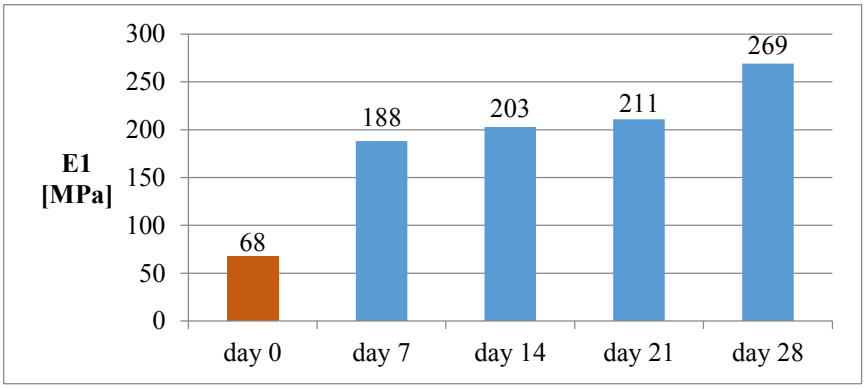

Figure 64 - Trend of E1 modules in the 28 days of curing

Volcanic ash considered until now a special waste with substantial environmental and economic costs for their disposal, can instead be reused in road sector and can provide the foundation layer in the road paving packages. This is definitely a good starting point which is among the objectives of sustainability: environmental, social and economic.

2.4 References

- AASHTO T 193, *Standard method of test for the California Bearing Ratio,* American Association of State Highway and Transportation Officials, January 2013.
- ASTM D 1883-16, *Standard Test Method for California Bearing Ratio (CBR) of Laboratory-Compacted Soils*, ASTM Volume 04.08 Soil and Rock (I): D421 – D5876, March 2016.
- ASTM D 422-63, *Standard Test Method for Particle-Size Analysis of Soils*, ASTM International, West Conshohocken, PA, 2007.
- ASTM D 6951-03, *Standard Test Method for Use of the Dynamic Cone Penetrometer in Shallow Pavement Applications*, ASTM International, West Conshohocken, PA, 2003.

- ASTM D 854-F12, *Standard test methods for specific gravity of soil solids by water pycnometer*, Annual Book of ASTM Standards, 2005.
- ASTM D 4318-84, *Standard Test Methods for Liquid Limit, Plastic Limit, and Plasticity Index of Soils*, ASTM International, West Conshohocken, PA.
- ASTM E2583/07, *Standard Test Method for Measuring Deflections with a Light Weight* Deflectometer *(LWD).* West Conshohocken, PA: ASTM International.
- Burrow, M.P.N., Chan, A.H.C. & Shein, A., *Deflectometer based analysis of ballasted railway tracks*, In: Proceedings of The Institution of Civil Engineersgeotechnical Engineering, 160(3), pp. 169-177, 2007.
- Cafiso S., Capace B., D'Agostino C., Delfino E., Di Graziano A., *Introduction of new systems for evaluation of ballast bearing capacity*, *BCRRA 2017* Tenth International Conference on the Bearing Capacity of Roads, Railways and Airfields, Athens, June 28/30, 2017.
- Cafiso S., Di Graziano A., D'Agostino C., Pappalardo G., Capace B., *Road Asset Management for Sustainable Development*, 2015 International Conference in Environmental Science and Sustainable Development (ICESSD 2015), Bangkok, Thailand, 25-26 October 2015.
- Cafiso, S., Capace, B., D'Agostino, C., Delfino, M., Di Graziano A., *Monitoring of railway track with light high efficiency systems*. International congress on transport infrastructure and systems 10^{th} – 12^{th} April 2017 Rome (Italy), 2017.
- Cafiso, S., Capace, B., D'Agostino, C., Delfino, M., Di Graziano A., *Application of NDT to railway track inspection*. International Conference on Traffic and Transport Engineering, 24th – 25th November 2016, Belgrade (Serbia), 2016a.
- Cafiso, S., D'Agostino, C., Capace, B., Motta, E., Capilleri, P., *Comparison of in situ devices for the assessment of pavement subgrade stiffness*. 1st IMEKO TC4 International Workshop on Metrology for Geotechnics Benevento, Italy, March 17-18, 2016 b.
- Cai, Z., *Modelling of rail track dynamics and wheel/rail interaction*. PhD thesis, Department of Civil Engineering, Queen's University, Ontario, Canada, 1992.
- Cerniglia, D., Garcia G., Kalay, S. & Prior, F., *Application of Laser Induced Ultrasound for Rail Inspection*. Railway Research Center, 2006.
- Chen, D. H., D. F. Lin, P. H. Liau, and J. Bilyeu, *A Correlation Between Dynamic Cone Penetrometer Values and Pavement Layer Moduli*, Geotechnical Testing Journal, Volume 28, Issue 1, pp. 42–49, January 2005.
- CNR UNI 10006, Costruzione e manutenzione delle strade. Tecniche di impiego delle terre. Road construction and maintenance. Technical provisions for use soils, June 2002.
- Corsaro G., *Compressione, compattazione e portanza di ceneri vulcaniche per il riutilizzo in ambito geotecnico e stradale*, Tesi di Laurea in Ingegneria Civile e Ambientale - Università di Catania, Relatori: Prof. Ing. Ernesto Motta, Prof. Ing. Salvatore Cafiso, Correlatori: Dott. Ing. Piera Paola Capilleri, Dott. Ing. Grazia La Cava, A.A. 2015/2016.

- Daniels, D.J., *Ground Penetrating Radar*, 2nd Edition. IET, 2004.
- De Chiara, F.*, Improvement of railway track diagnosis using ground penetrating radar*, (PhD Thesis). Dissertation partially developed at Laboratório Nacional de Engenharia Civil (LNEC), submitted to the University of Rome "Sapienza" for the degree of Doctor of Philosophy in Civil Engineering, May 2014.
- Dynatest International, *LWDmod Manual.*
- Eriksen, A., Gascoyne, J., & Al-Nuaimy, W., *Improved Productivity & Reliability of Ballast Inspection using Road-Rail Multi-Channel GPR*. Preceedings of Railway Engineering. London, UK: IEEE, 2004.
- Fernandes, J., Paixão, S. Fontul, & Fortunato. E., *The Falling Weight Deflectometer: Application to Railway Substructure Evaluation*, In: Proceedings of the First International Conference on Railway Technology: Research, Development and Maintenance, Civil-Comp Press, Stirlingshire, UK, Paper 130, 2012.
- Fleming, P.R., M. W Frost; and C.D.F Rogers*, A Comparison of Devices for Measuring Stiffness In- situ,* Proceedings of the Fifth International Conference on Unbound Aggregate in Roads, Nottingham, United Kingdom, 2000.
- Gallagher, G.P., Leiper, Q., Williamson, R., Clark, M.R., Forde, M.C., *The application of time domain ground penetrating radar to evaluate railway track ballast*. NDT E Int. 32, 463–468, 1999.
- George K. P., *Falling Weight Deflectometer for Estimating Subgrade Resilient Moduli*, Final Report conducted by the Department of Civil Engineering, University of Mississippi, The Mississippi Department of Transportation, U. S. Department of Transportation, FHWA, October 2003.
- Göbel, C., Hellmann, R., Petzold, H., *Georadar model and in-situ investigations for inspection of railway tracks*, in: Fifth International Conferention on Ground Penetrating Radar, 1994.
- Grassie, S.L. & Cox, S.J., *The dynamic response of railway track with flexible sleepers to high frequency vertical excitation*. Proc Inst Mech Eng Part D; 24:77–90, 1984.
- Hamed F. Kashani, Carlton L. Ho, William P. Clement, and Charles Oden, *Evaluating The Correlation Between Geotechnical Index and Electromagnetic Properties of Fouled Ballasted Track by Full Scale Laboratory Model*, TRB 2016 Annual Meeting.
- Horníček, L. & Břešťovský, P., *Using the Lightweight Falling Deflectometer for Monitoring Trial Railway Sections with Under-Ballast Geocomposites*, Published in: Railway Condition Monitoring (RCM 2014), 6th IET Conference on, 2014.
- Huang, Y. H., *Pavement analysis and design*, Prentice-Hall, 815 p. 1993.
- Hugenschmid, J., *Railway track inspection using GPR. Journal of Applied Geophysics*, 147-155, 1999.

- Humphrey, A., SWOT *Analysis for Management Consulting. SRI Alumni Newsletter*. SRI International.: 7-8, December 2005.
- Jack, R. and Jackson, P., *Imaging attributes of railway track formation and ballast using ground probing radar*, NDT&E International, No. 32, pp. 457-462, 1999.
- Kashani, F.H.; Ho, C.L.; Clement, W.P.; Oden, C., *Evaluating The Correlation Between Geotechnical Index and Electromagnetic Properties of Fouled Ballasted Track by Full Scale Laboratory Model*, In Proceedings of the TRB 2016 Annual Meeting.
- Konur, D., Long, S., Qui, R., Elmore C. & Farhangi H., *Track Inspection Planning and Risk Measurement Analysis*, Missouri University of Science and Technology, Engineering Management and Systems Engineering Department, Final Report Prepared for Missouri Department of Transportation, Project TR201409, Report cmr15-005, 2015.
- Lee, W., Lee, J., Henderson, C., Taylor, H. F. & James, R., Lee, C. E. et al., *Railroad bridge instrumentation with fiber-optic sensors*. Applied Optics, 38(7), 1110-1114.
- Isola M., Betti G., Marradi A., Tebaldi G., *Evaluation of cement treated mixtures with high percentage of reclaimed asphalt pavement*, Construction and Building Materials 48 (2013) 238–247, 2013.
- Mallela, J. & George, K.P., *Three-Dimensional Dynamic Response Model for Rigid Pavements*, Transportation Research Record No. 1448, Transportation Research Board, Washington, D.C. 1994.
- Marradi A., Pinori U., Betti G., *Subgrade and foundation dynamic performance evaluation by means of light weight deflectometer tests*, TRB 2014 Annual Meeting.
- Minnesota Department of transportation, *User Guide to the Dynamic Cone Penetrometer*, 1999, March 1. http://www.dot.state.mn.us/materials/researchdocs/User_Guide.pdf
- Nazzal M.D., M.Y. Abu-Farsakh, K. Alshibli, and L. Mohammad, *Evaluating the light falling weight deflectometer device for in situ measurement of elastic modulus of pavement layers*, Transportation Research Record: Journal of the Transportation Research Board, No. 2016, pp. 13–22. Washington, DC: Transportation Research Board of the National Academies, 2007.
- NDT, H., *A document outlining the emergence of the eddy current NDT inspection method as an important part of rail maintenance and safety,* 2014.
- Neupane, M., Parsons, R.L. & Han, J., *Rapid estimation of fouled ballast material properties.* Transportation Research Board of the National Accademy, Washington DC, Annual Meeting 2016.
- Olhoeft, G. R., and Selig, E. T., *Ground penetrating radar evaluation of railroad track substructure conditions*. Proc. Of the 9th Int'l Conf. on Ground Penetrating Radar, Santa Barbara, CA, April, S. K. Koppenjan and H. Lee, eds., Proc. of SPIE, vol. 4758, p. 48-53, 2002.

- Saaranketo, T., *Electrical properties of road materials and subgrade soils and the use of ground penetrating radar in traffic infrastructure surveys* (PhD Thesis). University of Oulu, 2006.
- Sanfilippo M., *Caratterizzazione in sito di ceneri vulcaniche stabilizzate a cemento per sottofondi stradale,* Tesi di Laurea in Ingegneria Civile e Ambientale - Università di Catania, Relatore: Prof. Ing. Salvatore Cafiso, Correlatori: Dott.ssa Ing. Brunella Capace, Dott. Ing. Carmelo D'Agostino, Dott. Ing. Emanuele Delfino, A.A. 2016/2017.
- Seed, S.B., Alavi, S.H., Ott, W.C., Mikhail, M., and Mactutis, J.A., *Evaluation of Laboratory Determined and Nondestructive Test Based Resilient Modulus Values from WesTrack Experiment,* Nondestructive Testing of Pavements and Backcalculation of Moduli: Third Volume, ASTM STP 1375.
- Selig, E. T. and Waters, J. M., *Track Geotechnology and Substructure Management*. Thomas Telford Services Ltd., London, 1994.
- Selig, E. T., Hyslip, J. P., Olhoeft, G. R., and Smith, Stan, *Ground penetrating radar for track substructure condition assessment.* Proc. Of Implementation of Heavy Haul Technology for Network Efficiency, Dallas, TX, May, p. 6.27-6.33, 2003.
- Sharpe, P.C. & Govan, R., *The use of Falling Weight Deflectometer to Assess the Suitability of Routes for Upgrading*, In: Proceedings of the Second International Conference on Railway Technology: Research, Development and Maintenance, Civil-Comp Press, Stirlingshire, UK, Paper 134, 2014.
- Shell Bitumen, *Bisar 3.0 User Manual.*
- Siekmeier, J., Pinta, C., Merth, S., Jensen, J., Davich, P., Camargo, F., Beyer, M., *Using the Dynamic Cone Penetrometer and Light Weight Deflectometer for Construction Quality Assurance*, Minnesota Department of Transportation, MN/RC 2009-12, Minnesota, 244p, 2009.
- Sundquist H., Byggande, *Drift och Underhåll av Järnvägsbanor*, TRITA-BKN, Rapport 57, KTH, Stockholm 2000 (Compendium in Swedish).
- Sussmann, T.R., Selig, E.T. & Hyslip, J.P., *Railway track condition indicators from ground penetrating radar*. NDT E Int. 36, 157–167, 2003.
- Timoshenko S., *Method of analysis of statistical and dynamical stresses in rail*. In: Proceedings of second international congress for applied mechanics, p. 407–18. Zurich, 1926.
- Tranchina G., *Riutilizzo di ceneri vulcaniche in ambito geotecnico-stradale mediante stabilizzazione a cemento*, Tesi di Laurea in Ingegneria Civile e Ambientale - Università di Catania, *Relatori:* Prof. Ing. Ernesto Motta, Prof. Ing. Salvatore Cafiso, *Correlatori:* Dott. Ing. Piera Paola Capilleri, Dott. Ing. Grazia La Cava, A.A. 2015/2016.
- Transportation, C. B., *Connecticut Railroad Bridge Management Program*, 2012.

- Ullidtz P. *Modelling flexible pavement response and performance*, Copenhagen: Polyteknisk Forlag; 1998.
- UNI EN 1097-1, *Determinazione della resistenza all'usura (Micro-Deval*), 2011.
- UNI EN 13286-47, *Miscele non legate e legate con leganti idraulici. Parte 47: Metodo di prova per la determinazione dell'indice di portanza immediata e del rigonfiamento,* 2012.
- Uzarski, D.R., Brown, D.G., Harris, R.W. & Plotkin, D.E., *Maintenance Management of U.S. Army Railroad Networks-the RAILER System: Detailed Track Inspection Manual*. Champaign, IL: US Army Corps of Engineers; Construction Engineering Research Laboratories, 1993.
- Van Deusan, D.A., Lenngren, C.A., and Newcomb, D.E., *A Comparison of Laboratory and Field Subgrade Moduli at the Minnesota Road Research Project,* Nondestructive Testing of Pavements and Backcalculation of Moduli, ASTM STP 1198, H.L. Von Quintus et al., eds., ASTM, 1994.
- Varrica R., *Caratterizzazione di laboratorio per la stabilizzazione a cemento delle ceneri vulcaniche dell'Etna,* Tesi di Laurea in Ingegneria Civile e Ambientale - Università di Catania, Relatore: Prof. Ing. Salvatore Damiano Cafiso, Correlatori: Dott. Ing. Emanuele Delfino, Dott. Ing. Piera Paola Capilleri, A.A. 2015/2016.
- Yohannes, B., Tan, D., Khazanovich, L. & Hill, K. M., *Mechanistic modelling of tests of unbound granular materials*, International Journal of Pavement Engineering, Vol 15 No 7, pp 584-598, 2014.

CHAPTER 3

QUALITY CONTROL EXPERIMENTAL APPLICATIONS FOR PERFORMANCE BASED SPECIFICATIONS

The construction of a road is aimed at realization of a work that meets the project requirements in all its parts. The control activities can be a precious guide for the improvement of the construction process itself. Since the beginning of the new millennium, even in road engineering, quality has become one of the determining factors for the management of design and construction processes.
Both the road authorities and the construction companies recognized the importance of an approach to controls "Quality Control" inserted into a "Quality Assurance" system.
In fact, a correct approach QA/QC is essential to ensure performance and quality of road infrastructure, which is why it is defined that ***QA+QC= High Quality Infrastructures***.
The road authorities have the maximum interest to acquire a work whose quality is assured by a system of continuous control of the constructive system and furthermore they are interested in reducing the risk of non-compliance in final acceptance checks.
Therefore, operating according to the principles of quality assurance, the construction companies have at their disposal a series of tools through which to improve the production process and reduce the risk of non-compliance that could result in penalties or the rejection of the road authorities.
The quality of a product or service can be defined on the basis of its being appropriate for use. For a road work this translates into the ability to perform the function for which it was conceived. It follows that in order to guarantee quality, it is necessary to control overall design, construction and maintenance activities. In this study the aspects related to quality control are treated in the phase of acceptance of the works that can therefore result in the development of a performance based QA/QC procedures for pavement construction with an applicability of the models in different transport infrastructures and main or local Road Administrations.
It is therefore essential to understand the parameters that most affect the life of road pavements (to program durability and maintenance) and consequently, as soon as this is understood, obtain the indicators and the relationships that can be calculated simply by NDT tests with high-efficiency equipment (Falling Weight Deflectometer, Light Weight Deflectometer, Georadar, Aran, etc..) and therefore in situ measurements.
This chapter covers multiple topics.
In general, the aim is to simulate load bearing capacity NDT tests on road pavements and from these to obtain Basin Indices that, through statistical models, can be correlated with the residual life of the pavements (Esals) and with the Structural Number which is an overall indicator of the structural characteristics of a road infrastructure.
In this way it is possible to predict both Esal and SN directly from NDT tests with Falling Weight Deflectometer.
Moreover, considering in the road works how important it is then that the projects are respected in order to don't have roads with structural deficits already since the works are delivered, and that unfortunately occur over time with consequent damages at the economic-environmental-social level, construction and maintenance costs, which manifests itself in advance respect to the project period due to the damage, have been studied.
From the estimation of costs and their relationship with the structural characteristics of the road pavement, Penalty/Bonus methods have been developed that can be applied in modern

performance-based specifications, implementing them with new indexes or combinations of them that can be even more a support for the delivery of work in a workmanlike manner.

Specifically, in paragraph 3.1, in order to make simulations of NDT tests on roads, a database of road pavements was developed considering the types existing in the Italian Catalog of Road Pavement (CNR).
Moreover, for the calculation of the various parameters that characterize roads, the empirical AASHTO approach was used, the modules of the various pavement layers were calculated (making them also vary in percentage to have a larger sample of data) and reported at the frequencies typical of traditional FWD tests of 16 Hz.
In paragraph 3.2 the Design Esals from the SN were calculated using the empirical AASHTO method. The FWD tests, in 3.3, were simulated using the multi-layer elastic model with the support of the BISAR software, thanks to which it was therefore possible to derive the deflections that are obtained as a result of these NDT tests.
In paragraph 3.4 the Basin Indexes were calculated according to the deflections deriving from FWD tests. At this point, in paragraph 3.5, it was possible to calculate the Design Esals from the SN derived from the NDT tests.
Statistical predictive models, in 3.6, of the Esals and the Structural Number have been obtained starting from the FWD indices.
In paragraphs 3.7 and 3.8, performance-based approaches are investigated using NDT techniques and acceptance requirements in the construction phase of new road pavements.
Two case studies, in 3.9, are developed in order to understand what happens when an as built road pavement has structural deficits. In this part two possible strategies of maintenance are studied: a net overlay on the road pavement built and a solution of milling and overlay with AC and a 40% of RAP.
An estimate of the economic and environmental costs is presented in paragraph 3.10.
In 3.11 are developed the Penalty / Bonus models developed and the results of this study that can be applied in performance-based performance specifications. References are reported in 3.12.

The aim of this Chapter 3 is to positively move the point of view of the specifications: from traditional to performance-based. With a performance-based approach it is certainly possible, with the support of NDT techniques and predictive models, to be able to monitor pavements from the moment they are built looking for, with penalty models or bonuses to avoid initial structural deficits that have consequences of damage accelerated over time, with a consequent shortening of life compared to the designed.

3.1 Calibration procedure for the creation of a database of Road Flexible Pavements

In order to make an analysis on pavements aimed at the development of performance-based specifications in Quality Control of road works, a database of pavements type was created and to do this some pavements were chosen from the Italian reference which is the *Italian Catalog of Road Pavements*. In the following paragraphs, in fact, a detailed analysis will be carried out and all the steps that have been performed to create a suitable database of pavements.

3.1.1 The Italian Catalog of Road Pavements

In this research work, the Italian Catalog of Road Pavements (Catalogo delle Pavimentazioni Stradali, 1995*)* drawn up by the National Research Council (CNR)[29] was chosen as the reference point, from which to start in terms of paving packages.
The scope of this catalog concerns the design of new road pavements and offers a range of solutions for various roads with different traffic and subgrade conditions.

The catalog considers flexible, rigid and semi-rigid pavements with already defined parameters such as traffic, the bearing capacity of the subgrade, the characteristics and the thickness of the layers.

In the present research work only flexible pavements will be considered.

The Italian Catalog of Road Pavements presents tables for 8 categories of road.
It also considers separately, among the rural two-lane secondary roads, those so-called "tourist" (because characterized only by traffic of cars) and, in urban areas, the preferential lanes for public transport.
For the traffic composition, the catalog assumes for each type of road the typical spectra of commercial vehicles with a total mass ≥ 3 tons.

The following Table 27 *and*
Table 28 shows the types of vehicles considered and their axle loads and their frequency, expressed as a percentage, on the total number of commercial vehicles.

Table 27 - Types of commercial vehicles, number of axles, distribution of axle loads. Source: Catalogo delle Pavimentazioni Stradali, 1995

Tipo di veicolo	N° Assi	Distribuzione dei carichi per asse in KN
1) autocarri leggeri	2	↓10 ↓20
2) " "	"	↓15 ↓30
3) autocarri medi e pesanti	"	↓40 ↓80
4) " " "	"	↓50 ↓110
5) autocarri pesanti	3	↓40 ↓80 ↓80
6) " "	"	↓60 ↓100 ↓100
7) autotreni e autoarticolati	4	↓40 ↓90 ↓80 ↓80
8) " "	"	↓60 ↓100 ↓100 ↓100
9) " "	5	↓40 ↓80 ↓80 ↓80 ↓80
10) " "	"	↓60 ↓90 ↓90 ↓100 ↓100
11) " "	"	↓40 ↓100 ↓80 ↓80 ↓80
12) " "	"	↓60 ↓110 ↓90 ↓90 ↓90
13) mezzi d'opera	"	↓50 ↓120 ↓130 ↓130 ↓130
14) autobus	2	↓40 ↓80
15) "	2	↓60 ↓100
16) "	2	↓50 ↓80

[29] The National Research Council (CNR) is the largest public research authority in Italy and has the task of carrying out, promoting, disseminating, transferring and enhancing scientific and technological research in the main areas of knowledge development and their applications for scientific and technological, economic and social development.

Table 28 - Typical traffic spectra of commercial vehicle for each type of road. Source: Catalogo delle Pavimentazioni Stradali, 1995

	Tipo di veicolo															
Tipo di strada	1	2	3	4	5	6	7	8	9	10	11	12	13	14	15	16
1) autostrade extraurbane	12.2	----	24.4	14.6	2.4	12.2	2.4	4.9	2.4	4.9	2.4	4.9	0.10	----	----	12.2
2) " urbane	18.2	18.2	16.5	----	----	----	----	----	----	----	----	----	1.6	18.2	27.3	----
3) strade extr. principali e secondarie a forte traffico	----	13.1	39.5	10.5	7.9	2.6	2.6	2.5	2.6	2.5	2.6	2.6	0.5	----	----	10.5
4) strade extraurb. second. ordin.	----	----	58.8	29.4	----	5.9	----	2.8	----	----	----	----	0.2	----	----	2.9
5) " extr. second.-turistiche	24.5	----	40.8	16.3	----	4.15	----	2	----	----	----	----	0.05	----	----	12.2
6) " urbane di scorrimento	18.2	18.2	16.5	----	----	----	----	----	----	----	----	----	1.6	18.2	27.3	----
7) " " di quartiere e locali	80	----	----	----	----	----	----	----	----	----	----	----	----	20	----	----
8) corsie preferenziali	----	----	---	----	----	----	----	---	----	----	---	----	----	47	53	----

The traffic that the road pavements can withstand is expressed in total number of passes of commercial vehicles transiting on the most loaded lane.

The 6 traffic levels are shown in Table 29.

Table 29 - Traffic levels on the most loaded lane. Source: Catalogo Italiano delle Pavimentazioni Stradali, 1995

Traffic Levels	N. of commercial vehicles
1°	400,000
2°	1,500,000
3°	4,000,000
4°	10,000,000
5°	25,000,000
6°	45,000,000

The parameter chosen in the catalog to characterize the bearing capacity of the subgrade is the "resilient modulus" Mr, which can be evaluated on the basis of experimental tests using the AASHTO T274-82 standard.

The choice of this parameter was dictated by the fact that it better represents the behavior of the subgrade, as it allows to take into account also the reversible viscous component of the deformation. In the catalogue three categories of subgrade of good, medium and low bearing capacity were considered, represented by the values of the resilient module Mr, respectively of 150, 90 and 30 N/mm^2.

The main physical-mechanical characteristics of the materials used in the catalog superstructures are shown Table 30, where different types of traffic T[30] are distinguished:

- PP (very heavy) → T > 22,000,000
- P (heavy) → 8,000,000 < T < 22,000,000
- M (medium) → 3,500,000 < T < 8,000,000
- L (low) → T < 3,500,000

[30] T is the traffic expressed in number of commercial vehicles on the most loaded lane. Source: Catalogo delle Pavimentazioni Stradali, 1995.

Table 30 - Physical-mechanical characteristics of the materials used in the Catalogue. Source: Catalogo Italiano delle Pavimentazioni Stradali, 1995

Conglomerato bituminoso per strato di usura

traffico (1)	granulometria (2)	bitume (%)	stabilità Marshall (75 colpi) (Kg)	stabilità Marshall (75 colpi) (daN)	rigidezza Marshall (Kg/mm)	vuoti residui Marshall (%)
PP	fig. 1	4.5÷6	≥1100	≥1080	300÷450	4÷6
P	"	"	≥1100	≥1080	300÷450	4÷6
M	"	"	≥1000	≥980	>300	3÷6
L	"	"	≥1000	≥980	>300	3÷6

Densità in opera (rispetto alla densità Marshall) ≥ 97%

Conglomerato bituminoso per strato di collegamento

traffico (1)	granulometria (2)	bitume (%)	stabilità Marshall (75 colpi) (Kg)	stabilità Marshall (75 colpi) (daN)	rigidezza Marshall (Kg/mm)	vuoti residui Marshall (%)
PP	fig.2	4.5÷5.5	≥1000	≥980	300÷450	3÷6
P	"	"	≥1000	≥980	300÷450	3÷6
M	"	4÷5.5	≥ 900	≥880	>300	3÷7
L	"	"	≥ 900	≥880	>300	.3÷7

Densità in opera (rispetto alla densità Marshall) ≥ 98%

Conglomerato bituminoso per strato di base

traffico (1)	granulometria (2)	bitume (%)	stabilità Marshall (75 colpi) (Kg)	stabilità Marshall (75 colpi) (daN)	rigidezza Marshall (Kg/mm)	vuoti residui Marshall (%)
PP	fig.3	4÷5	≥800	≥780	>250	4÷7
P	"	"	≥800	≥780	"	"
M	"	3.5÷4.5	≥700	≥690	"	"
L	"	"	≥700	≥690	"	"

Densità in opera (rispetto alla densità Marshall) ≥ 98%

Misto granulare non legato		
CBR (dopo 4gg di immersione in acqua)	CBR ≥ 30%	
Densità (rispetto alla densità AASHTO modificata)	≥ 98%	
Misto cementato	Semirigide	Rigide
Classe di cemento	cemento 197/1 tipo 1÷5	cemento 197/1 tipo 1÷5
Contenuto di cemento	2.5÷3.5%	3.5÷5
Resistenza media a compressione a 7gg	$2.5 \le \sigma_{cm} \le 4.5$ N/mm^2	$4.0 \le \sigma_{cm} \le 7.0$ N/mm^2
Conglomerato cementizio		
Resistenza media a trazione per flessione	$f_{cfm} = 5.5$ N/mm^2 (*) (•)	$f_{cfm} = 4.0$ N/mm^2 (**) (•)
Modulo elastico	E = 47000 N/mm^2 (*)	E = 34000 N/mm^2 (**)
Coefficiente di Poisson	υ = 0.2 (*)	υ = 0.2 (**)

(1) Traffico (T) in numero di autoveicoli commerciali sulla corsia più caricata:

PP (molto pesante)	T > 22.000.000
P (pesante)	8.000.000 < T < 22.000.000
M (medio)	3.500.000 < T < 8.000.000
L (leggero)	T < 3.500.000

(2) Le caratteristiche degli aggregati delle miscele da adottare sono quelle indicate nelle norme CNR per le categorie di traffico PP, P, M ed L individuate in funzione del traffico commerciale complessivo secondo la nota 1.

(*) Per le autostrade extraurbane ed urbane, per le strade extraurbane principali e secondarie a forte traffico e per le urbane di scorrimento.
(**) Per le strade extraurbane secondarie sia ordinarie che turistiche, per le urbane di quartiere e locali e per le corsie preferenziali.
(•) Valori corrispondenti approssimativamente a resistenze caratteristiche cubiche Rck rispettivamente di 55 e 30 N/mm^2.

In addition, the catalog takes into account values of reliability and the Present Serviceability Index PSI, in Table 31, differentiated for the different type of road according to the AASHTO Guide for Design of Pavement Structures.

Table 31 - Reliability and PSI. Source: Catalogo delle Pavimentazioni Stradali, 1995

Tipo di strada	Affidabilità (%)	PSI
1) Autostrade extraurbane	90	3
2) " urbane	95	3
3) Strade extr. principali e secondarie a forte traffico	90	2.5
4) Strade extraurbane secondarie - ordinarie	85	2.5
5) " " " -turistiche	80	2.5
6) Strade urbane di scorrimento	95	2.5
7) " " di quartiere e locali	90	2
8) Corsie preferenziali	95	2.5

The highest reliability values were assumed for the roads located in the urban area, to reduce the risk of the need for reinforcements before the expected deadline, with the consequent serious penalties to traffic.
With regard to the PSI index, higher values have been adopted for motorways to ensure high safety and comfort standards for circulation throughout their entire life cycle.
The pavements of the catalog are included in tables and are identified with an alphanumeric code (with numbers from 1 to 8 indicating the type of road, as indicated in Table 31), and an alphabetical part indicating the type of superstructure:
- F = flexible;
- SR = semi-rigid;
- RG = non-armed rigid;
- RC = rigid with continuous armor.

For each pavement, depending on the subgrade category and the traffic class, the thicknesses and materials constituting the different layers of the pavements are indicated.
In the following Table 32, a solution for a type of road is shown, in order to understand the organization of the range of pavement solutions of the Italian Catalog.
Specifically, the example concerns the Extra-Urban Highways “Autostrade Extraurbane”, with flexible pavement type and different values of subgrade modulus Mr and traffic expressed in number of passages of commercial vehicles.

Table 32 - A solution of the Italian Catalog of Road Pavements for flexible pavements in "Autostrade Extraurbane". Source: Catalogo delle pavimentazioni stradali, 1995.

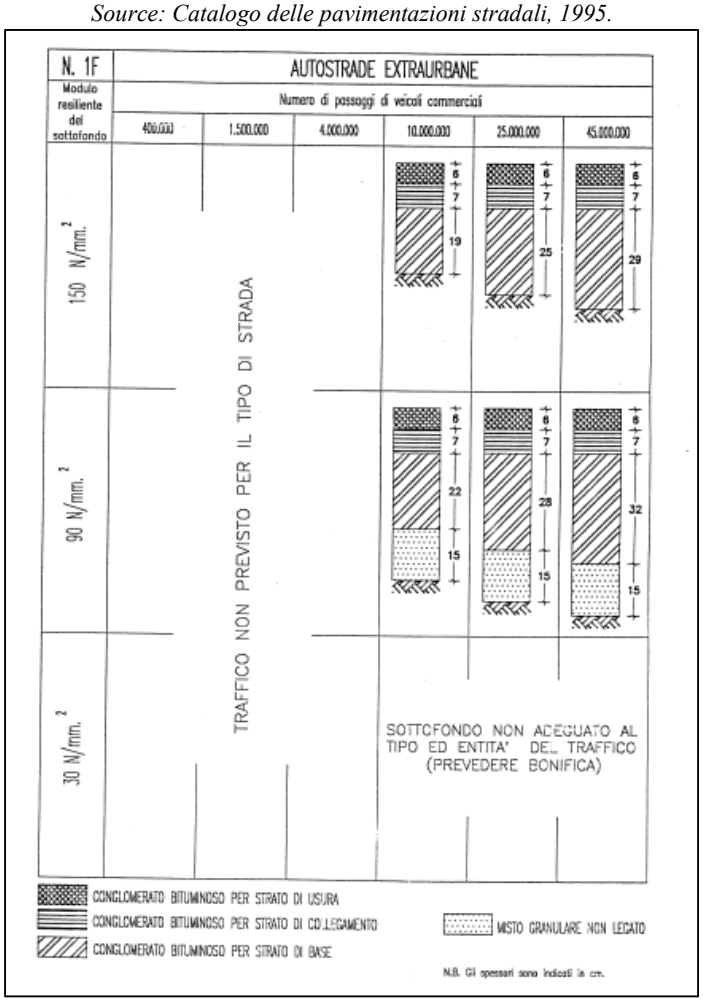

3.1.2 Application of the AASHTO Empirical approach

The Italian Catalog of Road Pavements was the reference for creating a database of flexible road pavements. It must be remembered that for each road pavement (flexible, rigid and semi-rigid) from the catalog were known: the type of road, the thicknesses for each layer (wear, binder, base and foundation if present), the resilient modulus of subgrade and the traffic expressed in number of commercial vehicle passages and type (very heavy, heavy, medium and low). The study that has been carried out concerns flexible pavements.

For these flexible road pavements with the application of the AASHTO empirical method (AASHTO Guide for Design of Pavement Structures, 1993), were calculated: the Structural Number, the ESAL and the traffic that was also possible compare with the solution of the Italian catalog and the modules of the various layers that make up each individual package.

Specifically, in the AASHTO Design Guide, according to the layer thicknesses, a structural indicator that is known as Structural Number SN, expresses the structural strength of the overall pavement. This indicator depends on the individual pavement thicknesses, on the layer coefficients that represent the relative strength of the material and on the drainage coefficients.

Although the empirical approach is now outdated, it certainly turns out to be an instrument of simple application in the calculation of some road parameters. In fact in this case, the reason why it was used is to verify the data deriving from the Italian Catalog for the different road types, calculating the traffic, the layer coefficients, the modules of the various layers and the Structural Number for different types of traffic, with the goal to calibrate a database of pavements comprehensive of different road types.

The Structural Number indicative of the total pavement thickness is:

$$SN = a_1 \cdot D_1 + a_2 \cdot D_2 \cdot m_2 + a_3 \cdot D_3 \cdot m_3$$

Where: $a_i = i^{th}$ layer coefficient; $D_i = i^{th}$ layer thickness; $m_i = i^{th}$ layer drainage coefficient.

Having made this important premise (hereafter will be more understandable the reasons), on all the flexible pavements present in the Italian catalog was iteratively defined (see **Appendix 1 and 2**) the values of layer coefficients that comply with the catalog design assumptions.

Two types of combinations were chosen: the first concerning pavements with very heavy and heavy traffic; the second with medium and low traffic.

The following a_i layer coefficients[31] depending on the type of traffic were selected:

- $a_1 = 0.43$, $a_2 = 0.26$, $a_3 = 0.12$ in cases of very heavy and heavy traffic;
- $a_1 = 0.41$, $a_2 = 0.24$, $a_3 = 0.11$ in cases of medium and low traffic;
- in case of road pavements without foundation obviously $a_3 = 0$.

As far as traffic calculations are concerned, the Esals derive from the following AASHTO equations:

$$\left.\begin{array}{l} \log_{10}\left(\frac{w_x}{w_{18}}\right) = 4,79\log_{10}(18+1) - 4,79\log_{10}(L_x + L_2) + 4,79\log_{10}(L_2) + \frac{G}{\beta_x} - \frac{G}{\beta_{18}} \\ \left\{\begin{array}{l} G = \log_{10}\left(\frac{4,2 - P_t}{4,2 - 1,5}\right) \\ \beta_x = 0,40 + \frac{0,081\cdot(L_x + L_2)^{3,23}}{(SN_f + 1)^{5,19}\cdot L_2^{\,3,23}} \\ \beta_{18} = 0,40 + \frac{0,081\cdot(L_x + L_2)^{3,23}}{(SN_f + 1)^{5,19}\cdot L_2^{\,3,23}} \qquad (L_2 = 1 \text{ (asse singolo)};\ L_x = 18 \text{ kips}) \end{array}\right. \end{array}\right\} \Rightarrow F.E._i = \frac{1}{\left(\frac{w_x}{w_{18}}\right)}$$

[31] Layer coefficients: a_1 is representative of wear and binder layer, a_2 of base layer, a_3 of foundation layer.

$$\log_{10}(w_{18}) = Z_R \cdot S_0 + 9,36\log_{10}(SN+1) - 0,20 + \frac{\log_{10}\left(\frac{\Delta PSI}{4,2-1,5}\right)}{0,40 + \frac{1094}{(SN+1)^{5,19}}} + 2,32\log_{10}(M_r) - 8,07$$

Where: w_{18} = predicted number of 18-kip equivalent single axle load applications, Z_R = standard normal deviate, S0 = combined standard error of the traffic prediction and performance prediction, ΔPSI = difference between the initial design serviceability index p_0 and the design terminal serviceability index p_t, M_R = resilient modulus (psi).

The amount of traffic in the catalog is a value proportional to the Esal, as in general $Esal_i = Traffic_i \cdot FE_i$.

Note all these relationships, it is clear that the calculations must be made for each individual type of road which in turn is made up of different vehicle traffic spectra typically present in different percentages. It was therefore simple to calculate for each different road the transformation coefficients FEi which allow to quickly switch from Esal to Traffic.

Details of the calculations for all catalog packages are in **Appendix 2** with the detail of calculation of traffic and layer coefficients: here it was possible to compare the traffic of the catalog with that calculated by AASHTO, thus finding the layer coefficients (traffic dependent) that best represent each road.

Given these values having made the investigation of all the solutions in the catalog, some packages representative of some SN values were selected, which are precisely those that make up the database on which to work for performance studies and quality control.

Once the database has been created and some pavement packages have been chosen (representative of very heavy and heavy, medium and low traffic), at this point knowing the layers' coefficient ai, from them it is possible to calculate the modules representing the stiffness characteristics of the various pavement layers that are wear, binder, base, subbase and subgrade.

Considering that the module of the subgrade is known, as already provided by the catalog solutions, then from the coefficients layers a_1, a_2, a_3 the modules of wear and binder, base and foundation, respectively, were calculated.

This was done with the AASHTO methodology that defines the following formulas:

$$a_1 = 0.3889 \cdot \log_{10}(M_{r1}) - 1.7608$$
$$a_2 = 0.00007 \cdot M_{r2}^{0.6613}$$
$$a_3 = 0.227 \cdot \log_{10}(E_{SB}) - 0.839$$

From the AASHTO formulas, it is possible to derive the Modules Mr1, Mr2, Mr3 of the pavement layers corresponding to the material coefficients ai assumed in the catalog:

1) $Mr1 = 10^{[(a1+1.7608)/0.3889]}$
2) $Mr2 = (a_2/0.00007)^{(1/0.6613)}$
3) $Mr3 = 10^{[(a3+0.389)/0.227]}$

It's good to remember that the resilient modulus of Asphalt layers is determined with a laboratory test performed at a frequency equivalent to 5Hz and at temperature of 20°C.

In Table 33 there are showed the results of the application of the AASHTO method for one of the road pavements of the Italian Catalog.

Table 33 – Application of the AASHTO Empirical Method to the road pavements of the Italian Catalog

ID Pav.	Case	a1	a2	a3	M1 [Mpa]	M2 [Mpa]	M3 [Mpa]	Ms [Mpa]	h1 [mm]	h2 [mm]	h3 [mm]	SN [cm]	SN [inch]
Ms 30 (M-L)	0	0.41	0.24	0.11	2632.89	1528.40	104.51	30	110	170	350	12.44	4.90
Ms 30 (PP-P)	0	0.43	0.26	0.12	2963.87	1725.06	115.67	30	110	220	350	14.65	5.77
Ms 90 (M-L)	0	0.41	0.24	0.11	2632.89	1528.40	104.51	90	130	160	150	10.82	4.26
Ms 90 (PP-P)	0	0.43	0.26	0.12	2963.87	1725.06	115.67	90	110	170	150	10.95	4.31
Ms 150 (M-L)	0	0.41	0.24		2632.89	1528.40		150	130	140		8.69	3.42
Ms 150 (PP-P)	0	0.43	0.26		2963.87	1725.06		150	110	170		9.15	3.60
MS 30 (L) 9-15-35	0	0.41	0.24	0.11	2632.89	1528.40	104.51	30	90	150	350	11.14	4.39
MS90 (L) 9-12-15	0	0.41	0.24	0.11	2632.89	1528.40	104.51	90	90	120	150	8.22	3.24
MS150 (L) 9-11	0	0.41	0.24		2632.89	1528.40		150	90	110		6.33	2.49
MS 30 (M) 13-20-35 (8F)	0	0.41	0.24	0.11	2632.89	1528.40	104.51	30	130	200	350	13.98	5.50
MS 90 (P) 11-18-15 (3F)	0	0.43	0.26	0.12	2963.87	1725.06	115.67	90	110	180	150	11.21	4.41
MS 90 (PP) 11-25-15 (6F)	0	0.43	0.26	0.12	2963.87	1725.06	115.67	90	110	250	150	13.03	5.13
MS 90 (M) 10-8-15 (7F)	0	0.41	0.24	0.11	2632.89	1528.40	104.51	90	100	80	150	7.67	3.02

Where: ID Pav. = identification name of each pavement package; a1, a2, a3 = layer coefficients; M1= wear and binder modulus; M2 = base modulus; M3 = foundation modulus; Ms = subgrade modulus; h1=wear + binder thickness; h2 = base thickness; h3 = foundation thickness; SN = Structural Number.

As anticipated, the purpose of this research work is to make surveys of a performance type, so it is necessary to know the indexes, related to the bearing capacity and the structural conditions, that can be related to the life of the pavement.
In the road sector, and as indicated in the ANAS specifications, but also in international specifications, the tests are carried out with high performance equipment such as Falling Weight Deflectometer, which returns stress and deformations in output that can then be processed to have structural indexes.
The FWD tests are actually done with frequencies of 16 Hz, so first of all the data, and therefore the modules must be referred at this frequency: all this will be discussed in the next paragraph.

3.1.3 Calculation of the layer's modules by using the Fonseca & Witczak model edited by NCHRP 1-37A 2004 with the MEPDG method and performance test considerations (AC wear and binder, AC base, granular foundation and subgrade)

In order to simulate FWD tests on the database of road pavements, from which to derive deflections and then calculate the basin indexes, it is necessary to consider that they are typical carried out at higher frequencies around 16 Hz. The empirical AASHTO method that has just been exposed and the procedure that has been followed refers to lower frequencies that are around 5 Hz,and it was used just to verify the data deriving from the Italian Catalog.
For this reason, with an MEPDG approach, the modules were obtained by making some hypothesis (volumetric, materials, etc.) for the layers in AC and estimates for the unbound layers such as subbase and subgrade. In this regard, the calculation was made at 16 Hz and a reference temperature of 20°C, in order to be in line with the performance specifications, with the 2 following formula and considerations:

- the dynamic modulus E* of bounded layers in AC, i.e. wear, binder, base, were calculated with the equation proposed by Fonseca and Witczak (1996) and used in the mechanistic empirical method (MEPDG) edited by NCHRP[32] 1-37 A 2004. Witczak and Fonseca have developed and modified a predictive equation for estimating |E*| of asphalt concrete as a function of mix design inputs and asphalt binder properties using a large database of thousands of dynamic modulus test data points:

$$\log E^* = 3.750063 + 0.02932\rho_{200} - 0.001767(\rho_{200})^2 - 0.002841\rho_4 - 0.058097V_a$$
$$- 0.802208\left(\frac{V_{beff}}{V_{beff} + V_a}\right) + \frac{3.871977 - 0.0021\rho_4 + 0.003958\rho_{38} - 0.000017(\rho_{38})^2 + 0.005470\rho_{34}}{1 + e^{(-0.603313 - 0.313351\log(f) - 0.393532\log(\eta))}}$$

where:

E* = dynamic modulus [10^5 psi]
ρ_{200} = % passing the no. 200 ASTM (0.075 mm) sieve, %
ρ_4 = % retained on the n. 4 ASTM (4.75 MM) SIEVE, %
ρ_{38} = % retained on the 3/8 in (9.5 mm) sieve, %
ρ_{34} = % retained on the 3/4 in (19.0 mm) sieve, %
V_v = void Volume, %
V_{be} = effective bitumen content, % by volume
f = loading frequency [Hz]
η = bitumen viscosity [10^6 poise]
log (log η) = A + VTS Log T_R; (A, VTS = regression parameters; T_R = Temperature [°R])

For this calculation, as as already mentioned, some hypothesis were made and the details of the parameters used for AC layers can be consulted in **Appendix 3.**

- For subbase and subgrade that are unbound layers in granular material, other considerations have been made.
  Considering that between the FWD tests and the AASHTO modules there are overestimations of about 33%, then the modules have been calculated dividing the modules in the catalog for 0.33. Simply by applying the following formula that allows to have the modules at a frequency of 16 Hz:

$$Mr_{FWD} = Mr_{AASHTO}/0.33$$

Each of these pavements, corresponding to the Italian catalog cases, have been defined as "Case 0". It's important to make this premise just to understand why these packages have been identified as "Case 0": they were so called 0, as a reference case, because later each of the calculated modules

[32] NCHRP: The NCHRP is administered by the Transportation Research Board (TRB) and sponsored by the member departments (i.e., individual state departments of transportation) of the American Association of State Highway and Transportation Officials (AASHTO), in cooperation with the Federal Highway Administration (FHWA). Individual projects are conducted by contractors with oversight provided by volunteer panels of expert stakeholders. the National Cooperative Highway Research Program (NCHRP) addresses issues integral to the state Departments of Transportation (DOTs) and transportation professionals at all levels of government and the private sector. The NCHRP provides practical, ready-to-implement solutions to pressing problems facing the industry.

has been changed in percentage in order to make simulations of as built differences. But, this will be explained in detail later.

At this point, selected the pavement packages, complete with all the layers of wear and binder, base, foundation, all the calculations have been made concerning the modules with the two procedures just explained for bound and unbound layers, and with these results clearly from the known formulas the layer coefficients have been obtained again.

The calculations for completeness have been done both at 5 and at 16 Hz for all the modules for the Case 0. In Table 34: N. is the number to which correspond an ID Pav. that is the identification name of each road pavement; a1, a2, a3 are the layer coefficients for the calculation of the SN; M1, M2, M3, Ms are the modulus of wear+binder, base, foundation and subgrade at 5 and 16 Hz; h1, h2, h3 represents the thickness of wear+ binder, base and foundation; SN is the Structural Number calculated in cm and in inch.

Table 34 –Results of Modules at 5 and 16 Hz with Fonseca & Witczak and performance test considerations

					5Hz				16 Hz								
N.	**Id.**	**a1**	**a2**	**a3**	**M1 [Mpa]**	**M2 [Mpa]**	**M3 [Mpa]**	**Ms [Mpa]**	**M1 [Mpa]**	**M2 [Mpa]**	**M3 [Mpa]**	**Ms [Mpa]**	**h1 [mm]**	**h2 [mm]**	**h3 [mm]**	**SN [cm]**	**SN [inch]**
1	Ms 30 (M-L)	0.42	0.33	0.11	2766	2505	104.5	30	3643	3342	316.69	90.9	110	170	350	14.11	5.55
2	Ms 30 (PP-P)	0.42	0.33	0.12	2766	2505	115.7	30	3643	3342	350.50	90.9	110	220	350	16.12	6.35
3	Ms 90 (M-L)	0.42	0.33	0.11	2766	2505	104.5	90	3643	3342	316.69	272.7	130	160	150	12.41	4.89
4	Ms 90 (PP-P)	0.42	0.33	0.12	2766	2505	115.7	90	3643	3342	350.50	272.7	110	170	150	12.06	4.75
5	MS 30 (L) 9-15-35	0.42	0.33	0.11	2766	2505	104.5	30	3643	3342	316.69	90.9	90	150	350	12.61	4.96
6	MS90 (L) 9-12-15	0.42	0.33	0.11	2766	2505	104.5	90	3643	3342	316.69	272.7	90	120	150	9.41	3.70
7	MS 30 (M) 13-20-35 (8F)	0.42	0.33	0.11	2766	2505	104.5	30	3643	3342	316.69	90.9	130	200	350	15.94	6.28
8	MS 90 (P) 11-18-15 (3F)	0.42	0.33	0.12	2766	2505	115.7	90	3643	3342	350.50	272.7	110	180	150	12.39	4.88
9	MS 90 (PP) 11-25-15 (6F)	0.42	0.33	0.12	2766	2505	115.7	90	3643	3342	350.50	272.7	110	250	150	14.72	5.80
10	MS 90 (M) 10-8-15 (7F)	0.42	0.33	0.11	2766	2505	104.5	90	3643	3342	316.69	272.7	100	80	150	8.50	3.34

In particular, for the research goal to simulate FWD tests, where chosen only the values of frequency of 16 Hz that are representative of these type of NDT tests.

For this reason, it was considered appropriate to carry out in situ tests with the Falling Weight Deflectometer at different loads and heights, in order to verify that the frequency is about 16 Hz.

The results in **Appendix 4** confirmed this frequency of 16 Hz, the tests were carried out with two types of load (at 250 and 400 Kg) to 4 different loading heights on which 4 drops were made each time.

The tests were carried out with the equipment FWD of the TI Lab of the University of Catania, with FWD Dynatest 8000.

3.1.4 Percentage variation of the individual layer modules for each pavement structure

The last step for the creation of a database with a high number of data and also a high variability with all the premises made up to now, is certainly to implement the data field for each road pavement.
Therefore, for each pavement structure the individual modules have been changed, let's see how.
Starting from each individual case called "Case 0", for each road pavement, it was made a variation of the individual layer modules with percentages of -20%, -10%, 0%, +15%.
In this way they were obtained 16 cases for each pavement with the variation of the single module leaving the rest constant, and another 2 cases per package with simultaneous variation of the modules M1(wear and binder) and M2 (base) of -20% and + 15%. In Table 35 the variation of the modules for a pavement package.

Table 35 - Variation of the individual layer modules in percentage of -20%, -10%, 0, +15% for a pavement package with 16 Hz frequency

					5 Hz				16 Hz							
Id. Pav.	**D**	**a1**	**a2**	**a3**	**M1 [Mpa]**	**M2 [Mpa]**	**M3 [Mpa]**	**Ms [Mpa]**	**M1 [Mpa]**	**M2 [Mpa]**	**M3 [Mpa]**	**Ms [Mpa]**	**h1 [mm]**	**h2 [mm]**	**h3 [mm]**	**D code**
Ms 30 (M-L)	***-20%***	0.38	0.33	0.11	2212.8	2505.0	104.5	30.0	2914.4	3342.0	316.7	90.9	110	170	350	**M1**
Ms 30 (M-L)	***-10%***	0.40	0.33	0.11	2489.4	2505.0	104.5	30.0	3278.7	3342.0	316.7	90.9	110	170	350	**M1**
Ms 30 (M-L)	***0%***	0.42	0.33	0.11	2766.0	2505.0	104.5	30.0	3643.0	3342.0	316.7	90.9	110	170	350	**O**
Ms 30 (M-L)	***15%***	0.44	0.33	0.11	3180.9	2505.0	104.5	30.0	4189.5	3342.0	316.7	90.9	110	170	350	**M1**
Ms 30 (M-L)	***-20%***	0.42	0.29	0.11	2766.0	2004.0	104.5	30.0	3643.0	2673.6	316.7	90.9	110	170	350	**M2**
Ms 30 (M-L)	***-10%***	0.42	0.31	0.11	2766.0	2254.5	104.5	30.0	3643.0	3007.8	316.7	90.9	110	170	350	**M2**
Ms 30 (M-L)	***0%***	0.42	0.33	0.11	2766.0	2505.0	104.5	30.0	3643.0	3342.0	316.7	90.9	110	170	350	**O**
Ms 30 (M-L)	***15%***	0.42	0.36	0.11	2766.0	2880.8	104.5	30.0	3643.0	3843.3	316.7	90.9	110	170	350	**M2**
Ms 30 (M-L)	***-20%***	0.42	0.33	0.09	2766.0	2505.0	83.6	30.0	3643.0	3342.0	253.4	90.9	110	170	350	**M3**
Ms 30 (M-L)	***-10%***	0.42	0.33	0.10	2766.0	2505.0	94.1	30.0	3643.0	3342.0	285.0	90.9	110	170	350	**M3**
Ms 30 (M-L)	***0%***	0.42	0.33	0.11	2766.0	2505.0	104.5	30.0	3643.0	3342.0	316.7	90.9	110	170	350	**O**
Ms 30 (M-L)	***15%***	0.42	0.33	0.12	2766.0	2505.0	120.2	30.0	3643.0	3342.0	364.2	90.9	110	170	350	**M3**
Ms 30 (M-L)	***-20%***	0.42	0.33	0.11	2766.0	2505.0	104.5	24.0	3643.0	3342.0	316.7	72.7	110	170	350	**Ms**
Ms 30 (M-L)	***-10%***	0.42	0.33	0.11	2766.0	2505.0	104.5	27.0	3643.0	3342.0	316.7	81.8	110	170	350	**Ms**
Ms 30 (M-L)	***0%***	0.42	0.33	0.11	2766.0	2505.0	104.5	30.0	3643.0	3342.0	316.7	90.9	110	170	350	**O**
Ms 30 (M-L)	***15%***	0.42	0.33	0.11	2766.0	2505.0	104.5	34.5	3643.0	3342.0	316.7	104.5	110	170	350	**Ms**

Where: D is the percentage of variation of modules; ai are the layer coefficients; M_i are the modules (at 5 Hz and 16 Hz) calculated with respect to the percentage of variation established, respectively of wear and binder, base, foundation, subgrade; h_i represents the layer thickness of wear and binder, base and foundation; Dcode is the code that indicates which of the modules has been changed in percentage, considering that the rest of the modules don't change.

The calculations forll road pavements analyzed are in **Appendix 5**, which represents the database of data with 180 configurations on which all the research studies are conducted, and therefore the sensitivity analyzes on the behavior of the various parameters. All this aimed at creating a protocol of rules on the control parameters/indexes to be adopted in the acceptance phase of the works with standardized procedures and methods.

3.2 Calculation of Design Esals from the AASHTO Structural Number

The database created at this point contains all the information for the calculation of the ESAL on the various pavements, which depend on two important fundamental parameters: the Subgrade Modulus and the Structural Number.
The Subgrade modulus Mr in the Esal calculation is in psi and derives from the input data of the Italian Catalog of Road Pavements.

The Structural Number, as we have already seen, depends on the layer coefficients a_i, the drainage coefficients m, the thickness of the pavement. The approach is that of the AASHTO method[33], where: SN = a1 · D1 + a2 · D2 · m2 + a3 · D3 · m3 (AASHTO Guide for Design of Pavement Structures, 1993). The drainage coefficients m are considered equal to 1; a_i are calculated from the AASHTO formulas; and D (or hi) is the layer thickness (ref. table above).
The Esal that derives from the following equation, as has already been widely explained, depend on SN and Mr in terms of the main parameters.

$$\log_{10}(w_{18}) = Z_R \cdot S_0 + 9,36\log_{10}(SN+1) - 0,20 + \frac{\log_{10}\left(\frac{\Delta PSI}{4,2-1,5}\right)}{0,40 + \frac{1094}{(SN+1)^{5,19}}} + 2,32\log_{10}(M_r) - 8,07$$

For the other parameters contained in the formula the following values have been assumed:
S_0=0.40; Z_R=0 (i.e. 50% reliability); ΔPSI = $p_0 - p_t$, where p_0 = 4.2, p_t = value dependent on the type of road, as reported in the Italian Catalog of road pavements.

Table 36 - Esals and Structural Number of a road pavements calculated from the Database

Id. Pav.	D	a1	a2	a3	h1 [mm]	h2 [mm]	h3 [mm]	Dcode	Esal0%	Esalmod	DEsal	Mr [psi]	SN [cm]	SN [inch]	DSN
Ms 30 (M-L)	*-20%*	0.38	0.33	0.11	110	170	350	M1	2.40E+07	1.93E+07	-20%	4350.98	13.69	5.39	-3%
Ms 30 (M-L)	*-10%*	0.40	0.33	0.11	110	170	350	M1	2.40E+07	2.17E+07	-10%	4350.98	13.91	5.48	-1%
Ms 30 (M-L)	*0%*	0.42	0.33	0.11	110	170	350	O	2.40E+07	2.40E+07	0%	4350.98	14.11	5.55	0%
Ms 30 (M-L)	*15%*	0.44	0.33	0.11	110	170	350	M1	2.40E+07	2.75E+07	14%	4350.98	14.37	5.66	2%
Ms 30 (M-L)	*-20%*	0.42	0.29	0.11	110	170	350	M2	2.40E+07	1.59E+07	-34%	4350.98	13.33	5.25	-6%
Ms 30 (M-L)	*-10%*	0.42	0.31	0.11	110	170	350	M2	2.40E+07	1.97E+07	-18%	4350.98	13.73	5.40	-3%
Ms 30 (M-L)	*0%*	0.42	0.33	0.11	110	170	350	O	2.40E+07	2.40E+07	0%	4350.98	14.11	5.55	0%
Ms 30 (M-L)	*15%*	0.42	0.36	0.11	110	170	350	M2	2.40E+07	3.18E+07	33%	4350.98	14.66	5.77	4%
Ms 30 (M-L)	*-20%*	0.42	0.33	0.09	110	170	350	M3	2.40E+07	1.60E+07	-33%	4350.98	13.34	5.25	-5%
Ms 30 (M-L)	*-10%*	0.42	0.33	0.10	110	170	350	M3	2.40E+07	1.99E+07	-17%	4350.98	13.74	5.41	-3%
Ms 30 (M-L)	*0%*	0.42	0.33	0.11	110	170	350	O	2.40E+07	2.40E+07	0%	4350.98	14.11	5.55	0%
Ms 30 (M-L)	*15%*	0.42	0.33	0.12	110	170	350	M3	2.40E+07	3.08E+07	28%	4350.98	14.59	5.74	3%
Ms 30 (M-L)	*-20%*	0.42	0.33	0.11	110	170	350	Ms	2.40E+07	1.43E+07	-40%	3480.78	14.11	5.55	0%
Ms 30 (M-L)	*-10%*	0.42	0.33	0.11	110	170	350	Ms	2.40E+07	1.88E+07	-22%	3915.88	14.11	5.55	0%
Ms 30 (M-L)	*0%*	0.42	0.33	0.11	110	170	350	O	2.40E+07	2.40E+07	0%	4350.98	14.11	5.55	0%
Ms 30 (M-L)	*15%*	0.42	0.33	0.11	110	170	350	Ms	2.40E+07	3.32E+07	38%	5003.63	14.11	5.55	0%

Where: Id.Pav = identification name of the pavement; ai = layer coefficients; hi = thickness of the layers; Dcode = code that indicates which of the modules has been changed in percentage; Esal0% = Esal calculated for Case 0; Esalmod = Esal calculated in individual cases that consider percentage variations; Desal = is the delta Esal in relation and with respect to Case 0; Mr = subgrade modulus in psi; SN = Structural Number in cm and in inch; DSN = delta SN in relation and with respect to case 0.

[33] Considering that the AASHTO method refers to a frequency of 5Hz, the layer coefficients are referred to this frequency and consequently also the reference modules. In the specific case, the only module that interests, given that it is finalized to Esal, is that of the subgrade calculated in psi.

The Table 36 shows the calculation details for one Id. Pav., the calculations on the whole database are shown in **Appendix 6**. In this way the Esal are calculated according to the Structural Number deriving from the layer's coefficients ai.

3.3 Falling Weight Deflectometer test simulations: deflections and strains

The database with the road pavement modules, with their variability, have been indispensable to simulate a FWD test through the theory of the elastic multilayer.
Therefore, in this regard, this was done with the dedicated Bisar software (Figure 65) which allowed the calculation of the deflections in a multilayer elastic system, where the thicknesses and the modules of the various pavement layers were used as input data. Surface deflections were used as simulated data of FWD test.

Figure 65 - Bisar 3.0 developed by Shell Bitumen, 1998

With Bisar it was also possible to obtain the strains at the critical points, i.e. the interface points of the base-subbase and subbase-subgrade, in order to be able to carry out subsequent checks as well. The use of Bisar makes it possible to have a large database of data and to simulate high-efficiency NDT tests as if they really had been carried out in situ with the Falling Weight Deflectometer.
To perform these tests, the input data of a typical FWD test were entered, and this for all the pavements of the database created with the variability of the modules, thus having a very large amount of data.

Input data:

- Load = 40 KN;
- Radius of loading plate = 0.15 m;
- Pressure P = 565.88 KPa;
- Spring compliance = 0;
- Poisson coefficients ν for each layer: ν1 (Wear+Binder)=0.45; ν2 (Base)=0.45; ν3 (Subbase)=0.30; ν4 (Subgrade)=0.35.
- Points for which to obtain with the simulations deflections and strains, (hereinafter in Figure 66 a scheme, the point 0 represents the center of the load plate):

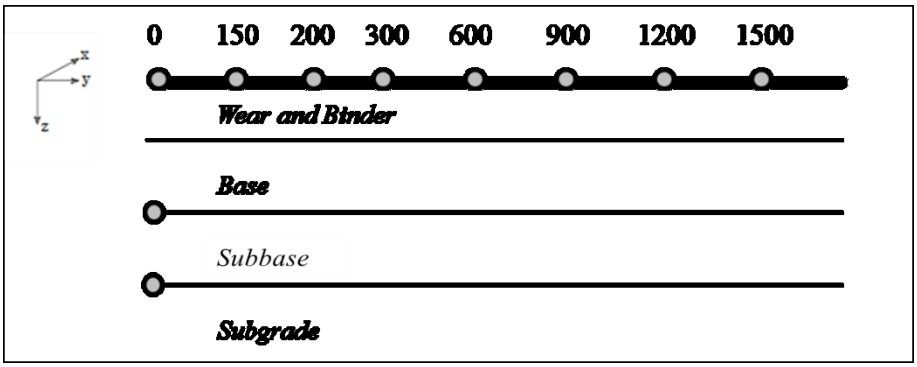

Figure 66 - Bisar control points used for FWD test simulations

In the scheme, the point 0 represents the center of the load plate, the other horizontal points are representative of the geophones positions. The vertical points are the critical points that will be used to obtain the strains at the interface base-foundation and foundation-subgrade.

- Thicknesses of layers;
- Modules of layers.

Output Data:

- Deflections at 0, 200, 300, 450, 600, 900, 1200, 1500 mm from the loading plate;
- Horizontal strain at the base-foundation interface and vertical strain at foundation-subgrade interface.

In Figure 67 a Bisar output for one road pavement of the database.

Project:	16hz 30 - MR1 M L -20%												
Calculated	31-Jan-2018 15.52.44												
System:	1: (untitled)												
		Modulus				Vertical	Vertical	Horz. (Shear)	Horz. (Shear)				Shear
Layer	Thickness	Elasticity	Poisson's		Load	Load	Stress	Load	Stress	Radius	X-Coordin	Y-Coordinate	Angle
Number	(m)	(MPa)	Ratio		Number	(kN)	(MPa)	(kN)	(MPa)	(m)	(m)	(m)	(Degrees)
1	0.11	2.91E+03	0.45		1	4.00E+01	5.66E-01	0.00E+00	0.00E+00	1.50E-01	0.00E+00	0.00E+00	0.00E+00
2	0.17	3.34E+03	0.45										
3	0.35	3.17E+02	0.3										
4		9.09E+01	0.35										
						Stress	Stress	Stress	Strain	Strain	Strain	Displacem	Displacement	Displacement
Position	Layer	X-Coordin	Y-Coordin	Depth		XX	YY	ZZ	XX	YY	ZZ	UX	UY	UZ
Number	Number	(m)	(m)	(m)		(MPa)	(MPa)	(MPa)	µstrain	µstrain	µstrain	(µm)	(µm)	(µm)
1	1	0.00E+00	0.00E+00	0.00E+00		-7.95E-01	-7.95E-01	-5.66E-01	-6.27E+01	-6.27E+01	5.13E+01	0.00E+00	0.00E+00	2.39E+02
2	1	0.00E+00	1.50E-01	0.00E+00		-5.20E-01	-4.83E-01	-2.83E-01	-6.04E+01	-4.18E+01	5.80E+01	0.00E+00	-9.05E+00	2.18E+02
3	1	0.00E+00	2.00E-01	0.00E+00		-2.38E-01	-1.90E-01	0.00E+00	-5.25E+01	-2.86E+01	6.63E+01	0.00E+00	-1.05E+01	2.05E+02
4	1	0.00E+00	3.00E-01	0.00E+00		-1.89E-01	-1.41E-01	0.00E+00	-4.31E+01	-1.92E+01	5.10E+01	0.00E+00	-1.29E+01	1.90E+02
5	1	0.00E+00	6.00E-01	0.00E+00		-8.51E-02	-3.04E-02	0.00E+00	-2.45E+01	2.70E+00	1.79E+01	0.00E+00	-1.47E+01	1.54E+02
6	1	0.00E+00	9.00E-01	0.00E+00		-4.14E-02	1.79E-03	0.00E+00	-1.45E+01	7.02E+00	6.13E+00	0.00E+00	-1.31E+01	1.25E+02
7	1	0.00E+00	1.20E+00	0.00E+00		-2.16E-02	1.07E-02	0.00E+00	-9.09E+00	7.04E+00	1.68E+00	0.00E+00	-1.09E+01	1.02E+02
8	1	0.00E+00	1.50E+00	0.00E+00		-1.18E-02	1.23E-02	0.00E+00	-5.96E+00	6.04E+00	-7.11E-02	0.00E+00	-8.94E+00	8.48E+01
9	2	0.00E+00	0.00E+00	2.80E-01		4.29E-01	4.29E-01	-5.88E-02	7.86E+01	7.86E+01	-1.33E+02	0.00E+00	0.00E+00	2.20E+02
10	3	0.00E+00	0.00E+00	2.80E-01		1.04E-02	1.04E-02	-5.88E-02	7.86E+01	7.86E+01	-2.05E+02	0.00E+00	0.00E+00	2.20E+02
11	3	0.00E+00	0.00E+00	6.30E-01		2.16E-02	2.16E-02	-1.38E-02	6.07E+01	6.07E+01	-8.44E+01	0.00E+00	0.00E+00	1.79E+02
12	4	0.00E+00	0.00E+00	6.30E-01		1.06E-03	1.06E-03	-1.38E-02	6.07E+01	6.07E+01	-1.60E+02	0.00E+00	0.00E+00	1.79E+02

Figure 67 - Bisar Output of a road pavement of the database

In this research work then the analysis of the output data will be done and will be correlated to the Esal in order to see what are the relationships and therefore the links between the performance indices and the life of the pavements for the creation of models that can be used as technical specifications by professionals in the sector.

In the following paragraph 3.3.1 there are the statistical analysis made on the database to obtain relationships between horizontal or vertical strains with FWD deflections and indices.

3.3.1 Prediction of horizontal and vertical strains from NDT Indices

With the data available in terms of strains from the calculations on the database of 180 pavements combinations with the Bisar simulation of a Falling Weight Deflectometer test, it was important to make a statistical analysis to see the relationship between the horizontal and vertical strain and different parameters deriving from non-destructive techniques.
From a literature review, it has been seen how at national and international level there are statistical models able to predict critical strains by linking them to the structural indices deriving from the deflection basins and also to the thickness of the layers.
Mallick et al. (2013), in "Pavement Engineering: Principle and Practice", an important book that is a good reference in the field of road paving studies, have reported relationships between deflection bowl parameters and stresses and strains at various locations in the pavement.
In particular, the horizontal tensile stresses and the vertical compression stresses were taken into consideration, for which the models that have developed in the critical points of the pavement layers are illustrated below:

1. **εxx_{AC} horizontal tensile strain at the bottom of the AC layer**

   LOG εxx_{AC} = −1.06755 + 0.56178*LOG(H1) + 0.03233*LOG(D1800) + 0.47462*LOG(SCI) + 1.15612*LOGBDI – 0.68266*LOGBCI
2. **εzz_F compressive vertical strain at the top of the subbase (foundation) layer**

   LOG εzz_F = 2.48589 + 0.34582*LOG(SCI) + 0.16638*LOG(D1800) – 0.68746*LOG(H1) + 0.47432*LOG(BDI)
3. **εzz_{SG} compressive vertical strain at the top of the subgrade layer**

   LOG εzz_{SG} = 2.48589 + 0.34582*LOG(SCI) + 0.16638*LOGD1800 – 0.68746*LOG(H1+H2) + 0.47432*LOGBDI

   where: εr1,0 is the maximum horizontal strain at the bottom of the asphalt layer (μm/m); H1 is the thickness of the asphalt mix layer (mm); Dr is the deflection at distance r of the load center (μm); SCI = D0 − D300 (μm); BDI = base damage index = D300 − D600 (μm); BCI = base curvature index = D600 − D900 (μm); εzz_F and εzz_{SG} are the compressive vertical strain at the top of foundation and at the top of subgrade (μm/m); H2 is the thickness of the foundation layer.

The models proposed by Losa (Losa et al., 2008), allow the estimation of critical strains, at a temperature of 20°C, on pavements taking into consideration variations in: thickness of the layers, stiffness, mechanical behavior of the pavement materials. All this is done on the basis of the deflection data and the thickness of the layers without making back analysis of results from surveys.In these models the strain values are dependent variables, the basin and thickness parameters are independent variables. The models that were derived from this study developed in 2008, just mentioned are:

1. **ε_{AC} horizontal strain at the bottom of the AC layer**

   LOG $\varepsilon_{AC=}$ 0.387*LOG(H1) + 0.108*LOG(H2) – 0.242*LOG(D900) + 0.080*LOG(D1800) + 0.446*LOG(SCI)+ 0.735*LOG(BDI) – 0.869
   R-square: 0.972

2. **ε_{SB} vertical strain at the top of the subbase (foundation) layer**

LOG $\varepsilon_{SB=}$ 0.103*LOG(H1) + 0.185*LOG(H2) + 1.443*LOG(D0) – 1.264*LOG(D300) + 0.883*LOG(BDI) –0.367

R-square: 0.982

3. **ε_{SG} vertical strain at the top of the subgrade layer**

LOG $\varepsilon_{SG=}$ -1.060*LOG(H1+H2) + 1.045*LOG(D0) + 0.178*LOG(D900) – 0.183*LOG(D1800) + 2.663

R-square: 0.950

where: H1 and H2 are the thickness (mm) of the AC layer and that of the subbase (foundation) layer respectively; Di (μm) is the deflection measured at distance i (mm) from the load centerplate; SCI=DO-D300 is the surface curvature index and BDI=D300-D600 is the base damage index: SCI and BDI are the deflection basin parameters considered in the model.

These studies were conducted to overcome the obstacles that are encountered during the assessment of structural conditions. These obstacles are generally:

- lack of spatial homogeneity of structural conditions due to variation in thickness and in values of mechanical parameters characterizing each pavement layer;
- variability of both the percentage of cracked area and the aging of asphalt concrete layers;
- presence of thin AC surface layers that make backanalysis unreliable;
- presence of layers composed of non-conventional materials;
- subgrade with cohesive materials having nonlinear mechanical behavior.

Starting from these premises and these studies conducted both internationally and nationally, statistical models were developed, on the database of 180 pavement combinations, for the direct evaluation of critical horizontal and vertical strains starting from the deflections measured with the Falling Weight test and from the layer thicknesses, in this way there is no need to back-calculate the layer modules.

The models developed in this thesis work, on the basis of the data obtained from the FWD simulations at the reference temperature of 20°C, try to overcome the difficulties that are usually encountered in the evaluation of the mechanical response of the pavements characterized by constructive and performance inhomogeneity.

Based on the models of Mallick and Losa, models were developed on the data available from the 180 FWD tests simulated, in terms of deflections, tensile horizontal strains and compressive vertical strains, which are shown below. It was decided to use the deflection 1500 mm away from the center plate, rather than the 1800 mm, since the response in the models was positive in terms of R-square and Adj. R-square; as far as the other variables are concerned, they are mostly those used in the Mallick et al. (Pavement Engineering book) and Losa models.

The numerical modeling was done considering that the pavements consist of layers of wear + binder of known thickness with a Poisson coefficient equal to 0.45, base with a Poisson coefficient of 0.45, subbase of 0.30 and a subgrade of 0.35.

As we will see in the developed models, both the absence and the presence of the bedrock at depths of 1.3 and 2.5 m, which are the min and max depths tested by Losa in its models, have been taken into consideration so that they can be compared.

The simulations were made using the Bisar software, which with the application of the LET[34] allowed to simulate the FWD test with the geophones positioned on the surface at different distances from the center plate from 0 to 1800 mm, and from thicknesses and from the modules of the layers considered as input, it was possible to obtain in output the deflections and the horizontal tensile strains at the bottom of the AC layers and the vertical compressive strains at the top of the subbase layers and at the top of the subgrade layers, which represent the most critical points of the layer pavements.
The BISAR calculation program was developed at the Koninklijke/Shell laboratory in Amsterdam and is one of the most used multi-layer programs for pavement design that adopt some simplifications. Bisar allow to calculate stresses, strains and displacements in an elastic multi-layer system which is defined by the following configuration and material behavior:

- the system consists of horizontal layers of uniform thickness resting on a semi-infinite base or half space;
- the layers extend infinitely in horizontal directions;
- the material of each layer is homogeneous and isotropic[35];
- the pavement structure can consist of at most 10 layers; the deeper layer ie the subgrade, is represented with a semi-infinite layer;
- the materials are elastic;
- the load is applied through a circular load surface with a constant contact pressure that depends on the radius of the circumference itself.

Two types of modeling were made based on the model form of Losa and Mallick as references, to see what happened in terms of response and reliability of the data: the result in both cases was positive. In the table are the results, respectively of the models developed using Mallick as reference (Mod. A) and then the models developed using Losa as reference (Mod. B).
The two types of models developed, without considering the presence of the bedrock, respond very well in terms of adj. R-square and therefore can be a valid support for the direct evaluation of critical strains starting from FWD type tests.

All the models were put together for completeness in the PhD research and comparison between the models developed in this thesis work and those of Mallick and Losa. This was done on a series of data, considering the "Cases 0" that correspond to the 10 types of simulated pavements, and considering among the 180 combinations also those 2 pavements that have a Structural Number maximum (6.68 inch) and minimum (3.06 inch). For all these 12 cases, 3 conditions were set:

- pavements without bedrock
- pavements with bedrock placed at 2.5 m
- pavements with bedrock placed at 1.3 m.

Thus, these last two conditions were also virtually simulated and other models coherently developed, and then each of these 3 conditions was directly compared with the Mallick models (graphically designated as “pav”) and Losa.

[34] Linear Elastic Theory.
[35] The distribution of strains and deformations is linear according to Hooke's law. Also for the unbound layers it is assumed, for simplicity, an elastic behavior and to them, consequently to the approximation made, a modulus of elasticity is associated.

The tables below (Table 37 and

Table 38) show the models developed without considering the bedrock (Mod A and Mod B) and the models considering the presence of the bedrock at 2.5 m (Mod. A 2.5m and Mod. B 2.5m) and 1.3 m (Mod A 1.3m and Mod B 1.3m).

Table 37 - Models developed for the prediction of horizontal and tensile strains from NDT tests (FWD) without considering the bedrock

MOD. A (no bedrock)
1. Horizontal strain at the bottom of the AC layer LOG10(Exxacb) = -0.478171 + 0.300301*LOG10(H1) - 0.0569384*LOG10(D1500) - 0.116566*LOG10(SCI) + 1.76207*Log10(BDI) - 0.555756*Log10(BCI) R-squared = 99.8432 percent R-squared (adjusted for d.f.) = 99.8387 percent **2. Vertical strain at the top of the subbase layer (subbase stiffer than subgrade)** LOG10(EzztopF) = 1.09016 + 0.122232*LOG10(SCI) - 0.218072*LOG10(d1500) - 0.100356*LOG10(H1) + 1.08588*LOG10(BDI) R-squared = 99.5849 percent R-squared (adjusted for d.f.) = 99.5743 percent **3. Vertical strain at the top of the subgrade layer** LOG10(EzztopSG) = 3.41849 + 0.359031*LOG10(SCI) + 0.461253*LOG10(d1500) - 1.1043*LOG10(H1+H2) + 0.264404*LOG10(BDI) R-squared = 99.7324 percent R-squared (adjusted for d.f.) = 99.7247 percent
MOD. B (no bedrock)
1. Horizontal strain at the bottom of the AC layer LOG10(Exxacb) = -0.277294 + 0.310212*Log10(H1) + 0.071345*Log10(H2) - 0.95426*Log10(D900) + 0.563388*Log10(D1500) - 0.0872768*Log10(Sci) + 1.46813*Log10(Bdi) R-squared = 99.8452 percent R-squared (adjusted for d.f.) = 99.8399 percent **2. Vertical strain at the top of the subbase layer** LOG10(EzztopF) = 1.28535 - 0.15956*LOG10(H1) + 0.176313*LOG10(H2) + 0.68027*LOG10(D0) - 1.18118*LOG10(D300) + 1.31777*LOG10(BDI) R-squared = 99.6443 percent R-squared (adjusted for d.f.) = 99.6329 percent **3. Vertical strain at the top of the subgrade layer** LOG10(EzztopSG) = 1.9735 - 0.845997*LOG10(H1+H2) + 1.06343*LOG10(D0) + 0.572799*LOG10(D900) - 0.578188*LOG10(D1500) R-squared = 99.5443 percent R-squared (adjusted for d.f.) = 99.5312 percent

The models considering the bedrock, as already anticipated, are hereafter and for each case the numbering 1, 2, 3 represents respectively: horizontal strain at the bottom of the AC layer, vertical strain at the top of the subbase layer, vertical strain at the top of the subgrade layer.

Table 38 - Models developed with bedrock at 2.5 m and at 1.3 m

BEDROCK AT 2.5 M
Mod. A 2.5m
1. LOG10(Exx ACb) = -2.06851 + 0.84416*LOG10(H1) + 0.00865327*LOG10(d1500) - 0.495886*LOG10(SCI) + 2.92951*LOG10(BDI) - 1.29611*LOG10(BCI)
2. LOG10(Ezz topF) = 0.731899 + 0.256317*LOG10(SCI) - 0.185027*LOG10(d1500) - 0.0361791*LOG10(H1) + 1.00471*LOG10(BDI)
3. LOG10(Ezz topSG) = 4.82176 + 0.465886*LOG10(SCI) + 0.617161*LOG10(d1500) - 1.60072*LOG10(H1+H2) + 0.0868575*LOG10(BDI)
Mod. B 2.5m
1. log10(Exx ACb) = -1.70261 + 0.610048*log10(H1) + 0.42099*log10(H2) - 0.817625*log10(d900) + 0.102669*log10(d1500) - 0.12954*log10(SCI) + 1.69105*log10(BDI)
2. LOG10(Ezz topF) = 1.1756 - 0.160746*LOG10(H1) - 1.85716*LOG10(H2) + 1.56138*LOG10(D0) + 1.8017*LOG10(d300) - 0.728178*LOG10(BDI)
3. LOG10(Ezz topSG) = 1.67255 - 0.68722*LOG10(H1+H2) + 1.13225*LOG10(D0) + 0.00637409*LOG10(d900) - 0.0683885*LOG10(d1500)
BEDROCK AT 1.3 M
Mod. A 1.3 m
1. LOG10(Exx ACb) = -2.65242 + 1.06908*LOG10(H1) + 0.0402706*LOG10(d1500) - 0.732012*LOG10(SCI) + 3.531*LOG10(BDI) - 1.69366*LOG10(BCI)
2. LOG10(Ezz topF) = 0.179386 + 0.191232*LOG10(SCI) - 0.165252*LOG10(d1500) + 0.145167*LOG10(H1) + 1.10458*LOG10(BDI)
3. LOG10(Ezz topSG) = 10.5134 + 0.967333*LOG10(SCI) + 1.18118*LOG10(d1500) - 3.76217*LOG10(H1+H2) - 0.583232*LOG10(BDI)
Mod. B 1.3 m
1. LOG10(Exx ACb) = -2.98297 + 1.25491*LOG10(H1) + 0.630338*LOG10(H2) - 2.48782*LOG10(d900) + 0.898152*LOG10(d1500) - 0.934811*LOG10(SCI) + 3.11985*LOG10(BDI)
2. LOG10(Ezz topF) = 1.46651 - 0.254*LOG10(H1) - 1.57966*LOG10(H2) + 1.44229*LOG10(D0) + 1.72563*LOG10(d300) - 0.80067*LOG10(BDI)
3. LOG10(Ezz topSG) = 2.76668 - 1.02122*LOG10(H1+H2) + 1.07986*LOG10(D0) - 0.221675*LOG10(d900) + 0.241243*LOG10(d1500)

The following part is a graphical summary in which is possible to see how the models behave in these 3 conditions.

Each chart is representative respectively of: horizontal strains at the bottom of the AC layer (Figure 68); vertical strains at the top of the foundation layer (Figure 69); vertical strains at the top of subgrade layer (Figure 70).

In all the graphs, the models developed for the PhD thesis (x axis) were compared with the Losa and Mallick models (y axis).

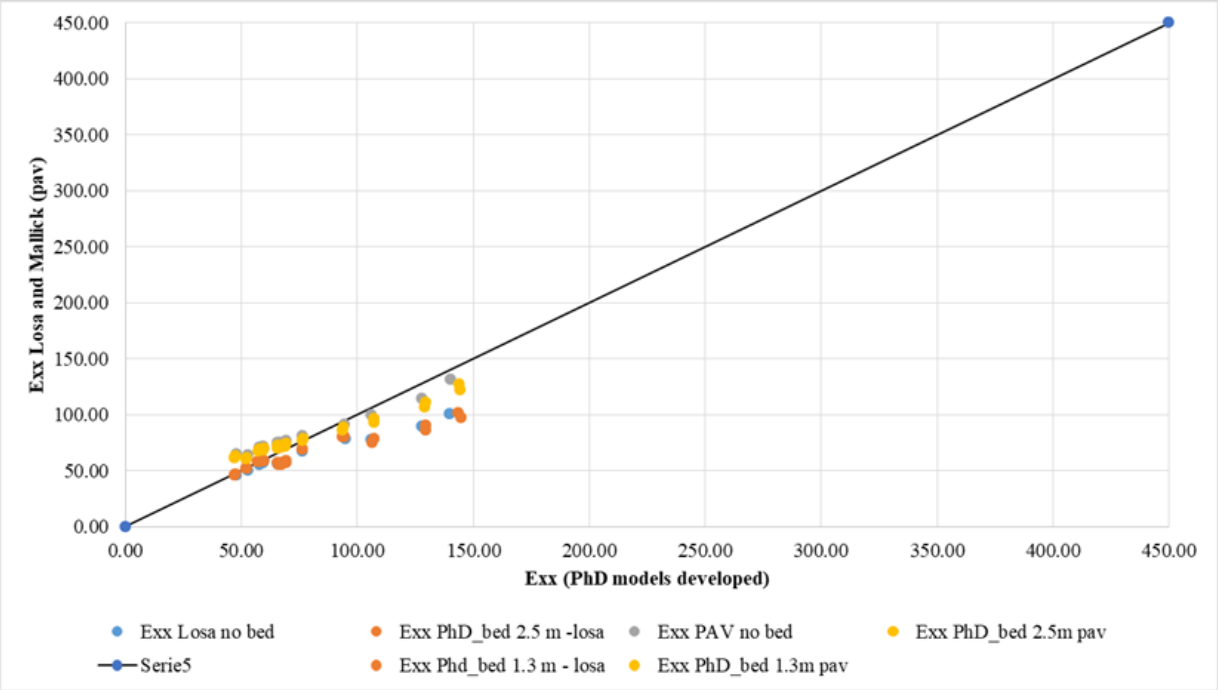

Figure 68 – Horizontal tensile strains Exx at the bottom of AC layers: comparison of PhD developed models with Losa and Mallick models (no bedrock, bedrock at 2.5 m, bedrock at 1.3 m)

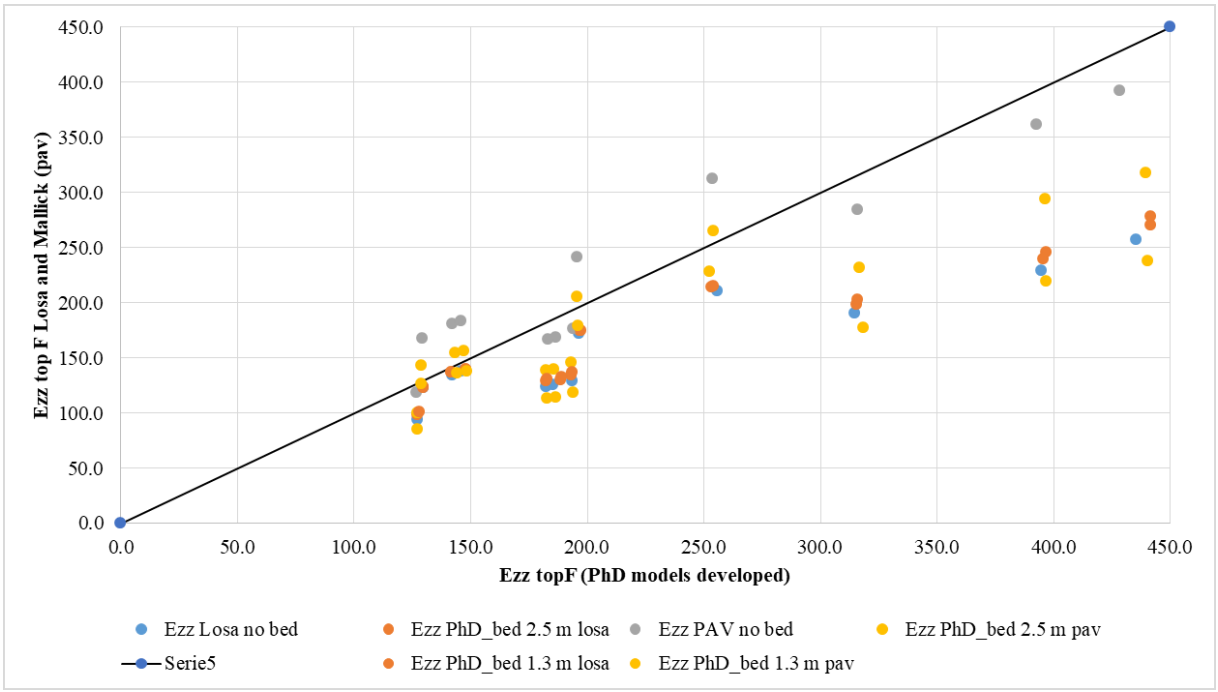

Figure 69 - Vertical compressive strains Ezz at the top of subbase layer: comparison of PhD developed models with Losa and Mallick models (no bedrock, bedrock at 2.5 m, bedrock at 1.3 m)

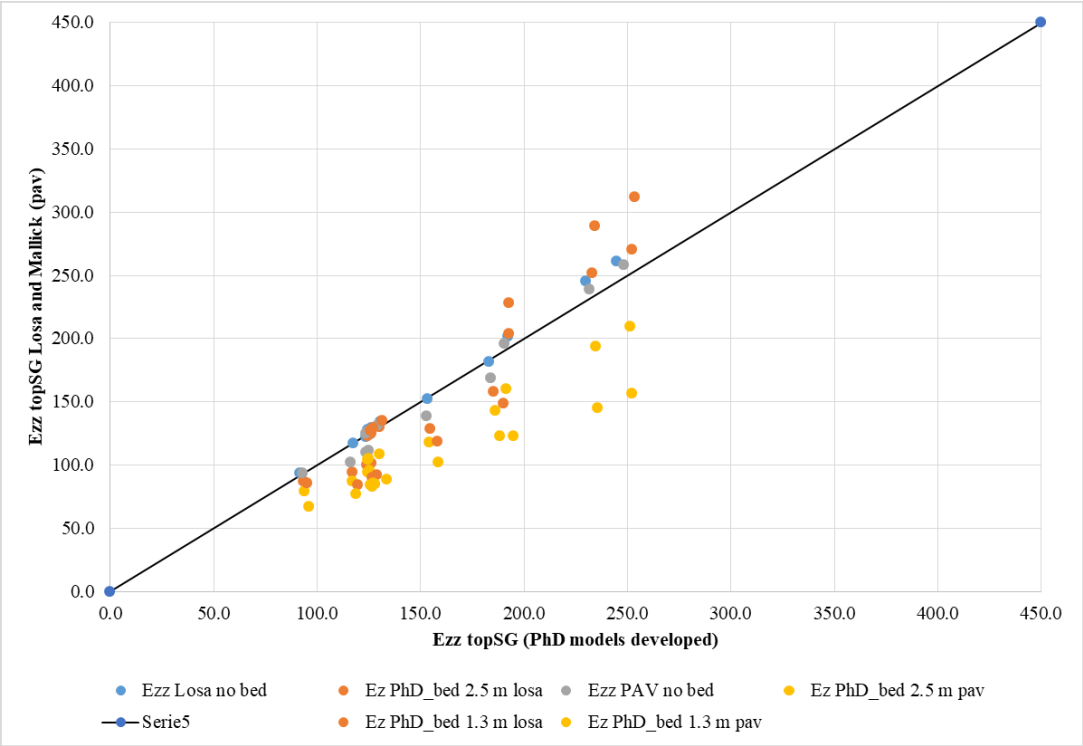

Figure 70 - Vertical compressive strains Ezz at the top of subgrade layer: comparison of PhD developed models with Losa and Mallick models (no bedrock, bedrock at 2.5 m, bedrock at 1.3 m)

From the results obtained, it can be noted graphically that the models without the presence of the bedrock respond better in terms of modeling. Especially for the subgrade, with the calculation of MAPE[36] in Table 39 (comparison with models developed with Losa and Mallick) it is possible to see how in cases with bedrock presence (at 2.5 and 1.3 m) it increases considerably compared to the case without bedrock.

Table 39 - Results of MAPE

	MAPE no bedrock [%]	**MAPE bedrock 2.5 m [%]**	**MAPE bedrock 1.3 m [%]**
Horiz. Tensile strains Phd – Losa	1.8	1.5	1.4
Horiz. Tensile strains Phd – Mallick	0.3	0.5	0.7
Vertical Compressive strains top subbase Phd – Losa	1.8	1.5	1.5
Vertical Compressive strains top subbase Phd – Mallick	1.6	0.3	0.9
Vertical Compressive strains top subgrade Phd – Losa	0.05	1.4	2.3
Vertical Compressive strains top subgrade Phd – Mallick	0.75	2.5	4.9

[36] MAPE: mean absolute percent error, in statistic is a measure of the size of the error in percentage terms.

The fact that models where there is no bedrock respond better is also confirmed by the direct comparison between the models of Losa and those of Mallick (pav), simulating the various cases of road pavements in the database and without considering the developed models, in all cases of horizontal and vertical strain is possible to see how the curve without bedrock stands always higher than the others where the bedrock is considered to be 1.3 and 2.5 meters deep. The following Figure 71 summarizes the graphic results, in each of them the Losa models are on the x axis, those of Mallick et al. on the y axis.

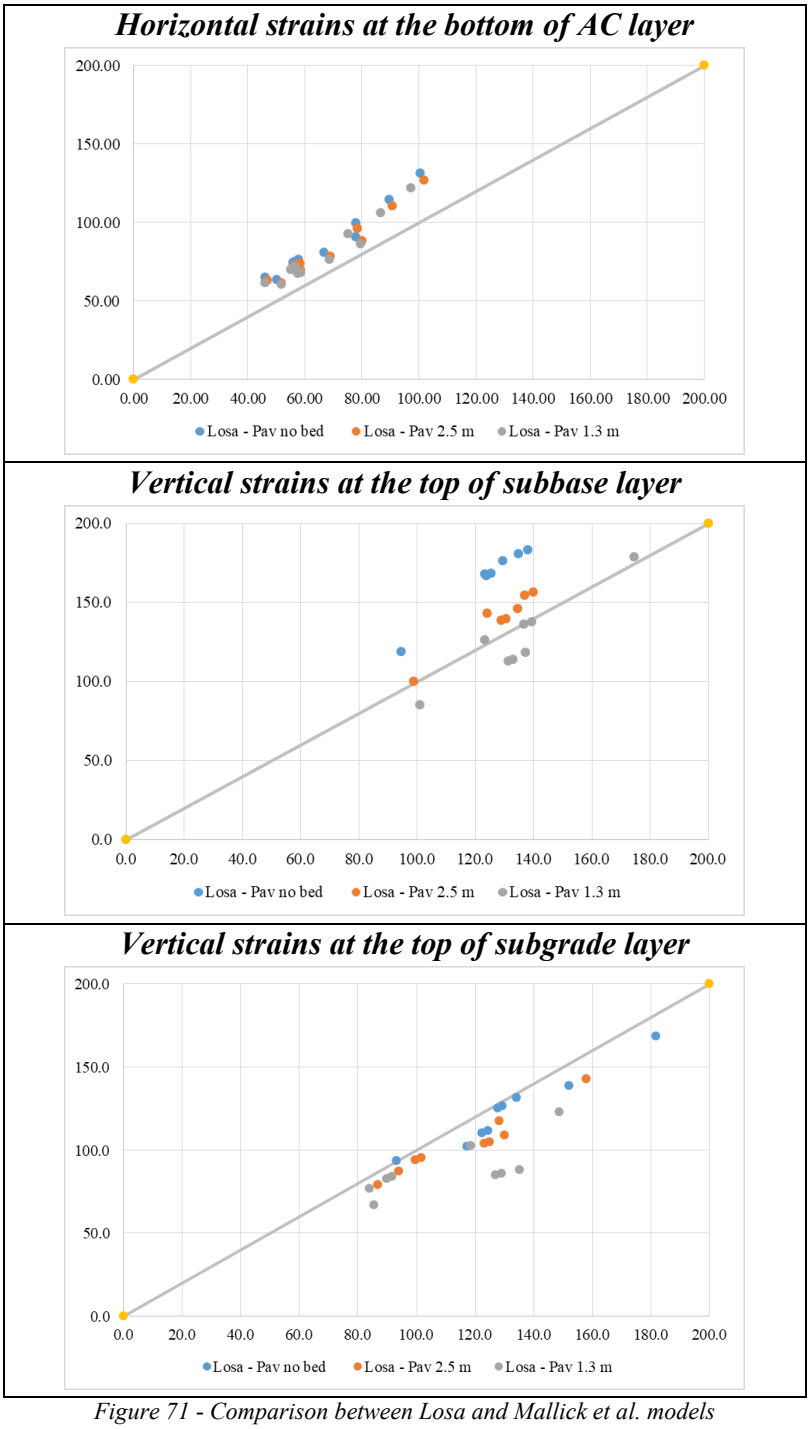

Figure 71 - Comparison between Losa and Mallick et al. models

In conclusion, the models developed without considering the presence of the bedrock can be considered a valid support for the technicians for the direct estimation of the tensions starting from

NDT Falling Weight Deflectometer tests. All this on the basis of the deflection data coming from the tests and the thickness data of the road pavements, without resorting to backanalysis and with the merit of having immediate results with reliable and effective models.

3.4 Basin Indexes from FWD simulations

The data of the road pavement modules, with their variability, have been indispensable to simulate a FWD test, that is an NDT test, through the theory of the elastic multilayer.
The Bisar software allowed the calculation of the deflections that are normally obtained with FWD in situ tests.
As already argued in paragraph 3.3.1, the modules used for the different pavement layers as input in Bisar were calculated at a frequency of 16 Hz and a reference temperature of 20°C was considered.
The values of the deflections have been calculated in the typical points of a standard configuration of Falling Weight Deflectometer test with the geophones placed at distances known from the center of the load plate (with radius of 150 mm), and therefore of 0, 200, 300, 450, 600, 900, 1200, 1500 mm. The Poisson Coefficients used were: $\nu_{bound\ layers}$ = 0.45; $\nu_{subbase}$= 0.30; $\nu_{subgrade}$=0.35.
Below, in Table 40 the deflections calculated for a road pavement of the database. In **Appendix 7** all the results for the whole database.

Table 40 - Deflections calculated with Bisar software for a road pavement.

Id. Pav.	D	D code	do [µm]	d150 [µm]	d200 [µm]	d300 [µm]	d600 [µm]	d900 [µm]	d1200 [µm]	d1500 [µm]
Ms 30 (M-L)	*-20%*	**M1**	239.30	218.40	204.80	189.60	153.50	124.70	102.20	84.78
Ms 30 (M-L)	*-10%*	**M1**	235.40	215.60	202.80	187.90	152.40	124.10	101.90	84.69
Ms 30 (M-L)	*0%*	**O**	232.20	213.20	201.00	186.40	151.40	123.60	101.70	84.60
Ms 30 (M-L)	*15%*	**M1**	228.00	210.00	198.60	184.30	150.10	122.80	101.30	84.48
Ms 30 (M-L)	*-20%*	**M2**	241.20	220.10	206.80	190.30	152.60	123.80	101.60	84.41
Ms 30 (M-L)	*-10%*	**M2**	236.30	216.40	203.70	188.10	152.00	123.70	101.60	84.52
Ms 30 (M-L)	*0%*	**O**	232.20	213.20	201.00	186.40	151.40	123.60	101.70	84.60
Ms 30 (M-L)	*15%*	**M2**	226.90	209.10	197.60	184.00	150.60	123.40	101.70	84.72
Ms 30 (M-L)	*-20%*	**M3**	240.80	221.40	209.00	193.70	156.40	126.40	103.10	85.14
Ms 30 (M-L)	*-10%*	**M3**	236.20	217.10	204.80	189.80	153.70	124.90	102.30	84.85
Ms 30 (M-L)	*0%*	**O**	232.20	213.20	201.00	186.40	151.40	123.60	101.70	84.60
Ms 30 (M-L)	*15%*	**M3**	226.90	208.10	196.10	181.90	148.40	121.80	100.80	84.30
Ms 30 (M-L)	*-20%*	**Ms**	262.40	243.20	230.90	215.90	179.40	149.20	124.70	105.00
Ms 30 (M-L)	*-10%*	**Ms**	245.90	226.80	214.50	199.70	164.00	135.10	112.00	93.72
Ms 30 (M-L)	*0%*	**O**	232.20	213.20	201.00	186.40	151.40	123.60	101.70	84.60
Ms 30 (M-L)	*15%*	**Ms**	215.10	196.20	184.10	169.60	135.70	109.30	88.98	73.49

Note: the other road pavements are reported in Appendix 7.

The FWD test simulations allowed the calculation of several Basin Indexes or known as Deflection Bowl Parameters starting from the deflections in µm obtained at the various distances from the center of the loading plate.

The Basin Indexes can be a fundamental tool for quality control during the acceptance phase of the works to identify the case in which compliance requirements are not met.

15 different basin indices were selected, which are reported in Table 41 with number, parameter Id, full name, significance and formula.

Table 41 - Basin Indexes: Description and equations

N. and [unit of measure]	Parameter Id	Name of the Index and significance	Formula
I1 [µm]	D_0'	First deflection under load	D_0'
I2 [mm]	RoC	Radius of Curvature	$RoC = L^2 / \left[2D_0 \left(1 - \frac{D_{300}}{D_0}\right)\right]$
I3 [Mpa]	Eeq	Equivalent Modulus characterizing the condition of all the layers of the pavement	$E_{eq} = \frac{2(1-\mu^2) a\, \sigma_0}{D_0}$
I4 [-]	AUPP	Area under pavement performance characterizing the condition of the pavement upper layer	$AUPP = \frac{5D_0 + 2D_{300} + 2D_{600} + D_{900}}{D_0}$
I5 [-]	Al_1	Area Indices characterizing the condition of upper layer	$Al_1 = \frac{D_0 + D_{300}}{2D_0}$
I6 [-]	Al_2	Area Indices characterizing the condition of middle layer	$Al_2 = \frac{D_{300} + D_{600}}{2D_0}$
I7 [-]	Al_3	Area Indices characterizing the condition of middle layer	$Al_3 = \frac{D_{600} + D_{900}}{2D_0}$
I8 [-]	Al_4	Area Indices characterizing the condition of lower layer	$Al_4 = \frac{D_{900} + D_{1200}}{2D_0}$
I9 [MPa]	E_{0r}	Modulus of Elasticity at 600 mm from center characterizing subgrade layer	$E_{0r} = \frac{(1-\mu^2) a^2\, \sigma_0}{r * D_{600}}$
I10 [µm]	IS300 SCI	Anas Index IS300 Surface Curvature Index characterizing the pavement layers	$IS300 = D_0 - D_{300}$
I11 [µm]	MLI	Middle Layer Index characterizing the condition of the base layer	$MLI = D_{300} - D_{600}$
I12 [µm]	LLI	Lower Layer Index characterizing the condition of the subgrade	$LLI = D_{1200} - D_{1500}$
I13 [µm]	IS200	Anas index IS200	$IS200 = D_0 - D_{200}$
I13c [µm]	IS_{200CF}	Anas Index IS_{200CF} correct with the subgrade	$IS_{200CF} = (1.94 - 0.5 * LOG(D_{900} - D_{1500})) * (D_0 - D_{200})$
I14 [-]	SF	Shape factor	$SF = (D_0 - D_{300}) / D_{200}$

Specifically, at National Level, as it has already been described, ANAS defines the indexes IS300, IS200, IS_{200CF} characterizing the surface layers of road pavements ("Linee Guida di Progetto e Norme Tecniche Prestazionali" (2008), "Capitolato Speciale D'Appalto - Norme Tecniche" (2009), "Capitolato Speciale D'Appalto - Norme Tecniche per l'esecuzione del contratto Parte 2" (Coordinamento Territoriale/Direzione IT.PRL.05.21, 2016)).

At International Level, from literature studies and then investigating the state of the art, it has instead highlighted that using the deflections noted at different sensors a serious of expressions can be used to determine relevant properties of the pavement (Mallik et al., 2013).
There is therefore a much wider picture than the Italian one, with different basin indexes, specifically characterizing all the layers that make up the road superstructure, thus investigating it in its totality from the most superficial layers to the subgrade (Horak et al., 2006; Solanki et al., 2016).
The basin indexes have been calculated for all the different road paving structures of the database, in which the module variations of the various layers have been considered in percentages ranging from -20% to + 15%. In Table 42 and Table 43 there is a road paving structure on which the previously explained Basin Indexes and the Delta Basin Indexes have been calculated.
The detail with the whole database is in **Appendix 8**.

Table 42 - Basin Indexes for a road pavement of the database

Id. Pav.	D	16hzM1 [Mpa]	16hz M2 [Mpa]	16hzM3 [Mpa]	16hz Ms [Mpa]	I1 [µm]	I2 [mm]	I3 [Mpa]	I4 [-]	I5 [-]	I6 [-]	I7 [-]	I8 [-]	I9 [MPa]	I10 [µm]	I11 [µm]	I12 [µm]	I13 [µm]	I13c [µm]	I14 [-]
Ms 30 (M-L)	-20%	2914.4	3342.0	316.7	90.9	228.85	1146496.82	623.15	8.54	0.91	0.75	0.61	0.50	121.31	39.25	36.10	17.42	24.05	27.40	0.19
Ms 30 (M-L)	-10%	3278.7	3342.0	316.7	90.9	225.50	1196808.51	632.40	8.57	0.92	0.75	0.61	0.50	122.19	37.60	35.50	17.21	22.70	25.93	0.19
Ms 30 (M-L)	0%	3643.0	3342.0	316.7	90.9	222.70	1239669.42	640.35	8.59	0.92	0.76	0.62	0.51	123.00	36.30	35.00	17.10	21.70	24.83	0.18
Ms 30 (M-L)	15%	4189.5	3342.0	316.7	90.9	219.00	1296829.97	651.17	8.61	0.92	0.76	0.62	0.51	124.06	34.70	34.20	16.82	20.40	23.43	0.17
Ms 30 (M-L)	-20%	3643.0	2673.6	316.7	90.9	230.65	1115241.64	618.28	8.51	0.91	0.74	0.60	0.49	122.03	40.35	37.70	17.19	23.85	27.24	0.20
Ms 30 (M-L)	-10%	3643.0	3007.8	316.7	90.9	226.35	1176470.59	630.03	8.55	0.92	0.75	0.61	0.50	122.51	38.25	36.10	17.08	22.65	25.90	0.19
Ms 30 (M-L)	0%	3643.0	3342.0	316.7	90.9	222.70	1239669.42	640.35	8.59	0.92	0.76	0.62	0.51	123.00	36.30	35.00	17.10	21.70	24.83	0.18
Ms 30 (M-L)	15%	3643.0	3843.3	316.7	90.9	218.00	1323529.41	654.16	8.64	0.92	0.77	0.63	0.52	123.65	34.00	33.40	16.98	20.40	23.38	0.17
Ms 30 (M-L)	-20%	3643.0	3342.0	253.4	90.9	231.10	1203208.56	617.08	8.58	0.92	0.76	0.61	0.50	119.06	37.40	37.30	17.96	22.10	25.02	0.18
Ms 30 (M-L)	-10%	3643.0	3342.0	285.0	90.9	226.65	1221166.89	629.19	8.58	0.92	0.76	0.61	0.50	121.16	36.85	36.10	17.45	21.85	24.88	0.18
Ms 30 (M-L)	0%	3643.0	3342.0	316.7	90.9	222.70	1239669.42	640.35	8.59	0.92	0.76	0.62	0.51	123.00	36.30	35.00	17.10	21.70	24.83	0.18
Ms 30 (M-L)	15%	3643.0	3342.0	364.2	90.9	217.50	1264044.94	655.66	8.60	0.92	0.76	0.62	0.51	125.48	35.60	33.50	16.50	21.40	24.67	0.18
Ms 30 (M-L)	-20%	3643.0	3342.0	316.7	72.7	252.80	1219512.20	564.11	8.72	0.93	0.78	0.65	0.54	103.80	36.90	36.50	19.70	21.90	24.47	0.16
Ms 30 (M-L)	-10%	3643.0	3342.0	316.7	81.8	236.35	1227830.83	603.37	8.65	0.92	0.77	0.63	0.52	113.55	36.65	35.70	18.28	21.85	24.73	0.17
Ms 30 (M-L)	0%	3643.0	3342.0	316.7	90.9	222.70	1239669.42	640.35	8.59	0.92	0.76	0.62	0.51	123.00	36.30	35.00	17.10	21.70	24.83	0.18
Ms 30 (M-L)	15%	3643.0	3342.0	316.7	104.5	205.65	1248266.30	693.44	8.50	0.91	0.74	0.60	0.48	137.23	36.05	33.90	15.49	21.55	25.06	0.20

Do, that is the index I1, has been calculated considering the average between the deflection and the deflection d150, just to take into account that the load has been applied on a load plate with a radius of 150 mm.

Table 43 - Delta Basin Indexes related to the Case 0 of a road pavement

Id. Pav.	D	16hzM1 [Mpa]	16hz M2 [Mpa]	16hzM3 [Mpa]	16hz Ms [Mpa]	D_I1	D_I2	D_I3	D_I4	D_I5	D_I6	D_I7	D_I8	D_I9	D_I10	D_I11	D_I12	D_I13	DI13c	D_I14
Ms 30 (M-L)	-20%	2914.4	3342.0	316.7	90.9	0.028	-0.075	-0.027	-0.005	-0.005	-0.012	-0.016	-0.020	-0.014	0.081	0.031	0.019	0.108	0.103	0.061
Ms 30 (M-L)	-10%	3278.7	3342.0	316.7	90.9	0.013	-0.035	-0.012	-0.002	-0.002	-0.005	-0.007	-0.009	-0.007	0.036	0.014	0.006	0.046	0.044	0.027
Ms 30 (M-L)	0%	3643.0	3342.0	316.7	90.9	0.000	0.000	0.000	0.000	0.000	0.000	0.000	0.000	0.000	0.000	0.000	0.000	0.000	0.000	0.000
Ms 30 (M-L)	15%	4189.5	3342.0	316.7	90.9	-0.017	0.046	0.017	0.003	0.002	0.007	0.009	0.011	0.009	-0.044	-0.023	-0.016	-0.060	-0.057	-0.033
Ms 30 (M-L)	-20%	3643.0	2673.6	316.7	90.9	0.036	-0.100	-0.034	-0.009	-0.007	-0.020	-0.030	-0.034	-0.008	0.112	0.077	0.005	0.099	0.097	0.080
Ms 30 (M-L)	-10%	3643.0	3007.8	316.7	90.9	0.016	-0.051	-0.016	-0.004	-0.003	-0.009	-0.014	-0.016	-0.004	0.054	0.031	-0.001	0.044	0.043	0.040
Ms 30 (M-L)	0%	3643.0	3342.0	316.7	90.9	0.000	0.000	0.000	0.000	0.000	0.000	0.000	0.000	0.000	0.000	0.000	0.000	0.000	0.000	0.000
Ms 30 (M-L)	15%	3643.0	3843.3	316.7	90.9	-0.021	0.068	0.022	0.005	0.004	0.012	0.018	0.021	0.005	-0.063	-0.046	-0.007	-0.060	-0.058	-0.047
Ms 30 (M-L)	-20%	3643.0	3342.0	253.4	90.9	0.038	-0.029	-0.036	-0.001	0.001	-0.001	-0.009	-0.018	-0.032	0.030	0.066	0.050	0.018	0.008	-0.009
Ms 30 (M-L)	-10%	3643.0	3342.0	285.0	90.9	0.018	-0.015	-0.017	-0.001	0.000	-0.001	-0.005	-0.009	-0.015	0.015	0.031	0.020	0.007	0.002	-0.004
Ms 30 (M-L)	0%	3643.0	3342.0	316.7	90.9	0.000	0.000	0.000	0.000	0.000	0.000	0.000	0.000	0.000	0.000	0.000	0.000	0.000	0.000	0.000
Ms 30 (M-L)	15%	3643.0	3342.0	364.2	90.9	-0.023	0.020	0.024	0.001	0.000	0.001	0.006	0.012	0.020	-0.019	-0.043	-0.035	-0.014	-0.006	0.005
Ms 30 (M-L)	-20%	3643.0	3342.0	316.7	72.7	0.135	-0.016	-0.119	0.015	0.009	0.031	0.053	0.071	-0.156	0.017	0.043	0.152	0.009	-0.015	-0.115
Ms 30 (M-L)	-10%	3643.0	3342.0	316.7	81.8	0.061	-0.010	-0.058	0.007	0.004	0.014	0.025	0.033	-0.077	0.010	0.020	0.069	0.007	-0.004	-0.054
Ms 30 (M-L)	0%	3643.0	3342.0	316.7	90.9	0.000	0.000	0.000	0.000	0.000	0.000	0.000	0.000	0.000	0.000	0.000	0.000	0.000	0.000	0.000
Ms 30 (M-L)	15%	3643.0	3342.0	316.7	104.5	-0.077	0.007	0.083	-0.010	-0.007	-0.021	-0.035	-0.047	0.116	-0.007	-0.031	-0.094	-0.007	0.009	0.084

Note: Each Delta Basin Index D_I_i is calculated with the formula $DI_i = (I_i - I_{case0})/I_{case0}$, where I_i is a basin index and I_{case0} is the basin index with D=0% (without any percentage variation in modules).

The calculation of the basin indices will prove to be fundamental to see the correlations they have with the Esal.

3.5 Calculation of Design Esals from the NDT Structural Number

For the calculation of the Esal for the FWD Tests, the AASHTO procedure was applied (AASHTO Guide for Design of Pavement Structures, 1993).

First of all, it's important to calculate the Structural Number SNeff, that, from the known relations it is:

$$SNeff=0.0045 \cdot D \cdot \sqrt[3]{Ep}$$

With: Ep= elastic modulus of the entire pavement on the subgrade; D=total thickness of pavement layers above the subgrade.

The Elastic Modulus Ep, that was calculated with an objective research[37], is contained in the formula:

$$d_0 = 1.5\,P\,a\left\{\frac{1}{M_R\sqrt{1+\left(\frac{D}{a}\times\sqrt[3]{\frac{E_P}{M_R}}\right)^2}}+\frac{\left[1-\frac{1}{\sqrt{1+\left(\frac{D}{a}\right)^2}}\right]}{E_P}\right.$$

Where:
do = deflection at the center of the loading plate [in];
p = pressure plate [psi];
a = radius of the loading plate [in];
D = total thickness of pavement layers above the subgrade [in];
M_R = resilient modulus of the subgrade;

The corrected Mr (0.33xMrdesign) (in psi) was used as a resilient module of the subgrade. That is possible assuming the value of Mr of subgrade as known and equal to the design one.

As different assumption for Mr, also a latter calculation of Ep was made, and then subsequently of SNeff, considering the back-calculated Mr (NCHRP study – Darter, Elliot and Hall, 1991 – revised part III of the AASHTO pavement Guide):

$$M_R = \frac{(1-\nu^2)\times P}{\pi \times d_r \times r}$$

$$a_{3e} = \sqrt{a^2+\left(D\sqrt[3]{\frac{Ep}{Mr}}\right)^2}$$

$$r > 0.7\,a_{3e}$$

where:
a_{3e} = radius of the bulb of the stresses on the subgrade;
dr = deflection at distance r [in];
r = distance from the center of the plate [in]

That hypothesis assumed the subgrade modulus un-known during the FWD control test.

[37] Ep was calculated with an objective research implemented with the software Matlab due to the large amount of data.

For this case study and the data available from the database: dr = d600 and r = 600 mm, for which Mr600 was also calculated and consequently Ep600 and SNeff600.
So in the end SNeff was calculated and, considering the verification of $r > 0.7\ a_{3e}$, also SN600 in the way that has just been explained.

Known the Structural Number, SNeff and SN600, calculated the respective Ep, and also known the modules, respectively the module of the design subgrade and that back-calculated by the deflection at 600 mm from the center plate, two estimations of Esal were obtained:

- Esal deriving from SNeff and design Ms
- Esal deriving from SN600 and Mr600

Below in Table 44 the calculations for a road pavement.
In **Appendix 9** there are the complete calculations on the whole sample of the database.

Table 44 - Esals and Structural Number derived from NDT of a road pavement calculated from the Database

Id. Pav.	D	16 hz Ms [psi]	Mr600 [psi]	EP [psi]	Sneff [inch]	ESAL Sneff	EP600 [psi]	Sneff 600 [inch]	ESAL Sneff600
Ms 30 (M-L)	***-20%***	13184.8	17594.60	165040.23	6.12	6.51E+08	136907.31	5.75	7.96E+08
Ms 30 (M-L)	***-10%***	13184.8	17721.59	169287.94	6.17	6.94E+08	139553.72	5.79	8.49E+08
Ms 30 (M-L)	***0%***	13184.8	17838.65	172988.09	6.22	7.34E+08	141798.01	5.82	8.96E+08
Ms 30 (M-L)	***15%***	13184.8	17993.14	178100.28	6.28	7.90E+08	144885.00	5.86	9.65E+08
Ms 30 (M-L)	***-20%***	13184.8	17698.37	162834.63	6.09	6.29E+08	134766.93	5.72	7.76E+08
Ms 30 (M-L)	***-10%***	13184.8	17768.23	168192.10	6.16	6.83E+08	138513.07	5.77	8.38E+08
Ms 30 (M-L)	***0%***	13184.8	17838.65	172988.09	6.22	7.34E+08	141798.01	5.82	8.96E+08
Ms 30 (M-L)	***15%***	13184.8	17933.41	179527.61	6.30	8.07E+08	146231.91	5.88	9.80E+08
Ms 30 (M-L)	***-20%***	13184.8	17268.36	162291.33	6.09	6.24E+08	136281.72	5.74	7.53E+08
Ms 30 (M-L)	***-10%***	13184.8	17571.70	167808.30	6.16	6.79E+08	139122.50	5.78	8.26E+08
Ms 30 (M-L)	***0%***	13184.8	17838.65	172988.09	6.22	7.34E+08	141798.01	5.82	8.96E+08
Ms 30 (M-L)	***15%***	13184.8	18199.27	180248.81	6.30	8.15E+08	145496.50	5.87	1.00E+09
Ms 30 (M-L)	***-20%***	10547.8	15054.46	163974.82	6.11	3.82E+08	128151.23	5.63	4.71E+08
Ms 30 (M-L)	***-10%***	11866.3	16468.12	168673.96	6.17	5.39E+08	135233.55	5.73	6.62E+08
Ms 30 (M-L)	***0%***	13184.8	17838.65	172988.09	6.22	7.34E+08	141798.01	5.82	8.96E+08
Ms 30 (M-L)	***15%***	15162.5	19902.51	179418.10	6.30	1.11E+09	150920.37	5.94	1.35E+09

Where: Id. Pav. = identification name of road pavement; D = percentage of variation of the individual modules (as explained in the previous paragraphs); 16hzMs = subgrade modulus at 16 Hz [psi]; Mr600 = subgrade modulus at r=600 mm [psi]; Ep, Ep600 = elastic modulus of the entire pavement on the subgrade at 16 Hz and at r=600 mm [psi]; SNeff, SNeff600 = Structural Number at 16 Hz and at r=600 mm [in]; ESALSneff, ESALSneff600 = Esal at 16 Hz and at r=600 mm.

At this point all the calculations have been made in terms of Esal, in the sense that in paragraph 3.2 the design Esal deriving from the a_i coefficients (and therefore according to the AASHTO Structural Number) were calculated, now the calculation has been made instead going to consider the carrying out of the FWD tests, calculating SNeff, which as already seen have assumed the performance considerations, also of the frequency of the 16 Hz tests.

For this last reason, in fact, the dynamic modules E* of the bounded layers were calculated with the Fonseca and Witczak equation, and then for unbound layers it was considered that between the FWD tests and the AASHTO modules there are overestimating about 33%. Therefore, the calculation of the Esal from the NDT Structural Number has allowed to have also this important parameter coherently with the FWD performance tests.

3.6 Statistical Models

In this part all the statistical regressions that have been made in order to develop predictive models among the different variables studied, such as Esal (which may be related to Residual Life), Basin Indices, Structural Number, will be exposed.

In multiple regression models, covariates (independent variables) to be included in the model were selected basing on criteria to both maximize the likelihood of the model to estimate the independent variable (e.g. maximum $R^2_{adjusted}$) and minimize the variance of the regression coefficients limiting the inclusion of correlated variables.

This is because for the development of efficient models there is the need to put together several variables that are not correlated to each other and the regression model must have high values of R-square, or even better, Adj. R-square.

Correlation was tested by correlation coefficients and pearson's p-values in the correlation matrix among variables. The logic used in the research studies conducted was generally that of retaining significant models with several variables with values of R-square (or Adj. R-square) of about 90% or more, and correlation coefficients less than 0.5. Table 45 with the descriptive statistics of the variables included in the models is reported below, where Ii are the basin indexes calculated and explained in paragraph 3.4.

Table 45 - Descriptive statistics.

	I1 = d0 [µm]	*I2 [mm]*	*I3 [Mpa]*	*I4 [-]*	*I5 [-]*	*I6 [-]*	*I7 [-]*
Count	180	180	180	180	180	180	180
Average	171.363	1.24352E6	892.794	8.12344	0.88478	0.671195	0.505746
Standard deviation	45.3851	230840.	235.77	0.428265	0.0287638	0.0790685	0.10676
Coeff. of variation	26.4848%	18.5634%	26.4081%	5.27197%	3.25096%	11.7802%	21.1094%
Minimum	101.91	719424.	511.869	7.35717	0.832351	0.52624	0.319995
Maximum	278.6	1.78678E6	1399.34	8.8091	0.929672	0.79617	0.67975
Range	176.69	1.06735E6	887.471	1.45193	0.0973214	0.26993	0.359756
Stnd. skewness	1.6294	-2.01937	1.4466	0.394024	0.936617	0.367794	0.23801
Stnd. kurtosis	-3.10671	-1.8239	-3.38361	-3.8367	-4.24117	-3.8662	-3.68405

	I8 [-]	*I9 [MPa]*	*I10 [µm]*	*I11 [µm]*	*I12 [µm]*	*I13 [µm]*	*I13c [µm]*
Count	180	180	180	180	180	180	180
Average	0.392593	214.473	37.6348	32.8141	11.3201	22.5527	27.8523
Standard deviation	0.109896	75.3209	8.01123	8.88502	4.46879	3.8525	5.16051
Coeff. of variation	27.9925%	35.1191%	21.2868%	27.0769%	39.4767%	17.0822%	18.5281%
Minimum	0.21777	97.9056	25.185	18.29	6.35	16.175	20.4166
Maximum	0.580731	341.368	62.55	53.38	21.4	35.65	45.9277
Range	0.362961	243.463	37.365	35.09	15.05	19.475	25.5111
Stnd. skewness	0.77899	-1.53325	5.67065	3.01049	2.95287	5.74251	6.92653
Stnd. kurtosis	-3.79351	-4.70764	0.619928	-2.30102	-4.02519	1.25159	2.6027

	I14 [-]
Count	180
Average	0.270536
Standard deviation	0.0765068
Coeff. of variation	28.2797%
Minimum	0.15405
Maximum	0.414513
Range	0.260463
Stnd. skewness	-0.879959
Stnd. kurtosis	-4.26767

The following part show how the variables were used and therefore the statistics with Esal, SN and Indices.

3.6.1 Prediction of design life (Esals) from FWD Indices

On the pavement structures analyzed in this research study, analyzes were carried out to see how loss of residual life, in terms of Esal, and the basin indices deriving from the FWD test simulation can be related. The basin indices used for the statically study were identified as follows in

Table *46*.

Table 46 - Basin Indices processed for statistical analysis

Id. Basin Index	**Name of the Index and significance**	**Formula**
A=I1 = d0 [µm]	First deflection under load	D_0
B=I2 [mm]	Radius of Curvature	$RoC = L^2/\left[2D_0\left(1-\frac{D_{300}}{D_0}\right)\right]$
C=I3 [Mpa]	Equivalent Modulus characterizing the condition of all the layers of the pavement	$E_{eq} = \frac{2(1-\mu^2)a\,\sigma_0}{D_0}$
D=I4 [-]	Area under pavement performance characterizing the condition of the pavement upper layer	$AUPP = \frac{5D_0 + 2D_{300} + 2D_{600} + D_{900}}{D_0}$
E=I6 [-]	Area Indices characterizing the condition of middle layer	$Al_2 = \frac{D_{300} + D_{600}}{2D_0}$
F=I5 [-]	Area Indices characterizing the condition of upper layer	$Al_1 = \frac{D_0 + D_{300}}{2D_0}$
G=I8 [-]	Area Indices characterizing the condition of lower layer	$Al_4 = \frac{D_{900} + D_{1200}}{2D_0}$
H=I9 [MPa]	Modulus of Elasticity at 600 mm from center characterizing subgrade layer	$E_{0r} = \frac{(1-\mu^2)a^2\,\sigma_0}{r * D_{600}}$
I=I10 [µm]	Anas Index IS300 Surface Curvature Index characterizing the pavement layers	$D_0 - D_{300}$
J=I11 [µm]	Middle Layer Index characterizing the condition of the base layer	$D_{300} - D_{600}$
K=I12 [µm]	Lower Layer Index characterizing the condition of the subgrade	$D_{1200} - D_{1500}$
L=I13 [µm]	Anas index IS200	$D_0 - D_{200}$
M=I13c [µm]	Anas Index IS_{200CF} correct with the subgrade	IS_{200CF}=(1.94-0.5*LOG(D_{900}-D_{1500}))*(D_0-D_{200})
N=I14 [-]	Shape factor	(D_0-D_{300})/D_{200}

Table 47 shows the correlation matrix of the Basin Indices.

Table 47 - Correlation matrix (in pairs) between the Basin Indices

	I1 = d0 [µm]	I2 [mm]	I3 [Mpa]	I4 [-]	I5 [-]	I6 [-]	I7 [-]	I8 [-]
I1 = d0 [µm]		-0.3773	-0.9759	0.6352	0.7140	0.6454	0.6037	0.6134
		(180)	(180)	(180)	(180)	(180)	(180)	(180)
		0.0000	0.0000	0.0000	0.0000	0.0000	0.0000	0.0000
I2 [mm]	-0.3773		0.4512	0.4643	0.3659	0.4528	0.4974	0.4840
	(180)		(180)	(180)	(180)	(180)	(180)	(180)
	0.0000		0.0000	0.0000	0.0000	0.0000	0.0000	0.0000
I3 [Mpa]	-0.9759	0.4512		-0.5644	-0.6510	-0.5747	-0.5310	-0.5453
	(180)	(180)		(180)	(180)	(180)	(180)	(180)
	0.0000	0.0000		0.0000	0.0000	0.0000	0.0000	0.0000
I4 [-]	0.6352	0.4643	-0.5644		0.9904	0.9997	0.9985	0.9966
	(180)	(180)	(180)		(180)	(180)	(180)	(180)
	0.0000	0.0000	0.0000		0.0000	0.0000	0.0000	0.0000
I5 [-]	0.7140	0.3659	-0.6510	0.9904		0.9932	0.9815	0.9789
	(180)	(180)	(180)	(180)		(180)	(180)	(180)
	0.0000	0.0000	0.0000	0.0000		0.0000	0.0000	0.0000
I6 [-]	0.6454	0.4528	-0.5747	0.9997	0.9932		0.9969	0.9943
	(180)	(180)	(180)	(180)	(180)		(180)	(180)
	0.0000	0.0000	0.0000	0.0000	0.0000		0.0000	0.0000
I7 [-]	0.6037	0.4974	-0.5310	0.9985	0.9815	0.9969		0.9988
	(180)	(180)	(180)	(180)	(180)	(180)		(180)
	0.0000	0.0000	0.0000	0.0000	0.0000	0.0000		0.0000
I8 [-]	0.6134	0.4840	-0.5453	0.9966	0.9789	0.9943	0.9988	
	(180)	(180)	(180)	(180)	(180)	(180)	(180)	
	0.0000	0.0000	0.0000	0.0000	0.0000	0.0000	0.0000	
I9 [MPa]	-0.9342	0.0607	0.9115	-0.8512	-0.9022	-0.8580	-0.8287	-0.8355
	(180)	(180)	(180)	(180)	(180)	(180)	(180)	(180)
	0.0000	0.4181	0.0000	0.0000	0.0000	0.0000	0.0000	0.0000
I10 [µm]	0.3185	-0.9786	-0.3929	-0.5198	-0.4295	-0.5108	-0.5485	-0.5301
	(180)	(180)	(180)	(180)	(180)	(180)	(180)	(180)
	0.0000	0.0000	0.0000	0.0000	0.0000	0.0000	0.0000	0.0000
I11 [µm]	0.5424	-0.9544	-0.5957	-0.2964	-0.1812	-0.2819	-0.3369	-0.3248
	(180)	(180)	(180)	(180)	(180)	(180)	(180)	(180)
	0.0000	0.0000	0.0000	0.0001	0.0149	0.0001	0.0000	0.0000
I12 [µm]	0.9089	0.0213	-0.8404	0.8856	0.9273	0.8925	0.8653	0.8653
	(180)	(180)	(180)	(180)	(180)	(180)	(180)	(180)
	0.0000	0.7762	0.0000	0.0000	0.0000	0.0000	0.0000	0.0000
I13 [µm]	0.2890	-0.9708	-0.3632	-0.5325	-0.4531	-0.5255	-0.5567	-0.5369
	(180)	(180)	(180)	(180)	(180)	(180)	(180)	(180)
	0.0001	0.0000	0.0000	0.0000	0.0000	0.0000	0.0000	0.0000
I13c [µm]	-0.0122	-0.8915	-0.0788	-0.7546	-0.6964	-0.7509	-0.7698	-0.7502
	(180)	(180)	(180)	(180)	(180)	(180)	(180)	(180)
	0.8712	0.0000	0.2933	0.0000	0.0000	0.0000	0.0000	0.0000
I14 [-]	-0.7222	-0.3525	0.6604	-0.9869	-0.9996	-0.9903	-0.9768	-0.9737
	(180)	(180)	(180)	(180)	(180)	(180)	(180)	(180)
	0.0000	0.0000	0.0000	0.0000	0.0000	0.0000	0.0000	0.0000

	I9 [MPa]	I10 [µm]	I11 [µm]	I12 [µm]	I13 [µm]	I13c [µm]	I14 [-]
I1 = d0 [µm]	-0.9342	0.3185	0.5424	0.9089	0.2890	-0.0122	-0.7222
	(180)	(180)	(180)	(180)	(180)	(180)	(180)
	0.0000	0.0000	0.0000	0.0000	0.0001	0.8712	0.0000
I2 [mm]	0.0607	-0.9786	-0.9544	0.0213	-0.9708	-0.8915	-0.3525
	(180)	(180)	(180)	(180)	(180)	(180)	(180)
	0.4181	0.0000	0.0000	0.7762	0.0000	0.0000	0.0000
I3 [Mpa]	0.9115	-0.3929	-0.5957	-0.8404	-0.3632	-0.0788	0.6604
	(180)	(180)	(180)	(180)	(180)	(180)	(180)
	0.0000	0.0000	0.0000	0.0000	0.0000	0.2933	0.0000
I4 [-]	-0.8512	-0.5198	-0.2964	0.8856	-0.5325	-0.7546	-0.9869
	(180)	(180)	(180)	(180)	(180)	(180)	(180)
	0.0000	0.0000	0.0001	0.0000	0.0000	0.0000	0.0000
I5 [-]	-0.9022	-0.4295	-0.1812	0.9273	-0.4531	-0.6964	-0.9996
	(180)	(180)	(180)	(180)	(180)	(180)	(180)
	0.0000	0.0000	0.0149	0.0000	0.0000	0.0000	0.0000
I6 [-]	-0.8580	-0.5108	-0.2819	0.8925	-0.5255	-0.7509	-0.9903
	(180)	(180)	(180)	(180)	(180)	(180)	(180)
	0.0000	0.0000	0.0001	0.0000	0.0000	0.0000	0.0000
I7 [-]	-0.8287	-0.5485	-0.3369	0.8653	-0.5567	-0.7698	-0.9768
	(180)	(180)	(180)	(180)	(180)	(180)	(180)
	0.0000	0.0000	0.0000	0.0000	0.0000	0.0000	0.0000
I8 [-]	-0.8355	-0.5301	-0.3248	0.8653	-0.5369	-0.7502	-0.9737
	(180)	(180)	(180)	(180)	(180)	(180)	(180)
	0.0000	0.0000	0.0000	0.0000	0.0000	0.0000	0.0000
I9 [MPa]		0.0051	-0.2360	-0.9737	0.0298	0.3228	0.9070
		(180)	(180)	(180)	(180)	(180)	(180)
		0.9460	0.0014	0.0000	0.6911	0.0000	0.0000
I10 [µm]	0.0051		0.9473	-0.0973	0.9922	0.9370	0.4175
	(180)		(180)	(180)	(180)	(180)	(180)
	0.9460		0.0000	0.1939	0.0000	0.0000	0.0000
I11 [µm]	-0.2360	0.9473		0.1585	0.9125	0.7825	0.1651
	(180)	(180)		(180)	(180)	(180)	(180)
	0.0014	0.0000		0.0336	0.0000	0.0000	0.0268
I12 [µm]	-0.9737	-0.0973	0.1585		-0.1203	-0.4159	-0.9305
	(180)	(180)	(180)		(180)	(180)	(180)
	0.0000	0.1939	0.0336		0.1076	0.0000	0.0000
I13 [µm]	0.0298	0.9922	0.9125	-0.1203		0.9520	0.4432
	(180)	(180)	(180)	(180)		(180)	(180)
	0.6911	0.0000	0.0000	0.1076		0.0000	0.0000
I13c [µm]	0.3228	0.9370	0.7825	-0.4159	0.9520		0.6890
	(180)	(180)	(180)	(180)	(180)		(180)
	0.0000	0.0000	0.0000	0.0000	0.0000		0.0000
I14 [-]	0.9070	0.4175	0.1651	-0.9305	0.4432	0.6890	
	(180)	(180)	(180)	(180)	(180)	(180)	
	0.0000	0.0000	0.0268	0.0000	0.0000	0.0000	

The model selection was performed evaluating the $R^2_{adjusted}$ for all the combinations of variables. A synthesis of the survey conducted in this terms is in Table 48.

Table 48 - Models with Adjusted R-Square and Correlations between the different combinations of variables pairs.

MSE	R-Squared	Adjusted R-Squared	Cp	Included Variables	
1,14084E15	92,2107	92,0327	74,926	CDGJ 3-4-8-11	3-4 64.6 c=-0.56 ; 3-8 66.1 c=-0.54 ; 3-11 57.5 c=-0.59; 4-8 17.1 c=0.99 ; 4-11 49.8 c=-0.296 ; 8-11 48.98 c=-0.32
1,15431E15	92,1187	91,9386	77,8192	CEGJ 3-6-8-11	3-6 64.1 c= -0.57 ; 3-8 66.1 c=-0.54 ; 3-11 57.5 c=-0.59; 6-8 21.2 c=0.99 ; 6-11 50.0 c=-0.28 ; 8-11 48.98 c=-0.32
1,29444E15	91,162	90,96	107,902	CDEJ 3-4-6-11	3-4 64.6 c=-0.56 ; 3-6 64.1 c=-0.57; 3-11 57.5 c=-0.59; 4-6 35.38 c=0.9997 ; 4-11 49.8 c=-0.296; 6-11 50.0 c=-0.28
1,30269E15	91,1056	90,9023	109,675	CFGJ 3-5-8-11	3-5 62.9 c=-0.65; 3-8 66.1 c=-0.54; 3-11 57.5 c=-0.59; 5-8 45.9 c=0.97; 5-11 51.0 c=-0.18; 8-11 48.98 c=-0.32
1,35692E15	90,7354	90,5236	121,317	CGJN 3-8-11-14	3-8 66.1 c=-0.54; 3-11 57.5 c=-0.59; 3-14 62.5 c=0.66 ; 8-11 48.98 c=-0.32 ; 8-14 44.6 c=-0.97 ; 11-14 51.1 c=0.16
1,41973E15	90,3065	90,0849	134,802	CGIL 3-8-10-13	3-8 66.1 c=-0.54; 3-10 57.4 c=-0.39; 3-13 57.01 c=-0.36; 8-10 43.5 c=-0.53; 8-13 40.2 c=-0.54; 10-13 31.0 c=0.99
1,43558E15	90,1983	89,9743	138,205	CGJM 3-8-11-13c	3-8 66.1 c=-0.54; 3-11 57.5 c=-0.59; 3-13c 58.3 c=-0.08; 8-11 48.98 c=-0.32; 8-13c 33.7 c=-0.54; 11-13c 47.9 c=0.78
2,20997E15	84,8248	84,5661	305,168	CDI 3-4-10	3-4 64.6 c=-0.56 ; 3-10 57.4 c= -0.39 ; 4-10 45.98 c=-0.52
2,28225E15	84,3285	84,0613	320,775	CGI 3-8-10	3-8 66.1 c=-0.54 ; 3-10 57.4 c=-0.39; 8-10 43.5 c=-0.53
2,31251E15	84,1207	83,85	327,309	GHJ 8-9-11	8-9 65.94 c=-0.83 ; 8-11 48.98 c=-0.32; 9-11 53.23 c=-0.24
2,35872E15	83,8034	83,5273	337,287	CEI 3-6-10	3-6 64.1 c=-0.57 ; 3-10 57.4 c=-0.39; 6-10 46.8 c=-0.5108
2,43267E15	83,2956	83,0109	353,253	CGJ 3-8-11	3-8 66.1 c=-0.54; 3-11 57.5 c=-0.59; 8-11 48.98 c=-0.32
2,48039E15	82,9679	82,6776	363,557	EHI 6-9-10	6-9 62.1 c=-0.86; 6-10 46.8 c=-0.51; 9-10 52.04 c=0.0051
2,52049E15	82,6925	82,3975	372,215	DHI 4-9-10	4-9 63.2 c= -0.85; 4-10 45.9 c=-0.51; 9-10 52.04 c=0.0051
4,451E15	69,2626	68,9153	792,506	AC 1-3	1-3 68.9 c=-0.97
4,84559E15	66,5377	66,1596	878,188	CG 3-8	3-8 66.1 c=-0.54
4,87592E15	66,3282	65,9478	884,774	GH 8-9	8-9 65.94 c=-0.83
4,89441E15	66,2006	65,8186	888,789	CK 3-12	3-12 65.82 c= -0.84
5,04253E15	65,1777	64,7842	920,952	CH 3-9	3-9 64.78 c=0.91
5,06977E15	64,9896	64,594	926,866	CD 3-4	3-4 64.6 c=-0.56
5,07238E15	64,9716	64,5758	927,433	BM 2-13c	2-13c 64.6 c=-0.89

Note: for each model the $R^2_{adjusted}$ and correlation coefficient for each pair of variables in the model is reported.

Among the combinations of variables, the variables with poor correlation (c) were chosen, i.e. with correlation less than or equal to about 0.5.
These combinations of variables were chosen as independent variables in the regressions that will be reported below for the search for the best models with the highest possible R-Square value.
For these it is therefore necessary to study a model with simple and multiple statistical regressions.
The combinations of the basin index variables (to be used as independent) are:

- CDI, (C=I3, D=I4, I=I10);
- CGI (C=I3, G=I8, I=I10);
- CEI (C=I3, E=I6, I=I10);
- CGJ (C=I3, G=I8, J=I11);
- CG (C=I3, G=I8);
- CD (C=I3, D=I4).

3.6.1.1 Simple Regressions Esal-Basin Indices

In order to compare simple and multiple variable regression and to identify opportunities for variable transformation, many simple regressions were calibrated to identify the variable transformation which maximize the R^2.
Based on the considerations just made on the combinations of basin indices simple regressions were made in which the variables were used as follows:

- Dependent Variable: Esalmod
- As regards the Independent Variables (X), which were individually coupled to the dependent variables for simple regression, the indices previously selected were taken: I3, I4, I6, I8, I10, I11. These last variables X, in order to make the regressions, have been

transformed into these forms: X; 1/X; LOG(X), that is the natural logarithm; Exp(X); X^2; LOG10(X).

On each simple regression between Esal (*Esalmod*) and the individual Basin Index (I_i) performed, the model type was chosen that maximizes the value of R-Square, in order to find the best equation that returns the best correlation between variables. The best models obtained for I3, I4, I10, I8, I6, I11 and their transformation, in terms of Adjusted R-Square, are summarized in Table 49.
Apart of I11, I3 and I10, single regression showed very low values of R2 even with the best variable transformation applied. For this reason, multiple statistical regressions will be made later.

Table 49 - Simple Regressions between Esal and Basin Indexes

Case	Dependent Variable	Independent Variable	Model Type	Equation of the Model	Adj. R-Square
1	Esalmod	$I3^2$	*Square root-Y squared-X* *Y = (a + b*X^2)^2*	Esalmod = (3342.83 + 4.99907E-9*(I3^2)^2)^2	78.7%
2	Esalmod	Exp(I4)	*Squared X* *Y = a + b*X^2*	Esalmod = 1.15113E8 - 1.78648*EXP(I4)^2	3.0%
3a	Esalmod	1/I10	*Logarithmic-Y squared-X* *Y=exp(a + b*X^2)*	Esalmod = exp(14.8862 + 3489.44*1/I10^2)	76.2%
3b	Esalmod	$I10^2$	*S-curve* *Y = exp(a + b/X)*	Esalmod = exp(14.8862 + 3489.44/I10^2)	76.2%
4a	Esalmod	1/I8	*Logarithmic-Y squared-X* *Y=exp(a + b*X^2)*	Esalmod = exp(18.1011 - 0.0552809*1/I8^2)	5.4%
4b	Esalmod	$I8^2$	*S-curve* *Y = exp(a + b/X)*	Esalmod = exp(18.1011 - 0.0552809/I8^2)	5.4%
5	Esalmod	$I6^2$	*Squared-X model* *Y = a + b*X^2*	Esalmod = 1.25394E8 - 1.76965E8*(I6^2)^2	1.6%
6	Esalmod	1/I11	*Exponential* *Y = exp (a + b*X)*	Esalmod = exp(13.5727 + 124.514*1/I11 [μm])	78.7%

Where: Dependent Variable: Esalmod=design Esals calculated from the AASHTO Structural Number. Independent Variables that include basin indices or their transformations: I3=equivalent modulus characterizing the conditions of all the layers of the pavement; I4=area under pavement performance characterizing the condition of the pavement upper layer; I10=Anas index IS300 that is the surface curvature index characterizing the pavement layers; I8=area indices characterizing the condition of lower layer; I6=area indices characterizing the condition of the middle layer; I11=middle layer index characterizing the condition of the base layer.

From these simple regressions it's possible to note that some of these models have very low Adjusted R-square. This was predictable, but it is important for a more complete understanding of research.
The situation will improve in terms of multiple regressions where these values will be higher and the model will respond better in terms of Esal predict starting from basin indices (the latter not very correlated with each other, so as to respond better in terms of statistical prediction).
Moreover, in Table 50 simple regressions without variable transformation were made between the Esal and the Anas Indices IS300, IS200 and $IS200_{CF}$ that have been identified, as already expressed in the summary table of the indices, with the following codes: IS300 = I10; IS200 = I13; $IS200_{CF}$ = I13c. Also in this case the dependent variable Y is represented by the Esal (Esalmod) and the independent variables X are the structural Anas indices.
As it can be seen, the transformation has a slight improvement in the R^2 and I300 (I.e. I10) remains the index with the best correlation with Esals.

Table 50 - Simple Regressions between Esal and Anas Indices

Case	Dependent Variable	Independent Variable	Model Type	Equation of the Model	Adj. R-Square
1	Esalmod	IS300 = I10	*S-curve model* *Y = exp(a + b/X)*	Esalmod = exp(12.5507 + 184.247/I10)	73.7%
2	Esalmod	IS200 = I13	*S-curve model* *Y = exp(a + b/X)*	Esalmod = exp(11.7652 + 129.174/I13)	65.7%
3	Esalmod	$IS200_{CF}$ = I13c	*Reciprocal-Y square root-X* *Y=1/(a+ b*sqrt(X))*	Esalmod = 1/(-1.92686E-7 + 4.35651E-8*sqrt(I13c))	33.4%

3.6.1.2 Multiple Regressions Esal-Basin Indices

As already explained above, the combinations of variables of the basin indices have been used as independent variables, so as to find the model that best meets the high R-Square value.
To do this it was tried to find the best transformations of variables that could give, in all their combinations, the most satisfying result.
The Dependent Variable Y is also in this case the Esal. The Independent Variables X, as has already been done for simple regression indices, have been transformed into these forms, obviously considering all the possible combinations between them:

- X;
- 1/X;
- LOG(X), that is the natural logarithm;
- Exp(X);
- X^2;
- LOG10(X).

Multiple regressions were made with the following basic combinations of independent variables, that are the variables with lower correlation value considered in pairs, which were then transformed as explained above:

1) I3, I4, I10;
2) I3, I8, I10;
3) I3, I6, I10;
4) I3, I8, I11;
5) I3, I8;
6) I3, I4.

In Table 51 there are the best results obtained with the combinations of transformed independent variables, and also are reported the results obtained with the combinations of simple variable.
In this way it is possible to compare the adjusted r-square between the simple case of combinations of independent non-transformed variables and the best model of the combinations of independent variables transformed.

Table 51 - Multiple Regressions performed between Esal and different combinations of Basin Indices

Case	Dependent Variable	Independent Variables	Model	Adj. R-Square
1a	Esalmod	I3, I4, I10	Esalmod = -9.32453E9 + 1.64983E6*I3 + 8.20628E8*I4 + 3.37912E7*I10	84.6%
1b	Esalmod	$I3^2$, $I4^2$, $I10^2$	Esalmod=-2.75827E9 + 599.229*I3^2 + 3.01189E7*I4^2 + 230332.*I10^2	88.4%
2a	Esalmod	I3, I8, I10	Esalmod = -3.13263E9 + 1.36312E6*I3 + 2.57148E9*I8 + 2.6374E7*I10	84.1%
2b	Esalmod	$I3^2$, I8, $I10^2$	Esalmod = -1.34349E9 + 541.625*I3^2 + 1.70281E9*I8+ 202539.*I10^2	88.5%
3a	Esalmod	I3, I6, I10	Esalmod = -5.82598E9 + 1.70618E6*I3 + 4.58939E9*I6 + 3.47766E7*I10	83.5%
3b	Esalmod	$I3^2$, $I6^2$, $I10^2$	Esalmod = -1.72066E9 + 622.758*I3^2 + 2.03468E9*I6^2 + 234456.*I10^2	88.5%
4a	Esalmod	I3, I8, I11	Esalmod = -3.15424E9 + 1.57605E6*I3 + 2.4872E9*I8 + 2.6122E7*I11	83.0%
4b	**Esalmod**	**1/I3, I8, 1/I11**	**Esalmod = -1.23954E9 + 8.17769E11*1/I3- 2.14686E9*I8+ 3.62946E10*1/I11**	**90.7%**
5a	Esalmod	I3, I8	Esalmod = -5.63868E8 + 493331.*I3 + 5.34657E8*I8	66.2%
5b	Esalmod	$I3^2$, $I8^2$	Esalmod = -2.58765E8 + 279.458*I3^2 + 6.44306E8*I8^2	73.2%
6a	Esalmod	I3, I4	Esalmod = -1.43295E9 + 493576.*I3 + 1.32796E8*I4	64.6%
6b	Esalmod	$I3^2$, $I4^2$	Esalmod = -6.44251E8 + 270.989*I3^2 + 7.55219E6*I4^2	71.3%

From the regressions seen, the combinations of three FWD indices (transformed and not) predict better the Esal. In general, the multiple regressions respond better than simple regressions and therefore the combination of FWD indices, that are not correlated to each other, is important for the Esal prediction. The best model, including 3 indices I3, I8 and I11, returns an Adj.-R^2=90.7%. Those indices are related respectively to upper (I3), middle (I11) and lower (I8) layers.

The best model just seen gave a good result, considering that I3 to be calculated includes several variables, including the Poisson coefficient which requires more hypotheses, then a further attempt was made to have a model of immediate and simpler resolution: the I1 index was used instead of I3, combined with I8 and I11.

The I1 index is the first deflection under load and therefore is obtained directly in the center of the LWD test plate. In Table 52 it can be seen how also the combination of the three indices I1, I8, I11 gave good results.

Table 52 - Multiple Regression performed between Esal and the combination of I1, I8, 1/I11 Basin Indexes

Case	Dependent Variable	Independent Variables	Model	Adj. R-Square
7	Esalmod	I1, I8, 1/I11	**Esalmod = -1.23954E9 + 5.73443E6*I1- 2.14686E9*I8 [-] + 3.62946E10*1/I11 [µm]**	**90.73%**

This combination, can be said to be the best and can be preferred compared to I3, I8, I11, as a simple calculation and predicts the Esal well with an Adj. R-square equal to 90.7% that is a good result.

3.6.1.3 Statistical analysis between Esal (AASHTO) and Esal SNeff (NDT)

As was previously reported, AASHTO guide for design of pavement structures (edition 1993) provide a procedure to estimate the SN of existing pavement by FWD tests.
Then a statistic study is also performed to understand the link between Esal calculated with the AASHTO method and those deriving from FWD tests with SNeff.
By using data from the numerical simulations, 2 types of regressions were analyzed:

1) Simple regressions between Esals deriving from the layer coefficients assumed as actual value (i.e. dependent variable) and Esal deriving from SNeff (independent variable) calculated with the AASHTO procedure assuming known values of Subgrade modulus (Esalmod vs. EsalSNeff);

2) Simple regressions between Esal deriving from the coefficients and Esal layers deriving from the AASHTO procedure with also the estimation of subgrade modulus from FWD data, SNeff600 (Esal vs. ESALSNeff600).

In both cases, to make simple regressions, comparisons were made between types of alternative variable transformations, so as to choose the one that returned the highest value of R-square. Here are the results of model calibrations (Table 53 and Table 54).

Table 53 - Comparison of alternative models Esalmod vs. EsalSNeff

Model	*Correlation*	*R-Squared*
Linear	0,9785	95,75%
Double square root	0,9735	94,77%
Double squared	0,9615	92,45%
Multiplicative	0,9566	91,51%
Squared-X	0,9494	90,14%
Square root-Y	0,9493	90,12%
Square root-X	0,9340	87,23%
Logarithmic-Y square root-X	0,9253	85,62%
Square root-Y logarithmic-X	0,9069	82,24%
Squared-Y	0,9058	82,05%
Double reciprocal	0,8559	73,26%
Square root-Y squared-X	0,8518	72,56%
Reciprocal-Y logarithmic-X	-0,8295	68,80%
Exponential	0,8237	67,85%
S-curve model	-0,8017	64,27%
Squared-Y square root-X	0,8002	64,03%
Logarithmic-X	0,7941	63,06%
Reciprocal-Y square root-X	-0,6860	47,06%
Logarithmic-Y squared-X	0,6656	44,31%
Square root-Y reciprocal-X	-0,6493	42,16%
Squared-Y logarithmic-X	0,6132	37,61%
Reciprocal-X	-0,4841	23,44%
Reciprocal-Y squared-X	-0,3404	11,59%
Squared-Y reciprocal-X	-0,3030	9,18%
Reciprocal-Y	<no fit>	
Logistic	<no fit>	
Log probit	<no fit>	

Table 54 - Comparison of alternative models Esalmod vs. EsalSNeff600

Model	*Correlation*	*R-Squared*
Linear	0,9680	93,69%
Double squared	0,9609	92,33%
Double square root	0,9535	90,92%
Squared-X	0,9493	90,12%
Square root-Y	0,9411	88,57%
Multiplicative	0,9285	86,22%
Square root-X	0,9125	83,27%
Logarithmic-Y square root-X	0,9113	83,05%
Squared-Y	0,8962	80,33%
Square root-Y logarithmic-X	0,8763	76,79%
Square root-Y squared-X	0,8530	72,76%
Exponential	0,8210	67,41%
Reciprocal-Y logarithmic-X	-0,8105	65,69%
Double reciprocal	0,8026	64,42%
Squared-Y square root-X	0,7822	61,19%
Logarithmic-X	0,7652	58,55%
S-curve model	-0,7590	57,60%
Reciprocal-Y square root-X	-0,6845	46,85%
Logarithmic-Y squared-X	0,6689	44,74%
Square root-Y reciprocal-X	-0,6150	37,82%
Squared-Y logarithmic-X	0,5908	34,91%
Reciprocal-X	-0,4580	20,98%
Reciprocal-Y squared-X	-0,3462	11,98%
Squared-Y reciprocal-X	-0,2860	8,18%
Reciprocal-Y	<no fit>	
Logistic	<no fit>	
Log probit	<no fit>	

From these comparisons the model that best predict the dependent variable was the linear type:

$$Y = a + b \cdot X$$

Where: Y = Esalmod as dependent variable; X = EsalSNeff or EsalSNeff600 as independent variable (depending on whether it is case 1 or case 2); a, b = regression coefficients.

Detailed data on the regression calibration are reported in the following:

1) <u>Esalmod vs. Esal SNeff</u>
   Dependent variable: Esalmod
   Independent variable: ESALSneff
   Linear model: Y = a + b*X

   In Table 55 there are coefficients and analysis of variance Esalmod vs. EsalSNeff.

Table 55 - Coefficients and analysis of variance Esalmod vs. Esal SNeff

	Least Squares	*Standard*	*T*	
Parameter	*Estimate*	*Error*	*Statistic*	*P-Value*
Intercept	-3,33482E6	2,32725E6	-1,43294	0,1536
Slope	0,0485346	0,00076677	63,2974	0,0000

Source	*Sum of Squares*	*Df*	*Mean Square*	*F-Ratio*	*P-Value*
Model	2,45407E18	1	2,45407E18	4006,57	0,0000
Residual	1,09027E17	178	6,12511E14		
Total (Corr.)	2,56309E18	179			

   R-squared = 95.75 percent
   R-squared (adjusted for d.f.) = 95.72 percent
   The equation of the fitted model is Esalmod = -3.33482E6 + 0.0485346*ESAL Sneff.

   In Figure 72 there is the plot of fitted model Esalmod vs. EsalSNeff.

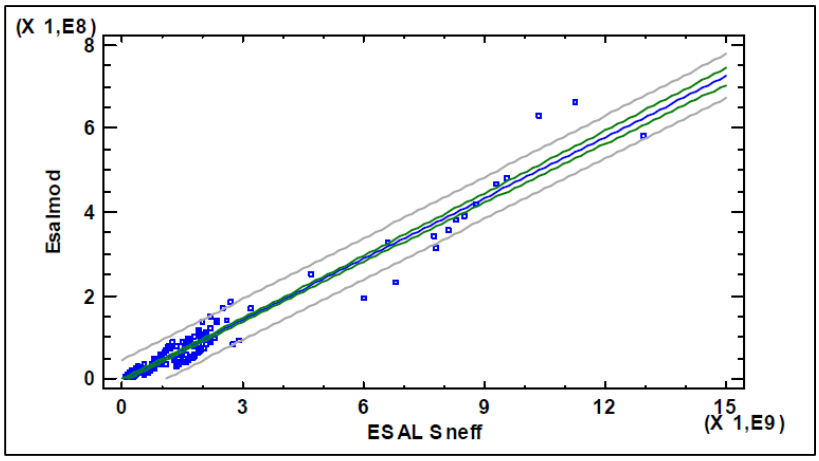

Figure 72 - Plot of fitted model Esalmod vs. EsalSNeff

2) Esalmod vs. Esal SNeff600

Dependent variable: Esalmod

Independent variable: ESALSneff600

Linear model: Y = a + b*X

Coefficients and analysis of variance Esalmod vs. EsalSNeff600 are reported in Table 56.

Table 56 - Coefficients and analysis of variance Esalmod vs. Esal SNeff600

	Least Squares	*Standard*	*T*	
Parameter	*Estimate*	*Error*	*Statistic*	*P-Value*
Intercept	-5,20805E6	2,86787E6	-1,816	0,0711
Slope	0,0450401	0,000875898	51,4217	0,0000

Source	*Sum of Squares*	*Df*	*Mean Square*	*F-Ratio*	*P-Value*
Model	2,40144E18	1	2,40144E18	2644,19	0,0000
Residual	1,61659E17	178	9,08194E14		
Total (Corr.)	2,56309E18	179			

R-squared = 93.69 percent

R-squared (adjusted for d.f.) = 93.66 percent

The equation of the fitted model is Esalmod = -5.20805E6 + 0.0450401*ESAL Sneff600.

In Figure 73 there is the plot of fitted model Esalmod vs. EsalSNeff.

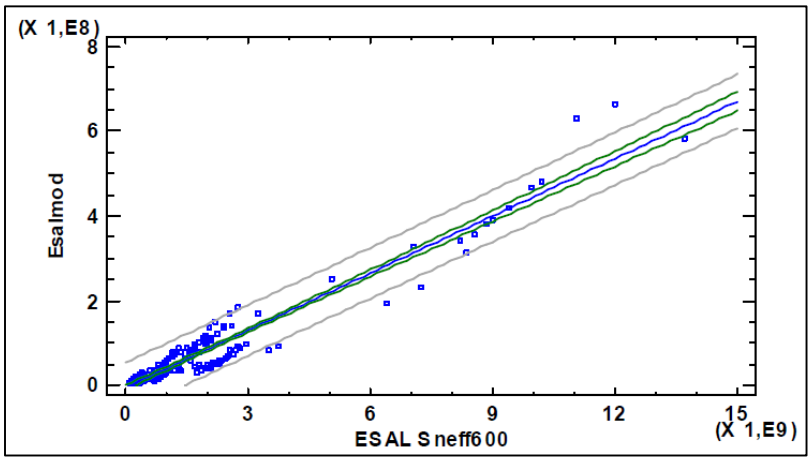

Figure 73 - Plot of fitted model Esalmod vs. EsalSNeff600

Analyzing the two cases it can be seen as the case Esalmod vs. EsalSNeff returns a higher R-square adjusted value, i.e. 95.72%. The other case has a slightly lower value, of 93.66%, but still significant and higher than the ones obtained with the basin indices. It is worth mentioning that the

AASHTO guide includes also a procedure to correct FWD estimation in function of Asphalt layers' temperatures different from 20°C.

3.6.1.4 Statistical analysis on the variation of Esals and Basin Indices

Another analysis on the Esal was conducted in terms of percentage variation of Esal (Delta) for changes in pavement moduli, this was done to verify how changes in the indices are able to capture variations in the number of Esal. The variations of Esal "DEsal" (dependent variable) have been related with the variation of the "DIi" basin index (independent variable), considering the indices from I1 to I14. The procedure for selection the best model form was the same as previously described.
Below are all the analyzes carried out, with all cases, and the results that may be considered significant in terms of Adj. R-square:

- **Case 1: Simple Regressions DEsal-DIndices on the 180 combinations of road pavements of the database**
  In this case, which considers in the 180 cases analyzed, the percentage variation of all the modules of the individual layers, only two relationships obtained can be considered of interest, with the indices I11 and I3. The best result was in the regression between the Desal and the delta of the I11 index, i.e. the middle layer index (D_{300}-D_{600}), characterizing the condition of the base layer. The subsequent regression to this in terms of high r-square value is that which analyzes the Desal with DI3, ie the Equivalent Modulus index characterizing the condition of all the layers' pavement.
  1. DEsal = -5.34221*D_I11 with **Adj. R-square=90.93%**
  2. DEsal = 5.41213*D_I3 with Adj. R-square=83.11%

- **Case 2: Comparison of regression DEsal-DIndices by Dcode**
  A comparison of regression models was made by categorizing pavements by a code (Dcode). The Delta Code is representative of what layer was effected by a variation of the module, since in the analyzed pavements some layers' modules have been made to vary individually or simultaneously, leaving the remaining modules unchanged.
  The Dcode meanings are reported in the following Table 57.

Table 57 - Meaning of Dcodes

Dcode	Meaning
M1	Variation in percentage of the module M1 (wear+binder) leaving the rest constant
M2	Variation in percentage of the module M2 (base) leaving the rest constant
M3	Variation in percentage of the module M3 (subbase) leaving the rest constant
Ms	Variation in percentage of the module Ms (subgrade) leaving the rest constant
M1 M2	Contemporary variation in percentage of the modules M1 and M2 (wear+binder and base) leaving the rest constant

Note: Dcode is an indicative code of the percentage variation (-20%, -10%, 0%, + 15%) of the pavement layer modules: each of the codes M1, M2, M3, Ms, M1M2 indicate which module has changed in percentage, leaving the others unchanged at the 0% reference case.

For each case analyzed, with the logic described above, on the road pavement packages studied, a total of 180 complete cases were analyzed. The significant results of the analysis with adj. r-square above 90% are reported.

1. DEsal = 0.0406017-8.078*D_I1 + 0.541734*D_I1*(Dcode=M1 M2) - 1.56926*D_I1*(Dcode=M2)-0.926954*D_I1*(Dcode=M3)+ 4.34099*D_I1*(Dcode= Ms)+ 33.9311*D_I1*(Dcode=O), Adj. R-square=95.65%
   Where the terms similar to Dcode=M1 M2 are indicator variables which take the value 1 if true and 0 if false. This corresponds to 6 lines with equal intercepts. For example, when Dcode=M1, the model reduces to DEsal = 0.0406017 - 8.078*D_I1. When Dcode=M1 M2, the model reduces to DEsal = 0.0406017 - 7.53626*D_I1.
2. DEsal=0.029191+3.08353*D_I2+0.183353*D_I2*(Dcode=M1M2) + 1.04541*D_I2*(Dcode=M2) + 6.96291*D_I2*(Dcode=M3) + 17.272*D_I2*(Dcode=Ms) + 21.1158*D_I2*(Dcode=O), Adj. R-square=93.11%
3. **DEsal=0.0314188+8.03369*D_I3-0.154061*D_I3*(Dcode=M1 M2)+ 1.79681*D_I3*(Dcode=M2) + 0.98496*D_I3*(Dcode=M3) - 4.03678*D_I3*(Dcode=Ms) - 28.0082*D_I3*(Dcode=O), Adj. R-square=96.99%**
4. DEsal=0.0305871+35.0838*D_I4-3.17469*D_I4*(Dcode=M1 M2) + 3.65615*D_I4*(Dcode=M2) + 99.8576*D_I4*(Dcode=M3) - 61.0247*D_I4*(Dcode=Ms) + 28.0462*D_I4*(Dcode=O), Adj. R-square=91.92%
5. DEsal=0.0285062+10.3415*D_I7-1.47918*D_I7*(Dcode=M1M2)- 0.0764718*D_I7*(Dcode=M2) + 9.42813*D_I7*(Dcode=M3) - 16.8157*D_I7*(Dcode=Ms) + 6.20444*D_I7*(Dcode=O), Adj. R-square=89.8%
6. DEsal=0.0301858+8.79297*D_I8- 1.02251*D_I8*(Dcode=M1 M2) + 0.31865*D_I8*(Dcode=M2) + 3.48315*D_I8*(Dcode=M3) - 13.9727*D_I8*(Dcode=Ms) + 5.66659*D_I8*(Dcode=O), Adj. R-square=92.11%
7. DEsal=0.0415766-3.04061*D_I10+0.114917*D_I10*(Dcode=M1M2)- 0.873091*D_I10*(Dcode=M2)-7.05176*D_I10*(Dcode=M3)- 17.2281*D_I10*(Dcode=Ms)-31.3848*D_I10*(Dcode=O), Adj. R-square=91.18%
8. DEsal=0.0341138-7.86079*D_I11+2.75947*D_I11*(Dcode=M1M2)+ 2.62149*D_I11* (Dcode=M2)+2.73028*D_I11*(Dcode=M3)+1.11244*D_I11*(Dcode=Ms)+38.8361*D _I11*(Dcode=O), Adj. R-square=93.54%
9. DEsal=0.032105-3.84297*D_I14-0.306887*D_I14*(Dcode=M1M2)- 1.91094*D_I14* (Dcode=M2)+32.3059*D_I14*(Dcode=M3)+7.94856*D_I14*(Dcode=Ms)- 6.57178*D_I14*(Dcode=O), Adj. R-square=92.63%

- **<u>Case 3: Comparison of multiple regression DEsal-DIndices by Dcode (Dcode <> "Ms")</u>**

  A comparison of regression lines was made between the Delta Esal (DEsal) as dependent variable, the Delta Deflection Basin Indexes (DIi) calculated as independent variable, and the Delta Code (Dcode) as Level codes, with a selection of the variable Dcode that is not equal to Ms (Ms=subgrade modulus).

  The significant results of the analysis with adj. r-square greater than 90% are reported below. Considering the Delta Code different from the subgrade module, the number of complete cases this time is 150.

1. DEsal=0.0342895-7.96225*D_I1 + 0.451866*D_I1*(Dcode=M1M2) - 1.6067*D_I1*(Dcode=M2) - 0.939517*D_I1*(Dcode=M3) + 29.7961*D_I1*(Dcode=O), Adj. R-square=95.06%
2. DEsal=0.0242897+3.04974*D_I2+0.211712*D_I2*(Dcode=M1M2) + 1.05526*D_I2*(Dcode=M2) + 6.90483*D_I2*(Dcode=M3) + 17.0865*D_I2*(Dcode=O), **Adj. R-square=96.41%**
3. DEsal=0.0282203+7.9763*D_I3- 0.107583*D_I3*(Dcode=M1 M2) + 1.81569*D_I3*(Dcode=M2) + 0.991359*D_I3*(Dcode=M3) - 25.9173*D_I3*(Dcode=O), Adj. R-square=96.21%
4. DEsal=0.0269139+34.7822*D_I4- 2.93326*D_I4*(Dcode=M1 M2) + 3.77414*D_I4*(Dcode=M2) + 99.2613*D_I4*(Dcode=M3) + 20.7666*D_I4*(Dcode=O), Adj. R-square=90.08%
5. DEsal=0.0257999+8.70582*D_I8- 0.950747*D_I8*(Dcode=M1M2) +0.355968*D_I8*(Dcode=M2) + 3.46934*D_I8*(Dcode=M3) + 3.65282*D_I8*(Dcode=O), Adj. R-square=91.12%
6. DEsal=0.0382765-3.01668*D_I10+0.0969563*D_I10*(Dcode=M1M2) - 0.879626*D_I10*(Dcode=M2) - 7.01278*D_I10*(Dcode=M3) - 28.6763*D_I10*(Dcode=O), Adj. R-square=93.83%
7. DEsal=0.0309074-7.80532*D_I11+2.71221*D_I11*(Dcode=M1M2) +2.58722* D_I11*(Dcode=M2) + 2.70428*D_I11*(Dcode=M3) +35.8693*D_I11*(Dcode=O), Adj. R-square=95.02%
8. DEsal=0.0299307-3.82242*D_I14-0.32209*D_I14*(Dcode=M1M2) - 1.91473*D_I14*(Dcode=M2) + 32.1889*D_I14*(Dcode=M3) - 5.88699*D_I14*(Dcode=O), Adj. R-square=90.21%

The generalized increase of adj. R^2 derived by the selecting evaluation of layers that have changed the modulus, confirms the sensitivity of indices to different pavement layers and subgrade.

- **<u>Case 4: Simple Regressions DEsal-DIndices (Dcode<>"Ms")</u>**

A simple regression was made between the Delta Esal (DEsal) as dependent variable and the Delta Deflection Basin Indexes (DIi) calculated as independent variable, with a linear model Y=b·X and a selection variable Dcode that is not equal to Ms. Therefore, the variation of the resilient module of the subgrade was not considered. The best results (i.e. adj. $R^2 \geq 90\%$) are:

1. DEsal = -7.88488*D_I1, with **Adj. R-square=92.77%**
2. DEsal = 3.4831*D_I2, with **Adj. R-square=89.98**%
3. DEsal = 8.21799*D_I3, with **Adj. R-square=94.50%**
4. DEsal = -5.08009*D_I11, with **Adj. R-square=93.10%**

Using as subset only the samples without a variation in the subgrade moduli, improve the prediction capability with an increase of adj. R^2.

- **<u>Case 5: Simple Regressions DEsal-DIndices (Dcode<>"Ms" & Dcode<>"M3")</u>**

In all cases, a simple regression was made between the Delta Esal (DEsal) as dependent variable and the Delta Deflection Basin Indexes (DIi) calculated as independent variable, with a linear model Y=b·X and a selection variable Dcode that is not equal to Ms (subgrade module) and to M3 (sub-base or foundation module). Therefore, the variation of the resilient

module of the subgrade and of the foundation were not considered. The best results with adj. r-square values greater than 90% are exposed below.

1. DEsal = -7.82252*D_I1, with Adj. R-square=92.54%
2. DEsal = 3.37696*D_I2, with Adj. R-square=95.73%
3. DEsal = 8.17565*D_I3, with Adj. R-square=94.43%
4. DEsal = 33.1471*D_I4, with Adj. R-square=94.43%
5. DEsal = 13.21*D_I6, with Adj. R-square=90.23%
6. DEsal = 9.17058*D_I7, with Adj. R-square=91.05%
7. DEsal = 8.03983*D_I8, with Adj. R-square=92.29%
8. DEsal = -3.04085*D_I10, with Adj. R-square=91.39%
9. DEsal = -5.12694*D_I11, with Adj. R-square=92.69%

In the latter case, compared to the previous ones, it is possible to note that all the models increased the adj. R^2 with values higher than 90% when, in addition to the subgrade, the subbase moduli variations were excluded in the regressions.

3.6.2 Prediction of SN from FWD Indexes

For completeness in the study it is also important to look at the correlation between Structural Numbers and FWD indices, in order to see at structural level which are the indexes most sensitive to changes in the bearing capacity of the road pavement. Similarly, to the studies made on Esal, also for the Structural number the independent variables to be included in the model (i.e. basin indices) were not correlated and the higher values of Adj. R-square for the regressions were selected (Table 58).

Table 58 - Models with Adjusted R-Square and Correlations between the different combinations of variables pairs

		Adjusted		*Included*
MSE	*R-Squared*	*R-Squared*	*Cp*	*Variables*
0.00281796	99.695	99.6898	297.112	CGK
0.00316987	99.6569	99.651	355.694	BDE
0.00359668	99.6107	99.604	426.745	GHK
0.00361726	99.6084	99.6018	430.172	BGN
0.0036304	99.607	99.6003	432.359	BEG
0.00776729	99.1544	99.1449	1126.38	GH
0.00790543	99.1394	99.1297	1149.51	AG
0.0115545	98.7422	98.7279	1760.42	FK
0.0118255	98.7127	98.6981	1805.79	CG
0.0128299	98.6033	98.5875	1973.95	BG
0.148523	83.7402	83.6489	24829.8	M
0.202108	77.8739	77.7496	33851.7	F
0.206148	77.4316	77.3048	34531.9	G
0.238473	73.8928	73.7461	39974.2	D
0.253741	72.2213	72.0652	42544.7	E
0.908334	0.0	0.0	153611.	

2-4-6 2-4 97.3 c=0.46 2-6:96.9 c=0.45 4-6 c=0.99 BD e BE

8-9 c=-0.8

1-8 c=0.6

7-12 c=0.8

3-8 c=-0.5

2-8 c=0.48

In the following part are exposed the models developed with simple and multiple regressions between SN (dependent variable) and Basin Indices (independent variables).

3.6.2.1 Simple Regressions SN-Basin Indices

For this case the simple regressions are summarized in Table 59, with the results in terms of linear model and the best model:

Table 59 - Prediction of SN from NDT Indexes: simple regressions

Case	Dependent Variable [Structural Number]	Independent Variable [Indexes]	Linear Model	Adj. R-Square [%]	Best Model	Adj. R-Square [%]
1	SN	I1 = D0	SN [inch] = 4.39129 + 0.00355896*D0	2.1	SN [inch] = sqrt(22.2364 + 0.00011756*D0^2)	3.3
2	SN	I2	SN [inch] = 0.801912 + 0.00000338268*I2 [mm]	68.2	SN [inch] = 1/(0.0224681 + 221653/I2 [mm])	78.2
3	SN	I3	SN [inch] = 5.3185 - 0.000357378*I3 [Mpa]	0.1	SN [inch] = sqrt(19.2862 + 5521.7/I3 [Mpa])	2.7
4	SN	I4	SN [inch] = -10.6505 + 1.92863*I4 [-]	74.3	SN [inch] = 20.8297 - 128.102/I4 [-]	75.8
5	SN	I5	SN [inch] = -18.2867 + 26.3395*I5 [-]	62.6	SN [inch] = 28.5661 - 20.8129/I5 [-]	63.5
6	SN	I6	SN [inch] = -1.91354 + 10.3258*I6 [-]	72.7	SN [inch] = exp(3.0928 - 0.992379/I6 [-])	76.7
7	SN	**I7**	SN [inch] = 0.998884 + 7.94228*I7 [-]	78.2	SN [inch] = exp(2.44039 - 0.409026/I7 [-])	**84.9**
8	SN	**I8**	SN [inch] = 1.99035 + 7.70373*I8 [-]	77.6	SN [inch] = 1/(0.0653744 + 0.0514462/I8 [-])	**86.2**
9	SN	I9	SN [inch] = 6.32711 - 0.00615473*I9 [MPa]	22.7	SN [inch] = sqrt(13.7692 + 2256.94/I9 [MPa])	26.6
10	SN	I10	SN [inch] = 8.72803 - 0.0987838*SCI I10 [µm]	69.9	SN [inch] = 1/(0.120632 + 0.0000589019*SCI I10 [µm]^2)	79.1
11	SN	I11	SN [inch] = 7.54913 - 0.0777706*BDI I11 [µm]	51.6	SN [inch] = 1/(0.143769 + 0.000056053*BDI I11 [µm]^2)	60.4
12	SN	I12	SN [inch] = 3.69417 + 0.116173*I12 [µm]	28.4	SN [inch] = sqrt(42.4357 - 161.591/I12 [µm])	34.5
13	SN	I13	SN [inch] = 9.53442 - 0.20034*I13 [µm]	67.9	SN [inch] = 1/(0.101266 + 0.000202964*I13 [µm]^2)	76.5
14	SN	**I13c**	SN [inch] = 9.62662 - 0.165317*I13c [µm]	82.9	SN [inch] = 1/(-0.267462 + 0.0903081*sqrt(I13c [µm]))	**91.2**
15	SN	I14	SN [inch] = 7.65434 - 9.74376*I14 [-]	60.8	SN [inch] = (2.56963 - 4.30055*I14 [-]^2)^2	64.2

From the results obtained there is not a high adj. R^2 with those indices that depend on the subgrade, and this is explained by the fact that the SN calculated with the empirical AASHTO method is not a function of the subgrade. I13c (I200c) returned the highest correlation with SN, followed by the area indices I7 (middle layer) and I8 (lower layer) with 84.9% and 86.2%. Likewise, the calculations were also made considering the correlations with SNeff and SNeff600 as independent variables.

3.6.2.2 Multiple Regressions SN-Basin Indices

At the multiple regression level, the dependent variable is the Structural Number SN, and the best results are given by the combinations of the following independent variables:

- 1/I3, I8

- I2, I8
- I2, I4
- I2, I6

In Table 60 the details of the results obtained with the highest values of Adj. R-square and the combination of independent variables that are not very correlated (i.e. with a correlation degree lower than 0.5).

Including just two variables in the model improves significantly the Adj. R-square, with values higher than 97%. Combining indices I3 or I2 with I8, that are related to upper and lower layers respectively, returns an Adj. R-square of about 99% .

The calculation was also made by combining I1 (D0 = first deflection under load) and I8 and also in this case Adj. R-square is 99.2% high.

Table 60 - Multiple regressions SN-Basin Indexes

Case	Dependent Variable	Independent Variables	Best Model	Adj. R-Square [%]
1	SN	1/I3, I8	SN [inch] = 2.90684 - 1773.21*1/I3 [Mpa] + 10.7882*I8 [-]	**99.1**
2	SN	I2, I8	SN [inch] = 0.206796 + 0.0000021348*I2 [mm] + 5.48892*I8 [-]	98.6
3	SN	I2, I4	SN [inch] = -8.79026 + 0.00000221485*I2 [mm] + 1.36074*I4 [-]	97.3
4	SN	I2, I6	SN [inch] = -2.66365 + 0.00000225665*I2 [mm] + 7.26419*I6 [-]	96.9
5	SN	I1=D0, I8	SN [inch] = 2.90684 - 0.0124342*D0 + 10.7882*I8 [-]	**99.2**

3.6.2.3 Statistical analysis between SN and SNeff

In this case was made the SN prediction as dependent variable, from SNeff once and then also SNeff600 considered as independent variables. The latter SNeff and SNeff600 are two parameters that derive from Falling Weight tests and, of course, are two indices that can be traced back to a wide range of temperatures as they derive from a procedure already codified by AASHTO (1993), that includes a procedure to correct the estimation of the FWD according to the temperatures of the asphalt layers other than 20 ° C. The results are reported in Table 61:

Table 61 - Prediction of SN from SNeff and SNeff600

Case	Dependent Variable [Structural Number]	Independent Variable [Indexes]	Linear Model	Adj. R-Square [%]	Best Model	Adj. R-Square [%]
1	SN	SNeff	SN [inch] = 0.583974 + 0.815243*Sneff [inch]	96.9	SN [inch] = 1/(0.0258222 + 0.93903/Sneff [inch])	**97.8**
2	SN	SNeff600	SN [inch] = -0.176684 + 0.989824*Sneff 600 [inch]	97.9	SN [inch] = 1/(-0.00358056 + 1.06683/Sneff 600 [inch])	**98.5**

In both cases, the regression returns Adj. R-square very high in both cases so both SNeff and SNeff600 can be evaluated as indices that directly allow SN to be predicted. The Adj. R-square are

equal to 97.8% in the case where SNeff is the independent variable, and equal to 98.5% in the case of SNeff600.

3.7 Performance based approach by NDT

In this thesis work a change of the point of view is brought out with a performance-based approach that is different from that of traditional specifications, therefore, in qualitative terms, attention has been placed in the quality controls by NDT in construction phase of the work and the consequent verification of the acceptance performance requirements.
In paragraphs 3.8, 3.9, 3.10, 3.11 will be illustrated the experimental cases and the models developed in terms of costs, or rather bonuses and penalties, which derive from changes in the Performance Indices respect to the project requirements and which are fundamental for the acceptance of the new construction works.
A performance-based approach aims at a long-term vision of the road superstructure throughout its entire life cycle, ranging from construction to laying materials, use, maintenance and rehabilitation and the end of life. A road that meets high performance requirements determines in users an improvement in the quality of life and a social, environmental and economic development that can therefore be said to be sustainable.

Why a performance-based approach and not a traditional? The Performance-Based Specifications are very advantageous compared to traditional ones, as they can overcome many limitations that have the traditional and certainly allow a much more immediate evaluation of the performance of a road pavement that would normally take much more time and costs. One of the main advantages is that the performance evaluation can be done by evaluating the residual life directly and therefore this allows a very quick understanding of the duration of a work and above all if it presents structural deficits, an estimation of the early decay and therefore the possible solutions of intervention in terms of costs, which should not be seen only as economic costs, but also as environmental and social costs with a view to sustainable development that is certainly one of the priorities at the international level in transport infrastructure.
From this it's easy to understand how a performance-based approach allows design flexibility and a variety of solutions that is certainly much more advanced than traditional approaches, in fact among the wide range of possible solutions the performance specifications allow the use of innovative materials, therefore not only technologically advanced, but also materials that can be recycled and therefore reused.

This is certainly an innovative factor because many of the materials that are not normally accepted at the traditional level, can be found with performance specifications employment with a significant saving of resources and the resulting benefits for the society, the environment, the client and the companies. Just thinking of the study done in this research work on volcanic ash, already presented in chapter 2, which is normally considered a waste to be treated appropriately, and instead if used with a stabilization as was done can be reused for the deeper layers of pavements (e.g. subbase and subgrade). Performance specifications are an opportunity and an element of innovation in road works.

Furthermore, a performance-based approach is faithful to the use of technologically advanced, non-destructive and high-performance instruments such as ARAN, FWD, LWD, GPR that allow a

simple execution of the surveys and have a high detail in the output in terms of grip, texture, unevenness, bearing capacity and thicknesses measured continuously without using a large number of cores.
But the reasons are manifold, among the advantages should certainly be emphasized these:

- speed of execution of the tests;
- possibility of carrying out a higher number of measurements and consequent extension of the survey campaigns;
- possibility to couple together several equipment during the tests and therefore have more results simultaneously with the advantage of being able to compare them together during the acquisition and processing phase;
- reduction of unit costs;
- continuous and detailed mapping of road infrastructure;
- performance measurement;
- possibility of using alternative materials with low environmental impact and that would not be applied according to the acceptance criteria of traditional specifications.

In Figure 74 some examples to demonstrate how advantageous the use of high speed NDT in performance approach is.
The simultaneous coupling of the Falling Weight Deflectometer and Ground Penetrating Radar allows the simultaneous detection of deflection basins and thicknesses, with a consequent rapidity of the on-site tests of those that appear to the operator with priority of intervention or to detect already detected critical issues from both devices. As regards the speed of the tests, it is shown that the load test on a plate in one point is performed in one hour, at the same time it is possible to make a large number of measurements with Light Weight Deflectometer over a large area and have a real and mapping of the bearing capacity of a test area, so the speed of the test allows in a short time to study a large amount of positions, to have a better distribution of data to describe the test area.

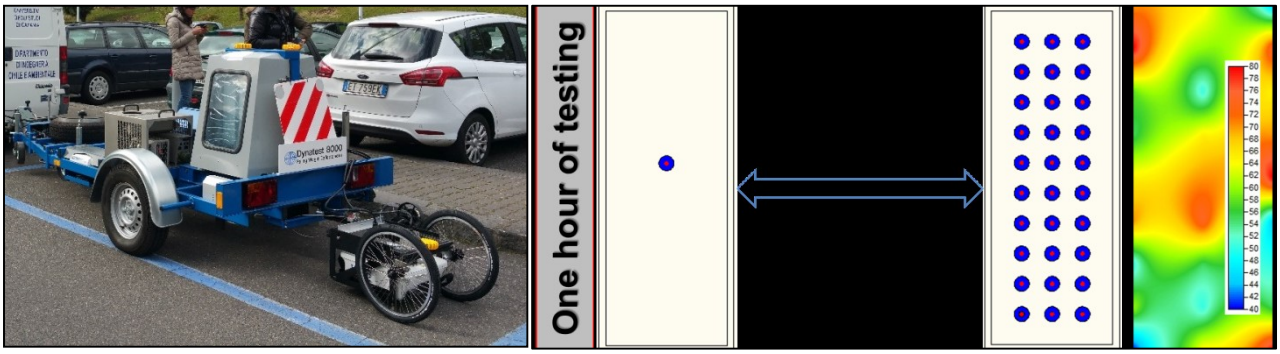

Figure 74 - FWD and GPR configuration in a test area of the University of Catania and comparison between a load plate and a LWD test in one hour of testing

As for the materials, it has already been seen (in Chapter 2) how the volcanic ash from waste can turn into a resource for our society: in the traditional specifications the volcanic ashes would never be accepted due to their poor mechanical characteristics and the high content of pollutants that have and would be destined to landfill, but it has been seen how their cement stabilization increases their performances making them suitable for their use in the realization of road foundations and subgrades.

These, like many other possible examples, make it possible to understand the importance of the performance of a road work when it is carried out, and how a change from a traditional to a performance point of view makes it possible to realize solutions that would normally not be accepted with positive consequences in terms of environmental, social and economic sustainability.

3.8 Basic considerations for the acceptance requirements for a new road surface: project period, PSI and Structural Number

The road pavements are designed by the technicians for a specific project period. During this period each pavement must guarantee adequate structural and functional characteristics until the limit value is reached, due to normal structural degradation (environment, materials, traffic, etc.), for which the restoration of these characteristics must be planned with the remaking of the same.
It is consequently clear that the respect of the project is fundamental to guaranteeing the functionality and reliability of the project over time, in this context the companies that carry out the construction work must take care to deliver the paving in the best way possible without incurring penalties due to construction deficits.
Acceptance of a work is regulated by specifications, and non-compliance with the project causes penalties or even demolition and reconstruction beyond certain limits.
The research project that was conducted during the PhD examines this topic, as the goal is to evaluate performance requirements and possible bonuses or penalties at the performance level.
What happens if the project is not respected and the work is delivered with an initial structural deficit? Following is the study that has been done and the graphic examples that help to understand and frame the problem. A deficit of initial structural capacity on a built road pavement produces a shortening of its residual life, this means that the final performance level (e.g. PSI) is reached in advance with respect to the design period for which the pavement was designed with the consequence that the maintenance treatment will be anticipated with increase od costs than the initial plan.
In the graph below (Figure 75), which explains the issue, it is possible to see how such a situation produces an unplanned intervention and therefore higher costs which, subsequently will be explained, can not only be understood only as economic costs.
On the x axis are shown the Esal in the analysis period (e.g. 15 years), and on the y axis the PSI (Present Serviceability Index, where: PSIi=initial PSI, PSIf=final PSI), or the degree of efficiency or functionality of the pavement.
In particular: ESAL0 represents the design ESALs in the base condition of the analysis design period; DESAL is the difference between ESAL0 and ESALi, where ESALi correspond to the achievement of the final PSI in advance and therefore the moment in which the pavement needs a maintenance intervention to restore the conditions for which it was designed; ESALt are the Esal correspondent to the terminal PSI of 1.5 at which the road needs demolition and reconstruction as at that level it is no longer accessible to users.
In fact, it can be seen that when the final PSIf is reached in advance, a maintenance intervention is needed to restore the project conditions until the end of the design analysis period.
The graph then becomes explanatory of why such a situation produces higher intervention costs that are not foreseen.

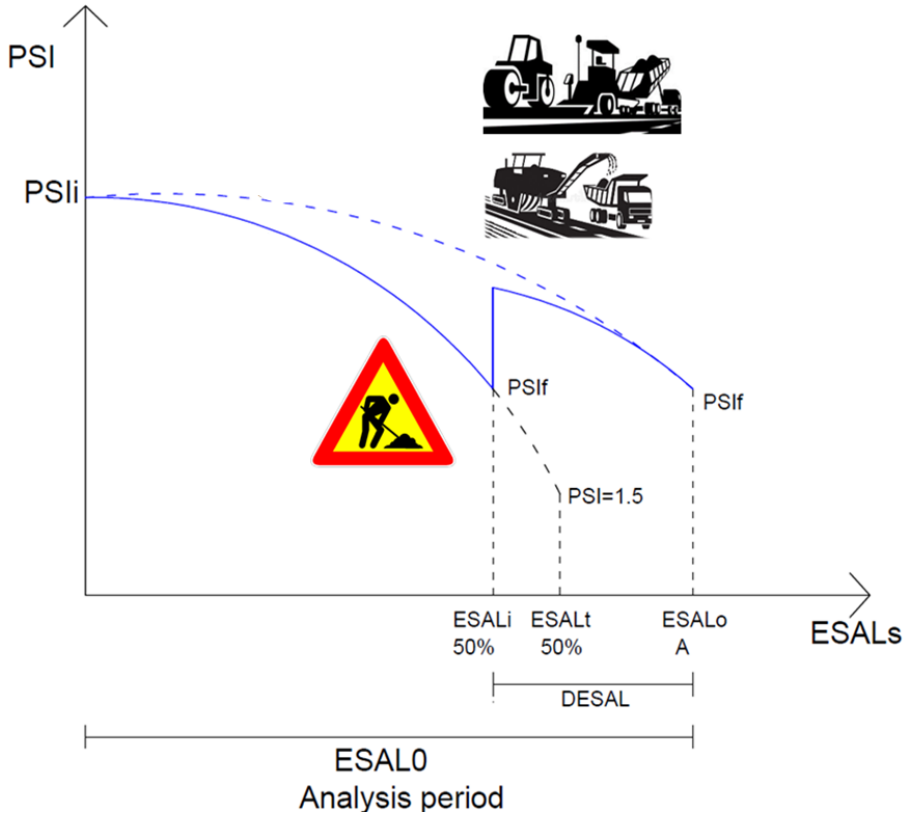

Figure 75 - Case with an initial constructive deficit: relationship between PSI and Esals

It should be remembered that the number of Esal is proportional to the pavement Life in years. Therefore, each reduction in the number of Esals (delta Esal) may be related to an equivalent reduction in the years to reach the final pavement condition.

That has been verified numerically and the results can be seen in the two graphs, in Figure 76 (a) and (b), where a period of analysis of 15 years (N) and a growth rate (GR) of 3% were considered.

The graphs have been obtained with the following considerations which are summarized by steps:

- Assuming Wx (Design ESALs in the base condition), GR and N (assumed values), it is possible to calculate W0 (ESALs in the initial year of the analysis period) $\sum_{0}^{N-1} W_{i_x} = \frac{w_{i_0} \times \left[(GR)^N - 1\right]}{GR - 1}$;
- Defined W0 for each value of Wxr (reduced number of design ESALs due to change in SN) it is possible to calculate N (Residual Life) given GR;
- Residual Life = number of years to the final PSI (PSIf);
- Residual Life [%]: percentage variation of RL with respect to the base condition;
- Delta ESALs [%]= (ESALo-ESALf)/ESALf: percentage variation of design ESAL (Mr, DPSI, Zr, So) between the base SNo condition (ESALo) and the reduced SNf (ESALf) (independent by Zr, So).

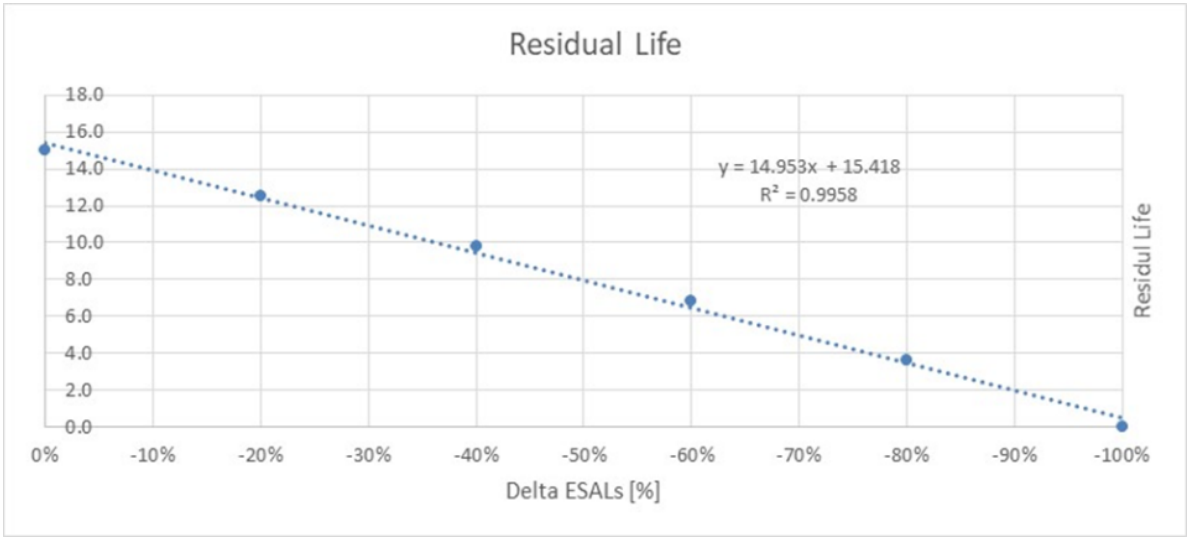

(a)

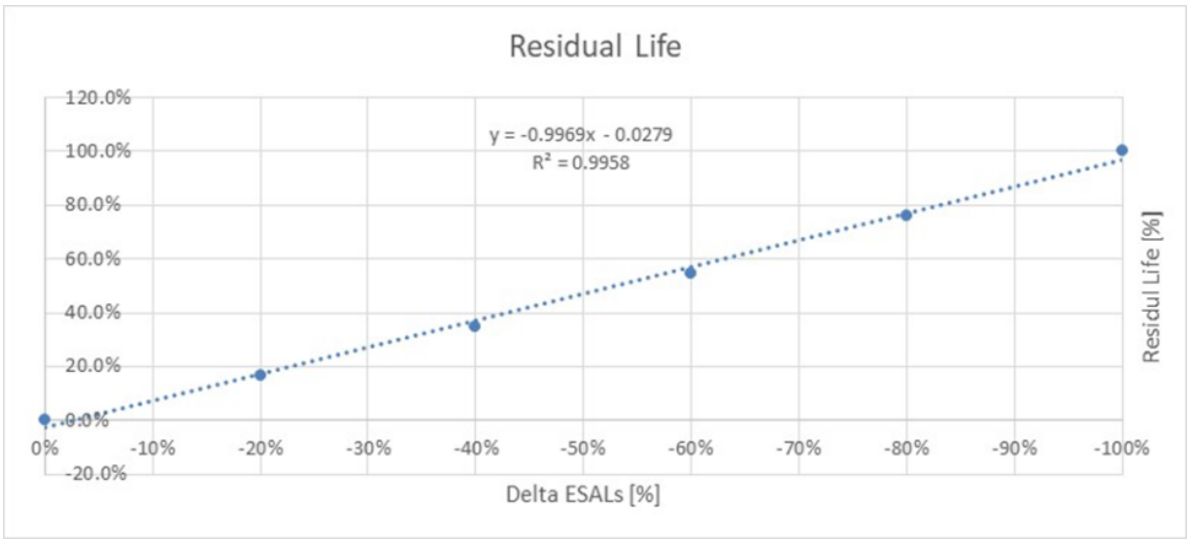

(b)

Figure 76 - Linear correlations: (a) Delta Esals [%] - Residual Life [years]; (b) Delta Esals [%] - Residual life [%]

The results allow to affirm that there is a linear correlation between Delta Esal and Residual life that is independent from Design ESALs and Analysis period values.
Having made these considerations and verified the proportionality between changes in Esal and Residual Life (i.e. Delta Esal=Delta Residual Life), the next step was to evaluate how changes in SN will effect changes in ESAL and Residual life.

The graph below (Figure 77) that has been constructed is conceptually explanatory of what happens. Similarly, to what was explained in the PSI graph, the initial defict in SN, due to construction errors, produces an early decay of the Structural Number curve and the need for an unplanned unticipated intervention (which generally translates into an overlay treatment) with the consequent restoration of performance to reach the end of the analysis period as designed.
For a better understanding of the phenomenon all the variables illustrated in the graph are explained along with their meaning:

- SNo: design SN of the base condition
- SNi: SN of the pavement as built

- DSNeff: reduction in SN at PSIf due to a reduced initial SN (DSNi)
- DSNi= SNo-SNi: reduction of SN due to construction errors
- ESALo: design ESAL for the base condition (A=50%)
- ESALi: design ESAL for the as built pavement (A=50%)
- Delta ESAL= ESALo-ESALi
- RL= 100*[1-ESALi(PSIi)]/ESALi(PSI=1.5) => CF
- SNeff = CF*SNi
- SNf: needed SN to reach the original design ESALo=ESALi+Delta ESAL
- A, Mr, PSI, Delta ESAl => SNf
- DSNeff = SNf-SNeff

These variables just described are explanatory of the phenomenon in terms of relations between the Structural Number (y-axis) and the ESALs (x-axis).

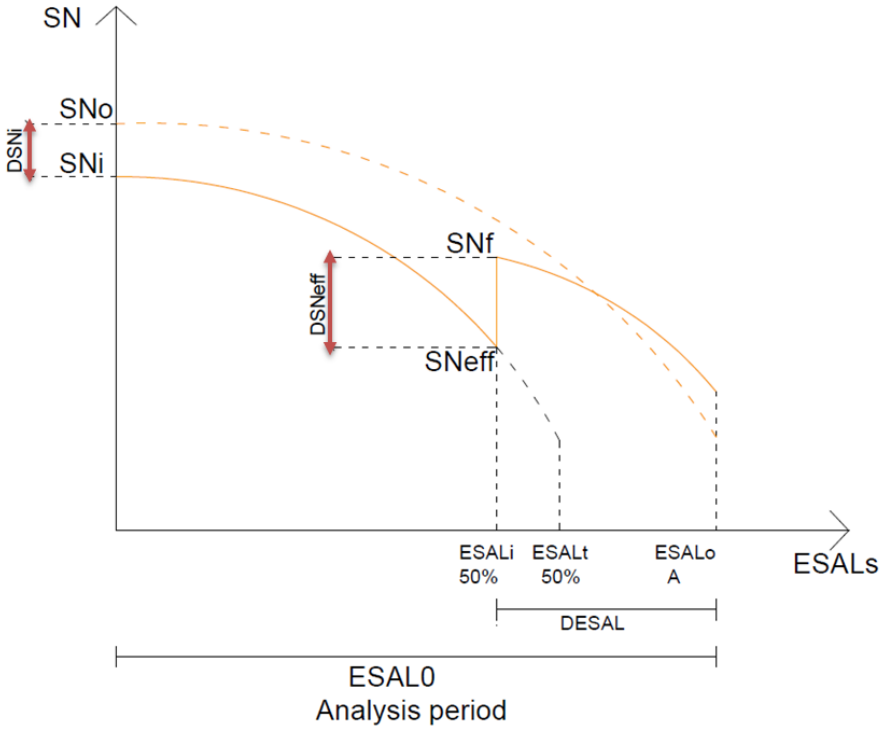

Figure 77 - Overlay intervention due to construction errors. Relationship between Structural Number and Esals.

The details of this study which clarify the operation of the graph and therefore of the variables can thus be explained in detail: the road pavements are designed to withstand over time, or better during the design period, to traffic loads, the external environmental conditions, and for this reason must have a structural strength that depends on the thickness of the layers, the structural strength of the materials and their sensitivity to the presence of water. So the structural design resistance of the road pavement is calculated in terms of the Structural Number SNo, which represents SN in the basic design condition.

If this requirement is not respected in the construction phase, then the pavement will present a deficit, which will occur over time after the road is put into operation, with a structural number SNi that will be smaller than the design one (SNo), for where the it will be built with a difference from the design one equal to DSNi = SNo-SNi, therefore there will be a reduction in the Structural

Number which is essentially due to construction errors. All this will result in an anticipated structural decay compared to the conditions for which the road was designed, therefore the reduction of structural number that will lead in advance to a SNeff involves the need for maintenance intervention with the achievement of SNf, as a new structural number starting condition, which will then allow the pavement to reach the original design ESALo over time.
SNeff is calculated with the Residual Life criterion of the AASHTO Guide (1993), in fact considering SNi and $SN_{1.5}$ is possible to calculate the ESALi (with PSIi) and $ESAL_{1.5}$ (with PSI=1.5). Consequently the Residual Life[38] is calculated as: $RL=100*(1-(N_p/N_{1.5})=100*(1-(ESALi/ESAL_{1.5})$, and considering SNeff=CF*SNi then CF is obtained from the graph (Figure 78).
The condition factor CF, in the AASHTO Guide (1993), is defined as a factor that is function of the Remaining (or residual) Life RL. It is defined by the equation CF=SCn/SCo, where: SCn is the pavement structural capacity after N_p ESAL, and SCo is the original structural capacity.
With RL determined, the designer may obtain the CF from Figure 78. The Condition Factor is obtained from the Remaining Life, in fact it is possible to see that when RL = 0 then CF = 0.5 that is the minimum value, and when RL = 100% consequently CF =1.

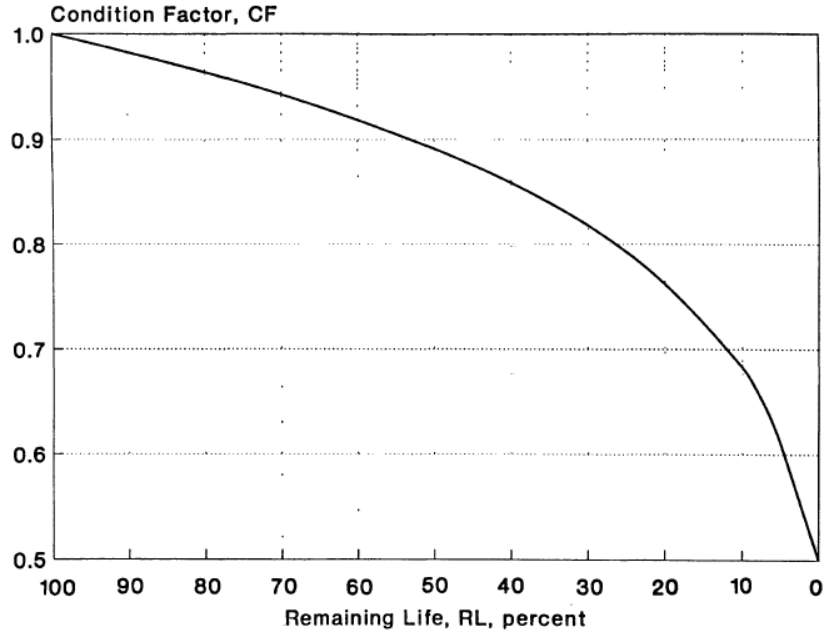

Figure 78 - Relationship between Condition Factor and Remaining Life. Source: AASHTO Guide, 1993.

The maintenance intervention to be made is therefore equal to a quantity DSNeff, i.e. the reduction in SN at PSIf two to a reduced initial SN (DSNi), where from the calculations made the relation, with this procedure used, between DSNeff and DSNi is: DSNeff = SNf- SNeff = 2.20362 * DSNi.
Therefore, the restoration work, with the new starting condition SNf, will have a new decay curve that will allow the pavement structure to reach the ESALs for which it was designed.
In general, what does it mean? Taking a simple example, if I have an initial deficit of 1 cm for a base layer, then when I have to do the intervention before the 15th year, for hypothesis at year 11, I will not have to restore 1 inch but more because the need for SN will be about more than double.

[38] The residual life (or remaining life) in the AASHTO Guide (1993) is defined as a function of N_p and $N_{1.5}$. Np is the total traffic to date and $N_{1.5}$ is the total traffc to pavement failure when the serviceability is equal to 1.5: they correspond in this work of research, respectively, to ESALi and $ESAL_{1.5}$.

This means that at 11 years to restore those 4 years is not enough to put what was missing at the time of construction, but we need to put more.
In short, this translates into the future in an intervention of about more than double in terms of thickness, and we will see later that it can reach up to four times in terms of costs.
All this once again demonstrates how important the respect of the project is, as it guarantees functionality, safety, significant economic savings because subsequently intervening has higher costs, avoiding not only unplanned maintenance, but also the application of penalties to the companies executing the works.
To better understand the problem and the extent of the effect it may have in delivering a new work with an initial structural deficit, experimental studies have been carried out on some pavements of the database, taking this condition into consideration. For this reason, some cases were studied in which it was necessary to intervene before the end of the design period.

3.9 New road pavements with as built structural deficit: performance and treatments

The delivery of a work in a workmanlike manner has seen that it is a guarantee of functionality, known and planned costs, reliability over time, but it is also an ethical and professional question in realizing something in the right way, respecting what it has done the designer, in the client and the end users that every day will follow a road and will have their perception of comfort that also determines an improvement in the quality of life.
All this, it's clear that it is part of the economic-environmental-social system of sustainable development.
Performance specifications or specifications in general are intended to verify that the works have been correctly delivered in compliance with the project, and they do so by imposing limits, acceptance requirements and penalties if certain conditions are not respected.

But what happens when a road pavement is delivered with an initial structural deficit, and therefore with a performance deficit?
The research was carried out on the database, on some pavement structures. In order to have a varied and representative sample of all the conditions, those pavements were selected with the maximum, average and minimum Structural Number among the database values.
On these pavements, some studies have been made considering that they are put in place with initial structural deficits (i.e. material moduli different than designed), and therefore with SN smaller than their design value, so with the relationships already seen (SN-Esal graph in the previous paragraph 3.8) they were calculated the year in which to carry out the maintenance treatment in advance of the 15-year design period and how many cm of overlay must be placed in, to intervene and restore the design conditions.
In this part are explained the selected pavements of the database and 2 case studies chosen in terms of different ways of overlay treatment so as to be able to estimate the costs connected to a deficit situation that produces unforeseen interventions and therefore expensive economically and environmentally.
Within the database the values of SN max, average and minimum [inch] are respectively: 6.35, 4.96, 3.34. These SN values are database road pavements numbered with n. 2-5-10.

In Table 62 there are the details of all the pavements with the corresponding SN values.

Table 62 - Road pavements of the database with the max, average and minimum value of SN

SN=6.35 (max) Pav. n. 2	SN=4.96 (average) Pav. n. 5	SN=3.34 (min) Pav. n. 10
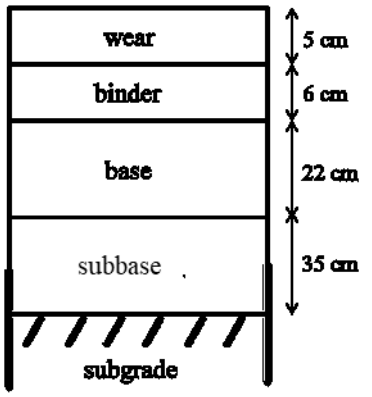	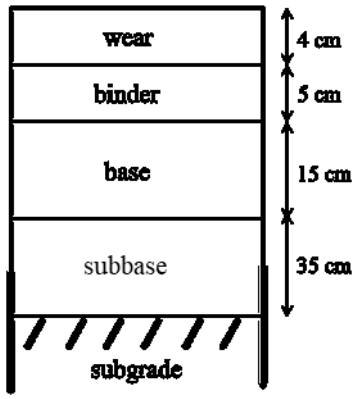	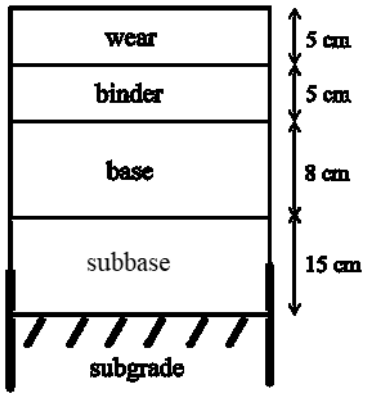

For these 3 road pavements two different case studies have been developed, considering that they have been put into operation with initial structural deficits and therefore these deficits lead to perform overlay maintenance interventions in advance over the years compared to the design period. The design period considered is 15 years.

- ***Case study 1:*** net overlay over the existing road pavement built that is made at year X (before the year 15th). So, in this case considering having an initial deficit, it was seen how much the road need to put in terms of new layers considering a net overlay.

- ***Case study 2:*** Milling and overlay maintaining a constant height of the pavement considering 4 cm of wear course realized with virgin AC and the rest of thickness composed by RAP at 40%.

It's good to remember that these are two possible hypothetical solutions and that clearly the range of solutions could be very wide and varied as technology and materials are constantly evolving.
The case study 1 is not a practical solution, but it was useful as minimum cost comparison.
Both solutions have been studied to have an estimate of the Economic and Environmental Costs of unscheduled interventions due to initial deficits that occur in the project period in advance with a deterioration that manifests itself before and a fall of the SN-Esal curve in a faster way.
The costs considered in this study are of two types:

1) **Economic:** the economic estimate (comprehensive of initial construction and maintenance) on the materials to be used and the works has been done taking into consideration the costs applied by ANAS (Price list 2018, Listino Prezzi 2018. Nuove Costruzioni - Manutenzione Straordinaria").
2) **Environmental:** environmental costs[39] are estimated both during construction and maintenance work and have a considerable impact in terms of materials production, materials transportation and processes (equipment).
   The calculated environmental impacts were: Energy consumption [MJ]; Water consumption [Kg]; CO2 emissions and Global Warming Potential; NOx emissions [Kg]; PM10 emissions [Kg]; SO2 emissions [Kg]; CO emissions [Kg]; Hg emissions [g]; Pb [g]; RCRA hazardous

[39] These environmental costs do not include traffic and accidents, it is an analysis made at the environmental level on the initial construction of the pavement and the unscheduled maintenance in terms of overlays due to initial structural deficits that occur before the design period.

waste generated; Human Toxicity Potential (cancer); Human Toxicity Potential (non-cancer).

The cost estimate calculations were made with the support of PaLATE[40] which is a Life-Cycle Assessment Tool for Environmental and Economic Effects in road applications. In Figure 79 are showed the life-cycle phases of road pavements.

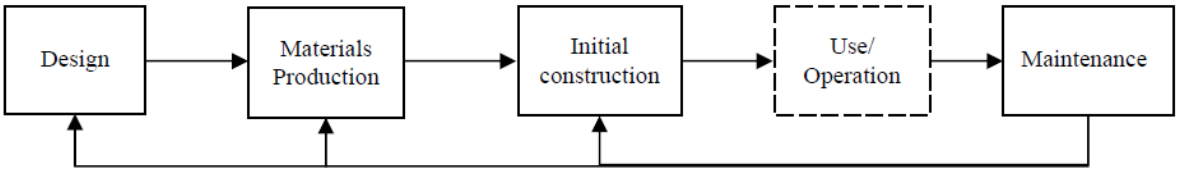

Figure 79 - Life-cycle phases of pavements. (Horvath, 2004).

The tool takes user input for the design, initial construction, maintenance, equipment use, and costs of a roadway, and characterizes the life-cycle environmental effects and costs of a given project (Horvath, 2004). These estimates have allowed to create bonus-penalty models that can be applied within performance specifications and which will be analyzed later in this chapter. In the following paragraphs the two case studies are presented.

3.9.1 Case Study 1: Net overlay on the road pavement built

In this first case it has been studied what can happen if a net overlay is performed.

A **Net Overlay** is a maintenance operation that is performed on the existing road pavement built, overlapping on the latter, without a milling being carried out. It is an intervention that in reality does not and must not be carried out, but here it is treated only for research purposes and to estimate both economic and environmental costs.

Assuming road pavements with initial construction deficits, for the three pavements with SN max, average, min, calculations were made considering that they have a lower structural number than the one designed, so they need an intervention before the 15th year. So, it was evaluated the year of intervention (early compared to the 15th year), the overlay thickness (cm), and then DSNeff, that is the reduction in SN due to a reduced initial SN (DSNi=SNo-SNi). The maintenance treatments that have been performed and planned in this case study on three road pavements are in Table 63, with the year of intervention and the thickness of the net overlay on each road pavement.

Table 63 - Net overlay interventions calculated on the 3 road pavements

		Overlay 3 cm			**Overlay 6 cm**			**Overlay 8 cm**			**Overlay 9 cm**		
Pav. N.	**SNo**	**SNi**	**DSNeff**	**Year**	**SNi**	**DSNeff**	**Year**	**SNi**	**DSNeff**	**Year**	**SNi**	**DSNeff**	**Year**
2	6.35	6.14	0.48	11	5.9	0.97	8	5.75	1.32	7	5.67	1.50	6
5	4.96	4.75	0.48	10	4.5	0.97	7	4.36	1.32	6			
10	3.34	3.13	0.48	9	2.9	0.97	5	2.74	1.32	4			

Where: SNo: design SN of the base condition; SNi: SN of the pavement as built; DSNeff: reduction in SN at PSIf due to a reduced initial SN (DSNi=SNo-SNi) is calculated as DSNeff=2.20362·DSNi; Year is the year of intervention with an overlay of X cm calculated with the relations for the residual life RL=100[1-ESALi(PSI=1.5)/ESALi(PSIi)].*

[40] PaLATE uses an LCA approach to model the environmental effects of road initial construction and maintenance. The user defines the design of the pavement, which results in a given type and volume of construction materials and its source (hauling distance), a given combination of construction activities, and a set of prescribed maintenance activities. It uses an alternative approach for assessing impacts from pavements construction and maintenance, which is based on the productivity and environmental implications caused by different types of equipment and materials.

As can be seen from the table, four overlay interventions for the road pavement n. 2 and three overlay interventions for the other two pavements (5 and 10).
Hypotheses were also made of the transport of materials for the initial construction and for the maintenance intervention: specifically, 10 km of distance were considered for aggregates and bitumen that make up the layers of AC, and 20 km of distance for the gravel that is used for the foundation. Furthermore, the composition of aggregates and bitumen for the AC layers is divided as follows: 89% aggregate and 11% bitumen for wear and binder, 84% aggregate and 16% bitumen for base layer. The foundation is composed by 100% gravel.
Cost estimates have been made in economic and environmental terms. In both types of costs there are therefore initial construction costs that are obviously related to the construction of the new pavement and maintenance costs related to the unscheduled intervention due to the restoration to be made due to the initial structural deficit. All the costs are made considering a surface of one square meter of pavement for the thickness of the various layers. This applies to all the case studies.

Economic costs

In these costs are considered all the real cost items used by ANAS in price lists, in this case both as regards the layers of AC (wear, binder and base, on which a weighted average has been made considering a price for AC), both for unbound layers such as the foundation.

The discount rate considered for each pavement are 3% and 5%.

In Table 64 there are the ANAS prices considered:

Table 64 - ANAS costs used for the economic evaluation

Pav n.	Wear [€/m³]	Binder [€/m³]	Base [€/m³]	Weighted average for AC (wear, binder and base) [€/m³]	Foundation [€/m³]
2	133.28	125.61	115.44	120.0	19.26
5	133.28	125.61	115.44	120.5	19.26
10	133.28	125.61	115.44	123.2	19.26

In Figure 80 the goodness of fit of the linear distribution of results (considering the Delta of the Structural Number and of the costs) and the detail of all calculations in Table 65, are reported:

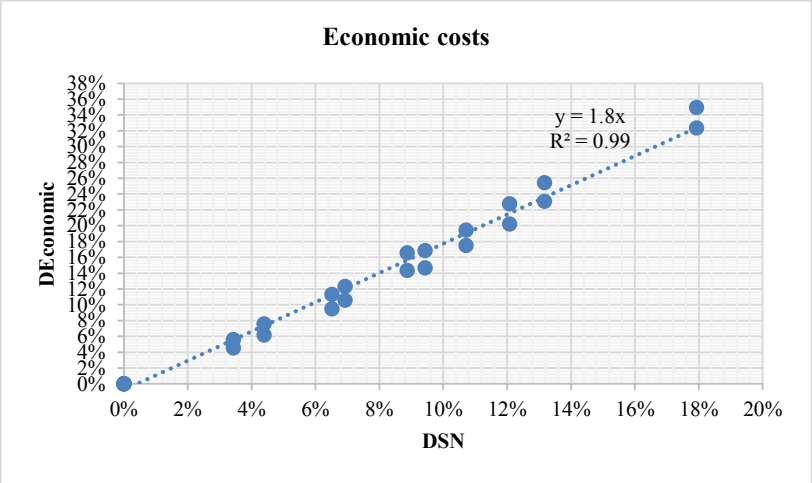

Figure 80 - Linear distribution DSN and DCosts (Case 1)

							initial construction							Overlay Maintenance AC						
ID PAV	Overlay tot AC [CM]	Discount Rate	Year	SN	DSNeff	DSN	Volume AC [m3]	Unit Cost AC [€/(m3)]	Actual Cost AC [€]	Volume SB [m3]	Unit Cost SB [€/(m3)]	Actual Cost SB [€]	NPV Init. constr.	Volume AC [m3]	Unit Cost AC [€/(m3)]	Actual Cost AC [€]	NPV TOT maintenance (overlay and no milling)	NPV maintenance overlay	NPV TOT constr.	Dcost
2	0	3%	0	6.35	0	0%	0.33	120.00	39.53	0.35	19.26	6.73	**46.3**	0.00	120.00	0.00	0.00	0.00	46.3	0%
2	0	5%	0	6.35	0	0%	0.33	120.00	39.53	0.35	19.26	6.73	**46.3**	0.00	120.00	0.00	0.00	0.00	46.3	0%
2	3	3%	11	6.35	0.48	3%	0.33	120.00	39.53	0.35	19.26	6.73	**46.3**	0.03	120.00	3.59	2.64	2.64	48.9	6%
2	3	5%	11	6.35	0.48	3%	0.33	120.00	39.53	0.35	19.26	6.73	**46.3**	0.03	120.00	3.59	2.14	2.14	48.4	5%
2	6	3%	8	6.35	0.97	7%	0.33	120.00	39.53	0.35	19.26	6.73	**46.3**	0.06	120.00	7.19	5.74	5.74	52.0	12%
2	6	5%	8	6.35	0.97	7%	0.33	120.00	39.53	0.35	19.26	6.73	**46.3**	0.06	120.00	7.19	4.94	4.94	51.2	11%
2	8	3%	7	6.35	1.32	9%	0.33	120.00	39.53	0.35	19.26	6.73	**46.3**	0.08	120.00	9.59	7.84	7.84	54.1	17%
2	8	5%	7	6.35	1.32	9%	0.33	120.00	39.53	0.35	19.26	6.73	**46.3**	0.08	120.00	9.59	6.84	6.84	53.1	15%
2	9	3%	6	6.35	1.50	11%	0.33	120.00	39.53	0.35	19.26	6.73	**46.3**	0.09	120.00	10.79	9.04	9.04	55.3	20%
2	9	5%	6	6.35	1.50	11%	0.33	120.00	39.53	0.35	19.26	6.73	**46.3**	0.09	120.00	10.79	8.14	8.14	54.4	18%
5	0	3%	0	4.96	0	0%	0.24	120.50	28.88	0.35	19.26	6.73	**35.6**	0.00	120.5	0.00	0.00	0.00	35.6	0%
5	0	5%	0	4.96	0	0%	0.24	120.50	28.88	0.35	19.26	6.73	**35.6**	0.00	120.5	0.00	0.00	0.00	35.6	0%
5	3	3%	10	4.96	0.48	4%	0.24	120.50	28.88	0.35	19.26	6.73	**35.6**	0.03	120.5	3.61	2.70	2.70	38.3	8%
5	3	5%	10	4.96	0.48	4%	0.24	120.50	28.88	0.35	19.26	6.73	**35.6**	0.03	120.5	3.61	2.20	2.20	37.8	6%
5	6	3%	7	4.96	0.97	9%	0.24	120.50	28.88	0.35	19.26	6.73	**35.6**	0.06	120.5	7.22	5.90	5.90	41.5	17%
5	6	5%	7	4.96	0.97	9%	0.24	120.50	28.88	0.35	19.26	6.73	**35.6**	0.06	120.5	7.22	5.10	5.10	40.7	14%
5	8	3%	6	4.96	1.32	12%	0.24	120.50	28.88	0.35	19.26	6.73	**35.6**	0.08	120.5	9.63	8.10	8.10	43.7	23%
5	8	5%	6	4.96	1.32	12%	0.24	120.50	28.88	0.35	19.26	6.73	**35.6**	0.08	120.5	9.63	7.20	7.20	42.8	20%
10	0	3%	0	3.34	0	0%	0.18	123.20	22.15	0.15	19.26	2.89	**25.0**	0.00	123.2	0.00	0.00	0.00	25.0	0%
10	0	5%	0	3.34	0	0%	0.18	123.20	22.15	0.15	19.26	2.89	**25.0**	0.00	123.2	0.00	0.00	0.00	25.0	0%
10	3	3%	9	3.34	0.48	7%	0.18	123.20	22.15	0.15	19.26	2.89	**25.0**	0.03	123.2	3.69	2.83	2.83	27.9	11%
10	3	5%	9	3.34	0.48	7%	0.18	123.20	22.15	0.15	19.26	2.89	**25.0**	0.03	123.2	3.69	2.38	2.38	27.4	10%
10	6	3%	5	3.34	0.97	13%	0.18	123.20	22.15	0.15	19.26	2.89	**25.0**	0.06	123.2	7.38	6.37	6.37	31.4	25%
10	6	5%	5	3.34	0.97	13%	0.18	123.20	22.15	0.15	19.26	2.89	**25.0**	0.06	123.2	7.38	5.78	5.78	30.8	23%
10	8	3%	4	3.34	1.32	18%	0.18	123.20	22.15	0.15	19.26	2.89	**25.0**	0.08	123.2	9.85	8.75	8.75	33.8	35%
10	8	5%	4	3.34	1.32	18%	0.18	123.20	22.15	0.15	19.26	2.89	**25.0**	0.08	123.2	9.85	8.10	8.10	33.1	32%
average	5	4%	6	5	1	7%	0.26	121	31	0	19	6	**36**	**0.0**	**121.1**	**5.6**	**4.3**	**4.3**	**40.8**	13%

Table 65 - Economic costs Case 1

The graph (Figure 80) shows the linear distribution of data by relating (for the three pavements considered) the differences (Delta) of the Structural number "DSN" and the cost differences "Dcost" calculated as explained in paragraph 3.8:

$$DSN=(DSNeff/2.204)/SNo$$

$$Dcost=(Total\ cost-Initial\ cost)/Initial\ cost$$

Where: DSNeff is the reduction in SN at PSIf due to a reduced initial SN; SNo is the design SN of the base condition; Total cost is the total cost including the construction cost and the unplanned maintenance cost; Initial cost represents the cost of road construction.

Making economic considerations, in Table 65 it's possible to see the cost details of the volumes considered during construction and maintenance in terms of Net Present Value NPV, Unit cost and Actual Cost, which are all variables that intervene when project periods are considered (in this case 15 years) taking into consideration the change in prices and the discount rate over the years.

Environmental costs

The environmental impacts calculated in terms of materials production, materials transportation and processes (equipment) were analyzed as the economic, taking into consideration the relations between DSN and DEnvironment (DEnergy, DWatercons., DCO2, etc.).
As for the Delta costs, the Delta Environment, that are environmental costs, have been calculated similarly:

$$DEnvironment=(Total\ cost-Initial\ cost)/Initial\ cost$$

In Table 66 and in Figure 81 there are the results and the distribution of data.

Table 66 - Results of Environmental Analysis for Case 1

ID PAV	DSN	DEnergy	DWaterCons.	DCO2	DNOx	DPM10	DSO2	DCO	DHg	DPb	DRCRA	DHTP (Cancer)	DHTP (Non-cancer)
2	0%	0.00	0.00	0.00	0.00	0.00	0.00	0.00	0.00	0.00	0.00	0.00	0.00
2	0%	0.00	0.00	0.00	0.00	0.00	0.00	0.00	0.00	0.00	0.00	0.00	0.00
2	3%	0.07	0.07	0.07	0.07	0.06	0.09	0.07	0.07	0.07	0.07	0.07	0.05
2	3%	0.07	0.07	0.07	0.07	0.06	0.09	0.07	0.07	0.07	0.07	0.07	0.05
2	7%	0.14	0.14	0.13	0.14	0.11	0.18	0.14	0.14	0.14	0.14	0.14	0.11
2	7%	0.14	0.14	0.13	0.14	0.11	0.18	0.14	0.14	0.14	0.14	0.14	0.11
2	9%	0.18	0.18	0.18	0.18	0.15	0.24	0.18	0.19	0.18	0.18	0.18	0.14
2	9%	0.18	0.18	0.18	0.18	0.15	0.24	0.18	0.19	0.18	0.18	0.18	0.14
2	11%	0.21	0.21	0.20	0.21	0.17	0.27	0.20	0.21	0.21	0.21	0.21	0.16
2	11%	0.21	0.21	0.20	0.21	0.17	0.27	0.20	0.21	0.21	0.21	0.21	0.16
5	0%	0.00	0.00	0.00	0.00	0.00	0.00	0.00	0.00	0.00	0.00	0.00	0.00
5	0%	0.00	0.00	0.00	0.00	0.00	0.00	0.00	0.00	0.00	0.00	0.00	0.00
5	4%	0.09	0.09	0.09	0.09	0.07	0.12	0.09	0.10	0.09	0.10	0.09	0.06
5	4%	0.09	0.09	0.09	0.09	0.07	0.12	0.09	0.10	0.09	0.10	0.09	0.06
5	9%	0.19	0.19	0.18	0.18	0.14	0.25	0.19	0.19	0.19	0.19	0.19	0.13
5	9%	0.19	0.19	0.18	0.18	0.14	0.25	0.19	0.19	0.19	0.19	0.19	0.13
5	12%	0.25	0.25	0.24	0.25	0.18	0.33	0.25	0.26	0.25	0.26	0.25	0.17
5	12%	0.25	0.25	0.24	0.25	0.18	0.33	0.25	0.26	0.25	0.26	0.25	0.17
10	0%	0.00	0.00	0.00	0.00	0.00	0.00	0.00	0.00	0.00	0.00	0.00	0.00
10	0%	0.00	0.00	0.00	0.00	0.00	0.00	0.00	0.00	0.00	0.00	0.00	0.00
10	7%	0.14	0.14	0.13	0.14	0.11	0.17	0.14	0.14	0.14	0.14	0.14	0.11
10	7%	0.14	0.14	0.13	0.14	0.11	0.17	0.14	0.14	0.14	0.14	0.14	0.11
10	13%	0.27	0.27	0.26	0.27	0.23	0.33	0.27	0.28	0.27	0.28	0.27	0.22
10	13%	0.27	0.27	0.26	0.27	0.23	0.33	0.27	0.28	0.27	0.28	0.27	0.22
10	18%	0.36	0.36	0.35	0.36	0.30	0.44	0.36	0.37	0.36	0.37	0.36	0.29
10	18%	0.36	0.36	0.35	0.36	0.30	0.44	0.36	0.37	0.36	0.37	0.36	0.29

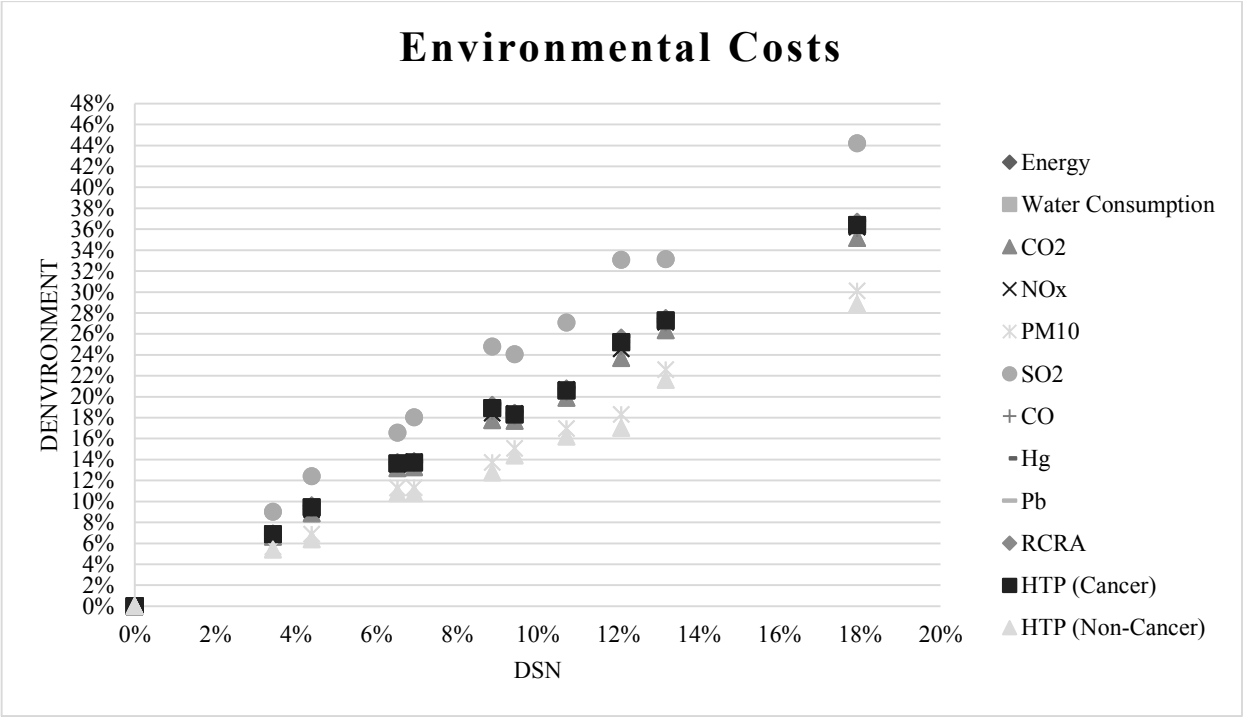

Figure 81 - Distribution of data, relation DSN-DEnvironment for the net overlay (Case 1)

Subsequently, both for case 1 and for case 2, statistical regressions were made and then the models were obtained that allow to know the relationship (in terms of delta) between the structural number and the economic or environmental costs that will be exposed later. Now the case 2, of milling and overlay is explained, the results will be exposed analogously to the case just presented, with graphs and tables, and the new details present for this specific intervention.

3.9.2 Case Study 2: Milling and overlay (AC + 40% RAP) on the road pavement built

Also in this case, as in case 1, the same intervention considerations were made before the end of the project period, the mode of intervention here was thought differently from a net overlay (which in reality is not done), this time with considerations closer to reality with **milling and overlay**.
The conditions considered are the following (Table 67):

Table 67 - Milling and overlay interventions calculated on the 3 road pavements

		Overlay 4 cm (4+0)			Overlay 8 cm (4+4)			Overlay 10 cm (4+6)			Overlay 13 cm (4+9)		
Pav. N.	**SNo**	**SNi**	**DSNeff**	**Year**	**SNi**	**DSNeff**	**Year**	**SNi**	**DSNeff**	**Year**	**SNi**	**DSNeff**	**Year**
2	6.35	6.23	0.27	13	6.1	0.54	11	6.05	0.67	10	5.96	0.87	9
5	4.96	4.84	0.27	12	4.7	0.54	10	4.66	0.67	9			
10	3.34	3.22	0.27	11	3.1	0.54	9	3.04	0.67	8			

Specifically, in this case the intervention is considered making a milling and an overlay at constant height of the pavement. The overlay is made of 4 cm of wear layer in AC, the rest of the cm of intervention with a 40% RAP (Reclaimed Asphalt Pavement)[41].

[41] Reclaimed asphalt pavement (RAP) is the term given to removed and/or reprocessed pavement materials containing asphalt and aggregates. These materials are generated when asphalt pavements are removed for reconstruction, resurfacing, or to obtain access to buried utilities. When properly crushed and screened, RAP consists of high-quality, well-graded aggregates coated by asphalt cement. sphalt pavement has been America's most recycled material for a long

This means that the 4 cm of milling will always go to landfill, the rest of the cm (depending on how much overlay is done) will go to landfill only 60%, 40% will not go to landfill because it is used to realize the overlay in RAP.
The composition of AC with aggregate and bitumen is the same concerning the Initial Construction that is the same (also for transportation distances), for the overlay of 4 cm in AC is considered 89% aggregate and 11% bitumen. Specifically, the distance of transportation of materials considered for the overlay in AC is 10 km. There is no transport distance for the RAP because everything happens in situ. Instead regarding transportation to landfill was considered that it is 20 km away.

Economic costs

Here the same considerations as in case 1 are valid, considering the prices applied by ANAS and updated to 2018. For the initial construction costs, the prices applied are the same as those previously seen. For overlay intervention costs including AC + RAP, this time too they have been considered weighted averages on the costs which are summarized in Table 68.

Table 68 - ANAS costs for overlay in AC and 40%RAP

Overlay Solution (AC+40%RAP) [cm]	**Wear [€/m³]**	**RAP [€/m³]**	**Weighted average for AC+40%RAP [€/m³]**
4+0	133.28	79.37	133.28
4+4	133.28	79.37	106.32
4+6	133.28	79.37	100.93
4+9	133.28	79.37	95.96

The ANAS cost for milling used is 42 €/m^3 that is comprehensive of the transportation to landfill.
Also in this case, in the following are reported the linear distribution of results (considering the Delta of the Structural Number and of the costs) and the detail of all calculations (Figure 82 and Table 69):

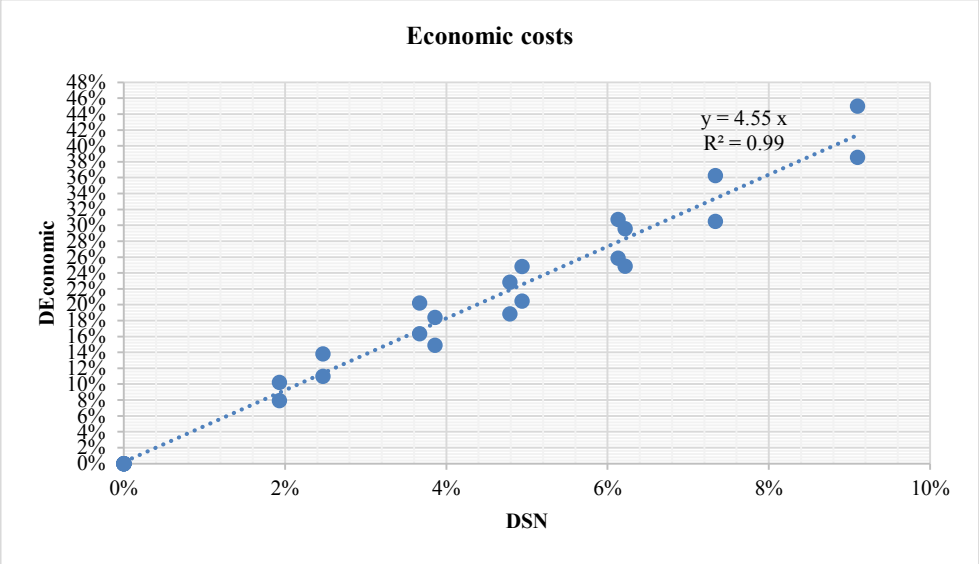

Figure 82 - Linear distribution DSN and DCosts (Case 2)

time. Using RAP material has well-recognized financial and environmental benefits. Although most of the produced RAP is recycled, a large portion of it is wasted or down-graded when used in landfills, embankment or base layers. Source: https://www.fhwa.dot.gov/publications/research/infrastructure/structures/97148/rap131.cfm

										initial construction							Overlay Maintenance AC + RAP at 40%			MILLING								
ID PAV	Overlay tot AC [CM]	Overlay wear [cm]	Overlay RAP at 40% [cm]	milling [cm]	Discount Rate	Year	SN	DSNeff	DSN	Volume AC [m3]	Unit Cost AC [€/(m3)]	Actual Cost AC [€]	Volume SB [m3]	Unit Cost SB [€/(m3)]	Actual Cost SB [€]	NPV Init. constr.	Volume AC+RAP [m3]	Unit Cost AC+RAP [€/(m3)]	Actual Cost AC+RAP [€]	Volume MILLING [m3]	Unit Cost MILLING [€/(m3)]	Actual Cost MILLING [€]	NPV TOT maintenance (overlay+milling)	NPV maintenance overlay	NPV maintenance milling and transportation to landfill	$ TOT constr.	Dcost
2	0	0	0	0	3%	0	6.35	0	0%	0.33	120.00	39.53	0.35	19.26	6.73	**46.3**	0.00	0	0.00	0.00	42	0.00	0.00	0.00	0.00	46.3	0%
2	0	0	0	0	5%	0	6.35	0	0%	0.33	120.00	39.53	0.35	19.26	6.73	**46.3**	0.00	0	0.00	0.00	42	0.00	0.00	0.00	0.00	46.3	0%
2	4	4	0	4	3%	13	6.35	0.27	2%	0.33	120.00	39.53	0.35	19.26	6.73	**46.3**	0.04	133.28	5.33	0.04	42	1.68	4.77	3.63	1.14	51.0	10%
2	4	4	0	4	5%	13	6.35	0.27	2%	0.33	120.00	39.53	0.35	19.26	6.73	**46.3**	0.04	133.28	5.33	0.04	42	1.68	3.71	2.82	0.89	50.0	8%
2	8	4	4	8	3%	11	6.35	0.54	4%	0.33	120.00	39.53	0.35	19.26	6.73	**46.3**	0.08	106.33	8.50	0.08	42	3.36	8.56	6.14	2.42	54.8	19%
2	8	4	4	8	5%	11	6.35	0.54	4%	0.33	120.00	39.53	0.35	19.26	6.73	**46.3**	0.08	106.33	8.50	0.08	42	3.36	6.93	4.97	1.96	53.2	15%
2	10	4	6	10	3%	10	6.35	0.67	5%	0.33	120.00	39.53	0.35	19.26	6.73	**46.3**	0.10	100.93	10.08	0.10	42	4.19	10.62	7.50	3.12	56.9	23%
2	10	4	6	10	5%	10	6.35	0.67	5%	0.33	120.00	39.53	0.35	19.26	6.73	**46.3**	0.10	100.93	10.08	0.10	42	4.19	8.76	6.19	2.57	55.0	19%
2	13	4	9	13	3%	9	6.35	0.87	6%	0.33	120.00	39.53	0.35	19.26	6.73	**46.3**	0.13	95.96	12.46	0.13	42	5.45	13.73	9.55	4.18	60.0	30%
2	13	4	9	13	5%	9	6.35	0.87	6%	0.33	120.00	39.53	0.35	19.26	6.73	**46.3**	0.13	95.96	12.46	0.13	42	5.45	11.55	8.03	3.52	57.8	25%
5	0	0	0	0	3%	0	4.96	0	0%	0.24	120.50	28.88	0.35	19.26	6.73	**35.6**	0.00	0	0.00	0.00	42	0.00	0.00	0.00	0.00	35.6	0%
5	0	0	0	0	5%	0	4.96	0	0%	0.24	120.50	28.88	0.35	19.26	6.73	**35.6**	0.00	0	0.00	0.00	42	0.00	0.00	0.00	0.00	35.6	0%
5	4	4	0	4	3%	12	4.96	0.27	2%	0.24	120.50	28.88	0.35	19.26	6.73	**35.6**	0.04	133.28	5.33	0.04	42	1.68	4.92	3.74	1.19	40.5	14%
5	4	4	0	4	5%	12	4.96	0.27	2%	0.24	120.50	28.88	0.35	19.26	6.73	**35.6**	0.04	133.28	5.33	0.04	42	1.68	3.91	2.97	0.94	39.5	11%
5	8	4	4	8	3%	10	4.96	0.54	5%	0.24	120.50	28.88	0.35	19.26	6.73	**35.6**	0.08	106.33	8.50	0.08	42	3.36	8.83	6.32	2.51	44.4	25%
5	8	4	4	8	5%	10	4.96	0.54	5%	0.24	120.50	28.88	0.35	19.26	6.73	**35.6**	0.08	106.33	8.50	0.08	42	3.36	7.29	5.22	2.07	42.9	20%
5	10	4	6	10	3%	9	4.96	0.67	6%	0.24	120.50	28.88	0.35	19.26	6.73	**35.6**	0.10	100.93	10.08	0.10	42	4.19	10.95	7.72	3.22	46.5	31%
5	10	4	6	10	5%	9	4.96	0.67	6%	0.24	120.50	28.88	0.35	19.26	6.73	**35.6**	0.10	100.93	10.08	0.10	42	4.19	9.21	6.50	2.71	44.8	26%
10	0	0	0	0	3%	0	3.34	0	0%	0.18	123.20	22.15	0.15	19.26	2.89	**25.0**	0.00	0	0.00	0.00	42	0.00	0.00	0.00	0.00	25.0	0%
10	0	0	0	0	5%	0	3.34	0	0%	0.18	123.20	22.15	0.15	19.26	2.89	**25.0**	0.00	0	0.00	0.00	42	0.00	0.00	0.00	0.00	25.0	0%
10	4	4	0	4	3%	11	3.34	0.27	4%	0.18	123.20	22.15	0.15	19.26	2.89	**25.0**	0.04	133.28	5.33	0.04	42	1.68	5.06	3.85	1.21	30.1	20%
10	4	4	0	4	5%	11	3.34	0.27	4%	0.18	123.20	22.15	0.15	19.26	2.89	**25.0**	0.04	133.28	5.33	0.04	42	1.68	4.09	3.11	0.98	29.1	16%
10	8	4	4	8	3%	9	3.34	0.54	7%	0.18	123.20	22.15	0.15	19.26	2.89	**25.0**	0.08	106.33	8.50	0.08	42	3.36	9.08	6.51	2.57	34.1	36%
10	8	4	4	8	5%	9	3.34	0.54	7%	0.18	123.20	22.15	0.15	19.26	2.89	**25.0**	0.08	106.33	8.50	0.08	42	3.36	7.64	5.48	2.16	32.7	31%
10	10	4	6	10	3%	8	3.34	0.67	9%	0.18	123.20	22.15	0.15	19.26	2.89	**25.0**	0.10	100.93	10.08	0.10	42	4.19	11.27	7.96	3.31	36.3	45%
10	10	4	6	10	5%	8	3.34	0.67	9%	0.18	123.20	22.15	0.15	19.26	2.89	**25.0**	0.10	100.93	10.08	0.10	42	4.19	9.66	6.82	2.84	34.7	39%
average	6	3	3	6	0	8	5	0	0	0.26	121	31	0	19	6	**36**	0	86	6.5	0.061	42	3	6	4	2	43	0

Table 69 - Economic costs case 2

Environmental costs

As for the previous case the calculations and distribution of data considering DSN and DEnvironment are, respectively, in Table 70 and in Figure 83.

Table 70 - Results for environmental costs for case 2

ID PAV	DSN	DEnergy	DWaterCons.	DCO2	DNOx	DPM10	DSO2	DCO	DHg	DPb	DRCRA	DHTP (Cancer)	DHTP (Non-cancer)
2	0%	0.0%	0.0%	0.0%	0.0%	0.0%	0.0%	0.0%	0.0%	0.0%	0.0%	0.0%	0.0%
2	0%	0.0%	0.0%	0.0%	0.0%	0.0%	0.0%	0.0%	0.0%	0.0%	0.0%	0.0%	0.0%
2	2%	9.3%	9.2%	9.0%	10.2%	7.9%	12.0%	9.2%	9.3%	9.2%	9.3%	9.2%	7.2%
2	2%	9.3%	9.2%	9.0%	10.2%	7.9%	12.0%	9.2%	9.3%	9.2%	9.3%	9.2%	7.2%
2	4%	10.4%	9.2%	9.4%	13.4%	8.1%	23.8%	9.5%	9.4%	9.3%	9.3%	9.6%	8.2%
2	4%	10.4%	9.2%	9.4%	13.4%	8.1%	23.8%	9.5%	9.4%	9.3%	9.3%	9.6%	8.2%
2	5%	11.0%	9.2%	9.7%	15.0%	8.3%	29.6%	9.6%	9.4%	9.3%	9.4%	9.9%	8.6%
2	5%	11.0%	9.2%	9.7%	15.0%	8.3%	29.6%	9.6%	9.4%	9.3%	9.4%	9.9%	8.6%
2	6%	11.9%	9.3%	10.0%	17.4%	8.5%	38.4%	9.7%	9.4%	9.3%	9.4%	10.2%	9.4%
2	6%	11.9%	9.3%	10.0%	17.4%	8.5%	38.4%	9.7%	9.4%	9.3%	9.4%	10.2%	9.4%
5	0%	0.0%	0.0%	0.0%	0.0%	0.0%	0.0%	0.0%	0.0%	0.0%	0.0%	0.0%	0.0%
5	0%	0.0%	0.0%	0.0%	0.0%	0.0%	0.0%	0.0%	0.0%	0.0%	0.0%	0.0%	0.0%
5	2%	12.5%	12.6%	12.0%	13.6%	9.6%	16.5%	12.6%	13.0%	12.7%	12.9%	12.6%	8.5%
5	2%	12.5%	12.6%	12.0%	13.6%	9.6%	16.5%	12.6%	13.0%	12.7%	12.9%	12.6%	8.5%
5	5%	14.1%	12.7%	12.6%	17.9%	9.9%	32.7%	12.9%	13.0%	12.8%	13.0%	13.3%	9.7%
5	5%	14.1%	12.7%	12.6%	17.9%	9.9%	32.7%	12.9%	13.0%	12.8%	13.0%	13.3%	9.7%
5	6%	14.9%	12.7%	12.9%	20.1%	10.0%	40.7%	13.1%	13.1%	12.8%	13.0%	13.6%	10.2%
5	6%	14.9%	12.7%	12.9%	20.1%	10.0%	40.7%	13.1%	13.1%	12.8%	13.0%	13.6%	10.2%
10	0%	0.0%	0.0%	0.0%	0.0%	0.0%	0.0%	0.0%	0.0%	0.0%	0.0%	0.0%	0.0%
10	0%	0.0%	0.0%	0.0%	0.0%	0.0%	0.0%	0.0%	0.0%	0.0%	0.0%	0.0%	0.0%
10	4%	18.3%	18.3%	17.8%	20.1%	15.8%	22.1%	18.3%	18.5%	18.3%	18.5%	18.2%	14.4%
10	4%	18.3%	18.3%	17.8%	20.1%	15.8%	22.1%	18.3%	18.5%	18.3%	18.5%	18.2%	14.4%
10	7%	20.6%	18.3%	18.8%	26.4%	16.3%	43.6%	18.8%	18.6%	18.4%	18.5%	19.2%	16.3%
10	7%	20.6%	18.3%	18.8%	26.4%	16.3%	43.6%	18.8%	18.6%	18.4%	18.5%	19.2%	16.3%
10	9%	21.8%	18.4%	19.2%	29.5%	16.5%	54.4%	19.0%	18.7%	18.4%	18.6%	19.6%	17.3%
10	9%	21.8%	18.4%	19.2%	29.5%	16.5%	54.4%	19.0%	18.7%	18.4%	18.6%	19.6%	17.3%

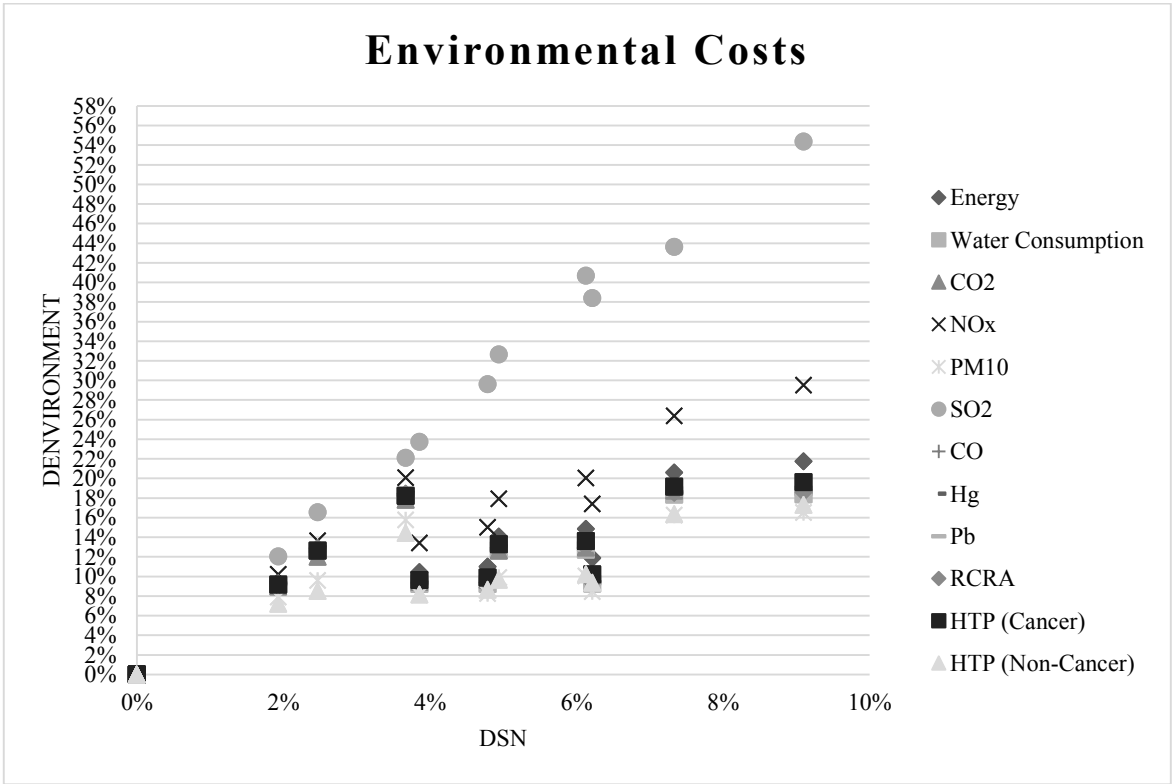

Figure 83- Distribution of data, relation DSN-DEnvironment for the Milling and overlay (AC + 40% RAP), (Case 2)

3.10 Estimate of the intervention costs and models for different solutions: net overlay vs. milling and overlay

A performance approach therefore makes it possible to estimate the higher intervention costs, and we have seen both at an economic and environmental level. The economic data just seen can be compared for the evaluation of the most advantageous solution. From the economic cost curves obtained it has been seen that intervening subsequently to repair an initial structural deficit (bearing capacity, thickness, etc.) can cost up to four times more. By putting the data together in the graph below (Figure 84), in fact, is possible to see the different slope of the curves that reach up to a quadrupling of costs for case 2.

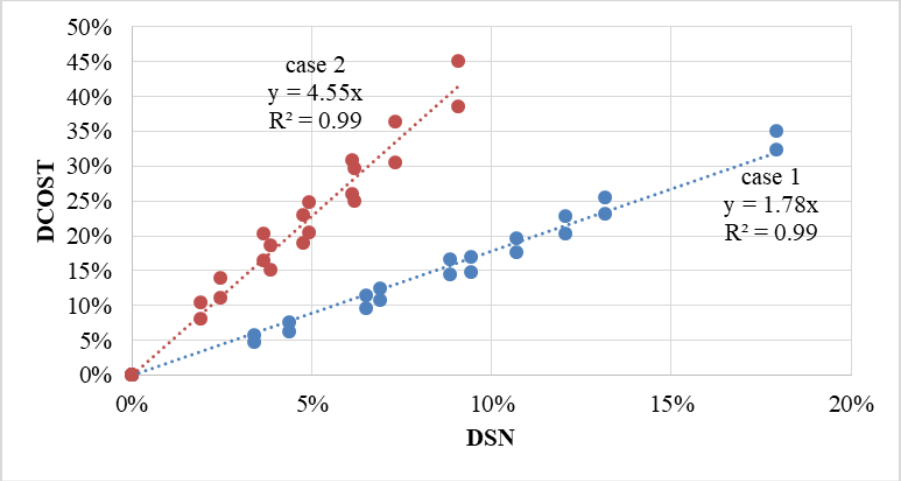

Figure 84 - Comparison of economic cost for the two case studies: 1)net overlay vs. 2)milling and overlay (AC+RAP).

In the economic costs the average of Net Present Value, Unit Costs and Actual costs[42] have been clearly taken into account to compare the two solutions studied.

To better understand what is happening, below in Table 71 there is an example of pavements studied with the net overlay solution (case 1), and with the milling + overlay solution (case 2).
In the two cases, therefore, there are two pavements with the same SNo = 3.34, and that have undergone very similar initial deficits and therefore require interventions, so in the first a net overlay of 6 cm was made, and in the second a milling and overlay 10 cm (4 cm in AC + 6 cm with 40% RAP).

Table 71 - Example of interventions in two pavements with built with similar initial deficit

Case	Type of intervention	Pav. N.	SNo	SNi	DSNeff	Year
1	Net overlay 6 cm	10	3.34	2.9	0.97	5
2	Milling and overlay 10 cm (4 cm + 6 cm)	10	3.34	3.04	0.67	8

Where: SNo: design SN of the base condition; SNi: SN of the pavement as built; DSNeff: reduction in SN at PSIf due to a reduced initial SN (DSNi=SNo-SNi) is calculated as DSNeff=2.20362·DSNi; Year is the year of intervention with an overlay of X cm calculated with the relations for the residual life RL=100[1-ESALi(PSI=1.5)/ESALi(PSIi)].*

From the results it's possible to see how comparing pavements that have in common the amount of initial deficit, between the two solutions, surely the second with the milling, having to remove part

[42] Actual cost= Volume[m^3]·Unit Cost[€/m^3]

of the pavement, requires much more important interventions in terms of costs, although certainly this solution can be said to be more realistic and environmentally sustainable, as 40% RAP is used.

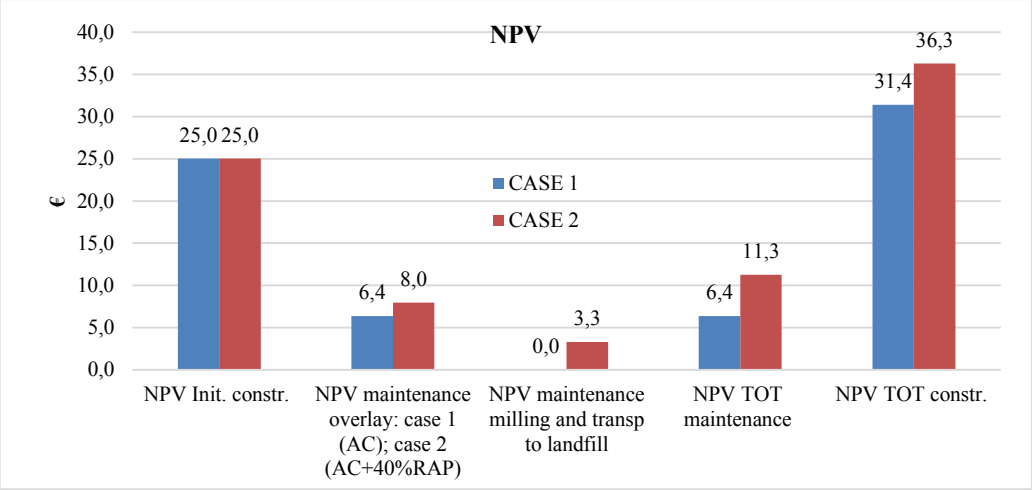

Figure 85 - Economic Estimation of solutions: Net Present Value

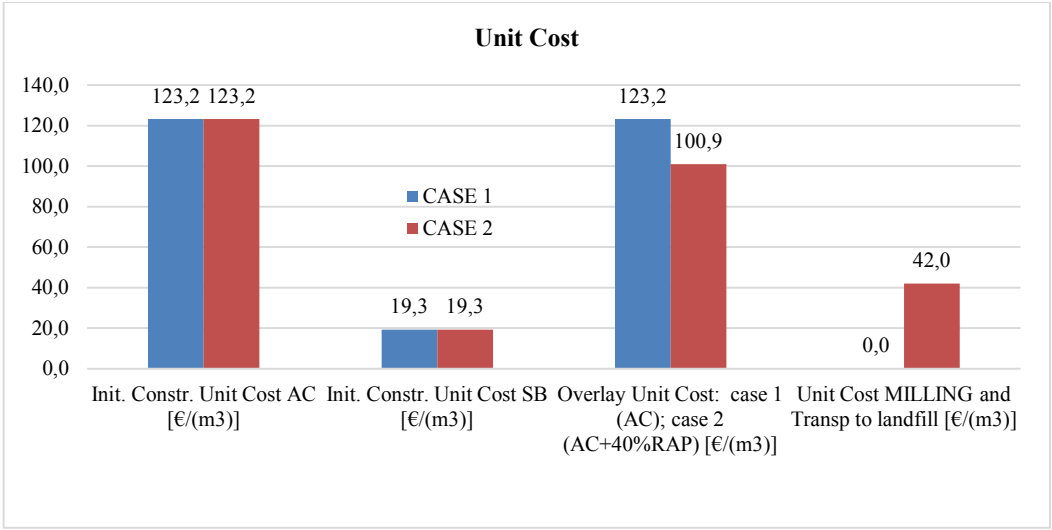

Figure 86 - Economic estimation of solutions: Anas Unit Costs

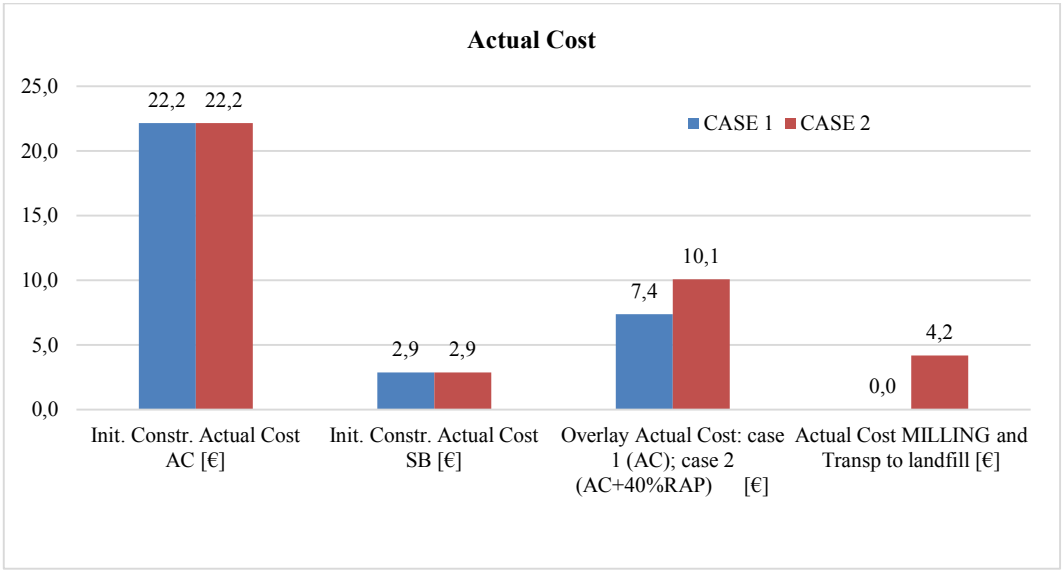

Figure 87 - Economic estimation of solutions: Actual Costs

In fact, from the histograms (Figure 85, Figure 86 and Figure 87) it can be seen that in both solutions the initial costs are the same, but the maintenance intervention done in different ways obviously generates different costs. Case 2 represents the most expensive intervention, as the milling is done that is not considered before, but also an overlay with new AC and a 40% RAP, considering therefore also costs of transport to landfill and additional variables. Although the cost in this last case is greater, it is certainly the intervention more adherent to reality, as a net overlay is never made over the pavement and therefore the milling is always necessary after a certain number of years.

The practical application is therefore exemplary of how an intervention can be done in different ways, generating different costs, and as therefore the initial costs of construction are added to the addition of interventions that are more, not budgeted and that serve to repair the deficit. This is why it is important to respect the project, it is also a guarantee of considerable cost savings.

In addition, models have been developed by relating the deltas relative to the structural number and those related to the economic and environmental costs, in order to compare and derive the best models and the different relationships according to the intervention solution before the 15th year to repair the initial construction deficit.

The models made with statistic regressions in the case of economic costs are exposed in Table 72:

Table 72 - Economic Models (statistical regressions)

Dependent variable (Economic costs)	**Independent variables**	**CASE 1 – Net Overlay**		**CASE 2 – Milling and overlay**	
		Models	**Adj. R^2 [%]**	**Models**	**Adj. R^2 [%]**
Dcost*100	DSN*100 DiscountRate*100	Dcost*100 = 2.28423 + 1.84935*DSN*100 - 0.763093*Discount Rate*100	99.208	Dcost*100 = 6.74855 + 4.52282*DSN*100 - 1.63956*Discount Rate*100	98.942
Dcost*100	DSN*100 DiscountRate*100	Dcost*100 = 1.8798*DSN*100 - 0.277145*Discount Rate*100	99.593	Dcost*100 = 4.69817*DSN*100 - 0.211729*Discount Rate*100	99.1277
Dcost*100	DSN*100	Dcost*100 = 1.78064*DSN*100	99.4083	Dcost*100 = 4.55499*DSN*100	99.1019

The economic costs can be noticed as they come to quadruple in the case 2 considering the milling and the overlay.

Clearly different solutions produce emissions and therefore different environmental impacts.
In

Table 73 the environmental models developed for the two cases.

Table 73 - Environmental Models (statistical regressions)

Dependent variable (Environmental costs)	Independent variables	CASE 1 – Net Overlay		CASE 2 – Milling and overlay	
		Models	Adj. R^2 [%]	Models	Adj. R^2 [%]
DEnergy*100	DSN*100	DEnergy*100 = 2.02*DSN*100	99.9357	[1] DEnergy*100 = 2.65619*DSN*100 [2] DEnergy*100 = 6.56809*sqrt(DSN*100)	92.9555 96.0855
DWaterCons.*100	DSN*100	DWaterCons.*100 = 2.03198*DSN*100	99.9054	[1] DWaterCons.*100 = 2.33338*DSN*100 [2] DWaterCons.*100 = 5.8293*sqrt(DSN*100)	88.6317 93.5131
DCO2*100	DSN*100	DCO2*100 = 1.95254*DSN*100	99.9354	[1] DCO2*100 = 2.38564*DSN*100 [2] DCO2*100 = 5.93063*sqrt(DSN*100)	90.5731 94.6267
DNOx*100	DSN*100	DNOx*100 = 2.01857*DSN*100	99.9481	[1] DNOx*100 = 3.46126*DSN*100 [2] DNOx*100 = 8.46045*sqrt(DSN*100)	96.7708 97.743
DPM10*100	DSN*100	DPM10*100 = 1.63183*DSN*100	99.8095	[1] DPM10*100 = 2.01216*DSN*100 [2] DPM10*100 = 4.99819*sqrt(DSN*100)	89.8373 93.7081
DSO2*100	DSN*100	DSO2*100 = 2.56765*DSN*100	99.7997	DSO2*100 = 6.17762*DSN*100	99.8176
DCO*100	DSN*100	DCO*100 = 2.01086*DSN*100	99.9134	[1] DCO*100 = 2.39512*DSN*100 [2] DCO*100 = 5.97065*sqrt(DSN*100)	89.5327 94.0575
DHg*100	DSN*100	DHg*100 = 2.06381*DSN*100	99.8842	[1] DHg*100 = 2.37438*DSN*100 [2] DHg*100 = 5.93275*sqrt(DSN*100)	88.6537 93.5685
DPb*100	DSN*100	DPb*100 = 2.03682*DSN*100	99.9009	[1] DPb*100 = 2.34214*DSN*100 [2] DPb*100 = 5.85095*sqrt(DSN*100)	88.6718 93.5485
DRCRA*100	DSN*100	DRCRA*100 = 2.05649*DSN*100	99.889	[1] DRCRA*100 = 2.36564*DSN*100 [2] DRCRA*100 = 5.91056*sqrt(DSN*100)	88.659 93.5634
DHTP (Cancer)*100	DSN*100	DHTP (Cancer)*100 = 2.0355*DSN*100	99.9043	[1] DHTP (Cancer)*100 = 2.4531*DSN*100 [2] DHTP (Cancer)*100 = 6.10271*sqrt(DSN*100)	90.4945 94.6802
DHTP (Non-cancer)*100	DSN*100	DHTP (Non-cancer)*100 = 1.55127*DSN*100	99.7187	[1] DHTP (Non-cancer) *100 = 2.03333*DSN*100 [2] DHTP (Non-cancer)*100 = 5.0076*sqrt(DSN*100)	93.0244 95.3809

All the developed models have very high Adj. R-square, of about 90% and over, there are all the solutions in terms of linear regressions and also other types of models (in case 2) that represent the modeling of the best models.

From these models it is therefore possible to foresee, starting from the structural number of a paving, those that may be the impacts in terms of emissions of a new road construction.
As already mentioned, the second solution with milling and overlay, is the one that is more representative of interventions that are done in reality and both at an economic and environmental level has shown how much the costs can increase when the project is not respected. But the analysis was also made considering the case of net overlay, which certainly generates lower costs, and allows to understand the variation range of the incidence of an unplanned intervention, also comparing it with the milling and overlay solution.

At this point, it is clear the need for a study on the penalties or bonuses that must be applied to companies if the works are not delivered as planned.
The final part of this thesis work, in the context of new constructions, focuses on which penalties or bonuses can be applied within specifications different from traditional ones, and which are therefore performance-based. These performance-based specifications consist of acceptance checks on structural indices deriving from NDT type tests. Each of these indices can be associated with a law that defines the quantification of bonus or penalties, the latter in case of inadequate delivery of works.

3.11 Penalty/bonus methods for performance specifications in new road construction

The correct execution of a work and the respect of a project, it has been specified several times, that is fundamental for the society, the road users, the customers and certainly implies savings in terms of both economic and environmental costs over time and consequently in the design period. If a road is delivered with defects, then it's seen how it will undergo an acceleration of its degradation process and will come to an end of life before the period for which it was designed.
But what to do then in case a work presents initial structural deficits? The approach used by all the specifications is certainly that of the penalty, whose discipline is functional to the provision of appropriate incentives for the proper performance of contractual services. It's important to understand how to measure performance variations that result in a reduction in the functionality of a work and quantify the economic damage that the contracting entity undergoes due to this effect. Paying a penalty by a company is certainly burdensome, but it is also a way to protect the client and ensure the delivery of a well-made, safe and long-lasting work.

3.11.1 Development of Penalty/Bonus models: results and conclusions

The application of penalties in the phase of acceptance of new construction works and in performance terms, is certainly not a new discipline both internationally and nationally.
From a literature review, some studies have been made to allow methodological considerations and to develop penalty/bonus curves on performance-type indices.
At international leve, the **NCHRP report n. 704** (2011) captures an interesting reality to be translated into practice in actions of penalties on the works, taking into consideration therefore that

the accelerating growth of higway transportation develop increasingly complex problems of wide interest to highway authority.

The purpose of NCHRP with a performance approach is to promote the construction of a quality pavement by measuring and evaluating characteristics directly related to its performance with key variables that are dependent on the distresses that a road pavement can have, considering that systematic, well-designed research provides the most effective approach to the solution of many problems facing highway administrators and engineers.

The National Cooperative Highway Research Program, in fact, proposes a **performance approach** for the **evaluation of the penalties/bonuses** to be applied to a work and which is **related to the residual life of a road pavement**.

To assess the difference between the as-designed and as-built distributions a variable called the Predicted Life Difference (PLD) is introduced and used as the basis for establishing the Pay Factor Penalty/Bonus.

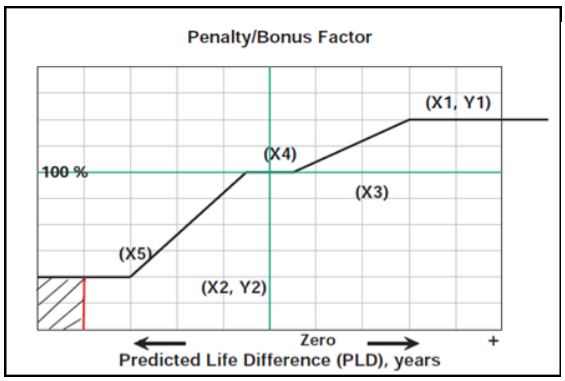

TYPICAL PAY ADJUSTMENT FACTORS	
Max. Bonus (%), Y1	7
Max. Penalty (%), Y2	20
Max. PLD (Years), X1	5
Min. PLD (Years), X2	-5
PLD for no Bonus, X3	2.5
PLD for no Penalty, X4	-2.5
PLD for Remove and Replace, X5	-10

Figure 88 - Penalty/Bonus versus pavement life difference relationship and typical value of pay adjustment factors. Source: NCHRP (2011).

Figure 88 shows typical values to set the Pay Factor-Predicted Life difference relationship derived from the NCHRP study. There is a region where there is no bonus or penalty, e.g., the region between (X3) and (X4). Also, there is a value (X5) at which removal and replacement of the as-built section is required. It's important to note that the precise coordinates of each point and of the shape of the relationship are defined by the user agency with reference to first, maximum and minimum Pay Factor values. After that NCHRP developed the relationships between the Predicted Life Difference and the Pay Adjustment factors.

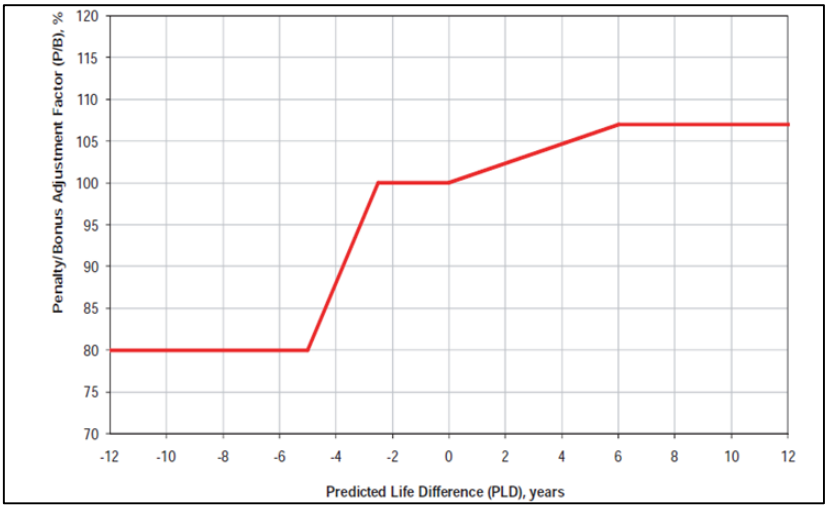

Figure 89 - Predicted life difference (PLD) vs. Penalty/Bonus adjustment factor (P/B). Source: NCHRP (2011).

In Figure 89, the residual life (x axis) is then put in relation to a penalty/bonus adjustment factor that indicates how much must be paid compared to the 100% value (pavement built respecting the project). So on the y axis, for example the 80% factor indicates that is paid a 80% value of the construction work, so consequently it can be stated that the penalty is 20%.
The graph clearly shows that the contractor is also compensated based upon the quality of a product (e.g., when the Predicted Life Difference is positive, Penalty/Bonus factor will be more than 100%).
The concept behind the **NCHRP payment system** is that the contractor's compensation is based on the expected performance difference, i.e., the Predicted Life Difference between as-designed and as-built. The conclusion of this study is that the purpose of a Performance Related Specification (PRS) like the Quality Related Specification (QRS) is to promote the construction of a quality pavement by measuring and evaluating characteristics directly related to its performance. The pavement performance is then predicted using key variables related to the pavement and consequently the quality of the as-built mix is converted into its predicted service life and is then compared with the as-designed mix.

On the basis of the models developed during the PhD and the NCHRP methodology it was possible to compare and study the Residual Life-Penalties relationships.
The residual life in this research study was obtained considering the 15-year project period and two types of possible interventions: net overlay (case 1) and milling + overlay (case 2).
The results are in Figure 90: in red the NCHRP curve and in grey (case 1) and blue (case 2) the developed models. In the x axis there is the residual life in terms of years of a pavement (RL=15*DEsal), in the y axis there are the Delta Costs calculated previously, as:

Case 1: Dcost=1.78*DSN
Case 2: Dcost=4.55*DSN

Where Dcost are the Penalty (if negative) or the Bonus (if positive) and DSN is the Delta Structural Number.

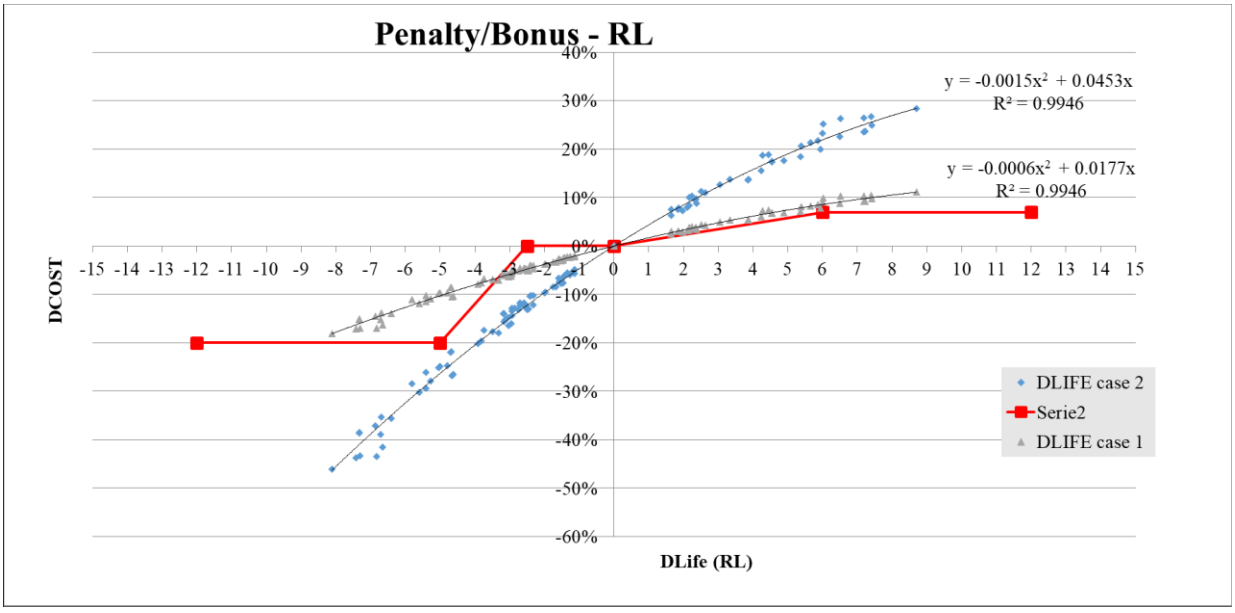

Figure 90 - Comparison between the models developed and the NCHRP performance related approach.

The negative part of the graph represents the penalties, the positive part represents the bonuses.

From the results obtained in Figure 90, it can be noted that the cases 1 and 2 studied give a variation range of the penalties or bonuses in relation to the residual life of the road pavements.
Comparing the two cases with the NCHRP curve, then the whole range of application of bonus or penalty, it is important to make 2 considerations, the first on penalties and the second on bonuses:

1) when it comes to restoring the damage suffered by the road authority due to initial structural deficits of construction, then it is important to find the most precautionary situation in terms of penalties, as the road authority needs to be reimbursed by the company for the higher costs that it will have in the future.
2) on the other hand, considering the bonuses, which are normally not required, there is not the same need for caution on the part of the road authority, so it is possible to give a reward to the company but with less restrictive conditions than the previous case. This means in any case that the company can gain an advantage when it realize a work with a surplus of quality and performance compared to the life for which it was designed.

In the graph is possible to see the grey curve of case 1 (net overlay) that has a good agreement, compared to NCHRP, especially in the part related to the bonuses, a little less in penalties.
For case 2, which is the solution that considers milling and overlay as an intervention, it is noted that the models developed in this thesis work responds in a fairly similar way as regards the penalties (especially the part that goes from 0 to -20% penalty, which are those that then at the max are recognized at the Italian level and we will see below with ANAS), a little less regarding the bonuses, and this can be explained by the fact that the NCHRP curve does not go beyond the 8% bonus. For this last case of milling + overlay the model used to calculate the Dcost (Penalty/Bonus) is therefore the one developed in this work of thesis that demonstrates a quadrupling of the costs[43].
From the two considerations made and the results obtained for the two cases, compared with the NCHRP curve which is constructed using rational methods, it can be deduced that the **P/B criterion** must be more restrictive when it comes to assigning penalties, less when it comes to bonuses, as these are a reward that the road authority recognizes to the company.
Thus, case 2 is more representative in terms of penalties, instead case 1 is in terms of bonus.
From the models obtained, it is suggested, for the purposes of the possible inclusion in performance specifications, to calculate the **Penalties**, which are in the negative part of the graph (x and y), such as:

$$\mathbf{Penalty=-0.0015*RL^2 + 0.0453*RL}$$

The **Bonuses**, in the positive part of the graph (x and y) can be recognized by road authorities towards companies such as:

$$\mathbf{Bonus = -0.0006*RL^2 + 0.0177*RL}$$

The regression models showed an excellent value of R-square equal to 99%.

This therefore means that negative differences in the life of the pavements generate penalties, however positive differences, representing a surplus compared to the design life, generate bonuses.

[43] Dcost = 4.55 * DSN (in percentage), calculated for all the combinations of the database of road pavements. Since Dcost is a function of the Structural Number, and as the Structural Number is the function of some variables related to the wear, binder, base and subbase layers, changes in the subgrade have not been considered.

At the Italian level, **ANAS** has recently introduced the performance approach, as well. This therefore emphasizes the use of new high-performance NDT technologies and quality controls on pavements that need to be done in terms of performance.
As previously explained ANAS uses two indices, IS200 and IS300, and considering that the thesis work is developed for new constructions, the comparison this time was done with IS300 which is the index for ANAS representative of new constructions in its performance specifications.
The **ANAS** curve, in red with continuous line in Figure 91, is constructed considering that **the increasing differences (delta) of the I300 index** compared to the prescribed value, **correspond to penalties equal to half of the percentage points of which the index differs**. If this difference exceeds 40%, then it will be necessary to demolish and rebuild the road; therefore, the maximum penalty will be 20%. Anas does not plan to recognize bonuses to companies in case of negative differences of Delta I300. But the Anas bonus curve was however built in red with dotted line to make comparisons with the cases 1 and two studied, but it is not foreseen in the performance specifications of this road authority.
In Figure 91 all this has been represented, ie the Anas model[44] together with the two models developed on the road pavement database studied in the thesis (case 1 and case 2). The negative part of the y axis represents the penalties, the positive part the bonuses.

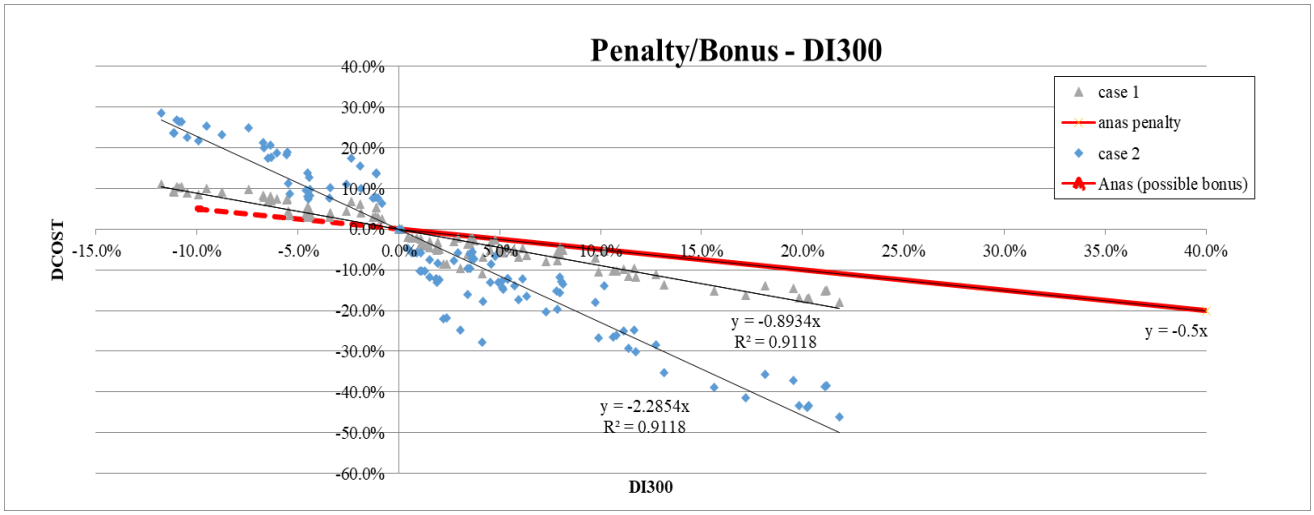

Figure 91 - Comparison between the models developed and the ANAS performance approach of Penalty/Bonus for the Structural Index I300

As can be seen from the graph, the trend obtained in the models related to cases 1 and 2 is very similar to that of Anas, but some considerations must be made in terms of slope of the curves.
The developed models have a greater slope with respect to Italian specifications with coefficients of 2.28 (case 2: intervention of milling and overlay) and 0.89 (case 1: net overlay) compared to 0.5 of ANAS. This implies with the models developed higher penalties or bonuses in terms of actual economic costs due to as built defects. The three models, with linear relationships, have the following equations:

1) **Anas:** Penalty = -0.5*DI300. Bonuses are not provided.
2) **Case 1:** Penalty/Bonus = -0.89*DI300
3) **Case 2:** Penalty/Bonus = -2.28*DI300

[44] Anas in its specifications does not provide a graphical representation, it was developed here to make a graphic comparison with the models developed with the data related to cases 1 and 2. In addition Anas only provides penalties for companies and does not consider the possibility of bonus.

It's clear that the DI300 is sensitive to the Delta Cost data, but that the criterion used by Anas is not very precautionary for itself, because the penalties applied are certainly lower than the models of case 1 and 2. The DI300 would seem to work in terms of trends, but penalties should be higher.
The criterion used by Anas in terms of trend is much closer to case 1 than to case 2, but it should be noted that surely with the developed models of this work of thesis, the road authority is better protected regarding the costs it must sustain in the future if the pavement has a structural deficit when it is built. Following are the considerations for penalties and bonuses, in order to be proposed for performance specifications.
A model like that of case 1 can be suggested within modern performance specifications, as it allows the road authority to better support the unforeseed maintenance costs of the road infrastructure due to initial structural deficits. Surely the data obtained with case 2 would be even more precautionary for the road authority, but with the consequence, however, that the penalties would be excessive for the companies compared to the existing specifications, and therefore difficult to sustain in economic terms. At the same time, the bonuses would be excessive and would be too much to the disadvantage of the road authority.
Case 1, chosen for performance specifications, is also very similar as a trend of values in terms of penalties for small differences of the I300 index (for example up to 5%) where companies would not be much penalized tolerating small differences, but when differences in the I300 index increase (after 5% for example), surely the road authority needs more protection, and then using this model developed with a coefficient 0.89 it would be possible to penalize more companies that do not deliver the work in a workmanlike manner according to project directions. The maximum acceptable penalty, as for Anas, must be 20%, limit beyond which the demolition is expected.
A suggestion could be that companies up to 5% of the difference in the I300 could not be penalized admitting in the specifications a tolerance from 0 to 5% and considering applying the penalties from 5% onwards, considering to arrive at a maximum penalty of 20%, beyond which the demolition must be foreseen.
In this way, using case 1 as a reference, it means that we are applying a penalty equal to the cost that the road authority will have to pay more for maintenance, due to the deficits.
In addition, the developed models provide the possibility of applying bonuses with a considerable advantage for companies. As seen from the models developed by NCHRP, the bonuses are always lower proportionally than the penalties, this happens because they are still a reward for companies that make work with a performance surplus that was not required. Considering the case 1, with equation y=-0.89*x as a reference, in the application of the bonuses it can be considered a 50%, i.e. y = (-0.89*0.5)*x = -0.4467*x (where y is the bonus and x is DI300), compared to the performance gain that will receive the road authority, and which is recognized to the company as a reward.
These bonuses are an advantage and would encourage companies, considering also that Anas at this moment does not foresee them in its specifications.
In the conclusions part the results will be shown graphically in Figure 96 compared to the models developed and these considerations.

The same considerations have been made in terms of **differences in thicknesses** of the AC layers (Figure 92) and of the subbase (Figure 93), by developing predictions of cost variations (DCOST) that are compared in the following graphs with the deductions made by **ANAS**.

Anas in its performance specifications **considers deductions and therefore penalties for asphalt concrete layers without making distinctions between the wear, binder and base layers**. Anas does not deal with the thickness of the subbase.

In Figure 92 the Anas criterion is compared with the cases 1 and 2. The penalties are in the negative part of the graph, instead the bonuse are in the positive part.

In the case, therefore, of the **asphalt concrete layers**, from the graph we note that the Anas criterion, as we can see in Figure 92, is more penalizing than the case studies developed in the thesis. In fact, in general Anas is more penalizing than model 1, but much less penalizing than model 2. Case 1 is shown in grey, case 2 in blue, the Anas case in orange.

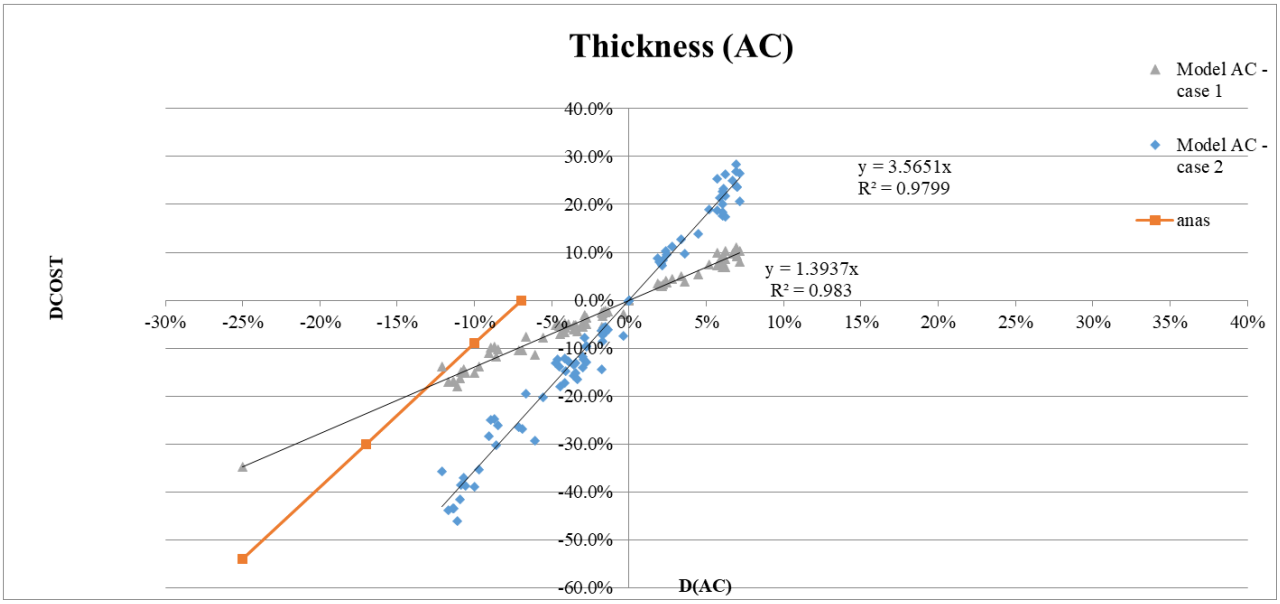

Figure 92 - Comparison between the models developed and the ANAS performance approach of Penalty/Bonus for the thickness of the AC layers

As it's possible to see, Anas considers an initial tolerance from 0% up to -7% difference compared to the project thicknesses and in this range does not apply any penalty; applies penalties from -7% to 25% difference in thickness, with a maximum penalty of 54%; moreover it does not provide any bonuses.
The case study n. 1 is the most similar to the deductions applied by Anas, both cases (case 1 and case Anas) reach a penalty of 20% with a negative difference in thickness of about 14%. For case 1, the maximum difference in the AC thickness of -25% generates lower penalties than Anas.
Case 2, compared to the Anas performance specifications is significantly more penalizing and therefore would be unsustainable in terms of costs for companies that carry out road construction works.
The models developed allow also to provide bonuses, and therefore case 1 can become a reference in the performance specifications to recognize bonuses to companies.

So, in general the best model developed for **AC layers** turns out to be **y=1.3937*x** related to case study 1 (with y=Dcost or P/B, and x=DeltaACthickness).

Similarly to the Anas criterion, from 0 to 7% of negative difference in thickness, can be considered a tolerance in the application of penalties to the companies.

Penalties apply from -7% to -25% of difference in the thickness of the layers in asphalt concrete. At 25% of difference in negative of the thickness will correspond a penalty of 35%, which is lower than that of Anas of 54%. Once the 25% difference in negative in the thickness is exceeded, the demolition must be foreseen. Moreover for the bonuses, similar to the previous case, we can estimate 50% of the income that will receive the institution, so the equation will be: y=(1.3937*0.5)*x → Bonus = (1.3937*0.5)*DACthickness = 0.6969*DACthickness.

Anas in its performance specifications does not consider deductions for the layers of **subbases**.
In this research work it was considered appropriate to study also this case, thus obtaining two models for the case 1 (gray) and the case 2 (in blue).
In the graph of Figure 93, the ANAS criterion, already seen previously in the AC case (Figure 92), has been reported in order to make some considerations and comparisons, in order to insert deductions also for the thickness of the subbase layers.
However, considering that the ANAS criterion does not apply to subbases, it has been reported in orange with a dotted line.

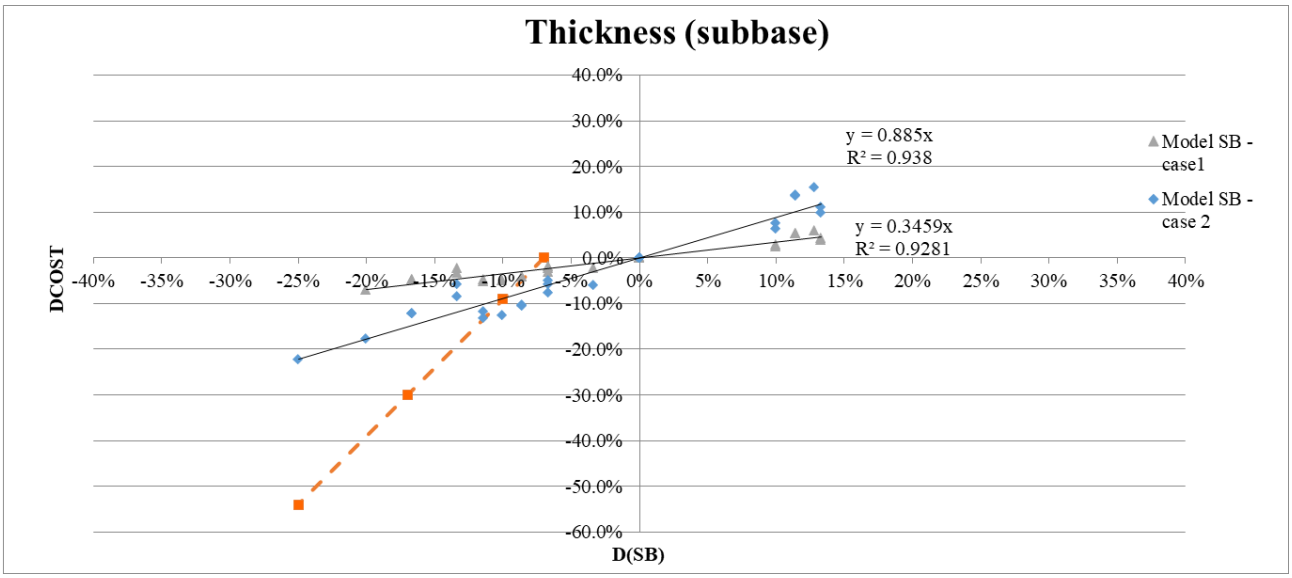

Figure 93 - Comparison between the models developed for the thickness of the subbase layer

Also this time, in the negative part x and y of the chart there are the penalties, in the positive part the bonuses.

In fact, in Figure 93, the penalty criterion that is outlined in orange is certainly much more penalizing than cases 1 and 2, this because the limit value of negative difference in thickness of 25% involves a penalty of 54%. This case is very penalizing, because comparing it also to cases 1 and 2, it is possible to note how the latter at the limit value of subbase thickness difference certainly have much lower penalties.

From the developed models of cases 1 and 2, surely one solution would be to choose an intermediate case. Case 1 would generate penalties that are too low. For this reason, an intermediate solution would be to adopt the criterion of case 2, since the limit of 25% of negative difference in subbase thickness implies a penalty of around 22%.

Certainly they are more reasonable values from the moment in which there is nothing in this sense in Italian specifications. Moreover, compared to the orange solution, differences of -10% in thickness would generate 9% penalties in both cases.
So for subbases, a good solution would be the one related to case 2 of equation y=0.885*x.
Similarly to what was done for the AC layers, with regard to the penalties, a tolerance of 0 to -7% is considered, and if this last value is exceeded the penalties will be applied. Penalties would be applied in the range of negative differences in thickness from 7% to 25%, over 25% should be considered demolition. The bonuses will also be lower here and again considered 50% compared to the model of penalties, as a reward for companies that build with higher performance even if not required, so: y=(0.885*0.5)*x → Bonus=(0.885*0.5)*DSBthickness=0.4425*DSBthickness.
The results with the graphic solutions accompanied by the equations for the thicknesses of AC and subbase layers are in Figure 97 and Figure 98.
All possible suggestions for performance specifications, as a result of these studies of Residual Life, I300 and AC or subbase thickness, will be presented in the conclusions.

Finally, Penalty/Bonus models have been developed for all the indexes studied in this research work (case 1 and case 2) and are shown in Table 74 and in **Appendix 10**.

Table 74 - Models Penalty/Bonus developed for Performance Specification of new road construction

Dependent Variable [Penalty/Bonus]	**Independent Variable [Delta Indexes]**	**Name of the Index and significance (Independent variable)**	**Best Models (Linear Regressions) Dcost=1.78DSN (case 1: net overlay)**	**Adj. R-Square [%]**	**Best Models (Linear Regressions) Dcost=4.55DSN (case 2: milling + overlay)**	**Adj. R-Square [%]**
Dcost	DI1 (I1=D_0')	First deflection under load	Dcost = -2.23442*DI1	**98.29**	Dcost=-5.71578*DI1	**98.29**
Dcost	DI2 (I2=RoC)	Radius of Curvature	Dcost = 0.971451*DI2	92.34	Dcost=2.48503*DI2	92.34
Dcost	DI3 (I3=Eq)	Equivalent Modulus characterizing the condition of all the layers of the pavement	Dcost = 2.3093*DI3	**98.44**	Dcost=5.90734*DI3	**98.44**
Dcost	DI4 (I4=AUPP)	Area under pavement performance characterizing the condition of the pavement upper layer	Dcost = 9.63501*DI4	90.55	Dcost=24.647*DI4	90.55
Dcost	DI5 (I5= Al_1)	Area Indices characterizing the condition of upper layer	Dcost = 11.2739*DI5	82.38	Dcost=28.8395*DI5	82.38
Dcost	DI6 (I6= Al_2)	Area Indices characterizing the condition of middle layer	Dcost = 3.82793*DI6	87.12	Dcost=9.7921*DI6	87.12
Dcost	DI7 (I7= Al_3)	Area Indices characterizing the condition of middle layer	Dcost = 2.68879*DI7	92.07	Dcost=6.8781*DI7	92.07
Dcost	DI8 (I8= Al_4)	Area Indices characterizing the condition of lower layer	Dcost = 2.34086*DI8	**95.10**	Dcost=5.98806*DI8	**95.10**
Dcost	DI9 (I9= E_{0r})	Modulus of Elasticity at 600 mm from center characterizing subgrade layer	Dcost = 4.75821*DI9	57.18	Dcost=12.1718*DI9	57.18

Dcost	DI10 (I10=IS300 or SCI)	**Anas Index IS300** Surface Curvature Index characterizing the pavement layers	Dcost = -0.893407*DI10	**91.76**	Dcost=-2.28539*DI10	**91.76**
Dcost	DI11 (I11=MLI)	Middle Layer Index characterizing the condition of the base layer	Dcost = -1.42324*DI11	**96.40**	Dcost=-3.64075*DI11	**96.40**
Dcost	DI12 (I12=LLI)	Lower Layer Index characterizing the condition of the subgrade	Dcost = -1.68199*DI12	13.60	Dcost=-4.30265*DI12	13.60
Dcost	DI13 (I13=IS200)	Anas index IS200	Dcost = -0.805616*DI13	86.20	Dcost=-2.06082*DI13	86.20
Dcost	DI13c ($I13c=IS_{200CF}$)	Anas Index IS_{200CF} correct with the subgrade	Dcost = -0.3734*DI13c	44.65	Dcost=-0.955182*DI13c	44.65
Dcost	DI14 (I14=SF)	Shape factor	Dcost = -1.19914*DI14	80.61	Dcost=-3.06747*DI14	80.61
Dcost	DSNeff	DSNeff from FWD test	Dcost=3.904*DSNeff	**97.50**	Dcost=9.987*DSNeff	**97.50**
Dcost	DSNeff600	DSNeff600 from FWD test	Dcost=4.435*DSNeff600	**95.40**	Dcost=11.346*DSNeff600	**95.40**
Dcost	DEsalSNeff	DEsalSNeff from FWD test	Dcost=0.564* DEsalSNeff	**97.10**	Dcost=1.443* DEsalSNeff	**97.10**
Dcost	DEsalSNeff 600	DEsalSNeff600 from FWD test	Dcost=0.561* DEsalSNeff600	**96.90**	Dcost=1.435* DEsalSNeff600	**96.90**
Dcost	DI1, DI8, DI11	Multiple regression with Delta Indices I1, I8, I11	Dcost = -1.10014*DI1 + 0.386319*DI8 - 0.513041*DI11	**98.82**	Dcost= -2.81422*DI1+0.988228*DI8 -1.31239*DI11	**98.82**
Dcost	DI1, DI8	Multiple regression with Delta Indices I1, I8, I11	Dcost = -2.19718*D_I1 + 0.0403397*DI8	**98.27**	Dcost=-5.62053*DI1+0.103192*DI8	**98.27**
Dcost	DISN	Where ISN in the Index that represents the multiple regression between SN (var. dep) and I1, I8: **ISN=SN=2.90684 - 0.0124342*I1 + 10.7882*I8 [-]** DISN is the Delta ISN	Dcost = 1.91*DISN	**97.00**	Dcost = 4.88*DISN	**97.00**

As already seen for the graph containing the I300 index of ANAS, the increasing differences in the indices (therefore positive) generate penalties (negative), vice versa generate bonuses (positive).
The calculations have been made, for research purposes, for all indexes considering the interventions in case 1 and 2, but for example the Anas I200 (DI13) index is only valid for superficial rehabilitation, so it does not fall within the categories covered by this study, ie new buildings, and presents an Adj. R-square equal to 86%.
From the results obtained, clearly as could be expected, there are regressions with Adj. R-Square weak for all those descriptive indices of the subgrade. This is explained by the fact that Dcost, as explained previously, was calculated without considering the variations of the subgrade for the road pavements of the database.

As for the other Penalty/Bonus curves relative to the other indices, the statistical regressions and therefore the models developed gave good results that are around 90% or even reach 98% which can be said to be an excellent result.
It's important to remember that the calculations have been made considering the interventions of Net Overlay (case 1) and those of Milling + Overlay (case 2). Milling + overlay interventions have higher costs in general but represent the most realistic solution.
There are excellent results for the regressions between Dcost with the indices deriving from FWD tests, ie the DSNeff, DSNeff600, DEsalSNeff, DEsalSneff600, with ADj. R-square respectively of 97.5%, 95.4%, 97.10%, 96.90%. Furthermore, the indices DI1, DI3, DI8, DI10, DI11 have values of Adj. R-square between 92% and 98%.
Multiple regressions were made combining DI1, DI8, DI11 and DI1, DI8 with Adj. R-square respectively of 98.82% and 98.27%.
Furthermore, the regression between Dcost and DISN returns a 97% Adj. R-square which is very high and represents a delta of the Structural Number, which was calculated according to the I1 and I8 indices.

In conclusion, this study shows that new performance indexes can be included in the Specifications to improve the correlation with performance measures, going to have a more complete vision and the performance guarantee of all the layers that rest on the road subgrades that are designed (bearing capacity, thickness, materials, etc.). Moreover, it was showed the importance to related the performance indicator to an estimation of actual costs related to as built defects: then in the conclusions are shown the best results and the possible suggestions for specifications.

3.12 References

- AASHTO T274-82*, Standard Method of Test for Resilient Modulus of Subgrade Soils.*
- AASHTO, *Guide for Design of Pavement Structures*, 1993.
- AASHTO*, Mechanistic – Empirical Pavement Design Guide. A Manual of Practice. Interim Edition,* July 2008.
- ANAS S.p.A., *Capitolato Speciale D'Appalto - Norme Tecniche per l'esecuzione del contratto Parte 2,* Coordinamento Territoriale/Direzione IT.PRL.05.21, 2016.
- ANAS S.p.A., *Capitolato Speciale D'Appalto. Norme Tecniche*, IT.CDGT.C.05.16-Rev.0-24/04/2009.
- ANAS S.p.A., *Gestione delle pavimentazioni stradali. Linee guida di progetto e norme tecniche prestazionali*, Ricerca & Innovazione – Centro Sperimentale Stradale, Novembre 2008.
- ANAS S.p.A., *Listino prezzi 2018. Nuove Costruzioni e Manutenzione Straordinaria,* Direzione Ingegneria e Verifiche, NC-MS 2018 – Rev.0, 2018.
- *Catalogo delle Pavimentazioni Stradali, 1995.*

- *CNR B.U. n. 60/78, Norme sulle caratteristiche geometriche e di traffico delle strade urbane,* 1978.
- CNR B.U. n. 78/80, *Norme sulle caratteristiche geometriche delle strade urbane*, 1980.
- Darter, M.I., Elliott, R.P., and Hall, K.T., *Revision of AASHTO Pavement Overlay Design Procedure*, Transportation Research Record 1374, p. 36–47, Transportation Research Board, Washington, DC., 1991.
- Horak E., Emery S., *Falling Weight Deflectometer Bowl Parameters as Analysis Tool for Pavement Structural Evaluations*, 22nd ARRB Conference – Research into Practice, Canberra Australia, 2006.
- Horvath, A Life-Cycle Analysis Model and Decision-Support Tool for Selecting Recycled Versus Virgin materials for Highway Applications, Final Report for RMRC Research Project No. 23, March 2004.
- Losa M., Bacci R., Leandri P.*, A Statistical Model for Prediction of Critical Strains in Pavements from Deflection Measurements,* Road Materials and Pavement Design, 9:sup1, 373-396, DOI: 10.1080/14680629.2008.9690175, 2008.
- Mallick Rajib B., El-Korchi Tahar, Pavement Engineering: Principles and Practice. Second Edition, CRC Press - Taylor & Francis Group, International Standard Book Number-13: 978-1-4398-7036-5 (eBook - PDF), 2013.
- NCHRP 1-37 A 2004, *Guide for Mechanistic – Empirical Design of new and rehabilitated pavement structures*, 2004.
- NCHRP Report 704, A *Performance-Related Specification for Hot-Mixed Asphalt*, TRB, Washington D.C., 2011.
- *Nuovo Codice della Strada, 1992.*
- Shell Bitumen, *Bisar 3.0 User Manual.*
- Solanki, U. J., Gundaliya P. J., Barasara M. D., *A Study on FWD Deflection Bowl Parameter to Assess Structural Condition of Flexible Pavement,* 2016.
- Statgraphics*, Centurion XVI User Manual*, 2009.

CONCLUSIONS

The PhD thesis work carried out has the aim of inserting and enriching, within road specifications, a performance approach that goes beyond and exceeds the limits of the traditional approaches in the accepting phase of new construction works.

The dissertation, making a big picture of the work done, consists of three macro-chapters: a flow chart of the different topics is exposed in Figure 94.

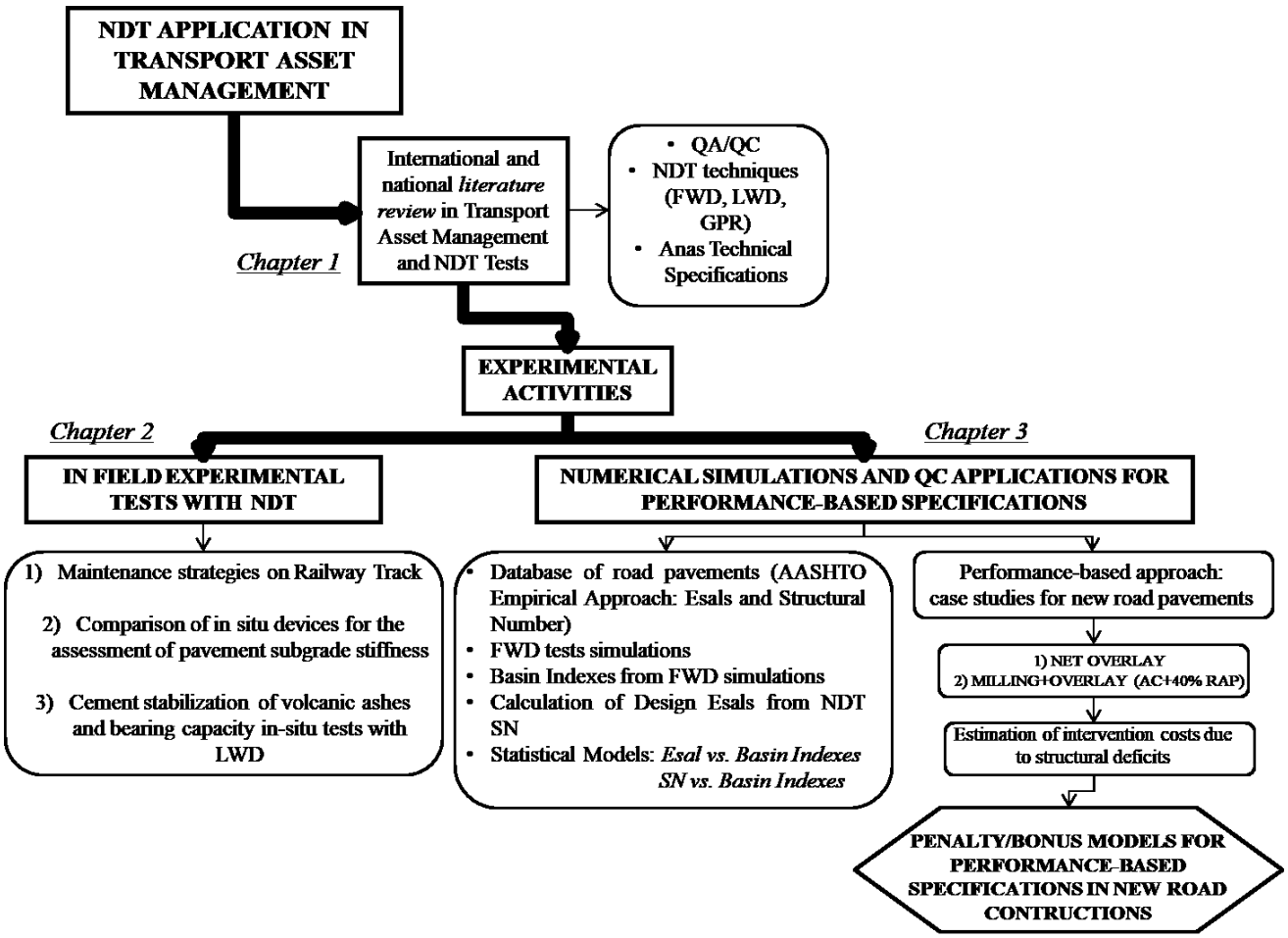

Figure 94 - Flow chart showing the different topics of the PhD dissertation

The first Chapter covers a state of the art in the field of **Transport Asset Management**, from which emerge the motivations of the research and the need for quality controls in road works through the use of non-destructive techniques.
In this part, the requirements of road infrastructures in terms of QA/QC are examined in depth, and the emerging international development of a **performance-based approach** as a requirement for acceptance of the works, together with **performance pay factors** to be applied in cases of non-acceptability and structural deficit on as built constructions.
The results of this research work refer both to an **experimental activity** and to a part of **numerical simulations**, which are the topics covered in chapters 2 and 3.
Chapter 2 includes experimental in field activities carried out using the high-efficient equipment of the Transport Infrastructure Laboratory (University of Catania). Specifically, maintenance strategies have been developed in the railway sector, studies on pavement subgrade stiffness, and the proposal

in road sector to re-use Etna volcanic ashes stabilized with cement that, from waste, can be transformed into a resource for our society.
Chapter 3 includes numerical applications and simulations aimed at developing performance-based methods that can be integrated into performance specifications with penalty/bonus models.

The results related to the experimental activity, which was also the subject of publications and presentation at international conferences, were obtained thanks to the use of various NDT equipment, (such as FWD, Georadar), and can be found in Chapter 2 where there are also the conclusions.

This part of conclusions refers to the numerical simulations discussed in Chapter 3.

In particular, the research work included a study on the state of the art in the field of NDT tests, QC and specifications, and in particular on ANAS specifications that are the reference for Italian road pavements, and also included an experimental investigation both with tests done in situ, and numerical simulations.
Emphasizing also the NDT techniques, the coupling of high efficiency equipment, the study of basin indices and the estimation of economic and environmental costs, it was possible to develop statistical predictive models of the residual life, in terms of Esal, of the Structural Number, tensile and compressive strains at critical points of pavement layers. Furthermore, the estimate of life cycle costs in relation to changes in the structural basin indexes of road pavements have allowed the development of statistical regressions and therefore Penalty/Bonus relationships that can be used in modern performance specifications.

Certainly, at performance level, structural NDT tests must be increasingly standardized to get an immediate idea of how the road construction work was done, and then to ascertain if there are initial structual deficits.

All this can be done in a very simple way, i.e., starting from deflections that can be obtained equally by all the technicians already allowing in the first instance to derive structural indexes to evaluate the structural conditions pavements and to verify the correct execution of works. With the advantage of not going from cumbersome back-calculation mechanisms that can range over multiple approaches and results sometimes difficult to compare.

From these premises, the study was then developed by directly assessing how a structural deficit of bearing capacity results in terms of additional economic and environmental costs. From the calculations made, it was seen that initial structural performance deficits translate into a shortening of the residual life, an achievement of the final PSI level in advance of the designed period, and at higher intervention costs compared to the initial deficit that can result in around double in terms of structural performance and up to 4.5 times in terms of costs.

The damage is that the performance deficit occurs after a few years from when the work is put into operation generating a shortening of the life of the road pavement.
A **performance-based approach** is therefore necessary for several reasons, as it considers a quantification of the bearing capacity with the evaluation of the effects over time, allows the

estimation of the greater costs of both economic and environmental intervention, allows the application of penalties commensurate with higher maintenance costs.

Starting from the assumption of how important the respect of the project is, and from the existing ANAS specifications, some critical issues emerged from this research work, which through some suggestions can be overcome.
Firstly, when a road is built, in a **performance-based perspective**, it would be good for the New Constructions to emphasize the **progressive importance of the controls** and therefore **the overall assessment of the pavement by step**, **i.e. by layers.**
The **performance checks** must be carried out as the construction of the road is made, starting from the subgrade and, once the appropriate structural checks have been made, go to the checks on the subbase and then to the base, binder and wear layers. This would certainly improve the accuracy and specifity of results of NDT tests that would be done with an overall knowledge of the road pavement. A **progressiveness of the tests by step**, allows not only to identify in advance where the problem is, but also to understand and interpret the test correctly, and therefore the structural indices that derive from it.

A literature review at international and national level was made and therefore a research aimed at the development of new performance-based specifications was carried out.

At international livel, **NCHRP** (2011), in the **report n. 704**, proposes a performance approach to promote the construction of a quality pavement by **measuring characteristics direcly related to its performance** evaluating penalty and bonuses to be applied to a new construction work and related to the residual life.

In Italy the **Anas** IS300 structural index, represents the reference control index for the bearing structural capacity of New Constructions, whose calculation is given by a difference in deflections: IS300 = do-d300. The deductions that Anas applies on I300 in terms of penalties, measured with FWD, correspond to half of the percentage points of which the index differs with respect to the limits, considering that if the differences reach 40% up, then the work will not be acceptable, with a penalty which therefore can reach about 20% at most.
As for the thicknesses, measured with a georadar device, the penalty will correspond to three times the percentage points of which the thickness decreases with respect to the design values, admitting a maximum tolerance of 7%; if, on the other hand, the difference reaches 25%, then the DL can ask for the remake, and in case the works are awarded with a discount of more than 30%, then the maximum value of the total deduction will be raised to a maximum of 30%.
Starting from this factual data of the International studies and Italian specifications, in this thesis work, various evaluations and models were developed to see the correlations between the indices, also combined, and ESALs (residual life), SN and associated life cycle costs.

By **correlating the ESALs** (dependent variable) **with the Basin Indexes** (independent variables), in Table 75, it has been seen that the combination of them related to specific layers works very well, with the following multiple regressions involving the combinations of I3 (upper layer), I8 (lower layer) and I11 (middle layer), but also I1 (first deflection under load), with I8 and I11. The regression between ESAL and ESALSNeff and ESALSNeff600 resulting from FWD tests also works better than others.

Table 75 - Best predictive models of ESALs from Basin Indexes

Case	Dependent Variable	Independent Variables	Best Models	Adj. R-Square
1.	Esalmod	1/I3, I8, 1/I11	Esalmod = -1.23954E9 + 8.17769E11*1/I3- 2.14686E9*I8+ 3.62946E10*1/I11	**90.7%**
2.	Esalmod	I1, I8, 1/I11	Esalmod = -1.23954E9 + 5.73443E6*I1- 2.14686E9*I8 [-] + 3.62946E10*1/I11 [µm]	**90.73%**
3.	Esalmod	ESAL Sneff	Esalmod = -3.33482E6 + 0.0485346*ESAL Sneff	**95.72%**
4.	Esalmod	ESAL Sneff600	Esalmod = -5.20805E6 + 0.0450401*ESAL Sneff600	**93.66%**

Among the first two models obtained, with Adj. R-square around 91%, the second combination is certainly more immediate, as the indices I1, I8, I11 can be directly deduced from the deflections of the Falling Weight Deflectometer NDT tests.

The deflections that make up these indices are very varied and allow to have an overall assessment of the entire pavement. The first model, also has good correlations, but contains within I3 which is the equivalent module, and being a function of several variables among which also the Poisson coefficient implies more hypotheses and considerations on the individual layers that can lead to a variability of results. For this reason, it is suggested to use the combination containing I1, I8, I11.
There also good results in the regressions between Esal and EsalSNeff, with adj. R-square of 95.72%; the use of EsalSNeff is better than EsalSNeff600, but the results are still high in both cases 3 and 4.

Among the models **developed correlating the Structural Number and the Basin Indexes**, in Table 76, also in this case the best results were obtained with multiple regressions containing combinations in pairs of structural indices, such as: I3-I8; I1-I8; I2(radius of curvature) with I8, I4 (upper layer), I6 (middle layer).
At the same time, the simple regression between SN and SNeff or SNeff 600 gave excellent results. The best models obtained for the prediction of SN from Basin Indexes are:

Table 76 - Best predictive models of SN from Basin Indexes

Case	Dependent Variable	Independent Variables	Best Model	Adj. R-Square [%]
1	SN	1/I3, I8	SN [inch] = 2.90684 - 1773.21*1/I3 [Mpa] + 10.7882*I8 [-]	**99.1**
2	SN	I2, I8	SN [inch] = 0.206796 + 0.0000021348*I2 [mm] + 5.48892*I8 [-]	98.6
3	SN	I2, I4	SN [inch] = -8.79026 + 0.00000221485*I2 [mm] + 1.36074*I4 [-]	97.3
4	SN	I2, I6	SN [inch] = -2.66365 + 0.00000225665*I2 [mm] + 7.26419*I6 [-]	96.9
5	SN	I1, I8	SN [inch] = 2.90684 - 0.0124342*I1 + 10.7882*I8 [-]	**99.2**
6	SN	Sneff	SN [inch] = 1/(0.0258222 + 0.93903/Sneff [inch])	**97.8**
7	SN	Sneff600	SN [inch] = 1/(-0.00358056 + 1.06683/Sneff 600 [inch])	**98.5**

Among these, good results in terms of Adj. R-square, although all are very high, are given by the independent variable combinations of I3 with I8 and I1 with I8; once again it is certainly easier to

obtain the model that combines I1 with I8 directly from NDT tests. But the best results were combining SN (dependent variable) with SNeff or SNeff600 (independent variable), with Adj. R-square values equal to 97.8% and 98.5%.

Significant results have also been achieved in terms of **Penalty/Bonus models**, which combine the changes in the Residual Life (DLife) and in the indices (DeltaIndex) together with changes in cost, or better penalties or bonuses (DCost).
A good agreement between the model developed in this research work (in blue in the graph) and the NCHRP model (in red) has been reached (Figure 95), taking into consideration the **penalties** to be associated with the **variations of Residual Life**, where the concept that emerges is that the contractor is compensated according to the quality of a product.
From this it follows that the concept behind the **NCHRP payment system** is that the contractor's compensation is based on the expected performance difference, i.e., the Predicted Life Difference between as-designed and as-built. For the **bonuses** the best agreement between the models developed and NCHRP was reached with the model in gray. The bonuses are clearly lower than the penalties as they have a character of reward for companies that perform work with higher performance than those required by the road authority.

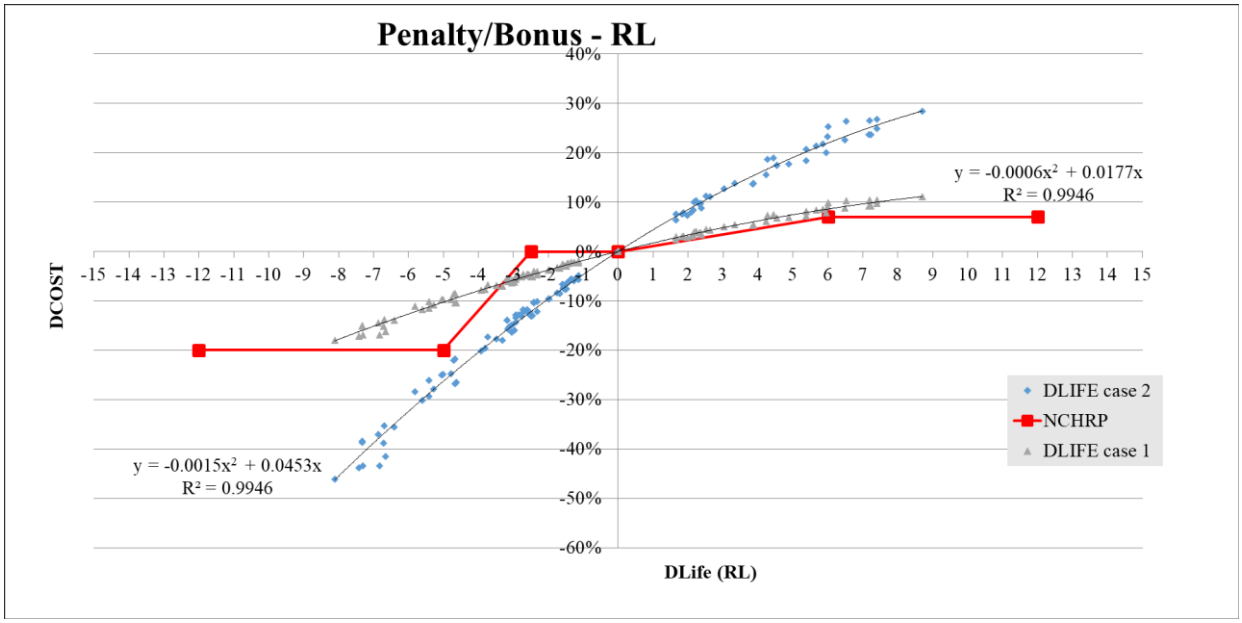

Figure 95 - P/B model developed and NCHRP performance approach

The penalties are in the negative part of the graph and the bonuses in the positive part.
In the case of penalties, 20% can be considered as the maximum applicable, whereas 10% for bonuses. The models will therefore be:

$$\textbf{Penalty} = -0.0015*RL^2 + 0.0453*RL$$
$$\textbf{Bonus} = -0.0006*RL^2 + 0.0177*RL$$

With RL=residual life.

However, from the considerations made on the **ANAS specifications**, changes can be suggested which certainly represent a major advantage for the road authority, which can therefore take greater precautions in case of costs not foreseen for future maintenance due to structural deficiencies during road paving construction. These suggestions in terms of penalty or bonus have been studied in the

new construction works, both for differences in the IS300 index, and for differences in the thickness of the AC layers, and for differences in the thickness of the subbase.

As far as the **IS300** index is concerned, several models developed in chapter 3 (paragraph 3.11) have already been seen, from which the best results and any tolerances to be considered before the possible application of penalties are deducted.
In this regard in Figure 96, therefore, a graphic solution of easy intuition has been developed and from which penalties and bonuses can be obtained when there are differences in the IS300 index. In the graph, in red, is also reported today's solution of ANAS, remembering that it does not provide bonuses but only penalties equal to half the percentage of which the index differs. The Penalty/Bonus model proposed with this research study is highlighted in black.

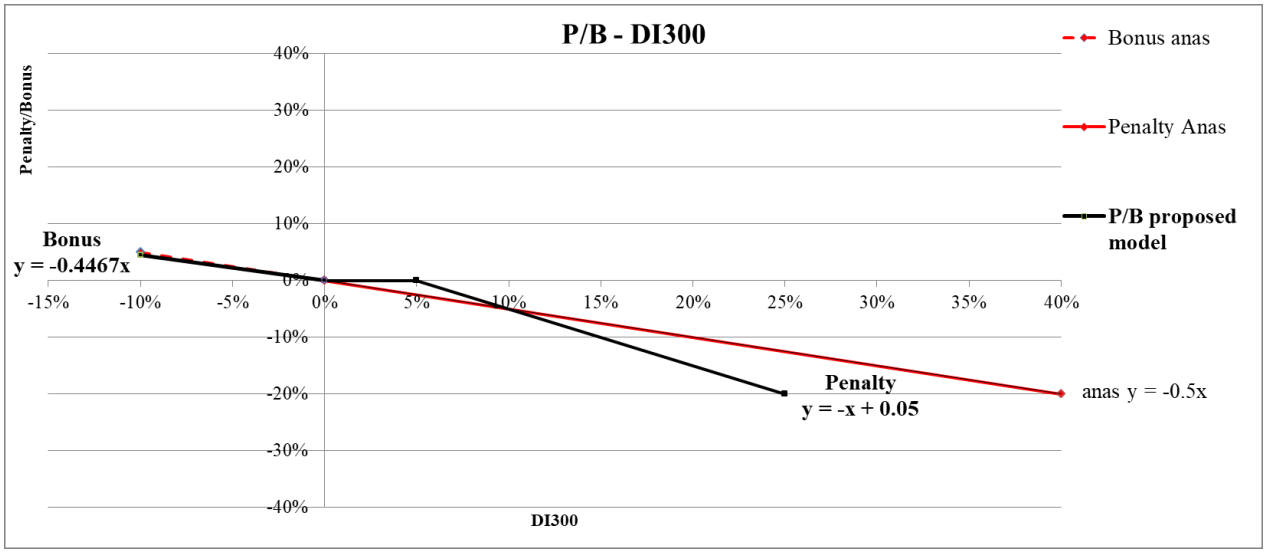

Figure 96 - Penalty/Bonus solution suggested for the Delta I300 in performance specifications

Negative index differences generate **bonuses**, vice versa differences in increase of the index generate penalties.
In terms of calculation, as regards **penalties**, a tolerance is suggested for differences in the index ranging from 0 to 5%, instead exceeding 5% penalties are applied, until the 20% of limit in the penalties. The maximum penalty that most applies with the proposed model is 20%, as for Anas, which corresponds to a maximum variation of the index of 25%.
This criterion is certainly more advantageous for the road authority that can thus be better protected when there are structural problems on the pavement built by the company. The equation of penalties will be:

$$\textbf{Penalty} = -\textbf{DI300} + 0.05$$

Therefore for the bonuses, is suggested a maximum limit of 10% in the difference of the IS300 index with the equation:

$$\textbf{Bonus} = -0.4467 * \textbf{DI300}$$

As it is possible to see, the bonuses are lower than the penalties because they are reward for companies that perform the road works with higher performance than those required by the road authority.

Regarding **differences in the thicknesses** in the construction of road pavements, **ANAS** never considering bonus, provides penalties only for the layers in AC, not making distinction between wear, binder and base. It does not provide anything for the subbase layers.

In this research study it was considered necessary not only to give suggestions on the **AC layers**, but also to provide models for the granular layers that make up the **subbases**.

In the graph in Figure 97 on the x axis there are the thickness differences, on the y axis the penalties or bonuses. The P/B proposed model is showe in black.

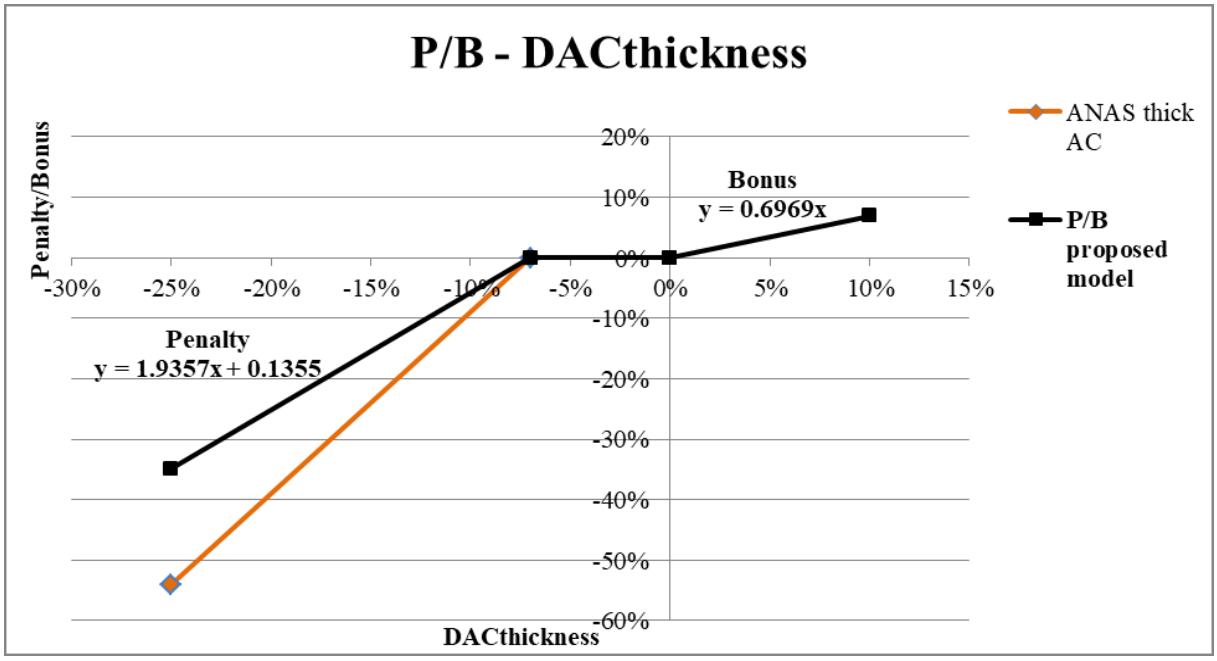

Figure 97 - Penalty/Bonus solution suggested for the Delta thickness of AC layers in performance specifications

Positive differences in the thickness generate bonuses, vice versa generate penalties.

Similarly to the previous case of DI300, **bonuses** are calculated considering maximum differences in thickness of 10%, and their equation, lower than penalties, is:

Bonus = 0.6969*DACthickness

In the case of penalties, also here as in ANAS, a tolerance of -7% of thickness variation of asphalt concrete layers was respected, beyond which penalties are applied that reach their maximum of 35% at the maximum limit of difference in negative of the thickness equal to 25%. The penalties, as well as graphically, can be obtained with the equation:

Penalty = 1.9357* DACthickness + 0.1355

For the subbase layers, in Figure 98 a bonus and penalty model was also obtained, although today ANAS does not provide it.
The construction logic is the same as the case in AC, but clearly was constructed with data on the results obtained on subbases.

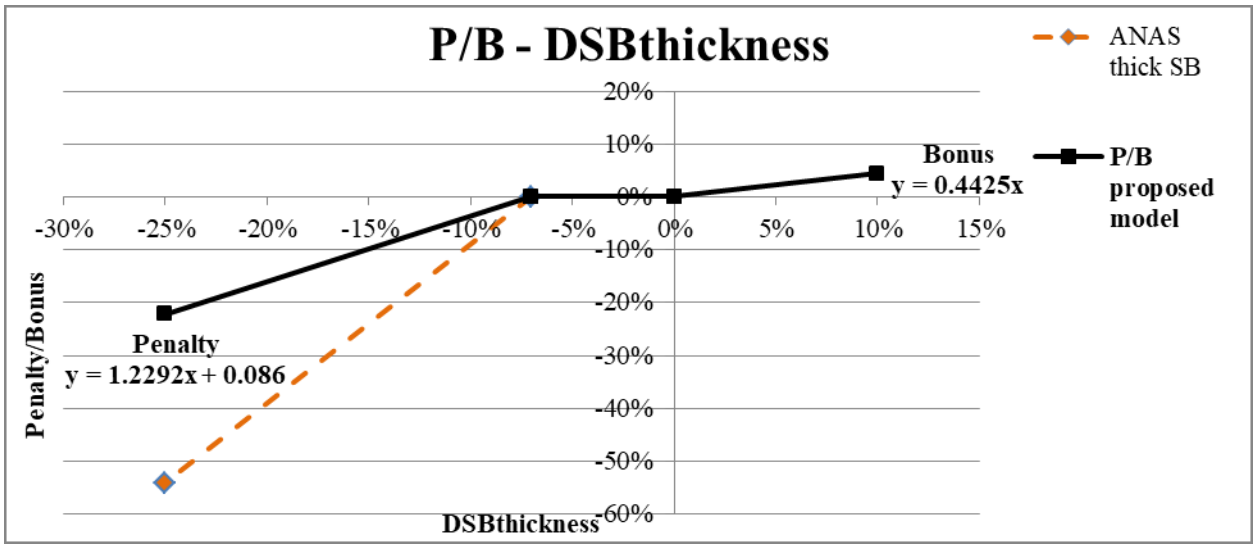

Figure 98 - Penalty/Bonus solution suggested for the Delta thickness of subbase layers in performance specifications

As previously penalties and bonuses can be obtained graphically, or alternatively calculated.
The equation to calculate the bonus is:

Bonus = 0.4425*DSBthickness

As for the penalties it was considered a tolerance from 0 to -7% of difference in the thickness of the subbase layer, and from -7% to -25% of difference in subbase thickness the penalty can be calculated as:

Penalty = 1.2292* DSBthickness + 0.086

The logic of the applied criteria with the models developed in this research study for Residual Life, IS300, AC and subbase layers, is to provide penalties commensurate with the costs that must support the road authority for maintenance that must be done if there are structural deficits under construction.

In addition, the introduction of bonuses even lower if compared to penalties, and which are not yet foreseen by Anas, has a character of economic reward for companies that perform road works with a performance surplus.

As for the **P/B models in relation to the Structural Indexes deriving from NDT tests**, many of the indexes have given significant results, but certainly combining the data deriving from the analyzes on the ESALs and the SNs, in order to suggest the inclusion of new indexes in the performance-based specifications, in addition to the existing I300 for new constructions, it's certainly important to suggest those indices which in the three cases have given a positive response.

Among the best models, once again those containing the variations of the indices I1, I3, I8, I11, turn out to be the most correlated and that also respond well in the prediction of the ESALs and the Structural Number.
It should also be remembered this time that I1 is preferred to I3 because this is less subject to interpretation elements and directly represents the deflection that is obtained under the FWD load plate.

But from the regressions obtained the results have shown that including the variations of DSNeff and DEsalSneff in the regressions with Dcost representing the Penalties/Bonuses to be applied according to the variations of the indexes we have seen how they respond very well, and with high values of Adj. R-square, and these may be better than the other indexes because they can work with any temperature, as they contain within them the procedure codified by AASHTO (1993). Therefore, among the analyzed indexes that have given excellent results, it is possible to state that the AASHTO procedure works very well and is applicable in all conditions.

Summing up the best results, in **Performance-Based Specifications**, existing penalty models may include new variations in the indices, which found highest values of Adj. R-square and a very varied application possibility in road pavements. Among these, deriving from the empirical AASHTO procedure, the following model, in Table 77, is suggested:

Table 77 - Proposal of SNeff and SNeff600 Indices to be included in performance based specifications: Penalty/Bonus models

Dependent Variable [Penalty/Bonus]	Independent Variable [Delta Indexes]	Best Models (Linear Regressions)	Adj. R-Square [%]
Dcost	DSNeff	**Dcost=9.987*DSNeff**	**97.50**
Dcost	DSNeff600	Dcost=11.346*DSNeff600	95.40

Note: For these indices, negative differences (in percentage) of the index generate penalties, vice versa generate bonuses. This can also be seen from the graphs in appendix 10.

DSNeff was preferred to DSNeff600 because showed higher Rsquare and it is not effected by the uncertainity of a double estimation of subgrade and pavement moduli. Of course, that approach is applicable only if the subgrade modulus was previously checked by diret tests (e.g. LWD) on the subgrade layer during pavement construction. If that check was not performed, DSNeff600, must be used.

Moreover**, indexes deriving directly from the deflections of FWD tests** have given also excellent results and are therefore easily obtained directly from the NDT load-bearing tests, even these are proposed to be inserted in the modern performance specifications. The results are in Table 78.

Table 78 - Proposal of I1, ISN Indices to be included in performance based specifications: Penalty/Bonus models

Dependent Variable [Penalty/Bonus]	Independent Variable [Delta Indexes]	Best Models (Linear Regressions)	Adj. R-Square [%]
Dcost	**DI1**	Dcost=-5.71578*DI1	**98.29**
Dcost	**DISN**	**Dcost=4.88*DISN**	**97.00**

Note: For I1 and I11, increasing differences in these indices generate penalties, conversely they generate bonuses. For I8 and ISN, negative differences (in percentage) of the index generate penalties, vice versa generate bonuses. This can also be seen from the graphs in appendix 10.

The inclusion of the **ISN Index** is very important because understanding a **combination of indices I1 and I8** becomes an **overall index** and that in a very simple way allows to monitor the conditions of the entire pavement. Even if it presents an Adj. R-square which is not the largest of all (DI1 has Adj. R-square = 98.29%) it is the one that is obtained in a simpler way and includes inside it indices (I1 and I8) that give information on all the road pavement and subgrade.
The formula for the calculation of ISN is:

ISN = 2.90684 - 0.0124342*I1 + 10.7882*I8 =

$$= 2.90684 - 0.0124342*d_0 + 10.7882*[(d_{900}+d_{1200})/2*d_0]$$

In the studies conducted on the specifications, various critical issues emerged, as well as important research cues that may lead more and more to an evolution as **further works and future needs** in this sense.

The design and evaluation of the road pavement has been addressed with the *AASHTO empirical method*, which has its limits, but at the same time has been fundamental since it has proved to be an immediate tool for the assessment of the structural features of the pavement and also of maintenance interventions with the overlay design procedure.
Having dealt with a comparative analysis, instead of a absolute evaluation of results, can still be considered valid, but certainly the ***Mechanistic Empirical (MEPDG) approach*** allows better to evaluate the relationships between the characteristics of the materials and volumetric properties of the AC mixes with their effects on performance.
Moreover, pavements built with **materials not included in the empirical approach** (e.g. modified bitumen, RAP, …) should show different performance relationships with initial bearing capacity derived by FWD tests that should be better evaluated by MEPDG.
Certain further investigations can be made on the **environmental aspects** and therefore the costs in terms of emissions resulting from unscheduled maintenance to restore the entire design life of the road pavements under examination: these assessments can have different impacts depending on the type of intervention, material and recovery time.

Despite these limitations, the simplicity and consistency of the empirical approach represents an added value for the understanding and transparency issues in the framework of construction contracts.

BIBLIOGRAPHY

- AASHTO Designation R 9-97, Standard Recommended Practice for Acceptance Sampling Plans for Highway Construction, *Standard Specifications for Transportation Materials and Methods of Sampling and Testing, Part I Specifications*, 24th Edition. AASHTO, Washington, D.C., 2004.
- AASHTO T 193, *Standard method of test for the California Bearing Ratio*, American Association of State Highway and Transportation Officials, January 2013.
- AASHTO T274-82*, Standard Method of Test for Resilient Modulus of Subgrade Soils.*
- AASHTO, *Guide for Design of Pavement Structures*, 1993.
- AASHTO*, Mechanistic – Empirical Pavement Design Guide. A Manual of Practice. Interim Edition,* July 2008.
- ANAS S.p.A., *Capitolato Speciale D'Appalto - Norme Tecniche per l'esecuzione del contratto Parte 2,* Coordinamento Territoriale/Direzione IT.PRL.05.21., 2016.
- ANAS S.p.A., *Capitolato Speciale D'Appalto. Norme Tecniche*, IT.CDGT.C.05.16-Rev.0-24/04/2009.
- ANAS S.p.A., *Gestione delle pavimentazioni stradali. Linee guida di progetto e norme tecniche prestazionali*, Ricerca & Innovazione – Centro Sperimentale Stradale, Novembre 2008.
- ANAS S.p.A., *Listino prezzi 2018. Nuove Costruzioni e Manutenzione Straordinaria,* Direzione Ingegneria e Verifiche, NC-MS 2018 – Rev.0, 2018.
- ASTM D 1883-16, *Standard Test Method for California Bearing Ratio (CBR) of Laboratory-Compacted Soils*, ASTM Volume 04.08 Soil and Rock (I): D421 – D5876, March 2016.
- ASTM D 422-63, *Standard Test Method for Particle-Size Analysis of Soils*, ASTM International, West Conshohocken, PA, 2007.
- ASTM D 4318-84, *Standard Test Methods for Liquid Limit, Plastic Limit, and Plasticity Index of Soils*, ASTM International, West Conshohocken, PA.
- ASTM D 6951-03, *Standard Test Method for Use of the Dynamic Cone Penetrometer in Shallow Pavement Applications*, ASTM International, West Conshohocken, PA, 2003.
- ASTM D4694-96, *Standard Test Method for Deflections with a Falling-Weight-Type Impulse Load Device.*
- ASTM D6432-11, *Standard Guide for Using the Surface Ground Penetrating Radar Method for Subsurface.*
- ASTM D854 10, *Standard test methods for specific gravity of soil solids by water pycnometer*, Annual Book of ASTM Standards, 2005.

- ASTM E2583/07, *Standard Test Method for Measuring Deflections with a Light Weight* Deflectometer *(LWD)*. West Conshohocken, PA: ASTM International.
- Austroads, *Development of Performance Contracts and Specifications - Full Report*, ISBN 0 85588 670 6, Austroads Project No. T&E.P.N.506, Austroads Publication No. AP–T25.1/03, Published by Austroads Incorporated, Sidney, 2003.
- Baltzer, S., Pratt, D., Weligamage, J., Adamsen, J., and Hildebrand, G., *Continuous bearing capacity profile of 18,000 km Australian road network in 5 months*, 24th ARRB conference proceedings, Melbourne, Australia, 2010.
- Burati, J. L., and C. S. Hughes. *Construction Quality Management for Managers*. Demonstration Project 89, Publication Number FHWA-SA-94-044. FHWA, Dec. 1993.
- Burrow, M.P.N., Chan, A.H.C. & Shein, A., Deflectometer- *based analysis of ballasted railway tracks*, In: Proceedings of The Institution of Civil Engineers Geotechnical Engineering, 160(3), 169-177, 2007.
- Cafiso S., Capace B., D'Agostino C., Delfino E., Di Graziano A., *Introduction of new systems for evaluation of ballast bearing capacity*, *BCRRA 2017* Tenth International Conference on the Bearing Capacity of Roads, Railways and Airfields, Athens, June 28/30, 2017b
- Cafiso S., Di Graziano A., D'Agostino C., Pappalardo G., Capace B., *Road Asset Management for Sustainable Development*, 2015 International Conference in Environmental Science and Sustainable Development (ICESSD 2015), Bangkok, Thailand, 25-26 October 2015.
- Cafiso, S., Capace, B., D'Agostino, C., Delfino, M., Di Graziano A., *Monitoring of railway track with light high efficiency systems*. International congress on transport infrastructure and systems 10^{th} – 12^{th} April 2017 Rome (Italy), 2017a.
- Cafiso, S., Capace, B., D'Agostino, C., Delfino, M., Di Graziano A., *Application of NDT to railway track inspection*. International Conference on Traffic and Transport Engineering, 24th – 25th November 2016, Belgrade (Serbia), 2016a.
- Cafiso, S., D'Agostino, C., Capace, B., Motta, E., Capilleri, P., *Comparison of in situ devices for the assessment of pavement subgrade stiffness*. 1st IMEKO TC4 International Workshop on Metrology for Geotechnics Benevento, Italy, March 17-18, 2016 b.
- Cai, Z., *Modelling of rail track dynamics and wheel/rail interaction*. PhD thesis, Department of Civil Engineering, Queen's University, Ontario, Canada, 1992.
- Carlson A., Folkeson L., *Sustainability and Energy Efficient Management of Roads*, ERA-NET Road – Energy, May 2014.
- *Catalogo delle Pavimentazioni Stradali, 1995.*
- Cerniglia, D., Garcia G., Kalay, S. & Prior, F., *Application of Laser Induced Ultrasound for Rail Inspection*. Railway Research Center, 2006.

- Cesolini E., Drusin S., *La capacità portante delle pavimentazioni misurata ad alto rendimento e collegata al capitolato d'appalto prestazionale*, Anas S.p.A., Centro Sperimentale Stradale – Cesano (Roma), Italy.
- Chai, G., and Roslie, N., *The Structural Response and Behavior Prediction of Subgrade Soils Using Falling Weight Deflectometer in Pavement Construction*, Proceedings, Third International Conference on Road & Airfield Pavement Technology, Beijing, China, April 1998.
- Chen, D. H., D. F. Lin, P. H. Liau, and J. Bilyeu, *A Correlation Between Dynamic Cone Penetrometer Values and Pavement Layer Moduli*, Geotechnical Testing Journal, Volume 28, Issue 1, January 2005, pp. 42–49, 2005.
- Chen, J., Hossain M., Latorella T.M., *Use of Falling Weight Deflectometer and Dynamic Cone Penetrometer in Pavement Evaluation,* Transportation Research Record, 1655, 145-151, 1999.
- CNR B.U. n. 60/78*, Norme sulle caratteristiche geometriche e di traffico delle strade urbane,* 1978.
- CNR B.U. n. 78/80, *Norme sulle caratteristiche geometriche delle strade urbane*, 1980.
- CNR UNI 10006*, Costruzione e manutenzione delle strade. Tecniche di impiego delle terre. Road construction and maintenance. Technical provisions for use soils*, June 2002.
- Corsaro G., *Compressione, compattazione e portanza di ceneri vulcaniche per il riutilizzo in ambito geotecnico e stradale*, Tesi di Laurea in Ingegneria Civile e Ambientale - Università di Catania, Relatori: Prof. Ing. Ernesto Motta, Prof. Ing. Salvatore Cafiso, Correlatori: Dott. Ing. Piera Paola Capilleri, Dott. Ing. Grazia La Cava, A.A. 2015/2016.
- Daniels, D.J., *Ground Penetrating Radar*, 2nd Edition, IET, 2004.
- Darter, M.I., Elliott, R.P., and Hall, K.T., *Revision of AASHTO Pavement Overlay Design Procedure*, Transportation Research Record 1374, p. 36–47, Transportation Research Board, Washington, DC., 1991.
- De Beer, M., *Use of dynamic cone penetrometer in the design of road structures. Geotechniques in African Environment*, Rotterdam: Balkema, 167–176, 1990.
- De Chiara, F., *Improvement of railway track diagnosis using ground penetrating radar,* (PhD Thesis). Dissertation partially developed at Laboratório Nacional de Engenharia Civil (LNEC), submitted to the University of Rome "Sapienza" for the degree of Doctor of Philosophy in Civil Engineering, May 2014.
- Decreto Legislativo 3 Aprile 2006, n. 152, *Norme in materia ambientale*, (G.U. n. 88 del 14 aprile 2006).
- Dynatest International, 1998. *ELMOD Quick Start Manual*.
- Dynatest International, *LWDmod Manual.*

- Dyson Robert G., *Strategic development and SWOT analysis at the University of Warwick*, http://dx.doi.org/10.1016/S0377-2217(03)00062-6, European Journal of Operational Research, Volume 152, Issue 3, Pages 631–640, Applications of Soft O.R. Methods, 1 February 2004
- Ehsan Kianirad, *Development and Testing of a Portable In-Situ Near-Surface Soil Characterization System*, Dissertation Presented to the Department of Civil and Environmental Engineering in partial fulfillment of the requirements for the degree of Doctor of Philosophy in the field of Geotechnical and Geo-Environmental Engineering, Northeastern University Boston, Massachusetts, April 2001.
- EN 13816: *Transportation Services. Public Service of passengers. Basic concepts, performance targets and service quality measurement,* 2002.
- Eriksen, A., Gascoyne, J., & Al-Nuaimy, W., *Improved Productivity & Reliability of Ballast Inspection using Road-Rail Multi-Channel GPR*. Preceedings of Railway Engineering. London, UK: IEEE, 2004.
- European Union Road Federation (ERF), International Road Federation (IRF), *Sustainable Roads and Optimal Mobility*, ERF Discussion paper, October 2009.
- European Union Road Federation, *European Road Statistics*, 11th edition ERF, 2013.
- European Union Road Federation, *Road Asset Management - An ERF position paper for maintaining and improving a sustainable and efficient road network*, 2014.
- Farshad Amini, *Potential Applications of Dynamic and Static Cone Penetrometers in Mdot Pavement Design and Construction*, Report FHWA/MS-DOT-RD-03-162 by Department of Civil Engineering Jackson State University In cooperation with the Mississippi Department of Transportation and the U.S. Department of Transportation Federal Highway Administration, September 2003.
- Fernandes, J., Paixão, S. Fontul, & Fortunato. E., *The Falling Weight Deflectometer: Application to Railway Substructure Evaluation*, In: Proceedings of the First International Conference on Railway Technology: Research, Development and Maintenance, Civil-Comp Press, Stirlingshire, UK, Paper 130, 2012.
- FHWA, *Long-Term Pavement Performance Program Manual for Falling Weight Deflectometer Measurements*, Publication No. FHWA-HRT-06-132, December 2006.
- FHWA, *MAP-21, the Moving Ahead for Progress in the 21st Century Act in USA*, source: http://www.fhwa.dot.gov/asset/plans.cfm, 2009.
- Fleming, P.R., M. W Frost; and C.D.F Rogers, *A Comparison of Devices for Measuring Stiffness In-situ*, Proceedings of the Fifth International Conference on Unbound Aggregate In Roads, Nottingham, United Kingdom, 2000.
- Gallagher, G.P., Leiper, Q., Williamson, R., Clark, M.R., Forde, M.C., *The application of time domain ground penetrating radar to evaluate railway track ballast*. NDT E Int. 32, 463–468, 1999.

- George K. P., *Falling Weight Deflectometer for Estimating Subgrade Resilient Moduli*, Final Report conducted by the Department of Civil Engineering, University of Mississippi, The Mississippi Department of Transportation, U. S. Department of Transportation, FHWA, October 2003.
- George, K.P., Uddin, W., *Subgrade Characterization for Highway Pavement Design*, Mississippi Department of Transportation, FHWA/MS-DOT-RD-00-131, Mississippi, 261p, 2000.
- Göbel, C., Hellmann, R., Petzold, H., *Georadar model and in-situ investigations for inspection of railway tracks*, in: Fifth International Conferention on Ground Penetrating Radar, 1994.
- Goulias D., Karimi S., *Risk Analysis for Highway Materials of flexible Pavement Structures*, Proceedings ATINER Annual Conference on Civil Engineering, Athens, GR, June 19-22, 2017.
- Goulias D., Shibeshi T., *Development of FHWA Manual incorporating NDT into the QA of Nonstructural Precast Concrete Products for Highway Construction*, Proceedings NDE/NDT for Highways and Bridges: Structural Materials Technology (SMT), Portland, OR, August 29-31, 2016.
- Grassie, S.L. & Cox, S.J., *The dynamic response of railway track with flexible sleepers to high frequency vertical excitation*. Proc Inst Mech Eng Part D; 24:77–90, 1984.
- Gudishala, R., *Development of Resilient Modulus Prediction Models for Base and Subgrade Pavement Layers from in Situ Devices Test Results*. Louisiana State University, Master of Science, 133p, Baton Rouge, 2004.
- Haas Ralph, Hudson W. Ronald with Falls Lynne Cowe, *Pavement Asset Management*, Scrivener Publishing Wiley, ISBN: 978-1-119-03870-2, May 2015.
- Hamed F. Kashani, Carlton L. Ho, William P. Clement, and Charles Oden, *Evaluating The Correlation Between Geotechnical Index and Electromagnetic Properties of Fouled Ballasted Track by Full Scale Laboratory Model*, In: TRB 2016 Annual Meeting, 2016.
- Hassan, A., T*he Effect of Material Parameters on Dynamic Cone Penetrometer Results for Fine-grained Soils and Granular Materials,* Oklahoma State University, PhD Dissertation, Stillwater, 1996.
- Hellier Charles, *Handbook of Nondestructive Evaluation*, McGraw-Hill. p. 1.1, ISBN 0-07-028121-1, 2003.
- Horak E., Emery S., *Falling Weight Deflectometer Bowl Parameters as Analysis Tool for Pavement Structural Evaluations*, 22nd ARRB Conference – Research into Practice, Canberra Australia, 2006.
- Horizon 2020, Work Programme 2014-2015, *Smart, green and integrated transport.*
- Horizon 2020, Work Programme 2016-2017, *Smart, green and integrated transport.*

- Horizon 2020, Work Programme 2018-2020, *Smart, green and integrated transport.*
- Horníček, L. & Břešťovský, P., *Using the Lightweight Falling Deflectometer for Monitoring Trial Railway Sections with Under-Ballast Geocomposites*, Published in: Railway Condition Monitoring (RCM 2014), 6th IET Conference on, 2014.
- Horvath, A Life-Cycle Analysis Model and Decision-Support Tool for Selecting Recycled Versus Virgin materials for Highway Applications, Final Report for RMRC Research Project No. 23, March 2004.
- Hossain M.S. and A.K. Apeagyei, *Evaluation of the Lightweight Deflectometer for In-Situ Determination of Pavement Layer Moduli*, Final Report VTRC 10-R. Charlottesville, VA: Virginia Transportation Research Council, 2010.
- Huang Y. H., *Pavement analysis and design*, Prentice-Hall, 815 p, 1993.
- Huang Yang H., *Pavement Analysis and Design*, Second Edition, Pearson Prentice Hall, International Edition, ISBN13: 978-0-13-272610-8, ISBN10: 0-13-272610-6, 2012.
- Hugenschmidt J., Railway track inspection using GPR, Journal of Applied Geophysics, vol. 43, n. 1-3, pp. 147-156, Mar. 2000.
- Humphrey, A., *SWOT Analysis for Management Consulting*. SRI Alumni Newsletter. SRI International. (2005): 7-8, December 2005.
- IDS Ingegneria dei sistemi, *K2 Fast Wave v. 02.00 – User manual,* Pisa, 2013.
- Isola M., Betti G., Marradi A., Tebaldi G., *Evaluation of cement treated mixtures with high percentage of reclaimed asphalt pavement*, Construction and Building Materials 48 (2013) 238–247, 2013.
- Jack, R. and Jackson, P., *Imaging attributes of railway track formation and ballast using ground probing radar*, NDT&E International, No. 32, pp. 457-462, 1999.
- Jol H. M., *Ground Penetrating Radar Theory and Applications*, 1st Edition, eBook ISBN 9780080951843, Hardcover ISBN 9780444533487, Elsevier Science, December 2008.
- Kashani, F.H.; Ho, C.L.; Clement, W.P.; Oden, C., *Evaluating The Correlation Between Geotechnical Index and Electromagnetic Properties of Fouled Ballasted Track by Full Scale Laboratory Model*, In Proceedings of the TRB 2016 Annual Meeting.
- Konur, D., Long, S., Qui, R., Elmore C. & Far-hangi H., *Track Inspection Planning and Risk Measurement Analysis*, Missouri University of Science and Technology, Engineering Management and Systems Engineering Department, Final Report Prepared for Missouri Department of Transportation, Project TR201409, Report cmr15-005, 2015.
- Kopac, P. A. *Performance-Related Quality Assurance Specifications*. Presented at the ASCE Convention, Dallas, Tex., Oct. 1993.

- Lambert J. P., Fleming P. R., Frost M. W., *The assessment of coarse granular materials for performance based pavement foundation design*, International Journal of Pavement Engineering, Vol 9, No3, pp 203-214, 2008.
- Lee, W., Lee, J., Henderson, C., Taylor, H. F. & James, R., Lee, C. E. et al., *Railroad bridge instrumentation with fiber-optic sensors*. Applied Optics, 38(7), 1110-1114. March 1, 1999.
- Local Government Victoria,. *Local Government Asset Management Better Practice Guide*, http://www.delwp.vic.gov.au, 2015.
- Losa M., Bacci R., Leandri P*., A Statistical Model for Prediction of Critical Strains in Pavements from Deflection Measurements,* Road Materials and Pavement Design, 9:sup1, 373-396, DOI: 10.1080/14680629.2008.9690175, 2008.
- Losert, Robert, (March 31, 2009), *Solution for NDT Inspection*, NDT Magazine. Retrieved December 15, 2010.
- Louis, Cartz, *Nondestructive Testing,* A S M International, ISBN 978-0-87170-517-4, 1995.
- Mallela, J. & George, K.P., *Three-Dimensional Dynamic Response Model for Rigid Pavements*, Transportation Research Record No. 1448, Transportation Research Board, Washington, D.C. 1994.
- Mallick Rajib B., El-Korchi Tahar, Pavement Engineering: Principles and Practice. Second Edition, CRC Press - Taylor & Francis Group, International Standard Book Number-13: 978-1-4398-7036-5 (eBook - PDF), 2013.
- Marradi A., G. Betti, C. Sangiorgi, and C. Lantieri, *Comparing light weight deflectometers to standardize their use in the compaction control*, Proceedings of the 5th International Conference 'Bituminous Mixtures and Pavements', Thessaloniki, Greece: Aristotle University of Thessaloniki, 2011.
- Marradi A., Pinori U., Betti G., *Subgrade and foundation dynamic performance evaluation by means of light weight deflectometer tests*, TRB 2014 Annual Meeting.
- Minnesota Department of Transportation, *User Guide to the Dynamic Cone Penetrometer*, http://www.dot.state.mn.us/materials/researchdocs/User_Guide.pdf
- Mohammad, L.N., Herath, A., Abu-Farsakh, M.Y., Gaspard, K., Gudishala, R., *Prediction of Resilient Modulus of Cohesive Subgrade Soils from Dynamic Cone Penetrometer Test Parameters*, Journal of Materials in Civil Engineering, 19(11), 986- 992, 2007.
- Nazzal M.D., M.Y. Abu-Farsakh, K. Alshibli, and L. Mohammad, *Evaluating the light falling weight deflectometer device for in situ measurement of elastic modulus of pavement layers*, Transportation Research Record: Journal of the Transportation Research Board, No. 2016, pp. 13–22. Washington, DC: Transportation Research Board of the National Academies, 2007.
- NCHRP 1-37 A 2004, *Guide for Mechanistic – Empirical Design of new and rehabilitated pavement structures*, 2004.

- NCHRP Report 704, *A Performance-Related Specification for Hot-Mixed Asphalt*, TRB, Washington D.C., 2011.
- NCHRP, Report *626: NDT Technology for Quality Assurance of HMA Pavement Construction,* Research sponsored by the American Association of State Highway and Transportation Officials in cooperation with the Federal Highway Administration, Transportation Research Board, Washington D.C., 2009.
- NDT, C., *Rail Inspection*, Retrieved from NDT Resource Center, 2013. http://www.ndted.org/AboutNDT/SelectedApplications/RailInspection/RailInspection.htm.
- NDT, H., *A document outlining the emergence of the eddy current NDT inspection method as an important part of rail maintenance and safety*, 2014.
- Neupane, M., Parsons, R.L. & Han, J., *Rapid estimation of fouled ballast material properties.* Transportation Research Board of the National Accademy, Washington DC, Annual Meeting 2016.
- *Nuovo Codice della Strada, 1992.*
- Olhoeft, G. R., and Selig, E. T., *Ground penetrating radar evaluation of railroad track substructure conditions*. Proc. Of the 9th Int'l Conf. on Ground Penetrating Radar, Santa Barbara, CA, April, S. K. Koppenjan and H. Lee, eds., Proc. of SPIE, vol. 4758, p. 48-53, 2002.
- Osita, Christian; Onyebuchi, Idoko; Justina, Nzekwe, *Organization's stability and productivity: the role of SWOT analysis*, International Journal of Innovative and Applied Research (2014): 23–32, January 31, 2014.
- Pajewski L., Benedetto A., Loizos A., Slob E., Tosti F., *Civil Engineering Applications of Ground Penetrating Radar: Research Perspectives in COST Action TU1208*, Geophysical Research Abstracts Vol. 15, EGU2013-13941, 2013.
- Pandey B.B., Srinivasa K.R., Sudhakar R.K., *Regression Models for Estimation of In Situ Subgrade Moduli from DCP Tests*, Indian Highways, 5-19, 2003.
- PIARC, *Asset Management Practice*, Technical Committee C4.1 Management of road infrastructure assets, Paris, 2008.
- Profillidis V. A., *Railway Management and Engineering: Fourth Edition*, London, UK: Ashgate, 2014.
- Saaranketo T., *Electrical properties of road materials and subgrade soils and the use of ground penetrating radar in traffic infrastructure surveys* (PhD Thesis). University of Oulu, 2006.
- Saarenketo T., *Electrical properties of water in clay and silty soils*, Journal of Applied Geophysics 40(1):73-88, DOI 10.1016/S0926-9851(98)00017-2, October 1998.
- Sanfilippo M., *Caratterizzazione in sito di ceneri vulcaniche stabilizzate a cemento per sottofondi stradale,* Tesi di Laurea in Ingegneria Civile e Ambientale - Università di

Catania, Relatore: Prof. Ing. Salvatore Cafiso, Correlatori: Dott.ssa Ing. Brunella Capace, Dott. Ing. Carmelo D'Agostino, Dott. Ing. Emanuele Delfino, A.A. 2016/2017.

- Santagata F. A., *Strade. Teoria e Tecnica delle costruzioni. Progettazione – Costruzione, (Vol. 1 – Vol. 2)*, Pearson Italia – Milano, Torino, ISBN: 8891903043, 9788891903044, 2016.
- Seed, S.B., Alavi, S.H., Ott, W.C., Mikhail, M., and Mactutis, J.A., *Evaluation of Laboratory Determined and Nondestructive Test Based Resilient Modulus Values from WesTrack Experiment*, Nondestructive Testing of Pavements and Backcalculation of Moduli: Third Volume, ASTM STP 1375.
- Selig, E. T. and Waters, J. M., *Track Geotechnology and Substructure Management*. Thomas Telford Services Ltd., London, 1994.
- Selig, E. T., Hyslip, J. P., Olhoeft, G. R., and Smith, Stan, *Ground penetrating radar for track substructure condition assessment.* Proc. Of Implementation of Heavy Haul Technology for Network Efficiency, Dallas, TX, May, p. 6.27-6.33, 2003.
- Sharpe, P.C. & Govan, R., *The use of Falling Weight Deflectometer to Assess the Suitability of Routes for Upgrading*, In: Proceedings of the Second International Conference on Railway Technology: Research, Development and Maintenance, Civil-Comp Press, Stirlingshire, UK, Paper 134, 2014.
- Shell Bitumen, *Bisar 3.0 User Manual.*
- Siekmeier, J., Pinta, C., Merth, S., Jensen, J., Davich, P., Camargo, F., Beyer, M., *Using the Dynamic Cone Penetrometer and Light Weight Deflectometer for Construction Quality Assurance*. Minnesota Department of Transportation, MN/RC 2009-12, Minnesota, 244p.
- Solanki, U. J., Gundaliya P. J., Barasara M. D., *A Study on FWD Deflection Bowl Parameter to Assess Structural Condition of Flexible Pavement,* 2016.
- Statgraphics*, Centurion XVI User Manual*, 2009.
- Sundquist H., Byggande, *Drift och Underhåll av Järnvägsbanor*, TRITA-BKN, Rapport 57, KTH, Stockholm 2000 (Compendium in Swedish).
- Sussmann T. R., Ebersöhn W., Selig E. T., *Fundamental Nonlinear Track Load-Deflection Behavior for Condition Evaluation*, Transportation Research Record 1742, Paper No. 01-2916, 2001.
- Sussmann, T.R., Selig, E.T. & Hyslip, J.P., *Railway track condition indicators from ground penetrating radar*. NDT E Int. 36, 157–167, 2003
- Timoshenko S., *Method of analysis of statistical and dynamical stresses in rail*. In: Proceedings of second international congress for applied mechanics, p. 407–18. Zurich, 1926.
- Tranchina G., *Riutilizzo di ceneri vulcaniche in ambito geotecnico-stradale mediante stabilizzazione a cemento*, Tesi di Laurea in Ingegneria Civile e Ambientale - Università di

Catania, *Relatori:* Prof. Ing. Ernesto Motta, Prof. Ing. Salvatore Cafiso, *Correlatori:* Dott. Ing. Piera Paola Capilleri, Dott. Ing. Grazia La Cava, A.A. 2015/2016.

- Transportation Research Circular E-C074, *Glossary of Highway Quality Assurance Terms*, Transportation Research Board, Washington D.C., May 2005.
- Transportation, C. B., *Connecticut Railroad Bridge Management Program*, 2012.
- Ullidtz P. *Modelling flexible pavement response and performance*, Copenhagen: Polyteknisk Forlag; 1998.
- UNI EN 1097-1, *Determinazione della resistenza all'usura (Micro-Deval)*, 2011.
- UNI EN 13286-47, *Miscele non legate e legate con leganti idraulici. Parte 47: Metodo di prova per la determinazione dell'indice di portanza immediata e del rigonfiamento,* 2012.
- Uz V. E., Saltan M., İ. Gokalp, *Comparison of DCP, CBR, and RLT Test Results for Granular Pavement Materials and Subgrade with Structural Perspective*, International Symposium Non-Destructive Testing in Civil Engineering (NDT-CE), Berlin, 15-17 September 2015.
- Uzarski, D.R., Brown, D.G., Harris, R.W. & Plotkin, D.E., *Maintenance Management of U.S. Army Railroad Networks-the RAILER System: Detailed Track Inspection Manual*. Champaign, IL: US Army Corps of Engineers; Construction Engineering Research Laboratories, 1993.
- Van Dam Thomas J., Harvey John T., Muench Stephen T., Smith Kurt D., Snyder Mark B., Al-Qadi Imad L., Ozer Hasan, Meijer Joep, V. Ram Prashant, R. Roesier Jeffery, Kendall Alissa, *Towards Sustainable Pavement Systems: A Reference Document*, FHWA-HIF-15-002, January 2015.
- Van Deusan, D.A., Lenngren, C.A., and Newcomb, D.E., *A Comparison of Laboratory and Field Subgrade Moduli at the Minnesota Road Research Project, Nondestructive Testing of Pavements and Backcalculation of Moduli*, ASTM STP 1198, H.L. Von Quintus et al., eds., ASTM, 1994.
- Varrica R., *Caratterizzazione di laboratorio per la stabilizzazione a cemento delle ceneri vulcaniche dell'Etna,* Tesi di Laurea in Ingegneria Civile e Ambientale - Università di Catania, Relatore: Prof. Ing. Salvatore Damiano Cafiso, Correlatori: Dott. Ing. Emanuele Delfino, Dott. Ing. Piera Paola Capilleri, A.A. 2015/2016.
- Volkan E Uz and M Saltan Granüler Yol Tabakalarının Yerinde Değerlendirme Yöntemleri, *Dinamik Koni Penetrometre (DCP) Testi*, SDU International Technologic Science, Vol 4 No 2, pp 70-88, 2012.
- Volkan E Uz, *Investigating the parameters that affect permanent deformation (rutting) in chip-sealed pavements*, Phd Thesis, Süleyman Demirel University, 207 p., 2012.
- Warsame A., *Framework for Quality Improvement of Infrastructure Projects*, Journal of Civil Engineering and Architecture, ISSN 1934-7359, Volume 7, No. 12 (Serial No. 73), pp. 1529-1539, USA, Dec. 2013.

- Webster, S. L., Grau, R. H., and Williams, T. P., *Description and Application of Dual Mass Dynamic Cone Penetrometer*, Report GL-92-3, Department of the Army, Washington, DC, pp 48., May 1992.
- Willenbrock, J. H., *Statistical Quality Control of Highway Construction*, Volume 2. FHWA, Jan. 1976.
- Witczak, M., Qi, X. and Mirza, M.W., *Use of Nonlinear Subgrade Modulus in AASHTO Design Procedure*, ASCE Journal of Transportation Engineering, Vol. 121, No. 3, 1995, pp. 273-282.
- World Commission on Environment and Development, *Our Common Future*, ISBN 019282080X, Oxford University press, 1987.
- Yohannes B., Tan D., Khazanovich L., Hill K. M., *Mechanistic modelling of tests of unbound granular materials*, International Journal of Pavement Engineering, Vol 15 No 7, pp 584-598, 2014.

APPENDIX 1

EQUATION FOR THE TRANSFORMATION OF ESAL IN TRAFFIC

The graphs below are related to the calculation of the transformation coefficient from Esal to Traffic related to different road types. Each graph contains the equation for each road, where y is the equation of the transformation coefficient of Esal in traffic, and x is the Structural Number.

1 – Road Type: Autostrade extraurbane

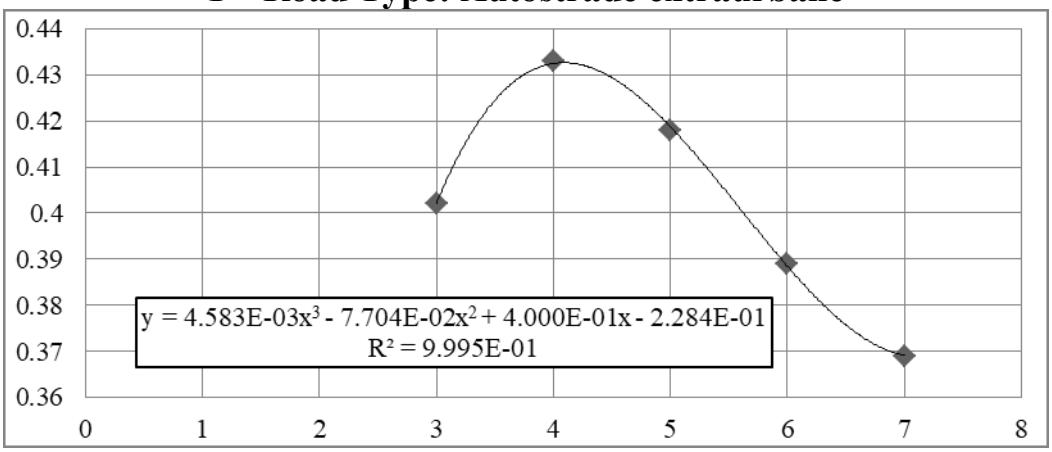

2 – Road Type: Autostrade urbane

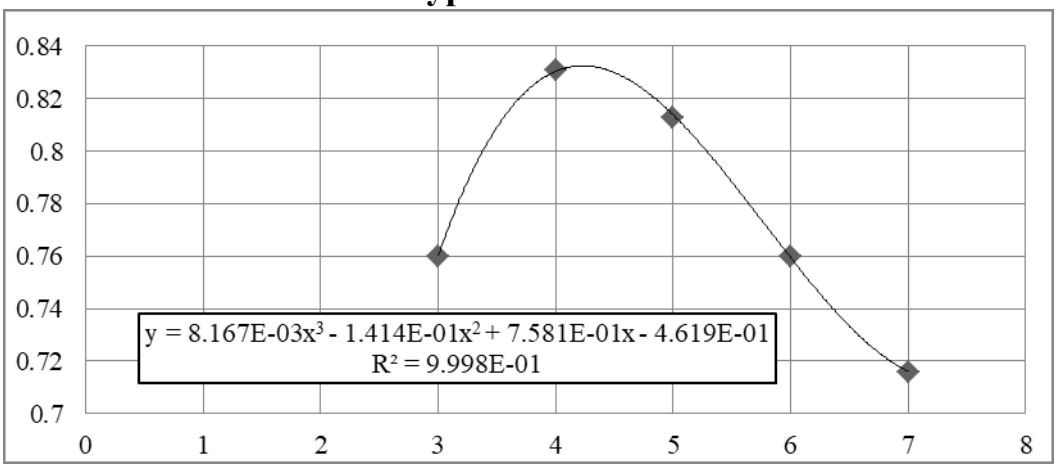

3 – Road Type: Strade extraurbane principali e secondarie a forte traffico

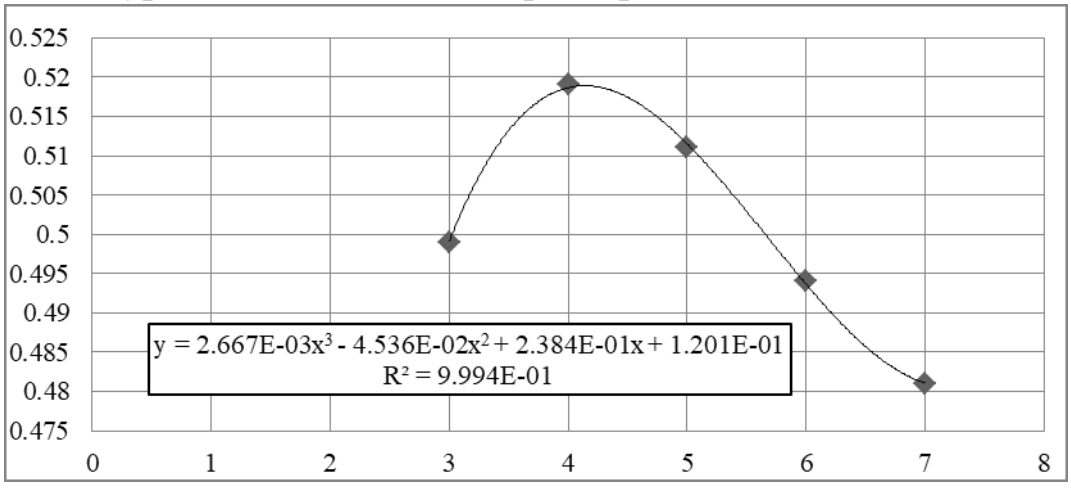

4 – Road Type: Strade extraurbane secondarie ordinarie

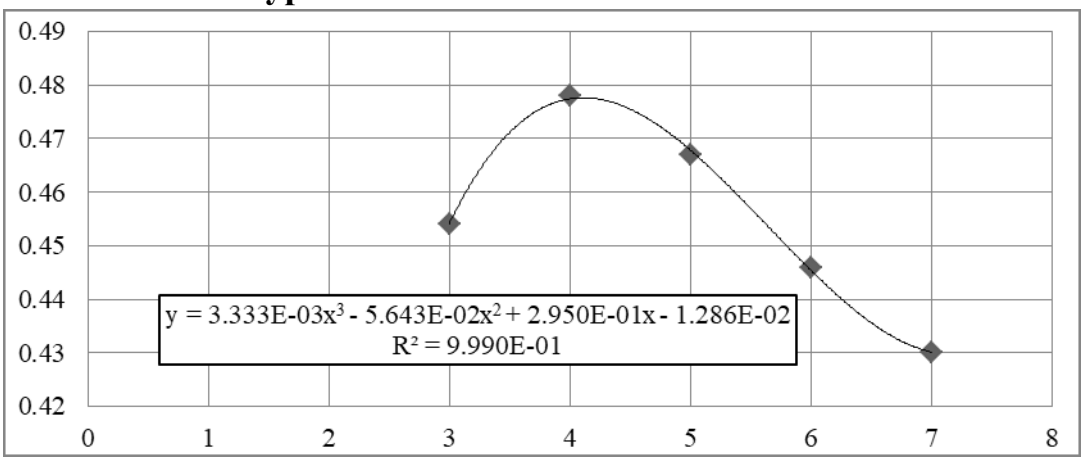

5 – Road Type: Strade extraurbane secondarie turistiche

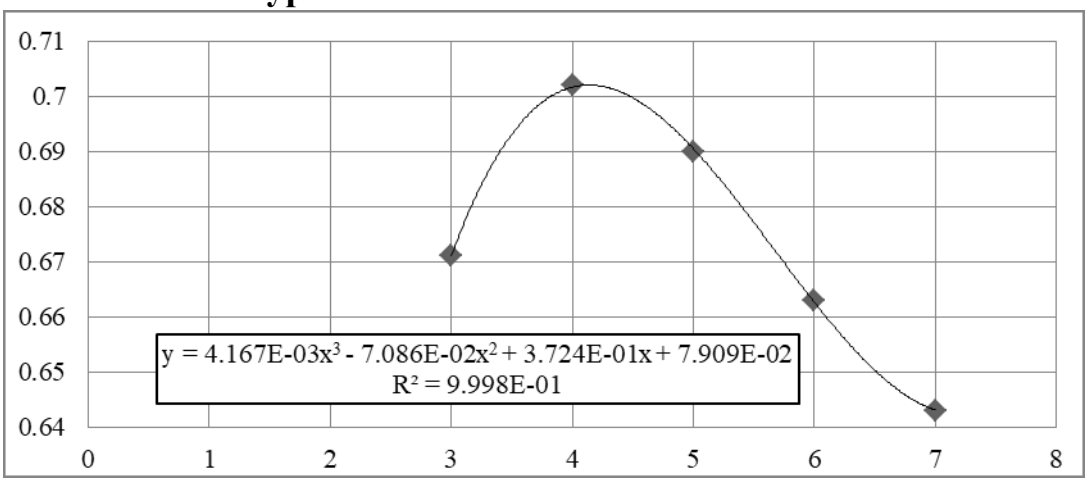

6 – Road Type: Strade urbane di scorrimento

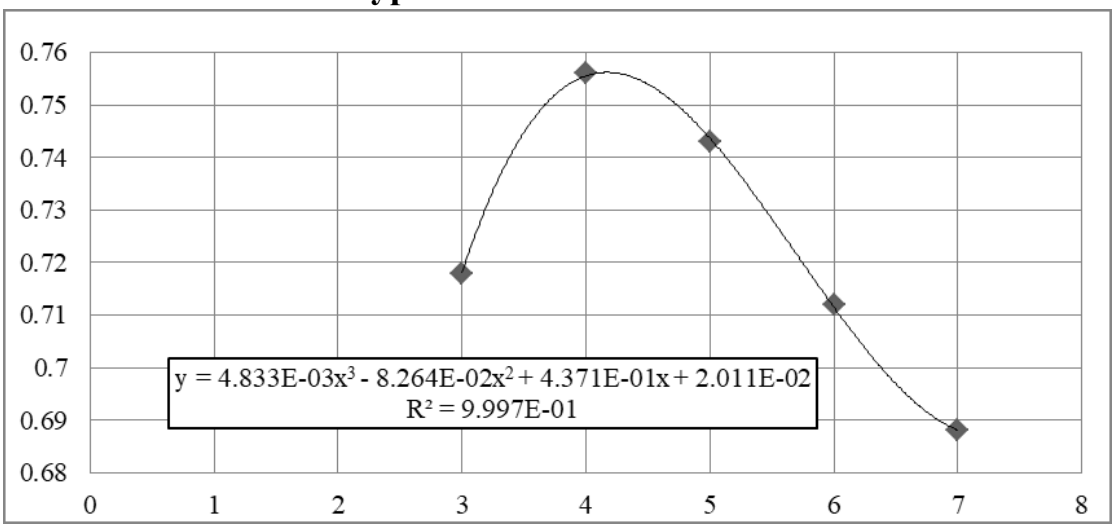

7 – Road Type: Strade urbane di quartiere e locali

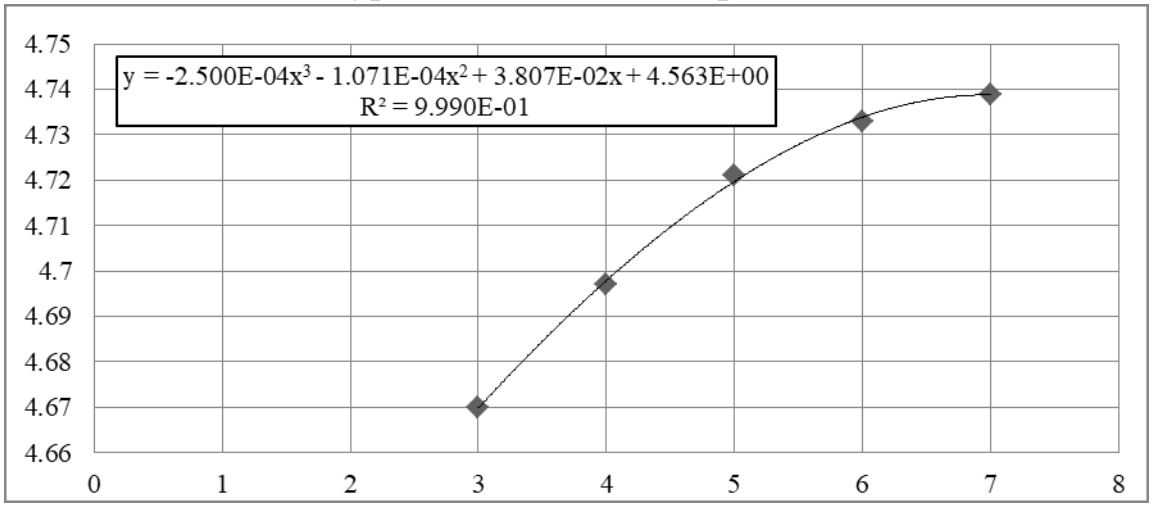

The coefficients are summarized in the following table, where y is the equation of the transformation coefficient of Esal in traffic, and x is the Structural Number. Just multiply the Esal by the coefficient y and it is possible to derive the traffic.

Equation for the transformation of Esal in traffic

Id	Type of road	PSI	Coefficient of transformation equation
1	Autostrade extraurbane	3	$y = 4.583 \cdot 10^{-3} \cdot x^3 - 7.704 \cdot 10^{-2} \cdot x^2 + 4 \cdot 10^{-1} \cdot x - 2.284 \cdot 10^{-1}$
2	Autostrade urbane	3	$y = 8.167 \cdot 10^{-3} \cdot x^3 - 1.414 \cdot 10^{-1} \cdot x^2 + 7.581 \cdot 10^{-1} \cdot x - 4.619 \cdot 10^{-1}$
3	Extraurbane principali e secondarie a forte traffico	2.5	$y = 2.667 \cdot 10^{-3} \cdot x^3 - 4.536 \cdot 10^{-2} \cdot x^2 + 2.384 \cdot 10^{-1} \cdot x + 1.201 \cdot 10^{-1}$
4	Extraurbane secondarie ordinarie	2.5	$y = 3.333 \cdot 10^{-3} \cdot x^3 - 5.643 \cdot 10^{-2} \cdot x^2 + 2.950 \cdot 10^{-1} \cdot x - 1.286 \cdot 10^{-2}$
5	Extraurbane secondarie turistiche	2.5	$y = 4.167 \cdot 10^{-3} \cdot x^3 - 7.086 \cdot 10^{-2} \cdot x^2 + 3.724 \cdot 10^{-1} \cdot x + 7.909 \cdot 10^{-2}$
6	Urbane di scorrimento	2.5	$y = 4.833 \cdot 10^{-3} \cdot x^3 - 8.264 \cdot 10^{-2} \cdot x^2 + 4.371 \cdot 10^{-1} \cdot x - 2.011 \cdot 10^{-2}$
7	Urbane di quartiere	2	$y = -2.50 \cdot 10^{-4} \cdot x^3 - 1.071 \cdot 10^{-4} \cdot x^2 + 3.807 \cdot 10^{-2} \cdot x + 4.563$

Having all the data and elements to do the calculations, trying different combinations of a_i have been found the ones that are better and that allow to obtain a traffic as close as possible to that of the catalog. All the flexible pavement in the catalog, since they depend on traffic, have been grouped according to the type of traffic (very heavy, heavy, medium, low), also distinguishing the cases of packages with and without foundation.

APPENDIX 2

CALCULATION OF TRAFFIC AND LAYER COEFFICIENTS

This appendix contains the details of the AASHTO traffic calculations and the coefficient layers with the most suitable solutions compared to the catalog traffic.

The following are the input data used according to the type of road, the reliability, the PSI and all the parameters that are related and that are a fundamental part for the calculation of the ESAL, the traffic and the Structural Number.

Subsequently, the tables containing all solutions of the Italian Pavement Catalog are shown, with the results of the layer coefficients, the Structural Number, the Esal and the traffic. The tables are divided for traffic type: PP=very heavy, P=heavy, M=medium, L=low. Two types of combinations of layer coefficients a_i were chosen:

1) $a_1 = 0.43$, $a_2 = 0.26$, $a_3 = 0.12$ in cases of very heavy and heavy traffic;
2) $a_1 = 0.41$, $a_2 = 0.24$, $a_3 = 0.11$ in cases of medium and low traffic;

Input Data: Reliability R, PSI, Z_R, S_0

Tipo di strada	Affidabilità (%)	PSI
1) Autostrade extraurbane	90	3
2) Autostrade urbane	95	3
3) Strade extraurbane principali e secondarie a forte traffico	90	2.5
4) Strade extraurbane secondarie – ordinarie	85	2.5
5) Strade extraurbane secondarie – turistiche	80	2.5
6) Strade urbane di scorrimento	95	2.5
7) Strade urbane di quartiere e locali	90	2
8) Corsie preferenziali	95	2.5

$S_0 = 0.4$

R (%)	50	60	70	75	80	85	90	92	95	98	99	99,9
Z_R	0,000	-0,253	-0,524	-0,674	-0,841	-1,037	-1,282	-1,405	-1,645	-2,054	-2,327	-3,090

Solutions for all Roads of the Italian Catalog of Road Pavements

Cases with foundation

Road Type	Traffic Type	d1	d2	d3	Mr [N/mm2]	Tc	ZrSo	DPSI	a1	a2	m2	a3	m3	SN	ESALs	Taashto
1	PP	13	28	15	90	2.50E+07	-0.5128	1.2	0.43	0.26	1	0.12	1	14.67	58,386,127	2.31E+07
1	PP	13	32	15	90	4.50E+07	-0.5128	1.2	0.43	0.26	1	0.12	1	15.71	95,518,987	3.66E+07
2	PP	13	16	15	90	2.50E+07	-0.658	1.2	0.43	0.26	1	0.12	1	11.55	8,813,397	7.31E+06
3	PP	11	23	15	90	2.50E+07	-0.5128	1.7	0.43	0.26	1	0.12	1	12.51	39,969,237	2.05E+07
6	PP	11	25	15	90	2.50E+07	-0.658	1.7	0.43	0.26	1	0.12	1	13.03	38,073,628	2.82E+07

Road Type	Traffic Type	d1	d2	d3	Mr [N/mm2]	Tc	ZrSo	DPSI	a1	a2	m2	a3	m3	SN	ESALs	Taashto
1	P	13	22	15	90	1.00E+07	-0.5128	1.2	0.43	0.26	1	0.12	1	13.11	27,176,945	1.13E+07
2	P	13	21	15	90	1.00E+07	-0.658	1.2	0.43	0.26	1	0.12	1	12.85	17,079,131	1.39E+07
3	P	11	18	15	90	1.00E+07	-0.5128	1.7	0.43	0.26	1	0.12	1	11.21	19,005,631	9.84E+06
4	P	11	17	15	90	1.00E+07	-0.4148	1.7	0.43	0.26	1	0.12	1	10.95	20,413,504	9.74E+06
4	P	11	22	35	30	1.00E+07	-0.4148	1.7	0.43	0.26	1	0.12	1	14.65	12,209,822	5.51E+06
6	P	11	20	15	90	1.00E+07	-0.658	1.7	0.43	0.26	1	0.12	1	11.73	18,412,085	1.39E+07

Road Type	Traffic Type	d1	d2	d3	Mr [N/mm2]	Tc	ZrSo	DPSI	a1	a2	m2	a3	m3	SN	ESALs	Taashto
2	M	13	16	15	90	4.00E+06	-0.658	1.2	0.41	0.24	1	0.11	1	10.82	6,026,153	5.02E+06
3	M	11	14	15	90	4.00E+06	-0.5128	1.7	0.41	0.24	1	0.11	1	9.52	6,687,742	3.46E+06
4	M	11	13	15	90	4.00E+06	-0.4148	1.7	0.41	0.24	1	0.11	1	9.28	7,155,166	3.39E+06
4	M	11	17	35	30	4.00E+06	-0.4148	1.7	0.41	0.24	1	0.11	1	12.44	3,766,078	1.77E+06
5	M	11	10	15	90	4.00E+06	-0.3364	1.7	0.41	0.24	1	0.11	1	8.56	5,227,777	3.60E+06
5	M	11	14	35	30	4.00E+06	-0.3364	1.7	0.41	0.24	1	0.11	1	11.72	3,001,126	2.10E+06
6	M	11	15	15	90	4.00E+06	-0.658	1.7	0.41	0.24	1	0.11	1	9.76	5,591,107	4.21E+06
7	M	10	8	15	90	4.00E+06	-0.5128	2.2	0.41	0.24	1	0.11	1	7.67	2,222,196	1.04E+07
7	M	10	9	35	30	4.00E+06	-0.5128	2.2	0.41	0.24	1	0.11	1	10.11	1,124,431	5.28E+06

Road Type	Traffic Type	d1	d2	d3	Mr [N/mm2]	Tc	ZrSo	DPSI	a1	a2	m2	a3	m3	SN	ESALs	Taashto
4	L	9	8	15	90	4.00E+05	-0.4148	1.7	0.41	0.24	1	0.11	1	7.26	1,613,370	7.21E+05
4	L	9	12	15	90	1.50E+06	-0.4148	1.7	0.41	0.24	1	0.11	1	8.22	3,413,070	1.58E+06
4	L	9	9	35	30	4.00E+05	-0.4148	1.7	0.41	0.24	1	0.11	1	9.7	736,262	3.51E+05
4	L	9	15	35	30	1.50E+06	-0.4148	1.7	0.41	0.24	1	0.11	1	11.14	1,786,561	8.52E+05
5	L	9	8	15	90	4.00E+05	-0.3364	1.7	0.41	0.24	1	0.11	1	7.26	1,932,564	1.28E+06
5	L	9	10	15	90	1.50E+06	-0.3364	1.7	0.41	0.24	1	0.11	1	7.74	2,842,426	1.92E+06
5	L	9	8	35	30	4.00E+05	-0.3364	1.7	0.41	0.24	1	0.11	1	9.46	754,595	5.27E+05
5	L	9	12	25	30	1.50E+06	-0.3364	1.7	0.41	0.24	1	0.11	1	9.32	688,070	4.80E+05
6	L	9	13	15	90	1.50E+06	-0.658	1.7	0.41	0.24	1	0.11	1	8.46	2,321,189	1.71E+06
7	L	12	0	15	90	4.00E+06	-0.5128	2.2	0.41	0	0	0.11	1	6.57	811,548	3.78E+06
7	L	9	8	15	90	1.50E+06	-0.5128	2.2	0.41	0.24	1	0.11	1	7.26	1,549,851	7.23E+06
7	L	12	0	35	30	4.00E+06	-0.5128	2.2	0.41	0	0	0.11	1	8.77	424,351	1.99E+06
7	L	9	8	35	30	1.50E+06	-0.5128	2.2	0.41	0.24	1	0.11	1	9.46	710,233	3.33E+06

Cases without foundation

Road Type	Traffic Type	d1	d2	d3	Mr [N/mm2]	Tc	ZrSo	DPSI	a1	a2	m2	a3	m3	SN	ESALs	Taashto
1	PP	13	25	0	150	2.50E+07	-0.5128	1.2	0.43	0.26	1	0	0	12.09	53,128,689	2.25E+07
1	PP	13	29	0	150	4.50E+07	-0.5128	1.2	0.43	0.26	1	0	0	13.13	89,789,484	3.71E+07
2	PP	13	25	0	150	2.50E+07	-0.658	1.2	0.43	0.26	1	0	0	12.09	38,030,243	3.13E+07
3	PP	11	22	0	150	2.50E+07	-0.5128	1.7	0.43	0.26	1	0	0	10.45	39,375,085	2.04E+07
6	PP	11	23	0	150	2.50E+07	-0.658	1.7	0.43	0.26	1	0	0	10.71	33,020,948	2.50E+07

Road Type	Traffic Type	d1	d2	d3	Mr [N/mm2]	Tc	ZrSo	DPSI	a1	a2	m2	a3	m3	SN	ESALs	Taashto
1	P	13	19	0	150	1.00E+07	-0.5128	1.2	0.43	0.26	1	0	0	10.53	23,623,763	1.02E+07
2	P	13	19	0	150	1.00E+07	-0.658	1.2	0.43	0.26	1	0	0	10.53	16,910,213	1.41E+07
3	P	11	17	0	150	1.00E+07	-0.5128	1.7	0.43	0.26	1	0	0	9.15	17,122,119	8.82E+06
4	P	11	16	0	150	1.00E+07	-0.4148	1.7	0.43	0.26	1	0	0	8.89	17,979,265	8.47E+06
6	P	11	18	0	150	1.00E+07	-0.658	1.7	0.43	0.26	1	0	0	9.41	14,570,036	1.09E+07

Road Type	Traffic Type	d1	d2	d3	Mr [N/mm2]	Tc	ZrSo	DPSI	a1	a2	m2	a3	m3	SN	ESALs	Taashto
2	M	13	14	0	150	4.00E+06	-0.658	1.2	0.41	0.24	1	0	0	8.69	6,038,768	4.85E+06
3	M	11	13	0	150	4.00E+06	-0.5128	1.7	0.41	0.24	1	0	0	7.63	5,681,899	2.84E+06
4	M	11	12	0	150	4.00E+06	-0.4148	1.7	0.41	0.24	1	0	0	7.39	5,872,865	2.64E+06
5	M	11	10	0	150	4.00E+06	-0.3364	1.7	0.41	0.24	1	0	0	6.91	4,694,812	3.06E+06
6	M	11	14	0	150	4.00E+06	-0.658	1.7	0.41	0.24	1	0	0	7.87	4,902,568	3.55E+06
7	M	10	8	0	150	4.00E+06	-0.5128	2.2	0.41	0.24	1	0	0	6.02	1,520,377	7.07E+06

Road Type	Traffic Type	d1	d2	d3	Mr [N/mm2]	Tc	ZrSo	DPSI	a1	a2	m2	a3	m3	SN	ESALs	Taashto
4	L	9	8	0	150	4.00E+05	-0.4148	1.7	0.41	0.24	1	0	0	5.61	1,122,137	4.48E+05
4	L	9	11	0	150	1.50E+06	-0.4148	1.7	0.41	0.24	1	0	0	6.33	2,312,978	9.79E+05
5	L	9	8	0	150	4.00E+05	-0.3364	1.7	0.41	0.24	1	0	0	5.61	1,344,144	8.08E+05
5	L	9	10	0	150	1.50E+06	-0.3364	1.7	0.41	0.24	1	0	0	6.09	2,196,686	1.37E+06
6	L	9	12	0	150	1.50E+06	-0.658	1.7	0.41	0.24	1	0	0	6.57	1,652,531	1.13E+06
7	L	12	0	0	150	4.00E+06	-0.5128	2.2	0.41			0	0	4.92	436,584	2.02E+06
7	L	9	8	0	150	1.50E+06	-0.5128	2.2	0.41	0.24	1	0	0	5.61	976,456	4.53E+06

Where: d1=thickness of wear and binder [cm]; d2=thickness of base [cm]; d3=thickness of foundation [cm]; Mr=subgrade modulus [N/mm2]; Tc=Traffic Catalog; DPSI=4.2-PSI; ai= i^{th} layer coefficients; mi= i^{th} layer drainage coefficient; SN=Structural Number [cm]; Esal= Esal calculated with AASHTO method; Taashto=traffic derived from the Esals calculated with AASHTO method.

APPENDIX 3

APPLICATION OF THE FONSECA AND WITCZAK METHOD FOR AC LAYERS

In the following tables there are all the results and details of parameter used for the application of the Fonseca and Witczak method edited by NCHRP 1-37A 2004.

$$\log E^* = 3.750063 + 0.02932\rho_{200} - 0.001767(\rho_{200})^2 - 0.002841\rho_4 - 0.058097V_a$$
$$- 0.802208\left(\frac{V_{beff}}{V_{beff} + V_a}\right) + \frac{3.871977 - 0.0021\rho_4 + 0.003958\rho_{38} - 0.000017(\rho_{38})^2 + 0.005470\rho_{34}}{1 + e^{(-0.603313 - 0.313351\log(f) - 0.393532\log(\eta))}}$$

E* = dynamic modulus [10^5 psi]
ρ_{200} = % passing the no. 200 ASTM (0.075 mm) sieve, %
ρ_4 = % retained on the n. 4 ASTM (4.75 MM) SIEVE, %
ρ_{38} = % retained on the 3/8 in (9.5 mm) sieve, %
ρ_{34} = % retained on the 3/4 in (19.0 mm) sieve, %
V_v = void Volume, %
V_{be} = effective bitumen content, % by volume
f = loading frequency [Hz]
η = bitumen viscosity [10^6 poise]
log (log η) = A + VTS Log T_R; (A, VTS = regression parameters; T_R = Temperature [°R])

The results show the calculations of the modules of the various layers both at 5 Hz and at 16 Hz frequencies.

Wear and binder modulus at 5 Hz

p200 %	r4 %	r3/8 %	r3/4 %	Va %	Vbe %	η [P10^6]	f [Hz]	VFA	VMA	log E*	E* [psi 10^5]	E* [Mpa]	Layer
7	55	15	0	4	11	1.59E+00	5	0.73	15.0	5.60E+00	401,160	2,766	Wear and binder

Wear and binder modulus at 16 Hz

p200 %	r4 %	r3/8 %	r3/4 %	Va %	Vbe %	η [P10^6]	f [Hz]	VFA	VMA	log E*	E* [psi 10^5]	E* [Mpa]	Layer
7	55	15	0	4	11	1.59E+00	16	0.73	15.0	5.72E+00	528,412	3,643	Wear and binder

Base modulus at 5 Hz

p200 %	r4 %	r3/8 %	r3/4 %	Va %	Vbe %	η [P10^6]	f [Hz]	VFA	VMA	log E*	E* [psi 10^5]	E* [Mpa]	Layer
5	70	48	21	6	16	1.59E+00	5	0.73	22.0	5.56E+00	363,252	2,505	Base

Base modulus at 16 Hz

p200 %	r4 %	r3/8 %	r3/4 %	Va %	Vbe %	η [P10^6]	f [Hz]	VFA	VMA	log E*	E* [psi 10^5]	E* [Mpa]	Layer
5	70	48	21	6	16	1.59E+00	16	0.73	22.0	5.69E+00	484,697	3,342	Base

Considering that log (log η) = A + VTS Log T_R, the graph and the table below are representative of the equation with the parameter used for the research work.

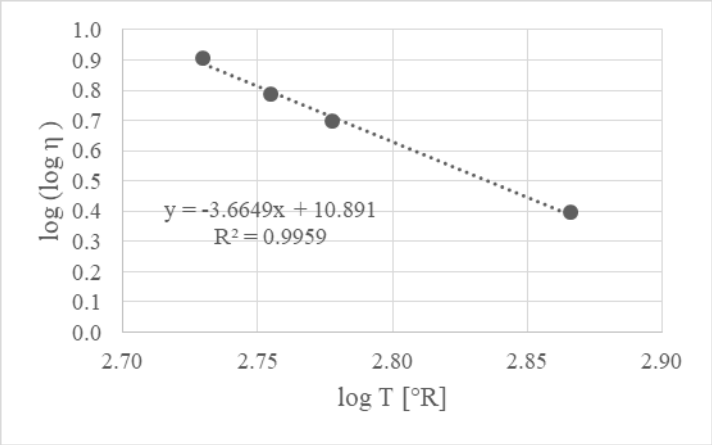

T°C	T°R	log T°R	η [cP]	log log η	A
25	536.67	2.73	9.92E+07	0.90290	10.891
43	569.07	2.76	1.30E+06	0.78632	**VTS**
60	599.67	2.78	9.00E+04	0.69498	-3.6649
135	734.67	2.87	3.00E+02	0.39395	
PEN	**log η**	**η [P]**	**η [cP]**	**h [P 10^6]**	**Pa s**
100	6.00	9.9E+05	9.9E+07	9.9E-01	9.9E+04

T [°C]	Pa s
25	9.9E+04
43	1300
60	90
135	0.3

APPENDIX 4

BEARING CAPACITY FWD TESTS

The tests were carried out with the FWD equipment of the TI Lab of the University of Catania, with the Falling Weight Deflectometer Dynatest 8000. The FWD tests were carried out at different loads and heights, in order to verify that the frequency is about 16 Hz.

FWD in situ test carried out aimed at verifying the frequency of 16 Hz

Tests were carried out with both 250 kg and 400 kg loads at 4 different loading heights, and for every height the mass has been dropped 4 times. Each of the tests returned a frequency of 16 Hz, with time histories showing that each drop takes place in a time 30 ms. The graph below represents a time histories of the tests carried out (Load = 250 Kg, last drop at the second loading height): the drop was recorded in a time of about 30 ms and the maximum recorded load value it is around 40 KN.

Time History of a FWD test carried out at University of Catania

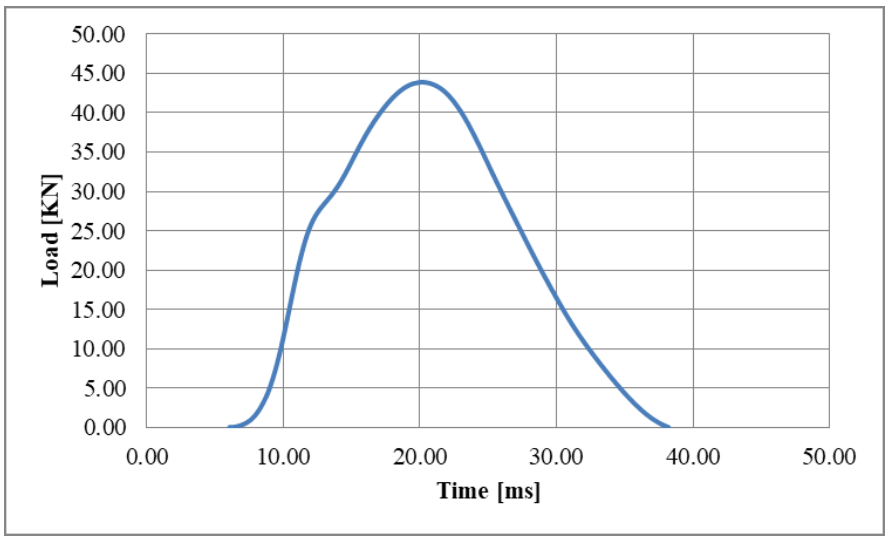

As said before, each drop takes place in a time of 30 ms and depending on the height clearly records a max at different load values. Below is a syntesis of the time and load values recorded in the tests carried out.

Bearing capacity tests performed with FWD Dynatest 8000

Falling Mass	Height N.	Time [ms]	Load [KN]
250 Kg	1	30	30
250 Kg	2	30	40
250 Kg	3	30	60
250 Kg	4	30	90
400 Kg	1	30	50
400 Kg	2	30	70
400 Kg	3	30	110
400 Kg	4	30	150

The detailed results of experimental tests with the FWD Dynatest 8000 are in the following tables, where there is the detail of Stress [Kpa], Loads (or Force) [KN], and Deflections Di [μm] recorded by the 15 geophones during the FWD tests performed in Catania.

Falling mass: 250 Kg

Height n.	DropID	Stress	Force	D1	D2	D3	D4	D5	D6	D7	D8	D9	D10	D11	D12	D13	D14	D15
1	1	433.00	30.57	217.10	172.90	144.60	108.30	82.00	60.50	48.60	36.30	28.50	22.70	18.70	15.10	13.00	11.00	9.70
1	2	429.00	30.29	214.50	169.90	142.20	106.60	80.70	59.50	48.30	36.20	28.10	22.50	18.90	14.90	12.80	11.00	9.20
1	3	425.00	30.03	210.90	168.20	139.00	105.30	79.00	58.90	45.80	35.50	27.80	22.00	17.90	14.40	12.60	10.50	8.90
1	4	425.00	30.01	210.20	167.80	138.90	105.30	79.30	58.50	46.10	35.50	28.20	22.10	17.70	14.60	12.40	10.20	9.00

Height n.	DropID	Stress	Force	D1	D2	D3	D4	D5	D6	D7	D8	D9	D10	D11	D12	D13	D14	D15
2	1	609.00	43.07	299.10	237.50	198.10	150.40	113.60	85.60	67.10	51.90	40.30	32.60	26.00	21.10	17.00	15.30	13.40
2	2	607.00	42.91	295.10	234.50	195.60	148.70	112.50	84.60	66.60	51.50	40.10	32.40	25.80	21.30	17.10	15.30	13.40
2	3	607.00	42.87	293.50	233.00	195.20	148.50	111.60	84.00	66.80	51.50	40.50	32.70	26.30	21.30	17.50	15.30	13.60
2	4	605.00	42.76	292.70	233.20	194.60	148.00	111.80	84.50	66.60	51.60	40.40	32.60	26.40	21.30	17.40	15.60	13.90

Height n.	DropID	Stress	Force	D1	D2	D3	D4	D5	D6	D7	D8	D9	D10	D11	D12	D13	D14	D15
3	1	889.00	62.80	424.90	339.60	283.60	215.80	164.30	124.60	97.80	76.20	59.30	47.60	38.60	31.80	26.50	23.40	20.50
3	2	889.00	62.80	422.20	337.20	281.60	215.10	163.80	124.00	96.90	76.10	59.50	47.80	38.40	31.70	26.60	23.40	20.20
3	3	887.00	62.66	421.10	337.10	281.60	215.00	164.20	124.30	97.30	76.10	59.90	47.90	38.80	32.10	26.80	23.80	20.90
3	4	885.00	62.58	420.30	335.70	280.50	214.70	163.30	123.60	96.90	76.00	59.60	47.70	38.60	31.60	26.50	23.20	20.30

Height n.	DropID	Stress	Force	D1	D2	D3	D4	D5	D6	D7	D8	D9	D10	D11	D12	D13	D14	D15
4	1	1296.00	91.61	596.80	475.70	398.50	303.30	232.50	176.20	139.20	108.80	85.10	68.40	55.30	44.60	38.30	33.60	30.00
4	2	1294.00	91.45	597.20	476.80	398.80	304.80	233.20	177.50	139.90	110.00	85.60	68.60	55.70	44.90	38.30	34.00	30.20
4	3	1297.00	91.68	599.30	478.70	400.80	306.30	234.50	178.60	140.80	110.30	86.20	69.10	56.20	45.50	38.80	34.10	30.60
4	4	1295.00	91.54	601.10	479.40	402.60	306.80	234.60	178.80	141.30	110.20	86.00	68.90	56.10	45.90	38.90	34.80	31.00

Falling mass: 400 Kg

Height n.	DropID	Stress	Force	D1	D2	D3	D4	D5	D6	D7	D8	D9	D10	D11	D12	D13	D14	D15
1	1	679.00	47.96	249.20	189.20	157.70	120.70	134.00	130.20	126.60	123.70	107.30	78.50	62.00	95.10	146.70	185.40	225.50
1	2	680.00	48.03	242.80	183.00	152.30	116.70	132.60	128.20	123.80	120.80	104.80	79.50	65.60	101.80	151.90	187.20	220.90
1	3	680.00	48.05	242.40	183.10	152.60	116.80	123.60	121.50	120.50	122.00	112.80	91.90	85.30	124.20	171.50	201.10	228.80
1	4	675.00	47.71	241.60	182.10	151.70	116.70	129.80	128.90	127.30	131.80	123.20	103.10	98.10	139.70	187.70	217.50	246.80

Height n.	DropID	Stress	Force	D1	D2	D3	D4	D5	D6	D7	D8	D9	D10	D11	D12	D13	D14	D15
2	1	1009.00	71.31	374.80	288.90	237.00	175.90	133.40	100.70	78.20	60.70	46.80	37.80	31.50	27.20	24.50	22.90	22.60
2	2	1013.00	71.57	378.10	291.60	239.10	177.80	134.30	101.40	78.80	60.30	47.20	37.80	31.80	27.60	25.00	23.30	22.30
2	3	1012.00	71.53	379.30	292.30	239.70	178.20	134.70	101.50	79.00	60.30	47.40	37.90	31.90	27.70	25.20	23.30	22.30
2	4	1013.00	71.63	381.00	293.10	240.60	178.80	135.30	102.00	79.20	60.60	47.40	37.90	32.00	27.80	25.10	23.30	22.50

Height n.	DropID	Stress	Force	D1	D2	D3	D4	D5	D6	D7	D8	D9	D10	D11	D12	D13	D14	D15
3	1	1525.00	107.82	594.00	471.40	393.90	290.80	217.50	163.50	127.80	94.70	74.00	57.90	52.50	44.10	39.10	34.90	36.40
3	2	1530.00	108.15	597.60	474.00	395.70	290.90	218.20	163.90	128.70	94.90	74.00	59.30	50.80	44.10	39.10	36.40	35.30
3	3	1535.00	108.50	604.00	478.50	398.60	292.30	219.50	164.50	128.40	95.40	74.20	59.70	49.70	44.10	39.10	37.00	35.00
3	4	1527.00	107.96	605.80	480.40	399.80	293.10	219.90	164.10	127.50	95.70	74.10	59.90	49.40	43.80	38.90	37.20	34.90

Height n.	DropID	Stress	Force	D1	D2	D3	D4	D5	D6	D7	D8	D9	D10	D11	D12	D13	D14	D15
4	1	2110.00	149.15	911.30	714.50	588.50	426.60	317.40	235.20	179.10	134.60	104.50	84.30	70.50	61.80	55.20	51.90	47.70
4	2	2172.00	153.49	930.20	728.30	601.00	433.90	321.90	237.80	183.00	136.20	105.60	85.70	72.40	63.40	57.50	54.30	50.10
4	3	2181.00	154.13	943.50	738.20	608.60	438.90	324.80	239.20	183.80	136.60	106.00	86.40	72.90	63.90	57.70	55.10	51.60
4	4	2094.00	148.02	952.90	744.60	614.50	442.40	327.10	240.40	184.10	137.00	106.40	86.80	73.20	64.30	58.20	55.40	51.80

As for the frequency, from the data of the tests, it can be obtained with various formulas:

$f = 0.496/t$

$f = 1/(2 \cdot t_{FWD})$

Applying both relationships in the various tests analyzed, the frequency has always been around 16 Hz, so having this check a positive result, then the pavements of the database can be studied with modules referred to this frequency value, which is precisely the tests which are conducted on roads with high efficiency FWD equipment for the verification of the load-bearing capacity and of the structural and performance characteristics.

APPENDIX 5
DATABASE OF PAVEMENTS

In the following Database of data: D is the percentage of variation of modules; ai are the layer coefficients; M_i are the modules (at 5 Hz and 16 Hz) calculated with respect to the percentage of variation established, respectively of wear and binder, base, foundation, subgrade; h_i represents the layer thickness of wear and binder, base and foundation; Dcode is the code that indicates which of the modules has been changed in percentage, considering that the rest of the modules don't change.

					5 Hz				16 Hz							
Id. Pav.	**D**	**a1**	**a2**	**a3**	**M1 [Mpa]**	**M2 [Mpa]**	**M3 [Mpa]**	**Ms [Mpa]**	**M1 [Mpa]**	**M2 [Mpa]**	**M3 [Mpa]**	**Ms [Mpa]**	**h1 [mm]**	**h2 [mm]**	**h3 [mm]**	**Dcode**
Ms 30 (M-L)	***-20%***	0.38	0.33	0.11	2212.8	2505.0	104.5	30.0	2914.4	3342.0	316.7	90.9	110	170	350	**M1**
Ms 30 (M-L)	***-10%***	0.40	0.33	0.11	2489.4	2505.0	104.5	30.0	3278.7	3342.0	316.7	90.9	110	170	350	**M1**
Ms 30 (M-L)	***0%***	0.42	0.33	0.11	2766.0	2505.0	104.5	30.0	3643.0	3342.0	316.7	90.9	110	170	350	**O**
Ms 30 (M-L)	***15%***	0.44	0.33	0.11	3180.9	2505.0	104.5	30.0	4189.5	3342.0	316.7	90.9	110	170	350	**M1**
Ms 30 (M-L)	***-20%***	0.42	0.29	0.11	2766.0	2004.0	104.5	30.0	3643.0	2673.6	316.7	90.9	110	170	350	**M2**
Ms 30 (M-L)	***-10%***	0.42	0.31	0.11	2766.0	2254.5	104.5	30.0	3643.0	3007.8	316.7	90.9	110	170	350	**M2**
Ms 30 (M-L)	***0%***	0.42	0.33	0.11	2766.0	2505.0	104.5	30.0	3643.0	3342.0	316.7	90.9	110	170	350	**O**
Ms 30 (M-L)	***15%***	0.42	0.36	0.11	2766.0	2880.8	104.5	30.0	3643.0	3843.3	316.7	90.9	110	170	350	**M2**
Ms 30 (M-L)	***-20%***	0.42	0.33	0.09	2766.0	2505.0	83.6	30.0	3643.0	3342.0	253.4	90.9	110	170	350	**M3**
Ms 30 (M-L)	***-10%***	0.42	0.33	0.10	2766.0	2505.0	94.1	30.0	3643.0	3342.0	285.0	90.9	110	170	350	**M3**
Ms 30 (M-L)	***0%***	0.42	0.33	0.11	2766.0	2505.0	104.5	30.0	3643.0	3342.0	316.7	90.9	110	170	350	**O**
Ms 30 (M-L)	***15%***	0.42	0.33	0.12	2766.0	2505.0	120.2	30.0	3643.0	3342.0	364.2	90.9	110	170	350	**M3**
Ms 30 (M-L)	***-20%***	0.42	0.33	0.11	2766.0	2505.0	104.5	24.0	3643.0	3342.0	316.7	72.7	110	170	350	**Ms**
Ms 30 (M-L)	***-10%***	0.42	0.33	0.11	2766.0	2505.0	104.5	27.0	3643.0	3342.0	316.7	81.8	110	170	350	**Ms**
Ms 30 (M-L)	***0%***	0.42	0.33	0.11	2766.0	2505.0	104.5	30.0	3643.0	3342.0	316.7	90.9	110	170	350	**O**
Ms 30 (M-L)	***15%***	0.42	0.33	0.11	2766.0	2505.0	104.5	34.5	3643.0	3342.0	316.7	104.5	110	170	350	**Ms**
Ms 30 (PP-P)	***-20%***	0.38	0.33	0.12	2212.8	2505.0	115.7	30.0	2914.4	3342.0	350.5	90.9	110	220	350	**M1**
Ms 30 (PP-P)	***-10%***	0.40	0.33	0.12	2489.4	2505.0	115.7	30.0	3278.7	3342.0	350.5	90.9	110	220	350	**M1**
Ms 30 (PP-P)	***0%***	0.42	0.33	0.12	2766.0	2505.0	115.7	30.0	3643.0	3342.0	350.5	90.9	110	220	350	**O**
Ms 30 (PP-P)	***15%***	0.44	0.33	0.12	3180.9	2505.0	115.7	30.0	4189.5	3342.0	350.5	90.9	110	220	350	**M1**
Ms 30 (PP-P)	***-20%***	0.42	0.29	0.12	2766.0	2004.0	115.7	30.0	3643.0	2673.6	350.5	90.9	110	220	350	**M2**
Ms 30 (PP-P)	***-10%***	0.42	0.31	0.12	2766.0	2254.5	115.7	30.0	3643.0	3007.8	350.5	90.9	110	220	350	**M2**
Ms 30 (PP-P)	***0%***	0.42	0.33	0.12	2766.0	2505.0	115.7	30.0	3643.0	3342.0	350.5	90.9	110	220	350	**O**
Ms 30 (PP-P)	***15%***	0.42	0.36	0.12	2766.0	2880.8	115.7	30.0	3643.0	3843.3	350.5	90.9	110	220	350	**M2**
Ms 30 (PP-P)	***-20%***	0.42	0.33	0.10	2766.0	2505.0	92.5	30.0	3643.0	3342.0	280.4	90.9	110	220	350	**M3**
Ms 30 (PP-P)	***-10%***	0.42	0.33	0.11	2766.0	2505.0	104.1	30.0	3643.0	3342.0	315.5	90.9	110	220	350	**M3**
Ms 30 (PP-P)	***0%***	0.42	0.33	0.12	2766.0	2505.0	115.7	30.0	3643.0	3342.0	350.5	90.9	110	220	350	**O**
Ms 30 (PP-P)	***15%***	0.42	0.33	0.13	2766.0	2505.0	133.0	30.0	3643.0	3342.0	403.1	90.9	110	220	350	**M3**
Ms 30 (PP-P)	***-20%***	0.42	0.33	0.12	2766.0	2505.0	115.7	24.0	3643.0	3342.0	350.5	72.7	110	220	350	**Ms**
Ms 30 (PP-P)	***-10%***	0.42	0.33	0.12	2766.0	2505.0	115.7	27.0	3643.0	3342.0	350.5	81.8	110	220	350	**Ms**
Ms 30 (PP-P)	***0%***	0.42	0.33	0.12	2766.0	2505.0	115.7	30.0	3643.0	3342.0	350.5	90.9	110	220	350	**O**
Ms 30 (PP-P)	***15%***	0.42	0.33	0.12	2766.0	2505.0	115.7	34.5	3643.0	3342.0	350.5	104.5	110	220	350	**Ms**
Ms 90 (M-L)	***-20%***	0.38	0.33	0.11	2212.8	2505.0	104.5	90.0	2914.4	3342.0	316.7	272.7	130	160	150	**M1**
Ms 90 (M-L)	***-10%***	0.40	0.33	0.11	2489.4	2505.0	104.5	90.0	3278.7	3342.0	316.7	272.7	130	160	150	**M1**
Ms 90 (M-L)	***0%***	0.42	0.33	0.11	2766.0	2505.0	104.5	90.0	3643.0	3342.0	316.7	272.7	130	160	150	**O**
Ms 90 (M-L)	***15%***	0.44	0.33	0.11	3180.9	2505.0	104.5	90.0	4189.5	3342.0	316.7	272.7	130	160	150	**M1**
Ms 90 (M-L)	***-20%***	0.42	0.29	0.11	2766.0	2004.0	104.5	90.0	3643.0	2673.6	316.7	272.7	130	160	150	**M2**
Ms 90 (M-L)	***-10%***	0.42	0.31	0.11	2766.0	2254.5	104.5	90.0	3643.0	3007.8	316.7	272.7	130	160	150	**M2**
Ms 90 (M-L)	***0%***	0.42	0.33	0.11	2766.0	2505.0	104.5	90.0	3643.0	3342.0	316.7	272.7	130	160	150	**O**
Ms 90 (M-L)	***15%***	0.42	0.36	0.11	2766.0	2880.8	104.5	90.0	3643.0	3843.3	316.7	272.7	130	160	150	**M2**
Ms 90 (M-L)	***-20%***	0.42	0.33	0.09	2766.0	2505.0	83.6	90.0	3643.0	3342.0	253.4	272.7	130	160	150	**M3**
Ms 90 (M-L)	***-10%***	0.42	0.33	0.10	2766.0	2505.0	94.1	90.0	3643.0	3342.0	285.0	272.7	130	160	150	**M3**
Ms 90 (M-L)	***0%***	0.42	0.33	0.11	2766.0	2505.0	104.5	90.0	3643.0	3342.0	316.7	272.7	130	160	150	**O**
Ms 90 (M-L)	***15%***	0.42	0.33	0.12	2766.0	2505.0	120.2	90.0	3643.0	3342.0	364.2	272.7	130	160	150	**M3**
Ms 90 (M-L)	***-20%***	0.42	0.33	0.11	2766.0	2505.0	104.5	72.0	3643.0	3342.0	316.7	218.2	130	160	150	**Ms**
Ms 90 (M-L)	***-10%***	0.42	0.33	0.11	2766.0	2505.0	104.5	81.0	3643.0	3342.0	316.7	245.5	130	160	150	**Ms**
Ms 90 (M-L)	***0%***	0.42	0.33	0.11	2766.0	2505.0	104.5	90.0	3643.0	3342.0	316.7	272.7	130	160	150	**O**

					5 Hz				16 Hz							
Id. Pav.	**D**	**a1**	**a2**	**a3**	**M1 [Mpa]**	**M2 [Mpa]**	**M3 [Mpa]**	**Ms [Mpa]**	**M1 [Mpa]**	**M2 [Mpa]**	**M3 [Mpa]**	**Ms [Mpa]**	**h1 [mm]**	**h2 [mm]**	**h3 [mm]**	**Dcode**
Ms 90 (M-L)	***15%***	0.42	0.33	0.11	2766.0	2505.0	104.5	103.5	3643.0	3342.0	316.7	313.6	130	160	150	**Ms**
Ms 90 (PP-P)	***-20%***	0.38	0.33	0.12	2212.8	2505.0	115.7	90.0	2914.4	3342.0	350.5	272.7	110	170	150	**M1**
Ms 90 (PP-P)	***-10%***	0.40	0.33	0.12	2489.4	2505.0	115.7	90.0	3278.7	3342.0	350.5	272.7	110	170	150	**M1**
Ms 90 (PP-P)	***0%***	0.42	0.33	0.12	2766.0	2505.0	115.7	90.0	3643.0	3342.0	350.5	272.7	110	170	150	**O**
Ms 90 (PP-P)	***15%***	0.44	0.33	0.12	3180.9	2505.0	115.7	90.0	4189.5	3342.0	350.5	272.7	110	170	150	**M1**
Ms 90 (PP-P)	***-20%***	0.42	0.29	0.12	2766.0	2004.0	115.7	90.0	3643.0	2673.6	350.5	272.7	110	170	150	**M2**
Ms 90 (PP-P)	***-10%***	0.42	0.31	0.12	2766.0	2254.5	115.7	90.0	3643.0	3007.8	350.5	272.7	110	170	150	**M2**
Ms 90 (PP-P)	***0%***	0.42	0.33	0.12	2766.0	2505.0	115.7	90.0	3643.0	3342.0	350.5	272.7	110	170	150	**O**
Ms 90 (PP-P)	***15%***	0.42	0.36	0.12	2766.0	2880.8	115.7	90.0	3643.0	3843.3	350.5	272.7	110	170	150	**M2**
Ms 90 (PP-P)	***-20%***	0.42	0.33	0.10	2766.0	2505.0	92.5	90.0	3643.0	3342.0	280.4	272.7	110	170	150	**M3**
Ms 90 (PP-P)	***-10%***	0.42	0.33	0.11	2766.0	2505.0	104.1	90.0	3643.0	3342.0	315.5	272.7	110	170	150	**M3**
Ms 90 (PP-P)	***0%***	0.42	0.33	0.12	2766.0	2505.0	115.7	90.0	3643.0	3342.0	350.5	272.7	110	170	150	**O**
Ms 90 (PP-P)	***15%***	0.42	0.33	0.13	2766.0	2505.0	133.0	90.0	3643.0	3342.0	403.1	272.7	110	170	150	**M3**
Ms 90 (PP-P)	***-20%***	0.42	0.33	0.12	2766.0	2505.0	115.7	72.0	3643.0	3342.0	350.5	218.2	110	170	150	**Ms**
Ms 90 (PP-P)	***-10%***	0.42	0.33	0.12	2766.0	2505.0	115.7	81.0	3643.0	3342.0	350.5	245.5	110	170	150	**Ms**
Ms 90 (PP-P)	***0%***	0.42	0.33	0.12	2766.0	2505.0	115.7	90.0	3643.0	3342.0	350.5	272.7	110	170	150	**O**
Ms 90 (PP-P)	***15%***	0.42	0.33	0.12	2766.0	2505.0	115.7	103.5	3643.0	3342.0	350.5	313.6	110	170	150	**Ms**
MS 30 (L) 9-15-35	***-20%***	0.38	0.33	0.11	2212.8	2505.0	104.5	30.0	2914.4	3342.0	316.7	90.9	90	150	350	**M1**
MS 30 (L) 9-15-35	***-10%***	0.40	0.33	0.11	2489.4	2505.0	104.5	30.0	3278.7	3342.0	316.7	90.9	90	150	350	**M1**
MS 30 (L) 9-15-35	***0%***	0.42	0.33	0.11	2766.0	2505.0	104.5	30.0	3643.0	3342.0	316.7	90.9	90	150	350	**O**
MS 30 (L) 9-15-35	***15%***	0.44	0.33	0.11	3180.9	2505.0	104.5	30.0	4189.5	3342.0	316.7	90.9	90	150	350	**M1**
MS 30 (L) 9-15-35	***-20%***	0.42	0.29	0.11	2766.0	2004.0	104.5	30.0	3643.0	2673.6	316.7	90.9	90	150	350	**M2**
MS 30 (L) 9-15-35	***-10%***	0.42	0.31	0.11	2766.0	2254.5	104.5	30.0	3643.0	3007.8	316.7	90.9	90	150	350	**M2**
MS 30 (L) 9-15-35	***0%***	0.42	0.33	0.11	2766.0	2505.0	104.5	30.0	3643.0	3342.0	316.7	90.9	90	150	350	**O**
MS 30 (L) 9-15-35	***15%***	0.42	0.36	0.11	2766.0	2880.8	104.5	30.0	3643.0	3843.3	316.7	90.9	90	150	350	**M2**
MS 30 (L) 9-15-35	***-20%***	0.42	0.33	0.09	2766.0	2505.0	83.6	30.0	3643.0	3342.0	253.4	90.9	90	150	350	**M3**
MS 30 (L) 9-15-35	***-10%***	0.42	0.33	0.10	2766.0	2505.0	94.1	30.0	3643.0	3342.0	285.0	90.9	90	150	350	**M3**
MS 30 (L) 9-15-35	***0%***	0.42	0.33	0.11	2766.0	2505.0	104.5	30.0	3643.0	3342.0	316.7	90.9	90	150	350	**O**
MS 30 (L) 9-15-35	***15%***	0.42	0.33	0.12	2766.0	2505.0	120.2	30.0	3643.0	3342.0	364.2	90.9	90	150	350	**M3**
MS 30 (L) 9-15-35	***-20%***	0.42	0.33	0.11	2766.0	2505.0	104.5	24.0	3643.0	3342.0	316.7	72.7	**90**	**150**	**350**	**Ms**
MS 30 (L) 9-15-35	***-10%***	0.42	0.33	0.11	2766.0	2505.0	104.5	27.0	3643.0	3342.0	316.7	81.8	90	150	350	**Ms**
MS 30 (L) 9-15-35	***0%***	0.42	0.33	0.11	2766.0	2505.0	104.5	30.0	3643.0	3342.0	316.7	90.9	90	150	350	**O**
MS 30 (L) 9-15-35	***15%***	0.42	0.33	0.11	2766.0	2505.0	104.5	34.5	3643.0	3342.0	316.7	104.5	90	150	350	**Ms**
MS90 (L) 9-12-15	***-20%***	0.38	0.33	0.11	2212.8	2505.0	104.5	90.0	2914.4	3342.0	316.7	272.7	90	120	150	**M1**
MS90 (L) 9-12-15	***-10%***	0.40	0.33	0.11	2489.4	2505.0	104.5	90.0	3278.7	3342.0	316.7	272.7	90	120	150	**M1**
MS90 (L) 9-12-15	***0%***	0.42	0.33	0.11	2766.0	2505.0	104.5	90.0	3643.0	3342.0	316.7	272.7	90	120	150	**O**
MS90 (L) 9-12-15	***15%***	0.44	0.33	0.11	3180.9	2505.0	104.5	90.0	4189.5	3342.0	316.7	272.7	90	120	150	**M1**
MS90 (L) 9-12-15	***-20%***	0.42	0.29	0.11	2766.0	2004.0	104.5	90.0	3643.0	2673.6	316.7	272.7	90	120	150	**M2**
MS90 (L) 9-12-15	***-10%***	0.42	0.31	0.11	2766.0	2254.5	104.5	90.0	3643.0	3007.8	316.7	272.7	90	120	150	**M2**
MS90 (L) 9-12-15	***0%***	0.42	0.33	0.11	2766.0	2505.0	104.5	90.0	3643.0	3342.0	316.7	272.7	90	120	150	**O**
MS90 (L) 9-12-15	***15%***	0.42	0.36	0.11	2766.0	2880.8	104.5	90.0	3643.0	3843.3	316.7	272.7	90	120	150	**M2**
MS90 (L) 9-12-15	***-20%***	0.42	0.33	0.09	2766.0	2505.0	83.6	90.0	3643.0	3342.0	253.4	272.7	90	120	150	**M3**

					5 Hz				16 Hz							
Id. Pav.	**D**	**a1**	**a2**	**a3**	**M1 [Mpa]**	**M2 [Mpa]**	**M3 [Mpa]**	**Ms [Mpa]**	**M1 [Mpa]**	**M2 [Mpa]**	**M3 [Mpa]**	**Ms [Mpa]**	**h1 [mm]**	**h2 [mm]**	**h3 [mm]**	**Dcode**
MS90 (L) 9-12-15	***-10%***	0.42	0.33	0.10	2766.0	2505.0	94.1	90.0	3643.0	3342.0	285.0	272.7	90	120	150	**M3**
MS90 (L) 9-12-15	***0%***	0.42	0.33	0.11	2766.0	2505.0	104.5	90.0	3643.0	3342.0	316.7	272.7	90	120	150	**O**
MS90 (L) 9-12-15	***15%***	0.42	0.33	0.12	2766.0	2505.0	120.2	90.0	3643.0	3342.0	364.2	272.7	90	120	150	**M3**
MS90 (L) 9-12-15	***-20%***	0.42	0.33	0.11	2766.0	2505.0	104.5	72.0	3643.0	3342.0	316.7	218.2	90	120	150	**Ms**
MS90 (L) 9-12-15	***-10%***	0.42	0.33	0.11	2766.0	2505.0	104.5	81.0	3643.0	3342.0	316.7	245.5	90	120	150	**Ms**
MS90 (L) 9-12-15	***0%***	0.42	0.33	0.11	2766.0	2505.0	104.5	90.0	3643.0	3342.0	316.7	272.7	90	120	150	**O**
MS90 (L) 9-12-15	***15%***	0.42	0.33	0.11	2766.0	2505.0	104.5	103.5	3643.0	3342.0	316.7	313.6	90	120	150	**Ms**
MS 30 (M) 13-20-35 (8F)	***-20%***	0.38	0.33	0.11	2212.8	2505.0	104.5	30.0	2914.4	3342.0	316.7	90.9	130	200	350	**M1**
MS 30 (M) 13-20-35 (8F)	***-10%***	0.40	0.33	0.11	2489.4	2505.0	104.5	30.0	3278.7	3342.0	316.7	90.9	130	200	350	**M1**
MS 30 (M) 13-20-35 (8F)	***0%***	0.42	0.33	0.11	2766.0	2505.0	104.5	30.0	3643.0	3342.0	316.7	90.9	130	200	350	**O**
MS 30 (M) 13-20-35 (8F)	***15%***	0.44	0.33	0.11	3180.9	2505.0	104.5	30.0	4189.5	3342.0	316.7	90.9	130	200	350	**M1**
MS 30 (M) 13-20-35 (8F)	***-20%***	0.42	0.29	0.11	2766.0	2004.0	104.5	30.0	3643.0	2673.6	316.7	90.9	130	200	350	**M2**
MS 30 (M) 13-20-35 (8F)	***-10%***	0.42	0.31	0.11	2766.0	2254.5	104.5	30.0	3643.0	3007.8	316.7	90.9	130	200	350	**M2**
MS 30 (M) 13-20-35 (8F)	***0%***	0.42	0.33	0.11	2766.0	2505.0	104.5	30.0	3643.0	3342.0	316.7	90.9	130	200	350	**O**
MS 30 (M) 13-20-35 (8F)	***15%***	0.42	0.36	0.11	2766.0	2880.8	104.5	30.0	3643.0	3843.3	316.7	90.9	130	200	350	**M2**
MS 30 (M) 13-20-35 (8F)	***-20%***	0.42	0.33	0.09	2766.0	2505.0	83.6	30.0	3643.0	3342.0	253.4	90.9	130	200	350	**M3**
MS 30 (M) 13-20-35 (8F)	***-10%***	0.42	0.33	0.10	2766.0	2505.0	94.1	30.0	3643.0	3342.0	285.0	90.9	130	200	350	**M3**
MS 30 (M) 13-20-35 (8F)	***0%***	0.42	0.33	0.11	2766.0	2505.0	104.5	30.0	3643.0	3342.0	316.7	90.9	130	200	350	**O**
MS 30 (M) 13-20-35 (8F)	***15%***	0.42	0.33	0.12	2766.0	2505.0	120.2	30.0	3643.0	3342.0	364.2	90.9	130	200	350	**M3**
MS 30 (M) 13-20-35 (8F)	***-20%***	0.42	0.33	0.11	2766.0	2505.0	104.5	24.0	3643.0	3342.0	316.7	72.7	130	200	350	**Ms**
MS 30 (M) 13-20-35 (8F)	***-10%***	0.42	0.33	0.11	2766.0	2505.0	104.5	27.0	3643.0	3342.0	316.7	81.8	130	200	350	**Ms**
MS 30 (M) 13-20-35 (8F)	***0%***	0.42	0.33	0.11	2766.0	2505.0	104.5	30.0	3643.0	3342.0	316.7	90.9	130	200	350	**O**
MS 30 (M) 13-20-35 (8F)	***15%***	0.42	0.33	0.11	2766.0	2505.0	104.5	34.5	3643.0	3342.0	316.7	104.5	130	200	350	**Ms**
MS 90 (P) 11-18-15 (3F)	***-20%***	0.38	0.33	0.12	2212.8	2505.0	115.7	90.0	2914.4	3342.0	350.5	272.7	110	180	150	**M1**
MS 90 (P) 11-18-15 (3F)	***-10%***	0.40	0.33	0.12	2489.4	2505.0	115.7	90.0	3278.7	3342.0	350.5	272.7	110	180	150	**M1**
MS 90 (P) 11-18-15 (3F)	***0%***	0.42	0.33	0.12	2766.0	2505.0	115.7	90.0	3643.0	3342.0	350.5	272.7	110	180	150	**O**
MS 90 (P) 11-18-15 (3F)	***15%***	0.44	0.33	0.12	3180.9	2505.0	115.7	90.0	4189.5	3342.0	350.5	272.7	110	180	150	**M1**
MS 90 (P) 11-18-15 (3F)	***-20%***	0.42	0.29	0.12	2766.0	2004.0	115.7	90.0	3643.0	2673.6	350.5	272.7	110	180	150	**M2**
MS 90 (P) 11-18-15 (3F)	***-10%***	0.42	0.31	0.12	2766.0	2254.5	115.7	90.0	3643.0	3007.8	350.5	272.7	110	180	150	**M2**
MS 90 (P) 11-18-15 (3F)	***0%***	0.42	0.33	0.12	2766.0	2505.0	115.7	90.0	3643.0	3342.0	350.5	272.7	110	180	150	**O**
MS 90 (P) 11-18-15 (3F)	***15%***	0.42	0.36	0.12	2766.0	2880.8	115.7	90.0	3643.0	3843.3	350.5	272.7	110	180	150	**M2**
MS 90 (P) 11-18-15 (3F)	***-20%***	0.42	0.33	0.10	2766.0	2505.0	92.5	90.0	3643.0	3342.0	280.4	272.7	110	180	150	**M3**
MS 90 (P) 11-18-15 (3F)	***-10%***	0.42	0.33	0.11	2766.0	2505.0	104.1	90.0	3643.0	3342.0	315.5	272.7	110	180	150	**M3**
MS 90 (P) 11-18-15 (3F)	***0%***	0.42	0.33	0.12	2766.0	2505.0	115.7	90.0	3643.0	3342.0	350.5	272.7	110	180	150	**O**
MS 90 (P) 11-18-15 (3F)	***15%***	0.42	0.33	0.13	2766.0	2505.0	133.0	90.0	3643.0	3342.0	403.1	272.7	110	180	150	**M3**
MS 90 (P) 11-18-15 (3F)	***-20%***	0.42	0.33	0.12	2766.0	2505.0	115.7	72.0	3643.0	3342.0	350.5	218.2	110	180	150	**Ms**

					5 Hz				16 Hz							
Id. Pav.	**D**	**a1**	**a2**	**a3**	**M1 [Mpa]**	**M2 [Mpa]**	**M3 [Mpa]**	**Ms [Mpa]**	**M1 [Mpa]**	**M2 [Mpa]**	**M3 [Mpa]**	**Ms [Mpa]**	**h1 [mm]**	**h2 [mm]**	**h3 [mm]**	**Dcode**
MS 90 (P) 11-18-15 (3F)	***-10%***	0.42	0.33	0.12	2766.0	2505.0	115.7	81.0	3643.0	3342.0	350.5	245.5	110	180	150	**Ms**
MS 90 (P) 11-18-15 (3F)	***0%***	0.42	0.33	0.12	2766.0	2505.0	115.7	90.0	3643.0	3342.0	350.5	272.7	110	180	150	**O**
MS 90 (P) 11-18-15 (3F)	***15%***	0.42	0.33	0.12	2766.0	2505.0	115.7	103.5	3643.0	3342.0	350.5	313.6	110	180	150	**Ms**
MS 90 (PP) 11-25-15 (6F)	***-20%***	0.38	0.33	0.12	2212.8	2505.0	115.7	90.0	2914.4	3342.0	350.5	272.7	110	250	150	**M1**
MS 90 (PP) 11-25-15 (6F)	***-10%***	0.40	0.33	0.12	2489.4	2505.0	115.7	90.0	3278.7	3342.0	350.5	272.7	110	250	150	**M1**
MS 90 (PP) 11-25-15 (6F)	***0%***	0.42	0.33	0.12	2766.0	2505.0	115.7	90.0	3643.0	3342.0	350.5	272.7	110	250	150	**O**
MS 90 (PP) 11-25-15 (6F)	***15%***	0.44	0.33	0.12	3180.9	2505.0	115.7	90.0	4189.5	3342.0	350.5	272.7	110	250	150	**M1**
MS 90 (PP) 11-25-15 (6F)	***-20%***	0.42	0.29	0.12	2766.0	2004.0	115.7	90.0	3643.0	2673.6	350.5	272.7	110	250	150	**M2**
MS 90 (PP) 11-25-15 (6F)	***-10%***	0.42	0.31	0.12	2766.0	2254.5	115.7	90.0	3643.0	3007.8	350.5	272.7	110	250	150	**M2**
MS 90 (PP) 11-25-15 (6F)	***0%***	0.42	0.33	0.12	2766.0	2505.0	115.7	90.0	3643.0	3342.0	350.5	272.7	110	250	150	**O**
MS 90 (PP) 11-25-15 (6F)	***15%***	0.42	0.36	0.12	2766.0	2880.8	115.7	90.0	3643.0	3843.3	350.5	272.7	110	250	150	**M2**
MS 90 (PP) 11-25-15 (6F)	***-20%***	0.42	0.33	0.10	2766.0	2505.0	92.5	90.0	3643.0	3342.0	280.4	272.7	110	250	150	**M3**
MS 90 (PP) 11-25-15 (6F)	***-10%***	0.42	0.33	0.11	2766.0	2505.0	104.1	90.0	3643.0	3342.0	315.5	272.7	110	250	150	**M3**
MS 90 (PP) 11-25-15 (6F)	***0%***	0.42	0.33	0.12	2766.0	2505.0	115.7	90.0	3643.0	3342.0	350.5	272.7	110	250	150	**O**
MS 90 (PP) 11-25-15 (6F)	***15%***	0.42	0.33	0.13	2766.0	2505.0	133.0	90.0	3643.0	3342.0	403.1	272.7	110	250	150	**M3**
MS 90 (PP) 11-25-15 (6F)	***-20%***	0.42	0.33	0.12	2766.0	2505.0	115.7	72.0	3643.0	3342.0	350.5	218.2	110	250	150	**Ms**
MS 90 (PP) 11-25-15 (6F)	***-10%***	0.42	0.33	0.12	2766.0	2505.0	115.7	81.0	3643.0	3342.0	350.5	245.5	110	250	150	**Ms**
MS 90 (PP) 11-25-15 (6F)	***0%***	0.42	0.33	0.12	2766.0	2505.0	115.7	90.0	3643.0	3342.0	350.5	272.7	110	250	150	**O**
MS 90 (PP) 11-25-15 (6F)	***15%***	0.42	0.33	0.12	2766.0	2505.0	115.7	103.5	3643.0	3342.0	350.5	313.6	110	250	150	**Ms**
MS 90 (M) 10-8-15 (7F)	***-20%***	0.38	0.33	0.11	2212.8	2505.0	104.5	90.0	2914.4	3342.0	316.7	272.7	100	80	150	**M1**
MS 90 (M) 10-8-15 (7F)	***-10%***	0.40	0.33	0.11	2489.4	2505.0	104.5	90.0	3278.7	3342.0	316.7	272.7	100	80	150	**M1**
MS 90 (M) 10-8-15 (7F)	***0%***	0.42	0.33	0.11	2766.0	2505.0	104.5	90.0	3643.0	3342.0	316.7	272.7	100	80	150	**O**
MS 90 (M) 10-8-15 (7F)	***15%***	0.44	0.33	0.11	3180.9	2505.0	104.5	90.0	4189.5	3342.0	316.7	272.7	100	80	150	**M1**
MS 90 (M) 10-8-15 (7F)	***-20%***	0.42	0.29	0.11	2766.0	2004.0	104.5	90.0	3643.0	2673.6	316.7	272.7	100	80	150	**M2**
MS 90 (M) 10-8-15 (7F)	***-10%***	0.42	0.31	0.11	2766.0	2254.5	104.5	90.0	3643.0	3007.8	316.7	272.7	100	80	150	**M2**
MS 90 (M) 10-8-15 (7F)	***0%***	0.42	0.33	0.11	2766.0	2505.0	104.5	90.0	3643.0	3342.0	316.7	272.7	100	80	150	**O**
MS 90 (M) 10-8-15 (7F)	***15%***	0.42	0.36	0.11	2766.0	2880.8	104.5	90.0	3643.0	3843.3	316.7	272.7	100	80	150	**M2**
MS 90 (M) 10-8-15 (7F)	***-20%***	0.42	0.33	0.09	2766.0	2505.0	83.6	90.0	3643.0	3342.0	253.4	272.7	100	80	150	**M3**
MS 90 (M) 10-8-15 (7F)	***-10%***	0.42	0.33	0.10	2766.0	2505.0	94.1	90.0	3643.0	3342.0	285.0	272.7	100	80	150	**M3**
MS 90 (M) 10-8-15 (7F)	***0%***	0.42	0.33	0.11	2766.0	2505.0	104.5	90.0	3643.0	3342.0	316.7	272.7	100	80	150	**O**
MS 90 (M) 10-8-15 (7F)	***15%***	0.42	0.33	0.12	2766.0	2505.0	120.2	90.0	3643.0	3342.0	364.2	272.7	100	80	150	**M3**
MS 90 (M) 10-8-15 (7F)	***-20%***	0.42	0.33	0.11	2766.0	2505.0	104.5	72.0	3643.0	3342.0	316.7	218.2	100	80	150	**Ms**
MS 90 (M) 10-8-15 (7F)	***-10%***	0.42	0.33	0.11	2766.0	2505.0	104.5	81.0	3643.0	3342.0	316.7	245.5	100	80	150	**Ms**
MS 90 (M) 10-8-15 (7F)	***0%***	0.42	0.33	0.11	2766.0	2505.0	104.5	90.0	3643.0	3342.0	316.7	272.7	100	80	150	**O**
MS 90 (M) 10-8-15 (7F)	***15%***	0.42	0.33	0.11	2766.0	2505.0	104.5	103.5	3643.0	3342.0	316.7	313.6	100	80	150	**Ms**

Below is the rest of the database where, the only difference with the table above, lies in the fact that the modules M1 and M2 have been changed at a rate of -20% and + 15% at the same time.

					5 Hz				16 Hz							
Id. Pav.	**D**	**a1**	**a2**	**a3**	**M1 [Mpa]**	**M2 [Mpa]**	**M3 [Mpa]**	**Ms [Mpa]**	**M1 [Mpa]**	**M2 [Mpa]**	**M3 [Mpa]**	**Ms [Mpa]**	**h1 [mm]**	**h2 [mm]**	**h3 [mm]**	**Dcode**
Ms 30 (M-L)	***-20%***	0.38	0.29	0.11	2212.8	2004.0	104.5	30.0	2914.4	2673.6	316.7	90.9	110	170	350	**M1 M2**
Ms 30 (M-L)	***15%***	0.44	0.36	0.11	3180.9	2880.8	104.5	30.0	4189.5	3843.3	316.7	90.9	110	170	350	**M1 M2**
Ms 30 (PP-P)	***-20%***	0.38	0.29	0.12	2212.8	2004.0	115.7	30.0	2914.4	2673.6	350.5	90.9	110	220	350	**M1 M2**
Ms 30 (PP-P)	***15%***	0.44	0.36	0.12	3180.9	2880.8	115.7	30.0	4189.5	3843.3	350.5	90.9	110	220	350	**M1 M2**
Ms 90 (M-L)	***-20%***	0.38	0.29	0.11	2212.8	2004.0	104.5	90.0	2914.4	2673.6	316.7	272.7	130	160	150	**M1 M2**
Ms 90 (M-L)	***15%***	0.44	0.36	0.11	3180.9	2880.8	104.5	90.0	4189.5	3843.3	316.7	272.7	130	160	150	**M1 M2**
Ms 90 (PP-P)	***-20%***	0.38	0.29	0.12	2212.8	2004.0	115.7	90.0	2914.4	2673.6	350.5	272.7	110	170	150	**M1 M2**
Ms 90 (PP-P)	***15%***	0.44	0.36	0.12	3180.9	2880.8	115.7	90.0	4189.5	3843.3	350.5	272.7	110	170	150	**M1 M2**
MS 30 (L) 9-15-35	***-20%***	0.38	0.29	0.11	2212.8	2004.0	104.5	30.0	2914.4	2673.6	316.7	90.9	90	150	350	**M1 M2**
MS 30 (L) 9-15-35	***15%***	0.44	0.36	0.11	3180.9	2880.8	104.5	30.0	4189.5	3843.3	316.7	90.9	90	150	350	**M1 M2**
MS90 (L) 9-12-15	***-20%***	0.38	0.29	0.11	2212.8	2004.0	104.5	90.0	2914.4	2673.6	316.7	272.7	90	120	150	**M1 M2**
MS90 (L) 9-12-15	***15%***	0.44	0.36	0.11	3180.9	2880.8	104.5	90.0	4189.5	3843.3	316.7	272.7	90	120	150	**M1 M2**
MS 30 (M) 13-20-35 (8F)	***-20%***	0.38	0.29	0.11	2212.8	2004.0	104.5	30.0	2914.4	2673.6	316.7	90.9	130	200	350	**M1 M2**
MS 30 (M) 13-20-35 (8F)	***15%***	0.44	0.36	0.11	3180.9	2880.8	104.5	30.0	4189.5	3843.3	316.7	90.9	130	200	350	**M1 M2**
MS 90 (P) 11-18-15 (3F)	***-20%***	0.38	0.29	0.12	2212.8	2004.0	115.7	90.0	2914.4	2673.6	350.5	272.7	110	180	150	**M1 M2**
MS 90 (P) 11-18-15 (3F)	***15%***	0.44	0.36	0.12	3180.9	2880.8	115.7	90.0	4189.5	3843.3	350.5	272.7	110	180	150	**M1 M2**
MS 90 (PP) 11-25-15 (6F)	***-20%***	0.38	0.29	0.12	2212.8	2004.0	115.7	90.0	2914.4	2673.6	350.5	272.7	110	250	150	**M1 M2**
MS 90 (PP) 11-25-15 (6F)	***15%***	0.44	0.36	0.12	3180.9	2880.8	115.7	90.0	4189.5	3843.3	350.5	272.7	110	250	150	**M1 M2**
MS 90 (M) 10-8-15 (7F)	***-20%***	0.38	0.29	0.11	2212.8	2004.0	104.5	90.0	2914.4	2673.6	316.7	272.7	100	80	150	**M1 M2**
MS 90 (M) 10-8-15 (7F)	***15%***	0.44	0.36	0.11	3180.9	2880.8	104.5	90.0	4189.5	3843.3	316.7	272.7	100	80	150	**M1 M2**

APPENDIX 6

ESAL DEPENDENT FROM THE STRUCTURAL NUMBER WITH THE AASHTO LAYER COEFFICIENTS

Id. Pav.	D	a1	a2	a3	h1 [mm]	h2 [mm]	h3 [mm]	Dcode	Esal0%	Esalmod	DEsal	Mr [psi]	SN [cm]	SN [inch]	DSN
Ms 30 (M-L)	***-20%***	0.38	0.33	0.11	110	170	350	**M1**	2.40E+07	1.93E+07	-20%	4350.98	13.69	5.39	-3%
Ms 30 (M-L)	***-10%***	0.40	0.33	0.11	110	170	350	**M1**	2.40E+07	2.17E+07	-10%	4350.98	13.91	5.48	-1%
Ms 30 (M-L)	***0%***	0.42	0.33	0.11	110	170	350	**O**	2.40E+07	2.40E+07	0%	4350.98	14.11	5.55	0%
Ms 30 (M-L)	***15%***	0.44	0.33	0.11	110	170	350	**M1**	2.40E+07	2.75E+07	14%	4350.98	14.37	5.66	2%
Ms 30 (M-L)	***-20%***	0.42	0.29	0.11	110	170	350	**M2**	2.40E+07	1.59E+07	-34%	4350.98	13.33	5.25	-6%
Ms 30 (M-L)	***-10%***	0.42	0.31	0.11	110	170	350	**M2**	2.40E+07	1.97E+07	-18%	4350.98	13.73	5.40	-3%
Ms 30 (M-L)	***0%***	0.42	0.33	0.11	110	170	350	**O**	2.40E+07	2.40E+07	0%	4350.98	14.11	5.55	0%
Ms 30 (M-L)	***15%***	0.42	0.36	0.11	110	170	350	**M2**	2.40E+07	3.18E+07	33%	4350.98	14.66	5.77	4%
Ms 30 (M-L)	***-20%***	0.42	0.33	0.09	110	170	350	**M3**	2.40E+07	1.60E+07	-33%	4350.98	13.34	5.25	-5%
Ms 30 (M-L)	***-10%***	0.42	0.33	0.10	110	170	350	**M3**	2.40E+07	1.99E+07	-17%	4350.98	13.74	5.41	-3%
Ms 30 (M-L)	***0%***	0.42	0.33	0.11	110	170	350	**O**	2.40E+07	2.40E+07	0%	4350.98	14.11	5.55	0%
Ms 30 (M-L)	***15%***	0.42	0.33	0.12	110	170	350	**M3**	2.40E+07	3.08E+07	28%	4350.98	14.59	5.74	3%
Ms 30 (M-L)	***-20%***	0.42	0.33	0.11	110	170	350	**Ms**	2.40E+07	1.43E+07	-40%	3480.78	14.11	5.55	0%
Ms 30 (M-L)	***-10%***	0.42	0.33	0.11	110	170	350	**Ms**	2.40E+07	1.88E+07	-22%	3915.88	14.11	5.55	0%
Ms 30 (M-L)	***0%***	0.42	0.33	0.11	110	170	350	**O**	2.40E+07	2.40E+07	0%	4350.98	14.11	5.55	0%
Ms 30 (M-L)	***15%***	0.42	0.33	0.11	110	170	350	**Ms**	2.40E+07	3.32E+07	38%	5003.63	14.11	5.55	0%
Ms 30 (PP-P)	***-20%***	0.38	0.33	0.12	110	220	350	**M1**	6.55E+07	5.37E+07	-18%	4350.98	15.71	6.18	-3%
Ms 30 (PP-P)	***-10%***	0.40	0.33	0.12	110	220	350	**M1**	6.55E+07	5.97E+07	-9%	4350.98	15.93	6.27	-1%
Ms 30 (PP-P)	***0%***	0.42	0.33	0.12	110	220	350	**O**	6.55E+07	6.55E+07	0%	4350.98	16.12	6.35	0%
Ms 30 (PP-P)	***15%***	0.44	0.33	0.12	110	220	350	**M1**	6.55E+07	7.42E+07	13%	4350.98	16.38	6.45	2%
Ms 30 (PP-P)	***-20%***	0.42	0.29	0.12	110	220	350	**M2**	6.55E+07	4.02E+07	-39%	4350.98	15.12	5.95	-6%
Ms 30 (PP-P)	***-10%***	0.42	0.31	0.12	110	220	350	**M2**	6.55E+07	5.17E+07	-21%	4350.98	15.63	6.15	-3%
Ms 30 (PP-P)	***0%***	0.42	0.33	0.12	110	220	350	**O**	6.55E+07	6.55E+07	0%	4350.98	16.12	6.35	0%
Ms 30 (PP-P)	***15%***	0.42	0.36	0.12	110	220	350	**M2**	6.55E+07	9.15E+07	40%	4350.98	16.83	6.63	4%
Ms 30 (PP-P)	***-20%***	0.42	0.33	0.10	110	220	350	**M3**	6.55E+07	4.51E+07	-31%	4350.98	15.35	6.04	-5%
Ms 30 (PP-P)	***-10%***	0.42	0.33	0.11	110	220	350	**M3**	6.55E+07	5.50E+07	-16%	4350.98	15.76	6.20	-2%
Ms 30 (PP-P)	***0%***	0.42	0.33	0.12	110	220	350	**O**	6.55E+07	6.55E+07	0%	4350.98	16.12	6.35	0%
Ms 30 (PP-P)	***15%***	0.42	0.33	0.13	110	220	350	**M3**	6.55E+07	8.23E+07	26%	4350.98	16.60	6.54	3%
Ms 30 (PP-P)	***-20%***	0.42	0.33	0.12	110	220	350	**Ms**	6.55E+07	3.91E+07	-40%	3480.78	16.12	6.35	0%
Ms 30 (PP-P)	***-10%***	0.42	0.33	0.12	110	220	350	**Ms**	6.55E+07	5.13E+07	-22%	3915.88	16.12	6.35	0%
Ms 30 (PP-P)	***0%***	0.42	0.33	0.12	110	220	350	**O**	6.55E+07	6.55E+07	0%	4350.98	16.12	6.35	0%
Ms 30 (PP-P)	***15%***	0.42	0.33	0.12	110	220	350	**Ms**	6.55E+07	9.06E+07	38%	5003.63	16.12	6.35	0%
Ms 90 (M-L)	***-20%***	0.38	0.33	0.11	130	160	150	**M1**	6.23E+07	4.86E+07	-22%	13052.94	11.92	4.69	-4%
Ms 90 (M-L)	***-10%***	0.40	0.33	0.11	130	160	150	**M1**	6.23E+07	5.54E+07	-11%	13052.94	12.18	4.80	-2%
Ms 90 (M-L)	***0%***	0.42	0.33	0.11	130	160	150	**O**	6.23E+07	6.23E+07	0%	13052.94	12.41	4.89	0%
Ms 90 (M-L)	***15%***	0.44	0.33	0.11	130	160	150	**M1**	6.23E+07	7.28E+07	17%	13052.94	12.72	5.01	2%
Ms 90 (M-L)	***-20%***	0.42	0.29	0.11	130	160	150	**M2**	6.23E+07	4.29E+07	-31%	13052.94	11.68	4.60	-6%
Ms 90 (M-L)	***-10%***	0.42	0.31	0.11	130	160	150	**M2**	6.23E+07	5.19E+07	-17%	13052.94	12.05	4.75	-3%

Id. Pav.	D	a1	a2	a3	h1 [mm]	h2 [mm]	h3 [mm]	Dcode	Esal0%	Esalmod	DEsal	Mr [psi]	SN [cm]	SN [inch]	DSN
Ms 90 (M-L)	***0%***	0.42	0.33	0.11	130	160	150	**O**	6.23E+07	6.23E+07	0%	13052.94	12.41	4.89	0%
Ms 90 (M-L)	***15%***	0.42	0.36	0.11	130	160	150	**M2**	6.23E+07	8.08E+07	30%	13052.94	12.93	5.09	4%
Ms 90 (M-L)	***-20%***	0.42	0.33	0.09	130	160	150	**M3**	6.23E+07	5.27E+07	-15%	13052.94	12.08	4.76	-3%
Ms 90 (M-L)	***-10%***	0.42	0.33	0.10	130	160	150	**M3**	6.23E+07	5.76E+07	-8%	13052.94	12.26	4.83	-1%
Ms 90 (M-L)	***0%***	0.42	0.33	0.11	130	160	150	**O**	6.23E+07	6.23E+07	0%	13052.94	12.41	4.89	0%
Ms 90 (M-L)	***15%***	0.42	0.33	0.12	130	160	150	**M3**	6.23E+07	6.92E+07	11%	13052.94	12.62	4.97	2%
Ms 90 (M-L)	***-20%***	0.42	0.33	0.11	130	160	150	**Ms**	6.23E+07	3.71E+07	-40%	10442.35	12.41	4.89	0%
Ms 90 (M-L)	***-10%***	0.42	0.33	0.11	130	160	150	**Ms**	6.23E+07	4.88E+07	-22%	11747.64	12.41	4.89	0%
Ms 90 (M-L)	***0%***	0.42	0.33	0.11	130	160	150	**O**	6.23E+07	6.23E+07	0%	13052.94	12.41	4.89	0%
Ms 90 (M-L)	***15%***	0.42	0.33	0.11	130	160	150	**Ms**	6.23E+07	8.62E+07	38%	15010.88	12.41	4.89	0%
Ms 90 (PP-P)	***-20%***	0.38	0.33	0.12	110	170	150	**M1**	1.01E+08	7.97E+07	-21%	13052.94	11.64	4.58	-3%
Ms 90 (PP-P)	***-10%***	0.40	0.33	0.12	110	170	150	**M1**	1.01E+08	9.04E+07	-11%	13052.94	11.86	4.67	-2%
Ms 90 (PP-P)	***0%***	0.42	0.33	0.12	110	170	150	**O**	1.01E+08	1.01E+08	0%	13052.94	12.06	4.75	0%
Ms 90 (PP-P)	***15%***	0.44	0.33	0.12	110	170	150	**M1**	1.01E+08	1.17E+08	16%	13052.94	12.32	4.85	2%
Ms 90 (PP-P)	***-20%***	0.42	0.29	0.12	110	170	150	**M2**	1.01E+08	6.46E+07	-36%	13052.94	11.28	4.44	-6%
Ms 90 (PP-P)	***-10%***	0.42	0.31	0.12	110	170	150	**M2**	1.01E+08	8.13E+07	-20%	13052.94	11.68	4.60	-3%
Ms 90 (PP-P)	***0%***	0.42	0.33	0.12	110	170	150	**O**	1.01E+08	1.01E+08	0%	13052.94	12.06	4.75	0%
Ms 90 (PP-P)	***15%***	0.42	0.36	0.12	110	170	150	**M2**	1.01E+08	1.37E+08	36%	13052.94	12.61	4.96	5%
Ms 90 (PP-P)	***-20%***	0.42	0.33	0.10	110	170	150	**M3**	1.01E+08	8.37E+07	-17%	13052.94	11.73	4.62	-3%
Ms 90 (PP-P)	***-10%***	0.42	0.33	0.11	110	170	150	**M3**	1.01E+08	9.25E+07	-8%	13052.94	11.90	4.69	-1%
Ms 90 (PP-P)	***0%***	0.42	0.33	0.12	110	170	150	**O**	1.01E+08	1.01E+08	0%	13052.94	12.06	4.75	0%
Ms 90 (PP-P)	***15%***	0.42	0.33	0.13	110	170	150	**M3**	1.01E+08	1.14E+08	12%	13052.94	12.26	4.83	2%
Ms 90 (PP-P)	***-20%***	0.42	0.33	0.12	110	170	150	**Ms**	1.01E+08	6.02E+07	-40%	10442.35	12.06	4.75	0%
Ms 90 (PP-P)	***-10%***	0.42	0.33	0.12	110	170	150	**Ms**	1.01E+08	7.91E+07	-22%	11747.64	12.06	4.75	0%
Ms 90 (PP-P)	***0%***	0.42	0.33	0.12	110	170	150	**O**	1.01E+08	1.01E+08	0%	13052.94	12.06	4.75	0%
Ms 90 (PP-P)	***15%***	0.42	0.33	0.12	110	170	150	**Ms**	1.01E+08	1.40E+08	38%	15010.88	12.06	4.75	0%
MS 30 (L) 9-15-35	***-20%***	0.38	0.33	0.11	90	150	350	**M1**	1.07E+07	8.88E+06	-17%	4350.98	12.27	4.83	-3%
MS 30 (L) 9-15-35	***-10%***	0.40	0.33	0.11	90	150	350	**M1**	1.07E+07	9.82E+06	-9%	4350.98	12.45	4.90	-1%
MS 30 (L) 9-15-35	***0%***	0.42	0.33	0.11	90	150	350	**O**	1.07E+07	1.07E+07	0%	4350.98	12.61	4.96	0%
MS 30 (L) 9-15-35	***15%***	0.44	0.33	0.11	90	150	350	**M1**	1.07E+07	1.21E+07	12%	4350.98	12.82	5.05	2%
MS 30 (L) 9-15-35	***-20%***	0.42	0.29	0.11	90	150	350	**M2**	1.07E+07	7.31E+06	-32%	4350.98	11.92	4.69	-5%
MS 30 (L) 9-15-35	***-10%***	0.42	0.31	0.11	90	150	350	**M2**	1.07E+07	8.90E+06	-17%	4350.98	12.27	4.83	-3%
MS 30 (L) 9-15-35	***0%***	0.42	0.33	0.11	90	150	350	**O**	1.07E+07	1.07E+07	0%	4350.98	12.61	4.96	0%
MS 30 (L) 9-15-35	***15%***	0.42	0.36	0.11	90	150	350	**M2**	1.07E+07	1.40E+07	30%	4350.98	13.09	5.15	4%
MS 30 (L) 9-15-35	***-20%***	0.42	0.33	0.09	90	150	350	**M3**	1.07E+07	6.96E+06	-35%	4350.98	11.84	4.66	-6%
MS 30 (L) 9-15-35	***-10%***	0.42	0.33	0.10	90	150	350	**M3**	1.07E+07	8.76E+06	-18%	4350.98	12.24	4.82	-3%
MS 30 (L) 9-15-35	***0%***	0.42	0.33	0.11	90	150	350	**O**	1.07E+07	1.07E+07	0%	4350.98	12.61	4.96	0%
MS 30 (L) 9-15-35	***15%***	0.42	0.33	0.12	90	150	350	**M3**	1.07E+07	1.40E+07	30%	4350.98	13.09	5.15	4%
MS 30 (L) 9-15-35	***-20%***	0.42	0.33	0.11	**90**	**150**	**350**	**Ms**	1.07E+07	6.40E+06	-40%	3480.78	12.61	4.96	0%
MS 30 (L) 9-15-35	***-10%***	0.42	0.33	0.11	90	150	350	**Ms**	1.07E+07	8.41E+06	-22%	3915.88	12.61	4.96	0%
MS 30 (L) 9-15-35	***0%***	0.42	0.33	0.11	90	150	350	**O**	1.07E+07	1.07E+07	0%	4350.98	12.61	4.96	0%

Id. Pav.	D	a1	a2	a3	h1 [mm]	h2 [mm]	h3 [mm]	Dcode	Esal0%	Esalmod	DEsal	Mr [psi]	SN [cm]	SN [inch]	DSN
MS 30 (L) 9-15-35	***15%***	0.42	0.33	0.11	90	150	350	**Ms**	1.07E+07	1.48E+07	38%	5003.63	12.61	4.96	0%
MS90 (L) 9-12-15	***-20%***	0.38	0.33	0.11	90	120	150	**M1**	2.02E+07	1.61E+07	-20%	13052.94	9.07	3.57	-4%
MS90 (L) 9-12-15	***-10%***	0.40	0.33	0.11	90	120	150	**M1**	2.02E+07	1.82E+07	-10%	13052.94	9.25	3.64	-2%
MS90 (L) 9-12-15	***0%***	0.42	0.33	0.11	90	120	150	**O**	2.02E+07	2.02E+07	0%	13052.94	9.41	3.70	0%
MS90 (L) 9-12-15	***15%***	0.44	0.33	0.11	90	120	150	**M1**	2.02E+07	2.32E+07	15%	13052.94	9.62	3.79	2%
MS90 (L) 9-12-15	***-20%***	0.42	0.29	0.11	90	120	150	**M2**	2.02E+07	1.40E+07	-31%	13052.94	8.86	3.49	-6%
MS90 (L) 9-12-15	***-10%***	0.42	0.31	0.11	90	120	150	**M2**	2.02E+07	1.69E+07	-16%	13052.94	9.14	3.60	-3%
MS90 (L) 9-12-15	***0%***	0.42	0.33	0.11	90	120	150	**O**	2.02E+07	2.02E+07	0%	13052.94	9.41	3.70	0%
MS90 (L) 9-12-15	***15%***	0.42	0.36	0.11	90	120	150	**M2**	2.02E+07	2.60E+07	29%	13052.94	9.79	3.86	4%
MS90 (L) 9-12-15	***-20%***	0.42	0.33	0.09	90	120	150	**M3**	2.02E+07	1.62E+07	-20%	13052.94	9.08	3.57	-4%
MS90 (L) 9-12-15	***-10%***	0.42	0.33	0.10	90	120	150	**M3**	2.02E+07	1.83E+07	-10%	13052.94	9.25	3.64	-2%
MS90 (L) 9-12-15	***0%***	0.42	0.33	0.11	90	120	150	**O**	2.02E+07	2.02E+07	0%	13052.94	9.41	3.70	0%
MS90 (L) 9-12-15	***15%***	0.42	0.33	0.12	90	120	150	**M3**	2.02E+07	2.32E+07	14%	13052.94	9.61	3.79	2%
MS90 (L) 9-12-15	***-20%***	0.42	0.33	0.11	90	120	150	**Ms**	2.02E+07	1.21E+07	-40%	10442.35	9.41	3.70	0%
MS90 (L) 9-12-15	***-10%***	0.42	0.33	0.11	90	120	150	**Ms**	2.02E+07	1.58E+07	-22%	11747.64	9.41	3.70	0%
MS90 (L) 9-12-15	***0%***	0.42	0.33	0.11	90	120	150	**O**	2.02E+07	2.02E+07	0%	13052.94	9.41	3.70	0%
MS90 (L) 9-12-15	***15%***	0.42	0.33	0.11	90	120	150	**Ms**	2.02E+07	2.80E+07	38%	15010.88	9.41	3.70	0%
MS 30 (M) 13-20-35 (8F)	***-20%***	0.38	0.33	0.11	130	200	350	**M1**	6.02E+07	4.74E+07	-21%	4350.98	15.45	6.08	-3%
MS 30 (M) 13-20-35 (8F)	***-10%***	0.40	0.33	0.11	130	200	350	**M1**	6.02E+07	5.38E+07	-11%	4350.98	15.71	6.19	-1%
MS 30 (M) 13-20-35 (8F)	***0%***	0.42	0.33	0.11	130	200	350	**O**	6.02E+07	6.02E+07	0%	4350.98	15.94	6.28	0%
MS 30 (M) 13-20-35 (8F)	***15%***	0.44	0.33	0.11	130	200	350	**M1**	6.02E+07	6.97E+07	16%	4350.98	16.25	6.40	2%
MS 30 (M) 13-20-35 (8F)	***-20%***	0.42	0.29	0.11	130	200	350	**M2**	6.02E+07	3.84E+07	-36%	4350.98	15.03	5.92	-6%
MS 30 (M) 13-20-35 (8F)	***-10%***	0.42	0.31	0.11	130	200	350	**M2**	6.02E+07	4.84E+07	-20%	4350.98	15.50	6.10	-3%
MS 30 (M) 13-20-35 (8F)	***0%***	0.42	0.33	0.11	130	200	350	**O**	6.02E+07	6.02E+07	0%	4350.98	15.94	6.28	0%
MS 30 (M) 13-20-35 (8F)	***15%***	0.42	0.36	0.11	130	200	350	**M2**	6.02E+07	8.17E+07	36%	4350.98	16.59	6.53	4%
MS 30 (M) 13-20-35 (8F)	***-20%***	0.42	0.33	0.09	130	200	350	**M3**	6.02E+07	4.13E+07	-31%	4350.98	15.17	5.97	-5%
MS 30 (M) 13-20-35 (8F)	***-10%***	0.42	0.33	0.10	130	200	350	**M3**	6.02E+07	5.04E+07	-16%	4350.98	15.58	6.13	-2%
MS 30 (M) 13-20-35 (8F)	***0%***	0.42	0.33	0.11	130	200	350	**O**	6.02E+07	6.02E+07	0%	4350.98	15.94	6.28	0%
MS 30 (M) 13-20-35 (8F)	***15%***	0.42	0.33	0.12	130	200	350	**M3**	6.02E+07	7.57E+07	26%	4350.98	16.43	6.47	3%
MS 30 (M) 13-20-35 (8F)	***-20%***	0.42	0.33	0.11	130	200	350	**Ms**	6.02E+07	3.58E+07	-40%	3480.78	15.94	6.28	0%
MS 30 (M) 13-20-35 (8F)	***-10%***	0.42	0.33	0.11	130	200	350	**Ms**	6.02E+07	4.71E+07	-22%	3915.88	15.94	6.28	0%
MS 30 (M) 13-20-35 (8F)	***0%***	0.42	0.33	0.11	130	200	350	**O**	6.02E+07	6.02E+07	0%	4350.98	15.94	6.28	0%
MS 30 (M) 13-20-35 (8F)	***15%***	0.42	0.33	0.11	130	200	350	**Ms**	6.02E+07	8.32E+07	38%	5003.63	15.94	6.28	0%

Id. Pav.	D	a1	a2	a3	h1 [mm]	h2 [mm]	h3 [mm]	Dcode	Esal0%	Esalmod	DEsal	Mr [psi]	SN [cm]	SN [inch]	DSN
MS 90 (P) 11-18-15 (3F)	***-20%***	0.38	0.33	0.12	110	180	150	**M1**	1.22E+08	9.64E+07	-21%	13052.94	11.98	4.72	-3%
MS 90 (P) 11-18-15 (3F)	***-10%***	0.40	0.33	0.12	110	180	150	**M1**	1.22E+08	1.09E+08	-10%	13052.94	12.20	4.80	-2%
MS 90 (P) 11-18-15 (3F)	***0%***	0.42	0.33	0.12	110	180	150	**O**	1.22E+08	1.22E+08	0%	13052.94	12.39	4.88	0%
MS 90 (P) 11-18-15 (3F)	***15%***	0.44	0.33	0.12	110	180	150	**M1**	1.22E+08	1.41E+08	16%	13052.94	12.65	4.98	2%
MS 90 (P) 11-18-15 (3F)	***-20%***	0.42	0.29	0.12	110	180	150	**M2**	1.22E+08	7.64E+07	-37%	13052.94	11.57	4.55	-7%
MS 90 (P) 11-18-15 (3F)	***-10%***	0.42	0.31	0.12	110	180	150	**M2**	1.22E+08	9.71E+07	-20%	13052.94	11.99	4.72	-3%
MS 90 (P) 11-18-15 (3F)	***0%***	0.42	0.33	0.12	110	180	150	**O**	1.22E+08	1.22E+08	0%	13052.94	12.39	4.88	0%
MS 90 (P) 11-18-15 (3F)	***15%***	0.42	0.36	0.12	110	180	150	**M2**	1.22E+08	1.68E+08	38%	13052.94	12.97	5.11	5%
MS 90 (P) 11-18-15 (3F)	***-20%***	0.42	0.33	0.10	110	180	150	**M3**	1.22E+08	1.01E+08	-17%	13052.94	12.06	4.75	-3%
MS 90 (P) 11-18-15 (3F)	***-10%***	0.42	0.33	0.11	110	180	150	**M3**	1.22E+08	1.12E+08	-8%	13052.94	12.24	4.82	-1%
MS 90 (P) 11-18-15 (3F)	***0%***	0.42	0.33	0.12	110	180	150	**O**	1.22E+08	1.22E+08	0%	13052.94	12.39	4.88	0%
MS 90 (P) 11-18-15 (3F)	***15%***	0.42	0.33	0.13	110	180	150	**M3**	1.22E+08	1.37E+08	12%	13052.94	12.60	4.96	2%
MS 90 (P) 11-18-15 (3F)	***-20%***	0.42	0.33	0.12	110	180	150	**Ms**	1.22E+08	7.26E+07	-40%	10442.35	12.39	4.88	0%
MS 90 (P) 11-18-15 (3F)	***-10%***	0.42	0.33	0.12	110	180	150	**Ms**	1.22E+08	9.54E+07	-22%	11747.64	12.39	4.88	0%
MS 90 (P) 11-18-15 (3F)	***0%***	0.42	0.33	0.12	110	180	150	**O**	1.22E+08	1.22E+08	0%	13052.94	12.39	4.88	0%
MS 90 (P) 11-18-15 (3F)	***15%***	0.42	0.33	0.12	110	180	150	**Ms**	1.22E+08	1.68E+08	38%	15010.88	12.39	4.88	0%
MS 90 (PP) 11-25-15 (6F)	***-20%***	0.38	0.33	0.12	110	250	150	**M1**	4.21E+08	3.40E+08	-19%	13052.94	14.31	5.63	-3%
MS 90 (PP) 11-25-15 (6F)	***-10%***	0.40	0.33	0.12	110	250	150	**M1**	4.21E+08	3.81E+08	-9%	13052.94	14.52	5.72	-1%
MS 90 (PP) 11-25-15 (6F)	***0%***	0.42	0.33	0.12	110	250	150	**O**	4.21E+08	4.21E+08	0%	13052.94	14.72	5.80	0%
MS 90 (PP) 11-25-15 (6F)	***15%***	0.44	0.33	0.12	110	250	150	**M1**	4.21E+08	4.79E+08	14%	13052.94	14.98	5.90	2%
MS 90 (PP) 11-25-15 (6F)	***-20%***	0.42	0.29	0.12	110	250	150	**M2**	4.21E+08	2.33E+08	-45%	13052.94	13.58	5.35	-8%
MS 90 (PP) 11-25-15 (6F)	***-10%***	0.42	0.31	0.12	110	250	150	**M2**	4.21E+08	3.16E+08	-25%	13052.94	14.16	5.57	-4%
MS 90 (PP) 11-25-15 (6F)	***0%***	0.42	0.33	0.12	110	250	150	**O**	4.21E+08	4.21E+08	0%	13052.94	14.72	5.80	0%
MS 90 (PP) 11-25-15 (6F)	***15%***	0.42	0.36	0.12	110	250	150	**M2**	4.21E+08	6.28E+08	49%	13052.94	15.53	6.11	5%
MS 90 (PP) 11-25-15 (6F)	***-20%***	0.42	0.33	0.10	110	250	150	**M3**	4.21E+08	3.55E+08	-15%	13052.94	14.39	5.67	-2%
MS 90 (PP) 11-25-15 (6F)	***-10%***	0.42	0.33	0.11	110	250	150	**M3**	4.21E+08	3.89E+08	-8%	13052.94	14.56	5.73	-1%
MS 90 (PP) 11-25-15 (6F)	***0%***	0.42	0.33	0.12	110	250	150	**O**	4.21E+08	4.21E+08	0%	13052.94	14.72	5.80	0%

Id. Pav.	D	a1	a2	a3	h1 [mm]	h2 [mm]	h3 [mm]	Dcode	Esal0%	Esalmod	DEsal	Mr [psi]	SN [cm]	SN [inch]	DSN
MS 90 (PP) 11-25-15 (6F)	***15%***	0.42	0.33	0.13	110	250	150	**M3**	4.21E+08	4.67E+08	11%	13052.94	14.93	5.88	1%
MS 90 (PP) 11-25-15 (6F)	***-20%***	0.42	0.33	0.12	110	250	150	**Ms**	4.21E+08	2.51E+08	-40%	10442.35	14.72	5.80	0%
MS 90 (PP) 11-25-15 (6F)	***-10%***	0.42	0.33	0.12	110	250	150	**Ms**	4.21E+08	3.29E+08	-22%	11747.64	14.72	5.80	0%
MS 90 (PP) 11-25-15 (6F)	***0%***	0.42	0.33	0.12	110	250	150	**O**	4.21E+08	4.21E+08	0%	13052.94	14.72	5.80	0%
MS 90 (PP) 11-25-15 (6F)	***15%***	0.42	0.33	0.12	110	250	150	**Ms**	4.21E+08	5.82E+08	38%	15010.88	14.72	5.80	0%
MS 90 (M) 10-8-15 (7F)	***-20%***	0.38	0.33	0.11	100	80	150	**M1**	1.43E+07	1.05E+07	-26%	13052.94	8.12	3.20	-4%
MS 90 (M) 10-8-15 (7F)	***-10%***	0.40	0.33	0.11	100	80	150	**M1**	1.43E+07	1.24E+07	-13%	13052.94	8.32	3.27	-2%
MS 90 (M) 10-8-15 (7F)	***0%***	0.42	0.33	0.11	100	80	150	**O**	1.43E+07	1.43E+07	0%	13052.94	8.50	3.34	0%
MS 90 (M) 10-8-15 (7F)	***15%***	0.44	0.33	0.11	100	80	150	**M1**	1.43E+07	1.72E+07	20%	13052.94	8.73	3.44	3%
MS 90 (M) 10-8-15 (7F)	***-20%***	0.42	0.29	0.11	100	80	150	**M2**	1.43E+07	1.06E+07	-25%	13052.94	8.13	3.20	-4%
MS 90 (M) 10-8-15 (7F)	***-10%***	0.42	0.31	0.11	100	80	150	**M2**	1.43E+07	1.24E+07	-13%	13052.94	8.32	3.27	-2%
MS 90 (M) 10-8-15 (7F)	***0%***	0.42	0.33	0.11	100	80	150	**O**	1.43E+07	1.43E+07	0%	13052.94	8.50	3.34	0%
MS 90 (M) 10-8-15 (7F)	***15%***	0.42	0.36	0.11	100	80	150	**M2**	1.43E+07	1.74E+07	22%	13052.94	8.75	3.45	3%
MS 90 (M) 10-8-15 (7F)	***-20%***	0.42	0.33	0.09	100	80	150	**M3**	1.43E+07	1.10E+07	-23%	13052.94	8.17	3.21	-4%
MS 90 (M) 10-8-15 (7F)	***-10%***	0.42	0.33	0.10	100	80	150	**M3**	1.43E+07	1.26E+07	-12%	13052.94	8.34	3.28	-2%
MS 90 (M) 10-8-15 (7F)	***0%***	0.42	0.33	0.11	100	80	150	**O**	1.43E+07	1.43E+07	0%	13052.94	8.50	3.34	0%
MS 90 (M) 10-8-15 (7F)	***15%***	0.42	0.33	0.12	100	80	150	**M3**	1.43E+07	1.68E+07	18%	13052.94	8.70	3.43	2%
MS 90 (M) 10-8-15 (7F)	***-20%***	0.42	0.33	0.11	100	80	150	**Ms**	1.43E+07	8.50E+06	-40%	10442.35	8.50	3.34	0%
MS 90 (M) 10-8-15 (7F)	***-10%***	0.42	0.33	0.11	100	80	150	**Ms**	1.43E+07	1.12E+07	-22%	11747.64	8.50	3.34	0%
MS 90 (M) 10-8-15 (7F)	***0%***	0.42	0.33	0.11	100	80	150	**O**	1.43E+07	1.43E+07	0%	13052.94	8.50	3.34	0%
MS 90 (M) 10-8-15 (7F)	***15%***	0.42	0.33	0.11	100	80	150	**Ms**	1.43E+07	1.97E+07	38%	15010.88	8.50	3.34	0%
Ms 30 (M-L)	***-20%***	0.38	0.29	0.11	110	170	350	**M1 M2**	2.40E+07	1.30E+07	-46%	4350.98	12.96	5.10	-8%
Ms 30 (M-L)	***15%***	0.44	0.36	0.11	110	170	350	**M1 M2**	2.40E+07	3.44E+07	43%	4350.98	14.81	5.83	5%
Ms 30 (PP-P)	***-20%***	0.38	0.29	0.12	110	220	350	**M1 M2**	6.55E+07	3.36E+07	-49%	4350.98	14.76	5.81	-8%
Ms 30 (PP-P)	***15%***	0.44	0.36	0.12	110	220	350	**M1 M2**	6.55E+07	9.71E+07	48%	4350.98	16.96	6.68	5%
Ms 90 (M-L)	***-20%***	0.38	0.29	0.11	130	160	150	**M1 M2**	6.23E+07	3.40E+07	-45%	13052.94	11.23	4.42	-10%
Ms 90 (M-L)	***15%***	0.44	0.36	0.11	130	160	150	**M1 M2**	6.23E+07	8.94E+07	43%	13052.94	13.13	5.17	6%
Ms 90 (PP-P)	***-20%***	0.38	0.29	0.12	110	170	150	**M1 M2**	1.01E+08	5.18E+07	-49%	13052.94	10.91	4.30	-10%
Ms 90 (PP-P)	***15%***	0.44	0.36	0.12	110	170	150	**M1 M2**	1.01E+08	1.49E+08	48%	13052.94	12.76	5.02	6%
MS 30 (L) 9-15-35	***-20%***	0.38	0.29	0.11	90	150	350	**M1 M2**	1.07E+07	6.15E+06	-43%	4350.98	11.62	4.57	-8%
MS 30 (L) 9-15-35	***15%***	0.44	0.36	0.11	90	150	350	**M1 M2**	1.07E+07	1.49E+07	39%	4350.98	13.21	5.20	5%
MS90 (L) 9-12-15	***-20%***	0.38	0.29	0.11	90	120	150	**M1 M2**	2.02E+07	1.13E+07	-44%	13052.94	8.55	3.37	-9%
MS90 (L) 9-12-15	***15%***	0.44	0.36	0.11	90	120	150	**M1 M2**	2.02E+07	2.84E+07	40%	13052.94	9.93	3.91	6%
MS 30 (M) 13-20-35 (8F)	***-20%***	0.38	0.29	0.11	130	200	350	**M1 M2**	6.02E+07	3.08E+07	-49%	4350.98	14.59	5.74	-8%
MS 30 (M) 13-20-35(8F)	***15%***	0.44	0.36	0.11	130	200	350	**M1 M2**	6.02E+07	8.90E+07	48%	4350.98	16.77	6.60	5%

Id. Pav.	D	a1	a2	a3	h1 [mm]	h2 [mm]	h3 [mm]	Dcode	Esal0%	Esalmod	DEsal	Mr [psi]	SN [cm]	SN [inch]	DSN
MS 90 (P) 11-18-15 (3F)	***-20%***	0.38	0.29	0.12	110	180	150	**M1 M2**	1.22E+08	6.15E+07	-49%	13052.94	11.20	4.41	-10 %
MS 90 (P) 11-18-15 (3F)	***15%***	0.44	0.36	0.12	110	180	150	**M1 M2**	1.22E+08	1.82E+08	49%	13052.94	13.12	5.17	6%
MS 90 (PP) 11-25-15 (6F)	***-20%***	0.38	0.29	0.12	110	250	150	**M1 M2**	4.21E+08	1.93E+08	-54%	13052.94	13.23	5.21	-10 %
MS 90 (PP) 11-25-15 (6F)	***15%***	0.44	0.36	0.12	110	250	150	**M1 M2**	4.21E+08	6.64E+08	58%	13052.94	15.64	6.16	6%
MS 90 (M) 10-8-15 (7F)	***-20%***	0.38	0.29	0.11	100	80	150	**M1 M2**	1.43E+07	7.88E+06	-45%	13052.94	7.77	3.06	-9%
MS 90 (M) 10-8-15 (7F)	***15%***	0.44	0.36	0.11	100	80	150	**M1 M2**	1.43E+07	2.00E+07	40%	13052.94	8.93	3.52	5%

Where: Id.Pav = identification name of the paving; ai = layer coefficients; hi = thickness of the layers; Dcode = code that indicates which of the modules has been changed in percentage; Esal0% = Esal calculated for Case 0; Esalmod = Esal calculated in individual cases that consider percentage variations; Desal = is the delta Esal in relation and with respect to Case 0; Mr = subgrade modulus in psi; SN = Structural Number in cm and in inch; DSN = delta SN in relation and with respect to case 0.

APPENDIX 7

DEFLECTIONS FROM FWD TEST SIMULATIONS

In the following, Id. Pav. Is the identification name of the road pavement analyzed; d_i are the deflections at different distances in mm from the center of the loading plate.

Id. Pav.	D	D code	do [µm]	d150 [µm]	d200 [µm]	d300 [µm]	d600 [µm]	d900 [µm]	d1200 [µm]	d1500 [µm]
Ms 30 (M-L)	-20%	M1	239.30	218.40	204.80	189.60	153.50	124.70	102.20	84.78
Ms 30 (M-L)	-10%	M1	235.40	215.60	202.80	187.90	152.40	124.10	101.90	84.69
Ms 30 (M-L)	0%	O	232.20	213.20	201.00	186.40	151.40	123.60	101.70	84.60
Ms 30 (M-L)	15%	M1	228.00	210.00	198.60	184.30	150.10	122.80	101.30	84.48
Ms 30 (M-L)	-20%	M2	241.20	220.10	206.80	190.30	152.60	123.80	101.60	84.41
Ms 30 (M-L)	-10%	M2	236.30	216.40	203.70	188.10	152.00	123.70	101.60	84.52
Ms 30 (M-L)	0%	O	232.20	213.20	201.00	186.40	151.40	123.60	101.70	84.60
Ms 30 (M-L)	15%	M2	226.90	209.10	197.60	184.00	150.60	123.40	101.70	84.72
Ms 30 (M-L)	-20%	M3	240.80	221.40	209.00	193.70	156.40	126.40	103.10	85.14
Ms 30 (M-L)	-10%	M3	236.20	217.10	204.80	189.80	153.70	124.90	102.30	84.85
Ms 30 (M-L)	0%	O	232.20	213.20	201.00	186.40	151.40	123.60	101.70	84.60
Ms 30 (M-L)	15%	M3	226.90	208.10	196.10	181.90	148.40	121.80	100.80	84.30
Ms 30 (M-L)	-20%	Ms	262.40	243.20	230.90	215.90	179.40	149.20	124.70	105.00
Ms 30 (M-L)	-10%	Ms	245.90	226.80	214.50	199.70	164.00	135.10	112.00	93.72
Ms 30 (M-L)	0%	O	232.20	213.20	201.00	186.40	151.40	123.60	101.70	84.60
Ms 30 (M-L)	15%	Ms	215.10	196.20	184.10	169.60	135.70	109.30	88.98	73.49
Ms 30 (PP-P)	-20%	M1	212.20	193.20	180.90	168.80	141.20	118.10	99.16	83.78
Ms 30 (PP-P)	-10%	M1	208.90	190.80	179.30	167.30	140.10	117.50	98.79	83.62
Ms 30 (PP-P)	0%	O	206.00	188.80	177.80	166.00	139.20	116.90	98.46	83.46
Ms 30 (PP-P)	15%	M1	202.30	186.10	175.80	164.20	137.80	116.00	97.99	83.23
Ms 30 (PP-P)	-20%	M2	215.10	195.90	183.80	170.10	140.80	117.40	98.56	83.36
Ms 30 (PP-P)	-10%	M2	210.20	192.00	180.50	167.90	139.90	117.10	98.51	83.42
Ms 30 (PP-P)	0%	O	206.00	188.80	177.80	166.00	139.20	116.90	98.46	83.46
Ms 30 (PP-P)	15%	M2	200.80	184.60	174.30	163.40	138.10	116.40	98.36	83.49
Ms 30 (PP-P)	-20%	M3	212.60	195.10	184.00	171.70	143.30	119.50	99.99	84.21
Ms 30 (PP-P)	-10%	M3	209.10	191.70	180.70	168.60	141.10	118.10	99.16	83.80
Ms 30 (PP-P)	0%	O	206.00	188.80	177.80	166.00	139.20	116.90	98.46	83.46
Ms 30 (PP-P)	15%	M3	202.00	184.90	174.00	162.40	136.60	115.20	97.54	83.02
Ms 30 (PP-P)	-20%	Ms	232.90	215.50	204.50	192.40	164.40	140.40	120.00	103.00
Ms 30 (PP-P)	-10%	Ms	218.20	200.90	189.90	177.90	150.60	127.50	108.10	92.19
Ms 30 (PP-P)	0%	O	206.00	188.80	177.80	166.00	139.20	116.90	98.46	83.46
Ms 30 (PP-P)	15%	Ms	190.80	173.60	162.70	151.00	124.90	103.70	86.51	72.76
Ms 90 (M-L)	-20%	M1	142.10	122.00	109.10	95.70	67.59	48.60	36.27	28.29
Ms 90 (M-L)	-10%	M1	139.00	120.10	108.00	94.92	67.27	48.55	36.30	28.34
Ms 90 (M-L)	0%	O	136.30	118.40	107.00	94.23	66.99	48.49	36.33	28.38
Ms 90 (M-L)	15%	M1	132.90	116.30	105.70	93.30	66.60	48.41	36.36	28.43
Ms 90 (M-L)	-20%	M2	143.10	123.60	111.30	96.95	67.42	48.29	36.05	28.17
Ms 90 (M-L)	-10%	M2	139.40	120.80	109.00	95.48	67.19	48.41	36.20	28.28

Id. Pav.	D	D code	do [µm]	d150 [µm]	d200 [µm]	d300 [µm]	d600 [µm]	d900 [µm]	d1200 [µm]	d1500 [µm]
Ms 90 (M-L)	0%	O	136.30	118.40	107.00	94.23	66.99	48.49	36.33	28.38
Ms 90 (M-L)	15%	M2	132.40	115.40	104.50	92.61	66.69	48.59	36.49	28.51
Ms 90 (M-L)	-20%	M3	139.30	121.30	109.70	96.57	68.25	49.00	36.43	28.30
Ms 90 (M-L)	-10%	M3	137.60	119.60	108.10	95.18	67.45	48.62	36.29	28.28
Ms 90 (M-L)	0%	O	136.10	118.20	106.80	93.99	66.78	48.32	36.19	28.27
Ms 90 (M-L)	15%	M3	134.20	116.40	105.10	92.52	65.98	47.98	36.09	28.27
Ms 90 (M-L)	-20%	Ms	152.80	134.70	123.10	109.90	80.63	59.78	45.45	35.74
Ms 90 (M-L)	-10%	Ms	143.50	125.50	114.00	101.00	72.87	53.34	40.23	31.51
Ms 90 (M-L)	0%	O	136.10	118.20	106.80	93.99	66.78	48.32	36.19	28.27
Ms 90 (M-L)	15%	Ms	127.00	109.30	97.92	85.42	59.39	42.30	31.39	24.43
Ms 90 (PP-P)	-20%	M1	143.10	122.90	109.90	96.27	67.45	48.27	35.96	28.07
Ms 90 (PP-P)	-10%	M1	140.40	121.30	109.00	95.56	67.15	48.22	36.00	28.11
Ms 90 (PP-P)	0%	O	138.10	119.80	108.10	94.93	66.88	48.17	36.02	28.15
Ms 90 (PP-P)	15%	M1	135.20	118.00	107.00	94.07	66.52	48.09	36.05	28.20
Ms 90 (PP-P)	-20%	M2	145.60	125.30	112.60	97.56	67.21	47.93	35.75	27.97
Ms 90 (PP-P)	-10%	M2	141.50	122.30	110.20	96.14	67.04	48.07	35.90	28.06
Ms 90 (PP-P)	0%	O	138.10	119.80	108.10	94.93	66.88	48.17	36.02	28.15
Ms 90 (PP-P)	15%	M2	133.80	116.60	105.60	93.34	66.64	48.29	36.18	28.26
Ms 90 (PP-P)	-20%	M3	141.50	123.00	111.10	97.54	68.29	48.76	36.20	28.15
Ms 90 (PP-P)	-10%	M3	139.70	121.30	109.50	96.11	67.51	48.43	36.09	28.15
Ms 90 (PP-P)	0%	O	138.10	119.80	108.10	94.93	66.88	48.17	36.02	28.15
Ms 90 (PP-P)	15%	M3	136.10	118.00	106.40	93.42	66.11	47.87	35.95	28.16
Ms 90 (PP-P)	-20%	Ms	155.30	136.80	124.90	111.20	80.96	59.72	45.29	35.59
Ms 90 (PP-P)	-10%	Ms	145.70	127.30	115.60	102.10	73.07	53.22	40.06	31.38
Ms 90 (PP-P)	0%	O	138.10	119.80	108.10	94.93	66.88	48.17	36.02	28.15
Ms 90 (PP-P)	15%	Ms	128.80	110.60	99.07	86.14	59.38	42.10	31.21	24.32
MS 30 (L) 9-15-35	-20%	M1	263.00	240.00	225.00	206.50	161.90	128.40	103.40	84.87
MS 30 (L) 9-15-35	-10%	M1	259.40	237.30	223.00	204.70	160.90	127.90	103.30	84.83
MS 30 (L) 9-15-36	0%	O	256.30	234.90	221.20	203.20	160.10	127.50	103.10	84.80
MS 30 (L) 9-15-37	15%	M1	252.30	231.80	218.80	201.10	158.90	126.90	102.90	84.74
MS 30 (L) 9-15-38	-20%	M2	266.10	242.00	226.90	206.70	160.80	127.50	102.90	84.62
MS 30 (L) 9-15-35	-10%	M2	260.80	238.20	223.80	204.80	160.50	127.50	103.00	84.71
MS 30 (L) 9-15-35	0%	O	256.30	234.90	221.20	203.20	160.10	127.50	103.10	84.80
MS 30 (L) 9-15-35	15%	M2	250.60	230.70	217.80	201.00	159.50	127.50	103.20	84.90
MS 30 (L) 9-15-35	-20%	M3	267.30	245.40	231.30	212.20	165.70	130.40	104.30	85.05
MS 30 (L) 9-15-35	-10%	M3	261.50	239.90	225.90	207.50	162.70	128.80	103.60	84.91
MS 30 (L) 9-15-35	0%	O	256.30	234.90	221.20	203.20	160.10	127.50	103.10	84.80
MS 30 (L) 9-15-35	15%	M3	249.60	228.60	215.10	197.70	156.70	125.80	102.40	84.66
MS 30 (L) 9-15-35	-20%	Ms	289.40	267.80	253.90	235.50	190.20	154.60	127.10	105.70

Id. Pav.	D	D code	do [µm]	d150 [µm]	d200 [µm]	d300 [µm]	d600 [µm]	d900 [µm]	d1200 [µm]	d1500 [µm]
MS 30 (L) 9-15-35	-10%	Ms	271.30	249.80	236.00	217.80	173.70	139.70	113.80	94.13
MS 30 (L) 9-15-35	0%	O	256.30	234.90	221.20	203.20	160.10	127.50	103.10	84.80
MS 30 (L) 9-15-35	15%	Ms	237.50	216.30	202.70	185.00	143.20	112.40	89.94	73.45
MS90 (L) 9-12-15	-20%	M1	175.10	150.40	134.30	114.20	71.96	48.08	34.87	27.20
MS90 (L) 9-12-15	-10%	M1	172.30	148.50	133.20	113.50	71.81	48.13	34.92	27.23
MS90 (L) 9-12-16	0%	O	170.00	146.90	132.30	112.80	71.68	48.16	34.97	27.25
MS90 (L) 9-12-17	15%	M1	166.90	144.90	130.90	111.80	71.48	48.20	35.03	27.28
MS90 (L) 9-12-18	-20%	M2	178.20	152.60	136.50	114.90	71.51	47.80	34.76	27.18
MS90 (L) 9-12-15	-10%	M2	173.70	149.50	134.20	113.70	71.61	48.00	34.87	27.21
MS90 (L) 9-12-15	0%	O	170.00	146.90	132.30	112.80	71.68	48.16	34.97	27.25
MS90 (L) 9-12-15	15%	M2	165.20	143.60	129.80	111.50	71.74	48.38	35.10	27.30
MS90 (L) 9-12-15	-20%	M3	175.70	152.10	137.10	116.70	73.30	48.58	34.96	27.15
MS90 (L) 9-12-15	-10%	M3	172.60	149.30	134.50	114.60	72.40	48.34	34.96	27.20
MS90 (L) 9-12-15	0%	O	170.00	146.90	132.30	112.80	71.68	48.16	34.97	27.25
MS90 (L) 9-12-15	15%	M3	166.60	144.00	129.50	110.50	70.82	47.97	34.99	27.31
MS90 (L) 9-12-15	-20%	Ms	191.40	168.00	153.00	132.50	87.69	60.37	44.21	34.43
MS90 (L) 9-12-15	-10%	Ms	179.50	156.20	141.40	121.50	78.69	53.48	38.98	30.36
MS90 (L) 9-12-15	0%	O	170.00	146.90	132.30	112.80	71.68	48.16	34.97	27.25
MS90 (L) 9-12-15	15%	Ms	158.30	135.60	121.10	102.10	63.21	41.82	30.22	23.57
MS 30 (M) 13-20-35 (8F)	-20%	M1	216.00	196.60	184.10	171.60	143.20	119.40	99.86	84.11
MS 30 (M) 13-20-35 (8F)	-10%	M1	212.00	193.80	182.10	169.90	142.00	118.70	99.47	83.94
MS 30 (M) 13-20-35 (8F)	0%	O	208.60	191.40	180.40	168.50	141.00	118.00	99.13	83.78
MS 30 (M) 13-20-35 (8F)	15%	M1	204.30	188.30	178.10	166.50	139.60	117.20	98.65	83.56
MS 30 (M) 13-20-35 (8F)	-20%	M2	217.00	198.20	186.30	172.70	142.60	118.60	99.20	83.65
MS 30 (M) 13-20-35 (8F)	-10%	M2	212.50	194.50	183.10	170.40	141.80	118.30	99.17	83.73
MS 30 (M) 13-20-35 (8F)	0%	O	208.60	191.40	180.40	168.50	141.00	118.00	99.13	83.78
MS 30 (M) 13-20-35 (8F)	15%	M2	203.80	187.50	177.00	165.90	139.90	117.60	99.05	83.84
MS 30 (M) 13-20-35 (8F)	-20%	M3	215.10	197.70	186.50	174.20	145.10	120.70	100.70	84.56
MS 30 (M) 13-20-35 (8F)	-10%	M3	211.70	194.40	183.30	171.20	142.90	119.30	99.86	84.14

Id. Pav.	D	D code	do [µm]	d150 [µm]	d200 [µm]	d300 [µm]	d600 [µm]	d900 [µm]	d1200 [µm]	d1500 [µm]
MS 30 (M) 13-20-35 (8F)	0%	O	208.60	191.40	180.40	168.50	141.00	118.00	99.13	83.78
MS 30 (M) 13-20-35 (8F)	15%	M3	204.60	187.50	176.60	164.90	138.40	116.40	98.20	83.33
MS 30 (M) 13-20-35 (8F)	-20%	Ms	235.80	218.50	207.40	195.20	166.50	141.80	120.90	103.40
MS 30 (M) 13-20-35 (8F)	-10%	Ms	221.00	203.70	192.60	180.60	152.50	128.80	108.90	92.56
MS 30 (M) 13-20-35 (8F)	0%	O	208.60	191.40	180.40	168.50	141.00	118.00	99.13	83.78
MS 30 (M) 13-20-35 (8F)	15%	Ms	193.20	176.10	165.20	153.30	126.60	104.80	87.10	73.04
MS 90 (P) 11-18-15 (3F)	-20%	M1	139.80	120.10	107.30	94.25	66.77	48.19	36.06	28.19
MS 90 (P) 11-18-15 (3F)	-10%	M1	137.20	118.50	106.40	93.55	66.46	48.12	36.09	28.23
MS 90 (P) 11-18-15 (3F)	0%	O	135.00	117.10	105.60	92.94	66.18	48.06	36.11	28.27
MS 90 (P) 11-18-15 (3F)	15%	M1	132.10	115.30	104.50	92.11	65.80	47.97	36.13	28.31
MS 90 (P) 11-18-15 (3F)	-20%	M2	142.60	122.70	110.10	95.65	66.57	47.85	35.84	28.07
MS 90 (P) 11-18-15 (3F)	-10%	M2	138.40	119.60	107.70	94.18	66.37	47.97	35.99	28.18
MS 90 (P) 11-18-15 (3F)	0%	O	135.00	117.10	105.60	92.94	66.18	48.06	36.11	28.27
MS 90 (P) 11-18-15 (3F)	15%	M2	130.60	113.80	103.00	91.31	65.90	48.16	36.27	28.39
MS 90 (P) 11-18-15 (3F)	-20%	M3	138.20	120.10	108.50	95.43	67.56	48.67	36.31	28.28
MS 90 (P) 11-18-15 (3F)	-10%	M3	136.40	118.40	106.90	94.07	66.80	48.33	36.19	28.27
MS 90 (P) 11-18-15 (3F)	0%	O	135.00	117.10	105.60	92.94	66.18	48.06	36.11	28.27
MS 90 (P) 11-18-15 (3F)	15%	M3	133.10	115.30	104.00	91.51	65.42	47.75	36.02	28.27
MS 90 (P) 11-18-15 (3F)	-20%	Ms	151.70	133.60	122.00	108.80	80.01	59.50	45.36	35.73
MS 90 (P) 11-18-15 (3F)	-10%	Ms	142.40	124.40	112.80	99.95	72.26	53.06	40.14	31.51
MS 90 (P) 11-18-15 (3F)	0%	O	135.00	117.10	105.60	92.94	66.18	48.06	36.11	28.27
MS 90 (P) 11-18-15 (3F)	15%	Ms	125.90	108.10	96.79	84.37	58.80	42.04	31.31	24.43
MS 90 (PP) 11-25-15 (6F)	-20%	M1	121.80	103.90	92.28	82.01	61.77	46.95	36.32	28.84
MS 90 (PP) 11-25-15 (6F)	-10%	M1	119.50	102.50	91.62	81.45	61.42	46.80	36.30	28.86
MS 90 (PP) 11-25-15 (6F)	0%	O	117.60	101.40	91.03	80.96	61.10	46.67	36.27	28.88
MS 90 (PP) 11-25-15 (6F)	15%	M1	115.20	99.85	90.22	80.28	60.67	46.48	36.22	28.90
MS 90 (PP) 11-25-15 (6F)	-20%	M2	125.50	107.20	95.85	84.06	61.89	46.69	36.06	28.65
MS 90 (PP) 11-25-15 (6F)	-10%	M2	121.20	104.00	93.22	82.37	61.48	46.69	36.18	28.77
MS 90 (PP) 11-25-15 (6F)	0%	O	117.60	101.40	91.03	80.96	61.10	46.67	36.27	28.88

Id. Pav.	D	D code	do [µm]	d150 [µm]	d200 [µm]	d300 [µm]	d600 [µm]	d900 [µm]	d1200 [µm]	d1500 [µm]
MS 90 (PP) 11-25-15 (6F)	15%	M2	113.10	97.98	88.25	79.12	60.57	46.62	36.38	29.01
MS 90 (PP) 11-25-15 (6F)	-20%	M3	119.80	103.40	93.02	82.76	62.27	47.32	36.58	28.99
MS 90 (PP) 11-25-15 (6F)	-10%	M3	118.60	102.30	91.94	81.78	61.63	46.96	36.40	28.93
MS 90 (PP) 11-25-15 (6F)	0%	O	117.60	101.40	91.03	80.96	61.10	46.67	36.27	28.88
MS 90 (PP) 11-25-15 (6F)	15%	M3	116.30	100.10	89.86	79.90	60.44	46.32	36.11	28.83
MS 90 (PP) 11-25-15 (6F)	-20%	Ms	131.60	115.20	104.80	94.45	73.30	57.23	45.19	36.34
MS 90 (PP) 11-25-15 (6F)	-10%	Ms	123.80	107.50	97.13	86.92	66.48	51.31	40.17	32.13
MS 90 (PP) 11-25-15 (6F)	0%	O	117.60	101.40	91.03	80.96	61.10	46.67	36.27	28.88
MS 90 (PP) 11-25-15 (6F)	15%	Ms	110.00	93.82	83.56	73.65	54.55	41.07	31.60	25.01
MS 90 (M) 10-8-15 (7F)	-20%	M1	195.20	166.10	147.60	122.60	72.68	47.34	34.30	26.95
MS 90 (M) 10-8-15 (7F)	-10%	M1	191.60	163.90	146.20	121.80	72.65	47.41	34.34	26.95
MS 90 (M) 10-8-15 (7F)	0%	O	188.50	161.90	145.00	121.10	72.61	47.47	34.37	26.96
MS 90 (M) 10-8-15 (7F)	15%	M1	184.50	159.30	143.40	120.20	72.56	47.55	34.41	26.96
MS 90 (M) 10-8-15 (7F)	-20%	M2	195.50	166.60	148.50	122.70	72.31	47.15	34.24	26.93
MS 90 (M) 10-8-15 (7F)	-10%	M2	191.70	164.10	146.60	121.90	72.48	47.33	34.31	26.94
MS 90 (M) 10-8-15 (7F)	0%	O	188.50	161.90	145.00	121.10	72.61	47.47	34.37	26.96
MS 90 (M) 10-8-15 (7F)	15%	M2	184.40	159.10	142.90	120.10	72.77	47.67	34.46	26.98
MS 90 (M) 10-8-15 (7F)	-20%	M3	195.90	168.40	150.90	125.80	74.15	47.70	34.26	26.84
MS 90 (M) 10-8-15 (7F)	-10%	M3	192.00	164.90	147.70	123.30	73.30	47.56	34.32	26.90
MS 90 (M) 10-8-15 (7F)	0%	O	188.50	161.90	145.00	121.10	72.61	47.47	34.37	26.96
MS 90 (M) 10-8-15 (7F)	15%	M3	184.30	158.10	141.60	118.50	71.82	47.39	34.45	27.03
MS 90 (M) 10-8-15 (7F)	-20%	Ms	212.50	185.30	167.90	142.80	89.42	59.77	43.46	33.97
MS 90 (M) 10-8-15 (7F)	-10%	Ms	199.10	172.20	155.10	130.70	79.97	52.83	38.31	30.00
MS 90 (M) 10-8-15 (7F)	0%	O	188.50	161.90	145.00	121.10	72.61	47.47	34.37	26.96
MS 90 (M) 10-8-15 (7F)	15%	Ms	175.60	149.30	132.70	109.50	63.76	41.11	29.71	23.36

Below, in the table, the deflections calculated for those pavements in which the M1 and M2 Modules of the layers in asphalt concrete have been changed at the same time, keeping the other modules constant.

Id. Pav.	D	D code	do [µm]	d150 [µm]	d200 [µm]	d300 [µm]	d600 [µm]	d900 [µm]	d1200 [µm]	d1500 [µm]
Ms 30 (M-L)	-20%	M1 M2	248.40	225.20	210.50	193.40	154.60	124.80	102.10	84.60
Ms 30 (M-L)	15%	M1 M2	222.70	205.90	195.10	181.80	149.30	122.60	101.30	84.59
Ms 30 (PP-P)	-20%	M1 M2	221.40	200.30	186.80	172.80	142.70	118.60	99.24	83.69
Ms 30 (PP-P)	15%	M1 M2	197.10	181.90	172.20	161.60	136.70	115.60	97.87	83.26
Ms 90 (M-L)	-20%	M1 M2	149.10	127.20	113.30	98.30	67.93	48.38	36.00	28.11
Ms 90 (M-L)	15%	M1 M2	129.00	113.30	103.20	91.63	66.27	48.50	36.53	28.56
Ms 90 (PP-P)	-20%	M1 M2	150.70	128.40	114.30	98.78	67.70	48.02	35.70	27.91
Ms 90 (PP-P)	15%	M1 M2	130.90	114.70	104.40	92.44	66.25	48.20	36.22	28.32
MS 30 (L) 9-15-35	-20%	M1 M2	272.80	247.00	230.50	209.80	162.60	128.30	103.30	84.72
MS 30 (L) 9-15-35	15%	M1 M2	246.60	227.60	215.40	198.90	158.30	126.90	103.00	84.85
MS90 (L) 9-12-15	-20%	M1 M2	183.50	155.90	138.40	116.20	71.74	47.73	34.69	27.15
MS90 (L) 9-12-15	15%	M1 M2	162.10	141.50	128.40	110.50	71.52	48.43	35.17	27.34
MS 30 (M) 13-20-35 (8F)	-20%	M1 M2	224.40	203.30	189.90	175.70	144.70	119.90	99.89	83.97
MS 30 (M) 13-20-35 (8F)	15%	M1 M2	199.50	184.30	174.60	163.90	138.50	116.70	98.55	83.61
MS 90 (P) 11-18-15 (3F)	-20%	M1 M2	147.60	125.70	111.70	96.84	67.09	47.96	35.80	28.01
MS 90 (P) 11-18-15 (3F)	15%	M1 M2	127.80	112.00	101.90	90.44	65.49	48.06	36.29	28.44
MS 90 (PP) 11-25-15 (6F)	-20%	M1 M2	129.80	109.80	97.07	85.03	62.50	46.93	36.10	28.62
MS 90 (PP) 11-25-15 (6F)	15%	M1 M2	110.70	96.49	87.42	78.41	60.12	46.42	36.33	29.03
MS 90 (M) 10-8-15 (7F)	-20%	M1 M2	202.30	170.80	150.90	124.00	72.34	47.05	34.20	26.94
MS 90 (M) 10-8-15 (7F)	15%	M1 M2	180.40	156.50	141.20	119.10	72.70	47.76	34.51	26.99

APPENDIX 8

BASIN INDEXES

In the tables, in the following pages, there are the Basin Indexes calculated starting from the deflections of the FWD test simulations.
The Indexes are from I1 to I14: I1=first deflection under load [µm]; I2=radius of curvature [mm]; I3=equivalent modulus [MPa]; I4=area under pavement performance; I5, I6, I7, I8= area indices; I9=modulus of elasticity at 600 mm from center [MPa]; I10= Anas IS300 or surface curvature index; I11=middle layer index; I12=lower layer index; I13=Anas IS200; I13c=Anas IS_{200CF} corrected with the subgrade; I14=shape factor.
The table below shows the equations of the basin indices for a better understanding of the results.

N. and [unit of measure]	Parameter Id	Name of the Index and significance	Formula
I1 [µm]	D_0'	First deflection under load	D_0'
I2 [mm]	RoC	Radius of Curvature	$RoC = L^2 / \left[2D_0 \left(1 - \frac{D_{300}}{D_0}\right)\right]$
I3 [Mpa]	Eeq	Equivalent Modulus characterizing the condition of all the layers of the pavement	$E_{eq} = \frac{2(1-\mu^2) a\, \sigma_0}{D_0}$
I4 [-]	AUPP	Area under pavement performance characterizing the condition of the pavement upper layer	$AUPP = \frac{5D_0 + 2D_{300} + 2D_{600} + D_{900}}{D_0}$
I5 [-]	Al_1	Area Indices characterizing the condition of upper layer	$Al_1 = \frac{D_0 + D_{300}}{2D_0}$
I6 [-]	Al_2	Area Indices characterizing the condition of middle layer	$Al_2 = \frac{D_{300} + D_{600}}{2D_0}$
I7 [-]	Al_3	Area Indices characterizing the condition of middle layer	$Al_3 = \frac{D_{600} + D_{900}}{2D_0}$
I8 [-]	Al_4	Area Indices characterizing the condition of lower layer	$Al_4 = \frac{D_{900} + D_{1200}}{2D_0}$
I9 [MPa]	E_{0r}	Modulus of Elasticity at 600 mm from center characterizing subgrade layer	$E_{0r} = \frac{(1-\mu^2) a^2\, \sigma_0}{r * D_{600}}$
I10 [µm]	IS300 SCI	Anas Index IS300 Surface Curvature Index characterizing the pavement layers	$IS300 = D_0 - D_{300}$
I11 [µm]	MLI	Middle Layer Index characterizing the condition of the base layer	$MLI = D_{300} - D_{600}$
I12 [µm]	LLI	Lower Layer Index characterizing the condition of the subgrade	$LLI = D_{1200} - D_{1500}$
I13 [µm]	IS200	Anas index IS200	$IS200 = D_0 - D_{200}$
I13c [µm]	IS_{200CF}	Anas Index IS_{200CF} correct with the subgrade	$IS_{200CF} = (1.94 - 0.5 * LOG(D_{900} - D_{1500})) * (D_0 - D_{200})$
I14 [-]	SF	Shape factor	$SF = (D_0 - D_{300}) / D_{200}$

Id. Pav.	D	16hzM1 [Mpa]	16hzM2 [Mpa]	16hzM3 [Mpa]	16hzMs [Mpa]	I1 [µm]	I2 [mm]	I3 [Mpa]	I4 [-]	I5 [-]	I6 [-]	I7 [-]	I8 [-]	I9 [MPa]	I10 [µm]	I11 [µm]	I12 [µm]	I13 [µm]	I13c [µm]	I14 [-]
Ms 30 (M-L)	**-20%**	2914.4	3342.0	316.7	90.9	228.85	1146496.82	623.15	8.54	0.91	0.75	0.61	0.50	121.31	39.25	36.10	17.42	24.05	27.40	0.19
Ms 30 (M-L)	**-10%**	3278.7	3342.0	316.7	90.9	225.50	1196808.51	632.40	8.57	0.92	0.75	0.61	0.50	122.19	37.60	35.50	17.21	22.70	25.93	0.19
Ms 30 (M-L)	**0%**	3643.0	3342.0	316.7	90.9	222.70	1239669.42	640.35	8.59	0.92	0.76	0.62	0.51	123.00	36.30	35.00	17.10	21.70	24.83	0.18
Ms 30 (M-L)	**15%**	4189.5	3342.0	316.7	90.9	219.00	1296829.97	651.17	8.61	0.92	0.76	0.62	0.51	124.06	34.70	34.20	16.82	20.40	23.43	0.17
Ms 30 (M-L)	**-20%**	3643.0	2673.6	316.7	90.9	230.65	1115241.64	618.28	8.51	0.91	0.74	0.60	0.49	122.03	40.35	37.70	17.19	23.85	27.24	0.20
Ms 30 (M-L)	**-10%**	3643.0	3007.8	316.7	90.9	226.35	1176470.59	630.03	8.55	0.92	0.75	0.61	0.50	122.51	38.25	36.10	17.08	22.65	25.90	0.19
Ms 30 (M-L)	**0%**	3643.0	3342.0	316.7	90.9	222.70	1239669.42	640.35	8.59	0.92	0.76	0.62	0.51	123.00	36.30	35.00	17.10	21.70	24.83	0.18
Ms 30 (M-L)	**15%**	3643.0	3843.3	316.7	90.9	218.00	1323529.41	654.16	8.64	0.92	0.77	0.63	0.52	123.65	34.00	33.40	16.98	20.40	23.38	0.17
Ms 30 (M-L)	**-20%**	3643.0	3342.0	253.4	90.9	231.10	1203208.56	617.08	8.58	0.92	0.76	0.61	0.50	119.06	37.40	37.30	17.96	22.10	25.02	0.18
Ms 30 (M-L)	**-10%**	3643.0	3342.0	285.0	90.9	226.65	1221166.89	629.19	8.58	0.92	0.76	0.61	0.50	121.16	36.85	36.10	17.45	21.85	24.88	0.18
Ms 30 (M-L)	**0%**	3643.0	3342.0	316.7	90.9	222.70	1239669.42	640.35	8.59	0.92	0.76	0.62	0.51	123.00	36.30	35.00	17.10	21.70	24.83	0.18
Ms 30 (M-L)	**15%**	3643.0	3342.0	364.2	90.9	217.50	1264044.94	655.66	8.60	0.92	0.76	0.62	0.51	125.48	35.60	33.50	16.50	21.40	24.67	0.18
Ms 30 (M-L)	**-20%**	3643.0	3342.0	316.7	72.7	252.80	1219512.20	564.11	8.72	0.93	0.78	0.65	0.54	103.80	36.90	36.50	19.70	21.90	24.47	0.16
Ms 30 (M-L)	**-10%**	3643.0	3342.0	316.7	81.8	236.35	1227830.83	603.37	8.65	0.92	0.77	0.63	0.52	113.55	36.65	35.70	18.28	21.85	24.73	0.17
Ms 30 (M-L)	**0%**	3643.0	3342.0	316.7	90.9	222.70	1239669.42	640.35	8.59	0.92	0.76	0.62	0.51	123.00	36.30	35.00	17.10	21.70	24.83	0.18
Ms 30 (M-L)	**15%**	3643.0	3342.0	316.7	104.5	205.65	1248266.30	693.44	8.50	0.91	0.74	0.60	0.48	137.23	36.05	33.90	15.49	21.55	25.06	0.20
Ms 30 (PP-P)	**-20%**	2914.4	3342.0	350.5	90.9	202.70	1327433.63	703.54	8.64	0.92	0.76	0.64	0.54	131.88	33.90	27.60	15.38	21.80	25.55	0.19
Ms 30 (PP-P)	**-10%**	3278.7	3342.0	350.5	90.9	199.85	1382488.48	713.57	8.66	0.92	0.77	0.64	0.54	132.92	32.55	27.20	15.17	20.55	24.15	0.18
Ms 30 (PP-P)	**0%**	3643.0	3342.0	350.5	90.9	197.40	1433121.02	722.43	8.68	0.92	0.77	0.65	0.55	133.78	31.40	26.80	15.00	19.60	23.09	0.18
Ms 30 (PP-P)	**15%**	4189.5	3342.0	350.5	90.9	194.20	1500000.00	734.33	8.71	0.92	0.78	0.65	0.55	135.14	30.00	26.40	14.76	18.40	21.75	0.17
Ms 30 (PP-P)	**-20%**	3643.0	2673.6	350.5	90.9	205.50	1271186.44	693.95	8.60	0.91	0.76	0.63	0.53	132.26	35.40	29.30	15.20	21.70	25.48	0.19
Ms 30 (PP-P)	**-10%**	3643.0	3007.8	350.5	90.9	201.10	1355421.69	709.13	8.64	0.92	0.77	0.64	0.54	133.11	33.20	28.00	15.09	20.60	24.23	0.18
Ms 30 (PP-P)	**0%**	3643.0	3342.0	350.5	90.9	197.40	1433121.02	722.43	8.68	0.92	0.77	0.65	0.55	133.78	31.40	26.80	15.00	19.60	23.09	0.18
Ms 30 (PP-P)	**15%**	3643.0	3843.3	350.5	90.9	192.70	1535836.18	740.05	8.73	0.92	0.78	0.66	0.56	134.84	29.30	25.30	14.87	18.40	21.74	0.17
Ms 30 (PP-P)	**-20%**	3643.0	3342.0	280.4	90.9	203.85	1399688.96	699.57	8.68	0.92	0.77	0.64	0.54	129.95	32.15	28.40	15.78	19.85	23.15	0.17
Ms 30 (PP-P)	**-10%**	3643.0	3342.0	315.5	90.9	200.40	1415094.34	711.61	8.68	0.92	0.77	0.65	0.54	131.97	31.80	27.50	15.36	19.70	23.10	0.18
Ms 30 (PP-P)	**0%**	3643.0	3342.0	350.5	90.9	197.40	1433121.02	722.43	8.68	0.92	0.77	0.65	0.55	133.78	31.40	26.80	15.00	19.60	23.09	0.18
Ms 30 (PP-P)	**15%**	3643.0	3342.0	403.1	90.9	193.45	1449275.36	737.18	8.69	0.92	0.77	0.65	0.55	136.32	31.05	25.80	14.52	19.45	23.07	0.18

Id. Pav.	D	M1	M2	M3	Ms	I1	I2	I3	I4	I5	I6	I7	I8	I9	I10	I11	I12	I13	I13c	I14
Ms 30 (PP-P)	**-20%**	3643.0	3342.0	350.5	72.7	224.20	1415094.34	636.07	8.81	0.93	0.80	0.68	0.58	113.27	31.80	28.00	17.00	19.70	22.73	0.16
Ms 30 (PP-P)	**-10%**	3643.0	3342.0	350.5	81.8	209.55	1421800.95	680.54	8.74	0.92	0.78	0.66	0.56	123.65	31.65	27.30	15.91	19.65	22.91	0.17
Ms 30 (PP-P)	**0%**	3643.0	3342.0	350.5	90.9	197.40	1433121.02	722.43	8.68	0.92	0.77	0.65	0.55	133.78	31.40	26.80	15.00	19.60	23.09	0.18
Ms 30 (PP-P)	**15%**	3643.0	3342.0	350.5	104.5	182.20	1442307.69	782.69	8.60	0.91	0.76	0.63	0.52	149.09	31.20	26.10	13.75	19.50	23.30	0.19
Ms 90 (M-L)	**-20%**	2914.4	3342.0	316.7	272.7	132.05	1237964.24	1079.95	7.84	0.86	0.62	0.44	0.32	275.51	36.35	28.11	7.98	22.95	29.52	0.33
Ms 90 (M-L)	**-10%**	3278.7	3342.0	316.7	272.7	129.55	1299451.34	1100.79	7.88	0.87	0.63	0.45	0.33	276.82	34.63	27.65	7.96	21.55	27.74	0.32
Ms 90 (M-L)	**0%**	3643.0	3342.0	316.7	272.7	127.35	1358695.65	1119.80	7.91	0.87	0.63	0.45	0.33	277.98	33.12	27.24	7.95	20.35	26.22	0.31
Ms 90 (M-L)	**15%**	4189.5	3342.0	316.7	272.7	124.60	1437699.68	1144.52	7.96	0.87	0.64	0.46	0.34	279.60	31.30	26.70	7.93	18.90	24.38	0.30
Ms 90 (M-L)	**-20%**	3643.0	2673.6	316.7	272.7	133.35	1236263.74	1069.42	7.83	0.86	0.62	0.43	0.32	276.20	36.40	29.53	7.88	22.05	28.40	0.33
Ms 90 (M-L)	**-10%**	3643.0	3007.8	316.7	272.7	130.10	1299826.69	1096.13	7.87	0.87	0.63	0.44	0.33	277.15	34.62	28.29	7.92	21.10	27.18	0.32
Ms 90 (M-L)	**0%**	3643.0	3342.0	316.7	272.7	127.35	1358695.65	1119.80	7.91	0.87	0.63	0.45	0.33	277.98	33.12	27.24	7.95	20.35	26.22	0.31
Ms 90 (M-L)	**15%**	3643.0	3843.3	316.7	272.7	123.90	1438159.16	1150.98	7.96	0.87	0.64	0.47	0.34	279.23	31.29	25.92	7.98	19.40	25.00	0.30
Ms 90 (M-L)	**-20%**	3643.0	3342.0	253.4	272.7	130.30	1334123.93	1094.45	7.91	0.87	0.63	0.45	0.33	272.84	33.73	28.32	8.13	20.60	26.41	0.31
Ms 90 (M-L)	**-10%**	3643.0	3342.0	285.0	272.7	128.60	1346499.10	1108.92	7.91	0.87	0.63	0.45	0.33	276.08	33.42	27.73	8.01	20.50	26.36	0.31
Ms 90 (M-L)	**0%**	3643.0	3342.0	316.7	272.7	127.15	1357056.69	1121.56	7.91	0.87	0.63	0.45	0.33	278.85	33.16	27.21	7.92	20.35	26.23	0.31
Ms 90 (M-L)	**15%**	3643.0	3342.0	364.2	272.7	125.30	1372788.29	1138.12	7.91	0.87	0.63	0.45	0.34	282.23	32.78	26.54	7.82	20.20	26.11	0.31
Ms 90 (M-L)	**-20%**	3643.0	3342.0	316.7	218.2	143.75	1329394.39	992.05	8.07	0.88	0.66	0.49	0.37	230.95	33.85	29.27	9.71	20.65	25.80	0.27
Ms 90 (M-L)	**-10%**	3643.0	3342.0	316.7	245.5	134.50	1343283.58	1060.27	7.98	0.88	0.65	0.47	0.35	255.55	33.50	28.13	8.72	20.50	26.04	0.29
Ms 90 (M-L)	**0%**	3643.0	3342.0	316.7	272.7	127.15	1357056.69	1121.56	7.91	0.87	0.63	0.45	0.33	278.85	33.16	27.21	7.92	20.35	26.23	0.31
Ms 90 (M-L)	**15%**	3643.0	3342.0	316.7	313.6	118.15	1374885.43	1207.00	7.81	0.86	0.61	0.43	0.31	313.55	32.73	26.03	6.96	20.23	26.58	0.33
Ms 90 (PP-P)	**-20%**	2914.4	3342.0	350.5	272.7	133.00	1225156.55	1072.23	7.82	0.86	0.62	0.44	0.32	276.08	36.73	28.82	7.89	23.10	29.74	0.33
Ms 90 (PP-P)	**-10%**	3278.7	3342.0	350.5	272.7	130.85	1275148.77	1089.85	7.86	0.87	0.62	0.44	0.32	277.31	35.29	28.41	7.89	21.85	28.15	0.32
Ms 90 (PP-P)	**0%**	3643.0	3342.0	350.5	272.7	128.95	1322751.32	1105.91	7.88	0.87	0.63	0.45	0.33	278.43	34.02	28.05	7.87	20.85	26.88	0.31
Ms 90 (PP-P)	**15%**	4189.5	3342.0	350.5	272.7	126.60	1383338.46	1126.44	7.92	0.87	0.63	0.45	0.33	279.94	32.53	27.55	7.85	19.60	25.30	0.30
Ms 90 (PP-P)	**-20%**	3643.0	2673.6	350.5	272.7	135.45	1187648.46	1052.84	7.79	0.86	0.61	0.43	0.31	277.07	37.89	30.35	7.78	22.85	29.47	0.34
Ms 90 (PP-P)	**-10%**	3643.0	3007.8	350.5	272.7	131.90	1258389.26	1081.17	7.84	0.86	0.62	0.44	0.32	277.77	35.76	29.10	7.84	21.70	27.98	0.32
Ms 90 (PP-P)	**0%**	3643.0	3342.0	350.5	272.7	128.95	1322751.32	1105.91	7.88	0.87	0.63	0.45	0.33	278.43	34.02	28.05	7.87	20.85	26.88	0.31
Ms 90 (PP-P)	**15%**	3643.0	3843.3	350.5	272.7	125.20	1412429.38	1139.03	7.94	0.87	0.64	0.46	0.34	279.44	31.86	26.70	7.92	19.60	25.27	0.30
Ms 90 (PP-P)	**-20%**	3643.0	3342.0	280.4	272.7	132.25	1296456.35	1078.31	7.88	0.87	0.63	0.44	0.32	272.68	34.71	29.25	8.05	21.15	27.13	0.31

Id. Pav.	D	M1	M2	M3	Ms	I1	I2	I3	I4	I5	I6	I7	I8	I9	I10	I11	I12	I13	I13c	I14
Ms 90 (PP-P)	**-10%**	3643.0	3342.0	315.5	272.7	130.50	1308519.92	1092.77	7.88	0.87	0.63	0.44	0.32	275.84	34.39	28.60	7.94	21.00	27.02	0.31
Ms 90 (PP-P)	**0%**	3643.0	3342.0	350.5	272.7	128.95	1322751.32	1105.91	7.88	0.87	0.63	0.45	0.33	278.43	34.02	28.05	7.87	20.85	26.88	0.31
Ms 90 (PP-P)	**15%**	3643.0	3342.0	403.1	272.7	127.05	1338090.99	1122.45	7.89	0.87	0.63	0.45	0.33	281.68	33.63	27.31	7.79	20.65	26.69	0.32
Ms 90 (PP-P)	**-20%**	3643.0	3342.0	350.5	218.2	146.05	1291248.21	976.42	8.04	0.88	0.66	0.48	0.36	230.01	34.85	30.24	9.70	21.15	26.41	0.28
Ms 90 (PP-P)	**-10%**	3643.0	3342.0	350.5	245.5	136.50	1308139.53	1044.74	7.96	0.87	0.64	0.46	0.34	254.85	34.40	29.03	8.68	20.90	26.55	0.30
Ms 90 (PP-P)	**0%**	3643.0	3342.0	350.5	272.7	128.95	1322751.32	1105.91	7.88	0.87	0.63	0.45	0.33	278.43	34.02	28.05	7.87	20.85	26.88	0.31
Ms 90 (PP-P)	**15%**	3643.0	3342.0	350.5	313.6	119.70	1340882.00	1191.37	7.78	0.86	0.61	0.42	0.31	313.60	33.56	26.76	6.89	20.63	27.13	0.34
MS 30 (L) 9-15-35	**-20%**	2914.4	3342.0	316.7	90.9	251.50	1000000.00	567.03	8.44	0.91	0.73	0.58	0.46	115.02	45.00	44.60	18.53	26.50	29.70	0.20
MS 30 (L) 9-15-35	**-10%**	3278.7	3342.0	316.7	90.9	248.35	1030927.84	574.22	8.46	0.91	0.74	0.58	0.47	115.73	43.65	43.80	18.47	25.35	28.47	0.20
MS 30 (L) 9-15-35	**0%**	3643.0	3342.0	316.7	90.9	245.60	1061320.75	580.65	8.48	0.91	0.74	0.59	0.47	116.31	42.40	43.10	18.30	24.40	27.44	0.19
MS 30 (L) 9-15-35	**15%**	4189.5	3342.0	316.7	90.9	242.05	1098901.10	589.16	8.50	0.92	0.74	0.59	0.47	117.19	40.95	42.20	18.16	23.25	26.22	0.19
MS 30 (L) 9-15-35	**-20%**	3643.0	2673.6	316.7	90.9	254.05	950369.59	561.33	8.40	0.91	0.72	0.57	0.45	115.81	47.35	45.90	18.28	27.15	30.51	0.21
MS 30 (L) 9-15-35	**-10%**	3643.0	3007.8	316.7	90.9	249.50	1006711.41	571.57	8.44	0.91	0.73	0.58	0.46	116.02	44.70	44.30	18.29	25.70	28.90	0.20
MS 30 (L) 9-15-35	**0%**	3643.0	3342.0	316.7	90.9	245.60	1061320.75	580.65	8.48	0.91	0.74	0.59	0.47	116.31	42.40	43.10	18.30	24.40	27.44	0.19
MS 30 (L) 9-15-35	**15%**	3643.0	3843.3	316.7	90.9	240.65	1134930.64	592.59	8.53	0.92	0.75	0.60	0.48	116.75	39.65	41.50	18.30	22.85	25.71	0.18
MS 30 (L) 9-15-35	**-20%**	3643.0	3342.0	253.4	90.9	256.35	1019252.55	556.30	8.46	0.91	0.74	0.58	0.46	112.38	44.15	46.50	19.25	25.05	27.85	0.19
MS 30 (L) 9-15-35	**-10%**	3643.0	3342.0	285.0	90.9	250.70	1041666.67	568.83	8.47	0.91	0.74	0.58	0.46	114.45	43.20	44.80	18.69	24.80	27.75	0.19
MS 30 (L) 9-15-35	**0%**	3643.0	3342.0	316.7	90.9	245.60	1061320.75	580.65	8.48	0.91	0.74	0.59	0.47	116.31	42.40	43.10	18.30	24.40	27.44	0.19
MS 30 (L) 9-15-35	**15%**	3643.0	3342.0	364.2	90.9	239.10	1086956.52	596.43	8.49	0.91	0.74	0.59	0.48	118.84	41.40	41.00	17.74	24.00	27.19	0.19
MS 30 (L) 9-15-35	**-20%**	3643.0	3342.0	316.7	72.7	278.60	1044083.53	511.87	8.61	0.92	0.76	0.62	0.51	97.91	43.10	45.30	21.40	24.70	27.06	0.17
MS 30 (L) 9-15-35	**-10%**	3643.0	3342.0	316.7	81.8	260.55	1052631.58	547.33	8.54	0.92	0.75	0.60	0.49	107.21	42.75	44.10	19.67	24.55	27.27	0.18
MS 30 (L) 9-15-35	**0%**	3643.0	3342.0	316.7	90.9	245.60	1061320.75	580.65	8.48	0.91	0.74	0.59	0.47	116.31	42.40	43.10	18.30	24.40	27.44	0.19
MS 30 (L) 9-15-35	**15%**	3643.0	3342.0	316.7	104.5	226.90	1073985.68	628.50	8.39	0.91	0.72	0.56	0.45	130.04	41.90	41.80	16.49	24.20	27.70	0.21
MS90 (L) 9-12-15	**-20%**	2914.4	3342.0	316.7	272.7	162.75	926879.51	876.23	7.58	0.85	0.57	0.37	0.25	258.78	48.55	42.24	7.67	28.45	36.42	0.36
MS90 (L) 9-12-15	**-10%**	3278.7	3342.0	316.7	272.7	160.40	959488.27	889.07	7.61	0.85	0.58	0.37	0.26	259.32	46.90	41.69	7.69	27.20	34.81	0.35
MS90 (L) 9-12-15	**0%**	3643.0	3342.0	316.7	272.7	158.45	985761.23	900.01	7.63	0.86	0.58	0.38	0.26	259.79	45.65	41.12	7.72	26.15	33.47	0.35
MS90 (L) 9-12-15	**15%**	4189.5	3342.0	316.7	272.7	155.90	1020408.16	914.73	7.66	0.86	0.59	0.38	0.27	260.52	44.10	40.32	7.75	25.00	31.99	0.34
MS90 (L) 9-12-15	**-20%**	3643.0	2673.6	316.7	272.7	165.40	891089.11	862.19	7.54	0.85	0.56	0.36	0.25	260.41	50.50	43.39	7.58	28.90	37.07	0.37
MS90 (L) 9-12-15	**-10%**	3643.0	3007.8	316.7	272.7	161.60	939457.20	882.47	7.59	0.85	0.57	0.37	0.26	260.04	47.90	42.09	7.66	27.40	35.10	0.36

Id. Pav.	D	M1	M2	M3	Ms	I1	I2	I3	I4	I5	I6	I7	I8	I9	I10	I11	I12	I13	I13c	I14
MS90 (L) 9-12-15	**0%**	3643.0	3342.0	316.7	272.7	158.45	985761.23	900.01	7.63	0.86	0.58	0.38	0.26	259.79	45.65	41.12	7.72	26.15	33.47	0.35
MS90 (L) 9-12-15	**15%**	3643.0	3843.3	316.7	272.7	154.40	1048951.05	923.62	7.69	0.86	0.59	0.39	0.27	259.57	42.90	39.76	7.80	24.60	31.44	0.33
MS90 (L) 9-12-15	**-20%**	3643.0	3342.0	253.4	272.7	163.90	953389.83	870.08	7.61	0.86	0.58	0.37	0.25	254.05	47.20	43.40	7.81	26.80	34.16	0.34
MS90 (L) 9-12-15	**-10%**	3643.0	3342.0	285.0	272.7	160.95	970873.79	886.03	7.62	0.86	0.58	0.38	0.26	257.21	46.35	42.20	7.76	26.45	33.79	0.34
MS90 (L) 9-12-15	**0%**	3643.0	3342.0	316.7	272.7	158.45	985761.23	900.01	7.63	0.86	0.58	0.38	0.26	259.79	45.65	41.12	7.72	26.15	33.47	0.35
MS90 (L) 9-12-15	**15%**	3643.0	3342.0	364.2	272.7	155.30	1004464.29	918.27	7.64	0.86	0.58	0.38	0.27	262.94	44.80	39.68	7.68	25.80	33.09	0.35
MS90 (L) 9-12-15	**-20%**	3643.0	3342.0	316.7	218.2	179.70	953389.83	793.58	7.79	0.87	0.61	0.41	0.29	212.36	47.20	44.81	9.78	26.70	32.92	0.31
MS90 (L) 9-12-15	**-10%**	3643.0	3342.0	316.7	245.5	167.85	970873.79	849.61	7.70	0.86	0.60	0.39	0.28	236.65	46.35	42.81	8.62	26.45	33.27	0.33
MS90 (L) 9-12-15	**0%**	3643.0	3342.0	316.7	272.7	158.45	985761.23	900.01	7.63	0.86	0.58	0.38	0.26	259.79	45.65	41.12	7.72	26.15	33.47	0.35
MS90 (L) 9-12-15	**15%**	3643.0	3342.0	316.7	313.6	146.95	1003344.48	970.44	7.53	0.85	0.56	0.36	0.25	294.60	44.85	38.89	6.65	25.85	33.85	0.37
MS 30 (M) 13-20-35 (8F)	**-20%**	2914.4	3342.0	316.7	90.9	206.30	1296829.97	691.26	8.63	0.92	0.76	0.64	0.53	130.04	34.70	28.40	15.75	22.20	25.89	0.19
MS 30 (M) 13-20-35 (8F)	**-10%**	3278.7	3342.0	316.7	90.9	202.90	1363636.36	702.84	8.66	0.92	0.77	0.64	0.54	131.14	33.00	27.90	15.53	20.80	24.32	0.18
MS 30 (M) 13-20-35 (8F)	**0%**	3643.0	3342.0	316.7	90.9	200.00	1428571.43	713.03	8.69	0.92	0.77	0.65	0.54	132.07	31.50	27.50	15.35	19.60	22.99	0.17
MS 30 (M) 13-20-35 (8F)	**15%**	4189.5	3342.0	316.7	90.9	196.30	1510067.11	726.47	8.72	0.92	0.78	0.65	0.55	133.39	29.80	26.90	15.09	18.20	21.41	0.17
MS 30 (M) 13-20-35 (8F)	**-20%**	3643.0	2673.6	316.7	90.9	207.60	1289398.28	686.93	8.61	0.92	0.76	0.63	0.52	130.59	34.90	30.10	15.55	21.30	24.88	0.19
MS 30 (M) 13-20-35 (8F)	**-10%**	3643.0	3007.8	316.7	90.9	203.50	1359516.62	700.77	8.65	0.92	0.77	0.64	0.53	131.32	33.10	28.60	15.44	20.40	23.88	0.18
MS 30 (M) 13-20-35 (8F)	**0%**	3643.0	3342.0	316.7	90.9	200.00	1428571.43	713.03	8.69	0.92	0.77	0.65	0.54	132.07	31.50	27.50	15.35	19.60	22.99	0.17
MS 30 (M) 13-20-35 (8F)	**15%**	3643.0	3843.3	316.7	90.9	195.65	1512605.04	728.89	8.73	0.92	0.78	0.66	0.55	133.11	29.75	26.00	15.21	18.65	21.93	0.17
MS 30 (M) 13-20-35 (8F)	**-20%**	3643.0	3342.0	253.4	90.9	206.40	1397515.53	690.92	8.68	0.92	0.77	0.64	0.54	128.34	32.20	29.10	16.14	19.90	23.10	0.17
MS 30 (M) 13-20-35 (8F)	**-10%**	3643.0	3342.0	285.0	90.9	203.05	1412872.84	702.32	8.68	0.92	0.77	0.65	0.54	130.31	31.85	28.30	15.72	19.75	23.05	0.17
MS 30 (M) 13-20-35 (8F)	**0%**	3643.0	3342.0	316.7	90.9	200.00	1428571.43	713.03	8.69	0.92	0.77	0.65	0.54	132.07	31.50	27.50	15.35	19.60	22.99	0.17
MS 30 (M) 13-20-35 (8F)	**15%**	3643.0	3342.0	364.2	90.9	196.05	1444622.79	727.40	8.69	0.92	0.77	0.65	0.55	134.55	31.15	26.50	14.87	19.45	22.96	0.18
MS 30 (M) 13-20-35 (8F)	**-20%**	3643.0	3342.0	316.7	72.7	227.15	1408450.70	627.81	8.81	0.93	0.80	0.68	0.58	111.84	31.95	28.70	17.50	19.75	22.67	0.15
MS 30 (M) 13-20-35 (8F)	**-10%**	3643.0	3342.0	316.7	81.8	212.35	1417322.83	671.56	8.74	0.93	0.78	0.66	0.56	122.11	31.75	28.10	16.34	19.75	22.92	0.16
MS 30 (M) 13-20-35 (8F)	**0%**	3643.0	3342.0	316.7	90.9	200.00	1428571.43	713.03	8.69	0.92	0.77	0.65	0.54	132.07	31.50	27.50	15.35	19.60	22.99	0.17
MS 30 (M) 13-20-35 (8F)	**15%**	3643.0	3342.0	316.7	104.5	184.65	1435406.70	772.31	8.60	0.92	0.76	0.63	0.52	147.09	31.35	26.70	14.06	19.45	23.13	0.19
MS 90 (P) 11-18-15 (3F)	**-20%**	2914.4	3342.0	350.5	272.7	129.95	1260504.20	1097.40	7.85	0.86	0.62	0.44	0.32	278.89	35.70	27.48	7.87	22.65	29.21	0.33
MS 90 (P) 11-18-15 (3F)	**-10%**	3278.7	3342.0	350.5	272.7	127.85	1311953.35	1115.42	7.88	0.87	0.63	0.45	0.33	280.19	34.30	27.09	7.86	21.45	27.69	0.32
MS 90 (P) 11-18-15 (3F)	**0%**	3643.0	3342.0	350.5	272.7	126.05	1359106.01	1131.35	7.91	0.87	0.63	0.45	0.33	281.38	33.11	26.76	7.84	20.45	26.42	0.31

Id. Pav.	D	M1	M2	M3	Ms	I1	I2	I3	I4	I5	I6	I7	I8	I9	I10	I11	I12	I13	I13c	I14
MS 90 (P) 11-18-15 (3F)	**15%**	4189.5	3342.0	350.5	272.7	123.70	1424501.42	1152.84	7.94	0.87	0.64	0.46	0.34	283.00	31.59	26.31	7.82	19.20	24.83	0.30
MS 90 (P) 11-18-15 (3F)	**-20%**	3643.0	2673.6	350.5	272.7	132.65	1216216.22	1075.06	7.81	0.86	0.61	0.43	0.32	279.73	37.00	29.08	7.77	22.55	29.13	0.34
MS 90 (P) 11-18-15 (3F)	**-10%**	3643.0	3007.8	350.5	272.7	129.00	1292360.71	1105.48	7.86	0.87	0.62	0.44	0.33	280.57	34.82	27.81	7.81	21.30	27.51	0.32
MS 90 (P) 11-18-15 (3F)	**0%**	3643.0	3342.0	350.5	272.7	126.05	1359106.01	1131.35	7.91	0.87	0.63	0.45	0.33	281.38	33.11	26.76	7.84	20.45	26.42	0.31
MS 90 (P) 11-18-15 (3F)	**15%**	3643.0	3843.3	350.5	272.7	122.20	1456782.13	1167.00	7.97	0.87	0.64	0.47	0.35	282.57	30.89	25.41	7.88	19.20	24.81	0.30
MS 90 (P) 11-18-15 (3F)	**-20%**	3643.0	3342.0	280.4	272.7	129.15	1334519.57	1104.20	7.90	0.87	0.63	0.45	0.33	275.63	33.72	27.87	8.03	20.65	26.54	0.31
MS 90 (P) 11-18-15 (3F)	**-10%**	3643.0	3342.0	315.5	272.7	127.40	1350135.01	1119.36	7.90	0.87	0.63	0.45	0.33	278.77	33.33	27.27	7.92	20.50	26.42	0.31
MS 90 (P) 11-18-15 (3F)	**0%**	3643.0	3342.0	350.5	272.7	126.05	1359106.01	1131.35	7.91	0.87	0.63	0.45	0.33	281.38	33.11	26.76	7.84	20.45	26.42	0.31
MS 90 (P) 11-18-15 (3F)	**15%**	3643.0	3342.0	403.1	272.7	124.20	1376567.76	1148.20	7.91	0.87	0.63	0.46	0.34	284.65	32.69	26.09	7.75	20.20	26.16	0.31
MS 90 (P) 11-18-15 (3F)	**-20%**	3643.0	3342.0	350.5	218.2	142.65	1329394.39	999.70	8.06	0.88	0.66	0.49	0.37	232.74	33.85	28.79	9.63	20.65	25.85	0.28
MS 90 (P) 11-18-15 (3F)	**-10%**	3643.0	3342.0	350.5	245.5	133.40	1345291.48	1069.02	7.98	0.87	0.65	0.47	0.35	257.70	33.45	27.69	8.63	20.60	26.23	0.30
MS 90 (P) 11-18-15 (3F)	**0%**	3643.0	3342.0	350.5	272.7	126.05	1359106.01	1131.35	7.91	0.87	0.63	0.45	0.33	281.38	33.11	26.76	7.84	20.45	26.42	0.31
MS 90 (P) 11-18-15 (3F)	**15%**	3643.0	3342.0	350.5	313.6	117.00	1379098.99	1218.86	7.81	0.86	0.61	0.43	0.31	316.69	32.63	25.57	6.88	20.21	26.62	0.34
MS 90 (PP) 11-25-15 (6F)	**-20%**	2914.4	3342.0	350.5	272.7	112.85	1459143.97	1263.68	7.96	0.86	0.64	0.48	0.37	301.47	30.84	20.24	7.48	20.57	26.97	0.33
MS 90 (PP) 11-25-15 (6F)	**-10%**	3278.7	3342.0	350.5	272.7	111.00	1522842.64	1284.75	8.00	0.87	0.64	0.49	0.37	303.19	29.55	20.03	7.44	19.38	25.45	0.32
MS 90 (PP) 11-25-15 (6F)	**0%**	3643.0	3342.0	350.5	272.7	109.50	1576734.41	1302.35	8.02	0.87	0.65	0.49	0.38	304.77	28.54	19.86	7.39	18.47	24.29	0.31
MS 90 (PP) 11-25-15 (6F)	**15%**	4189.5	3342.0	350.5	272.7	107.53	1651679.21	1326.27	8.05	0.87	0.66	0.50	0.38	306.93	27.25	19.61	7.32	17.31	22.80	0.30
MS 90 (PP) 11-25-15 (6F)	**-20%**	3643.0	2673.6	350.5	272.7	116.35	1393620.32	1225.67	7.91	0.86	0.63	0.47	0.36	300.88	32.29	22.17	7.41	20.50	26.89	0.34
MS 90 (PP) 11-25-15 (6F)	**-10%**	3643.0	3007.8	350.5	272.7	112.60	1488587.50	1266.49	7.97	0.87	0.64	0.48	0.37	302.89	30.23	20.89	7.41	19.38	25.45	0.32
MS 90 (PP) 11-25-15 (6F)	**0%**	3643.0	3342.0	350.5	272.7	109.50	1576734.41	1302.35	8.02	0.87	0.65	0.49	0.38	304.77	28.54	19.86	7.39	18.47	24.29	0.31
MS 90 (PP) 11-25-15 (6F)	**15%**	3643.0	3843.3	350.5	272.7	105.54	1703255.11	1351.21	8.09	0.87	0.66	0.51	0.39	307.44	26.42	18.55	7.37	17.29	22.77	0.30
MS 90 (PP) 11-25-15 (6F)	**-20%**	3643.0	3342.0	280.4	272.7	111.60	1560332.87	1277.84	8.02	0.87	0.65	0.49	0.38	299.05	28.84	20.49	7.59	18.58	24.31	0.31
MS 90 (PP) 11-25-15 (6F)	**-10%**	3643.0	3342.0	315.5	272.7	110.45	1569584.93	1291.14	8.02	0.87	0.65	0.49	0.38	302.15	28.67	20.15	7.47	18.51	24.29	0.31
MS 90 (PP) 11-25-15 (6F)	**0%**	3643.0	3342.0	350.5	272.7	109.50	1576734.41	1302.35	8.02	0.87	0.65	0.49	0.38	304.77	28.54	19.86	7.39	18.47	24.29	0.31
MS 90 (PP) 11-25-15 (6F)	**15%**	3643.0	3342.0	403.1	272.7	108.20	1590106.01	1317.99	8.02	0.87	0.65	0.49	0.38	308.10	28.30	19.46	7.28	18.34	24.18	0.31
MS 90 (PP) 11-25-15 (6F)	**-20%**	3643.0	3342.0	350.5	218.2	123.40	1554404.15	1155.65	8.18	0.88	0.68	0.53	0.41	254.05	28.95	21.15	8.85	18.60	23.81	0.28
MS 90 (PP) 11-25-15 (6F)	**-10%**	3643.0	3342.0	350.5	245.5	115.65	1566307.00	1233.09	8.10	0.88	0.66	0.51	0.40	280.11	28.73	20.44	8.04	18.52	24.05	0.30
MS 90 (PP) 11-25-15 (6F)	**0%**	3643.0	3342.0	350.5	272.7	109.50	1576734.41	1302.35	8.02	0.87	0.65	0.49	0.38	304.77	28.54	19.86	7.39	18.47	24.29	0.31
MS 90 (PP) 11-25-15 (6F)	**15%**	3643.0	3342.0	350.5	313.6	101.91	1592356.69	1399.34	7.92	0.86	0.63	0.47	0.36	341.37	28.26	19.10	6.59	18.35	24.54	0.34

Id. Pav.	D	M1	M2	M3	Ms	I1	I2	I3	I4	I5	I6	I7	I8	I9	I10	I11	I12	I13	I13c	I14
MS 90 (M) 10-8-15 (7F)	**-20%**	2914.4	3342.0	316.7	272.7	180.65	775193.80	789.41	7.42	0.84	0.54	0.33	0.23	256.21	58.05	49.92	7.35	33.05	42.48	0.39
MS 90 (M) 10-8-15 (7F)	**-10%**	3278.7	3342.0	316.7	272.7	177.75	804289.54	802.29	7.45	0.84	0.55	0.34	0.23	256.32	55.95	49.15	7.39	31.55	40.53	0.38
MS 90 (M) 10-8-15 (7F)	**0%**	3643.0	3342.0	316.7	272.7	175.20	831792.98	813.97	7.48	0.85	0.55	0.34	0.23	256.46	54.10	48.49	7.41	30.20	38.78	0.37
MS 90 (M) 10-8-15 (7F)	**15%**	4189.5	3342.0	316.7	272.7	171.90	870406.19	829.59	7.52	0.85	0.56	0.35	0.24	256.64	51.70	47.64	7.45	28.50	36.57	0.36
MS 90 (M) 10-8-15 (7F)	**-20%**	3643.0	2673.6	316.7	272.7	181.05	771208.23	787.67	7.41	0.84	0.54	0.33	0.22	257.53	58.35	50.39	7.31	32.55	41.90	0.39
MS 90 (M) 10-8-15 (7F)	**-10%**	3643.0	3007.8	316.7	272.7	177.90	803571.43	801.61	7.45	0.84	0.55	0.34	0.23	256.92	56.00	49.42	7.37	31.30	40.23	0.38
MS 90 (M) 10-8-15 (7F)	**0%**	3643.0	3342.0	316.7	272.7	175.20	831792.98	813.97	7.48	0.85	0.55	0.34	0.23	256.46	54.10	48.49	7.41	30.20	38.78	0.37
MS 90 (M) 10-8-15 (7F)	**15%**	3643.0	3843.3	316.7	272.7	171.75	871248.79	830.32	7.52	0.85	0.56	0.35	0.24	255.90	51.65	47.33	7.48	28.85	36.99	0.36
MS 90 (M) 10-8-15 (7F)	**-20%**	3643.0	3342.0	253.4	272.7	182.15	798580.30	782.91	7.46	0.85	0.55	0.33	0.22	251.13	56.35	51.65	7.42	31.25	40.01	0.37
MS 90 (M) 10-8-15 (7F)	**-10%**	3643.0	3342.0	285.0	272.7	178.45	815956.48	799.14	7.47	0.85	0.55	0.34	0.23	254.05	55.15	50.00	7.42	30.75	39.43	0.37
MS 90 (M) 10-8-15 (7F)	**0%**	3643.0	3342.0	316.7	272.7	175.20	831792.98	813.97	7.48	0.85	0.55	0.34	0.23	256.46	54.10	48.49	7.41	30.20	38.78	0.37
MS 90 (M) 10-8-15 (7F)	**15%**	3643.0	3342.0	364.2	272.7	171.20	853889.94	832.98	7.50	0.85	0.56	0.35	0.24	259.28	52.70	46.68	7.42	29.60	38.05	0.37
MS 90 (M) 10-8-15 (7F)	**-20%**	3643.0	3342.0	316.7	218.2	198.90	802139.04	716.98	7.64	0.86	0.58	0.38	0.26	208.25	56.10	53.38	9.49	31.00	38.26	0.33
MS 90 (M) 10-8-15 (7F)	**-10%**	3643.0	3342.0	316.7	245.5	185.65	818926.30	768.15	7.55	0.85	0.57	0.36	0.25	232.86	54.95	50.73	8.31	30.55	38.52	0.35
MS 90 (M) 10-8-15 (7F)	**0%**	3643.0	3342.0	316.7	272.7	175.20	831792.98	813.97	7.48	0.85	0.55	0.34	0.23	256.46	54.10	48.49	7.41	30.20	38.78	0.37
MS 90 (M) 10-8-15 (7F)	**15%**	3643.0	3342.0	316.7	313.6	162.45	849858.36	877.85	7.39	0.84	0.53	0.32	0.22	292.06	52.95	45.74	6.35	29.75	39.13	0.40

In the following table, the deflection bowl parameters calculated considering the simultaneous variation of the M1 and M2 modules.

Id. Pav.	D	16hzM1 [Mpa]	16hzM2 [Mpa]	16hzM3 [Mpa]	16hzMs [Mpa]	I1 [µm]	I2 [mm]	I3 [Mpa]	I4 [-]	I5 [-]	I6 [-]	I7 [-]	I8 [-]	I9 [MPa]	I10 [µm]	I11 [µm]	I12 [µm]	I13 [µm]	I13c [µm]	I14 [-]
Ms 30 (M-L)	**-20%**	2914.40	2673.60	316.7	90.9	236.80	1036866.36	602.22	8.47	0.91	0.73	0.59	0.48	120.45	43.40	38.80	17.50	26.30	29.93	0.21
Ms 30 (M-L)	**15%**	4189.50	3843.30	316.7	90.9	214.30	1384615.38	665.45	8.66	0.92	0.77	0.63	0.52	124.73	32.50	32.50	16.71	19.20	22.08	0.17
Ms 30 (PP-P)	**-20%**	2914.40	2673.60	350.5	90.9	210.85	1182654.40	676.34	8.56	0.91	0.75	0.62	0.52	130.50	38.05	30.10	15.55	24.05	28.10	0.20
Ms 30 (PP-P)	**15%**	4189.50	3843.30	350.5	90.9	189.50	1612903.23	752.54	8.76	0.93	0.79	0.67	0.56	136.22	27.90	24.90	14.61	17.30	20.50	0.16
Ms 90 (M-L)	**-20%**	2914.40	2673.60	316.7	272.7	138.15	1129234.63	1032.26	7.76	0.86	0.60	0.42	0.31	274.13	39.85	30.37	7.89	24.85	31.97	0.35
Ms 90 (M-L)	**15%**	4189.50	3843.30	316.7	272.7	121.15	1524390.24	1177.11	8.01	0.88	0.65	0.47	0.35	281.00	29.52	25.36	7.97	17.95	23.16	0.29
Ms 90 (PP-P)	**-20%**	2914.40	2673.60	350.5	272.7	139.55	1103752.76	1021.90	7.73	0.85	0.60	0.41	0.30	275.06	40.77	31.08	7.79	25.25	32.53	0.36
Ms 90 (PP-P)	**15%**	4189.50	3843.30	350.5	272.7	122.80	1482213.44	1161.29	7.98	0.88	0.65	0.47	0.34	281.08	30.36	26.19	7.90	18.40	23.75	0.29
MS 30 (L) 9-15-35	**-20%**	2914.40	2673.60	316.7	90.9	259.90	898203.59	548.70	8.36	0.90	0.72	0.56	0.45	114.52	50.10	47.20	18.58	29.40	32.94	0.22
MS 30 (L) 9-15-35	**15%**	4189.50	3843.30	316.7	90.9	237.10	1178010.47	601.46	8.55	0.92	0.75	0.60	0.48	117.64	38.20	40.60	18.15	21.70	24.48	0.18
MS90 (L) 9-12-15	**-20%**	2914.40	2673.60	316.7	272.7	169.70	841121.50	840.35	7.50	0.84	0.55	0.35	0.24	259.57	53.50	44.46	7.54	31.30	40.17	0.39
MS90 (L) 9-12-15	**15%**	4189.50	3843.30	316.7	272.7	151.80	1089588.38	939.44	7.72	0.86	0.60	0.40	0.28	260.37	41.30	38.98	7.83	23.40	29.90	0.32
MS 30 (M) 13-20-35 (8F)	**-20%**	2914.40	2673.60	316.7	90.9	213.85	1179554.39	666.85	8.56	0.91	0.75	0.62	0.51	128.69	38.15	31.00	15.92	23.95	27.84	0.20
MS 30 (M) 13-20-35 (8F)	**15%**	4189.50	3843.30	316.7	90.9	191.90	1607142.86	743.13	8.76	0.93	0.79	0.66	0.56	134.45	28.00	25.40	14.94	17.30	20.42	0.16
MS 90 (P) 11-18-15 (3F)	**-20%**	2914.40	2673.60	350.5	272.7	136.65	1130369.25	1043.59	7.75	0.85	0.60	0.42	0.31	277.56	39.81	29.75	7.79	24.95	32.19	0.36
MS 90 (P) 11-18-15 (3F)	**15%**	4189.50	3843.30	350.5	272.7	119.90	1527494.91	1189.38	8.00	0.88	0.65	0.47	0.35	284.34	29.46	24.95	7.85	18.00	23.29	0.29
MS 90 (PP) 11-25-15 (6F)	**-20%**	2914.40	2673.60	350.5	272.7	119.80	1294219.15	1190.37	7.85	0.85	0.62	0.46	0.35	297.95	34.77	22.53	7.48	22.73	29.75	0.36
MS 90 (PP) 11-25-15 (6F)	**15%**	4189.50	3843.30	350.5	272.7	103.60	1786777.84	1376.58	8.12	0.88	0.67	0.51	0.40	309.74	25.19	18.29	7.30	16.18	21.35	0.29
MS 90 (M) 10-8-15 (7F)	**-20%**	2914.40	2673.60	316.7	272.7	186.55	719424.46	764.44	7.36	0.83	0.53	0.32	0.22	257.42	62.55	51.66	7.26	35.65	45.93	0.41
MS 90 (M) 10-8-15 (7F)	**15%**	4189.50	3843.30	316.7	272.7	168.45	911854.10	846.58	7.56	0.85	0.57	0.36	0.24	256.14	49.35	46.40	7.52	27.25	34.91	0.35

Below the DIi = delta Index in relation and with respect to case 0 for each road pavement.

Id. Pav.	D	16hzM1 [Mpa]	16hzM2 [Mpa]	16hzM3 [Mpa]	16hzMs [Mpa]	D_I1	D_I2	D_I3	D_I4	D_I5	D_I6	D_I7	D_I8	D_I9	D_I10	D_I11	D_I12	D_I13	DI13c	D_I14
Ms 30 (M-L)	**-20%**	2914.4	3342.0	316.7	90.9	0.028	-0.075	-0.027	-0.005	-0.005	-0.012	-0.016	-0.020	-0.014	0.081	0.031	0.019	0.108	0.103	0.061
Ms 30 (M-L)	**-10%**	3278.7	3342.0	316.7	90.9	0.013	-0.035	-0.012	-0.002	-0.002	-0.005	-0.007	-0.009	-0.007	0.036	0.014	0.006	0.046	0.044	0.027
Ms 30 (M-L)	**0%**	3643.0	3342.0	316.7	90.9	0.000	0.000	0.000	0.000	0.000	0.000	0.000	0.000	0.000	0.000	0.000	0.000	0.000	0.000	0.000
Ms 30 (M-L)	**15%**	4189.5	3342.0	316.7	90.9	-0.017	0.046	0.017	0.003	0.002	0.007	0.009	0.011	0.009	-0.044	-0.023	-0.016	-0.060	-0.057	-0.033
Ms 30 (M-L)	**-20%**	3643.0	2673.6	316.7	90.9	0.036	-0.100	-0.034	-0.009	-0.007	-0.020	-0.030	-0.034	-0.008	0.112	0.077	0.005	0.099	0.097	0.080
Ms 30 (M-L)	**-10%**	3643.0	3007.8	316.7	90.9	0.016	-0.051	-0.016	-0.004	-0.003	-0.009	-0.014	-0.016	-0.004	0.054	0.031	-0.001	0.044	0.043	0.040
Ms 30 (M-L)	**0%**	3643.0	3342.0	316.7	90.9	0.000	0.000	0.000	0.000	0.000	0.000	0.000	0.000	0.000	0.000	0.000	0.000	0.000	0.000	0.000
Ms 30 (M-L)	**15%**	3643.0	3843.3	316.7	90.9	-0.021	0.068	0.022	0.005	0.004	0.012	0.018	0.021	0.005	-0.063	-0.046	-0.007	-0.060	-0.058	-0.047
Ms 30 (M-L)	**-20%**	3643.0	3342.0	253.4	90.9	0.038	-0.029	-0.036	-0.001	0.001	-0.001	-0.009	-0.018	-0.032	0.030	0.066	0.050	0.018	0.008	-0.009
Ms 30 (M-L)	**-10%**	3643.0	3342.0	285.0	90.9	0.018	-0.015	-0.017	-0.001	0.000	-0.001	-0.005	-0.009	-0.015	0.015	0.031	0.020	0.007	0.002	-0.004
Ms 30 (M-L)	**0%**	3643.0	3342.0	316.7	90.9	0.000	0.000	0.000	0.000	0.000	0.000	0.000	0.000	0.000	0.000	0.000	0.000	0.000	0.000	0.000
Ms 30 (M-L)	**15%**	3643.0	3342.0	364.2	90.9	-0.023	0.020	0.024	0.001	0.000	0.001	0.006	0.012	0.020	-0.019	-0.043	-0.035	-0.014	-0.006	0.005
Ms 30 (M-L)	**-20%**	3643.0	3342.0	316.7	72.7	0.135	-0.016	-0.119	0.015	0.009	0.031	0.053	0.071	-0.156	0.017	0.043	0.152	0.009	-0.015	-0.115
Ms 30 (M-L)	**-10%**	3643.0	3342.0	316.7	81.8	0.061	-0.010	-0.058	0.007	0.004	0.014	0.025	0.033	-0.077	0.010	0.020	0.069	0.007	-0.004	-0.054
Ms 30 (M-L)	**0%**	3643.0	3342.0	316.7	90.9	0.000	0.000	0.000	0.000	0.000	0.000	0.000	0.000	0.000	0.000	0.000	0.000	0.000	0.000	0.000
Ms 30 (M-L)	**15%**	3643.0	3342.0	316.7	104.5	-0.077	0.007	0.083	-0.010	-0.007	-0.021	-0.035	-0.047	0.116	-0.007	-0.031	-0.094	-0.007	0.009	0.084
Ms 30 (PP-P)	**-20%**	2914.4	3342.0	350.5	90.9	0.027	-0.074	-0.026	-0.005	-0.004	-0.011	-0.014	-0.018	-0.014	0.080	0.030	0.025	0.112	0.107	0.061
Ms 30 (PP-P)	**-10%**	3278.7	3342.0	350.5	90.9	0.012	-0.035	-0.012	-0.002	-0.002	-0.005	-0.006	-0.008	-0.006	0.037	0.015	0.011	0.048	0.046	0.028
Ms 30 (PP-P)	**0%**	3643.0	3342.0	350.5	90.9	0.000	0.000	0.000	0.000	0.000	0.000	0.000	0.000	0.000	0.000	0.000	0.000	0.000	0.000	0.000
Ms 30 (PP-P)	**15%**	4189.5	3342.0	350.5	90.9	-0.016	0.047	0.016	0.003	0.002	0.006	0.007	0.010	0.010	-0.045	-0.015	-0.016	-0.061	-0.058	-0.034
Ms 30 (PP-P)	**-20%**	3643.0	2673.6	350.5	90.9	0.041	-0.113	-0.039	-0.010	-0.007	-0.021	-0.032	-0.037	-0.011	0.127	0.093	0.013	0.107	0.104	0.091
Ms 30 (PP-P)	**-10%**	3643.0	3007.8	350.5	90.9	0.019	-0.054	-0.018	-0.005	-0.003	-0.010	-0.015	-0.017	-0.005	0.057	0.045	0.006	0.051	0.050	0.042
Ms 30 (PP-P)	**0%**	3643.0	3342.0	350.5	90.9	0.000	0.000	0.000	0.000	0.000	0.000	0.000	0.000	0.000	0.000	0.000	0.000	0.000	0.000	0.000
Ms 30 (PP-P)	**15%**	3643.0	3843.3	350.5	90.9	-0.024	0.072	0.024	0.006	0.004	0.012	0.018	0.022	0.008	-0.067	-0.056	-0.009	-0.061	-0.058	-0.048
Ms 30 (PP-P)	**-20%**	3643.0	3342.0	280.4	90.9	0.033	-0.023	-0.032	-0.001	0.001	-0.001	-0.006	-0.013	-0.029	0.024	0.060	0.052	0.013	0.003	-0.011
Ms 30 (PP-P)	**-10%**	3643.0	3342.0	315.5	90.9	0.015	-0.013	-0.015	0.000	0.000	0.000	-0.003	-0.006	-0.013	0.013	0.026	0.024	0.005	0.000	-0.004
Ms 30 (PP-P)	**0%**	3643.0	3342.0	350.5	90.9	0.000	0.000	0.000	0.000	0.000	0.000	0.000	0.000	0.000	0.000	0.000	0.000	0.000	0.000	0.000

Id. Pav.	D	M1	M2	M3	Ms	D_I1	D_I2	D_I3	D_I4	D_I5	D_I6	D_I7	D_I8	D_I9	D_I10	D_I11	D_I12	D_I13	D_I13c	D_I14
Ms 30 (PP-P)	**15%**	3643.0	3342.0	403.1	90.9	-0.020	0.011	0.020	0.000	-0.001	0.000	0.003	0.008	0.019	-0.011	-0.037	-0.032	-0.008	-0.001	0.010
Ms 30 (PP-P)	**-20%**	3643.0	3342.0	350.5	72.7	0.136	-0.013	-0.120	0.014	0.009	0.029	0.048	0.065	-0.153	0.013	0.045	0.133	0.005	-0.016	-0.119
Ms 30 (PP-P)	**-10%**	3643.0	3342.0	350.5	81.8	0.062	-0.008	-0.058	0.007	0.004	0.014	0.023	0.031	-0.076	0.008	0.019	0.061	0.003	-0.008	-0.056
Ms 30 (PP-P)	**0%**	3643.0	3342.0	350.5	90.9	0.000	0.000	0.000	0.000	0.000	0.000	0.000	0.000	0.000	0.000	0.000	0.000	0.000	0.000	0.000
Ms 30 (PP-P)	**15%**	3643.0	3342.0	350.5	104.5	-0.077	0.006	0.083	-0.010	-0.007	-0.021	-0.033	-0.043	0.114	-0.006	-0.026	-0.083	-0.005	0.009	0.086
Ms 90 (M-L)	**-20%**	2914.4	3342.0	316.7	272.7	0.037	-0.089	-0.036	-0.009	-0.009	-0.023	-0.030	-0.035	-0.009	0.098	0.032	0.004	0.128	0.126	0.076
Ms 90 (M-L)	**-10%**	3278.7	3342.0	316.7	272.7	0.017	-0.044	-0.017	-0.004	-0.004	-0.011	-0.014	-0.017	-0.004	0.046	0.015	0.001	0.059	0.058	0.036
Ms 90 (M-L)	**0%**	3643.0	3342.0	316.7	272.7	0.000	0.000	0.000	0.000	0.000	0.000	0.000	0.000	0.000	0.000	0.000	0.000	0.000	0.000	0.000
Ms 90 (M-L)	**15%**	4189.5	3342.0	316.7	272.7	-0.022	0.058	0.022	0.005	0.005	0.014	0.018	0.021	0.006	-0.055	-0.020	-0.003	-0.071	-0.070	-0.043
Ms 90 (M-L)	**-20%**	3643.0	2673.6	316.7	272.7	0.047	-0.090	-0.045	-0.011	-0.007	-0.026	-0.043	-0.050	-0.006	0.099	0.084	-0.009	0.084	0.083	0.057
Ms 90 (M-L)	**-10%**	3643.0	3007.8	316.7	272.7	0.022	-0.043	-0.021	-0.005	-0.003	-0.012	-0.020	-0.024	-0.003	0.045	0.039	-0.004	0.037	0.037	0.026
Ms 90 (M-L)	**0%**	3643.0	3342.0	316.7	272.7	0.000	0.000	0.000	0.000	0.000	0.000	0.000	0.000	0.000	0.000	0.000	0.000	0.000	0.000	0.000
Ms 90 (M-L)	**15%**	3643.0	3843.3	316.7	272.7	-0.027	0.058	0.028	0.006	0.004	0.016	0.026	0.031	0.004	-0.055	-0.048	0.004	-0.047	-0.046	-0.033
Ms 90 (M-L)	**-20%**	3643.0	3342.0	253.4	272.7	0.023	-0.018	-0.023	-0.001	0.001	-0.001	-0.008	-0.016	-0.018	0.018	0.040	0.023	0.012	0.007	-0.007
Ms 90 (M-L)	**-10%**	3643.0	3342.0	285.0	272.7	0.010	-0.009	-0.010	-0.001	0.000	-0.001	-0.005	-0.009	-0.007	0.009	0.018	0.008	0.007	0.005	-0.001
Ms 90 (M-L)	**0%**	3643.0	3342.0	316.7	272.7	-0.002	-0.001	0.002	0.000	0.000	-0.001	-0.002	-0.002	0.003	0.001	-0.001	-0.004	0.000	0.001	0.003
Ms 90 (M-L)	**15%**	3643.0	3342.0	364.2	272.7	-0.016	0.010	0.016	0.000	-0.001	-0.001	0.003	0.007	0.015	-0.010	-0.026	-0.016	-0.007	-0.004	0.008
Ms 90 (M-L)	**-20%**	3643.0	3342.0	316.7	218.2	0.129	-0.022	-0.114	0.019	0.014	0.047	0.077	0.099	-0.169	0.022	0.075	0.221	0.015	-0.016	-0.112
Ms 90 (M-L)	**-10%**	3643.0	3342.0	316.7	245.5	0.056	-0.011	-0.053	0.009	0.006	0.021	0.035	0.045	-0.081	0.011	0.033	0.097	0.007	-0.007	-0.051
Ms 90 (M-L)	**0%**	3643.0	3342.0	316.7	272.7	-0.002	-0.001	0.002	0.000	0.000	-0.001	-0.002	-0.002	0.003	0.001	-0.001	-0.004	0.000	0.001	0.003
Ms 90 (M-L)	**15%**	3643.0	3342.0	316.7	313.6	-0.072	0.012	0.078	-0.013	-0.010	-0.032	-0.051	-0.064	0.128	-0.012	-0.044	-0.125	-0.006	0.014	0.080
Ms 90 (PP-P)	**-20%**	2914.4	3342.0	350.5	272.7	0.031	-0.074	-0.030	-0.007	-0.007	-0.019	-0.025	-0.030	-0.008	0.080	0.027	0.003	0.108	0.106	0.062
Ms 90 (PP-P)	**-10%**	3278.7	3342.0	350.5	272.7	0.015	-0.036	-0.015	-0.004	-0.003	-0.009	-0.012	-0.014	-0.004	0.037	0.013	0.003	0.048	0.047	0.029
Ms 90 (PP-P)	**0%**	3643.0	3342.0	350.5	272.7	0.000	0.000	0.000	0.000	0.000	0.000	0.000	0.000	0.000	0.000	0.000	0.000	0.000	0.000	0.000
Ms 90 (PP-P)	**15%**	4189.5	3342.0	350.5	272.7	-0.018	0.046	0.019	0.004	0.004	0.011	0.015	0.018	0.005	-0.044	-0.018	-0.003	-0.060	-0.059	-0.034
Ms 90 (PP-P)	**-20%**	3643.0	2673.6	350.5	272.7	0.050	-0.102	-0.048	-0.012	-0.009	-0.031	-0.047	-0.054	-0.005	0.114	0.082	-0.011	0.096	0.096	0.069
Ms 90 (PP-P)	**-10%**	3643.0	3007.8	350.5	272.7	0.023	-0.049	-0.022	-0.006	-0.004	-0.014	-0.022	-0.025	-0.002	0.051	0.037	-0.004	0.041	0.041	0.031
Ms 90 (PP-P)	**0%**	3643.0	3342.0	350.5	272.7	0.000	0.000	0.000	0.000	0.000	0.000	0.000	0.000	0.000	0.000	0.000	0.000	0.000	0.000	0.000
Ms 90 (PP-P)	**15%**	3643.0	3843.3	350.5	272.7	-0.029	0.068	0.030	0.007	0.005	0.018	0.029	0.033	0.004	-0.063	-0.048	0.006	-0.060	-0.060	-0.041

Id. Pav.	D	M1	M2	M3	Ms	D_I1	D_I2	D_I3	D_I4	D_I5	D_I6	D_I7	D_I8	D_I9	D_I10	D_I11	D_I12	D_I13	D_I13c	D_I14
Ms 90 (PP-P)	**-20%**	3643.0	3342.0	280.4	272.7	0.026	-0.020	-0.025	-0.001	0.001	-0.001	-0.008	-0.016	-0.021	0.020	0.043	0.023	0.014	0.009	-0.007
Ms 90 (PP-P)	**-10%**	3643.0	3342.0	315.5	272.7	0.012	-0.011	-0.012	-0.001	0.000	-0.001	-0.004	-0.008	-0.009	0.011	0.020	0.009	0.007	0.005	-0.002
Ms 90 (PP-P)	**0%**	3643.0	3342.0	350.5	272.7	0.000	0.000	0.000	0.000	0.000	0.000	0.000	0.000	0.000	0.000	0.000	0.000	0.000	0.000	0.000
Ms 90 (PP-P)	**15%**	3643.0	3342.0	403.1	272.7	-0.015	0.012	0.015	0.001	-0.001	0.001	0.006	0.010	0.012	-0.011	-0.026	-0.010	-0.010	-0.007	0.004
Ms 90 (PP-P)	**-20%**	3643.0	3342.0	350.5	218.2	0.133	-0.024	-0.117	0.020	0.015	0.049	0.080	0.101	-0.174	0.024	0.078	0.233	0.014	-0.018	-0.113
Ms 90 (PP-P)	**-10%**	3643.0	3342.0	350.5	245.5	0.059	-0.011	-0.055	0.009	0.007	0.023	0.037	0.047	-0.085	0.011	0.035	0.103	0.002	-0.012	-0.054
Ms 90 (PP-P)	**0%**	3643.0	3342.0	350.5	272.7	0.000	0.000	0.000	0.000	0.000	0.000	0.000	0.000	0.000	0.000	0.000	0.000	0.000	0.000	0.000
Ms 90 (PP-P)	**15%**	3643.0	3342.0	350.5	313.6	-0.072	0.014	0.077	-0.013	-0.010	-0.031	-0.050	-0.062	0.126	-0.014	-0.046	-0.125	-0.011	0.009	0.076
MS 30 (L) 9-15-35	**-20%**	2914.4	3342.0	316.7	90.9	0.024	-0.058	-0.023	-0.004	-0.003	-0.010	-0.014	-0.018	-0.011	0.061	0.035	0.013	0.086	0.082	0.043
MS 30 (L) 9-15-35	**-10%**	3278.7	3342.0	316.7	90.9	0.011	-0.029	-0.011	-0.002	-0.002	-0.005	-0.007	-0.008	-0.005	0.029	0.016	0.009	0.039	0.037	0.021
MS 30 (L) 9-15-35	**0%**	3643.0	3342.0	316.7	90.9	0.000	0.000	0.000	0.000	0.000	0.000	0.000	0.000	0.000	0.000	0.000	0.000	0.000	0.000	0.000
MS 30 (L) 9-15-35	**15%**	4189.5	3342.0	316.7	90.9	-0.014	0.035	0.015	0.003	0.002	0.005	0.008	0.011	0.008	-0.034	-0.021	-0.008	-0.047	-0.045	-0.024
MS 30 (L) 9-15-35	**-20%**	3643.0	2673.6	316.7	90.9	0.034	-0.105	-0.033	-0.010	-0.008	-0.022	-0.031	-0.034	-0.004	0.117	0.065	-0.001	0.113	0.112	0.089
MS 30 (L) 9-15-35	**-10%**	3643.0	3007.8	316.7	90.9	0.016	-0.051	-0.016	-0.005	-0.004	-0.010	-0.014	-0.016	-0.002	0.054	0.028	-0.001	0.053	0.053	0.042
MS 30 (L) 9-15-35	**0%**	3643.0	3342.0	316.7	90.9	0.000	0.000	0.000	0.000	0.000	0.000	0.000	0.000	0.000	0.000	0.000	0.000	0.000	0.000	0.000
MS 30 (L) 9-15-35	**15%**	3643.0	3843.3	316.7	90.9	-0.020	0.069	0.021	0.006	0.004	0.013	0.018	0.021	0.004	-0.065	-0.037	0.000	-0.064	-0.063	-0.050
MS 30 (L) 9-15-35	**-20%**	3643.0	3342.0	253.4	90.9	0.044	-0.040	-0.042	-0.002	0.000	-0.003	-0.014	-0.025	-0.034	0.041	0.079	0.052	0.027	0.015	-0.004
MS 30 (L) 9-15-35	**-10%**	3643.0	3342.0	285.0	90.9	0.021	-0.019	-0.020	-0.001	0.000	-0.002	-0.007	-0.013	-0.016	0.019	0.039	0.021	0.016	0.011	-0.002
MS 30 (L) 9-15-35	**0%**	3643.0	3342.0	316.7	90.9	0.000	0.000	0.000	0.000	0.000	0.000	0.000	0.000	0.000	0.000	0.000	0.000	0.000	0.000	0.000
MS 30 (L) 9-15-35	**15%**	3643.0	3342.0	364.2	90.9	-0.026	0.024	0.027	0.002	0.000	0.002	0.009	0.016	0.022	-0.024	-0.049	-0.031	-0.016	-0.009	0.004
MS 30 (L) 9-15-35	**-20%**	3643.0	3342.0	316.7	72.7	0.134	-0.016	-0.118	0.016	0.010	0.033	0.057	0.077	-0.158	0.017	0.051	0.169	0.012	-0.014	-0.114
MS 30 (L) 9-15-35	**-10%**	3643.0	3342.0	316.7	81.8	0.061	-0.008	-0.057	0.008	0.005	0.016	0.027	0.036	-0.078	0.008	0.023	0.075	0.006	-0.006	-0.055
MS 30 (L) 9-15-35	**0%**	3643.0	3342.0	316.7	90.9	0.000	0.000	0.000	0.000	0.000	0.000	0.000	0.000	0.000	0.000	0.000	0.000	0.000	0.000	0.000
MS 30 (L) 9-15-35	**15%**	3643.0	3342.0	316.7	104.5	-0.076	0.012	0.082	-0.011	-0.007	-0.022	-0.038	-0.050	0.118	-0.012	-0.030	-0.099	-0.008	0.009	0.078
MS90 (L) 9-12-15	**-20%**	2914.4	3342.0	316.7	272.7	0.027	-0.060	-0.026	-0.006	-0.006	-0.018	-0.025	-0.029	-0.004	0.064	0.027	-0.006	0.088	0.088	0.048
MS90 (L) 9-12-15	**-10%**	3278.7	3342.0	316.7	272.7	0.012	-0.027	-0.012	-0.003	-0.003	-0.008	-0.011	-0.013	-0.002	0.027	0.014	-0.004	0.040	0.040	0.020
MS90 (L) 9-12-15	**0%**	3643.0	3342.0	316.7	272.7	0.000	0.000	0.000	0.000	0.000	0.000	0.000	0.000	0.000	0.000	0.000	0.000	0.000	0.000	0.000
MS90 (L) 9-12-15	**15%**	4189.5	3342.0	316.7	272.7	-0.016	0.035	0.016	0.004	0.003	0.010	0.015	0.018	0.003	-0.034	-0.019	0.004	-0.044	-0.044	-0.024
MS90 (L) 9-12-15	**-20%**	3643.0	2673.6	316.7	272.7	0.044	-0.096	-0.042	-0.012	-0.010	-0.032	-0.046	-0.049	0.002	0.106	0.055	-0.018	0.105	0.108	0.072

Id. Pav.	D	M1	M2	M3	Ms	D_I1	D_I2	D_I3	D_I4	D_I5	D_I6	D_I7	D_I8	D_I9	D_I10	D_I11	D_I12	D_I13	D_I13c	D_I14
MS90 (L) 9-12-15	**-10%**	3643.0	3007.8	316.7	272.7	0.020	-0.047	-0.019	-0.006	-0.005	-0.015	-0.021	-0.023	0.001	0.049	0.024	-0.008	0.048	0.049	0.034
MS90 (L) 9-12-15	**0%**	3643.0	3342.0	316.7	272.7	0.000	0.000	0.000	0.000	0.000	0.000	0.000	0.000	0.000	0.000	0.000	0.000	0.000	0.000	0.000
MS90 (L) 9-12-15	**15%**	3643.0	3843.3	316.7	272.7	-0.026	0.064	0.026	0.007	0.006	0.019	0.029	0.031	-0.001	-0.060	-0.033	0.010	-0.059	-0.061	-0.042
MS90 (L) 9-12-15	**-20%**	3643.0	3342.0	253.4	272.7	0.034	-0.033	-0.033	-0.002	0.000	-0.004	-0.017	-0.028	-0.022	0.034	0.055	0.012	0.025	0.021	-0.002
MS90 (L) 9-12-15	**-10%**	3643.0	3342.0	285.0	272.7	0.016	-0.015	-0.016	-0.001	0.000	-0.002	-0.008	-0.014	-0.010	0.015	0.026	0.005	0.011	0.010	-0.001
MS90 (L) 9-12-15	**0%**	3643.0	3342.0	316.7	272.7	0.000	0.000	0.000	0.000	0.000	0.000	0.000	0.000	0.000	0.000	0.000	0.000	0.000	0.000	0.000
MS90 (L) 9-12-15	**15%**	3643.0	3342.0	364.2	272.7	-0.020	0.019	0.020	0.002	0.000	0.003	0.011	0.018	0.012	-0.019	-0.035	-0.005	-0.013	-0.011	0.003
MS90 (L) 9-12-15	**-20%**	3643.0	3342.0	316.7	218.2	0.134	-0.033	-0.118	0.020	0.015	0.052	0.089	0.109	-0.183	0.034	0.090	0.267	0.021	-0.016	-0.106
MS90 (L) 9-12-15	**-10%**	3643.0	3342.0	316.7	245.5	0.059	-0.015	-0.056	0.009	0.007	0.024	0.041	0.050	-0.089	0.015	0.041	0.117	0.011	-0.006	-0.050
MS90 (L) 9-12-15	**0%**	3643.0	3342.0	316.7	272.7	0.000	0.000	0.000	0.000	0.000	0.000	0.000	0.000	0.000	0.000	0.000	0.000	0.000	0.000	0.000
MS90 (L) 9-12-15	**15%**	3643.0	3342.0	316.7	313.6	-0.073	0.018	0.078	-0.013	-0.010	-0.034	-0.055	-0.066	0.134	-0.018	-0.054	-0.139	-0.011	0.011	0.073
MS 30 (M) 13-20-35 (8F)	**-20%**	2914.4	3342.0	316.7	90.9	0.032	-0.092	-0.031	-0.006	-0.006	-0.014	-0.017	-0.021	-0.015	0.102	0.033	0.026	0.133	0.126	0.079
MS 30 (M) 13-20-35 (8F)	**-10%**	3278.7	3342.0	316.7	90.9	0.015	-0.045	-0.014	-0.003	-0.003	-0.007	-0.008	-0.010	-0.007	0.048	0.015	0.012	0.061	0.058	0.038
MS 30 (M) 13-20-35 (8F)	**0%**	3643.0	3342.0	316.7	90.9	0.000	0.000	0.000	0.000	0.000	0.000	0.000	0.000	0.000	0.000	0.000	0.000	0.000	0.000	0.000
MS 30 (M) 13-20-35 (8F)	**15%**	4189.5	3342.0	316.7	90.9	-0.018	0.057	0.019	0.004	0.003	0.008	0.010	0.013	0.010	-0.054	-0.022	-0.017	-0.071	-0.068	-0.042
MS 30 (M) 13-20-35 (8F)	**-20%**	3643.0	2673.6	316.7	90.9	0.038	-0.097	-0.037	-0.009	-0.006	-0.019	-0.028	-0.034	-0.011	0.108	0.095	0.013	0.087	0.082	0.073
MS 30 (M) 13-20-35 (8F)	**-10%**	3643.0	3007.8	316.7	90.9	0.018	-0.048	-0.017	-0.004	-0.003	-0.009	-0.013	-0.016	-0.006	0.051	0.040	0.006	0.041	0.039	0.035
MS 30 (M) 13-20-35 (8F)	**0%**	3643.0	3342.0	316.7	90.9	0.000	0.000	0.000	0.000	0.000	0.000	0.000	0.000	0.000	0.000	0.000	0.000	0.000	0.000	0.000
MS 30 (M) 13-20-35 (8F)	**15%**	3643.0	3843.3	316.7	90.9	-0.022	0.059	0.022	0.005	0.003	0.010	0.016	0.020	0.008	-0.056	-0.055	-0.009	-0.048	-0.046	-0.037
MS 30 (M) 13-20-35 (8F)	**-20%**	3643.0	3342.0	253.4	90.9	0.032	-0.022	-0.031	-0.001	0.001	0.000	-0.006	-0.012	-0.028	0.022	0.058	0.051	0.015	0.005	-0.011
MS 30 (M) 13-20-35 (8F)	**-10%**	3643.0	3342.0	285.0	90.9	0.015	-0.011	-0.015	0.000	0.000	0.000	-0.003	-0.006	-0.013	0.011	0.029	0.024	0.008	0.003	-0.005
MS 30 (M) 13-20-35 (8F)	**0%**	3643.0	3342.0	316.7	90.9	0.000	0.000	0.000	0.000	0.000	0.000	0.000	0.000	0.000	0.000	0.000	0.000	0.000	0.000	0.000
MS 30 (M) 13-20-35 (8F)	**15%**	3643.0	3342.0	364.2	90.9	-0.020	0.011	0.020	0.000	-0.001	0.000	0.004	0.008	0.019	-0.011	-0.036	-0.031	-0.008	-0.001	0.010
MS 30 (M) 13-20-35 (8F)	**-20%**	3643.0	3342.0	316.7	72.7	0.136	-0.014	-0.120	0.014	0.009	0.029	0.048	0.065	-0.153	0.014	0.044	0.140	0.008	-0.014	-0.118
MS 30 (M) 13-20-35 (8F)	**-10%**	3643.0	3342.0	316.7	81.8	0.062	-0.008	-0.058	0.007	0.004	0.014	0.023	0.031	-0.075	0.008	0.022	0.064	0.008	-0.003	-0.056
MS 30 (M) 13-20-35 (8F)	**0%**	3643.0	3342.0	316.7	90.9	0.000	0.000	0.000	0.000	0.000	0.000	0.000	0.000	0.000	0.000	0.000	0.000	0.000	0.000	0.000
MS 30 (M) 13-20-35 (8F)	**15%**	3643.0	3342.0	316.7	104.5	-0.077	0.005	0.083	-0.010	-0.007	-0.020	-0.032	-0.043	0.114	-0.005	-0.029	-0.084	-0.008	0.006	0.087
MS 90 (P) 11-18-15 (3F)	**-20%**	2914.4	3342.0	350.5	272.7	0.031	-0.073	-0.030	-0.007	-0.007	-0.018	-0.024	-0.029	-0.009	0.078	0.027	0.004	0.108	0.106	0.061
MS 90 (P) 11-18-15 (3F)	**-10%**	3278.7	3342.0	350.5	272.7	0.014	-0.035	-0.014	-0.003	-0.003	-0.009	-0.011	-0.014	-0.004	0.036	0.012	0.003	0.049	0.048	0.028

Id. Pav.	D	M1	M2	M3	Ms	D_I1	D_I2	D_I3	D_I4	D_I5	D_I6	D_I7	D_I8	D_I9	D_I10	D_I11	D_I12	D_I13	D_I13c	D_I14
MS 90 (P) 11-18-15 (3F)	**0%**	3643.0	3342.0	350.5	272.7	0.000	0.000	0.000	0.000	0.000	0.000	0.000	0.000	0.000	0.000	0.000	0.000	0.000	0.000	0.000
MS 90 (P) 11-18-15 (3F)	**15%**	4189.5	3342.0	350.5	272.7	-0.019	0.048	0.019	0.004	0.004	0.011	0.015	0.018	0.006	-0.046	-0.017	-0.003	-0.061	-0.060	-0.036
MS 90 (P) 11-18-15 (3F)	**-20%**	3643.0	2673.6	350.5	272.7	0.052	-0.105	-0.050	-0.013	-0.009	-0.031	-0.048	-0.055	-0.006	0.117	0.087	-0.009	0.103	0.103	0.072
MS 90 (P) 11-18-15 (3F)	**-10%**	3643.0	3007.8	350.5	272.7	0.023	-0.049	-0.023	-0.006	-0.004	-0.014	-0.022	-0.025	-0.003	0.052	0.039	-0.004	0.042	0.042	0.031
MS 90 (P) 11-18-15 (3F)	**0%**	3643.0	3342.0	350.5	272.7	0.000	0.000	0.000	0.000	0.000	0.000	0.000	0.000	0.000	0.000	0.000	0.000	0.000	0.000	0.000
MS 90 (P) 11-18-15 (3F)	**15%**	3643.0	3843.3	350.5	272.7	-0.031	0.072	0.032	0.008	0.006	0.019	0.030	0.035	0.004	-0.067	-0.050	0.005	-0.061	-0.061	-0.043
MS 90 (P) 11-18-15 (3F)	**-20%**	3643.0	3342.0	280.4	272.7	0.025	-0.018	-0.024	-0.001	0.001	0.000	-0.007	-0.015	-0.020	0.018	0.041	0.024	0.010	0.005	-0.009
MS 90 (P) 11-18-15 (3F)	**-10%**	3643.0	3342.0	315.5	272.7	0.011	-0.007	-0.011	0.000	0.001	0.000	-0.003	-0.006	-0.009	0.007	0.019	0.010	0.002	0.000	-0.006
MS 90 (P) 11-18-15 (3F)	**0%**	3643.0	3342.0	350.5	272.7	0.000	0.000	0.000	0.000	0.000	0.000	0.000	0.000	0.000	0.000	0.000	0.000	0.000	0.000	0.000
MS 90 (P) 11-18-15 (3F)	**15%**	3643.0	3342.0	403.1	272.7	-0.015	0.013	0.015	0.001	0.000	0.001	0.005	0.010	0.012	-0.013	-0.025	-0.011	-0.012	-0.010	0.003
MS 90 (P) 11-18-15 (3F)	**-20%**	3643.0	3342.0	350.5	218.2	0.132	-0.022	-0.116	0.020	0.015	0.049	0.079	0.101	-0.173	0.022	0.076	0.228	0.010	-0.021	-0.115
MS 90 (P) 11-18-15 (3F)	**-10%**	3643.0	3342.0	350.5	245.5	0.058	-0.010	-0.055	0.009	0.007	0.023	0.037	0.046	-0.084	0.010	0.035	0.101	0.007	-0.007	-0.054
MS 90 (P) 11-18-15 (3F)	**0%**	3643.0	3342.0	350.5	272.7	0.000	0.000	0.000	0.000	0.000	0.000	0.000	0.000	0.000	0.000	0.000	0.000	0.000	0.000	0.000
MS 90 (P) 11-18-15 (3F)	**15%**	3643.0	3342.0	350.5	313.6	-0.072	0.015	0.077	-0.013	-0.009	-0.031	-0.049	-0.061	0.126	-0.014	-0.044	-0.122	-0.012	0.008	0.075
MS 90 (PP) 11-25-15 (6F)	**-20%**	2914.4	3342.0	350.5	272.7	0.031	-0.075	-0.030	-0.007	-0.007	-0.018	-0.021	-0.026	-0.011	0.081	0.019	0.012	0.114	0.110	0.066
MS 90 (PP) 11-25-15 (6F)	**-10%**	3278.7	3342.0	350.5	272.7	0.014	-0.034	-0.014	-0.003	-0.003	-0.008	-0.009	-0.012	-0.005	0.035	0.009	0.007	0.049	0.048	0.029
MS 90 (PP) 11-25-15 (6F)	**0%**	3643.0	3342.0	350.5	272.7	0.000	0.000	0.000	0.000	0.000	0.000	0.000	0.000	0.000	0.000	0.000	0.000	0.000	0.000	0.000
MS 90 (PP) 11-25-15 (6F)	**15%**	4189.5	3342.0	350.5	272.7	-0.018	0.048	0.018	0.004	0.004	0.010	0.013	0.015	0.007	-0.045	-0.013	-0.009	-0.063	-0.061	-0.037
MS 90 (PP) 11-25-15 (6F)	**-20%**	3643.0	2673.6	350.5	272.7	0.063	-0.116	-0.059	-0.014	-0.010	-0.033	-0.052	-0.061	-0.013	0.131	0.116	0.003	0.110	0.107	0.075
MS 90 (PP) 11-25-15 (6F)	**-10%**	3643.0	3007.8	350.5	272.7	0.028	-0.056	-0.028	-0.006	-0.005	-0.015	-0.024	-0.028	-0.006	0.059	0.052	0.003	0.049	0.048	0.034
MS 90 (PP) 11-25-15 (6F)	**0%**	3643.0	3342.0	350.5	272.7	0.000	0.000	0.000	0.000	0.000	0.000	0.000	0.000	0.000	0.000	0.000	0.000	0.000	0.000	0.000
MS 90 (PP) 11-25-15 (6F)	**15%**	3643.0	3843.3	350.5	272.7	-0.036	0.080	0.038	0.008	0.006	0.020	0.032	0.038	0.009	-0.074	-0.066	-0.003	-0.064	-0.062	-0.045
MS 90 (PP) 11-25-15 (6F)	**-20%**	3643.0	3342.0	280.4	272.7	0.019	-0.010	-0.019	0.000	0.001	0.002	-0.002	-0.007	-0.019	0.011	0.032	0.027	0.006	0.001	-0.011
MS 90 (PP) 11-25-15 (6F)	**-10%**	3643.0	3342.0	315.5	272.7	0.009	-0.005	-0.009	0.000	0.001	0.001	-0.001	-0.004	-0.009	0.005	0.015	0.011	0.002	0.000	-0.005
MS 90 (PP) 11-25-15 (6F)	**0%**	3643.0	3342.0	350.5	272.7	0.000	0.000	0.000	0.000	0.000	0.000	0.000	0.000	0.000	0.000	0.000	0.000	0.000	0.000	0.000
MS 90 (PP) 11-25-15 (6F)	**15%**	3643.0	3342.0	403.1	272.7	-0.012	0.008	0.012	0.000	-0.001	0.000	0.003	0.006	0.011	-0.008	-0.020	-0.015	-0.007	-0.004	0.005
MS 90 (PP) 11-25-15 (6F)	**-20%**	3643.0	3342.0	350.5	218.2	0.127	-0.014	-0.113	0.020	0.015	0.048	0.075	0.096	-0.166	0.014	0.065	0.198	0.007	-0.020	-0.119
MS 90 (PP) 11-25-15 (6F)	**-10%**	3643.0	3342.0	350.5	245.5	0.056	-0.007	-0.053	0.009	0.007	0.022	0.035	0.044	-0.081	0.007	0.029	0.088	0.003	-0.010	-0.057
MS 90 (PP) 11-25-15 (6F)	**0%**	3643.0	3342.0	350.5	272.7	0.000	0.000	0.000	0.000	0.000	0.000	0.000	0.000	0.000	0.000	0.000	0.000	0.000	0.000	0.000

Id. Pav.	D	M1	M2	M3	Ms	D_I1	D_I2	D_I3	D_I4	D_I5	D_I6	D_I7	D_I8	D_I9	D_I10	D_I11	D_I12	D_I13	D_I13c	D_I14
MS 90 (PP) 11-25-15 (6F)	**15%**	3643.0	3342.0	350.5	313.6	-0.069	0.010	0.074	-0.013	-0.010	-0.030	-0.047	-0.059	0.120	-0.010	-0.038	-0.108	-0.006	0.010	0.079
MS 90 (M) 10-8-15 (7F)	**-20%**	2914.4	3342.0	316.7	272.7	0.031	-0.068	-0.030	-0.008	-0.007	-0.022	-0.031	-0.033	-0.001	0.073	0.029	-0.008	0.094	0.095	0.054
MS 90 (M) 10-8-15 (7F)	**-10%**	3278.7	3342.0	316.7	272.7	0.015	-0.033	-0.014	-0.004	-0.004	-0.011	-0.015	-0.015	-0.001	0.034	0.014	-0.003	0.045	0.045	0.026
MS 90 (M) 10-8-15 (7F)	**0%**	3643.0	3342.0	316.7	272.7	0.000	0.000	0.000	0.000	0.000	0.000	0.000	0.000	0.000	0.000	0.000	0.000	0.000	0.000	0.000
MS 90 (M) 10-8-15 (7F)	**15%**	4189.5	3342.0	316.7	272.7	-0.019	0.046	0.019	0.005	0.005	0.014	0.019	0.021	0.001	-0.044	-0.018	0.005	-0.056	-0.057	-0.034
MS 90 (M) 10-8-15 (7F)	**-20%**	3643.0	2673.6	316.7	272.7	0.033	-0.073	-0.032	-0.009	-0.008	-0.026	-0.037	-0.038	0.004	0.079	0.039	-0.013	0.078	0.080	0.053
MS 90 (M) 10-8-15 (7F)	**-10%**	3643.0	3007.8	316.7	272.7	0.015	-0.034	-0.015	-0.004	-0.004	-0.012	-0.017	-0.018	0.002	0.035	0.019	-0.005	0.036	0.037	0.024
MS 90 (M) 10-8-15 (7F)	**0%**	3643.0	3342.0	316.7	272.7	0.000	0.000	0.000	0.000	0.000	0.000	0.000	0.000	0.000	0.000	0.000	0.000	0.000	0.000	0.000
MS 90 (M) 10-8-15 (7F)	**15%**	3643.0	3843.3	316.7	272.7	-0.020	0.047	0.020	0.006	0.005	0.016	0.023	0.024	-0.002	-0.045	-0.024	0.009	-0.045	-0.046	-0.031
MS 90 (M) 10-8-15 (7F)	**-20%**	3643.0	3342.0	253.4	272.7	0.040	-0.040	-0.038	-0.003	0.000	-0.007	-0.024	-0.037	-0.021	0.042	0.065	0.001	0.035	0.032	0.001
MS 90 (M) 10-8-15 (7F)	**-10%**	3643.0	3342.0	285.0	272.7	0.019	-0.019	-0.018	-0.002	0.000	-0.004	-0.012	-0.018	-0.009	0.019	0.031	0.001	0.018	0.017	0.001
MS 90 (M) 10-8-15 (7F)	**0%**	3643.0	3342.0	316.7	272.7	0.000	0.000	0.000	0.000	0.000	0.000	0.000	0.000	0.000	0.000	0.000	0.000	0.000	0.000	0.000
MS 90 (M) 10-8-15 (7F)	**15%**	3643.0	3342.0	364.2	272.7	-0.023	0.027	0.023	0.002	0.001	0.005	0.016	0.023	0.011	-0.026	-0.037	0.001	-0.020	-0.019	-0.002
MS 90 (M) 10-8-15 (7F)	**-20%**	3643.0	3342.0	316.7	218.2	0.135	-0.036	-0.119	0.020	0.016	0.056	0.094	0.111	-0.188	0.037	0.101	0.281	0.026	-0.013	-0.104
MS 90 (M) 10-8-15 (7F)	**-10%**	3643.0	3342.0	316.7	245.5	0.060	-0.015	-0.056	0.010	0.008	0.026	0.044	0.051	-0.092	0.016	0.046	0.121	0.012	-0.007	-0.050
MS 90 (M) 10-8-15 (7F)	**0%**	3643.0	3342.0	316.7	272.7	0.000	0.000	0.000	0.000	0.000	0.000	0.000	0.000	0.000	0.000	0.000	0.000	0.000	0.000	0.000
MS 90 (M) 10-8-15 (7F)	**15%**	3643.0	3342.0	316.7	313.6	-0.073	0.022	0.078	-0.013	-0.010	-0.035	-0.058	-0.067	0.139	-0.021	-0.057	-0.143	-0.015	0.009	0.069

In conclusion, the results of delta indexes in relation and with respect to case 0 for each road pavement, calculated considering the simultaneous variation of the M1 and M2 modules:

Id. Pav.	D	16hzM1 [Mpa]	16hzM2 [Mpa]	16hzM3 [Mpa]	16hzMs [Mpa]	D_I1	D_I2	D_I3	D_I4	D_I5	D_I6	D_I7	D_I8	D_I9	D_I10	D_I11	D_I12	D_I13	DI13c	D_I14
Ms 30 (M-L)	-20%	2914.40	2673.60	316.7	90.9	0.063	-0.164	-0.060	-0.014	-0.011	-0.031	-0.044	-0.053	-0.021	0.196	0.109	0.023	0.212	0.205	0.142
Ms 30 (M-L)	15%	4189.50	3843.30	316.7	90.9	-0.038	0.117	0.039	0.009	0.006	0.019	0.027	0.033	0.014	-0.105	-0.071	-0.023	-0.115	-0.111	-0.078
Ms 30 (PP-P)	-20%	2914.40	2673.60	350.5	90.9	0.068	-0.175	-0.064	-0.015	-0.012	-0.032	-0.045	-0.053	-0.025	0.212	0.123	0.037	0.227	0.132	0.153
Ms 30 (PP-P)	15%	4189.50	3843.30	350.5	90.9	-0.040	0.125	0.042	0.009	0.006	0.018	0.026	0.033	0.018	-0.111	-0.071	-0.026	-0.117	-0.174	-0.083
Ms 90 (M-L)	-20%	2914.40	2673.60	316.7	272.7	0.085	-0.169	-0.078	-0.020	-0.016	-0.050	-0.072	-0.083	-0.014	0.203	0.115	-0.008	0.221	0.287	0.136
Ms 90 (M-L)	15%	4189.50	3843.30	316.7	272.7	-0.049	0.122	0.051	0.012	0.009	0.030	0.045	0.054	0.011	-0.109	-0.069	0.003	-0.118	-0.068	-0.076
Ms 90 (PP-P)	-20%	2914.40	2673.60	350.5	272.7	0.082	-0.166	-0.076	-0.019	-0.016	-0.049	-0.071	-0.081	-0.012	0.198	0.108	-0.010	0.211	0.310	0.133
Ms 90 (PP-P)	15%	4189.50	3843.30	350.5	272.7	-0.048	0.121	0.050	0.012	0.010	0.030	0.045	0.053	0.010	-0.108	-0.066	0.004	-0.118	-0.044	-0.076
MS 30 (L) 9-15-35	-20%	2914.40	2673.60	316.7	90.9	0.058	-0.154	-0.055	-0.014	-0.011	-0.031	-0.044	-0.051	-0.015	0.182	0.095	0.015	0.205	0.326	0.134
MS 30 (L) 9-15-35	15%	4189.50	3843.30	316.7	90.9	-0.035	0.110	0.036	0.008	0.006	0.018	0.027	0.033	0.011	-0.099	-0.058	-0.008	-0.111	-0.014	-0.075
MS90 (L) 9-12-15	-20%	2914.40	2673.60	316.7	272.7	0.071	-0.147	-0.066	-0.018	-0.016	-0.049	-0.069	-0.074	-0.001	0.172	0.081	-0.023	0.197	0.617	0.120
MS90 (L) 9-12-15	15%	4189.50	3843.30	316.7	272.7	-0.042	0.105	0.044	0.011	0.009	0.030	0.045	0.050	0.002	-0.095	-0.052	0.014	-0.105	0.204	-0.068
MS 30 (M) 13-20-35 (8F)	-20%	2914.40	2673.60	316.7	90.9	0.069	-0.174	-0.065	-0.015	-0.011	-0.032	-0.045	-0.053	-0.026	0.211	0.127	0.037	0.222	0.121	0.151
MS 30 (M) 13-20-35 (8F)	15%	4189.50	3843.30	316.7	90.9	-0.041	0.125	0.042	0.009	0.006	0.018	0.027	0.033	0.018	-0.111	-0.076	-0.027	-0.117	-0.178	-0.082
MS 90 (P) 11-18-15 (3F)	-20%	2914.40	2673.60	350.5	272.7	0.084	-0.168	-0.078	-0.020	-0.016	-0.050	-0.071	-0.082	-0.014	0.202	0.112	-0.006	0.220	0.296	0.137
MS 90 (P) 11-18-15 (3F)	15%	4189.50	3843.30	350.5	272.7	-0.049	0.124	0.051	0.012	0.010	0.030	0.045	0.054	0.011	-0.110	-0.068	0.001	-0.120	-0.062	-0.078
MS 90 (PP) 11-25-15 (6F)	-20%	2914.40	2673.60	350.5	272.7	0.094	-0.179	-0.086	-0.021	-0.017	-0.051	-0.072	-0.085	-0.022	0.218	0.134	0.012	0.231	0.198	0.142
MS 90 (PP) 11-25-15 (6F)	15%	4189.50	3843.30	350.5	272.7	-0.054	0.133	0.057	0.013	0.010	0.031	0.045	0.055	0.016	-0.118	-0.079	-0.012	-0.124	-0.140	-0.081
MS 90 (M) 10-8-15 (7F)	-20%	2914.40	2673.60	316.7	272.7	0.065	-0.135	-0.061	-0.017	-0.016	-0.048	-0.066	-0.068	0.004	0.156	0.065	-0.020	0.180	0.849	0.111
MS 90 (M) 10-8-15 (7F)	15%	4189.50	3843.30	316.7	272.7	-0.039	0.096	0.040	0.010	0.009	0.030	0.043	0.046	-0.001	-0.088	-0.043	0.015	-0.098	0.406	-0.063

APPENDIX 9

ESAL DEPENDENT FROM THE STRUCTURAL NUMBER DERIVED FROM NDT

Id. Pav.	D	16 hz Ms [psi]	Mr600 [psi]	EP [psi]	Sneff [inch]	ESAL Sneff	EP600 [psi]	Sneff 600 [inch]	ESAL Sneff600
Ms 30 (M-L)	***-20%***	13184.8	17594.60	165040.23	6.12	6.51E+08	136907.31	5.75	7.96E+08
Ms 30 (M-L)	***-10%***	13184.8	17721.59	169287.94	6.17	6.94E+08	139553.72	5.79	8.49E+08
Ms 30 (M-L)	***0%***	13184.8	17838.65	172988.09	6.22	7.34E+08	141798.01	5.82	8.96E+08
Ms 30 (M-L)	***15%***	13184.8	17993.14	178100.28	6.28	7.90E+08	144885.00	5.86	9.65E+08
Ms 30 (M-L)	***-20%***	13184.8	17698.37	162834.63	6.09	6.29E+08	134766.93	5.72	7.76E+08
Ms 30 (M-L)	***-10%***	13184.8	17768.23	168192.10	6.16	6.83E+08	138513.07	5.77	8.38E+08
Ms 30 (M-L)	***0%***	13184.8	17838.65	172988.09	6.22	7.34E+08	141798.01	5.82	8.96E+08
Ms 30 (M-L)	***15%***	13184.8	17933.41	179527.61	6.30	8.07E+08	146231.91	5.88	9.80E+08
Ms 30 (M-L)	***-20%***	13184.8	17268.36	162291.33	6.09	6.24E+08	136281.72	5.74	7.53E+08
Ms 30 (M-L)	***-10%***	13184.8	17571.70	167808.30	6.16	6.79E+08	139122.50	5.78	8.26E+08
Ms 30 (M-L)	***0%***	13184.8	17838.65	172988.09	6.22	7.34E+08	141798.01	5.82	8.96E+08
Ms 30 (M-L)	***15%***	13184.8	18199.27	180248.81	6.30	8.15E+08	145496.50	5.87	1.00E+09
Ms 30 (M-L)	***-20%***	10547.8	15054.46	163974.82	6.11	3.82E+08	128151.23	5.63	4.71E+08
Ms 30 (M-L)	***-10%***	11866.3	16468.12	168673.96	6.17	5.39E+08	135233.55	5.73	6.62E+08
Ms 30 (M-L)	***0%***	13184.8	17838.65	172988.09	6.22	7.34E+08	141798.01	5.82	8.96E+08
Ms 30 (M-L)	***15%***	15162.5	19902.51	179418.10	6.30	1.11E+09	150920.37	5.94	1.35E+09
Ms 30 (PP-P)	***-20%***	13184.8	19127.27	189998.66	6.93	1.70E+09	150492.65	6.41	2.19E+09
Ms 30 (PP-P)	***-10%***	13184.8	19277.45	194684.69	6.98	1.81E+09	153166.89	6.45	2.33E+09
Ms 30 (PP-P)	***0%***	13184.8	19402.09	198878.11	7.03	1.91E+09	155568.66	6.48	2.47E+09
Ms 30 (PP-P)	***15%***	13184.8	19599.21	204599.44	7.10	2.06E+09	158675.17	6.52	2.66E+09
Ms 30 (PP-P)	***-20%***	13184.8	19181.61	185584.86	6.87	1.59E+09	147120.45	6.36	2.08E+09
Ms 30 (PP-P)	***-10%***	13184.8	19305.01	192604.65	6.96	1.76E+09	151580.87	6.42	2.28E+09
Ms 30 (PP-P)	***0%***	13184.8	19402.09	198878.11	7.03	1.91E+09	155568.66	6.48	2.47E+09
Ms 30 (PP-P)	***15%***	13184.8	19556.63	207381.59	7.13	2.14E+09	160791.05	6.55	2.74E+09
Ms 30 (PP-P)	***-20%***	13184.8	18846.97	188163.69	6.90	1.65E+09	150388.70	6.41	2.11E+09
Ms 30 (PP-P)	***-10%***	13184.8	19140.83	193764.63	6.97	1.79E+09	153111.62	6.45	2.29E+09
Ms 30 (PP-P)	***0%***	13184.8	19402.09	198878.11	7.03	1.91E+09	155568.66	6.48	2.47E+09
Ms 30 (PP-P)	***15%***	13184.8	19771.38	205982.28	7.11	2.10E+09	158863.55	6.52	2.72E+09
Ms 30 (PP-P)	***-20%***	10547.8	16428.05	188283.13	6.90	9.87E+08	139985.43	6.26	1.28E+09
Ms 30 (PP-P)	***-10%***	11866.3	17933.41	193810.11	6.97	1.40E+09	148093.84	6.37	1.81E+09
Ms 30 (PP-P)	***0%***	13184.8	19402.09	198878.11	7.03	1.91E+09	155568.66	6.48	2.47E+09
Ms 30 (PP-P)	***15%***	15162.5	21623.47	206472.67	7.12	2.92E+09	165980.23	6.62	3.75E+09
Ms 90 (M-L)	***-20%***	39554.4	39958.14	258790.38	4.97	9.05E+08	256826.75	4.96	9.12E+08
Ms 90 (M-L)	***-10%***	39554.4	40148.22	267633.86	5.02	9.72E+08	264623.19	5.00	9.83E+08
Ms 90 (M-L)	***0%***	39554.4	40316.03	275862.45	5.07	1.04E+09	271853.55	5.05	1.05E+09
Ms 90 (M-L)	***15%***	39554.4	40552.12	286786.73	5.14	1.13E+09	281280.97	5.11	1.15E+09
Ms 90 (M-L)	***-20%***	39554.4	40058.90	254391.45	4.94	8.73E+08	252004.14	4.92	8.81E+08
Ms 90 (M-L)	***-10%***	39554.4	40196.03	265643.39	5.01	9.57E+08	262429.24	4.99	9.68E+08
Ms 90 (M-L)	***0%***	39554.4	40316.03	275862.45	5.07	1.04E+09	271853.55	5.05	1.05E+09

Id. Pav.	D	16 hz Ms [psi]	Mr600 [psi]	EP [psi]	Sneff [inch]	ESAL Sneff	EP600 [psi]	Sneff 600 [inch]	ESAL Sneff600
Ms 90 (M-L)	***15%***	39554.4	40497.39	289688.22	5.16	1.15E+09	284401.56	5.13	1.17E+09
Ms 90 (M-L)	***-20%***	39554.4	39571.74	264925.99	5.01	9.51E+08	264837.55	5.01	9.52E+08
Ms 90 (M-L)	***-10%***	39554.4	40041.08	271133.88	5.05	1.00E+09	268612.37	5.03	1.01E+09
Ms 90 (M-L)	***0%***	39554.4	40442.81	276632.37	5.08	1.04E+09	271956.13	5.05	1.06E+09
Ms 90 (M-L)	***15%***	39554.4	40933.18	283935.40	5.12	1.10E+09	276519.75	5.08	1.13E+09
Ms 90 (M-L)	***-20%***	31643.5	33495.86	265225.39	5.01	5.68E+08	253207.93	4.93	5.88E+08
Ms 90 (M-L)	***-10%***	35598.9	37062.86	271841.06	5.05	7.87E+08	263320.73	5.00	8.08E+08
Ms 90 (M-L)	***0%***	39554.4	40442.81	276632.37	5.08	1.04E+09	271956.13	5.05	1.06E+09
Ms 90 (M-L)	***15%***	45487.5	45475.18	283152.97	5.12	1.52E+09	283209.56	5.12	1.52E+09
Ms 90 (PP-P)	***-20%***	39554.4	40041.08	260357.02	4.86	1.56E+09	257923.71	4.85	1.57E+09
Ms 90 (PP-P)	***-10%***	39554.4	40219.97	268002.03	4.91	1.67E+09	264555.31	4.89	1.69E+09
Ms 90 (PP-P)	***0%***	39554.4	40382.34	275089.55	4.95	1.78E+09	270664.36	4.93	1.80E+09
Ms 90 (PP-P)	***15%***	39554.4	40600.89	284317.51	5.01	1.92E+09	278499.35	4.97	1.94E+09
Ms 90 (PP-P)	***-20%***	39554.4	40184.06	252097.67	4.81	1.45E+09	249102.79	4.79	1.47E+09
Ms 90 (PP-P)	***-10%***	39554.4	40285.96	264220.27	4.89	1.62E+09	260514.35	4.87	1.63E+09
Ms 90 (PP-P)	***0%***	39554.4	40382.34	275089.55	4.95	1.78E+09	270664.36	4.93	1.80E+09
Ms 90 (PP-P)	***15%***	39554.4	40527.78	290073.71	5.04	2.01E+09	284495.74	5.01	2.03E+09
Ms 90 (PP-P)	***-20%***	39554.4	39548.56	262980.27	4.88	1.60E+09	263010.12	4.88	1.60E+09
Ms 90 (PP-P)	***-10%***	39554.4	40005.49	269283.62	4.92	1.69E+09	266916.02	4.91	1.70E+09
Ms 90 (PP-P)	***0%***	39554.4	40382.34	275089.55	4.95	1.78E+09	270664.36	4.93	1.80E+09
Ms 90 (PP-P)	***15%***	39554.4	40852.68	282509.21	5.00	1.89E+09	275410.45	4.96	1.92E+09
Ms 90 (PP-P)	***-20%***	31643.5	33359.33	263270.02	4.88	9.56E+08	251969.98	4.81	9.77E+08
Ms 90 (PP-P)	***-10%***	35598.9	36961.42	270181.46	4.92	1.33E+09	262126.84	4.88	1.36E+09
Ms 90 (PP-P)	***0%***	39554.4	40382.34	275089.55	4.95	1.78E+09	270664.36	4.93	1.80E+09
Ms 90 (PP-P)	***15%***	45487.5	45482.84	281804.58	4.99	2.60E+09	281826.34	4.99	2.60E+09
MS 30 (L) 9-15-35	***-20%***	13184.8	16681.72	148558.61	5.54	3.07E+08	126970.05	5.25	3.63E+08
MS 30 (L) 9-15-35	***-10%***	13184.8	16785.40	151834.45	5.58	3.24E+08	129086.04	5.28	3.83E+08
MS 30 (L) 9-15-35	***0%***	13184.8	16869.28	154799.49	5.61	3.39E+08	131026.27	5.31	4.01E+08
MS 30 (L) 9-15-35	***15%***	13184.8	16996.67	158780.18	5.66	3.61E+08	133527.57	5.34	4.27E+08
MS 30 (L) 9-15-35	***-20%***	13184.8	16795.84	145996.56	5.50	2.94E+08	124412.26	5.22	3.51E+08
MS 30 (L) 9-15-35	***-10%***	13184.8	16827.23	150623.93	5.56	3.17E+08	127933.08	5.27	3.77E+08
MS 30 (L) 9-15-35	***0%***	13184.8	16869.28	154799.49	5.61	3.39E+08	131026.27	5.31	4.01E+08
MS 30 (L) 9-15-35	***15%***	13184.8	16932.73	160399.63	5.68	3.71E+08	135106.29	5.36	4.36E+08
MS 30 (L) 9-15-35	***-20%***	13184.8	16299.16	143751.60	5.48	2.83E+08	124880.66	5.22	3.30E+08
MS 30 (L) 9-15-35	***-10%***	13184.8	16599.70	149378.73	5.55	3.11E+08	128010.16	5.27	3.66E+08
MS 30 (L) 9-15-35	***0%***	13184.8	16869.28	154799.49	5.61	3.39E+08	131026.27	5.31	4.01E+08
MS 30 (L) 9-15-35	***15%***	13184.8	17235.30	162226.60	5.70	3.81E+08	135034.46	5.36	4.53E+08

Id. Pav.	D	16 hz Ms [psi]	Mr600 [psi]	EP [psi]	Sneff [inch]	ESAL Sneff	EP600 [psi]	Sneff 600 [inch]	ESAL Sneff600
MS 30 (L) 9-15-35	***-20%***	10547.8	14199.64	147006.63	5.52	1.78E+08	118903.52	5.14	2.14E+08
MS 30 (L) 9-15-35	***-10%***	11866.3	15548.48	151087.48	5.57	2.51E+08	125243.66	5.23	2.98E+08
MS 30 (L) 9-15-35	***0%***	13184.8	16869.28	154799.49	5.61	3.39E+08	131026.27	5.31	4.01E+08
MS 30 (L) 9-15-35	***15%***	15162.5	18860.13	160371.42	5.68	5.12E+08	139055.98	5.42	6.00E+08
MS90 (L) 9-12-15	***-20%***	39554.4	37531.56	209578.44	3.79	3.05E+08	219211.43	3.85	2.96E+08
MS90 (L) 9-12-15	***-10%***	39554.4	37609.96	215277.09	3.82	3.22E+08	224863.71	3.88	3.14E+08
MS90 (L) 9-12-15	***0%***	39554.4	37678.17	220211.14	3.85	3.38E+08	229735.31	3.91	3.30E+08
MS90 (L) 9-12-15	***15%***	39554.4	37783.59	226962.66	3.89	3.60E+08	236302.46	3.94	3.52E+08
MS90 (L) 9-12-15	***-20%***	39554.4	37767.74	203457.13	3.75	2.87E+08	211554.42	3.80	2.79E+08
MS90 (L) 9-12-15	***-10%***	39554.4	37715.00	212334.30	3.81	3.13E+08	221198.74	3.86	3.05E+08
MS90 (L) 9-12-15	***0%***	39554.4	37678.17	220211.14	3.85	3.38E+08	229735.31	3.91	3.30E+08
MS90 (L) 9-12-15	***15%***	39554.4	37646.65	231101.72	3.91	3.74E+08	241467.75	3.97	3.66E+08
MS90 (L) 9-12-15	***-20%***	39554.4	36845.44	206883.57	3.77	2.97E+08	219858.93	3.85	2.86E+08
MS90 (L) 9-12-15	***-10%***	39554.4	37303.47	213919.67	3.81	3.18E+08	225037.31	3.88	3.09E+08
MS90 (L) 9-12-15	***0%***	39554.4	37678.17	220211.14	3.85	3.38E+08	229735.31	3.91	3.30E+08
MS90 (L) 9-12-15	***15%***	39554.4	38135.71	228602.95	3.90	3.65E+08	236069.91	3.94	3.59E+08
MS90 (L) 9-12-15	***-20%***	31643.5	30799.08	211661.61	3.80	1.85E+08	217028.50	3.83	1.83E+08
MS90 (L) 9-12-15	***-10%***	35598.9	34321.65	216703.21	3.83	2.56E+08	223925.75	3.87	2.52E+08
MS90 (L) 9-12-15	***0%***	39554.4	37678.17	220211.14	3.85	3.38E+08	229735.31	3.91	3.30E+08
MS90 (L) 9-12-15	***15%***	45487.5	42726.96	224982.43	3.88	4.89E+08	237077.37	3.95	4.72E+08
MS 30 (M) 13-20-35 (8F)	***-20%***	13184.8	18860.13	184356.85	6.86	1.57E+09	147582.67	6.37	2.02E+09
MS 30 (M) 13-20-35 (8F)	***-10%***	13184.8	19019.51	189677.28	6.92	1.69E+09	150726.57	6.41	2.17E+09
MS 30 (M) 13-20-35 (8F)	***0%***	13184.8	19154.40	194433.01	6.98	1.80E+09	153526.30	6.45	2.31E+09
MS 30 (M) 13-20-35 (8F)	***15%***	13184.8	19346.50	200812.82	7.05	1.96E+09	157170.22	6.50	2.52E+09
MS 30 (M) 13-20-35 (8F)	***-20%***	13184.8	18939.49	182391.65	6.83	1.52E+09	145830.83	6.34	1.97E+09
MS 30 (M) 13-20-35 (8F)	***-10%***	13184.8	19046.34	188718.84	6.91	1.67E+09	149925.59	6.40	2.15E+09
MS 30 (M) 13-20-35 (8F)	***0%***	13184.8	19154.40	194433.01	6.98	1.80E+09	153526.30	6.45	2.31E+09
MS 30 (M) 13-20-35 (8F)	***15%***	13184.8	19305.01	201971.65	7.07	1.99E+09	158169.70	6.52	2.54E+09

Id. Pav.	D	16 hz Ms [psi]	Mr600 [psi]	EP [psi]	Sneff [inch]	ESAL Sneff	EP600 [psi]	Sneff 600 [inch]	ESAL Sneff600
MS 30 (M) 13-20-35 (8F)	***-20%***	13184.8	18613.17	184204.36	6.85	1.56E+09	148534.87	6.38	1.99E+09
MS 30 (M) 13-20-35 (8F)	***-10%***	13184.8	18899.73	189436.87	6.92	1.68E+09	151075.23	6.42	2.15E+09
MS 30 (M) 13-20-35 (8F)	***0%***	13184.8	19154.40	194433.01	6.98	1.80E+09	153526.30	6.45	2.31E+09
MS 30 (M) 13-20-35 (8F)	***15%***	13184.8	19514.24	201257.14	7.06	1.97E+09	156734.38	6.50	2.55E+09
MS 30 (M) 13-20-35 (8F)	***-20%***	10547.8	16220.85	183952.45	6.85	9.28E+08	138137.84	6.23	1.20E+09
MS 30 (M) 13-20-35 (8F)	***-10%***	11866.3	17709.97	189354.78	6.92	1.32E+09	146081.27	6.34	1.70E+09
MS 30 (M) 13-20-35 (8F)	***0%***	13184.8	19154.40	194433.01	6.98	1.80E+09	153526.30	6.45	2.31E+09
MS 30 (M) 13-20-35 (8F)	***15%***	15162.5	21333.10	201847.31	7.07	2.75E+09	163792.19	6.59	3.51E+09
MS 90 (P) 11-18-15 (3F)	***-20%***	39554.4	40448.87	266183.68	5.01	1.93E+09	261724.96	4.99	1.96E+09
MS 90 (P) 11-18-15 (3F)	***-10%***	39554.4	40637.54	273953.89	5.06	2.07E+09	268363.72	5.03	2.10E+09
MS 90 (P) 11-18-15 (3F)	***0%***	39554.4	40809.47	280934.70	5.11	2.19E+09	274259.15	5.06	2.23E+09
MS 90 (P) 11-18-15 (3F)	***15%***	39554.4	41045.15	290526.60	5.16	2.37E+09	282274.87	5.11	2.42E+09
MS 90 (P) 11-18-15 (3F)	***-20%***	39554.4	40570.39	256743.69	4.95	1.78E+09	251948.90	4.92	1.80E+09
MS 90 (P) 11-18-15 (3F)	***-10%***	39554.4	40692.65	269650.50	5.04	1.99E+09	263915.10	5.00	2.02E+09
MS 90 (P) 11-18-15 (3F)	***0%***	39554.4	40809.47	280934.70	5.11	2.19E+09	274259.15	5.06	2.23E+09
MS 90 (P) 11-18-15 (3F)	***15%***	39554.4	40982.87	296951.16	5.20	2.50E+09	288783.09	5.15	2.54E+09
MS 90 (P) 11-18-15 (3F)	***-20%***	39554.4	39975.89	269097.89	5.03	1.98E+09	266932.83	5.02	1.99E+09
MS 90 (P) 11-18-15 (3F)	***-10%***	39554.4	40430.70	275670.55	5.07	2.10E+09	271078.88	5.05	2.12E+09
MS 90 (P) 11-18-15 (3F)	***0%***	39554.4	40809.47	280934.70	5.11	2.19E+09	274259.15	5.06	2.23E+09
MS 90 (P) 11-18-15 (3F)	***15%***	39554.4	41283.57	288438.51	5.15	2.33E+09	279031.38	5.09	2.38E+09
MS 90 (P) 11-18-15 (3F)	***-20%***	31643.5	33755.42	268988.54	5.03	1.18E+09	255152.81	4.94	1.21E+09
MS 90 (P) 11-18-15 (3F)	***-10%***	35598.9	37375.74	275898.53	5.07	1.65E+09	265451.88	5.01	1.68E+09
MS 90 (P) 11-18-15 (3F)	***0%***	39554.4	40809.47	280934.70	5.11	2.19E+09	274259.15	5.06	2.23E+09
MS 90 (P) 11-18-15 (3F)	***15%***	45487.5	45931.48	288012.64	5.15	3.22E+09	285950.45	5.14	3.23E+09
MS 90 (PP) 11-25-15 (6F)	***-20%***	39554.4	43723.02	302057.99	6.06	7.73E+09	282305.48	5.93	8.22E+09
MS 90 (PP) 11-25-15 (6F)	***-10%***	39554.4	43972.17	310689.48	6.12	8.30E+09	289050.14	5.97	8.84E+09
MS 90 (PP) 11-25-15 (6F)	***0%***	39554.4	44202.47	318013.02	6.17	8.81E+09	294628.99	6.01	9.39E+09
MS 90 (PP) 11-25-15 (6F)	***15%***	39554.4	44515.76	328130.88	6.23	9.54E+09	302262.23	6.06	1.02E+10

Id. Pav.	D	16 hz Ms [psi]	Mr600 [psi]	EP [psi]	Sneff [inch]	ESAL Sneff	EP600 [psi]	Sneff 600 [inch]	ESAL Sneff600
MS 90 (PP) 11-25-15 (6F)	***-20%***	39554.4	43638.24	286840.55	5.96	6.78E+09	268820.99	5.83	7.24E+09
MS 90 (PP) 11-25-15 (6F)	***-10%***	39554.4	43929.26	303199.53	6.07	7.80E+09	282475.35	5.93	8.33E+09
MS 90 (PP) 11-25-15 (6F)	***0%***	39554.4	44202.47	318013.02	6.17	8.81E+09	294628.99	6.01	9.39E+09
MS 90 (PP) 11-25-15 (6F)	***15%***	39554.4	44589.25	338884.44	6.30	1.04E+10	311467.23	6.12	1.10E+10
MS 90 (PP) 11-25-15 (6F)	***-20%***	39554.4	43371.94	307842.85	6.10	8.11E+09	289079.45	5.97	8.57E+09
MS 90 (PP) 11-25-15 (6F)	***-10%***	39554.4	43822.34	313339.95	6.14	8.48E+09	292094.55	6.00	9.01E+09
MS 90 (PP) 11-25-15 (6F)	***0%***	39554.4	44202.47	318013.02	6.17	8.81E+09	294628.99	6.01	9.39E+09
MS 90 (PP) 11-25-15 (6F)	***15%***	39554.4	44685.16	324609.89	6.21	9.28E+09	298381.93	6.04	9.94E+09
MS 90 (PP) 11-25-15 (6F)	***-20%***	31643.5	36845.44	304805.83	6.08	4.71E+09	272715.86	5.86	5.07E+09
MS 90 (PP) 11-25-15 (6F)	***-10%***	35598.9	40625.32	312449.96	6.13	6.59E+09	284550.14	5.94	7.07E+09
MS 90 (PP) 11-25-15 (6F)	***0%***	39554.4	44202.47	318013.02	6.17	8.81E+09	294628.99	6.01	9.39E+09
MS 90 (PP) 11-25-15 (6F)	***15%***	45487.5	49510.01	325867.05	6.22	1.30E+10	308141.76	6.10	1.37E+10
MS 90 (M) 10-8-15 (7F)	***-20%***	39554.4	37159.75	185608.57	3.33	1.83E+08	196285.00	3.40	1.80E+08
MS 90 (M) 10-8-15 (7F)	***-10%***	39554.4	37175.10	191345.51	3.37	1.96E+08	202404.26	3.43	1.93E+08
MS 90 (M) 10-8-15 (7F)	***0%***	39554.4	37195.58	196644.91	3.40	2.09E+08	208021.87	3.46	2.05E+08
MS 90 (M) 10-8-15 (7F)	***15%***	39554.4	37221.21	203883.92	3.44	2.26E+08	215701.14	3.51	2.23E+08
MS 90 (M) 10-8-15 (7F)	***-20%***	39554.4	37349.90	184840.33	3.33	1.82E+08	194547.52	3.39	1.78E+08
MS 90 (M) 10-8-15 (7F)	***-10%***	39554.4	37262.29	191041.37	3.37	1.96E+08	201638.76	3.43	1.92E+08
MS 90 (M) 10-8-15 (7F)	***0%***	39554.4	37195.58	196644.91	3.40	2.09E+08	208021.87	3.46	2.05E+08
MS 90 (M) 10-8-15 (7F)	***15%***	39554.4	37113.80	204223.71	3.44	2.27E+08	216660.77	3.51	2.24E+08
MS 90 (M) 10-8-15 (7F)	***-20%***	39554.4	36423.07	182755.47	3.32	1.77E+08	196783.29	3.40	1.73E+08
MS 90 (M) 10-8-15 (7F)	***-10%***	39554.4	36845.44	189933.25	3.36	1.93E+08	202542.71	3.43	1.89E+08
MS 90 (M) 10-8-15 (7F)	***0%***	39554.4	37195.58	196644.91	3.40	2.09E+08	208021.87	3.46	2.05E+08
MS 90 (M) 10-8-15 (7F)	***15%***	39554.4	37604.72	205477.88	3.45	2.30E+08	215324.64	3.50	2.27E+08
MS 90 (M) 10-8-15 (7F)	***-20%***	31643.5	30203.21	189363.59	3.36	1.14E+08	198140.74	3.41	1.13E+08
MS 90 (M) 10-8-15 (7F)	***-10%***	35598.9	33772.30	193762.40	3.38	1.58E+08	203624.82	3.44	1.56E+08
MS 90 (M) 10-8-15 (7F)	***0%***	39554.4	37195.58	196644.91	3.40	2.09E+08	208021.87	3.46	2.05E+08
MS 90 (M) 10-8-15 (7F)	***15%***	45487.5	42358.39	200492.02	3.42	3.01E+08	213427.99	3.49	2.94E+08

Below, in the table, the calculations for those pavements that are referred to M1 and M2 changed at the same time, keeping the other modules constant.

Id. Pav.	D	16 hz Ms [psi]	Mr600 [psi]	EP [psi]	Sneff [inch]	ESAL Sneff	EP600 [psi]	Sneff 600 [inch]	ESAL Sneff600
Ms 30 (M-L)	***-20%***	13184.8	17469.41	155676.72	6.00	5.62E+08	130272.77	5.66	6.92E+08
Ms 30 (M-L)	***15%***	13184.8	18089.56	184987.17	6.36	8.71E+08	149506.92	5.92	1.06E+09
Ms 30 (PP-P)	***-20%***	13184.8	18926.22	177637.05	6.77	1.42E+09	142448.33	6.29	1.86E+09
Ms 30 (PP-P)	***15%***	13184.8	19756.92	213543.52	7.20	2.31E+09	164104.03	6.60	2.95E+09
Ms 90 (M-L)	***-20%***	39554.4	39758.15	239229.40	4.84	7.67E+08	238337.49	4.83	7.71E+08
Ms 90 (M-L)	***15%***	39554.4	40754.05	301596.63	5.23	1.26E+09	294537.22	5.19	1.28E+09
Ms 90 (PP-P)	***-20%***	39554.4	39893.22	239259.27	4.73	1.29E+09	237749.03	4.72	1.30E+09
Ms 90 (PP-P)	***15%***	39554.4	40766.35	300423.74	5.10	2.18E+09	293184.54	5.06	2.21E+09
MS 30 (L) 9-15-35	***-20%***	13184.8	16609.91	140403.71	5.43	2.68E+08	120765.11	5.17	3.19E+08
MS 30 (L) 9-15-35	***15%***	13184.8	17061.09	164638.35	5.73	3.95E+08	137758.12	5.40	4.65E+08
MS90 (L) 9-12-15	***-20%***	39554.4	37646.65	194157.83	3.69	2.60E+08	202288.76	3.74	2.53E+08
MS90 (L) 9-12-15	***15%***	39554.4	37762.46	238589.25	3.96	4.00E+08	248724.07	4.01	3.92E+08
MS 30 (M) 13-20-35 (8F)	***-20%***	13184.8	18664.62	173439.16	6.72	1.33E+09	140434.32	6.26	1.73E+09
MS 30 (M) 13-20-35 (8F)	***15%***	13184.8	19500.15	208892.64	7.15	2.18E+09	162096.54	6.57	2.78E+09
MS 90 (P) 11-18-15 (3F)	***-20%***	39554.4	40255.94	243793.61	4.87	1.58E+09	240687.32	4.85	1.59E+09
MS 90 (P) 11-18-15 (3F)	***15%***	39554.4	41239.44	307293.49	5.26	2.71E+09	297265.56	5.20	2.76E+09
MS 90 (PP) 11-25-15 (6F)	***-20%***	39554.4	43212.34	273120.88	5.86	6.00E+09	257896.30	5.75	6.39E+09
MS 90 (PP) 11-25-15 (6F)	***15%***	39554.4	44923.00	350036.07	6.37	1.13E+10	319715.27	6.18	1.20E+10
MS 90 (M) 10-8-15 (7F)	***-20%***	39554.4	37334.41	174805.07	3.27	1.60E+08	183855.68	3.32	1.57E+08
MS 90 (M) 10-8-15 (7F)	***15%***	39554.4	37149.53	211949.65	3.49	2.47E+08	224829.32	3.56	2.44E+08

APPENDIX 10

PENALTY/BONUS MODELS DEVELOPED FOR PERFORMANCE SPECIFICATION OF NEW ROAD CONSTRUCTION

In the graphs below: DCOST= Penalty/Bonus and DIi = Delta Indexes (from I1 to I14).

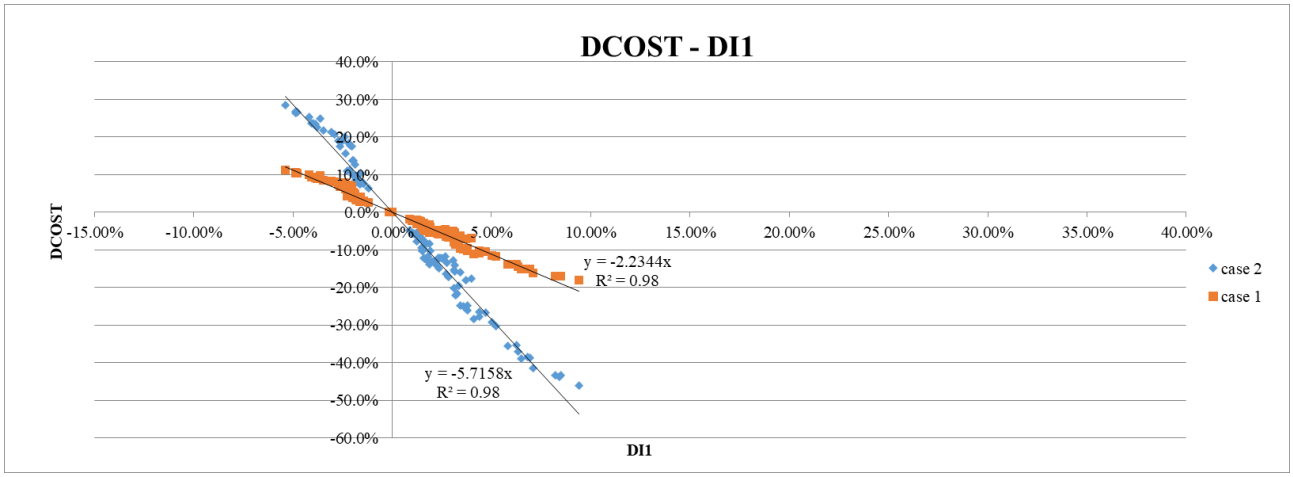

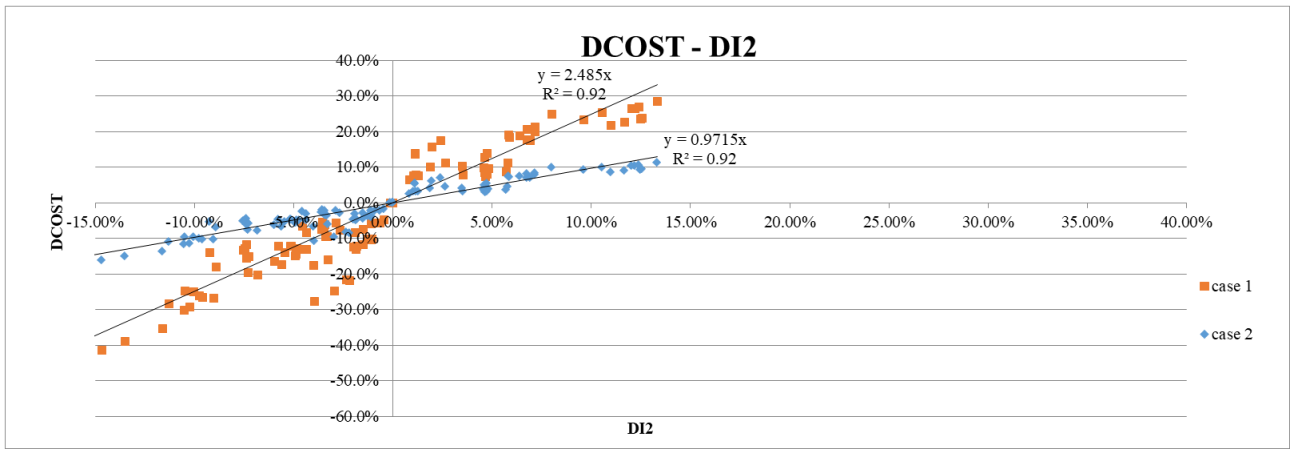

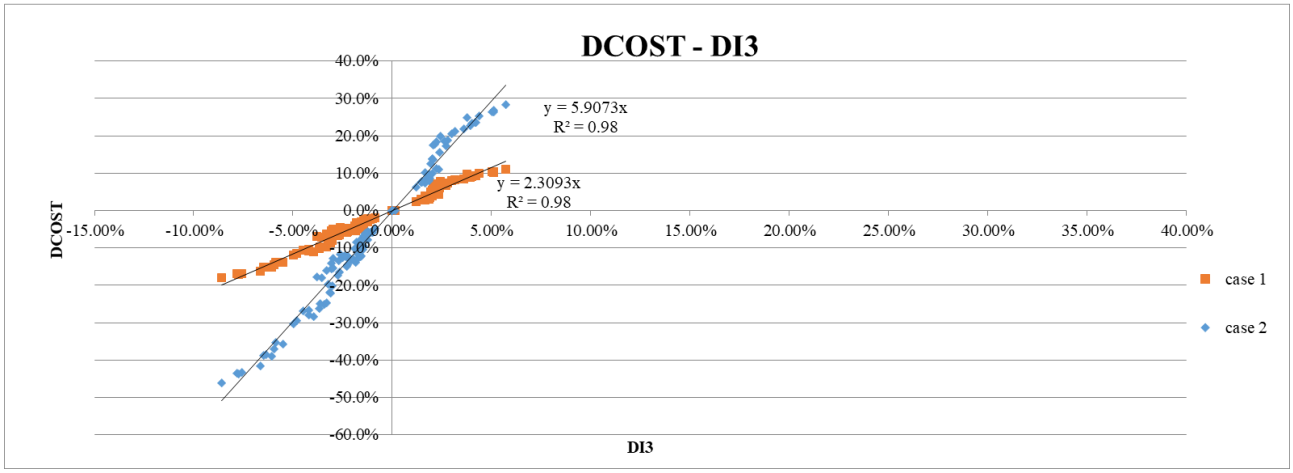

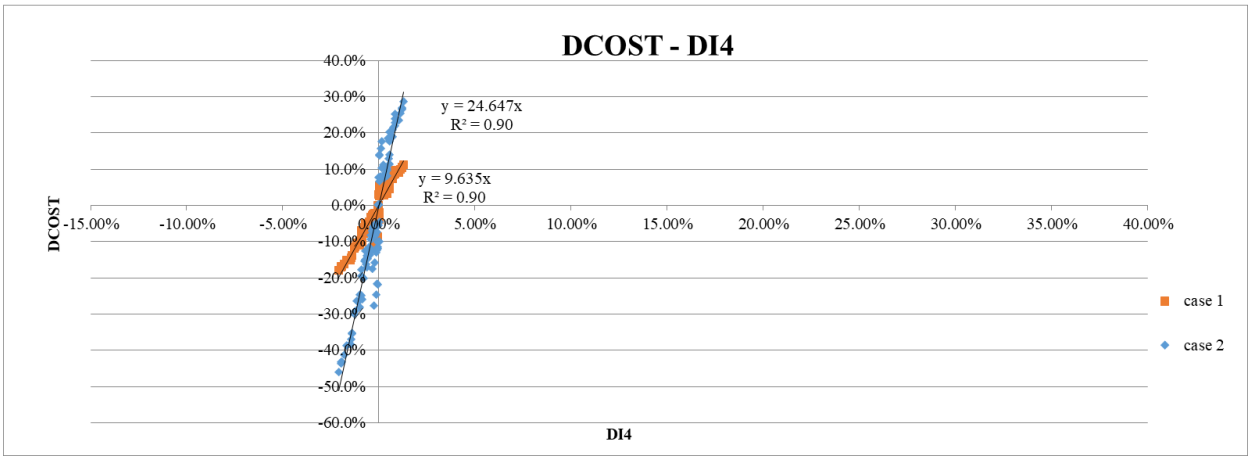
DCOST - DI4
y = 24.647x
R² = 0.90
y = 9.635x
R² = 0.90
DCOST
DI4
case 1
case 2

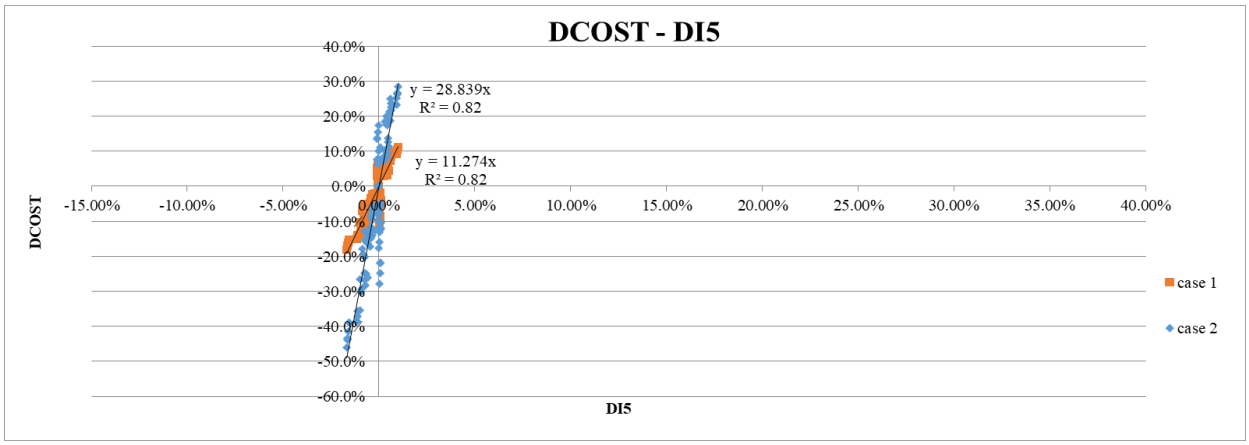
DCOST - DI5
y = 28.839x
R² = 0.82
y = 11.274x
R² = 0.82
DCOST
DI5
case 1
case 2

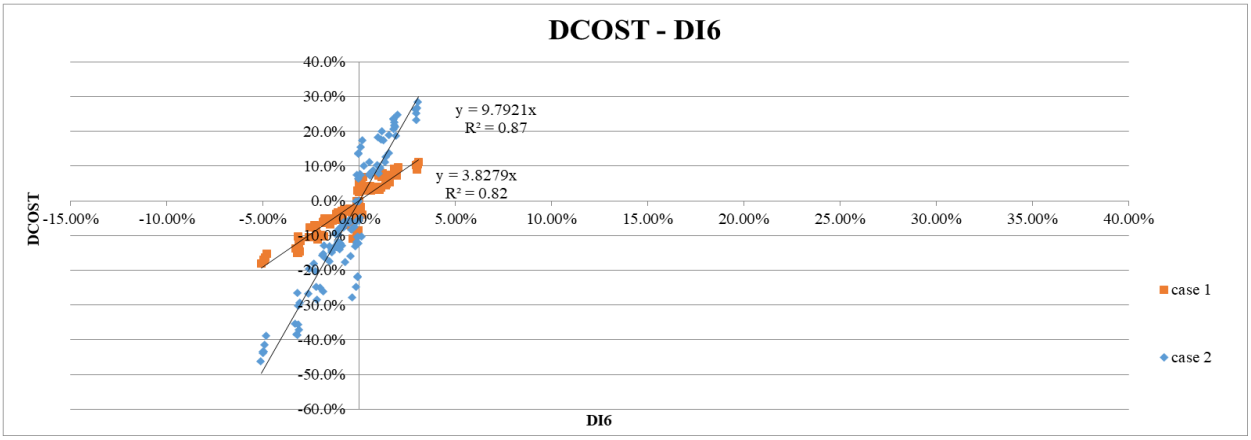
DCOST - DI6
y = 9.7921x
R² = 0.87
y = 3.8279x
R² = 0.82
DCOST
DI6
case 1
case 2

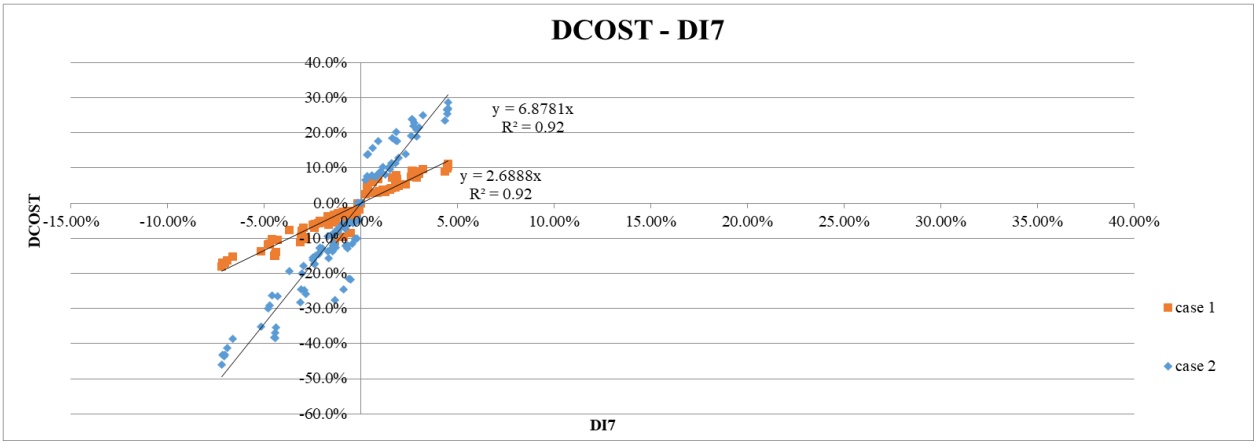
DCOST - DI7
y = 6.8781x
R² = 0.92
y = 2.6888x
R² = 0.92
DCOST
DI7
case 1
case 2

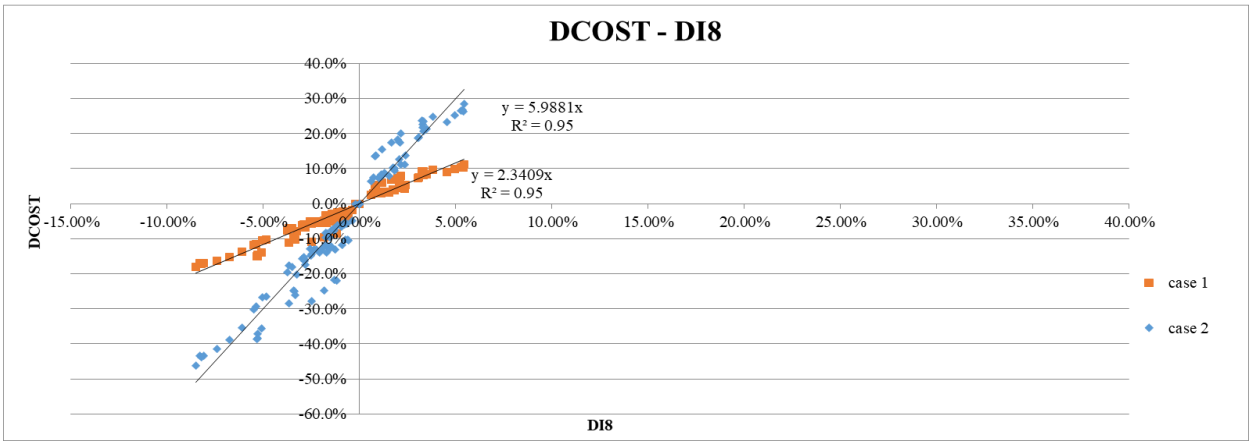
DCOST - DI8
y = 5.9881x
R² = 0.95
y = 2.3409x
R² = 0.95
DCOST
DI8
case 1
case 2

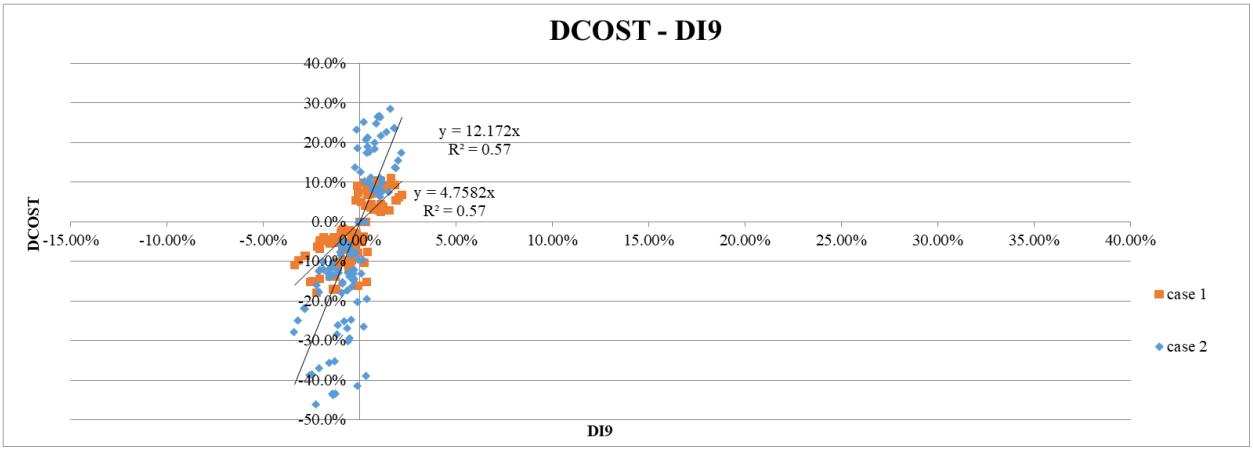
DCOST - DI9
y = 12.172x
R² = 0.57
y = 4.7582x
R² = 0.57
DCOST
DI9
case 1
case 2

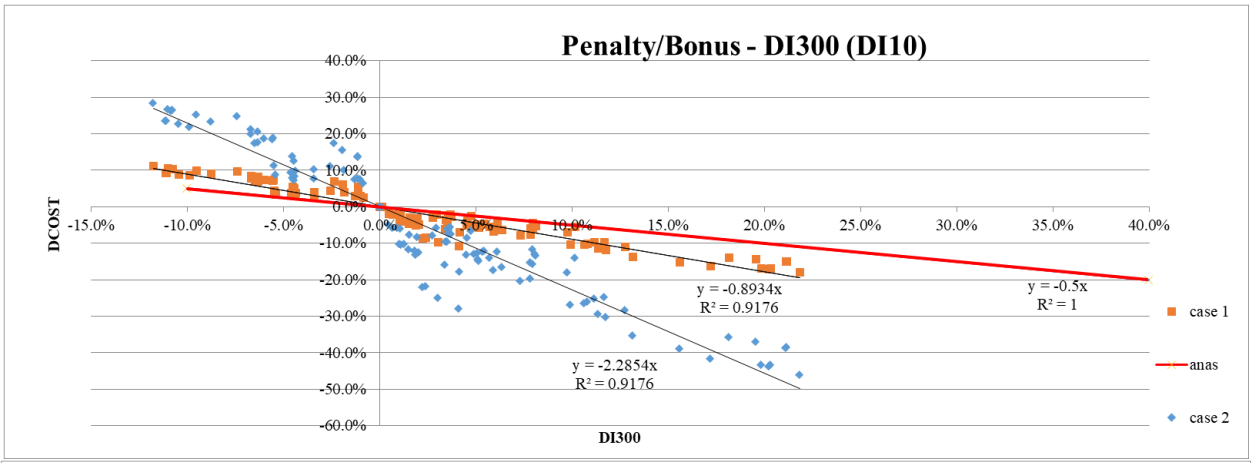
Penalty/Bonus - DI300 (DI10)
y = -0.8934x
R² = 0.9176
y = -0.5x
R² = 1
y = -2.2854x
R² = 0.9176
DCOST
DI300
case 1
anas
case 2

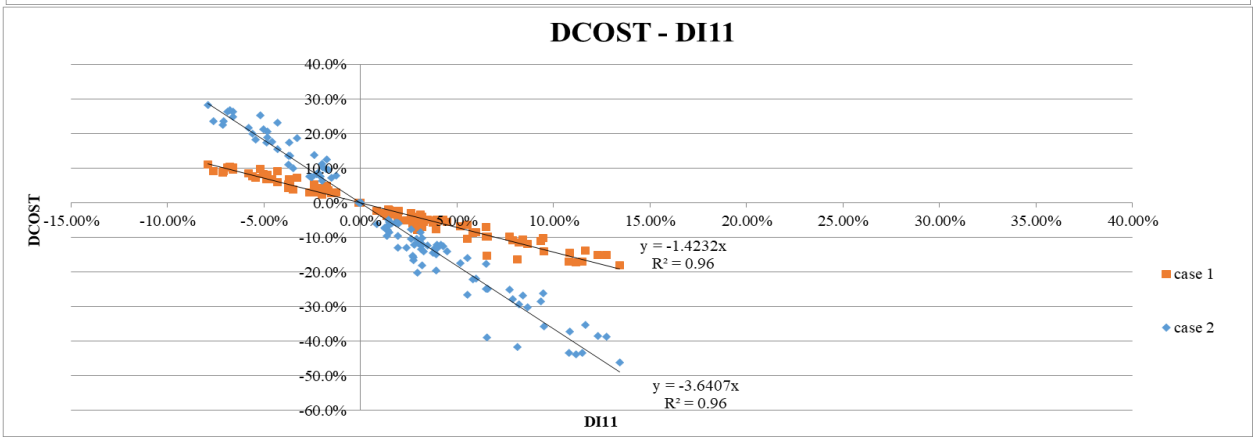
DCOST - DI11
y = -1.4232x
R² = 0.96
y = -3.6407x
R² = 0.96
DCOST
DI11
case 1
case 2

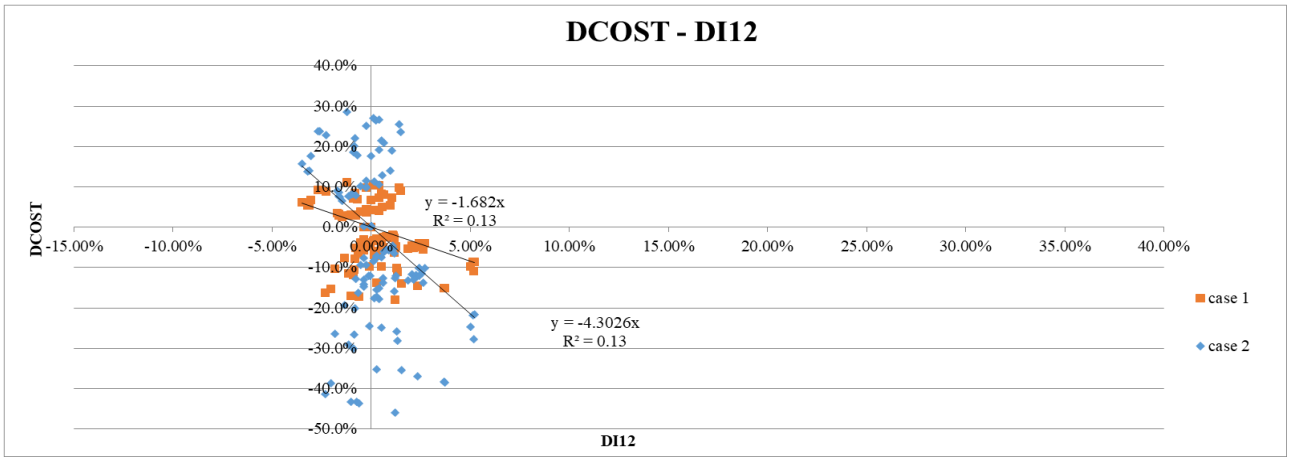
DCOST - DI12
DCOST
DI12
y = -1.682x
R² = 0.13
y = -4.3026x
R² = 0.13
case 1
case 2

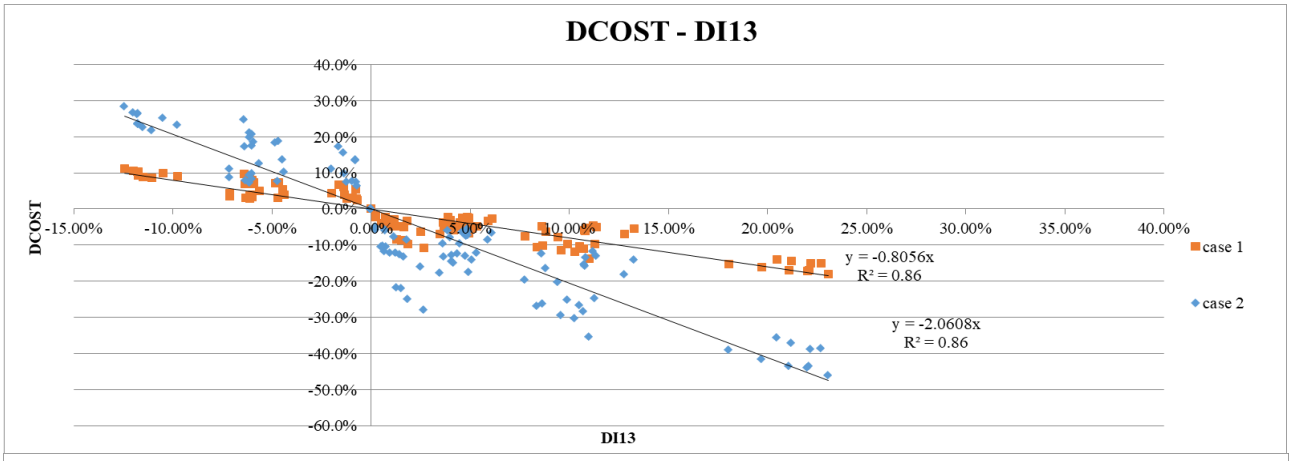
DCOST - DI13
DCOST
DI13
y = -0.8056x
R² = 0.86
y = -2.0608x
R² = 0.86
case 1
case 2

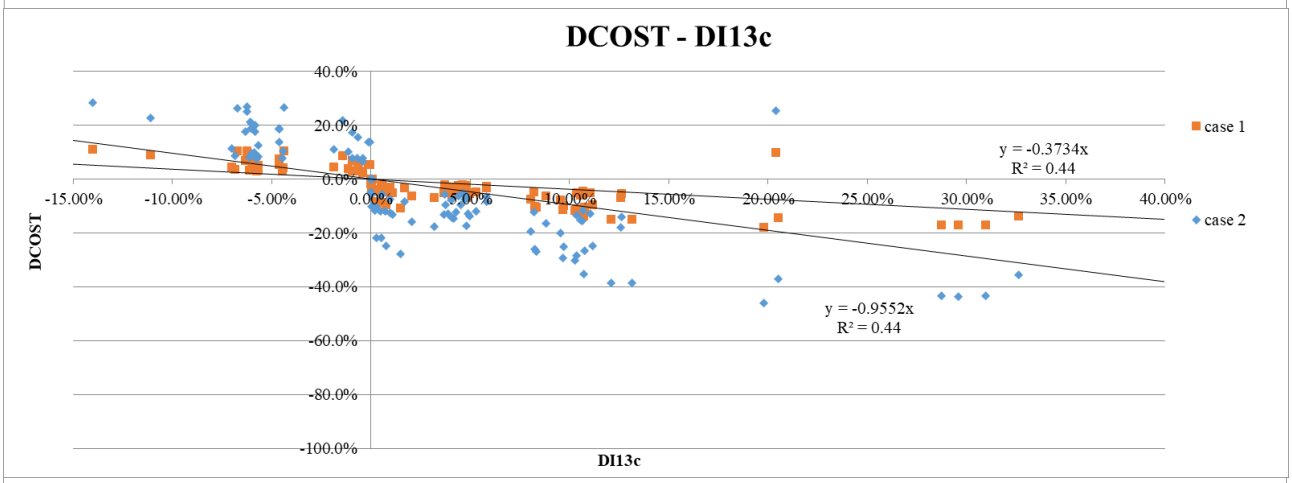
DCOST - DI13c
DCOST
DI13c
y = -0.3734x
R² = 0.44
y = -0.9552x
R² = 0.44
case 1
case 2

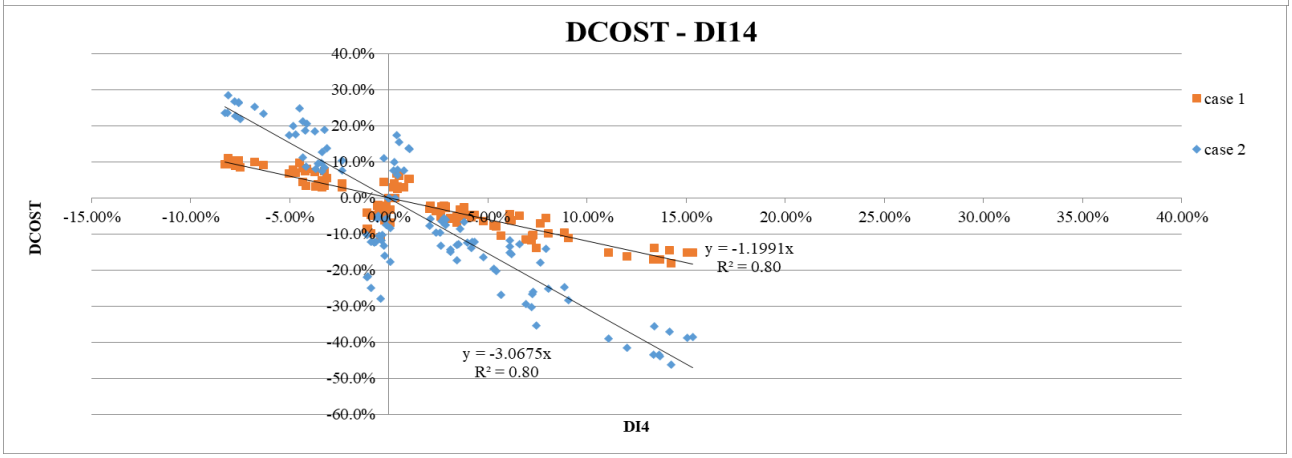
DCOST - DI14
DCOST
DI4
y = -1.1991x
R² = 0.80
y = -3.0675x
R² = 0.80
case 1
case 2

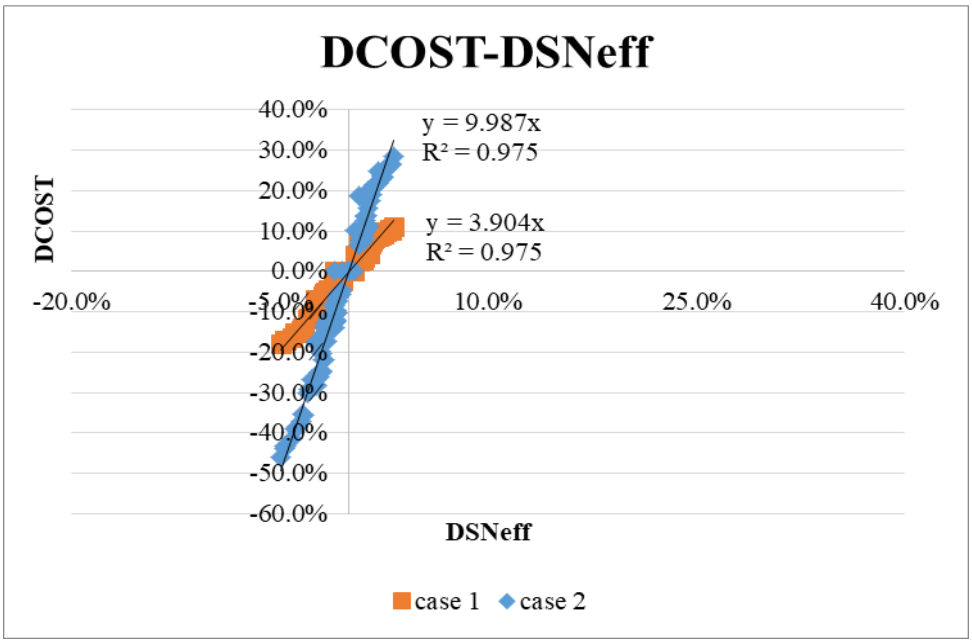
DCOST-DSNeff
y = 9.987x
R² = 0.975
y = 3.904x
R² = 0.975
DCOST
DSNeff
case 1
case 2

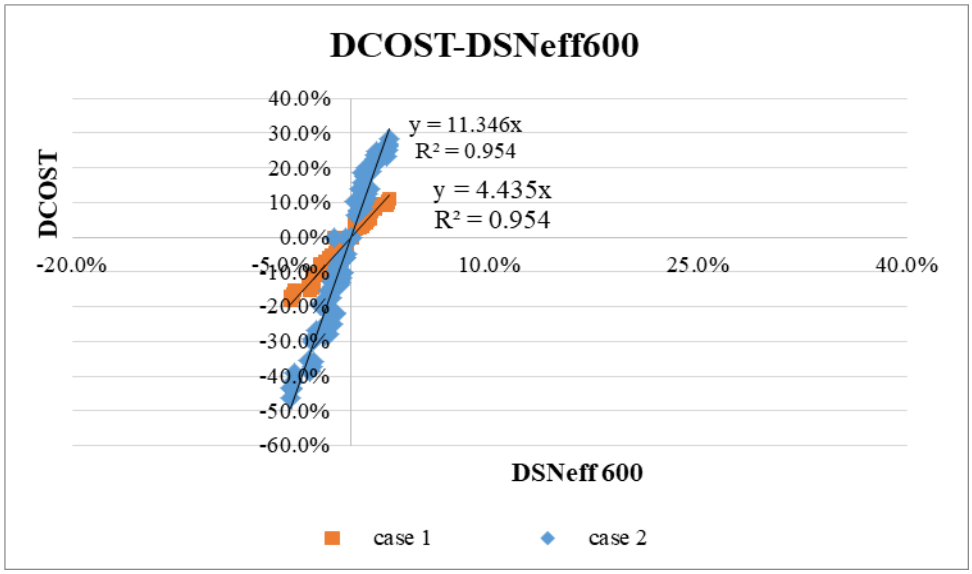
DCOST-DSNeff600
y = 11.346x
R² = 0.954
y = 4.435x
R² = 0.954
DCOST
DSNeff 600
case 1
case 2

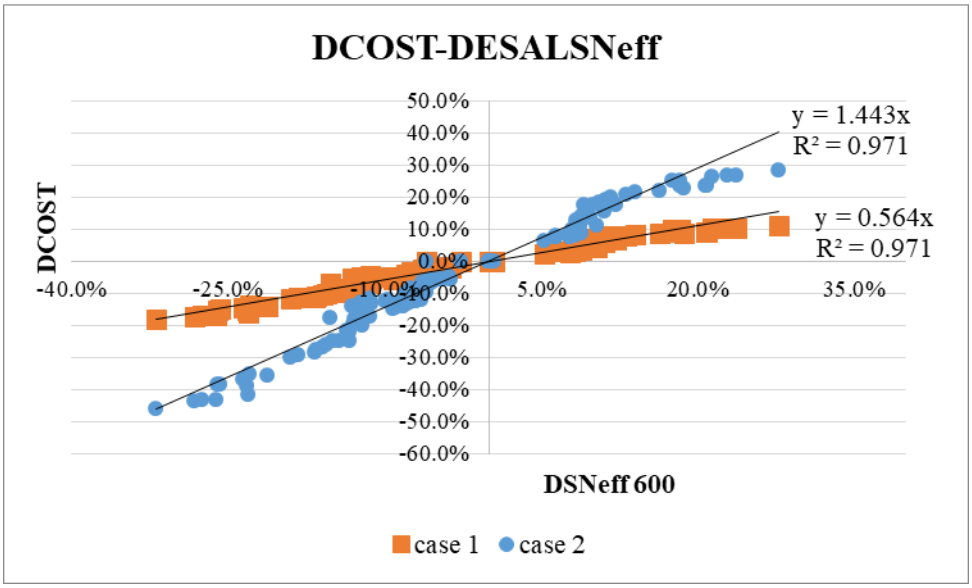
DCOST-DESALSNeff
y = 1.443x
R² = 0.971
y = 0.564x
R² = 0.971
DCOST
DSNeff 600
case 1
case 2

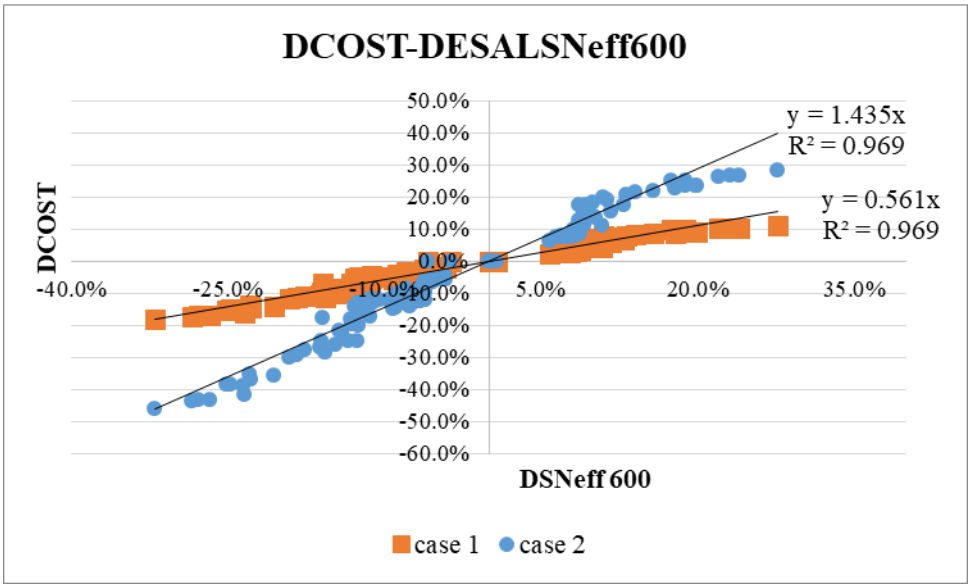
DCOST-DESALSNeff600
y = 1.435x
R² = 0.969
y = 0.561x
R² = 0.969
DCOST
DSNeff 600
case 1
case 2

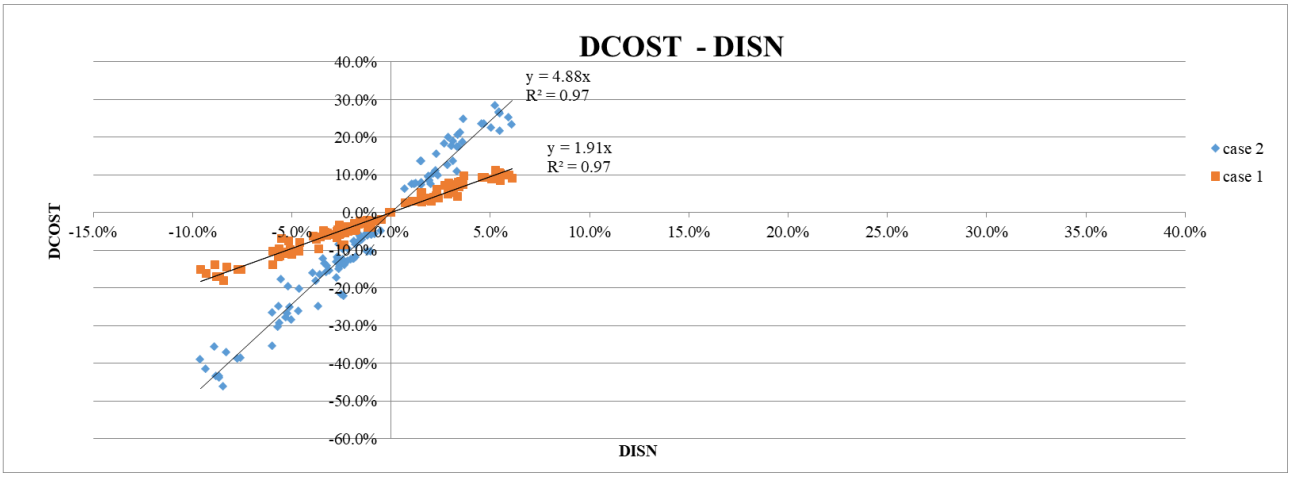
DCOST - DISN
y = 4.88x
R² = 0.97
y = 1.91x
R² = 0.97
DCOST
DISN
case 2
case 1